

AD-A062 609

DYNAMICS RESEARCH CORP WILMINGTON MASS SYSTEMS DIV
AN ANALYSIS OF FUEL CONSERVING OPERATIONAL PROCEDURES AND DESIG--ETC(U)
JUL 78 R K AGGARWAL

F/G 1/3

F33615-76-C-3104

UNCLASSIFIED

R-247U

AFFDL-TR-78-96-VOL-2

NL

1 OF 6
ADA
062609



AD A062609

DDC FILE COPY

18 19
AFFDL-TR-78-96 - VOL-2
Volume II

LEVEL III

125
D D C

DEC 21 1978

6
**AN ANALYSIS OF FUEL CONSERVING OPERATIONAL
PROCEDURES AND DESIGN MODIFICATIONS FOR
BOMBER / TRANSPORT AIRCRAFT.**

Volume II.

10
Romesh / Aggarwal
DYNAMICS RESEARCH CORPORATION
SYSTEMS DIVISION
60 CONCORD STREET
WILMINGTON, MASSACHUSETTS 01887

11
JUL 78

12 500 p.

14 R-247U

9
TECHNICAL REPORT AFFDL-TR-78-96, Volume II - Technical Report
Final Report for June 76 - July 78.

15 F33615-76-C-3144

16 2404

17 07

Approved for public release; distribution unlimited.

vol -1 - A061 746
AIR FORCE FLIGHT DYNAMICS LABORATORY
AIR FORCE SYSTEMS COMMAND
WRIGHT-PATTERSON AIR FORCE BASE, OHIO 45433

408 218

78 12 21 038

mt

NOTICE

When Government drawings, specifications, or other data are used for any purpose other than in connection with a definitely related Government procurement operation, the United States Government thereby incurs no responsibility nor any obligation whatsoever; and the fact that the government may have formulated, furnished, or in any way supplied the said drawings, specifications, or other data, is not to be regarded by implication or otherwise as in any manner licensing the holder or any other person or corporation, or conveying any rights or permission to manufacture, use, or sell any patented invention that may in any way be related thereto.

This report has been reviewed by the Information Office (OI) and is releasable to the National Technical Information Service (NTIS). At NTIS, it will be available to the general public, including foreign nations.

This technical report has been reviewed and is approved for publication.

L. E. Miller

L.E. MILLER, PhD
Project Engineer

Arnold G. Crowder

ARNOLD G. CROWDER, MAJ, USAF
Chief, High Speed Aero Perf. Br.

FOR THE COMMANDER

Melvin L. Buck

MELVIN L. BUCK
Chief, Aeromechanics Division

"If your address has changed, if you wish to be removed from our mailing list, or if the addressee is no longer employed by your organization please notify _____, W-PAFB, OH 45433 to help us maintain a current mailing list".

Copies of this report should not be returned unless return is required by security considerations, contractual obligations, or notice on a specific document.

REPORT DOCUMENTATION PAGE		READ INSTRUCTIONS BEFORE COMPLETING FORM
1. REPORT NUMBER AFFDL-TR-78-96 Vol II ✓	2. GOVT ACCESSION NO.	3. RECIPIENT'S CATALOG NUMBER
4. TITLE (and Subtitle) An Analysis of Fuel Conserving Operational Procedures and Design Modifications for Bomber/Transport Aircraft <i>Abbl 746</i>		5. TYPE OF REPORT & PERIOD COVERED Final 7 June 76 - 7 July 78
6. AUTHOR(s) R. Aggarwal, et. al.		7. PERFORMING ORG. REPORT NUMBER R-247U
8. PERFORMING ORGANIZATION NAME AND ADDRESS Dynamics Research Corporation 60 Concord Street Wilmington, Massachusetts 01887		9. CONTRACT OR GRANT NUMBER(s) F33615-76-C-3104 ✓
10. CONTROLLING OFFICE NAME AND ADDRESS Air Force Flight Dynamics Laboratory Air Force Systems Command Wright-Patterson AFB, Ohio 45433		11. PROGRAM ELEMENT, PROJECT, TASK AREA & WORK UNIT NUMBERS Project: 2404 Task: 240407 Work Unit: 24040707
12. MONITORING AGENCY NAME & ADDRESS (if different from Controlling Office)		13. REPORT DATE July, 1978
		14. NUMBER OF PAGES
		15. SECURITY CLASS. (of this report) Unclassified
		16. DECLASSIFICATION/DOWNGRADING SCHEDULE
17. DISTRIBUTION STATEMENT (of this Report) Approved for public release: distribution unlimited.		
18. DISTRIBUTION STATEMENT (of the abstract entered in Block 20, if different from Report)		
19. SUPPLEMENTARY NOTES		
20. KEY WORDS (Continue on reverse side if necessary and identify by block number)		
21. ABSTRACT (Continue on reverse side if necessary and identify by block number) Various proposed improvements in the design and operational procedures for bomber/transport aircraft are evaluated. The evaluation is performed in terms of the estimated savings in fuel consumption and in Direct Operating Cost (DOC). As an aid in the evaluation of design modifications, graphs of fuel and DOC savings as a function of the design parameters are developed. <i>OVER</i>		

These graphs are based on actual mission trajectory data rather than some typical trajectory profile. The actual mission data is presented in terms of histograms which provide statistical information concerning altitude, air speed, take-off weight, landing weight, and mission time. Separate analyses are performed on the following aircraft: the B-52G, the B-52H, the KC-135, the C-141, the C-130, and the C-5A.

UNCLASSIFIED

FORWARD

This report was prepared by the Dynamics Research Corporation (DRC), 60 Concord Street, Wilmington, Massachusetts, under Contract No. F33615-76-C-3104, for the Air Force Flight Dynamics Laboratory, Wright-Patterson Air Force Base, Ohio. Dr. L. E. Miller (AFFDL/FXG) was the Technical Monitor for this contract.

This report was submitted by the authors in July 1978 and covers the period of performance from June 1976 to July 1978.

The study was directed by Dr. John P. Matuszewski. Dr. Romesh K. Aggarwal was the principal investigator with engineering support from Mr. R. Dowd, Mr. John C. Goclowski, Mr. Harry Hubbard, Dr. Anthony J. Calise and Dr. Jason Speyer. In addition, Mr. Stanley J. Jakimczyk assisted in the computer program development.

ACCESSION for _____
N.Y.S. _____ White Section ☒
_____ B.H.F. Section ☐

APPROVED BY _____
DATE OF APPROVAL _____

SERIAL NO. _____

EXHIBIT TO PROCEEDINGS IN RE _____
SPECIAL

A

TABLE OF CONTENTS

SECTION	PAGE
1. INTRODUCTION	1-1
2. AIRCRAFT MISSION PROFILE AND DIRECT OPERATION COST MODELS*	2-1
2.1 MISSILE MODELS	2-1
2.1.1 Command Mission Statements	2-1
2.1.2 Data Sources	2-5
2.1.3 Data Analysis	2-7
2.1.4 Characteristics of Aircraft Missions	2-7
2.2 DIRECT OPERATING COST MODEL	2-8
2.2.1 Cost of Fuel and Oil Per Flight Hours (FH)	2-13
2.2.2 Cost of Flight Crew per Flight Hour (FH)	2-13
2.2.3 Maintenance Costs	2-13
2.2.4 Derivation of DOC Model	2-14
3. MATHEMATICAL MODELING, ANALYSIS AND SIMULATION *	3-1
3.1 MEASURE OF PERFORMANCE	3-2
3.2 AERODYNAMIC AND PROPULSION MODELS	3-3
3.2.1 Aerodynamics	3-4
3.2.2 Propulsion	3-11
3.3 EQUATIONS OF MOTION	3-16
3.4 DEFINITION OF FLIGHT SEGMENTS	3-17
3.4.1 Departure	3-17
3.4.2 Climb	3-19
3.4.3 Cruise	3-19

* Actual models given in Section 7 where each aircraft is discussed separately

TABLE OF CONTENTS (cont'd)

SECTION	PAGE
3.4.4 Descent	3-19
3.4.5 Acceleration/Deceleration	3-20
3.4.6 Turning	3-20
3.4.7 Approach	3-20
3.5 MODELING OF CONVENTIONAL FLIGHT PROCEDURES	3-20
3.5.1 Constraints	3-21
3.5.2 Thrust, Altitude, Velocity Procedure Information	3-22
3.6 MODELING OF OPTIMAL FLIGHT PROCEDURES	3-22
3.6.1 Extended Energy Management (EEM Solutions)	3-23
3.6.2 Constrained and Unconstrained Optimal Solutions	3-23
3.6.3 Modeling Mass Variations	3-24
3.6.4 Constrained Solutions	3-25
3.7 MISSION PROFILE ANALYSIS PROGRAM	3-26
3.7.1 Discussion of Program	3-26
3.7.2 Verification of Simulation Results	3-29
3.8 MISSION SPECTRUM ANALYSIS PROGRAM	3-35
4. ANALYSIS APPROACH AND DEFINITION OF OPERATIONAL PROCEDURES THAT CONSERVE FUEL	4-1
4.1 ANALYSIS OF AIRBORNE PROCEDURES REQUIRING TRAJECTORY OPTIMIZATION	4-1
4.1.1 Departure	4-2
4.1.2 Approach	4-3
4.1.3 Cruise	4-4
4.1.4 Climb	4-10
4.1.5 Descent	4-11
4.1.6 Integrated Trajectories	4-14
4.2 ANALYSIS OF OTHER FUEL CONSERVING AIRBORNE PROCEDURES	4-19
4.2.1 Procedures Which Reduce Drag	4-19
4.2.2 Procedures Which Reduce Engine Load	4-21

TABLE OF CONTENTS (cont'd)

SECTION	PAGE
4.2.3 Speed Management	4-23
4.2.4 Precision Navigation	4-23
4.3 ANALYSIS OF GROUND PROCEDURES	4-24
4.3.1 Maintenance	4-24
4.3.2 Ground Handling	4-29
4.3.3 Removing Excess Equipment	4-30
4.3.4 Cargo Loading	4-32
4.3.5 Computerized Flight Planning	4-32
4.3.6 Reduced Reserve Fuel	4-33
4.3.7 Alternate Fuel: Use of JP-8 Fuel	4-36
5. ANALYSIS APPROACH AND DEFINITION OF DESIGN MODIFICATIONS THAT CONSERVE FUEL	5-1
5.1 PARAMETRIC ANALYSIS OF AERODYNAMIC DESIGN CHANGES	5-2
5.2 PARAMETRIC ANALYSIS OF PROPULSION DESIGN CHANGES	5-3
5.3 DATA SOURCES	5-4
5.3.1 Data Required for Reengining Studies	5-4
5.3.2 Data Required for Evaluation of Winglets	5-6
6. SENSITIVITY ANALYSIS APPROACH	6-1
6.1 UNCERTAINTIES IN AIRCRAFT PARAMETERS	6-1
6.1.1 Sensitivity to Zero-Lift Drag	6-1
6.1.2 Sensitivity to Induced Drag	6-2
6.1.3 Sensitivity to Fuel Flow Rate	6-2
6.1.4 Sensitivity to Weight Variations	6-3
6.1.5 Sensitivity to Thrust Variations	6-3
6.2 SENSITIVITY TO ENVIRONMENTAL FACTORS	6-4
6.2.1 Sensitivity to Atmospheric Variations	6-4

TABLE OF CONTENTS (cont'd)

SECTION	PAGE
6.2.2 Sensitivity to Traffic Density	6-6
6.2.3 Impact of Optimal Procedures on Noise and Air Pollution	6-8
6.3 SENSITIVITY TO INSTRUMENT ERRORS	6-10
6.3.1 Sensitivity to Errors in Cruise Mach	6-10
6.3.2 Sensitivity to Errors in Cruise Altitude	6-12
6.4 SENSITIVITY TO UNCERTAINTIES IN DESIGN MODIFICATIONS	6-13
7. RESULTS OF FUEL/DOC TRADE-OFF STUDIES AND SENSITIVITY ANALYSIS BY AIRCRAFT TYPE	7-1
7.1 C-141	7-1
7.1.1 C-141 Design Missions	7-1
7.1.2 C-141 Mission Models	7-3
7.1.3 C-141 DOC Model	7-18
7.1.4 C-141 Aerodynamic and Propulsion Models	7-19
7.1.5 Evaluation of Airborne and Ground Operational Procedures	7-22
7.1.6 Evaluation of Design Modifications	7-44
7.1.7 Sensitivity Analysis	7-52
7.1.8 Conclusions for the C-141	7-64
7.2 C-5A AIRCRAFT	7-69
7.2.1 Design Mission Data	7-69
7.2.2 Mission Model	7-69
7.2.3 DOC Model	7-74
7.2.4 C-5A Characteristics	7-84
7.2.5 Evaluations of Airborne and Ground Operational Procedures	7-86
7.2.6 Evaluation of Design Modifications	7-107
7.2.7 Sensitivity Analysis	7-114
7.2.8 Conclusions for the C-5	7-123
7.3 C-130 AIRCRAFT	7-127
7.3.1 Design Mission Data	7-127

TABLE OF CONTENTS (cont'd)

SECTION	PAGE
7.3.2 Mission Model	7-127
7.3.3 DOC Model	7-139
7.3.4 C-130E Characteristics	7-139
7.3.5 Evaluation of Airborne and Ground Operational Procedures	7-143
7.3.6 Evaluation of Design Modification	7-158
7.3.7 Sensitivity Analysis	7-163
7.3.8 Conclusions for the C-130E	7-172
7.4 B-52G AIRCRAFT	7-177
7.4.1 Design Mission	7-177
7.4.2 Mission Model	7-177
7.4.3 DOC Model	7-179
7.4.4 B-52G Characteristics	7-183
7.4.5 Evaluation of Airborne and Ground Operational Procedures	7-186
7.4.6 Evaluation of Design Modifications	7-199
7.4.7 Sensitivity Analysis	7-204
7.4.8 Conclusions for the B-52G	7-213
7.5 B-52H AIRCRAFT	7-218
7.5.1 Design Mission	7-218
7.5.2 Mission Model	7-218
7.5.3 DOC Model	7-220
7.5.4 B-52H Characteristics	7-220
7.5.5 Evaluation of Airborne and Ground Operational Procedures	7-223
7.5.6 Evaluation of Design Modifications	7-233
7.5.7 Sensitivity Analysis	7-238
7.5.8 Conclusions for the B-52H	7-245
7.6 KC-135 AIRCRAFT UTILIZATION MODEL	7-250
7.6.1 Design Missions	7-250
7.6.2 Mission Model	7-250
7.6.3 DOC Model	7-263
7.6.4 KC-135 Characteristics	7-264

TABLE OF CONTENTS (cont'd)

SECTION	PAGE
7.6.5 Evaluation of Airborne and Ground Operational Procedures	7-267
7.6.6 Evaluation of Design Modifications	7-282
7.6.7 Sensitivity Analysis	7-292
7.6.8 Conclusions for the KC-135	7-302
8. IMPACT OF REDUCED FUEL ALLOCATIONS ON OPERATIONAL READINESS	8-1
8.1 OPERATIONAL EFFECTIVENESS	8-3
8.2 SIMULATORS	8-7
9. CONCLUSIONS AND RECOMMENDATIONS	9-1
REFERENCES	R-1
APPENDIX A	A-1
DERIVATION OF OPTIMAL FLIGHT PROCEDURES	
APPENDIX B	B-1
OPTIMALITY OF CRUISE SOLUTION	
APPENDIX C	C-1
FUNCTIONAL RELATIONSHIPS BETWEEN DESIGN MODIFICATIONS AND IMPROVEMENTS IN PERFORMANCE/COST	
APPENDIX D	D-1
CENTER-OF-GRAVITY SHIFT EFFECTS ON FUEL CONSUMPTION	
APPENDIX E	E-1
SUMMARY OF VISITS	

LIST OF ILLUSTRATIONS

FIGURE		PAGE
2.1-1	MAC Global Organization	2-3
2.1-2	SAC B-52G/H, KC-135 Organizations	2-4
2.2-1	DOC As a Function of Flight Time	2-11
2.2-2	Cost of Jet Fuel	2-12
3.2-1	C-141 Aerodynamic Data	3-5
3.2-2	Military Rated Thrust vs. Mach for B-52G	3-12
3.2-3	Normal Rated Thrust vs. Mach for B-52G	3-13
3.4-1	Typical Mission Profile	3-18
3.7-1	Feedback Implementation of the EEM Solution	3-28
4.1-1	Best Cruise Mach Numbers for Minimum Fuel Cruise for C-141	4-6
4.1-2	Range Factor for Minimum Fuel Cruise for C-141	4-7
4.1-3	Altitude-Mach Profiles for Long Range Optimal and Conventional Trajectories	4-17
4.2-1	Secondary Power System Energy Diagram, Typical Subsonic Cruise Mach 0.8 Transport	4-22
5.2-1	Illustration of a Break-Even Analysis Presentation of Acquisition and Maintenance Cost	5-5
6.2-1	Effect of Wind on Optimum Cruise Mach Number	6-7
7.1-1	C-141 Typical Airlift Mission	7-4
7.1-2	C-141 Typical Exercise Mission	7-5
7.1-3	C-141 Typical Training Mission	7-6
7.1-4	C-141 Distribution of Level Off Altitudes (less than 200,000 lbs)	7-9
7.1-5	C-141 Distribution of Level Off Altitudes (200,000 lbs)	7-10
7.1-6	C-141 Distribution of Level Off Altitudes (240,000 lbs)	7-11

LIST OF ILLUSTRATIONS (cont'd)

FIGURE		PAGE
7.1-7	C-141 Distribution of Level Off Altitudes (280,000 lbs)	7-12
7.1-8	C-141 Distribution of Level Off Altitudes (200,000 lbs)	7-13
7.1-9	C-141 Distribution of Level Off Altitudes (240,000 lbs)	7-14
7.1-10	C-141 Distribution of Level Off Altitudes (280,000 lbs)	7-15
7.1-11	C-141 Distribution of Level Off Altitudes (240,000 lbs)	7-16
7.1-12	C-141 Distribution of Level Off Altitudes (280,000 lbs)	7-17
7.1-13	Fuel/Time Trade-Off for the C-141 Cruise Solution	7-24
7.1-14	Fuel/DOC Savings Due to Reduced Speed - C-141 Long Range Missions	7-35
7.1-15	Fuel/DOC Savings Due to Reduced Speed and Increased Altitudes C-141 Medium Range Missions	7-36
7.1-16	Sensitivity of Fuel/DOC to Variations in Zero Lift Drag C-141A	7-45
7.1-17	Sensitivity of Fuel/DOC to Variations in Induced Drag C-141A	7-46
7.1-18	Sensitivity of Fuel/DOC to Variations in Thrust Specific Fuel Consumption C-141A	7-47
7.1-19	Sensitivity of Fuel/DOC to Variations in Weight C-141	7-48
7.1-20	Savings Due to Retrofitting C-141 with Winglets	7-50
7.1-21	Savings Due to Re-engining C-141	7-53
7.1-22	C-141 Vortex Generator Removal	7-54
7.1-23	C-141 Fillet Revision	7-55
7.1-24	Sensitivity of Range Factor to Variations in Zero-Lift Drag for C-141	7-57
7.1-25	Sensitivity of Range Factor to Variations in Induced Drag for C-141	7-58
7.1-26	Impact of Thrust Variations on Cruise Ceiling for C-141	7-60
7.1-27	Impact of Wind on Optimum Cruise Mach Number for C-141	7-62

LIST OF ILLUSTRATIONS (cont'd)

FIGURE		PAGE
7.1-28	Impact of Wind on Range Factor for C-141	7-63
7.1-29	Decrease in Range Factor Due to Flying Off Optimum Cruise Mach Number	7-66
7.1-30	Decrease in Range Factor Due to Flying Off Optimum Cruise Altitude	7-67
7.2-1	C-5 Typical Airlift Mission	7-71
7.2-2	C-5 Typical Training Mission	7-73
7.2-3	C-5 Distribution of Level Off Altitudes (450,000 lbs)	7-75
7.2-4	C-5 Distribution of Level Off Altitudes (450,000 - 550,000 lbs)	7-76
7.2-5	C-5 Distribution of Level Off Altitudes (550,000 - 650,000 lbs)	7-77
7.2-6	C-5 Distribution of Level Off Altitudes (up to 450,000 lbs)	7-78
7.2-7	C-5 Distribution of Level Off Altitudes (450,000- 550,000 lbs)	7-79
7.2-8	C-5 Distribution of Level Off Altitudes (550,000 - 650,000 lbs)	7-80
7.2-9	C-5 Distribution of Level Off Altitudes (450,000 - 550,000 lbs)	7-81
7.2-10	C-5 Distribution of Level Off Altitudes (550,000 - 650,000 lbs)	7-82
7.2-11	C-5 Distribution of Level Off Altitudes (650,000 lbs)	7-83
7.2-12	Fuel/Time Trade-Off for the C-5 Cruise Solution	7-88
7.2-13	Fuel/DOC Savings Due to Reduced Speed and Increased Altitudes C-5A Long Range Missions	7-97
7.2-14	Fuel/DOC Savings Due to Reduced Speed and Increased Altitude C-5A Medium Range Missions	7-98
7.2-15	Fuel/DOC Savings Due to Reduced Speed and Increased Altitude C-5A Short Range Missions	7-99
7.2-16	Sensitivity of Fuel/DOC to Variations in Zero-Lift Drag C-5A	7-108

LIST OF ILLUSTRATIONS (cont'd)

FIGURE		PAGE
7.2-17	Sensitivity of Fuel/DOC to Variations in Induced Drag C-5A	7-109
7.2-18	Sensitivity of Fuel/DOC in Thrust Specific Fuel Consumption C-5A	7-110
7.2-19	Sensitivity of Fuel/DOC to Variations in Weight C-5A	7-111
7.2-20	Savings Due to Winglets for C-5A	7-113
7.2-21	Sensitivity of Range Factor to Variations in Zero-Lift Drag for C-5A	7-115
7.2-22	Sensitivity of Range Factor to Variations in Induced Drag for C-5	7-116
7.2-23	Impact of Thrust Variation of Cruise Ceiling for C-5	7-119
7.2-24	Impact of Wind On Optimum Cruise Mach Number for C-5	7-121
7.2-25	Impact of Winds on Range Factor for C-5	7-122
7.2-26	Decrease in Range Factor Due to Flying Off Optimum Cruise Mach Number C-5A	7-124
7.2-27	Decrease in Range Factor Due to Flying Off Optimum Cruise Altitude C-5A	7-125
7.3-1	C-130 Typical Airlift Mission	7-129
7.3-2	C-130 Distribution of Level Off Altitudes (Up to 100,000 lbs)	7-131
7.3-3	C-130 Distribution of Level Off Altitudes (100,000 - 130,000 lbs)	7-132
7.3-4	C-130 Distribution of Level Off Altitudes (130,000 - 160,000 lbs)	7-133
7.3-5	C-130 Distribution of Level Off Altitudes (up to 100,000 lbs)	7-134
7.3-6	C-130 Distribution of Level Off Altitudes (100,000 - 130,000 lbs)	7-135
7.3-7	C-130 Distribution of Level Off Altitudes (130,000 - 160,000 lbs)	7-136
7.3-8	C-130 Distribution of Level Off Altitudes (100,000 - 130,000 lbs)	7-137

LIST OF ILLUSTRATIONS (cont'd)

FIGURE		PAGE
7.3-9	C-130 Distribution of Level Off Altitudes (130,000 - 160,000 lbs)	7-138
7.3-10	Fuel/Time Trade-Off for the C-130E Cruise Solution	7-145
7.3-11	Fuel/DOC Savings Due to Reduced Speed and Increased Altitude C-130E Long Range Missions	7-151
7.3-12	Fuel/DOC Savings Due to Reduced Speed and Increased Altitude C-130E Medium Range Missions	7-152
7.3-13	Fuel/DOC Savings Due to Reduced Speed and Increased Altitude C-130E Short Range Missions	7-153
7.3-14	Sensitivity of Fuel/DOC to Variations in Zero Life Drag C-130E	7-159
7.3-15	Sensitivity of Fuel/DOC to Variations in Induced Drag C-130E	7-160
7.3-16	Sensitivity of Fuel/DOC to Variations in Specific Fuel Consumption per Horse Power C-130E	7-161
7.3-17	Sensitivity of Fuel/DOC to Variations in Weight C-130E	7-162
7.3-18	Savings Due to C-130E Aft Body Strakes	7-164
7.3-19	Sensitivity of Range Factor to Variations in Zero Lift Drag for C-130E	7-165
7.3-20	Sensitivity of Range Factor to Variations in Induced Drag C-130E	7-167
7.3-21	Impact of Variations in Maximum Continuous Power of Cruise Ceiling	7-168
7.3-22	Sensitivity of Range Factor to Atmospheric Winds C-130E	7-170
7.3-23	Impact of Ambient Temperatures on Cruise Ceiling C-130E	7-171
7.3-24	Impact of Flying Off Optimum Cruise Speed on Range Factor C-130E	7-173
7.3-25	Impact of Flying Off Optimum Cruise Altitude on Range Factor C-130E	7-174
7.4-1	B-52 Normal Profile Mission	7-180

LIST OF ILLUSTRATIONS (cont'd)

FIGURE		PAGE
7.4-2	B-52 Training (No Low Level)	7-181
7.4-3	B-52 Pilot Proficiency Mission	7-182
7.4-4	Fuel/Time Trade-Off for the B-52G Cruise Solution	7-187
7.4-5	Sensitivity of Fuel/DOC to Variations in Zero-Lift Drag - B-52G	7-200
7.4-6	Sensitivity of Fuel/DOC to Variations in Induced Drag - B-52G	7-201
7.4-7	Sensitivity of Fuel/DOC to Variations in Thrust Specific Fuel Consumption - B-52G	7-202
7.4-8	Sensitivity of Fuel/DOC to Variations in Weight - B-52G	7-203
7.4-9	Savings Due to Manual Surge Bleed Valve Override	7-205
7.4-10	Sensitivity of Range Factor to Variations in Zero-Lift Drag - B-52G	7-206
7.4-11	Sensitivity of Range Factor to Variations in Induced Drag - B-52G	7-208
7.4-12	Impact of Variations in NRT on Cruise Ceiling for B-52G	7-209
7.4-13	Impact of Wind On Optimum Cruise Mach Number for B-52G	7-211
7.4-14	Impact of Wind on the Specific Range for B-52G	7-212
7.4-15	Impact of Flying Off Optimum Cruise Mach on Range Factor B-52G	7-214
7.4-16	Impact of Flying Off Optimum Cruise Altitude on Range Factor - B-52G	7-215
7.5-1	Fuel/Time Trade-Off for the B-52H Cruise Solution	7-224
7.5-2	Sensitivity of Fuel/DOC to Variations in Zero-Lift Drag B-52H	7-234
7.5-3	Sensitivity of Fuel/DOC to Variations in Induced Drag B-52H	7-235
7.5-4	Sensitivity of Fuel/DOC to Variations in Thrust Specific Fuel Consumption - B-52H	7-236
7.5-5	Sensitivity of Fuel/DOC to Variations in Weight-B-52H	7-237

LIST OF ILLUSTRATIONS (cont'd)

FIGURE		PAGE
7.5-6	Sensitivity of Range Factor to Variations in Zero-Lift Drag Coefficient for B-52H	7-239
7.5-7	Sensitivity of Range Factor to Variations in Induced Drag Coefficient for B-52H	7-240
7.5-8	Impact of Variations in NRT on Cruise Ceiling for B-52H	7-242
7.5-9	Impact of Wind on Range Factor for a B-52H Aircraft	7-243
7.5-10	Impact of Wind on Optimum Cruise Mach Number for B-52H Aircraft	7-244
7.5-11	Impact of Flying Off Optimum Cruise Mach Number on Range Factor B-52H	7-246
7.5-12	Impact of Flying Off Optimum Cruise Altitude on Range Factor B-52H	7-247
7.6-1	KC-135 Average Air Refueling (34%)	7-252
7.6-2	KC-135 Average Air Refueling (13%)	7-253
7.6-3	KC-135 Average Non-Refueling (45%)	7-254
7.6-4	KC-135 Average Non-Refueling (8%)	7-255
7.6-5	KC-135 Distribution of Take-Off Gross Weight	7-257
7.6-6	KC-135 Distribution of Level Off Altitudes (Climb) (140,000)	7-258
7.6-7	KC-135 Distribution of Level-Off Altitudes (Climb) (180,000)	7-259
7.6-8	KC-135 Distribution of Level Off Altitude (Climb) (220,000)	7-260
7.6-9	KC-135 Distribution of Level Off Altitude (Climb) (260,000)	7-261
7.6-10	KC-135 Distribution of Landing Gross Weights	7-262
7.6-11	Fuel/Time Trade-Off for the KC-135 Cruise Solution	7-268
7.6-12	Sensitivity of Fuel/DOC to Variations in Zero Lift Drag - KC-135	7-284

LIST OF ILLUSTRATIONS (cont'd)

FIGURE		PAGE
7.6-13	Sensitivity of Fuel/DOC to Variations in Induced Drag - KC-135	7-285
7.6-14	Sensitivity of Fuel/DOC to Variations in Thrust Specific Fuel Consumption - KC-135	7-286
7.6-15	Sensitivity of Fuel/DOC to Variations in Weight - KC-135	7-287
7.6-16	Retrofitting KC-135 with Winglets	7-289
7.6-17	Savings Due to Re-engining KC-135 with TF-33	7-291
7.6-18	Sensitivity of Range Factor to Variations in Zero-Lift Drag KC-135A	7-293
7.6-19	Sensitivity of Range Factor to Variations in Induced Drag KC-135A	7-294
7.6-20	Impact of Thrust Variations on Cruise Ceiling for KC-135	7-296
7.6-21	Impact of Wind on Optimum Cruise Mach Number for KC-135	7-298
7.6-22	Impact of Wind on Range Factor for KC-135	7-299
7.6-23	Decrease in Range Factor Due to Flying Off Optimum Cruise Mach Number - KC-135	7-300
7.6-24	Decrease in Range Factor Due to Flying Off Optimum Cruise Altitude - KC-135	7-301
8.1-1	Aircraft Fuel Consumption FY 1976	8-4
8.1-2	Fuel Utilization (FY 1976) by Command	8-5
8.2-1	General Electric Compu-Scope Display System	8-12
A-1	Short Range Solutions	A-11
B-1	T_{min} and T_{max} Curves in (E, f) Space	B-7
B-2	Relaxed Steady State Cruise vs Energy for the C-141 Transport	B-11
B-3	Relaxed Steady State Cruise vs Energy for the C-5A Transport	B-12

TABLES

TABLE		PAGE
2.1-1	ASIMIS Tape Data	2-6
2.1-2	Fuel Conservation Study Aircraft Information Active Duty Aircraft in Operational Roles	2-9
3.2-1	Example C_D Aerodynamic Data for the C-141	3-7
3.2-2	Parabolic Representation Coefficients of C_D for the C-141	3-8
3.2-3	Percentage Error in Theoretical C_D Model for the C-141 Aircraft, $M^* = 0.9$	3-9
3.2-4	Percentage Error in Theoretical C_D Model for the C-141 Aircraft, $M^* = 0.95$	3-10
3.2-5	Comparison of Actual and Theoretical NRT Values for B-52G	3-15
3.7-1	Comparison of Actual, Simulated and Performance Chart Trajectories for C-5A	3-30
3.7-2	Comparison of Actual, Simulated and Performance Chart Trajectories for C-130E	3-31
3.7-3	Comparison of Actual, Simulated and Performance Chart Trajectories for KC-135	3-32
3.7-4	Comparison of Fuel Consumed for EEM and Gradient Solutions	3-34
4.1-1	Comparison of Constant Mach vs. Variable Mach Cruise for C-141 Aircraft	4-9
4.1-2	Procedures for Various Conventional Descents for C-141 Aircraft	4-13
4.1-3	Comparison of EEM and Conventional Trajectories for C-141 Aircraft	4-16
4.3-1	Jet Fuel Data	4-37
7.1-1	Typical Mission Data for C-141	7-2
7.1-2	ASIMIS Tape Data Bands for C-141 Aircraft	7-8
7.1-3	Comparison of Optimum vs. Conventional Climb - C-141	7-27

TABLES (cont'd)

TABLE		PAGE
7.1-4	Fuel/DOC Savings Due to Optimal Climb for C-141	7-29
7.1-5	Comparison of Optimum vs. Conventional Descent C-141	7-31
7.1-6	Fuel/DOC Savings Due to Optimal Descent - C-141	7-32
7.1-7	Comparison of the Fuel/DOC for the Best and Worst Cruise Altitudes with Respect to Nominal Operating Altitudes for C-141	7-34
7.1-8	C-141 Annual Savings Due to Increased Altitudes and Reduced Speed	7-38
7.1-9	Annual Fuel/DOC Savings Due to Delayed Flap Approach - C-141	7-39
7.1-10	Fuel/DOC Savings Due to Reducing Reserve Fuel to Requirements for C-141	7-42
7.1-11	Estimated Fuel Savings for the C-141	7-68
7.2-1	C-5A Typical Mission Data	7-70
7.2-2	Comparison of Optimum vs. Conventional Climb - C-5A	7-91
7.2-3	Fuel/DOC Savings Due to Optimal Climb for C-5A	7-92
7.2-4	Comparison of Optimal vs. Conventional Descent - C-5A	7-94
7.2-5	Fuel/DOC Savings Due to Optimal Descent - C-5A	7-95
7.2-6	C-5A Annual Savings Due to Increased Altitudes and Reduced Speed	7-101
7.2-7	Annual Fuel/DOC Savings Due to Delayed Flap Approach - C-5A	7-102
7.2-8	Fuel/DOC Savings Due to Reducing Reserve Fuel for C-5A	7-105
7.2-9	Estimated Fuel Savings for the C-5A	7-126
7.3-1	C-130E Typical Mission Data	7-128
7.3-2	Comparison of Optimum vs. Conventional Climb C-130E	7-147
7.3-3	Comparison of Optimal vs. Conventional Descent - C-130E	7-149

TABLES (cont'd)

TABLE		PAGE
7.3-4	C-130E Annual Fuel Savings Due to Increased Altitude and Reduced Speed	7-154
7.3-5	Annual Fuel/DOC Savings Due to Reduced Reserve Fuel for C-130E	7-156
7.3-6	Estimated Fuel Savings for the C-130E	7-176
7.4-1	B-52G Typical Mission Data	7-178
7.4-2	Comparison of Optimum Climb vs. Conventional Climb-B-52G	7-190
7.4-3	Comparison of Optimal vs. Conventional Descent B-52G	7-193
7.4-4	Annual Fuel/DOC Savings Due to Clean Aircraft Configuration During Descent - B-52G	7-194
7.4-5	Annual Fuel/DOC Savings Due to Delayed Flap Approach - B-52G	7-196
7.4-6	Estimated Fuel Savings for the B-52G	7-217
7.5-1	B-52H Typical Mission Data	7-219
7.5-2	Comparison of Optimum vs. Conventional Climb - B-52H	7-226
7.5-3	Comparison of Optimal vs. Conventional Descent - B-52H	7-228
7.5-4	Annual Fuel/DOC Savings Due to Clean Aircraft Configuration During Descent - B-52H	7-229
7.5-5	Annual Fuel/DOC Savings Due to Delayed Flap Approach - B-52H	7-231
7.5-6	Estimated Fuel Savings for the B-52H	7-249
7.6-1	KC-135A Typical Mission Data	7-251
7.6-2	Comparison of Optimum vs. Conventional Climb - KC-135	7-272
7.6-3	Fuel/DOC Savings Due to Optimum Climb for KC-135	7-272
7.6-4	Comparison of Optimum vs. Conventional Descent KC-135	7-275

TABLES (cont'd)

TABLE		PAGE
7.6-5	Annual Fuel/DOC Savings Due to Trajectory Optimization for KC-135	7-278
7.6-6	Annual Fuel/DOC Savings Due to Delayed Flap Approach - KC-135	7-279
7.6-7	Estimated Fuel Savings for the KC-135	7-303
8.1-1	Flying Hours vs. Fuel Consumption (USAF)	8-2
8.2-1	Simulator Technology Assessment	8-10
8.2-2	Savings Per Flight Hour Utilizing Simulators by Aircraft Type	8-15
8.2-3	Projected FY78 Fuel Savings Due to Simulators	8-16
B-1	Aerodynamic and Engine Data	B-10
E-1	Base Checklist (Maintenance)	E-2

SECTION 1

INTRODUCTION

This study was motivated by a concern for energy conservation and a concern for the escalating cost of fuel. It is estimated that over 54% of the fuel requirements of the Air Force are consumed by the following five aircraft: the B-52, the KC-135, the C-141, the C-130, and the C-5A. The scope of this fuel conservation study is confined to addressing these five aircraft.

The objective of the study is two-fold:

1. Quantify how improvements in design or operational procedures will impact fuel consumption and direct operating costs (DOC).
2. Determine the sensitivity of the fuel consumption and DOC results to uncertainties (variations) in the aircraft parameters, instrumentation errors, and environmental conditions.

A major contribution of this study is the approach taken to generate the effect of design changes on fuel consumption and direct operating cost. With this approach the design change is first broken down into its effect on the design parameters (i. e., aerodynamic parameters, engine parameters, weight, etc.). Then sensitivity plots of fuel and DOC savings as a function of each design parameter are generated for each aircraft type. These sensitivity plots are based on actual mission trajectory data, as opposed to "typical" mission trajectory profiles. To evaluate the impact of some new design modification in the fleet, the procedure thus consists of determining how the individual design parameters are effected. Then the appropriate sensitivity plots are entered, and the contributions from each plot (positive or negative) are combined to obtain the total effect on fuel and DOC savings. Within this study the sensitivity plots are employed to evaluate specific design modifications.

It is important to note that the sensitivity plots employed in the above procedure are based on how the aircraft were actually flown, not on some typical or optimum flight profile. Thus the results of the design modification impact analyses presented here are the fuel and DOC savings expected if the aircraft continue to be flown the way they have been flown in the past. This realistic approach is in contrast to prior studies in which estimated fuel savings are based on a particular flight profile, one which often cannot be flown as a result of ATC or other restrictions.

Prior studies were limited to typical or optimum flight profiles because actual flight profile data were not available. As part of this study, DRC undertook a task to locate and incorporate into the study actual mission profile data for the five aircraft. The data found has been transformed into histograms, thus providing spectra of the mission profile parameters, such as altitude, air speed, take-off weight, landing weight, and mission time. Several sources of data were used and cross-checked to determine the data's validity and applicability to the study. By means of an Interim Mission and Cost Data Analysis Report, DRC Report M-314U dated August 1977, coordination was obtained with the using commands on the mission data and operational procedures to be used for the final results of the study. The resulting data base, which represents actual Air Force fleet operation for the five aircraft types, is in itself a major contribution.

Many fuel conservation operational changes and design modifications have been identified and proposed by prior studies. These studies are summarized and referenced in this report. Thus, the purpose of this study is not so much to discover new procedures for fuel conservation as it is to evaluate procedures identified and proposed in prior studies. Various operational procedures to be evaluated include trajectory optimization while airborne and improved ground handling procedures prior to take-off and after landing. Various design modifications to be evaluated include the addition of winglets and the replacement of current engines with more efficient engines. As an alternative, the effect of a reduction in fuel allocation is also evaluated.

The optimal control methodology employed for developing the mission spectrum analysis computer program is a unique approach based on singular perturbation theory (SPT). Optimal flight trajectories are dependent on many factors such as external configuration, engine performance characteristics, system weight, air traffic control (ATC) constraints, atmospheric conditions, and mission requirements. The derivation of the optimal trajectory must reflect the differences among aircraft/missions in those factors. The SPT Methodology (called Extended Energy Management, EEM), is unique in that it provides an inherently analytic solution to the optimal control problem that satisfies all necessary and sufficiency conditions for a complete nonlinear dynamic model, while enforcing a broad class of state and control variable constraints. Since the solution is largely analytic, it can be used directly for on-board digital control. Significant contributions have been made with this methodology in being able to overcome the historic difficulties in obtaining rapid solutions to nonlinear, constrained optimal control problems. This EEM SPT Methodology was utilized in this study to obtain the trajectory optimization results for the five aircraft types. Sensitivity results are given to determine the impact of optimal operating procedures relative to existing air traffic control requirements. In addition, an appendix presents results regarding a recent controversy in the literature about the optimality of cruise. This appendix describes under what condition cruise is not optimizing and gives results for two aircraft considered in this study. This report is organized into two volumes. Volume I is a separate executive summary of the major objectives and results. Volume II is the detailed technical report. Sections 2 through 6 of Volume II present general information about the aircraft, models, procedures and the analysis approach utilized; then Section 7 provides the specific numerical results. Section 2 gives the data sources and a general description of the mission profiles and operating cost models. Section 3 gives the analytical problem formulation, definitions of terms, and describes the mission spectrum analysis simulation tool that was developed. Section 4 gives the analysis approach for assessing operational procedures (airborne and ground) that conserve fuel. Section 5 discusses the analytical approach for addressing design modifications, and Section 6 describes the sensitivity analysis approach.

Section 7 then provides numerical results for each aircraft in separate sub-sections. Included for each aircraft type are the mission spectrum data and the fuel and DOC savings resulting from specific design modifications and operational procedure changes. Conclusions are given for each aircraft separately. Section 8 discusses the impact of reduced fuel allocation on operational readiness, and Section 9 presents the overall study conclusions and recommendations.

SECTION 2

AIRCRAFT MISSION PROFILES AND DIRECT OPERATING COST MODELS

This section contains information regarding Air Force usage of the aircraft covered under this study. The acquisition of required data for this study was undertaken using three basic approaches; first, all data available in published form was collected directly from the Offices of Primary Responsibility (OPRs) within the Air Force or other appropriate agencies; second, samples from USAF data systems were collected on tape or in their raw form, as available; and third, personal visits were made to a varied cross-section of agencies where interviews were conducted with both cognizant technical and management personnel. A continuous cross-checking and comparison of information gathered was undertaken which provided a measurement of the data's validity and the scope of its application. The two major Sub-sections described below are mission models and direct operating cost models.

2.1 MISSION MODELS

Detailed mission data by aircraft was obtained in two forms: First, typical mission profiles were obtained with average flight parameter values; Second distribution data of mission profiles was obtained for each aircraft. In addition, descriptive information on aircraft operations was obtained. This section describes the data and aircraft operations but specific data by aircraft appears in Section 7.

2.1.1 Command Mission Statements

Before looking at typical mission profiles flown by the various aircraft in this study, or the data supplied on each flight phase, it is necessary to become familiar with the various major Air Commands that control and operate these aircraft. The two in question are: (1) the Military Airlift Command (MAC), headquartered at Scott AFB in Illinois, and (2) the Strategic Air Command (SAC), headquartered at Offutt AFB, Nebraska.

2.1.1.1 Military Airlift Command (MAC)

MAC's primary mission is the deployment and resupply of combat forces and their support equipment. Strategic airlift missions are flown by C-5 and C-141 aircraft while MAC's tactical mission is flown by C-130 aircraft. The peacetime airlift mission of MAC is to maintain itself in a constant state of war-readiness. The airlift capability must be able to fulfill all tasks assigned by the Joint Chiefs of Staff, and the Air Force, ranging from global airlift of combat forces and equipment, to aerial drops in combat zones. As a by-product of the constant training required for the global airlift mission, MAC routinely supports Department of Defense logistic needs on a worldwide basis. Figure 2.1-1 is an organizational chart showing the placement of Global Airlift units within the Command.

2.1.1.2 Strategic Air Command (SAC)

The Strategic Air Command serves as one of the cornerstones of the United States nuclear deterrent force. Their mission is to:

- deter nuclear attacks on the United States
- help deter conventional and nuclear attacks on U.S. allies
- strengthen U. S. power and influence in world affairs
- engage in nuclear wars should deterrence fail.

Deterring nuclear attack on the United States has been the primary reason for maintaining an arsenal of nuclear weapons and sophisticated weapon system delivery vehicles for those nuclear arms. While supplemented by the smaller, faster, limited range FB-111As, the present mainstay of SAC's bomber force is the B-52 with the B52G/H models armed with the capability of deploying the inertially guided, high-speed, Short-Range Attack Missile (SRAM). SAC is the single manager for all of the Air Force's KC-135 tankers, and supports its bomber force and the tactical and cargo forces of other commands with aerial refueling capabilities. Figure 2.1-2 is an organizational chart depicting B-52G/H and KC-135 dispersion within the command.

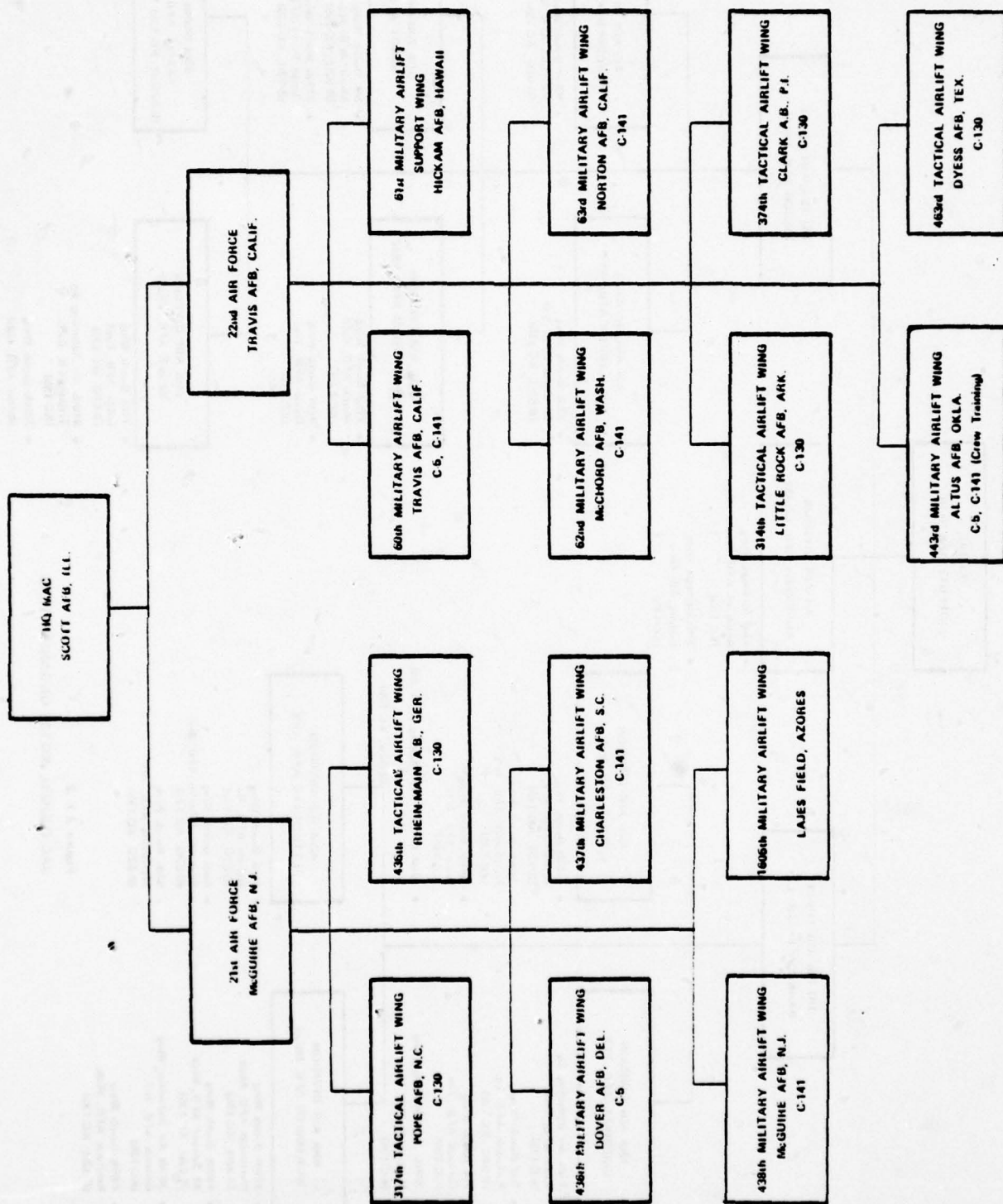


Figure 2.1-1 MAC GLOBAL ORGANIZATIONS

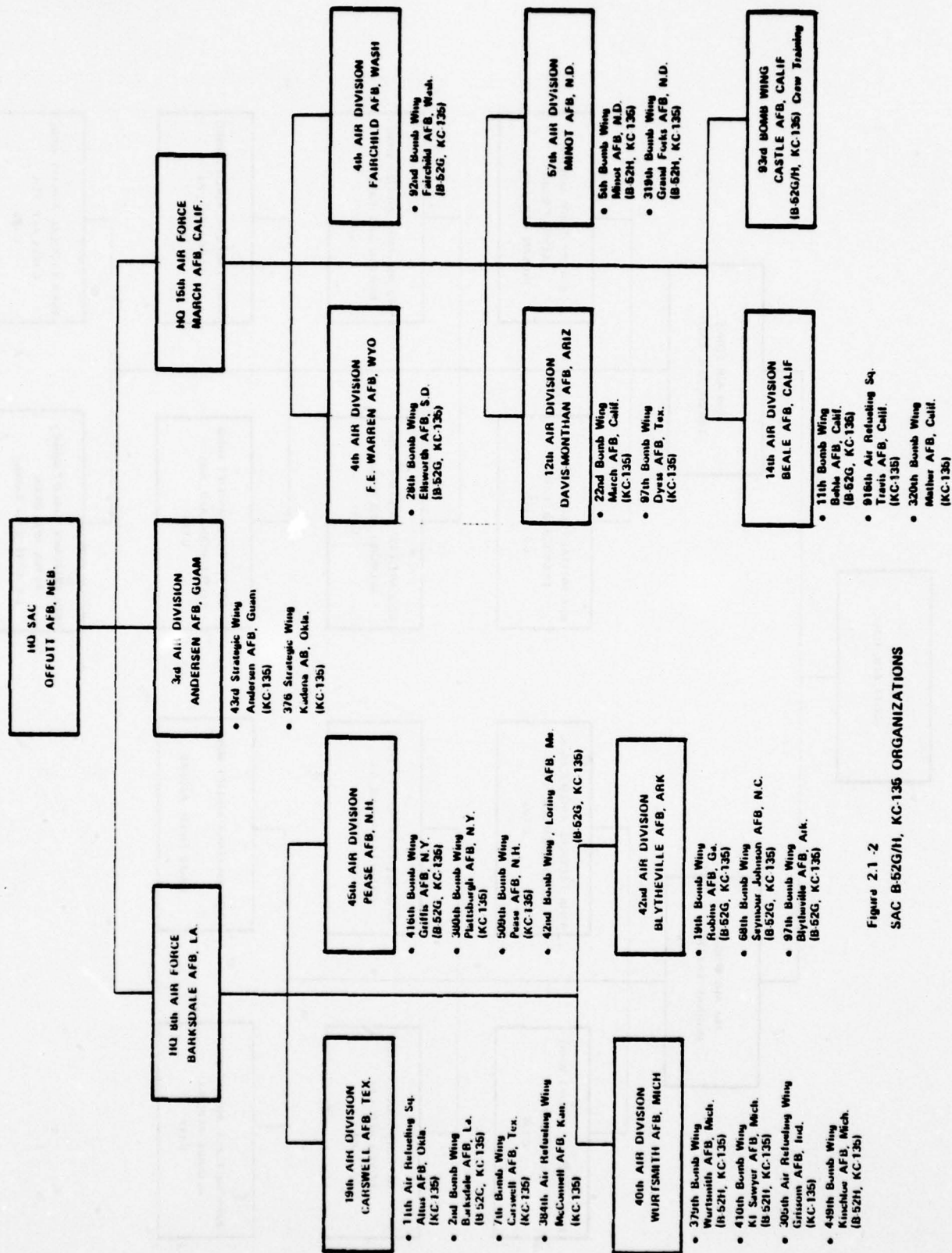


Figure 2.1-2
SAC B-52G/H, KC-135 ORGANIZATIONS

2.1.2 Data Sources

Data utilized in this report to develop the various mission models was acquired from the following sources:

- Magnetic tape data detailing aircraft usage
- Information obtained from major commands (MAC & SAC)
- Personnel interviews conducted during visits to operating units

Data items and information obtained from these various sources are described below:

2.1.2.1 Aircraft Structural Integrity Management Information Systems (ASIMIS)

This activity is a part of the Air Force Structural Integrity Program (ASIP) as provided for in AFR 80-13. The ASIMIS collects various data relating to aircraft usage through forms completed during flight by aircrew members. These forms are reviewed by appropriate AFLC engineering personnel and then input to the ASIMIS computer programs at the Oklahoma City Air Logistics Center. The normal use of this data is to compute fatigue accumulation factors by individual aircraft in order to track remaining service life. DRC acquired the basic data tapes for each type aircraft, and developed programs to adapt the raw information to a useable form for purposes of flight profile information. Each type aircraft is managed separately, and the data elements and format varies considerably from one aircraft to the other. Table 2.1-1 indicates the data elements available by type aircraft.

2.1.2.2 Major Air Commands

Considerable information was received from headquarters of both the Military Air Command and the Strategic Air Command regarding mission procedures, constraints, and flying activity. Of particular interest and importance to this study were the various mission profiles, sortie distributions, and pertinent policy/procedure regulations. These are given in detail for each aircraft in Section 7.

FLIGHT DATA									
Aircraft	Fuel Wgt.	Cargo/ Payload Wgt.	Phase Data					End Wgt.	Comments
			Duration	Altitude	Mach/Speed	CG	Wgt.		
C-5	X	X	X	X	X	X	X	X	good data
C-130	X	X	X	X	X	X	X	X	good data but not for all phases
C-141	X	X	X	X	X	0	X	X	data in lands & not for all phases
B-52	0	0	X	X	X	0	X	X	refueling & low level only
KC-135	X	0	X	X	X	X	X	X	fuel offload not available

X - INDICATES AVAILABLE (POSSIBLY INCOMPLETE) DATA

0 - INDICATES UNAVAILABLE DATA

TABLE 2.1-1
ASIMIS TAPE DATA

2.1.2.3 Operating Units

Several air bases were visited to conduct interviews with MAC and SAC aircrew personnel. The purpose of these interviews was to gain further insight into flight profiles flown by the various aircraft and to collect pertinent procedural information utilized by these organizations. Standard flight plans and actual flight logs were collected for further analysis and use in this study. In addition, local directives and policy regulations followed by these various wings were collected for comparison and possible fuel utilization impact.

2.1.3 Data Analysis

The entire collection of aircraft usage information was analyzed, and it was felt that the most detailed source of actual profile and phase distribution would be the ASIMIS tapes. For this reason, data for all aircraft under study was processed. The results are presented in Section 7 by aircraft type. However, as indicated in Table 2.1-1 mission profile information available for B-52 aircraft from ASIMIS tapes is incomplete. Also, for KC-135, fuel off-load data is not given on the ASIMIS tapes. Thus the tapes could not be used to construct complete profiles and distributions for these aircraft. Instead, only average mission profiles are shown (in Section 7) for B-52G, B-52H and KC-135 aircraft. These profiles were developed from the information received from MAC and SAC operating units and were reviewed by the two major air commands. This report incorporates their recommendations in order to best reflect actual aircraft usage.

2.1.4 Characteristics of Aircraft Missions

The following subsection contains general information regarding aircraft populations and operating constraints. The detailed information on each aircraft mission profile is presented in Section 7 for each mission type flown, as well as for the percentage of total sorties that the mission is flown.

2.1.4.1 Aircraft Population

It has been necessary to carefully define the aircraft types to be included in this study in order to arrive at a measure of commonality identifiable to typical missions and procedures. For example, there are a large number of aircraft designated as EC, WC, RC or C-135 models, as well as KC models, which are used for other than tanker purposes. For the purposes of this study, only KC-135A aircraft in the primary role of SAC tanker are considered. Similarly, only C-130E aircraft actually performing a MAC airlift mission are considered. All MAC C-5 and C-141 aircraft are included as well as all SAC B-52G and B-52H bombers. Table 2.1-2 shows aircraft quantity, flying hour and fuel consumption information.

2.1.4.2 General Constraints

There are three basic operating constraints imposed by the Federal Aviation Administration (FAA) upon all aircraft operating in controlled air space which is under FAA jurisdiction. First, aircraft operating below 10,000 feet are not permitted to exceed 250 knots indicated airspeed (KIAS), under normal conditions. Second, turbine powered aircraft are required to limit airspeed to 200 KIAS or less, within an airport area. Both of these restrictions are for the specific purpose of providing sufficient clearance and reaction time between aircraft at congested altitudes and in heavy traffic areas to take advantage of see-and-be-seen safety principle. Third, altitude is assigned with 2,000 ft spacing below 29,000 ft and with 4000-ft. spacing above. SAC aircraft are not restricted by the 250 KIAS constraint.

2.2 DIRECT OPERATING COST MODEL

Total operating cost of an aircraft can be broken down into two cost categories, namely, indirect operating costs (IOC) and direct operating costs (DOC). IOC is comprised of items such as ground support equipment, base operating costs, i.e., functions that cannot be impacted by this fuel conservation study. DOC is comprised of flight crew costs, fuel costs, and aircraft maintenance costs which can be impacted by this study.

Table 2.1-2
FUEL CONSERVATION STUDY AIRCRAFT INFORMATION
ACTIVE DUTY AIRCRAFT IN OPERATIONAL ROLES

AIRCRAFT	NO. ASSIGNED	FY76		FY77 PLANNING FACTOR (GAL/HR)
		FLYING HOURS	FUEL CONSUMED (Million of Gallons)	
B-52G	172	70,664	283.30	4,005
B-52H	97	36,280	123.17	3,390
C-130E	217	147,888	116.09	785
C-5	76	42,236	142.64	3,455
C-141	272	298,657	600.82	2,025
KC-135	572	178,154	458.12	2,415

Figure 2.2-1 graphically displays how DOC varies as a function of flight time. As flight time increases, fuel cost decreases up to a point, while other direct operating costs increase. The resultant total DOC decreases to a minimum point and then begins to climb again. For maximum efficiency an aircraft should operate at the minimum DOC point. In the analysis of DOC for the aircraft under study, time-related cost/flight hour will be broken out of total DOC.

The largest singular increase in DOC is the cost of fuel. Since March 1973 the cost per gallon of JP-4 has increased from approximately 12 cents to 42 cents (Figure 2.2-2) or a 350 percent increase in three years. Fuel costs now comprise over 50 percent of DOC.

Crew costs have also increased because of pay raises. Over the past 20 years, the yearly base pay of an Air Force captain with over six years experience has increased over 300 percent from \$4867.20 to \$15,159.60.

A typical staff sergent with over ten years experience during the same time frame has increased over 260 percent from \$2901.60 to \$7725.00. This increased cost, coupled with the increased fuel cost, has forced DOC to climb significantly.

Maintenance costs, while also increasing over time, will be the area least impacted by this study. There are two reasons: First, over 54 percent of all maintenance performed on aircraft is non-flight related; Secondly, the increased costs lie in parts and labor which are functions not affected by this study.

To obtain the DOC of each aircraft, it was necessary to derive the cost of fuel and oil per flight hour, the cost of flight crew per flight hour, and the cost of direct maintenance operations per flight hour. In the following subsections the data utilized to derive these figures and the sources of that data will be explained.

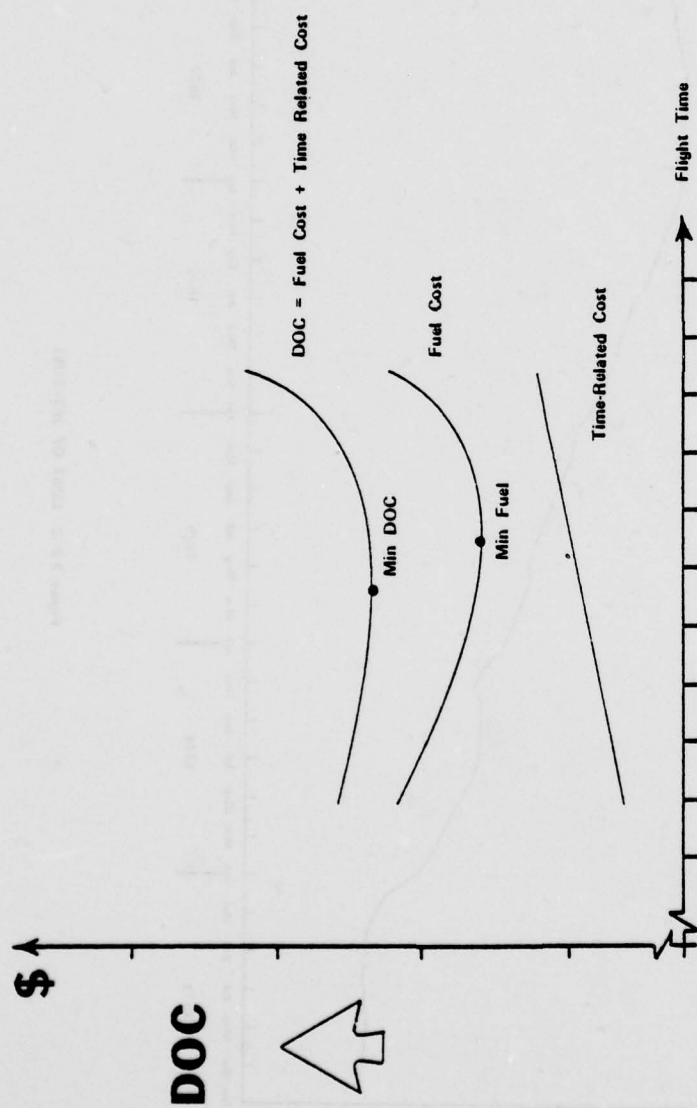


Figure 2.2-1 DOC AS A FUNCTION OF FLIGHT TIME

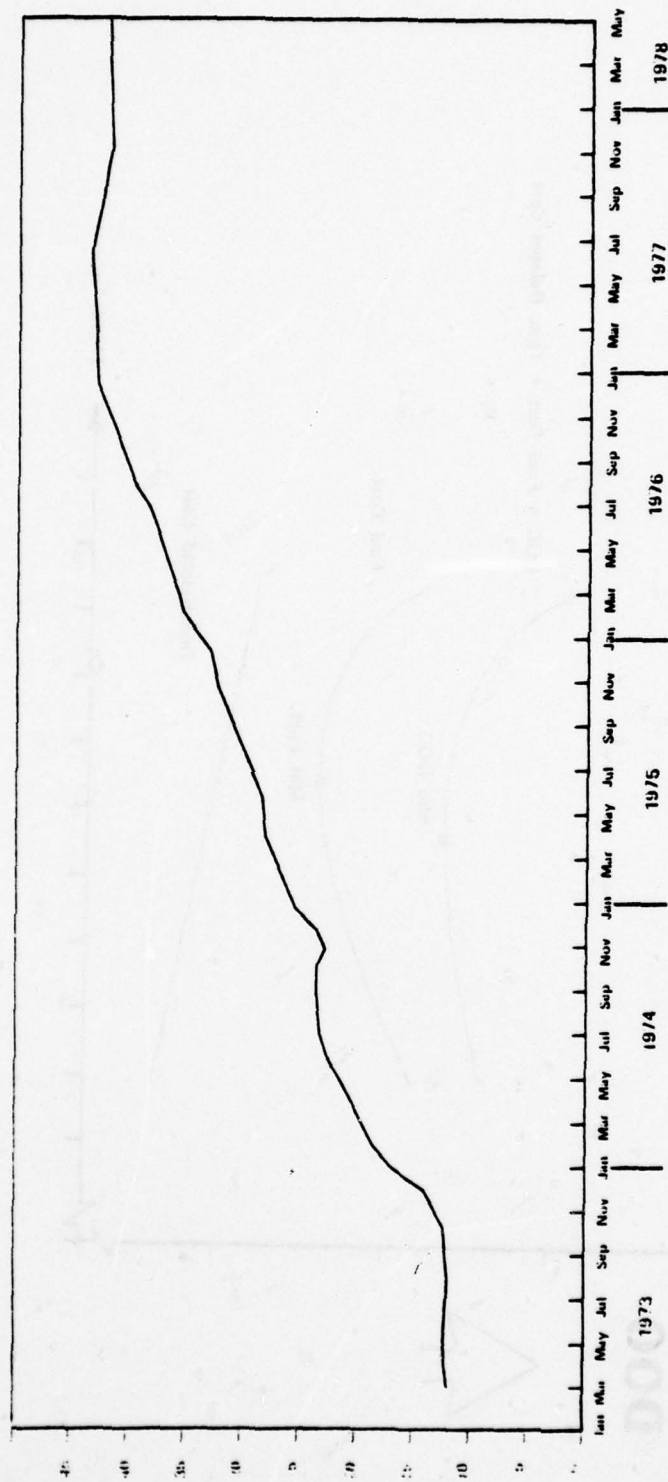


Figure 2.2-2 COST OF JET FUEL

2.2.1 Cost of Fuel and Oil Per Flight Hours (FH)

Fuel and oil costs were derived by utilizing the following formulas:

$$\begin{aligned}\text{Fuel Cost/FH} &= \text{Fuel Consumption/FH} \times \$ \text{Cost/Gal. of Fuel} \\ \text{Oil Cost/FH} &= \text{Oil Consumption/FH} \times \$ \text{Cost/Gal. of Oil}\end{aligned}$$

The cost values utilized to derive fuel and oil costs per flight hour were \$0.42/gal. and \$9.35 gallon, respectively. Fuel and oil prices plus consumption data were acquired from Headquarters San Antonio Air Force Logistics Center (AFLC), Kelley Air Force Base, Texas. The resultant fuel and oil costs per flight hour are considered representative of the present (1978) costs to the Air Force.

2.2.2 Cost of Flight Crew per Flight Hour (FH)

Flight crew costs are not a direct function of the number of hours the aircraft is flown in any given year. Air crew salaries are a constant, regardless of the number of hours spent in the air. To obtain a figure for flight crew per hour it was necessary to have information on the average seniority of each flight crew position, and the number of flight crews per aircraft. This information was obtained from MAC and SAC Headquarters for this study.

Salary information to match against the above data was supplied by the USAF Office of Accounting and Finance. Multiplying crew data by cost data gives crew cost per flight hour.

$$\text{Flight Crew Cost/FH} =$$

$$\frac{\text{Cost per crew/yr.} \times \text{no. of aircraft} \times \text{no. of crews assigned/aircraft}}{\text{Total no. of FH/yr}}$$

2.2.3 Maintenance Costs

For Direct Maintenance Operations figures, IROS (Increase Reliability of Operational System) data were utilized. IROS provides logistic support costs in accordance with AFR 400-46 and Air Force Logistics Command Regulation 400-16. Due to the fact that certain base-level costs for unscheduled

maintenance, and certain depot-level costs are not included in IROS cost data [1]*, the IROS figures have been adjusted upwards by a factor of two to reflect more realistic Direct Maintenance Operations costs. This factor was selected based on published information and discussions with MAC and SAC personnel.

2.2.4 Derivation of DOC Model

Utilizing the formulas previously mentioned, DOC for each aircraft can be derived. Maintenance costs for the various aircraft in the study were taken directly from IROS KO51 type data. The latest figures (1978) available were utilized and present representative costs of maintenance per flight hour.

For Air Force operations only a part of flight crew salary and direct maintenance cost are affected by the number of flight hours. Thus for the direct operating cost (DOC) model, it was assumed that 25% of flight crew salary and direct maintenance cost are considered as time related. However, due to uncertainties in this assumption, DOC1, DOC2 and DOC3 models are also developed which respectively take 50, 75 and 100 percent of flight crew and maintenance cost as time related cost. Each of these direct operating cost models include oil cost as time related cost.

The following example illustrates the derivation of direct operating cost models for C-5A.

*Numbers in brackets refer to the references

Crew Salary	\$ 401/FH
Maintenance Cost from IROS Data	\$1183/FH
Direct Maintenance Operations Cost (2 x IROS cost)	\$2366/FH
Oil Cost	\$ 6/FH

Using these figures time related cost/FH for various direct operating cost models are obtained as follows:

<u>Model Type</u>	Component of Time Related Cost	Cost - \$
DOC	Crew Salary (.25 x 401)	100
	Direct Maintenance Cost (.25 x 2366)	592
	Oil Cost	<u>6</u>
	Total	698
DOC1	Crew Salary (.5 x 401)	201
	Direct Maintenance Cost (.5 x 2366)	1183
	Oil Cost	<u>6</u>
	Total	1390
DOC2	Crew Salary (.75 x 401)	301
	Direct Maintenance Cost (.75 x 2366)	1774
	Oil Cost	<u>6</u>
	Total	2081
DOC3	Crew Salary (1 x 401)	401
	Direct Maintenance Cost (1 x 2366)	2366
	Oil Cost	<u>6</u>
	Total	2773

The specific direct operating cost models for the aircraft under study are given in Section 7 by aircraft type.

SECTION 3

MATHEMATICAL MODELING, ANALYSIS AND SIMULATION

A major portion of this study is directed at evaluating changes in operational flight procedures and the impact that design modifications and fuel and cost parameter changes have on fuel and Direct Operating Cost(DOC). DRC's approach to this work was to develop a trajectory simulation program using a Singular Perturbation Theory (SPT) Optimal Control methodology for trajectory optimization to minimize DOC. Then this optimal trajectory simulation was exercised for each aircraft type, for each mission, and for each of the design parameters of interest. Singular Perturbation Theory is a reduced order analysis technique that avoids the historical time and convergence problems associated with numerical techniques of optimal control solution (such as gradient techniques) and results in a fast, efficient simulation tool for evaluating the impact of optimal flight profiles in reducing fuel consumption and DOC.

An aircraft trajectory is characterized by the time histories of its state (altitude, velocity, flight path angle, etc.) and control (angle-of-attack, thrust setting, etc.) variables. Aircraft equations of motion define the dynamics relationships between state and control variables. By varying the control inputs to the aircraft equations of motion, different trajectories are obtained to accomplish a given mission. The optimal trajectory is the one which minimizes the cost function used as the measure of performance. Moreover, no two aircraft missions are alike, therefore the effect on performance of operational/design modifications were evaluated for a spectrum of aircraft missions. This section details the equations of motion and the aerodynamic and propulsion models used to characterize an aircraft in the Mission Profile Analysis (MPA) Computer Simulation Program. It also describes this simulation program, the measure of performance, and the method used to optimize aircraft trajectories.

3.1 MEASURE OF PERFORMANCE

While fuel conservation is the overall objective of this effort, it is necessary to formulate aircraft direct operating cost (DOC) as part of the performance index in order to carry out a fuel versus DOC trade-off analysis. Thus a DOC model is required in formulating a suitable performance index for optimization. The DOC models for the aircraft under study are described in Subsection 2.2. The total DOC model can be described mathematically as:

$$\text{DOC} = c_F F + c_T T + c_o \quad (3.1)$$

where F represents fuel consumed, T represents time of flight and c_F and c_T are the cost coefficients associated with fuel and flight hours, respectively. The c_o coefficient represents cost components not affected by the aircraft trajectory. For example, for KC-135 aircraft, c_F is \$.42/gallon and c_T is \$354/flight hour, as described in Subsection 7.2. This value of c_T is obtained by considering 25% of flight crew and maintenance costs as time related cost. In this case c_o may be considered as flight crew and maintenance cost components which are mission related rather than time related. For the aircraft under study the c_o component is zero because no appreciable cost components were found which could be considered as mission related. Thus, since minimization of DOC depends only on c_F/c_T , a suitable performance index for optimization is

$$J = \int_0^T [\theta f + (1-\theta)] dt; \quad 0 \leq \theta \leq 1 \quad (3.2)$$

where f is fuel flow rate. The variable θ can be expressed in terms of c_F and c_T as

$$\theta = \frac{c_F/c_T}{1 + c_F/c_T} \quad (3.3)$$

and total mission cost is given by

$$\text{DOC} = (c_F + c_T) J \quad (3.4)$$

The values $\theta=0$ and $\theta=1$ correspond to minimum time and minimum fuel, respectively.

The performance index selected for optimization plays an important role in the fuel/DOC trade-off studies. Since fuel cost, c_F , is escalating at a higher rate than time-related cost c_T , the value θ that minimizes DOC will increase in the future. Moreover, there are uncertainties in the value of c_T because it is not possible to precisely estimate how much of flight crew and maintenance cost is time related. These uncertainties can be accounted for by optimizing the solution for a range of the parameter θ in equation (3.2). This sensitivity is given in the numerical results.

3.2 AERODYNAMIC AND PROPULSION MODELS

This subsection describes the models and modeling methods used to represent aerodynamic and propulsion characteristics of the aircraft under study. The basic aerodynamic data is made up of the lift and drag aerodynamic force co-efficients as functions of Mach number, angle of attack and flap setting. With the exception of the C-130E, standard day propulsion data provides normal, military and take-off rated thrust and idle thrust as functions of mach and altitude, and fuel flow rate as function of mach, altitude and thrust setting. For the C-130E which has turbo prop engines, propulsion data is given for indicated torque, net jet thrust and fuel flow as functions of mach, altitude and turbine inlet temperature (T_{in}). Most of the aerodynamic and propulsion data was obtained from the Aeronautical Systems Division and is given as curves in the appropriate parameters. Since a part of this study entails performing sensitivity analysis by variation of aircraft aerodynamic and propulsion characteristics, it was decided to use a parametric representation of aerodynamic and propulsion data, as opposed to table look up and interpolation schemes. Consequently parametric aerodynamic and propulsion models were developed from the original aircraft data.

3.2.1 Aerodynamics

For an aircraft in clean configuration, aerodynamic drag coefficient (C_D) is a function of aircraft Mach number and lift coefficient (C_L). Fig. 3.2-1 illustrates the drag coefficient C_D as a function of lift coefficient C_L for various Mach numbers. This data is for the C-141 aircraft and is representative of all the aircraft under study. It is assumed that at a given Mach number, C_D is parabolic in C_L , thus

$$C_D = C_{D_0} - 2K C'_L C_L + K C_L^2 \quad (3.5)$$

where

C_{D_0} = zero-lift drag coefficient

K = induced drag factor

C'_L = lift coefficient for minimum drag coefficient

This form was found to be adequate for C_D .

Rewriting C_D in equation (3.5) as

$$C_D = A_1 + A_2 C_L + A_3 C_L^2 \quad (3.6)$$

the parameters A_i ($i=1, 3$) were determined by least squares fit of (3.6) to the aerodynamic data at each Mach number (M).

The coefficients A_i ($i=1, 3$), were taken as functions of M only, and assumed to have the following functional form

$$A_i(M) = A_i(M_0) + \alpha_i (M^* - M)^{\beta_i} \quad i = 1, 3 \quad (3.7)$$

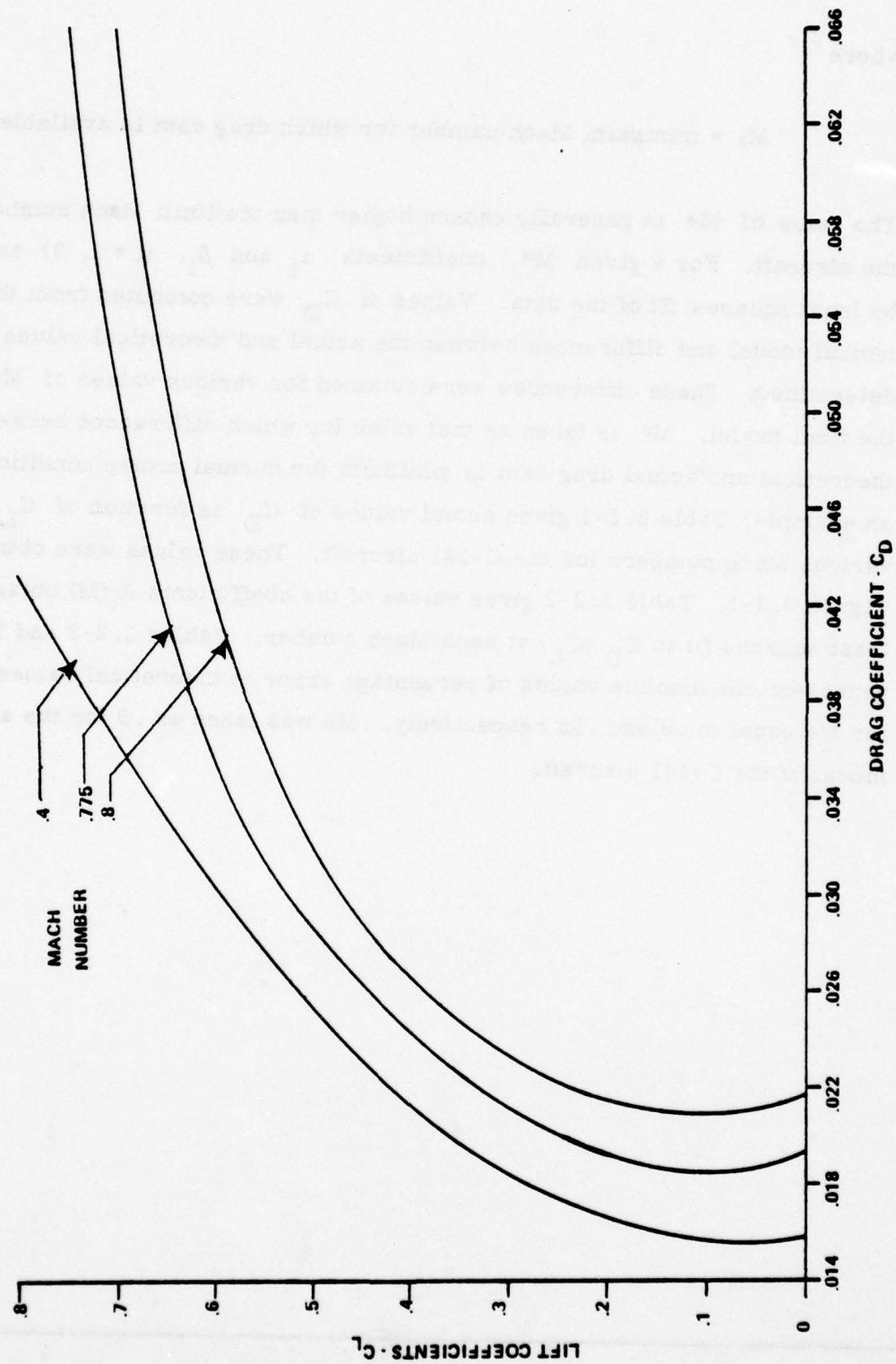


Figure 3.2.1 C-141 AERODYNAMIC DATA

where

M_0 = minimum Mach number for which drag data is available.

The value of M^* is generally chosen higher than the limit Mach number of the aircraft. For a given M^* , coefficients α_i and β_i , ($i = 1, 3$) are obtained by least squares fit of the data. Values of C_D were computed from the theoretical model and differences between the actual and theoretical values were determined. These differences were obtained for various values of M^* . For the final model, M^* is taken as that value for which differences between the theoretical and actual drag data is minimum for normal cruise conditions. As an example, Table 3.2-1 gives actual values of C_D as function of C_L for various Mach numbers for the C-141 aircraft. These values were obtained from Figure 3.2-1. Table 3.2-2 gives values of the coefficients $A_i(M)$ obtained by least squares fit to $C_D(C_L)$ at each Mach number. Tables 3.2-3 and 3.2-4 represent the absolute values of percentage error in theoretical values of C_D for M^* equal to .9 and .95 respectively. M^* was taken as .9 for the aerodynamic model of the C-141 aircraft.

Mach C _L	.55	.6	.65	.7	.725	.75	.775	.8
.0	.0162	.0165	.0167	.0172	.0176	.0182	.0193	.0217
.1	.0158	.0160	.0162	.0167	.0170	.0176	.0185	.0208
.2	.0167	.0169	.0170	.0175	.0177	.0182	.0192	.0215
.3	.0188	.0190	.0192	.0195	.0198	.0201	.0212	.0233
.4	.0221	.0221	.0225	.0228	.0230	.0233	.0242	.0265
.5	.0263	.0263	.0266	.0269	.0273	.0276	.0286	.0319
.6	.0314	.0314	.0318	.0323	.0327	.0333	.0354	.0424

Table 3.2-1 EXAMPLE C_D AERODYNAMIC DATA FOR THE C-141

Mach Coefficient	.55	.6	.65	.7	.725	.75	.775	.8
A ₁	.0161	.0167	.0166	.0171	.0175	.0182	.0193	.0224
A ₂	-.0072	-.0079	-.0082	-.0092	-.0103	-.0121	-.0145	-.0267
A ₃	.055	.0552	.0564	.0576	.0594	.0620	.0675	.0958

Table 3.2-2 PARABOLIC REPRESENTATION COEFFICIENTS OF C_D
FOR THE C-141

Mach C _L	.55	.6	.65	.7	.725	.75	.775	.8
0	.41	.75	.70	1.03	.88	.19	1.09	3.12
.1	1.64	.93	.71	.2	.01	.15	.81	.87
.2	1.54	.76	.95	.3	.16	.14	.09	.5
.3	.84	.07	.40	.68	.88	.10	.07	4.11
.4	.17	.03	1.35	1.64	1.33	.19	1.83	9.17
.5	.11	.02	.80	1.03	1.35	.12	3.14	11.68
.6	.58	.67	.35	1.06	1.10	.14	1.09	4.59

Table 3.2-3 PERCENTAGE ERROR IN THEORETICAL C_D MODEL

FOR THE C-141 AIRCRAFT, M* = 0.9

Note: Current Mach number is approximately 0.75

Mach C _L	.55	.6	.65	.7	.725	.75	.775	.8
0	.28	.84	.71	.85	.58	.2	1.22	1.50
.1	1.54	.85	.7	.06	.26	.18	.94	.46
.2	1.45	.70	.94	.19	.37	.43	.25	.79
.3	.78	.03	.42	.59	.70	.38	.27	2.59
.4	.21	.01	1.36	1.57	1.17	.11	2.08	7.25
.5	.14	.01	.82	0.97	1.18	.45	3.44	9.37
.6	.56	.65	.36	1.0	.92	.23	1.42	2.13

Table 3.2-4 PERCENTAGE ERROR IN THEORETICAL C_D MODEL
FOR C-141 AIRCRAFT, M^{*}=0.95

Note: Current Mach number is approximately 0.75

3.2.2 Propulsion

There is a limit on the amount of thrust available from each engine. Under normal operating conditions this limit is called the normal rated thrust (NRT). Although thrust higher than NRT is also available for the aircraft under study, engine operations above NRT are not advised because engine performance deteriorates rapidly if engines are operated continuously above NRT. Maximum available thrust from each engine is called military rated thrust (MRT). Figures 3.2-2 and 3.2-3 illustrate MRT and NRT respectively for the B-52G aircraft. These figures are representative of all aircraft under study except the C-130E (discussed in Section 7.3). On a standard day NRT and MRT are functions of Mach and altitude. Both MRT and NRT are strongly affected by altitude but are only weak functions of Mach. Both MRT and NRT were represented as multinomials in altitude and Mach. The following representation is used for NRT

$$\text{NRT} = B_1 + B_2 M + B_3 H + B_4 M^2 + B_5 MH + B_6 H^2 + B_7 M^2 H + B_8 MH^2 + B_9 H^2 M^2 \quad (3.8-a)$$

where

$$H = \text{Altitude}/40000. \quad (3.8-b)$$

Altitude was scaled down such that the range of values of M and H is almost equal. This is done to avoid ill-conditioning of matrices in the least-squares algorithm which is used to obtain the unknown coefficients B_i ($i=1, 9$). MRT is represented by the same functional form as NRT except that coefficients B_i are different. This representation of MRT and NRT was found to be adequate for the aircraft under study in the troposphere. However above the tropopause the dependence of MRT and NRT on altitude and Mach Number changes for almost all aircraft under study. Therefore separate models were developed for NRT for altitudes above and below the tropopause. The functional form of NRT remains the same, but the coefficients (B_i) are different. This resulted in a discontinuity in NRT at the tropopause.

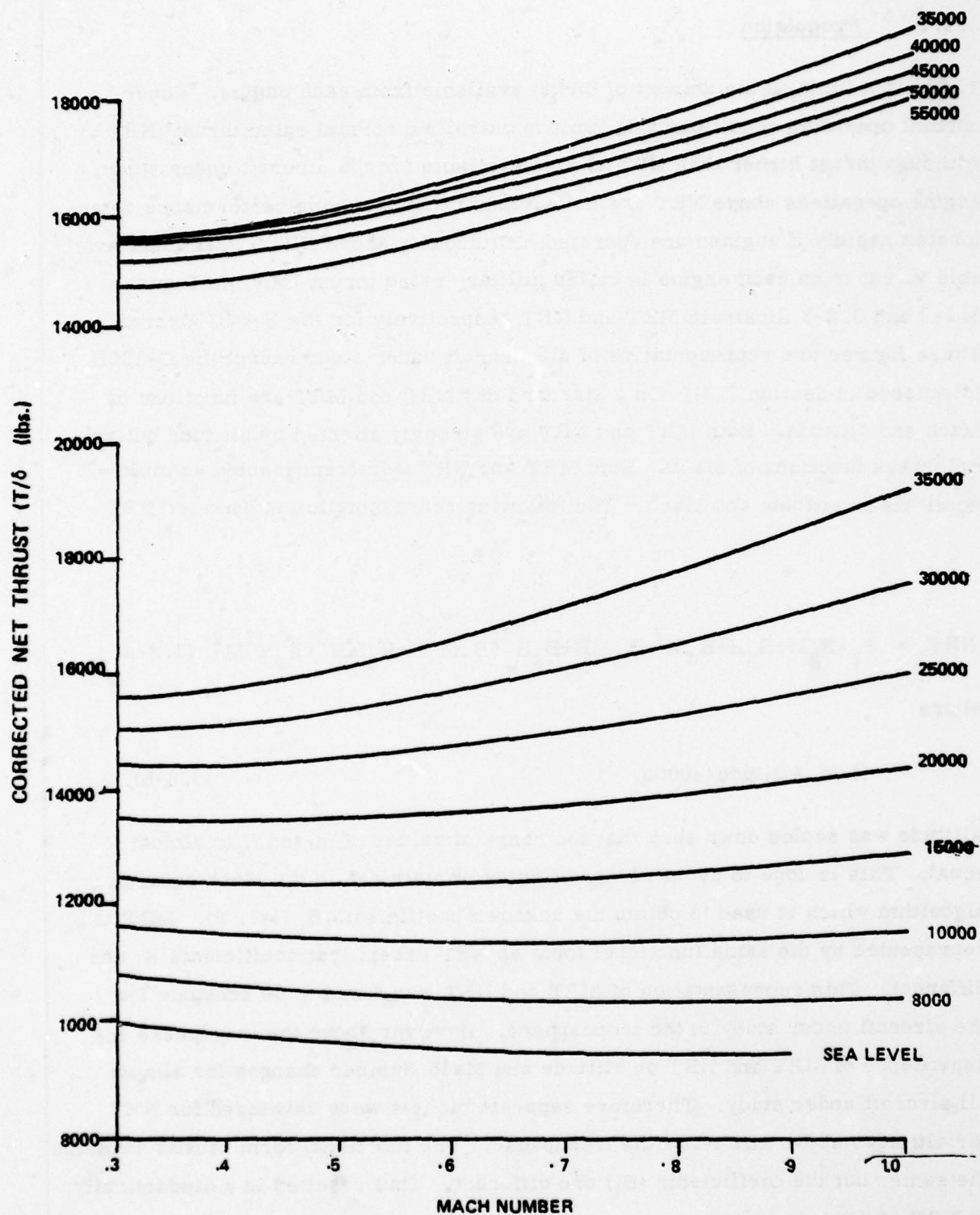


Figure 3.2-2 MILITARY RATED THRUST VS. MACH FOR B-52G

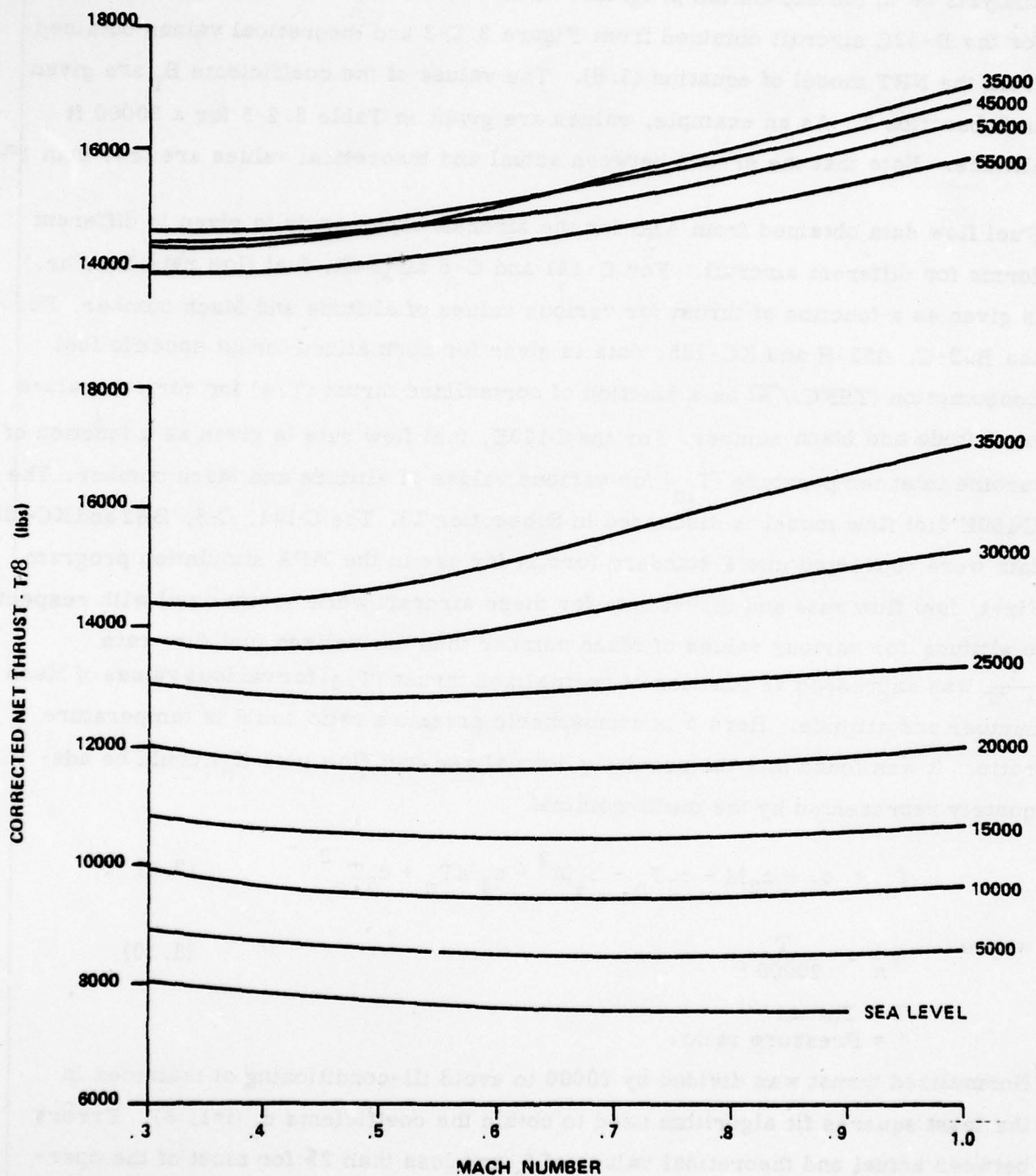


Figure 3.2-3 NORMAL RATED THRUST VS. MACH FOR B-52G

However this discontinuity does not create any problems in the optimal trajectory analysis or in the simulation program. Table 3.2-5 shows actual values of NRT for the B-52G aircraft obtained from Figure 3.2-3 and theoretical values obtained from the NRT model of equation (3.8). The values of the coefficients B_i are given in Subsection 7. As an example, values are given in Table 3.2-5 for a 30000 ft altitude. Note that the errors between actual and theoretical values are less than 1%.

Fuel flow data obtained from ASD for the aircraft under study is given in different forms for different aircraft. For C-141 and C-5 aircraft, fuel flow rate (lbs./hr.) is given as a function of thrust for various values of altitude and Mach number. For the B52-G, B52-H and KC-135, data is given for normalized thrust specific fuel consumption ($TSFC/\sqrt{\theta}$) as a function of normalized thrust (T/δ) for various values of altitude and Mach number. For the C-130E, fuel flow rate is given as a function of turbine inlet temperature (T_{in}) for various values of altitude and Mach number. The C-130E fuel flow model is discussed in Subsection 7.3. The C-141, C-5, B-52 and KC-135 data were converted into a standard format for use in the MPA simulation program. First, fuel flow rate and thrust data for these aircraft were normalized with respect to altitude for various values of Mach number then normalized fuel flow rate $\frac{f}{\delta \sqrt{\theta}}$ was expressed as function of normalized thrust (T/δ) for various values of Mach number and altitude. Here δ is atmospheric pressure ratio and θ is temperature ratio. It was found that the resulting normalized fuel flow rate (f_n) could be adequately represented by the multi-nominal

$$f_n = c_1 + c_2 M + c_3 T_n + c_4 M^2 + c_5 M T_n + c_6 T_n^2 \quad (3.9)$$

where $T_n = \frac{T}{20000}$ (3.10)

T = Thrust

δ = Pressure ratio

Normalized thrust was divided by 20000 to avoid ill-conditioning of matrices in the least squares fit algorithm used to obtain the coefficients c_i ($i=1, 6$). Errors between actual and theoretical values of f_n are less than 2% for most of the operating conditions, except close to idle thrust setting where larger errors were

ALTITUDE 30000 FT

MACH	ACTUAL NRT	NRT FROM THEORETICAL MODEL	% ERROR
.3	4128	4098	-.73
.4	4113	4114	.02
.5	4143	4145	.05
.6	4203	4191	-.28
.7	4277	4251	-.59
.8	4351	4327	-.56
.9	4425	4417	-.19

Table 3.2-5 COMPARISON OF ACTUAL AND THEORETICAL
NRT VALUES FOR B-52G

obtained. Therefore a separate model was developed for normalized idle fuel flow rate using idle thrust and fuel flow data for the aircraft. The functional form of the idle fuel flow model is the same as in equation (3.9) but the coefficients change. This discontinuity in the fuel flow model did not create any problems in the optimal trajectory analysis or in the aircraft simulation program.

3.3 EQUATIONS OF MOTION

In this subsection "point-mass" two-degree-of-freedom (2-DOF) equations of motion describing aircraft motion in a vertical plane are presented. These equations provide the basis for all aircraft trajectory simulation performed in this report.

The point-mass 2-DOF equations of motion for an aircraft are:

$$\dot{x} = V \cos \gamma \quad (3.11)$$

$$\dot{E} = [T \cos \alpha - .5 \rho V^2 S C_D] V / W \quad (3.12)$$

$$\dot{h} = V \sin \gamma \quad (3.13)$$

$$\dot{\gamma} = g[(T \sin \alpha + .5 \rho V^2 C_L) / W - \cos \gamma] / V \quad (3.14)$$

$$\dot{W} = -f \quad (3.15)$$

where the state variables are

- x = Range, ft
- E = Aircraft specific energy/unit weight
- h = Altitude, ft
- γ = Flight path angle, rad
- W = Aircraft weight, lbs

Velocity can be expressed as a function of E and h using the relation

$$V = [2g(E - h)]^{1/2} \quad (3.16)$$

Aircraft model parameters include engine thrust (T), lift and drag coefficients (C_L and C_D), angle of attack (α), reference area (S), atmospheric density (ρ) and gravitational acceleration (g). Thrust (T) and angle of attack (α) are the control variables. Fuel flow rate (\dot{f}) is a function of altitude, Mach number and engine thrust setting.

For transport/bomber aircraft, the flight path angle (γ) is generally small. Therefore γ dynamics can be ignored in the simulation without appreciably affecting the simulation results. Thus for this effort γ dynamics were ignored and flight path angle (γ) is obtained using Eq. (3.13) where altitude rate is determined from the optimization algorithm or based on a standard flight profile.

3.4 DEFINITION OF FLIGHT SEGMENTS

Although from take-off to touchdown the aircraft mission profile is a continuous trajectory, various parts of this trajectory have different characteristics. Thus the aircraft mission profile can be decomposed sometimes into various segments whose performance characteristics can be evaluated separately. These segments include departure, climb, cruise, acceleration, descent, turning and approach. These segments when added together define an aircraft mission profile as shown in Fig. 3.4-1. Note that acceleration, deceleration and turning may not occur as shown in Fig. 3.4-1 and for some missions may not occur at all. The cruise segment need not be a constant altitude cruise. There can be cruise-climb or step climb segment. Short range missions may not have a cruise segment. These various mission segments and their characteristics are described further below.

3.4.1 Departure

The departure segment considered in this study consists of take-off, landing gear retraction, climbout to flap retraction height, acceleration to flap retraction speed, flap retraction and then acceleration to normal climbout speed. Normal climbout speed for C-5 and C-141 is 250 KCAS below 10000 feet altitude due to

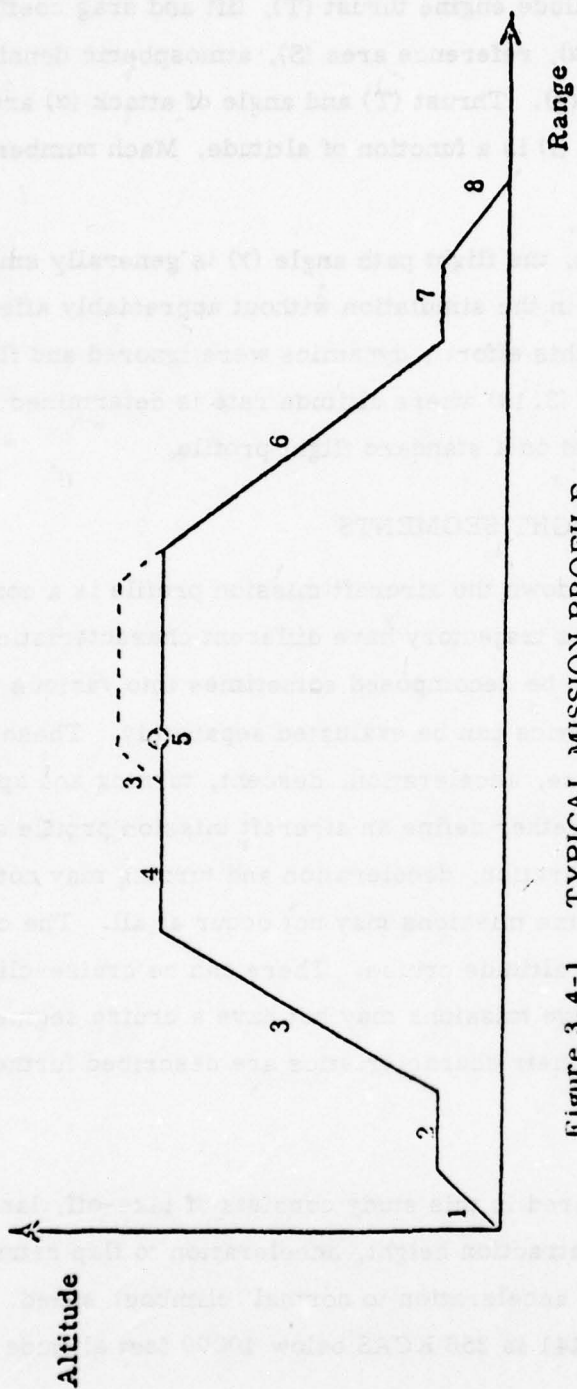


Figure 3.4-1 TYPICAL MISSION PROFILE

- 1 Departure
- 2 Acceleration
- 3 Climb/Step Climb
- 4 Cruise
- 5 Turns
- 6 Deceleration
- 7 Deceleration
- 8 Approach

ATC constraints. The C-130E is not affected by this constraint and the B-52G, B-52H, and KC-135 aircraft are not required to follow this constraint according to SAC regulations.

3.4.2 Climb

During climb the aircraft is in a clean configuration. Conventional flight procedures follow a specified speed schedule and thrust setting during climb, whereas for optimal flight procedures, both aircraft thrust setting and speed schedule is obtained from the optimization algorithm (described in Appendix A). Maximum climb speed for C-5 and C-141 aircraft is limited to 250 KCAS below 10000 ft altitude by ATC restrictions.

3.4.3 Cruise

Because of Air Traffic Control (ATC) restrictions, cruise is generally performed at constant altitude and airspeed. These ATC restrictions are defined in the next subsection. However, both constrained and unconstrained cruise solutions have been evaluated in this study and the results are given in Section 7.

3.4.4 Descent

Like climb, conventional descents are performed at specified speed and thrust settings. Some aircraft use airbrakes during normal descent (B-52G and B-52H). But most aircraft have a clean configuration during descent. Conventional thrust setting during descent is aircraft dependent. For example, for the C-141 two engines are set at idle thrust and two engines are set at a fuel flow of 1500 lb/hrs.

For optimal descent, the aircraft is in a clean configuration and both aircraft speed and thrust setting are obtained from the optimization algorithm. Maximum descent speed for C-5, C-141 and C-130 aircraft is limited to 250 KCAS below 10000 ft altitude.

3.4.5 Acceleration/Deceleration

Level acceleration and deceleration form a very small portion of total mission profile. Acceleration/deceleration are performed at a specified thrust setting. For simulation, thrust setting for acceleration is taken as NRT and for deceleration thrust is taken equal to descent thrust setting.

3.4.6 Turning

Based on the information obtained on current operational procedures/missions, the time spent in turning during a mission by bomber/transport aircraft is negligible compared to total mission time. Savings in fuel by optimizing turning for the aircraft under study will be insignificant. Therefore improved turning procedures were not evaluated in this study.

3.4.7 Approach

The approach procedure considered in this study is the instrument landing approach. The approach on the ILS glide path begins at 3000 feet altitude and about 10 n.m. from touchdown. The conventional approach is flown at constant airspeed and high thrust settings throughout the approach. The optimal approach begins at a higher initial airspeed and decelerates at idle thrust through most of the approach.

3.5 MODELING OF CONVENTIONAL FLIGHT PROCEDURES

The conventional flight profiles simulated in this study closely approximate the mission profiles obtained by processing the ASIMIS Data tapes (See Section 2.1.2). Most of the information required to simulate conventional flights was obtained from these ASIMIS tapes. Any remaining required data was obtained from performance handbooks (T.O. 's) for the aircraft under study and from discussions with various using commands during the course of this study.

3.5.1 Constraints

Aircraft flight procedures are constrained due to factors such as airframe, ATC, using commands and manufacturers. These are described next.

3.5.1.1 Airframe

Aircraft limits of operation are defined by flap placard, maximum lift (stall angle-of-attack), maximum load factor, maximum mach number, maximum and minimum in flight power settings and maximum take-off/landing weight.

3.5.1.2 Air Traffic Control (ATC)

ATC presents one of the most restrictive constraints on aircraft operations. These constraints arise from environmental pollution, noise, air traffic density and safety considerations during departure, approach and in cruise. In this study ATC constraints are treated as variables which can be altered and influenced to achieve fuel conservation objectives. ATC constraints on jet transport air speed within the terminal area are imposed on all conventional flights simulated. However the constraint on air speed to be less than 250 KCAS below 10000 feet altitude is imposed on the C-5, C-141 and C-130E aircraft only. B-52 and KC-135 aircraft are not restricted by this requirement. Cruise altitudes for conventional flights were obtained from the ASIMIS tape data. The ATC constraint on constant altitude cruise with 2000 feet spacing below 29,000 feet and 4000 feet above that altitude is imposed on all conventional flights.

3.5.1.3 Military Operational Constraints

These constraints are imposed to ensure flight conditions consistent with mission requirements and maintenance policies. These constraints include performance ceilings and constraints on use of military thrust. The performance ceiling constraint imposed in the simulation is a cruise ceiling which is the altitude where the airplane has an available rate of climb of 300 feet per minute at normal rated thrust.

3.5.2 Thrust, Altitude and Velocity Procedures Information

The ASIMIS tapes do not provide any information on thrust settings used during a mission. Therefore thrust setting information required to simulate conventional flights was obtained from the T.O.'s. All aircraft generally use normal rated thrust during climb. Cruise altitude and speed information was obtained from the ASIMIS tapes when available. Thrust setting for conventional descents simulated in this study vary from aircraft to aircraft and are described separately for each aircraft in Section 7.

3.6 MODELING OF OPTIMAL FLIGHT PROCEDURES

The modeling of the optimal flight procedures is dependent on the method of optimization employed. Today several algorithms exist which can numerically solve trajectory optimization problems. However, the scope of this study places severe requirements on the method of optimization. Thus, the method must be computationally efficient so that the optimal solution can be generated for the large spectrum of missions (obtained from processing data tapes) for each aircraft type under study. Also, the method must be flexible enough to permit a wide variety of constraints on the state and control variables, i.e., constraints on altitude, air speed, minimum and maximum thrust setting, etc.

The above requirements suggested that gradient-type optimization techniques should not be used as the main approach to solving the two point boundary value (TPBV) problem associated with the optimal control problem in this effort. A TPBV problem is one in which some of the initial conditions and some of the final conditions are undefined. This situation requires that some type of iterative technique be employed in which either the set of initial (or final) conditions are guessed and then the set of equations are integrated either forward (or backward) to the other end condition. The process is repeated until the given conditions are satisfied. For the aircraft optimal trajectory problem the initial and final conditions for the state equations are known; it is the end conditions for the adjoint

equations which give rise to a TPBV problem. The energy management techniques offered an appealing alternative to the numerical gradient techniques. Several papers have discussed the use of energy management reduced order modeling techniques in the solution of minimum fuel trajectories [2-4]. These methods embody the use of total aircraft energy (kinetic plus potential) as a state variable and reductions in model order resulting from ignoring altitude, flight path angle and mass variations. Even with these simplifications a two point boundary value (TPBV) problem results when position dynamics are modeled.

3.6.1 Extended Energy Management (EEM) Solutions

In Ref. [5] an extended energy management (EEM) method of analysis is developed that is based on concepts taken from singular perturbation theory [6, 7]. This method offers the advantage that the fast dynamics ignored in a reduced order formulation [e. g. like energy management] can later be accounted for through a separate "boundary layer" analysis. The result is that the solution of a high order problem is approximated by the solution of a series of problems of lower order. When the dynamics are ordered on separate time scales such that only one state equation appears in each boundary layer, then the original TPBV problem is reduced to a series of point-wise extremizations of algebraic functions. This allows the solution to be mechanized in a feedback form suitable for on-board digital implementation. Thus the EEM method was selected for use in optimizing the aircraft flight profiles.

3.6.2 Constrained and Unconstrained Optimal Solutions

Appendix A derives the EEM solution for optimal climb, cruise and descent procedures for the aircraft under study. Using the necessary conditions for optimality results in a cruise solution given by Eqs. (A-28) to (A-31). This solution is based on the assumption that cruise is actually part of the total optimal trajectory. The analysis in Reference [8] shows that cruise is not minimizing for a wide

class of drag models. The optimal solution appears to be one in which the velocity oscillates at the cruise energy level between maximum energy rate at maximum thrust setting and the minimum drag at idle thrust setting. Optimality of steady state cruise for the aircraft under study was investigated by determining the relaxed steady state cruise fuel consumption assuming an infinite chattering between minimum and maximum thrust and the corresponding velocities described above. Although this is not an implementable path, it serves as a lower bound on fuel performance for the cruise arc. As shown in Appendix B for the C-5A and C-141 transports, steady-state cruise is a fuel minimizing path. Since these two aircraft are representative of the aircraft under study, it is most likely that steady-state cruise is optimal for all aircraft under study.

3.6.3 Modeling Mass Variations

The mass variation equation is not explicitly taken into consideration in the derivation of optimal control algorithm in Appendix A. One approach would have been to include the mass variation equation (3.15) as part of the slow dynamics and carrying the outer expansion and first boundary layer solution to first order. Reference [9] derives the optimal minimum fuel solution for transport/ bomber aircraft using this approach. To zero order, mass variation appears in the cruise portion of the solution. In the first order solution mass variations during climb and descent are computed and used to correct the zero order cruise solution and then to correct the climb and descent solutions. However for the performance index given by Eq. (3.2), inclusion of Eq. (3.15) as part of the slow dynamics leads to a two point boundary value problem. Another approach which avoids the two point boundary value problem, consists of applying the control solution in (A-47) to a detailed aircraft simulation that integrates W along with the other state variables. The control solution is then updated periodically using the current weight and energy state. The updated solution is then used as the control input over the next short interval of time. Both of these procedures were applied to the minimum fuel problem. The difference between fuel consumed using these techniques was negligible, thus the latter approach was used for the results obtained in this report.

3.6.4 Constrained Solutions

Depending on the cruise constraints that are enforced, the optimum cruise solution obtained by using the control algorithm of Eq. (A-31) results in either a cruise climb, step climb or constant altitude cruise. If the ATC constraint of constant altitude cruise is not enforced and if the optimum altitude obtained from Eq. (A-31) is less than cruise ceiling altitude, then the optimum cruise solution is an unconstrained cruise climb path. However, if the optimum cruise altitude is constrained by cruise ceiling, then the optimum cruise is a cruise climb path along the cruise ceiling. On a standard day the B-52G, B-52H, KC-135 and C-141 are not constrained by cruise ceiling, but the C-5 and C-130E can be constrained by cruise ceiling. When the ATC constraint of constant altitude cruise with 2000 feet spacing below 29,000 feet and 4000 feet above is enforced, then optimization in Eq. (A-31) is performed using discrete steps in altitude. When the optimum cruise climb altitude is constrained by cruise ceiling then the constant cruise altitude will be less than the optimum cruise climb altitude. Otherwise the best cruise altitude could be higher or lower than the optimum cruise climb altitude depending upon where the *maximum* of Eq. (A-31) is obtained. Note that as the aircraft flies its weight will decrease and the optimum altitude from Eq. (A-31) may jump to a higher level indicating a need for a step climb. In fact for this weight aircraft should be at new altitude and then step climb is initiated in anticipation. ATC regulations implicitly assume that a step climb will be accomplished in a minimum amount of time. Thus, it is assumed that the step climb will be performed at the NRT setting. Fuel consumed during step climb is anticipated and the climb is initiated when the solution of Eq. (A-31) for the current aircraft weight less anticipated climb fuel results in the next altitude step. Each of these solutions imply a time varying velocity. However, Air Force regulations require constant Mach/KCAS during cruise. For this case cruise velocity is set to a constant value in the optimization algorithm and the optimum constant velocity is obtained by repeating the solution for a range of Mach numbers.

3.7 MISSION PROFILE ANALYSIS PROGRAM

Generation of aircraft trajectories is an important part of the analysis of fuel conserving operational procedures and design modifications. This subsection describes the aircraft trajectory simulation program used in this study.

3.7.1 Discussion of Program

The Mission Profile Analysis Program developed for this fuel conservation study simulates both conventional as well as optimal trajectories with and without the constraints imposed by ATC and the using commands. The vehicle equations of motion used in the simulation were discussed in subsection 3.3. Aerodynamic and propulsion characteristics of the aircraft under study are described by the mathematical models in this simulation. These models are discussed in subsection 3.2. The program simulates all flight segments discussed in subsection 3.4. Aircraft control algorithms required to generate conventional flights are based mostly on information available from processing ASIMIS tapes and in part on conventional flight procedures described in Technical Orders [10 - 15] for each type aircraft. All aircraft under study follow a constant KCAS/Mach speed schedule during climb. Under normal operating conditions, climb is performed at NRT setting. Thus the program simulates conventional climb at NRT setting, although it has the capability to generate conventional climb at MRT setting. The program simulates conventional cruise at specified altitude and air speed. It also simulates a conventional step climb when specified. Thrust setting to simulate C-141 conventional descent is obtained by setting two engines at idle and two engines at 1500 lb/hrs fuel flow rate. The thrust value corresponding to 1500 lbs/hr fuel flow is obtained from the mathematical model of fuel flow rate as a function of thrust and Mach. This thrust is used to simulate a C-141 conventional descent. Similarly, conventional descents for KC-135 are simulated by setting two engines at idle thrust and two at specified thrust settings (to insure that sufficient power is available for operating secondary systems). The program simulates conventional descent for the remaining aircraft at idle thrust settings. The speed schedule followed to simulate conventional descent is similar to climb

and is obtained from the ASIMIS tapes or average mission profiles given in Section 7. The Mission Profile Analysis Program simulates conventional departure according to procedures outlined in the T.O.s. The approach segment simulated in the program is an instrument landing system (ILS) approach.

Aircraft optimum cruise altitudes, speed schedule and thrust settings required to simulate optimal climb, cruise and descents are obtained using the control algorithms defined by Eq. (A-31) and (A-47). There are two essential results. Equation (A-31) is the calculation of the optimal cruise condition, which entails maximization of the following function with respect to altitude (h) and velocity (V)

$$h_o, v_o = \arg \max_{h, v} [V/[\sigma \theta f + 1 - 0]], T = D \quad (3.17)$$

In the above equation f is the fuel/flow rate, T is thrust and D is drag. Equation (A-47) involves the calculation of optimal altitude (h_o^1) and thrust setting (T_o^1) driving climb and descent. These are obtained from the following minimization

$$h_o^1, T_o^1 = \arg \max_{h, T} \left[\frac{(T-D)V/W}{\lambda_x V + \theta f + 1 - \theta} \right]_E \quad (3.18)$$

$$\text{where } \lambda_x = - \frac{\sigma \theta f_o + 1 - \theta}{V_o} \quad (3.19)$$

and f_o is the fuel flow rate during cruise.

The minimization in Eq. (3.18) is done for the current energy E. In general there are two solutions to Eq. (3.18), one for climb and one for descent. It is necessary to update these solutions as a function of the aircraft energy level. The result is the optimal scheduling of h and T as a function of energy level.

The flow diagram in Figure 3.7-1 illustrates the computational scheme used in the Mission Profile Analysis Program to simulate optimal trajectories

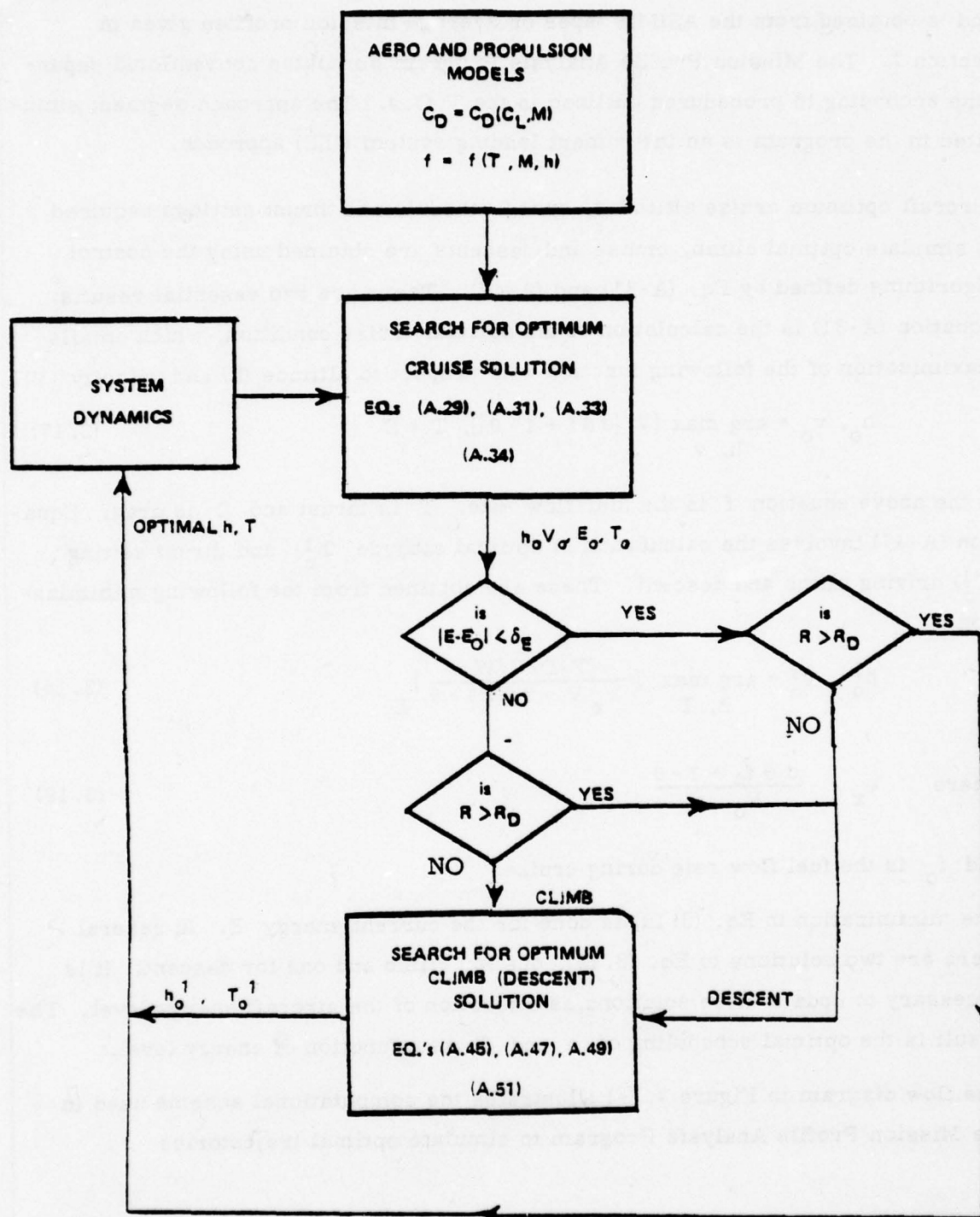


Figure 3.7-1 FEEDBACK IMPLEMENTATION OF THE EEM SOLUTION

As shown in Figure 3.7-1 the climb solution is used until cruise energy level (E_o) is reached, where

$$E_o = h_o + \frac{V_o^2}{2g} \quad (3.20)$$

At this point only the cruise solution is required. An estimate of distance traveled during descent (R_D) is obtained by integrating the aircraft trajectory forward in time. Cruise is maintained until Range-to-go (R) is less than R_D . At this point the control solution returns to the descent solution of (A.47).

3.7.2 Verification of Simulation Results

3.7.2.1 Conventional Flight Profiles

The Mission Profile Analysis Program was used to simulate representative conventional mission profiles for C-5, KC-135 and C-130E aircraft. For these aircraft actual mission profile data obtained from the ASIMIS tapes contained most of the information required to simulate a conventional trajectory. A three way comparison was made. First, actual mission data was obtained from ASIMIS tapes. Besides TOGW, cruise altitude, and air speed, this data provides information on fuel consumed and time spend during various mission segments. Using this data and performance curves given in the T.O.'s, aircraft trajectories were synthesized. From the performance curves, range travelled, fuel consumed and time spent during various mission segments were obtained. Allowance was made for fuel consumed during taxi out, take-off, approach and landing. Conventional trajectories were also simulated using the mission profile analysis program. Tables 3.7-1, 3.7-2 and 3.7-3 provide a comparison of results using these three methods (actual, simulated, and performance chart trajectories) for C-5A, C-130E and KC-135 aircraft respectively. Since the data for actual fuel consumed and time spent for the climb segment includes taxi out and take-off, a comparison of actual, simulated performance chart data for this segment usually indicates differences due to the many unknown components involved. Comparison of the cruise segment is the most valid comparison, since altitude, air speed, and cruise time are the same for all three (actual, simulated and performance

Aircraft Serial No. 680212
 Mission Date 8/9/76
 Mission Duration 6 hrs. 49 min.

TOGW 592,000 lbs
 TOFW 195,600 lbs
 LFW 52,000 lbs

Mission Segment	Altitude and Air Speed	Actual			Performance Charts			Trajectory Simulation		
		Range N. M.	Fuel lbs.	Time min.	Range N. M.	Fuel lbs.	Time min.	Range N. M.	Fuel lbs.	Time min.
Taxi Take-off Climb	Sea Level	-	17,200	49	161	17,800	49	159	17,830	49
Cruise	33,000 ft .77 Mach	2500	117,620	335	2,500	115,000	335	2500	117,850	335
Descent and Landing	Sea Level	-	8,780	25	91	6,250	25	93	7,089	25
Total		-	143,600	409	2,752	139,050	409	2,752	142,769	409

Table 3.7-1 Comparison of Actual, Simulated and Performance Chart Trajectories for C-5A

Aircraft Serial No.	5600514	TOGW	118,000 lbs
Mission Date	4/19/76	TOFW	43,000 lbs
Mission Duration	6 hrs. 20 min	LFW	19,000 lbs

Mission Segment	Altitude and Air Speed	Actual		Performance Charts			Trajectory Simulation			
		Range N. M.	Fuel lbs.	Time min.	Range N. M.	Fuel lbs.	Time min.	Range N. M.	Fuel lbs.	Time min.
Taxi		-	-	10	-	-	10	-	-	10
Take-off		-	-	-	-	1,300	-	-	1,300	-
Climb		-	-	20	50	1,400	15	50	1,560	15
Cruise	22,000 ft	-	-	-	1551	21,700	335	1551	21,800	335
Descent	196 KIAS	-	-	341	24	160	5	24	150	5
Landing		-	-	9	10	1,000	10	10	1,000	10
Total		-	24,000	380	1629	25,560	375	1629	25,810	375

Table 3.7-2 Comparison of Actual, Simulated and Performance Chart Trajectories for C-130E

Aircraft Serial No. 6203503
 Mission Date
 Mission Duration 6 hrs. 11 min.

TOGW 251,600
 TOFW 130,600
 LFW 45,000

Mission Segment	Altitude and Air Speed	Actual			Performance Charts			Trajectory Simulation		
		Range N.M.	Fuel lbs.	Time min.	Range N.M.	Fuel lbs.	Time min.	Range N.M.	Fuel lbs.	Time min.
Taxi Take-off Climb	285 KLAS	-	10600	22	113	9400	20	116	10380	20
Cruise	25000									
	290 KLAS	-	70000	326	2254	68300	326	2254	70050	326
Descent Approach Landing	220 KLAS									
		-	5000	23	120	4640	21	114	4670	27
Total		-	85600	371	2487	82310	367	2484	85100	373

Table 3.7-3 Comparison of Actual, Simulated and Performance Chart Trajectories for KC-135

chart) trajectories. Again descent data includes approach, landing and taxi-in fuel and time, and may show large differences due to the many unknowns involved. For C-5A difference between fuel during cruise phase of actual and simulated trajectory is less than 0.2%. However fuel consumed obtained from performance charts is approximately 2.2% less than actual value.

For the C-130E aircraft, the actual data does not provide information on the cruise segment separately. In fact, fuel consumption information is given for the total mission only. Moreover take-off fuel weight and landing fuel weight data is given to the nearest 1000 lbs. Thus there could be a 1000 lbs. difference between actual fuel consumed and the recorded data. Table 3.7-2 indicates almost 1800 lbs. difference between fuel consumed for actual and simulated trajectories. However the difference between fuel consumed during cruise for simulated and performance chart trajectories is less than 0.5%. For the KC-135 aircraft, performance charts indicated a 9% allowance for surge-bleed valve operation for the mission considered. Using this allowance in cruise, Table 3.7-3 indicates that the difference between the actual and simulated trajectory is negligible during the cruise segment.

3.7.2.2 Optimal Flight Profiles

Reference [16] obtains the minimum-fuel solutions for a C-141 type transport aircraft using a steepest-descent optimization method. In order to compare the EEM solution with the gradient solution, aircraft aerodynamic and propulsion characteristics given in [16] were used, and both long range (500-nm) and short range (200-nm) EEM solutions were obtained for the initial and terminal conditions given in this reference. Fuel consumption results for both cases are summarized in Table 3.7-4. From this table it is observed that fuel consumption for the EEM trajectories compares very well with the fuel consumption for the steepest descent trajectories.

Flight path dynamics are modeled in [16] and are ignored in the EEM analysis. Since the fuel consumption is almost the same in both cases, it indicates that these dynamics do not play an important role in fuel conservation studies in transport aircraft.

SOLUTION TYPE	Fuel Consumed (Lbs)	
	Short Range (200 nm)	Long Range (500 nm)
Steepest Descent	7,420	15,248
EEM	7,416	15,268

TABLE 3.7-4 COMPARISON OF FUEL CONSUMED FOR
EEM AND GRADIENT SOLUTIONS

The Mission Profile Analysis Program is an integral part of the mission spectrum analysis program. The mission spectrum analysis program analyses a spectrum of mission profiles obtained by processing ASIMIS tape data for each aircraft type. Thus trajectory information and frequency of each mission type is stored on a file and the mission spectrum analysis program generates results for each mission using the mission profile analysis program, and computes total results by summing over the spectrum of missions.

SECTION 4

ANALYSIS APPROACH AND DEFINITION OF OPERATIONAL PROCEDURES THAT CONSERVE FUEL

This section defines various operational procedures that potentially can result in fuel/DOC savings and describes the analysis approach to evaluate the improvements in performance/cost which can be expected by implementing these procedures. Operational procedures considered in this section include both airborne and ground procedures. In airborne procedures flight path optimization is one operational procedure that can result in significant fuel savings. Other airborne procedures which result in fuel/DOC savings are the procedures which reduce drag and the procedures which reduce engine load. Ground procedures which offer potential fuel/DOC savings are improved maintenance and ground handling techniques.

4.1 ANALYSIS OF AIRBORNE PROCEDURES REQUIRING TRAJECTORY OPTIMIZATION

Optimization of the aircraft's trajectory during flight is one operational procedure that can result in fuel savings. The flight profiles for the aircraft under study can be divided into the following flight modes for individual analysis:

- Departure
- Climb
- Cruise (constant altitude, cruise-climb, step climb)
- Descent
- Approach

The characteristics of these flight modes were described in the previous section. The trajectory optimization program described in subsection 3.7 can be employed to analyze various flight segments individually. The results of the optimization of individual flight segments can be implemented directly or can be used to assist in complete trajectory optimization. This subsection (1) identifies the airborne procedures that can benefit from trajectory optimization and (2) describes

the analysis approach for evaluating the fuel savings, which may be achieved by implementing these procedures.

4.1.1 Departure

Conventional departures for each aircraft under study are simulated following the procedures outlined in their respective performance manuals. These procedures are already close to optimal. It has been suggested that deploying flaps gradually during ground roll and reduced power take-off procedures offer fuel savings. These procedures are described next.

4.1.1.1 Deploying Flaps Gradually During Ground Roll

Deployment of flaps results in increased aerodynamic drag. If the flaps are deployed gradually during ground roll when the aircraft is accelerating, it will result in reduced drag. Thus fuel consumed and time spent during ground roll are also reduced. The fuel savings depend on aircraft weight, runway conditions and ambient temperature. However for some aircraft (B-52G and B-52H) partial deployment of flaps results in higher drag than fully deployed flaps. Evaluating this procedure in this study for the C-141 aircraft using trajectory optimization program resulted in average fuel savings per mission of less than one gallon, which is negligible. Also due to safety considerations the procedure may not be feasible. Therefore the procedure was not evaluated for the other aircraft under study.

4.1.1.2 Reduced Power Take-off

The original concept of using reduced engine pressure ratio (EPR) for take - off, where possible, was to extend engine life by reducing turbine creep and engine deterioration resulting from high temperatures and stress [17]. The side benefits of this procedure are the savings in fuel actually used during the take-off and the decreased SFC of operating engines which have less deterioration. Actual fuel savings due to reduced power takeoff were estimated for the aircraft under study by simulating the takeoffs using the mission profile analysis program. Actual fuel savings due to reduced power takeoff were found to be less than one half gallon per mission for all aircraft under study. Reduced power takeoff also increases takeoff time slightly. However the indirect benefit of reduced power takeoff

(the decreased SFC of operating engines) has been estimated at 2% by Braniff Airlines [17].

4.1.2 Approach

The procedures for landing jet transports have evolved from landing concepts originally developed for propeller aircraft. The conventional instrument landing approach procedure requires high thrust settings for an extended time with the accompanying noise impact, air pollution and high fuel consumption. The noise problem has been successfully attacked in recent years with the development of the two segment approach which brings the aircraft in at a steeper angle initially thereby achieving noise reduction through lower thrust settings and higher altitudes. A further reduction in noise and significant reduction in fuel consumption can be achieved with the delayed flap approach concept developed by NASA [18].

In contrast to a conventional ILS approach which is flown at a constant airspeed and high thrust settings through out the approach, the delayed flap approach begins at a higher initial airspeed and in a drag configuration that allows for low thrust. The landing flaps are then lowered at the appropriate time so that the airspeed slowly decelerates to approach speed at a specified altitude above the runway. At this point the pilot advances the throttles to approach power and the last portion of the approach is flown at a stabilized airspeed similar to a conventional approach. Note that since the delayed flap approach is executed at higher average airspeed than the conventional approach, time spent during the approach segment is also reduced, resulting in reduced holding times and less congestion near the terminal area.

Fuel/DOC savings due to the delayed flap approach procedure are evaluated for the aircraft under study by simulating this approach procedure in the mission profile analysis program. A 3° ILS glide slope is considered in the simulation. The altitude where the aircraft achieves stabilized approach speed in landing configuration is a variable parameter in the simulation. For the conventional approach this altitude is taken as 1,500 feet. Fuel/DOC savings due to delayed flap approach are evaluated by varying this altitude to 1,000 feet,

500 feet and 0 feet respectively. Fuel and DOC savings increase as this altitude is lowered.

4.1.3 Cruise

The cruise segment can have various flight modes depending upon the constraints imposed on the cruise altitude and air speed. The altitude constraint can be due to cruise ceiling, ATC constraint on altitude (described in Section 2) or a specified altitude. Air speed constraints can be due to a requirement of constant Mach/TAS cruise or a specified cruise Mach number. The following describes the cruise solution under these various constraints.

4.1.3.1 Optimal Cruise-Climb Solution

Appendix A derives the control algorithm for aircraft trajectory optimization. Optimum altitude and air speed for cruising flight are obtained by point extremization of function defined by equation (A.31). The solution of this equation depends upon the fuel/time tradeoff parameter θ defined in Subsection 3.1. Varying the parameter θ produces a curve of fuel consumption as a function of mission time. The solution corresponding to $\theta = 0$ is the minimum time solution. As the value of θ is increased fuel consumption decreases, however the mission time increases. The solution, corresponding to $\theta = 1$ is the minimum fuel solution.

Optimum cruise altitude and airspeed obtained from Equation (A.31) vary with aircraft weight. As an aircraft burns fuel its weight decreases and the optimum cruise altitude increases. Thus the optimum cruise solution is a climbing cruise flight path. For the aircraft whose optimum cruise altitude is constrained by cruise ceiling (C-5 and C-130E) this path lies along the cruise ceiling.

It is proven in Appendix A that for modern jet transports whose aerodynamic parameters C_D , K , and C_L' are independent of altitude and whose optimum cruise altitude is not constrained by cruise ceiling, some parameters remain unchanged for the minimum fuel cruise-climb solution. These parameters are cruise Mach

number, W/δ (weight over atmospheric pressure ratio) and range factor where range factor is defined as distance traveled per pound of fuel multiplied by aircraft weight. For example, values of these parameters for the C-141 are as follows.

- Mach number = 0.717
- W/δ = 1.24×10^6 lb.
- Range factor = 9226 n.mi.

This value of range factor is based upon the horizontal flight path assumption of Equation (A.29). However for a cruise climb profile, average value of flight path for C-141 is approximately 0.02 degrees and the value of range factor reduces by 0.7% due to increased thrust required for energy gain during cruise-climb.

4.1.3.2 Constant Altitude Variable Mach Number Cruise

If the aircraft is constrained to fly at a constant altitude, the optimum air speed is obtained by extremization of Equation (A.31) with h_0 fixed. As the aircraft burns fuel its weight decreases and the optimum air speed varies. Thus cruise Mach number for an optimum cruise trajectory under the constant altitude constraint varies along the trajectory. For the minimum fuel cruise solution of jet transports, the optimum cruise Mach number is a function of W/δ . Figure 4.1-1 and 4.1-2 illustrate best cruise Mach number and range factor as function of W/δ for a C-141 aircraft. Note that as the aircraft burns fuel, W/δ decreases resulting in a change in best cruise Mach number and range factor. The values of range factor shown in Figure 4.1-2 are based on the assumption of Equation (A.29) that thrust is equal to drag during cruise. However, the thrust required is smaller than drag due to the continuous decrease in cruise Mach

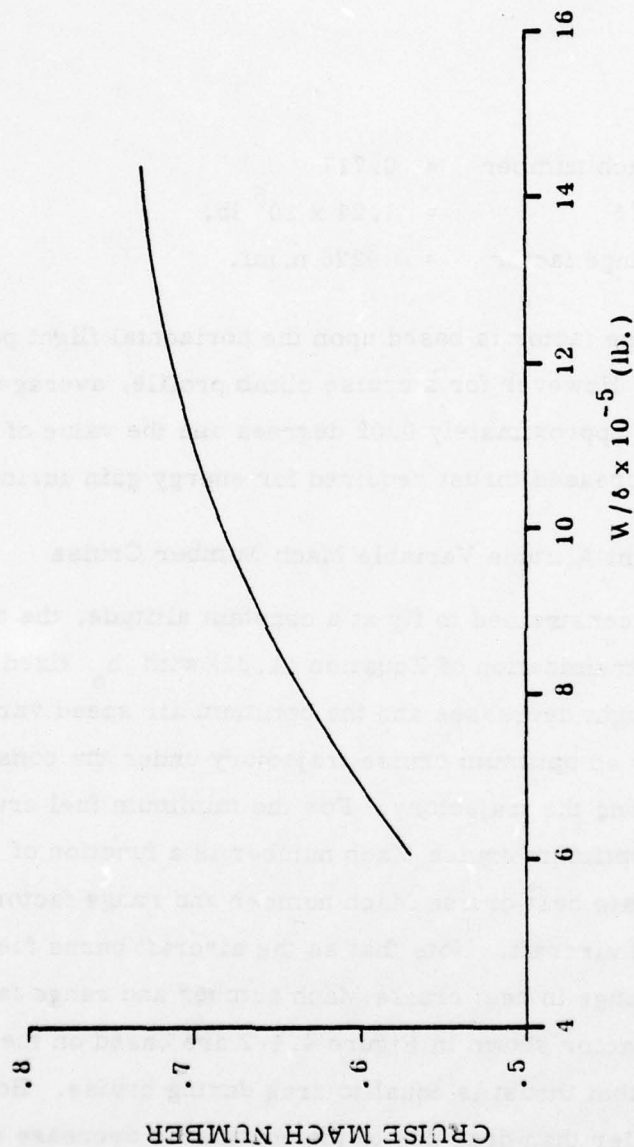


Figure 4.1-1 BEST CRUISE MACH NUMBERS FOR MINIMUM
FUEL CRUISE FOR C-141

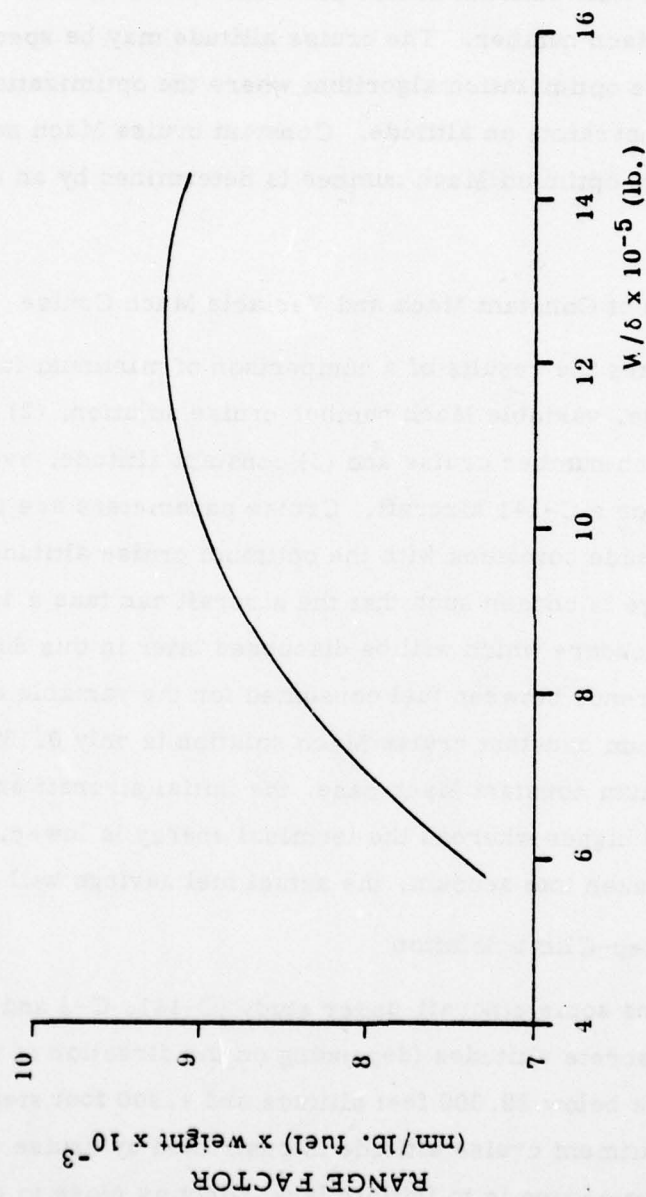


Figure 4.1-2 RANGE FACTOR FOR MINIMUM FUEL CRUISE
FOR C-141

number. Thus actual range factor is higher than shown in Figure 4.1-2 by approximately 0.1%.

4.1.3.3 Constant Altitude-Constant Mach Cruise

Cruise segments under conventional cruise procedures are flown at constant altitude and constant Mach number. The cruise altitude may be specified or determined from the optimization algorithm where the optimization is performed under ATC constraints on altitude. Constant cruise Mach number may be specified or an average optimum Mach number is determined by an iterative process.

4.1.3.4 Comparison of Constant Mach and Variable Mach Cruise

Table 4.1-1 summarizes the results of a comparison of minimum fuel consumed for (1) constant altitude, variable Mach number cruise solution, (2) constant altitude, specified Mach number cruise and (3) constant altitude, average optimum Mach number cruise for a C-141 aircraft. Cruise parameters are indicated on the table. Cruise altitude coincides with the optimum cruise altitude for initial aircraft weight. Range is chosen such that the aircraft can take a 4,000 foot step for the step-climb procedure which will be discussed later in this Subsection. Observe that the difference between fuel consumed for the variable cruise Mach solution and the optimum constant cruise Mach solution is only 0.13%. Also compared to the optimum constant Mach case, the initial aircraft energy for the variable Mach case is higher whereas the terminal energy is lower. If this energy difference is taken into account, the actual fuel savings will be negligible.

4.1.3.5 Optimum Step-Climb Solution

Due to ATC regulations some aircraft under study (C-141, C-5 and C-130E) are restricted to fly at discrete altitudes (depending on the direction of flight) with 2,000 foot step-climbs below 29,000 feet altitude and 4,000 foot steps above it. For aircraft whose optimum cruise altitude is restricted by cruise ceiling, the optimum step climb procedure is to initiate level flight as close to cruise ceiling as possible. Subsequent step-climbs would be initiated as soon as gross

Initial Weight 293,600 lbs.
 Altitude 35,000 feet
 Range 860 n. m.

CRUISE TYPE	FUEL CONSUMED LBS	% INCREASE OVER VARIABLE MACH
Optimum Variable Mach Cruise (.717 - .7)	26,142	0
Optimum Constant Mach Cruise (.71)	26,177	0.13
Specified Mach Cruise (.717)	26,193	0.19

Table 4.1-1 COMPARISON OF CONSTANT MACH VS. VARIABLE
 MACH CRUISE FOR C-141 AIRCRAFT

weight decreases to a value that allows a step climb. Climb is performed at NRT thrust setting as required by ATC regulations. This procedure is applicable to C-5 and C-130E aircraft. Note that the increase in fuel consumption due to flying off optimum cruise altitude is parabolic as a function of altitude. For aircraft whose cruise ceiling is more than 2,000 feet above optimum cruise altitude (C-141, B-52, KC-135), the optimum step-climb procedure is to initiate a level flight as close as possible to 2,000 feet above the cruise-climb altitude (cruise-climb altitude for these aircraft is higher than 29,000 feet). Subsequent step-climbs would be initiated as soon as gross weight decreases to a value that allows a step-climb of 4,000 feet to the next level flight altitude that is less than 2,000 feet above the cruise climb ceiling. Section 7.1 presents a comparison of cruise-climb vs step-climb procedure for a typical C-141 cruise. The step-climb procedure results in approximately 0.3% increase in fuel consumption over the optimum cruise-climb procedure.

4.1.4 Climb

During climb, the aircraft's altitude and air speed change from their take-off values to the values at the initiation of the cruise segment (for the short range case there may not be a cruise segment). During climb, the aircraft is in a clean configuration. The climb options considered in this study are described below.

4.1.4.1 Conventional Climb

Conventional climbs are generally executed at NRT power setting and a specified airspeed schedule (except C-130E which follows a airspeed schedule resulting in maximum rate of climb) consisting of a constant - IAS mode followed by a constant Mach number segment. However, due to the ATC constraint, airspeed of C-141 and C-5 aircraft below 10,000 feet altitude is restricted to 250 KIAS. Airspeed schedules for the aircraft under study were obtained from their respective performance manuals (from ASIMIS tape data for KC-135) and are given in Section 7 by aircraft type.

4.1.4.2 Optimal Climb

The optimum climb algorithm developed in Appendix A provides optimum air speed and thrust setting for optimal climb segments. The ATC constraint on maximum climb speed can be enforced in the optimization algorithm. Thus both constrained and unconstrained optimum climb solutions have been obtained to assess the impact of ATC constraint on optimal climb procedures. In general, both airspeed and throttle setting vary continuously for optimal trajectories.

4.1.4.3 Parametric Optimal Climb

Parametric optimal climb is similar to conventional climb. They both employ NRT power setting, and follow a constant KCAS-constant Mach airspeed schedule. The difference is that constant Mach number is equal to optimum cruise Mach number, and the value of constant-KCAS is determined by parametric optimization. The parametric optimum climb takes less time than the optimal climb solution and is easier to implement. Moreover the difference in fuel consumed between optimum and parametric optimum is small as shown by the comparison results given in Section 7 for each aircraft type.

4.1.5 Descent

During the descent segment, the aircraft's altitude decreases from the cruise levels to a value at which the approach phases can be initiated. As in the case of the climb segment, various descent procedures are examined in this study. These procedures are described below.

4.1.5.1 Conventional Descent

There are various conventional descent procedures for each aircraft type. These procedures are described in the performance manuals of the aircraft. For example the C-141 aircraft can execute the following four types of conventional descents.

- Enroute descent
- Penetration descent
- Rapid-with spoilers
- Rapid-clean

Table 4.1-2 lists the procedures for the C-141 conventional descent. The difference in the performance of these descent procedures is primarily dependent upon the thrust of the engines, the aircraft configuration and the air speed schedule. The use of drag devices (airbrakes, spoilers, etc.) and high airspeed result in rapid descents. However, under normal conditions the enroute descent procedure is employed. This descent procedure results in relatively low rate of descent.

The ASIMIS tape data does not provide information on the type of descent procedure used during a mission. Therefore conventional descent procedures considered in this study are the ones employed under normal conditions. The procedures are described for each aircraft in Section 7.

4.1.5.2 Optimal Descent

Optimal descent is performed in clean aircraft configuration. Optimum airspeed and thrust settings are obtained from the optimum descent algorithm of Appendix A. Both optimal airspeed and thrust setting vary along an optimal descent path. The ATC constraint on maximum airspeed 250 KCAS below 10,000 feet can be enforced in the optimization algorithm.

4.1.5.3 Parametric Optimum Descent

The parametric optimum descent is executed at idle thrust setting with aircraft in the clean configuration. Airspeed schedule is constant Mach-constant KCAS where the constant Mach number is the optimum cruise Mach and KCAS is determined by parametric optimization. As shown in Section 7, the difference in fuel consumed for optimal descent and parametric optimal descent is small. However, both descent procedures result in increased mission times. Thus direct operating cost savings due to optimum descent procedures are small. The results of comparison of various descent procedures are given in Section 7 for each aircraft.

Descent Type	Aircraft Configuration	Thrust Setting	Airspeed Schedule
Enroute Descent	Clean	Two Engines at Idle Two Engines at Fuel Flow of 1500 lb./hrs.	.74M/300 KCAS 250 KCAS Below 10,000 feet Altitude
Penetration Descent	Spoilers Deployed	Four Engines at Idle	.75M/250 KCAS
Rapid Descent - with Spoilers	Spoilers Deployed	Four Engines at Idle	.75M/350 KCAS
Rapid Descent - Clean Configuration	Clean	Two Engines at Idle Two Engines at Fuel Flow of 1500 lb./hrs.	.825M/350 KCAS

Table 4.1-2 PROCEDURES FOR VARIOUS CONVENTIONAL
DESCENTS FOR C-141 AIRCRAFT

4.1.6 Integrated Trajectories

Previous subsections described the fuel savings potential on individual aircraft segments through optimization procedures. This subsection discusses both the conventional and the optimal integrated trajectory profiles.

4.1.6.1 Conventional Profiles

As mentioned earlier the ASIMIS tape data for the aircraft under study contains information on the flight parameters (e.g. TOGW, altitude, airspeed mission duration, fuel consumed etc.) of the actual missions flown. These missions are categorized according to mission duration, take-off gross weight and cruise altitude. The ASIMIS tapes for each aircraft are processed to obtain mission spectrum data. Thus conventional missions simulated in this study represent the actual aircraft operations. The mission spectrum information is stored in the mission spectrum analysis program. This information is used in the mission profile analysis program to simulate the integrated conventional flight profiles from take-off to touch down.

4.1.6.2 Integrated Optimal Trajectories

As mentioned earlier fuel savings for optimal departure procedures is negligible. Therefore, the departure segment of the optimal trajectories used the conventional departure procedures. The optimal control algorithm developed in Appendix A provides airspeed and thrust setting for optimal trajectories during the climb, cruise and descent segments. These control parameters are used in the mission profile analysis program to simulate optimal flight paths. ATC constraint on cruise altitude as well as maximum airspeed (i.e., of 250 KIAS below 10,000 feet altitude) can be enforced during the optimization process. For the approach segment delayed flap approach procedures is simulated where the altitude above the runway where the aircraft attains stable configuration is an input variable in the simulation program.

If the distance traversed during climb to optimum cruise altitude and descent from that altitude to terminal altitude is greater than the specified mission range then the optimal aircraft trajectory cannot attain the optimal cruise altitude. The constrained matching technique, described in Appendix A, is used to obtain the optimum short range solution.

4.1.6.3 Comparison of Integrated Optimal and Conventional Profiles

The following example summarizes the results of a comparison of optimal and conventional trajectories. Both long range and short range minimum fuel trajectories were simulated for a C-141 aircraft using optimal and conventional procedures.

The initial and terminal conditions chosen for these trajectories are shown in Table 4.1-3. The aircraft is in a clean configuration at these values of altitude and airspeed. The long range solutions were obtained for a 1,000 nm. flight. The solid curve DEFG on Figure 4.1-3 shows the altitude Mach number profile for the long range optimal (EEM) solution. The optimum solution calls for the use of NRT power setting during climb from point D to point E and an idle thrust setting below point F during descent. Between points E and F the thrust setting lies between the maximum and minimum values. The aircraft Mach number increases during climb, remains constant during cruise and decreases during descent up to point P. However, the aircraft gains speed during descent below point P. This occurs because idle fuel flow rate is high at low altitudes and the aircraft minimizes fuel consumption by increasing speed. The dotted curve on Figure 4.1-3 illustrates the altitude Mach number profile for a conventional trajectory. Below 10,000 feet altitude, airspeed is 250KCAS. Above that altitude the climb segment follows a 280 KCAS/.7 Mach speed schedule. For this example cruise Mach number is taken as 0.74. Conventional descent is performed at 0.74M/300 KCAS speed schedule up to 10,000 feet altitude, and 250 KCAS below that altitude. Fuel optimal (EEM) trajectory consumed 1,462 lbs less fuel than conventional (28,020 - 26,558); however it took 502 seconds more mission time.

Initial Conditions

Altitude 3,000 feet
 Airspeed 440 ft./sec.
 Weight 260,000 lbs.

Terminal Conditions
 Altitude 3,000 feet

Trajectory Type	Fuel Consumed	Flight Time	DOC \$
200-nm RANGE EEM TRAJECTORY CONVENTIONAL TRAJECTORY	7,155 LBS. 7,908 LBS.	2,160 SEC. 2,040 SEC.	587.1 628.8
1,000-nm RANGE EEM TRAJECTORY CONVENTIONAL TRAJECTORY	26,558 LBS. 28,020 LBS.	9,133 SEC. 8,631 SEC.	2243.7 2309.2

Table 4.1-3 COMPARISON OF EEM AND CONVENTIONAL
 TRAJECTORIES FOR C-141 AIRCRAFT

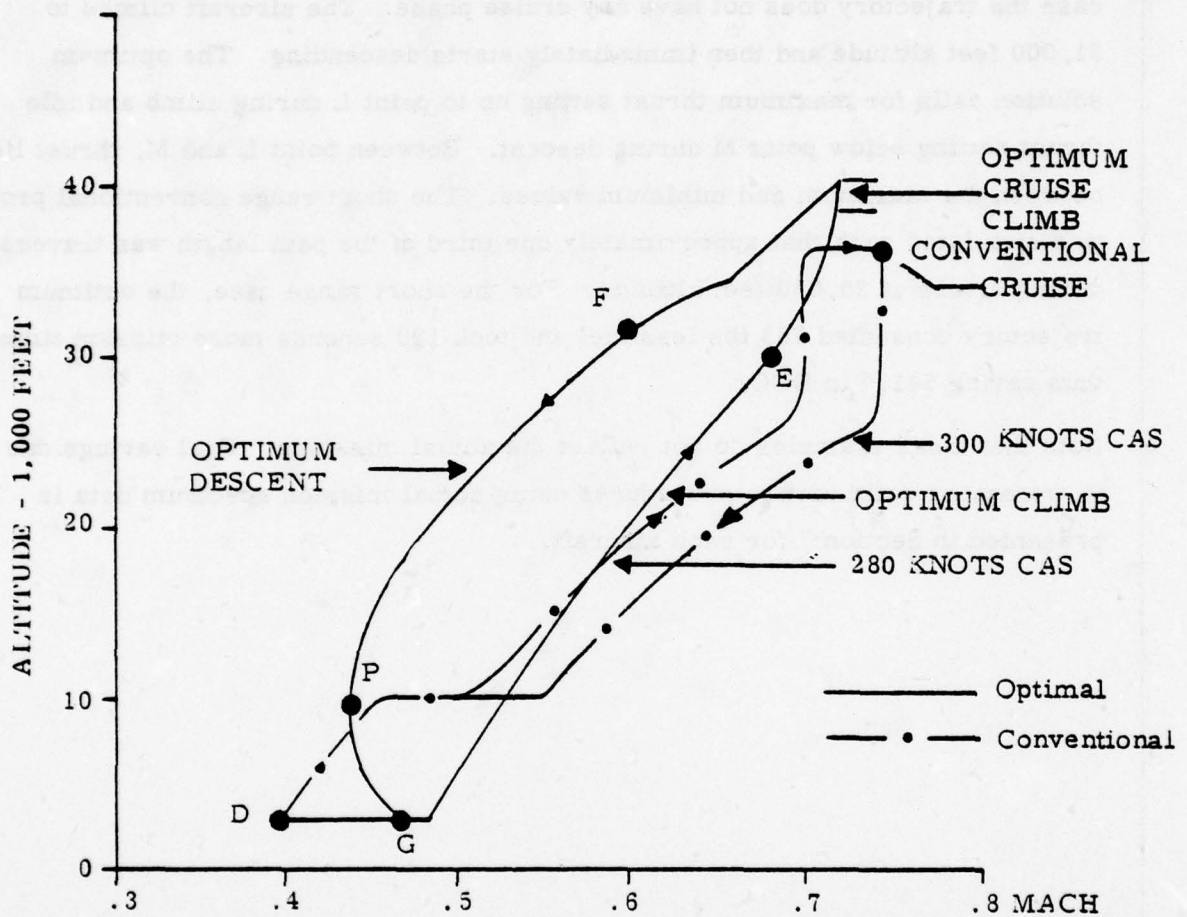


Figure 4.1-3 ALTITUDE - MACH PROFILES FOR LONG RANGE
OPTIMAL AND CONVENTIONAL TRAJECTORIES

The net result is that trajectory optimization resulted in a direct operating cost (DOC) savings of \$65.5 for the single trajectory. The solid curve KLMN on Figure A-1, Appendix A, is a 200-nm range optimal (EEM) trajectory. In this case the trajectory does not have any cruise phase. The aircraft climbs to 31,000 feet altitude and then immediately starts descending. The optimum solution calls for maximum thrust setting up to point L during climb and idle thrust setting below point M during descent. Between point L and M, thrust lies between the maximum and minimum values. The short range conventional profile was simulated such that approximately one third of the path length was traversed during cruise at 25,000 feet altitude. For the short range case, the optimum trajectory consumed 753 lbs less fuel and took 120 seconds more mission time thus saving \$41.7 in DOC.

Note that these examples do not reflect the actual missions. Fuel savings due to trajectory optimization procedures using actual mission spectrum data is presented in Section 7 for each aircraft.

4.2 ANALYSIS OF OTHER FUEL CONSERVING AIRBORNE PROCEDURES

Many candidate airborne procedures exist that are not directly related to trajectory optimization. This section discusses the properties of these procedures and evaluates fuel savings which may result by implementing them.

4.2.1 Procedures Which Reduce Drag

Drag can be reduced during flight by tighter fuel management, retrimming the aircraft for changes in operating conditions and burning fuel towards an aft c.g.

4.2.1.1 Tighter Fuel Management

Aircraft weight imbalance resulting from uneven fuel distribution about the aircraft centerline necessitates the need for trim with a corresponding increase in drag. By applying appropriate fuel expenditure management techniques, the imbalance of fuel in the tanks can be kept to a minimum. While this technique should be pre-planned in terms of the mission profile and the anticipated fuel consumption, its implementation is accomplished while the aircraft is airborne. A quantitative estimate of fuel savings due to this procedure requires an in-depth study of aircraft weight balance and fuel balance distributions over an entire mission and for a spectrum of missions. This type of data is not available at present for the aircraft under study. Since optimum fuel management techniques result in reduction of trim drag due to reduction in trim surface deflection, its effect is similar to aft c.g. operations. Therefore, evaluation of tighter fuel management is encompassed by the evaluation done for aft c.g. operations.

4.2.1.2 Retrimming

Since the aerodynamic forces on an aircraft vary with altitude, velocity, weight, and atmospheric conditions, it is desirable to retrim as speed changes are made. In some extreme cases trim changes are mandatory to provide aerodynamic stability.

AD-A062 609

DYNAMICS RESEARCH CORP WILMINGTON MASS SYSTEMS DIV
AN ANALYSIS OF FUEL CONSERVING OPERATIONAL PROCEDURES AND DESIG--ETC(U)
JUL 78 R K AGGARWAL

F/G 1/3

F33615-76-C-3104

UNCLASSIFIED

R-247U

AFFDL-TR-78-96-VOL-2

NL

2 OF 6
ADA
062609



When flying with an autopilot it is necessary, if fuel conservation measures are to be stressed, that the autopilot be disengaged and manual retrimming on all three axes be done each time power or speed changes are made. Analysis of the potential fuel savings requires a comparison of fuel consumption under such situations and of fuel consumed using current practice. Discussions with pilots indicated that current retrimming procedures are adequate.

4.2.1.3 AFT C.G. Operations

The operation of an aircraft with the center of gravity as near the aft limit as possible minimizes the distance between c.g. and the center of lift, and thus reduces the nose down trim. This in turn, has the effect of reducing the angle-of-attack for the horizontal stabilizer, minimizing the effect of induced drag on the tail surfaces and thereby reducing total aircraft drag. Therefore, operational procedures which shift aircraft c.g. near the aft limit result in fuel savings. Loading aircraft fuel and cargo towards an aft c.g. is a ground handling procedure and is discussed in Subsection 4.3.4. Where appropriate, it is desirable to burn fuel towards an aft c.g. during flight to enable reduced fuel consumption.

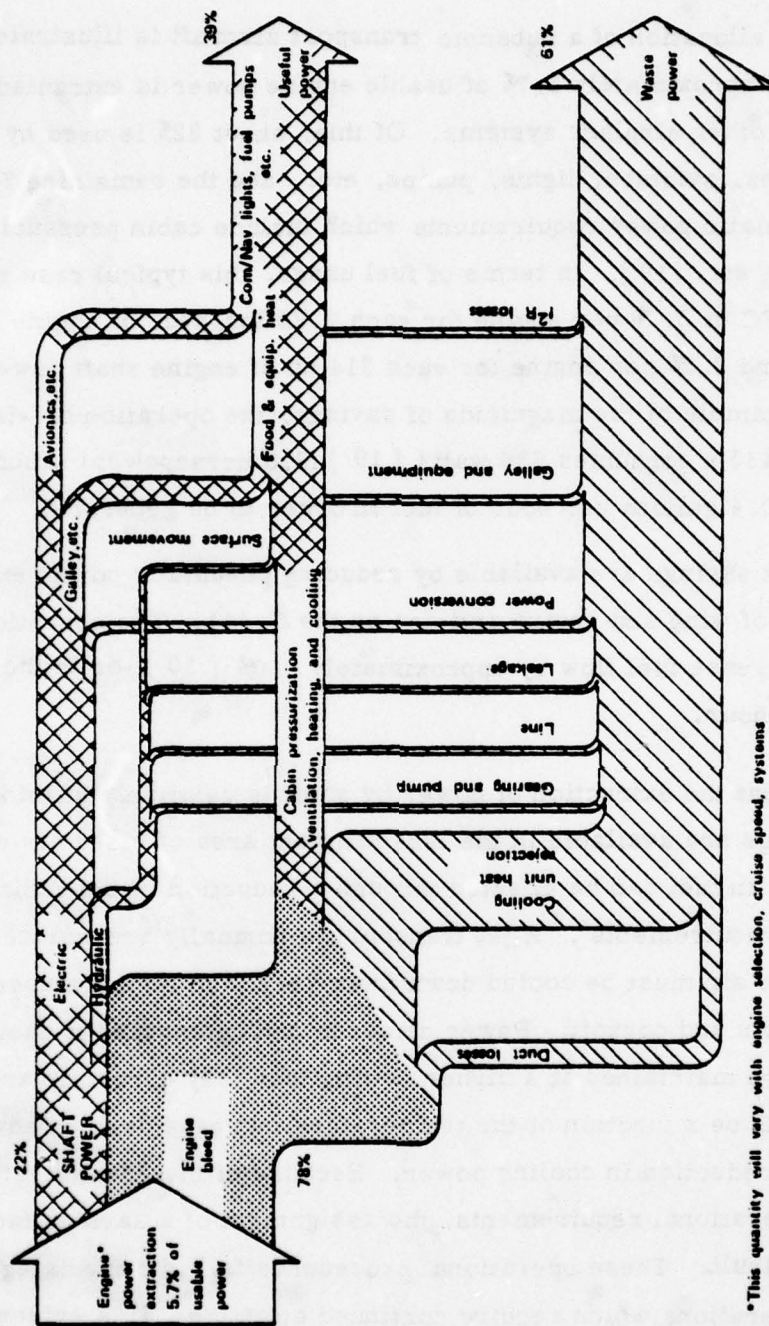
Analysis of fuel savings due to aft c.g. operations is accomplished by obtaining the savings in fuel consumed as a function of the shift in c.g. from the current c.g. Using the equations given in Appendix D these savings are obtained for an average cruise weight during the cruise segment of a mission and annual savings are obtained by averaging over the mission spectrum. Thus fuel savings results are portrayed in terms of the sensitivity of fuel savings to shift in c.g. For the C-130E aircraft, a 5% (percent MAC) shift in c.g. toward aft amounts to 0.55% savings in fuel cost.

4.2.2 Procedures Which Reduce Engine Load

A typical power allocation of a subsonic transport aircraft is illustrated in Figure 4.2-1. Approximately 5.7% of usable engine power is extracted to operate various other airplane systems. Of this, about 22% is used by hydraulic, electrical devices, avionics, lights, pumps, etc., and the remaining 78% goes to provide pneumatic power requirements which include cabin pressurization, air conditioning, etc. [19]. In terms of fuel usage, this typical case results in a decrease in SFC of 5.5% per engine for each 2.20 lbs/sec. of engine bleed air extracted, and 2.5% per engine for each 214 hp of engine shaft power used [19]. As an example of the magnitude of savings, the operation of window anti-ice on KC-135's consumes 636 watts [19] (8.5 horsepower) which requires on the order of 0.4 gallons per hour of fuel in order to be generated.

More significant savings are available by reducing pneumatic power extraction such as the use of wing and engine anti-ice on the C-141. The operation of these two systems increase fuel flow by approximately 9.0% [10], or in the area of 170 gallons per hour.

It can be seen that the extraction of power by shaft is relatively efficient and that more savings are available in the less efficient area of bleed air extraction. Thus, a savings in fuel can be effected through a reduction in the cabin pressurization requirements. A jet transport is normally pressurized at all times and engine air must be cooled down from very high temperatures before it enters the cabin and cockpit. Power demands can be reduced if cabin temperatures are maintained at a higher setting than they currently are. Fuel savings will be a function of the temperature increase deemed advisable and consequent reduction in cooling power. Because of the great diversity of systems and operational requirements, the assignment of a savings factor in this case is difficult. These operational procedures fall into the category of fuel conservation operations which require continued attention. It is evident however, that savings are available and their pursuit would be worthwhile.



*This quantity will vary with engine selection, cruise speed, systems configurations, airplane design, and other similar factors.

Figure 4.2-1 Secondary Power System Energy Diagram, Typical Subsonic Cruise Mach 0.8 Transport

4.2.3 Speed Management

By closely managing aircraft speed to close to optimum speed, a pilot can assure a more efficient use of power and thus minimizes fuel consumption. Airspeed indicators should be used when establishing cruise since Mach meters tend to read low. This may, in turn, result in flying at a faster speed than desired and thus in increased fuel consumption. The impact of flying faster than optimum cruise Mach number is discussed in Subsection 4.3.1.3. under instrument calibration. Another recommended technique for speed management is to allow the aircraft to bracket the desired airspeed by $\pm .01$ Mach (3 KIAS) rather than making frequent throttle adjustments to be precisely on speed. In order to keep constant speed during a constant altitude cruise, thrust required is equal to drag. However as the aircraft consumes fuel its weight, and thus drag, decrease. Thus a precise speed regulation will require a continuous adjustment in throttle setting. However, the desired throttle setting can only be obtained within certain tolerances. Thus a precise regulation of cruise speed implies an constant movement of throttle control, which is not a practical procedure. Also, the accuracy of airspeed measurement is $\pm .01$ Mach and, thus aircraft speed can only be adjusted to within that accuracy. Moreover, increase in fuel consumption due to flying off optimum cruise speed by $\pm .01$ Mach is approximately 0.2% which is not significant. Therefore, from a practical point of view, aircraft speed may be allowed to drift within $\pm .01$ Mach of the optimum cruise Mach number.

4.2.4 Precision Navigation

The ability of an aircraft to fly an optimized flight path is really the determinate of mission efficiency in terms of distance versus fuel consumed. The ability to precisely follow a prescribed routing is a major contributor to this efficiency. MAC has conducted extensive testing which showed that the current navigational capability of the C-141 is in the area of ± 7 nautical miles (nm), while with the added capability of inertial or Omega navigation systems, an accuracy of better than ± 2.5 nm can be expected [20].

In addition to the benefits of improved accuracy with precise navigation capability the aircraft can take advantage of the ATC Area Navigation (RNAV) procedure. Use of RNAV permits flying of direct routes between preselected points rather than having to fly along selected airways. This capability allows a reduction in actual distance flown and attendant fuel savings.

There are several efforts under way to provide improved navigation capabilities for the aircraft under study. A C-141 OT&E program is being conducted by MAC and extensive LCC analysis has been completed for B-52 and KC-135 aircraft [21]. The primary contribution to fuel conservation of precise navigation capability is the ability to fly optimal routes with the least possible deviations from the planned track.

Fuel savings attendant with precision navigation are evaluated by estimating the reduction in actual distance flown. The reduction in actual distances depends upon the route in question, but in general extensive fuel savings using this approach are not possible [22].

4.3 ANALYSIS OF GROUND OPERATIONS

This section deals with those techniques where savings may be effected by altering aircraft operations on the ground. These operations include aircraft and engine maintenance, instrument calibration, reduced engine warm-up and taxi time, improved cargo loading procedures which result in moving aircraft, c.g. to an aft position, and computerized flight planning. Although analysis of fuel savings due to reduced reserve fuel requires trajectory simulation the procedure itself is basically a ground procedure and is therefore described in this subsection.

4.3.1 Maintenance

Improved maintenance procedures which result in fuel conservation are described below.

4.3.1.1 Maintenance to Reduce Drag

One of the easier ways of reducing fuel consumption is through careful maintenance of the aerodynamically important parts of the aircraft. The areas to be considered are aircraft surface irregularities, control surface rigging, and seal leakages. Surface irregularities which have the greatest adverse effect on airplane fuel consumption are poor fit of doors and radomes, surface mismatch, rough points, rough external skin patches, dents and unfilled or overfilled skin gaps.

In evaluating the effect of skin irregularities, the following example is provided: a 10 square foot patch of rough paint (.0015 inches high) on a Boeing 707 upper wing critical area will waste 18.5 lbs/hr [23]. Another way to look at it is to consider the fact that a minor skin imperfection that creates just one pound of drag on a C-141 will increase fuel flow by approximately 0.5 pounds per hour [24].

In order to provide a measure of the importance of control surface rigging the following examples are given. A 1° sideslip on a Boeing 707, caused by misrigged controls, costs 85 lbs of fuel per hour. On the same aircraft, a single spoiler floating 1 inch at the trailing edge, will result in 17 lb/hr of additional fuel flow [23]. Attention should also be given to unnecessary down rigged flaps, and both up and down rigged ailerons and elevators.

Aerodynamic seals prevent air in a high pressure region or within an aerodynamic surface from leaking to areas of lower pressure thus disturbing airflow along the surface. Aerodynamic seals particularly along the wing leading edge and trailing edge flap cavities must be preserved.

Effective sealing of the pressurized compartment is important in preventing drag increases. Cabin air exiting through excessive gaps in door or window seals can disturb air flow along the fuselage to the point of air flow separation.

A direct quantification of savings due to aircraft maintenance for drag reduction is not possible due to the variables and uncertainties involved. During field visits the observed aircraft appeared to be in a good state of maintenance in regard to surface irregularities and control surface rigging. A continued emphasis on maintaining high degree of aerodynamic cleanliness is required. Discussions with maintenance and operations personnel have indicated that there may be some problems with pressurization losses. This would appear to be an area of potential savings and worthy of further investigation.

Fuel/DOC savings due to aircraft maintenance which reduces drag are portrayed in terms of the sensitivity of fuel/DOC to reduction in zero lift drag. These savings are obtained from the sensitivity results which were averaged over the mission spectrum data. Thus using Figure 7.1-16, for example, a 1% reduction in zero-lift drag due to aircraft maintenance amounts to 0.7% reduction in annual fuel consumption for the C-141 aircraft.

4.3.3.2 Engine Maintenance

Degradation of engine TSFC can significantly increase fuel consumption. There are several areas within the engine that can contribute to an increase in TSFC. As the time in service is extended, deterioration in TSFC can occur due to dirt buildup on the blades and vanes, erosion of airfoils and/or seals and high temperature effects in the turbine. Scheduled maintenance procedures improve engine fuel efficiency to some degree. Periodic engine cleaning by water wash, parts replacement and various functional and leakage checks are obvious procedures [25]. The deterioration of engine TSFC on J-57 and TF-33 engines between overhauls is between 3 - 6%.

During overhaul, only approximately one half of this loss is restored. Because of parts replacements over a series of overhauls the average engine performance level has deteriorated 5% from the original level [26]. A specific approach to reducing engine deterioration at the operating units is an engine trending technique used by the airlines. SAC has done considerable work in this area and has their entire KC-135 fleet participating in an Engine

Inflight Monitoring System [27]. It is believed that a better understanding of engine component deterioration and revised maintenance procedures to incorporate more fuel efficient components could result in 1-3% fuel savings [28].

United Airlines developed a procedure which uses flight crew data recorded in stabilized flight as an indication of engine out-of-trim condition. Throttle mismatch at a given engine operating condition has been found to be a valid indicator of the need for engine trimming. This data is then used as the basis for adjusting engine fuel control, followed by a throttle system rig check and idle run. This procedure is used after engine installation, fuel control change or whenever a throttle alignment discrepancy is written up. In the first two cases, the test cell engine trim and fuel control calibration are adequate for the first flight, after which a partial trim is performed if required. A takeoff power check is made prior to the first flight. A savings of between 370 and 600 gallons per trim has been experienced using this procedure [29], not including those instances when no trim at all is required. It is cautioned however that fuel economy trim procedures may have adverse side effects related to engine operation [30].

Fuel savings can also be realized by reducing engine and auxiliary power unit operation during maintenance. Commercial power or ground power units may be used to provide electric power for maintenance when the airplane is on the ground. Fuel/DOC savings due to improved maintenance procedures is presented in terms of sensitivity of fuel/DOC to improvements in TSFC due to these revised maintenance procedures. Thus using Figure 7.1-18, for example, a 1.5% improvement in TSFC results in 1.4% reduction in annual fuel cost for the C-141 aircraft.

4.3.1.3 Instrument Calibration

The need to keep instruments within calibration tolerances can be seen when considering the cost in fuel due to instrument errors. Speed measuring instruments have the most significant impact on fuel usage. Use of inaccurate speed indication (whether Mach or KIAS) for maintaining desired cruise

speeds has the same effect as deliberately flying faster or slower than the intended speed. To evaluate the impact of flying off speed for minimum fuel cruise, the sensitivity results given in Section 7 can be used for the aircraft under study. The impact of flying off speed depends upon the desired speed itself. If the desired speed is higher than the minimum fuel speed, an error in speed indication may result in flying slower than desired and thus result in fuel savings. Accuracy of speed indicators is generally within $\pm .01$ Mach. The fuel penalty for the aircraft under study due to $\pm .01$ Mach error in speed indicators is about .2% at minimum fuel flight conditions. Because of the impact of flying off speed, it is suggested that Mach and airspeed indicators be crosschecked frequently in flight.

Fuel consumed during a minimum fuel flight is less sensitive to flying off altitude. Section 6 describes the sensitivity of fuel consumed to errors in optimum cruise altitudes and these sensitivity results are given in Section 7 for each of the aircraft under study. The accuracy of an altimeter varies with pressure altitude, the tolerance being higher at higher altitudes. The maximum altitude tolerance for the aircraft under study is ± 250 feet. From the sensitivity results given in Section 7 it is seen that the increase in fuel consumed due to altimeter errors is within 0.1%.

It appeared during field trips that base level maintenance of instrument systems was good. There may be some problems with fuel quantity indications which could result in aircraft carrying more fuel than necessary. This has its own penalty, and is discussed in Section 4.3.6. It may also result in flying off optimum cruise altitude due to an error in aircraft weight estimation. However, fuel consumed in minimum fuel cruise is not very sensitive to W/δ as is shown in Section 6. Thus an error in aircraft weight estimation does not increase the fuel consumption significantly.

4.3.2 Ground Handling

Fuel consumed during ground handling depends on many factors: engine starting methods and warm-up time, taxi distance and the terrain on which the taxi is made, aircraft weight and the tire pressure. The following ground handling measures result in fuel/DOC savings.

4.3.2.1 Reducing Engine Use and Taxi Time

The use of external power instead of aircraft engine or aircraft auxiliary power units will result in fuel savings. In nearly every case the use of an electrical power cart or external air source will save fuel. There are times when the unavailability of maintenance manpower or the lack of equipment will make it necessary to use aircraft systems. An even greater savings is available if the Air Force were to connect to Diesel ground power units [31].

Engine starts should be delayed as long as possible and traffic control delays should be absorbed at the gate or in a specific area where the engines can be shut down. Auxiliary power units should be shut down as soon as possible after engine start. A minimum warm-up time should be used. Taxi distances should be shortened if possible by taking the shortest route available to the runway/ramp. The use of intersections for take-off where sufficient runway is available can reduce taxi time and in addition decrease airfield congestion and associated ATC delays. This concept would probably not be generally applicable to the B-52 and KC-135 because the majority of their missions depart at high gross weights. Furthermore, the C-5 should probably not participate if higher take-off power settings are required because of structural considerations.

Fuel/DOC savings due to improved ground handling procedures which reduce engine use and taxi time varies from mission to mission due to variations in starting methods, fuel flow rate while taxiing or idling, taxi distance and terrain, and aircraft fuel load and payload. An average fuel flow rate is assumed over the spectrum of missions for each aircraft under study and fuel savings are evaluated in terms of an average reduction of taxi time for the entire fleet. For

example, average fuel flow rate during ground operations for the C-141 is 15.4 gallons/minute and during 1976, 81,000 sorties were flown by C-141. Based on these figures every minute of reduced taxi time results in a fuel savings of 1.25 million gallons annually for the C-141 fleet.

4.3.2.2 Partial Engine Taxi

It is possible that the shutting down of two engines (four for B-52s) for taxi-in and parking is an acceptable means of reducing fuel consumption. This operational procedure can amount to significant fuel savings. For example, two-engine taxi for an average five minute taxi time can save about 3.12 million gallons of fuel annually for the C-141 fleet.

4.3.3 Removing Excess Equipment

Fuel mileage of an aircraft flying in a given set of altitude, temperature and speed conditions is a direct function of airplane gross weight. The higher the weight, the greater the fuel required to fly a given distance. Thus carrying of excess equipment causes the burning of additional fuel to carry that weight. Removal of equipment not required for a specific mission (e.g., galley, oven, over-water gear, tie down chains, etc.) appears to have substantial merit. By comparing the manhours required for removal and replacement of the equipment with the dollar value of savings, the advisability of taking that action can be assessed. However, it should be noted that the removal of excess equipment can present logistic problems which may be a significant drawback for military applications. Of course, other considerations such as aircraft downtime required and frequency of type mission changes also enter the decision process. An estimate of fuel/DOC savings due to removal of excess equipment for each aircraft under study was obtained by assuming an average reduction in operational empty weight (OEW) of aircraft for a spectrum of aircraft missions. Then the mission spectrum analysis program was used to evaluate annual fuel/DOC savings due to reduced excess equipment for an aircraft fleet. Reference [32] indicates that 6477 pounds maximum weight reduction is possible for C-141 aircraft. Out of the 6477 pounds only 282 pounds weight reduction is possible for all missions and the remaining

6195 pounds is mission oriented equipment. Assuming an average weight reduction of 2000 pounds for each C-141 due to removal of excess equipment, a 4.2 million gallon annual savings in fuel consumed is possible for the C-141 aircraft fleet.

For a specified mission flying under optimum cruise conditions, savings in fuel consumption due to removal of excess equipment can be obtained analytically. From Appendix A

$$R = RF \log \frac{W_i}{W_f} \quad (4.1)$$

where

R, RF, W_i and W_f are specified mission range, range factor, takeoff gross weight and landing weight respectively. Expressing W_i as

$$W_i = W_f + F \quad (4.2)$$

where F is fuel consumed during the mission, and differentiating Eq. (4.1) results in

$$\frac{dF}{F} = \frac{dW_f}{W_f} \quad (4.3)$$

Thus the savings in fuel is proportional to the reduction in landing weight. Assuming 200,000 pounds average landing weight for C-141, a 2000 pounds average reduction in excess equipment results in 1% savings in fuel consumed.

Differentiation of equation (4.1) also results in

$$dW_i = dW_f e^{R/RF} \quad (4.4)$$

If R/RF is small equation (4.4) may be written as

$$dW_i = dW_f [1 + R/RF] \quad (4.5)$$

Equation (4.5) expresses the reduction in TOGW due to removal of excess weight. Reduction in TOGW is equal to the reduction in excess equipment plus the savings in fuel as a result of reduced aircraft weight along the mission. Note that the reduction in TOGW is a function of mission range. Thus the longer the mission, the higher are the savings in fuel due to removal of excess weight.

4.3.4 Cargo Loading

As discussed in Subsection 4.2.1, the operation of aircraft with the center of gravity (c.g.) further aft than those now being used and as near the aft limit as possible can result in fuel savings. Aft c.g. operations would require the loading to be done in the aft c.g. regions of the aircraft. Aft c.g. operations seem most appropriate for cargo aircraft because of the ability to influence the c.g. by cargo load distribution. Thus, this procedure is applicable to C-141, C-5 and C-130E aircraft. A quantitative estimate of fuel savings due to aft c.g. operations requires an in-depth study of the aircraft weight and balance distribution due to improved loading procedures. In the case of the C-141 aircraft such a study has been performed that indicates a potential savings of 1% for cargo missions [33]. The analysis described in Subsection 4.2.1 is used to obtain estimates for the C-130E and C-5 aircraft.

4.3.5 Computerized Flight Planning

Flight plan optimization with respect to fuel consumption can contribute to fuel savings. Certain wind patterns may make it more economical to fly indirect routes or suboptimal altitudes in order to minimize the net fuel consumption for an entire mission. Atmospheric temperatures which are colder than standard have the effect of increasing the cruise altitude ceiling. Cruising at higher altitudes in turn may reduce fuel consumption for aircraft constrained by cruise ceiling such as the C-5 and C-130E. Thus sometimes it may pay to fly indirect routes through colder air masses. The flight plan should be optimized while taking into account the relevant meteorological data. Current Air Force flight

planning is accomplished through a combined manual/computer system. There are flight planners assigned at both the 21st Air Force, McGuire Air Force Base, New Jersey, and at the 22nd Air Force, Travis Air Force Base, California. These planners input numerous standard flight plans and receive a "time and route" bulletin. The flight planners determine the best routes and altitude, within the constraints resulting from weather factors such as storms and winds, and air traffic control limitations. The minimum time route is selected, the estimated aircraft gross weight on a specific mission is determined and a flight plan is then ordered approximately three hours before departure time.

This system is working very well; however, as fuel considerations become more and more important, additional sophistication could yield substantial improvements in mission efficiency. The Military Airlift Command and Air Force Weather Service are deeply involved in efforts to upgrade the computerized flight planning system. Any approach to provide real time selection of flight path, altitude, airspeed and fuel required to take advantage of meteorological factors and aircraft performance characteristics, would provide significant improvement. Also instead of minimum time routes, minimum fuel/DOC routes would provide additional savings. The specific savings is unknown, but it depends upon the capability of the computerized flight planning system to upgrade the plan in real time and the capability of an aircraft and the ability of a pilot or automatic flight system to follow the optimum flight plan.

4.3.6 Reduced Reserve Fuel

The landing fuel data obtained from the ASIMIS tapes for C-141, C-5, C-130E and KC-135 aircraft (no data is available for B-52's) indicates that the reserve fuel carried by these aircraft is much higher than required. Since it takes fuel to carry fuel, savings can be realized by reducing the reserve fuel to requirements. Reference [34] outlines the reserve fuel requirements for MAC operations. The following briefly describes these requirements.

- En Route Reserve - - An en route fuel reserve consisting of 10 percent of flight time over a route is required only when radio aids to navigation, excluding Loran, aircraft radar and DME, are inadequate to determine aircraft position accurately once an hour. This 10% is not to exceed the fuel required to fly one hour at normal cruise.
- Approach and Missed Approach at Original Destination - - Additional fuel is added to accomplish a penetration/en route descent, approach and missed approach at original destination when forecast ceiling is less than ceiling value.
- Destination to Alternate - - Fuel from overhead destination/initial penetration altitude to alternate is required.
- Holding - - Holding fuel is computed at maximum endurance speed plus 10 KCAS at predicted gross weight over the destination or alternate as appropriate (except the C-130's will use fuel flow at terminal cruise altitude and airspeed). Holding time for turbo jets is 45 minutes and for others 1 hour and 15 minutes. Similar requirements exist for SAC aircraft operation.

In determining reserve fuel requirements in this study it is assumed that an alternate is available within 200 nm. of the original destination. Generally an alternate airfield within 200 nm. of original destination is available within the United States and for most of the overseas operations with the exception of some overseas islands like the Azores, Goose Bay near Labrador and the Phillipine Islands.

The aircraft under study have adequate navigational equipment, thus en route reserve fuel may not be required. Also the fuel required for missed approach at the original destination has been neglected in this study. Here it is assumed that aircraft is carrying extra fuel for an alternate destination. If the aircraft lands at the original destination, it has an extra amount of fuel which can be used in case of missed approach. Holding time requirements appear excessive especially when an alternate is available.

Fuel savings due to reducing reserve fuel are determined in this study by successively relaxing each of the components that make up the reserve fuel requirements. In the first case, the reserve fuel requirements include fuel required for 200 nm. alternate plus en route reserve plus fuel required for maximum holding time. For the next case, en route reserve fuel is not considered. Then holding time requirements are evaluated by successive one-half hour segment reductions from the original stated requirement (e.g. 1 1/4 hrs., 3/4 hr., 1/4 hr.). Finally the reserve fuel requirements for only a 200 nm. alternate are evaluated. Once the reserve fuel requirements for each option have been determined, take-off fuel is adjusted such that when the mission is simulated again the landing fuel is equal to the required reserve fuel. For example, Table 7.1-10 summarizes the fuel and direct operating cost savings for the C-141 estimated by reducing the reserve fuel to the requirements established by the four options listed in column one of this table. Actual landing fuel for each mission type obtained from the ASIMIS tapes is shown in the C-141 histograms given in Subsection 7.1.2. From Table 7.1-10 note that 3.7% fuel savings can be achieved by reducing the reserve fuel to maximum requirements which include fuel for 200 nm. alternate, 45 minute holding time and en route reserve. However fuel savings increase to 5.7% if reserve fuel requirements are relaxed such that reserve fuel is required only for a 200 nm. alternate.

4.3.7 Alternate Fuel: Use of JP-8 Fuel

The fuel currently in general use by the Air Force is grade JP-4. Grade JP-5 is in limited Air Force use such as in "Air Force One" because of its high density and high temperature flash point. The Navy uses JP-5 for all jet aircraft shipboard operations. There are other fuels, as well as JP-5 that offer savings in terms of volume consumed because of their higher density. Table 4.3-1 provides comparison data between JP-4 and three alternate fuels.

In order to determine the relationship of a fuel's density to its rate of consumption, the following equation can be applied:

$$T = k \frac{V \cdot D}{R}$$

where

- T = length of time an engine can run on a given volume of fuel
- R = rate of fuel consumption at a given power setting measured in terms of weight per time
- D = density of a fuel measured in terms of weight per volume
- V = volume of fuel
- k = constant relating the equation to the operating parameters of a given engine

This equation assumes that the various fuels are equal in terms of energy content per pound. It can be seen that as the density increases, the run time increases for a given power setting and volume. Conversely for a given run time, if the power setting remains constant, then the volume of fuel required will decrease as the density increases.

Table 4.3-1 JET FUEL DATA

Grade	Type	Specific Gravity grams/cc (Max-Min @60°F)	Freeze Point C°	Average Heating Value BTUs/lb.	Flash Point
JP-4	Wide Cut gasoline	.802 - .751	-57	18,600	-20°F
JP-5	kerosene	.845 - .788	-46	18,500	140°F
Comm- ercial					
Jet A-1	kerosene	.830 - .775	-50	18,500	100°F
JP-8 **	kerosene	.830 - .775	-50	18,500	100°F

*High content of Butanes and Pentanes is reason for low flash point.

**Proposed fuel, chemically identical to Jet A-1.

It appears that the higher freeze point of the kerosene based fuels would have little impact on mission performance of most Air Force aircraft. In general terms, after 5 or 6 hours of flight, regardless of fuel temperature at takeoff, the temperature of aircraft fuel may be assumed to be equal to the indicated free air temperature. The indicated free air temperature in flight is several degrees warmer than the true outside air temperature because of the airspeed ram effect.

For example, at a true temperature of -40°C and a speed of MACH 0.8, the indicated free air temperature would be -15°C [15]. It follows that after cold soaking on the ground, fuel could reach the indicated free air temperature much sooner than the 5 or 6 hours, effectively restricting cruise altitude to a level at which the indicated temperature is above the freeze point.

It should be noted that in a standard atmosphere the true outside air temperature (OAT) at 37,000 feet and above, is -56°C . In addition, during engine start on the ground, at ambient air temperatures below -30°C , and engine start inflight at low temperatures, difficulty in obtaining engine light-off may be experienced. The incorporation of a higher energy ignition source, such as what the Navy uses in their aircraft, would improve both ground starting and the altitude relight capability.

The current (1978) price of the four grades of fuel listed in Table 4.3-1 is approximately 42 cents per gallon. The price varies on a day-to-day, and region-to-region basis, but there is very little difference in cost between the four grades. In addition, the slightly lower heating value of the kerosene type fuels is insignificant in terms of engine power output. Consequently, JP-5 would appear to be the optimum choice of available fuels because it has both the highest density and the highest flash point. However, JP-5 draws on very select crude oils which restrict its availability to a level inadequate to satisfy the Air Force's needs [35]. The use of JP-8 appears to be a logical compromise in terms of safety and density, and it is available in the quantities required. Theoretically,

a savings in fuel of approximately 3.3% could be realized, based on a mid-point comparison of the specific gravities. For the aircraft under study 3.3% savings in full amounts to 57.2 million gallons reduction in annual fuel consumption.*

*

In an effort toward standardization with NATO the U.S. Air Force will be shifting from JP-4 to JP-8 at its bases in Britain effective May 1978 [Aviation Week, April 10, 1978].

SECTION 5

ANALYSIS APPROACH AND DEFINITION OF DESIGN MODIFICATIONS THAT CONSERVE FUEL

New advances are being made in all areas of aeronautical technology to design and develop fuel efficient aircraft and improve the existing ones. This section presents the analysis approach for determining the benefits that may accrue from design modifications peculiar to the aircraft types under study.

Any parametric, hypothetical change considered should be realistic. Because of the highly coupled effects of almost any parameter change upon other parameters (such as operational empty weight), a viable design modification should take into account these coupled effects. A rigorous design analysis was not performed in this study. Instead, the fuel and DOC savings impact of parametric changes were treated independently. Thus the user of the results can account for all effects (positive and negative) of specific proposed design changes. The unique advantage to the parametric approach provided here is that the fuel and DOC computations will be based on the actual mission spectrum for each aircraft type, instead of a typical or hypothetical mission profile which may not be representative of how the Air Force actually flies its missions. This was accomplished by using the mission spectrum analysis program described in Section 3.8, and by using the mission spectrum profiles obtained by processing the ASIMIS tape data. The effect of winglet additions and re-engining of the C-141 and the KC-135 are separately examined in Sections 7.1 and 7.6. In particular, it was found that winglet additions for the current mission spectrum results in approximately 3% savings in fuel consumption for each aircraft. However, a recent Boeing report [36] predicts a potential improvement of 8% in range factor under optimum cruise-climb flight conditions which may result in a 7.8% savings in fuel consumption. The difference in savings is due to the difference in how the Air Force actually flies its missions and the optimal cruise-climb solution.

An alternative analytical approach for developing a relationship between aircraft parameter variations and aircraft range factor is derived in Appendix C. A

calculation of % improvement that results from retrofitting winglets on the KC-135 is carried out that shows a potential savings of approximately 8% at optimum cruise conditions.

5.1 PARAMETRIC ANALYSIS OF AERODYNAMIC DESIGN CHANGES

For an existing Air Force inventory aircraft any aerodynamic design modification which results in radical changes in aircraft structure does not appear to be cost effective. Thus, for example, replacing an existing wing with an advanced supercritical airfoil is not considered a viable design modification. Winglets (vortex diffusers) on the other hand offer potential fuel savings without radical structural changes. In general, any aerodynamic design change may be represented as a change in aerodynamic parameters and operational empty weight. After determining these first order effects of a design modification the fuel savings due to a proposed design modification could be evaluated using the mission spectrum analysis program described in Section 3. However, there are always uncertainties involved in any potential design modification. Thus evaluation of a design modification will require a repeated use of the mission spectrum analysis program to reflect those uncertainties. An alternative approach, which is taken in this study, involves parametric analysis of aerodynamic design changes. Aircraft zero lift drag and induced drag parameters are varied between $\pm 15\%$ of the baseline values, in increments of 5% change in the aerodynamic parameters. The mission spectrum analysis program was used to obtain the corresponding change in fuel cost and DOC. Thus generic plots of percentage variation in cost as a function of % variation in zero lift drag and induced drag are generated for each aircraft under study. In order to account for the change in aircraft OEW due to a design modification, generic plots representing variation in fuel cost and DOC as a function of the variation in aircraft weight were also generated. For example Figures 7.1-17, 7.1-18, 7.1-20 represent % variation in fuel cost and DOC as a function of % variation in zero lift drag, induced drag and change in aircraft weight for the total spectrum of C-141 missions. These plots can be used to evaluate the first order effects of any aerodynamic design modification.

As an example consider the winglet design for C-141 aircraft. Reference [36] indicates that a winglet design for C-141 will result in 1.5% reduction in zero lift drag and 11.0% reduction in induced drag for that aircraft. Also aircraft operational empty weight will increase by approximately 700 lbs. From Figure 7.1-17 a 1.5% reduction in zero lift drag will result in 1.05% saving in fuel cost. Fuel savings due to 11% reduction in induced drag obtained from Figure 7.1-18 are 1.77%. Increase in operational empty weight due to winglets amounts to .14% increase in fuel cost. Thus the total fuel savings due to retrofitting the C-141 fleet with winglets obtained by summing up savings and losses due to the individual parameter changes is 2.68%. Note that these generic plots have been generated using a spectrum of missions obtained from the ASIMIS tapes. Thus the fuel saving results are based on the current operational usage for the entire fleet of a specific aircraft type.

5.2 PARAMETRIC ANALYSIS OF PROPULSION DESIGN CHANGES

Retrofitting engines on an existing aircraft involves a detailed analysis of inlet design, engine and supporting structure weight change and its effect on wing bending and torsion moments, etc. A proper matching of aerodynamics and propulsion is required. For most existing engines, specific fuel consumption and thrust data at various altitudes and speeds is available and this data can be used in the mission spectrum analysis program to evaluate a propulsion plant modification. Uninstalled engine weight data is also available. However, changes in aircraft OEW due to changes in the propulsion plant is still required. Another approach for evaluating propulsion modifications is similar to the one for aerodynamic modifications. Specific fuel consumption for the existing engines is varied $\pm 15\%$ of the baseline value at 5% intervals, and corresponding values of variations in fuel cost and DOC are obtained using the mission spectrum analysis program. The generic plot of % change in fuel cost and DOC as a function of % change in SFC (see for example Figure 7.1-19), and the previously mentioned plot of % change in fuel cost and DOC as a function of change in aircraft weight (See for example Figure 7.1-20) are used to evaluate any propulsion design modifications for the given aircraft type.

Another aspect of design modification evaluation involves associated acquisition cost and maintenance considerations. Figure 5.2-1 illustrates a "breakeven" analysis presentation of acquisition and maintenance cost. Accumulated costs with and without design modifications are first determined after adjustment for inflationary factors. The total period of time should cover the life expectancy of the aircraft. The acquisition cost then establishes the breakeven point in time (T_{BE}). Hence, the total curve represents the functional relationship between T_{BE} and acquisition cost. This type of curve is particularly useful when acquisition and maintenance costs are not precisely known.

5.3 DATA SOURCES

There are only a few specific fuel conservative design modifications being considered for the aircraft under study. These include reengining the C-141 and KC-135 aircraft with more fuel efficient engines and retrofitting winglets on KC-135 and C-141 aircraft. These design modifications are evaluated in detail in Sections 7.1 and 7.6. Data required for this evaluation was obtained from the following sources.

5.3.1 Data Required for Reengining Studies

It has been suggested that the C-141 be reengined to take advantage of the greatly improved performance of the latest technology high by-pass turbo-fan engines. By replacing the currently installed TF-33-P7 with the TF-39 on a 2- for -1 basis, a 25% reduction in specific fuel consumption is predicted [37]. In considering the TF-39 engine there is the obvious advantage in that the engine is already developed and non-recurring development costs do not have to be expanded. Since the C-5A aircraft under study is powered by TF-39 engines, installed engine thrust and fuel flow models for the C-5A may be used for the C-141 reengining study. Although installation losses will be different for the C-141, as a first order approximation, the C-5A propulsion model will be adequate for this study. Engine weight information was obtained from Reference [38]. Several alternatives for reengining the KC-135 have been studied. The replacement of all four J-57s by two TF-39s

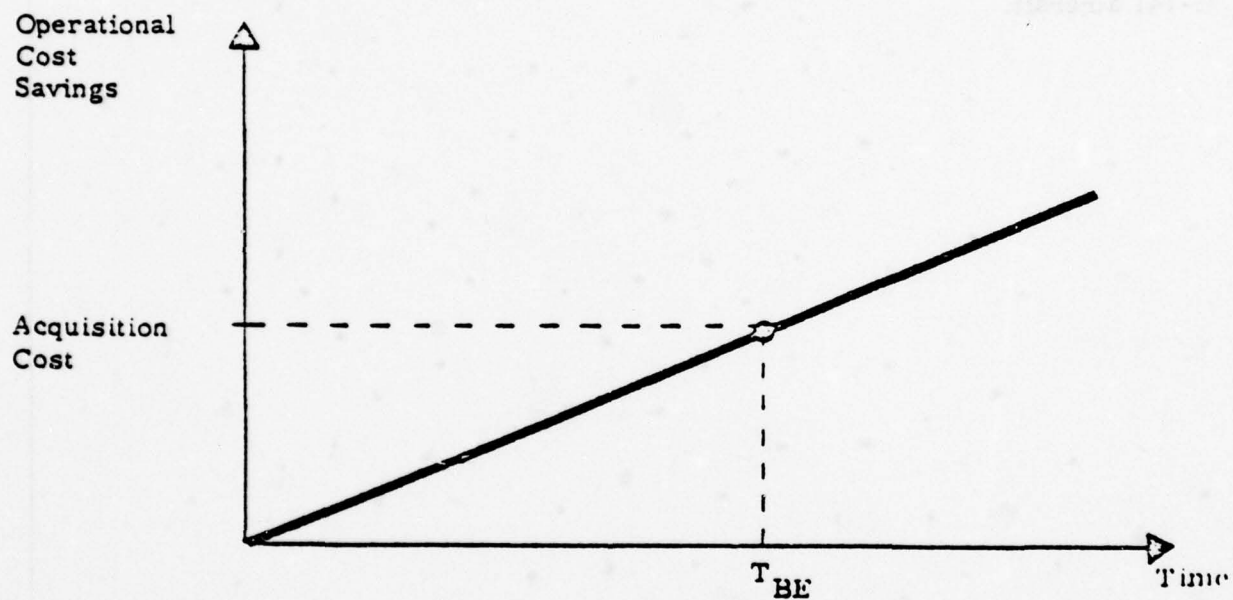
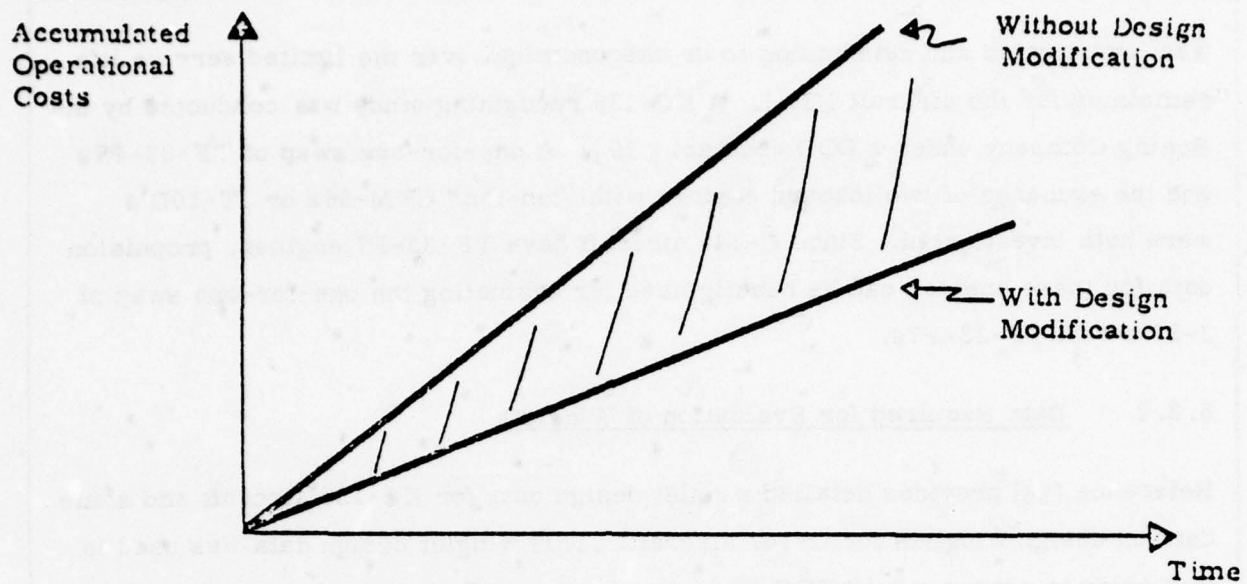


Figure 5.2-1 Illustration of a Break-Even Analysis Presentation of Acquisition and Maintenance Cost

was investigated and determined to be uneconomical over the limited service life remaining for the aircraft [37]. A KC-135 reengining study was conducted by the Boeing Company under a DOD contract [39]. A one-for-one swap of TF-33-P7s and the exchange of two inboard engines with "ten-ton" CFM-56s or JT-10D's were both investigated. Since C-141 aircraft have TF-33-P7 engines, propulsion data for these engines can be readily used for evaluating the one-for-one swap of J-57's with TF-33-P7s.

5.3.2 Data Required for Evaluation of Winglets

Reference [36] provides detailed winglet design data for KC-135 aircraft and some data on design winglets for C-141 aircraft. This winglet design data was used in this study to estimate fuel/DOC savings due to retrofitting winglets on KC-135 and C-141 aircraft.

SECTION 6

SENSITIVITY ANALYSIS APPROACH

Fuel consumption and DOC for a specified mission can vary from day to day and are different for two aircraft of the same type. This is due to changes in environmental conditions, differences between like aircraft, instrumentation errors, etc. Thus a sensitivity analysis is required to predict the first order changes in fuel consumption and DOC due to these uncertainties. Also, there may be uncertainties in improvements in performance/DOC due to design changes; sensitivity results are required as a function of possible improvements. The following describes the sensitivity studies for the aircraft under study.

6.1 UNCERTAINTIES IN AIRCRAFT PARAMETERS

The sensitivity of fuel consumption and DOC have been determined for variations in aerodynamics, engine performance and system weight. Aerodynamic and propulsion math models have been developed to represent the existing aircraft. These are described in Section 3.2. Sensitivity to variations in zero-lift drag, induced drag, fuel flow rate and system weight are determined for best cruise performance by varying the math model coefficients about their nominal values. Analytical functional relationships derived in Appendix C were used to obtain sensitivity of performance/DOC to variation in aerodynamic parameters, fuel flow rate and the system weight.

6.1.1 Sensitivity to Zero-Lift Drag

An increase in zero-lift drag coefficient results in an increase in fuel consumed to accomplish a mission. From Eq. C.17, Appendix C, it can be seen that an increase in C_{D_0} results in an increase in optimum cruise altitude. Variations in C_{D_0} do not cause significant change in optimum mach. If the coefficient B in the drag

model of Section 3.2 is assumed to be zero then Equation (C.18) implies that a 10% increase in C_{D_0} will result in a 5% decrease in range factor. However for the aircraft under study the decrease in range factor is close to 6.7% because the coefficient B is not zero and zero-lift drag is almost two-thirds of total drag at optimum cruise conditions.

6.1.2 Sensitivity to Induced Drag

An increase in induced drag coefficient also results in increased fuel consumption for a given mission. However the impact of variations in induced drag coefficient on optimum altitude is opposite to that of C_{D_0} . From equation (C.17) an increase in induced drag coefficient K implies a decrease in optimum cruise altitude. Again variations in induced drag coefficient do not change optimum Mach significantly. For most of the aircraft under study a 10% increase in induced drag results in approximately 3.3% decrease in range factor under optimum cruise conditions.

6.1.3 Sensitivity to Fuel Flow Rate

A uniform increase in fuel flow rate across all the operating conditions does not have any impact on optimum cruise conditions except that an increase in fuel flow rate results in a decrease in range factor and thus an increase in fuel required to accomplish a specified mission. Equation (C.25) can be used to derive the sensitivity of fuel consumed to variation in fuel flow rate. If mission range R and take-off gross weight remain constant, then from Equation (C.25)

$$\frac{dF}{F} = - \frac{dRF}{RF} \left[\frac{R}{RF} \frac{1}{e^{R/RF} - 1} \right]$$

which may be approximated by

$$\frac{dF}{F} = - \frac{dRF}{RF} \left[1 - .5 \frac{R}{RF} \right] \quad (6.1)$$

where F is the fuel consumed and RF is the range factor.

Equation (6.1) gives the sensitivity of fuel consumed for a variation in range factor as a function of aircraft range. For small values of $\frac{R}{RF}$ the difference between the exact solution and the approximate expression in Eq. (6.1) is very small. For example, for a 3000 nm. mission for the C-141 aircraft, a 10% increase in fuel flow rate amounts to an 8.46% increase in fuel consumed from the exact expression and an 8.37% increase from the approximate expression. However if it is known before hand that the zero-lift drag coefficient of a particular aircraft is less than nominal value, take-off fuel weight may be reduced accordingly. Assuming that the landing weight remains the same, fuel savings may be estimated using the following approximate expression:

$$\frac{dF}{F} = \frac{dRF}{RF} \left[1 + 0.5 \frac{R}{RF} \right] \quad (6.2)$$

6.1.4 Sensitivity to Weight Variations

An increase in aircraft weight also results in increased fuel consumption for a specified mission. Increase in aircraft weight results in a decrease in optimum cruise altitude; however, the optimum cruise Mach remains constant. Using Eq. (C.24) the increase in fuel consumed due to variations in aircraft initial weight is given by

$$\frac{dF}{F} = \frac{dW_i}{W_i} \quad (6.3)$$

Note that for a given mission this variation is independent of mission range. Variations in fuel consumed due to variations in landing weight may be obtained by the following solution:

$$\frac{dF}{F} = \frac{dW_f}{W_f} \quad (6.4)$$

6.1.5 Sensitivity to Thrust Variations

Variation in maximum thrust T_{\max} (h, M) impact the optimum cruise performance through its effect on the cruise ceiling. So long as the optimum cruise

altitude is not constrained by the cruise ceiling, the variation in T_{max} does not have any effect on the cruise solution. However if an aircraft altitude is constrained by the cruise ceiling (such as for the C-5A and C-130E aircraft), an increase in available power will increase the cruise ceiling. Thus aircraft performance will improve due to increase in cruise altitude. A decrease in T_{max} results in a decrease in cruise ceiling. Thus for the C-5A and C-130E aircraft, whose cruise altitudes are already constrained by cruise ceiling, a decrease in T_{max} further deteriorates the cruise performance. A decrease in cruise ceiling for other aircraft may constrain their optimum cruise altitude and thus degrade their cruise performance. Thus the sensitivity of the cruise solution to variations in T_{max} has been evaluated by determining its impact on cruise ceiling and thus on the optimum cruise altitude. If the optimum cruise altitude is constrained by the cruise ceiling, then the variation in fuel consumed and DOC due to variations in T_{max} are obtained for a typical mission.

Variations in T_{max} (maximum power for the C-130E) impact the climb performance of all aircraft. Sensitivity of climb performance to variations in T_{max} is determined by varying the parameters of the T_{max} model in the mission profile analysis program and simulating the climb profile for a typical mission.

6.2 SENSITIVITY TO ENVIRONMENTAL FACTORS

In this section sensitivity of optimal operational procedures to environmental factors is described and the impact of optimal operational procedures on noise and air pollution is discussed.

6.2.1 Sensitivity to Atmospheric Variations

Atmospheric variations which impact the optimal flight procedures are the deviations in temperature from the 1962 Standard Atmosphere Model and the wind velocities.

6.2.1.1 Temperature Effects

Atmospheric temperatures which are warmer than standard have the effect of decreasing the cruise altitude ceiling. For the C-141, at 300,000 pounds take-off gross weight, a temperature of 10° above standard lowers the cruise ceiling by approximately 1000 feet while a temperature of 20° above standard lowers the cruise ceiling by nearly 3000 feet. From the fuel flow model described in Section 3.2, normalized fuel flow rate (f_n) is independent of temperature; thus actual fuel flow rate (f) which is equal to

$$f = \sqrt{\theta} f_n \quad (6.5)$$

varies as the square root of the temperature. However, the speed of sound, and therefore the true airspeed at constant mach, varies directly with the square root of the temperature. Therefore these two effects would cancel, causing the nautical miles per pound of fuel to be independent of temperature for cruise at a given mach, gross weight and pressure altitude.

Thus temperature affects the cruise fuel consumption as a result of its effect on cruise ceiling. For C-141, KC-135, B-52A and B-52H aircraft, warmer temperatures may constrain their optimum cruise altitude and thus increase the fuel consumption. For C-5A and C-130E aircraft which are already constrained by cruise altitude ceiling, warmer temperatures further lower their cruise altitudes and thus increase the fuel consumed during flight. On the other hand, lower-than-standard temperatures reduce the fuel consumption for the C-5A and C-130E aircraft due to an increase in optimum cruise altitude. For constant mach cruise, mission flight time varies inversely as the square root of the temperature. The following approximate relation may be used to estimate change in mission time for a change in temperature:

$$\frac{dt}{t} = - .5 \frac{d \text{Temp}}{\text{Temp}} \quad (6.6)$$

where t , Temp are the mission time and ambient temperature in absolute units for a standard day. dt and $d \text{Temp}$ are the corresponding variations for a

non-standard day. Deviations in atmospheric temperatures have a big impact on take-off and climb performance. However, changes in total fuel consumption will be negligible.

6.2.1.2 Wind Effects

Atmospheric winds have a large effect on the fuel consumed in flying between two points. However the effect of wind on the optimum cruise conditions, i.e., optimum mach and altitude, is relatively minor. Head winds and tail winds cause a small shift in optimum cruise mach. Figure 6.2-1 illustrates the fuel consumption per hour for an aircraft at a given altitude as a function of mach number. A tangent line to the curve from the origin will define the mach number (M_1) which provides minimum fuel consumption per air mile. Minimum fuel per ground mile for a given wind condition can be obtained by shifting the horizontal scale by an amount equal to the wind speed. The resulting tangent line on Figure 6.2-1 is for a head wind and defines M_2 . It is apparent that, because of the shape of the curve, the optimum mach number increases from its nominal value for a head wind and reduces for a tail wind.

6.2.2 Sensitivity to Traffic Density

Delays in take-off and landing time schedules at a particular airport depend to a large extent on the amount of air traffic near that airport. For example, the possibility of delay in take-off/landing time at JFK airport is much higher than at Bangor, Maine. Since delays in take-off/landing times result in increased fuel consumption /DOC, air traffic density has an impact on fuel conservation. In this subsection the approach to the sensitivity analysis of fuel/DOC to variations in air traffic is presented.

6.2.2.1 Impact on Holding Time

If the number of aircraft waiting to land at a particular airport increases, it results in an increase in holding time for the newly arriving aircraft and thus in an increase in fuel consumption and DOC. This implies that the impact of air traffic density on fuel cost/DOC can be expressed in terms of sensitivity of fuel/DOC to variations in holding time. Therefore, the sensitivity analysis is

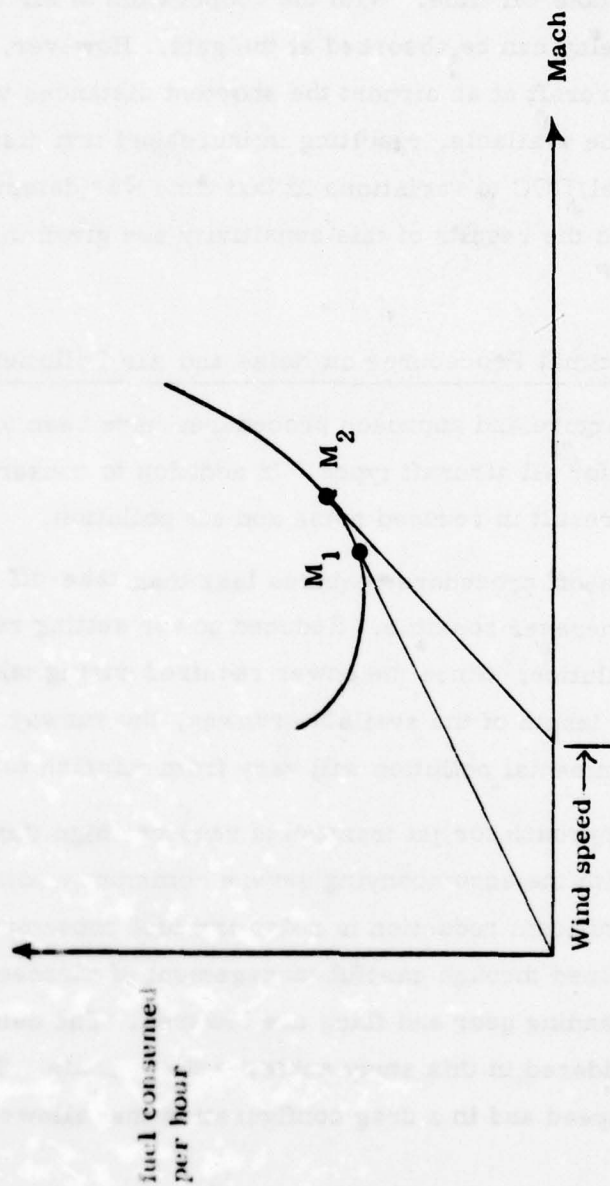


Figure 6.2-1 Effect of Wind on Optimum Cruise Mach Number

conducted to determine the variation in fuel/DOC due to variations in holding for each aircraft under study.

6.2.2.2 Impact on Taxi Time

If the number of airplanes waiting to take off from a particular airport increases, it results in a delay in take-off time. With the cooperation of air traffic controllers some of this delay can be absorbed at the gate. However, due to the increased number of aircraft at an airport the shortest distances to a particular runway/ramp may not be available, resulting in increased taxi distances and time. Sensitivity of fuel/DOC to variations in taxi time was determined for each aircraft under study and the results of this sensitivity are given in Section 7 for each aircraft type.

6.2.3 Impact of Optimal Procedures on Noise and Air Pollution

Fuel conservative departure and approach procedures have been identified and evaluated in this study for all aircraft types. In addition to conserving fuel, these procedures also result in reduced noise and air pollution.

The reduced power take-off procedure requires less than take-off rated thrust (TRT) power setting whenever possible. Reduced power setting results in reduced noise and air pollution. Since the power required during take-off depends on aircraft weight, the length of the available runway, the runway condition, etc., the reduction in environmental pollution will vary from mission to mission.

The conventional ILS approach for jet transports requires high thrust settings for an extended time with the accompanying severe community noise impact and high air pollution. Significant reduction in noise and fuel consumption (reduced air pollution) can be gained through careful management of airspeed profile and the point at which the landing gear and flaps are lowered. The delayed flap approach procedure considered in this study achieves these goals. The approach is initiated at high airspeed and in a drag configuration that allows for low thrust.

Thus both approach time and thrust settings are reduced, resulting in reduced noise and engine emissions. Reference [18] carried out a detailed analysis of the impact of the delayed flap approach on noise and air pollution. The delayed flap approach considered in the reference reduced the effective perceived noise by about 8 dB over the conventional approach at the 1 nm. point. Also the nitrous oxide output of the conventional ILS approach is higher than that of the delayed flap approach due to high thrust settings required for the conventional approach.

The overall conclusion is that the optimal departure and approach procedures identified in this study result in reduced environmental pollution.

6.3 SENSITIVITY TO INSTRUMENT ERRORS

Errors in airspeed indicator, mach indicator, and altimeters can result in flying aircraft at off-optimal cruise conditions. It is important to estimate variations in fuel consumed and DOC due to variations in optimum cruise conditions. This helps determine the accuracy to be expected of measuring instruments. In this section the sensitivity of the optimum solution to variations in speed and altitude is derived.

6.3.1 Sensitivity to Errors in Cruise Mach

Minimum fuel cruise is very sensitive to changes in mach. Ref. [40] indicates that for altitude close to the optimum cruise altitude, mach must be held at optimum mach $\pm .015$ in order to remain above 99 percent of optimum specific range. Equation (6.1) defines the change in fuel consumed due to a change in range factor RF. Thus the sensitivity of fuel consumed and DOC to variations in mach can be obtained by determining the sensitivity of range factor (RF) to variations in mach. From Appendix C the range factor (RF) is given by

$$RF = \frac{a_0 M W}{f_n \delta} \quad (6.7)$$

where the variables are defined in that appendix. Optimum pressure altitude and mach are obtained by maximizing RF with respect to mach and W/δ . At an optimum cruise mach

$$\frac{\partial RF}{\partial M} = 0 \quad (6.8)$$

Thus the variation of RF due to a variation in optimum mach (M^*) can be written as

$$dRF = \frac{1}{2} \frac{\partial^2 RF}{\partial M^2} (dM)^2 \quad (6.9)$$

where the second partial of RF with respect to M is evaluated at optimum mach M*. Since RF is maximum at mach M*, $\frac{\partial^2 RF}{\partial M^2}$ will be negative. Thus the optimum range factor decreases when mach number deviates from optimum cruise mach (M*) and a decrease in RF is proportional to the square of mach deviation. Since analytical models have been developed for normalized fuel flow and aerodynamic drag, an analytical expression for $\frac{\partial^2 RF}{\partial M^2}$ can be obtained and its value can be computed. For B-52H aircraft this value was obtained as -3660. Using this value for B-52H aircraft

$$\frac{dRF}{RF} = - .18 (dM)^2 \quad (6.10)$$

Equation (6.9) is obtained from a Taylor series expansion of RF about its optimum value where terms higher than second order have been neglected. For small deviations in Mach from its optimum value results obtained from Eq. (6.9) are fairly accurate. However for large variations in Mach number, results obtained from Eq. (6.9) have substantial errors. Thus the sensitivity of RF to variations in Mach have been obtained using the simulation. Figure 7.5-11 illustrates percentage variation in RF due to a variation in Mach number. From that figure it is observed that for $\pm .01$ Mach deviation, results obtained by using Eq. (6.10) and the figure are almost identical. However for a $\pm .05$ Mach deviation, Eq. (6.10) gives a value of 4.5% decrease in RF, but from Fig. 7.5-11 a .05 Mach decrease in optimum cruise Mach number (M*) results in a 3.27% decrease in RF whereas a .05 Mach increase results in a 7.07% decrease in RF. Thus for large variations in Mach, deviations in RF should be obtained using the sensitivity plots for this study. Once the deviation in RF has been determined, Eq. (6.1) can be used to obtain the increase in fuel consumed due to deviations in optimum Mach.

Variations in optimum Mach also affect the total mission time. Percentage increase/decrease in mission time is equal to percentage increase/decrease in optimum Mach. After obtaining changes in fuel consumed and mission time, sensitivity of DOC to changes in Mach can be obtained using the DOC model described in Section 2. For the aircraft under study, aircraft instruments determine cruise

speed to within $\pm .01$ Mach. Plots illustrating the impact of flying off optimum cruise Mach number on range factor are given in Section 7. These plots indicate that for the aircraft under study the increase in fuel consumed due to instrument errors is less than .25%.

6.3.2 Sensitivity to Errors in Cruise Altitude

The optimum cruise solution is not very sensitive to variations in normalized weight (W/δ) and thus to variations in optimum cruise altitude. For most of the aircraft under study (B-52G, B-52H, KC-135 and C-141), a ± 2000 foot deviation in optimum cruise altitude or a $\pm 8\%$ deviation in W/δ results in less than a 1% increase in total fuel consumed. This is fortunate since it is difficult to know aircraft weight (W) exactly, whereas air data computers (ADC) aboard aircraft provide altitude information to within ± 250 feet. Since RF is optimized with respect to W/δ , variation of RF due to the variation in optimum normalized weight (W/δ)* can be written as

$$dRF = \frac{1}{2} \frac{\partial^2 RF}{\partial (W/\delta)^2} \left(d \frac{W}{\delta}\right)^2 \quad (6.11)$$

Again the second partial of RF with respect to W/δ will be negative, and a decrease in RF due to deviations in W/δ is proportional to the square of the deviations. If the aircraft weight is assumed to be known exactly then (6.11) can be written as

$$dRF = \frac{1}{2} \frac{\partial^2 RF}{\partial (W/\delta)^2} \mu^2 (W/\delta)^2 (dh)^2 \quad (6.12)$$

where μ is defined in Appendix C.

Again an analytical expression for $\frac{\partial^2 RF}{\partial (W/\delta)^2}$ can be obtained using the aerodynamic and propulsion models of Section 3.2 and its value can be computed. However those results will be valid only for small values of dh . Therefore the sensitivity of RF to variations in altitude have been obtained using the simulation. Fig. 7.5-12 illustrates percentage variations in RF due to variations in altitude for B-52H aircraft. For this aircraft, cruising 2000 feet below optimum cruise altitude,

(which is equivalent to an 8.1% decrease in W/δ), results in a .63% increase in RF, and the increase in RF due to cruising 2000 feet above optimum cruise altitude (8.1% increase in W/δ in the troposphere) is 0.7%.

Assuming that aircraft weight is known exactly, errors in altitude estimates from air data computer (ADC) results in approximately .01% increase in fuel consumed, which is very small.

6.4 SENSITIVITY TO UNCERTAINTIES IN DESIGN MODIFICATIONS

Section 5 describes the analysis approach to design modifications. Since design changes impact the fuel and cost performance of an entire fleet of modified aircraft, these changes are evaluated by averaging over a spectrum of mission profiles for each aircraft. However there can be uncertainties in improvements in performance/DOC due to design changes. These uncertainties in predicted and actual improvements can be due to many factors, e. g. accuracy of the prediction technique, manufacturing tolerances, etc. Sensitivity results have been obtained which can be used to represent these uncertainties. Sensitivity of fuel/DOC to variations in zero-lift drag, induced drag, aircraft weight and fuel flow rate has been obtained by averaging over a mission spectrum. These plots are used to determine sensitivity of fuel savings/DOC to uncertainties in design change. Thus for example, Ref. [36] predicts an 11% reduction in induced drag by retrofitting C-141 with winglets. From Fig. 7.1-7 an 11% reduction in induced drag for the C-141 amounts to 1.8% savings in annual fuel cost. However, if the actual reduction in induced drag due to winglets is less than predicted, Fig. 7.1-7 can be used to estimate the difference between actual and predicted fuel savings. The detailed sensitivity results for design modifications are presented in Section 7 for each aircraft type.

SECTION 7

RESULTS OF FUEL/DOC TRADE-OFF STUDIES AND SENSITIVITY ANALYSIS BY AIRCRAFT TYPE

Sections 2 through 6 described various fuel conservative operational techniques/design modifications and outlined the approach taken to evaluate their fuel savings potential. This section presents results of fuel/DOC trade-off studies by aircraft and quantifies potential fuel/DOC savings due to operational/design modifications. Also presented in this section for each aircraft under study are the results of sensitivity analysis conducted to determine variations in fuel consumptions and DOC due to (1) environmental variations, (2) differences between like aircraft and (3) uncertainties in improvements that result from design modifications.

7.1 C-141

The Lockheed C-141 Starlifter is a four-engine cargo/troop transport aircraft whose primary mission is strategic airlift. The C-141 is powered by Pratt & Whitney TF-33-P-7 turbofan engines which are rated at 21,000 pounds of thrust each. A total of 284 C-141s were purchased by the Air Force, of which 272 were operating at time of this study. These A series aircraft have a maximum takeoff gross weight of 316,600 pounds, a floor length of 70 feet and carry ten cargo pallets. A stretched version has been prototyped which adds 23.3 feet to the fuselage length, allowing the C-141 to carry 13 cargo pallets. An aerial refueling capability has also been added to this stretched version. If prototype testing is successful, modification of all C-141's is planned.

7.1.1 C-141 Design Missions

Table 7.1-1 presents the design mission data for C-141 aircraft [41]. The basic mission has a 1000 n.m. combat radius and a 2040 n.mi. combat range.

CONDITIONS	BASIC MISSION	MAXIMUM CARGO	DESIGN RANGE	DESIGN RANGE	AIR DROP MISSION	FERRY MISSION
TAKE-OFF WEIGHT lbs.	270,390	316,600	316,600	305,544	316,600	284,744
Fuel lbs.	67,170	111,980	126,094	153,538	113,380	153,538
Payload lbs.	72,014	72,014	59,300	20,800	72,014	0
COMBAT RANGE n.mi.	2,040	3,453	4,000	5,500	-	5,974
Average Cruising Speed kn	430.7	433.5	431.0	419.6	-	409.2
Initial Cruising Altitude ft.	37,479	34,157	34,157	34,913	-	36,434
Final Cruising Altitude ft.	41,000	41,000	41,000	41,000	-	41,000
Total Mission Time hr.	4.78	8.02	9.34	13.15	-	14.63
FIRST LANDING WEIGHT	237,224	255,519	248,594	225,101	-	-
COMBAT RADIUS n.mi.	1000	1823	2079	2704	1309	-
Average Cruising Speed kn	411.5	416.0	417.2	418.9	413.5	-
Initial Cruising Altitude ft.	37,479	34,157	34,157	34,913	34,200	-
Final Cruising Altitude ft.	41,000	41,000	41,000	41,000	41,000	-
Total Mission Time hr.	4.93	8.85	10.06	13.0	6.83	-
LANDING WEIGHT lbs.	141,169	143,353	143,991	145,369	143,353	145,369

* Take-off Weight Does Not Include 1,400 lbs of Ramp Fuel
 OEW = 132,606 lb.

Table 7.1-1 TYPICAL MISSION DATA FOR C-141

The maximum take-off gross weight for the C-141 is 316,600 lbs and operational empty weight is 132,606 lbs. Maximum payload is 72,014 lbs, maximum fuel capacity is 23,620 gallons and maximum ferry range is 5,974 n.mi.

7.1.2 C-141 Mission Model

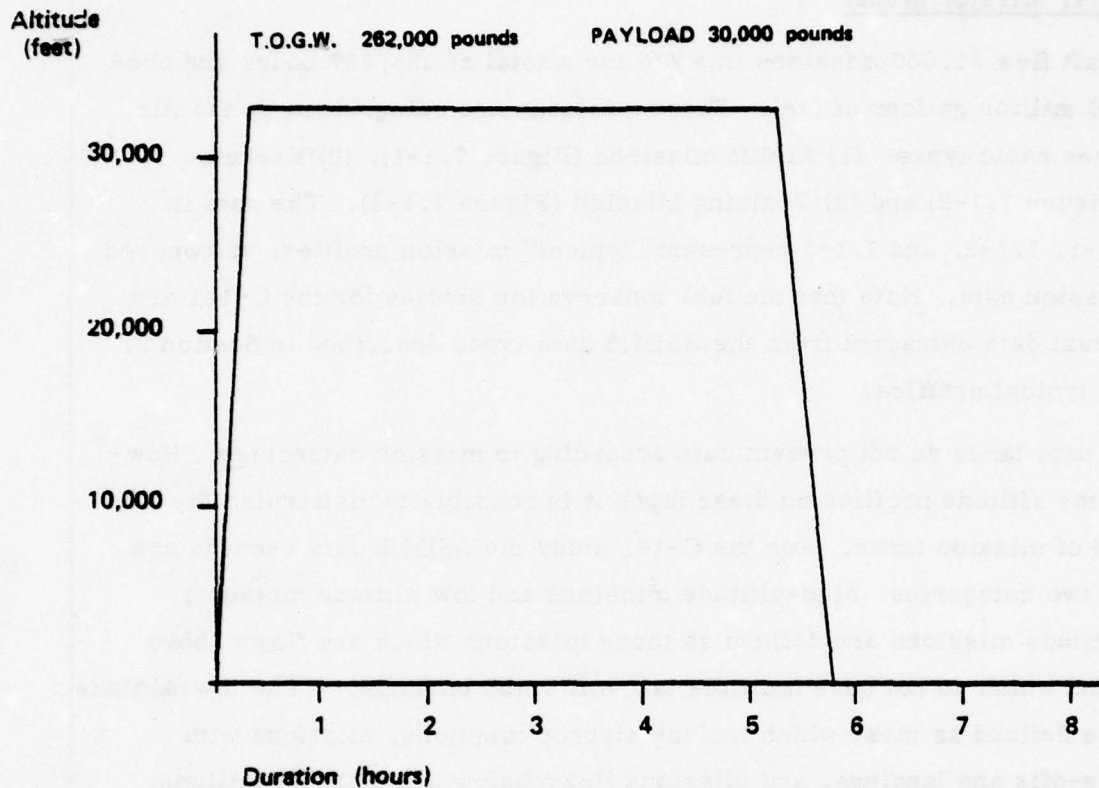
C-141 aircraft flew 81,000 missions in FY76 for a total of 298,657 hours and consumed 600.8 million gallons of fuel. These missions are categorized by the Air Force in three basic types: (1) Airlift missions (Figure 7.1-1), (2) Exercise missions (Figure 7.1-2) and (3) Training Mission (Figure 7.1-3). The data in Figures 7.1-1, 7.1-2, and 7.1-3 represent "typical" mission profiles, as opposed to actual mission data. Note that the fuel conservation studies for the C-141 are based on actual data extracted from the ASIMIS data types described in Section 2, not on these typical profiles.

The ASIMIS data tapes do not present data according to mission categories. However, from the altitude profiles on these tapes it is possible to distinguish the general type of mission flown. For the C-141 study the ASIMIS data records are divided into two categories: high-altitude missions and low altitude missions. The high-altitude missions are defined as those missions which are flown above 7,000 feet and which do not have multiple take-off's and landings. The low-altitude missions are defined as those which include airdrop missions, missions with multiple take-offs and landings, and missions flown below a 7,000 feet altitude.

Since the low-altitude type of missions are generally constrained to particular flight paths and altitudes, there is little or no opportunity for flight path optimization. Thus, it is the high-altitude type of missions which are used in the study of optimal flight procedures for the C-141. These high altitude missions comprise 86.3% of the total C-141 missions on the data tapes and 91.9% of the flying hours.

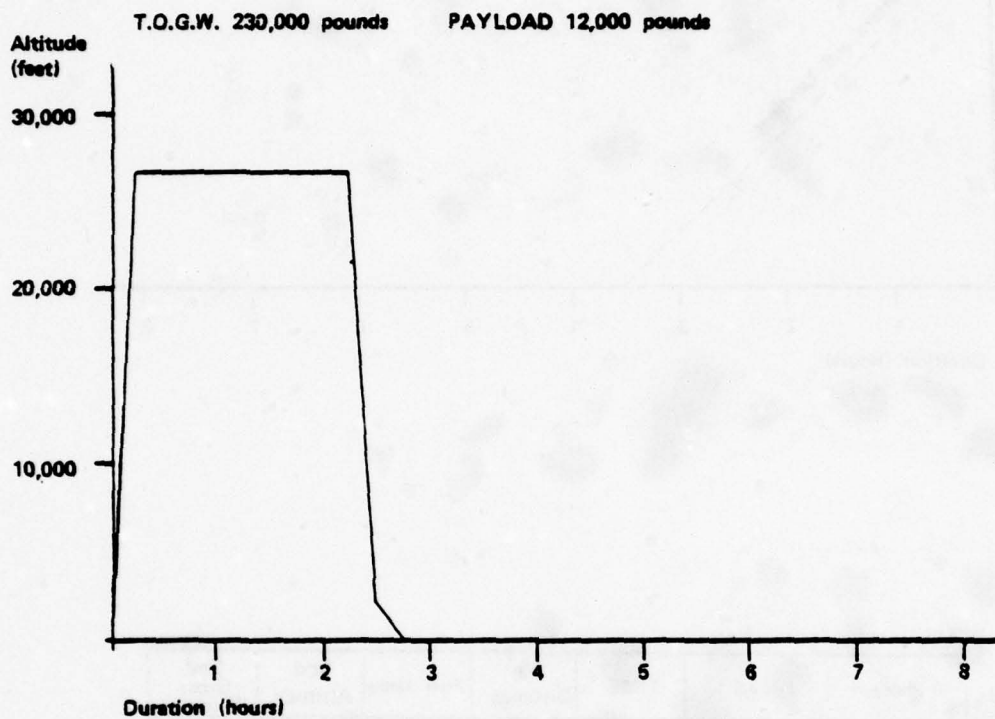
The data tapes used were for the period April through June 1976 and at the time of the data processing this was the latest information available. There were a total of 7618 sortie records of which 114 were discarded due to incomplete data.

Figure 7.1-1 C-141 TYPICAL AIRLIFT MISSION



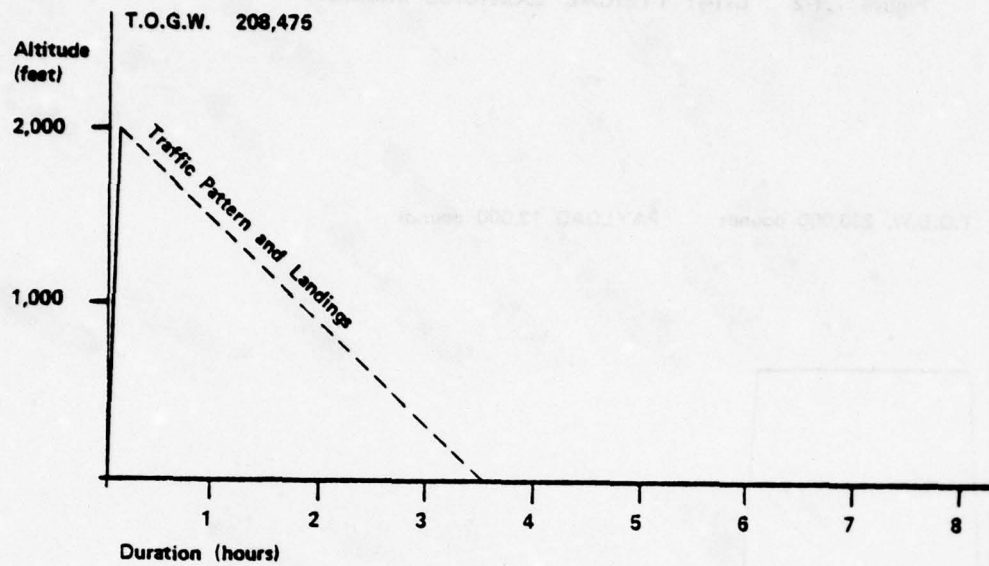
PHASE	IAS	TIME	Air Distance	Fuel Used	End Altitude	End Gross Weight
TAKEOFF/ CLIMBOUT	160	.10	16	2,000	3,000	260,000
CLIMB	280	.25	91	6,300	33,000	253,700
CRUISE	.767	4.95	2214	61,000	33,000	192,700
DESCENT	300	.25	84	1,200	3,000	191,500
TRAFFIC PATTERN	160	.25	41	2,500	0	189,000
TOTAL		5.8	2446	73,000		

Figure 7.1-2 C-141 TYPICAL EXERCISE MISSION



Phase	IAS	TIME	Air Distance	Fuel Used	End Altitude	End Gross Weight
Climb	280	0.20	53	6,200	26,600	223,800
Cruise	280	2.07	850	30,630	26,600	193,170
Descent	300	0.28	86	1,360	2,000	191,810
Traffic Pattern	180	.25	41	2,500	0	189,310
TOTAL		2.80	1030	40,690		

Figure 7.1-3 C-141 TYPICAL TRAINING MISSION



Phase	IAS	TIME	Air Distance	Fuel Used	End Altitude	End Gross Weight
Takeoff/ Climbout	160	.10	16	1,900	2,000	208,575
Traffic Pattern	160	3.59	603	42,680	0	163,895
TOTAL		3.69	619	44,580		

For the ASIMIS data on the C-141 aircraft, mission parameter information was recorded in weight bands, altitude bands and airspeed bands as shown in Table 7.1-2. In processing this data, altitude bands were kept the same, however, middle values of weight and airspeed bands were taken to obtain average weights and airspeeds.

The histograms contained in this section represent the distribution of various missions parameters obtained by processing data tapes for airlift missions. The missions were first separated according to mission duration. Missions of less than 3 hours duration are called short range missions; medium range missions have a mission duration of 3-6 hours; and the missions of more than 6 hours duration are called long range missions. Missions are further subdivided according to TOGW. The weight bands considered are less than 200,000 lbs, 200,000-240,000 lbs, 240,000-280,000 lbs and more than 280,000 lbs.

Figures 7.1-4 through 7.1-7 show the histograms of level off altitude for short range missions. Take-off fuel weight, landing fuel weight and average mission duration information is also shown on these histograms. For each mission type, three numbers are shown above each column: the number on the top is takeoff fuel weight, the middle number is landing fuel weight and the bottom number is the mission duration.

Figures 7.1-8 through 7.1-10 are the level off altitude histograms for medium range missions. Since there were only 3 medium range missions for TOGW less than 200,000 lbs, they were excluded from analysis.

Figures 7.1-11 and 7.1-12 are the level-off altitude histograms for long range missions. Since there were only 6 long range missions for TOGW less than 280,000 lbs, they were excluded from the analysis.

MISSION PARAMETER	DATA BANDS ON ASIMIS TAPES		
	VARIABLE RANGE	BAND WIDTH	BAND NUMBER
Fuel Weight Bands lbs	0 - 137,000	12,000 for odd band 13,000 for even band	1-11
	137,000 +	-	12
Payload lbs	0 - 20,000	5,000	1-4
	20,000 - 27,000 27,000 - 35,000 35,000 +	7,000 8,000 -	5 6 7
Altitude ft	Contour	-	1
	0 - 2,000 2,000 - 22,000 22,000 - 32,000 32,000 - above	1,000 ft 5,000 ft 10,000 ft -	2-3 4-7 8 9
Airspeed Mach	0 - .37	.37	1
	.37 - .45 .45 - .54 .54 - .61 .61 - .71 .71 - .8 .8+	.08 .09 .08 .1 .09	2 3 4 5 6 7

Table 7.1-2 ASIMIS TAPE DATA BANDS FOR C-141 AIRCRAFT

Figure 7.1-4

C-141
DISTRIBUTION OF LEVEL OFF ALTITUDES
TAKE OFF GROSS WEIGHT - up to 200,000 pounds
MISSION DURATION - less than 3 hours

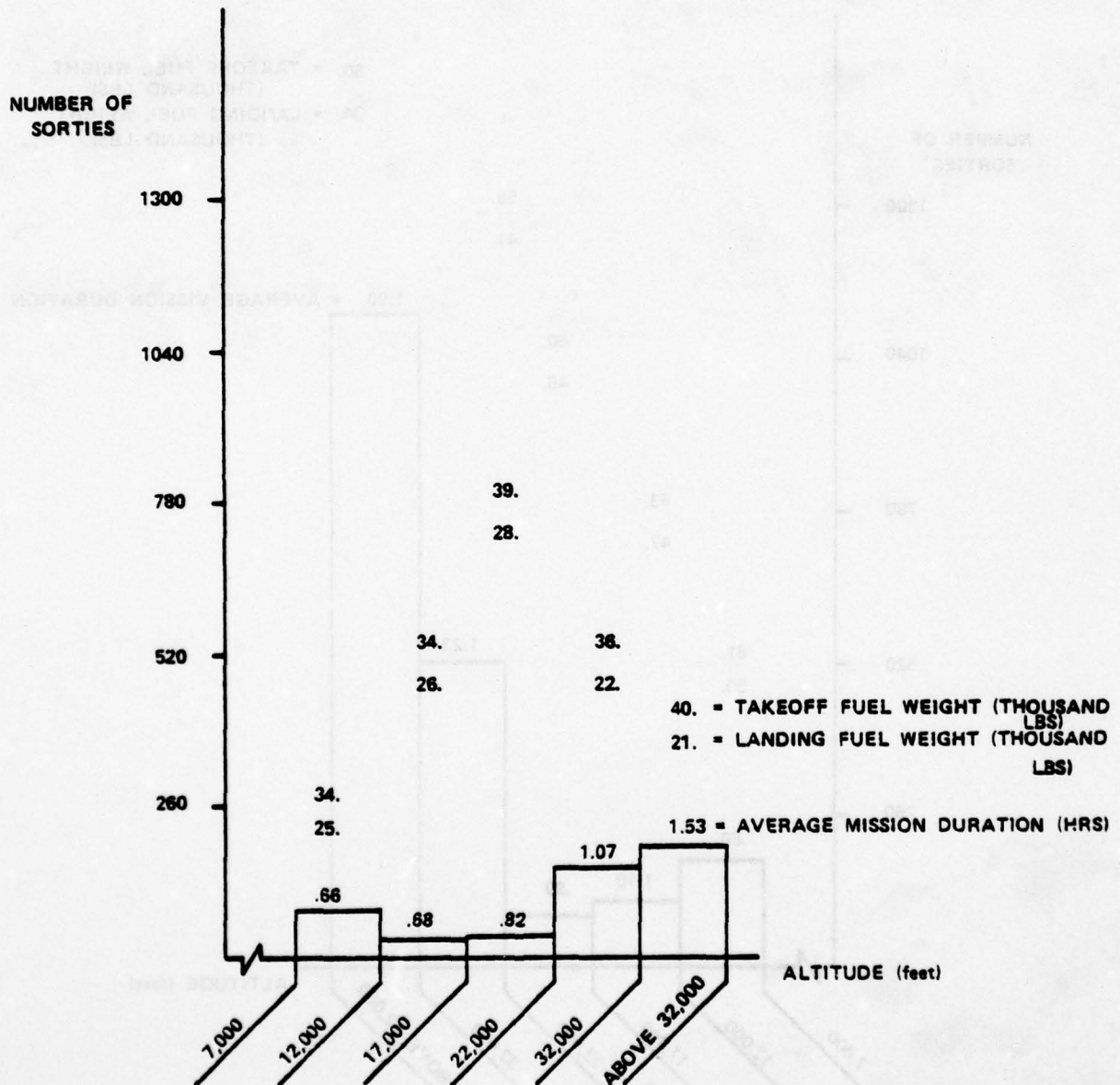


Figure 7.1-5

C-141
DISTRIBUTION OF LEVEL OFF ALTITUDES
TAKE OFF GROSS WEIGHT - 200,000 - 240,000 pounds
MISSION DURATION - less than 3 hours

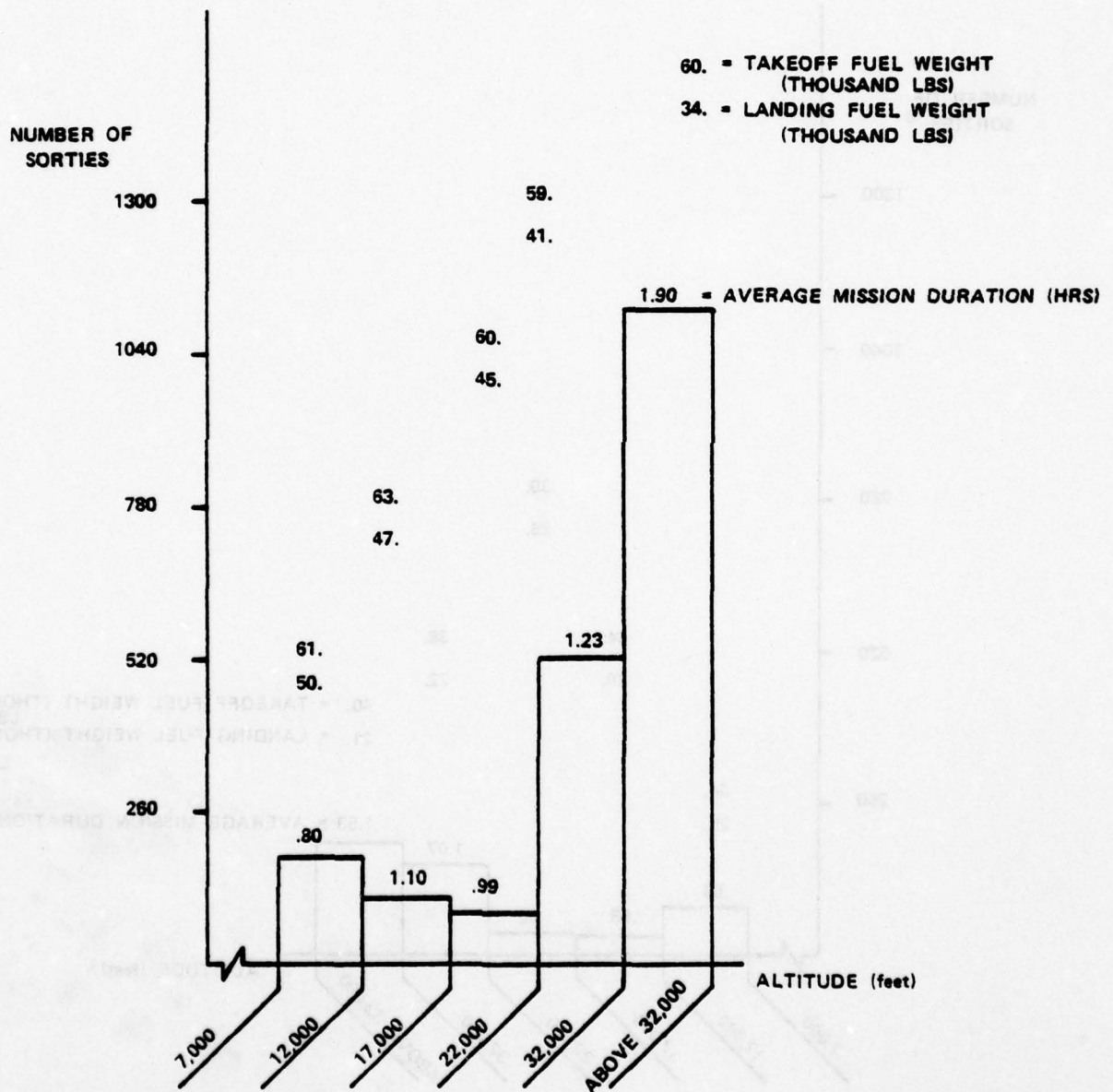


Figure 7.1-6

C-141

DISTRIBUTION OF LEVEL OFF ALTITUDES

TAKE OFF GROSS WEIGHT - 240,000 - 280,000 pounds

MISSION DURATION - less than 3 hours

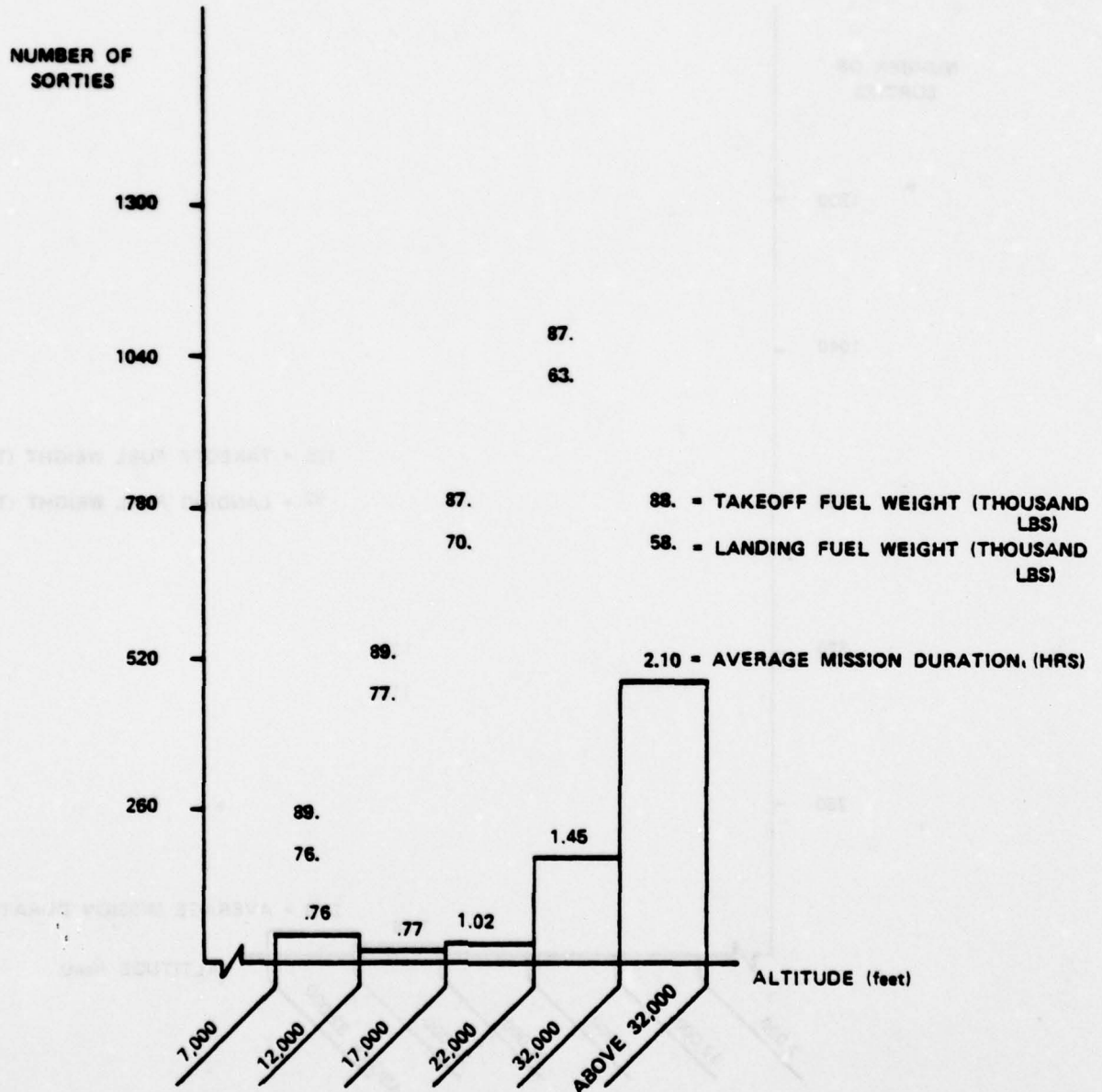


Figure 7.1-7

C-141
DISTRIBUTION OF LEVEL OFF ALTITUDES
TAKE OFF GROSS WEIGHT - 280,000 AND ABOVE
MISSION DURATION - less than 3 hours

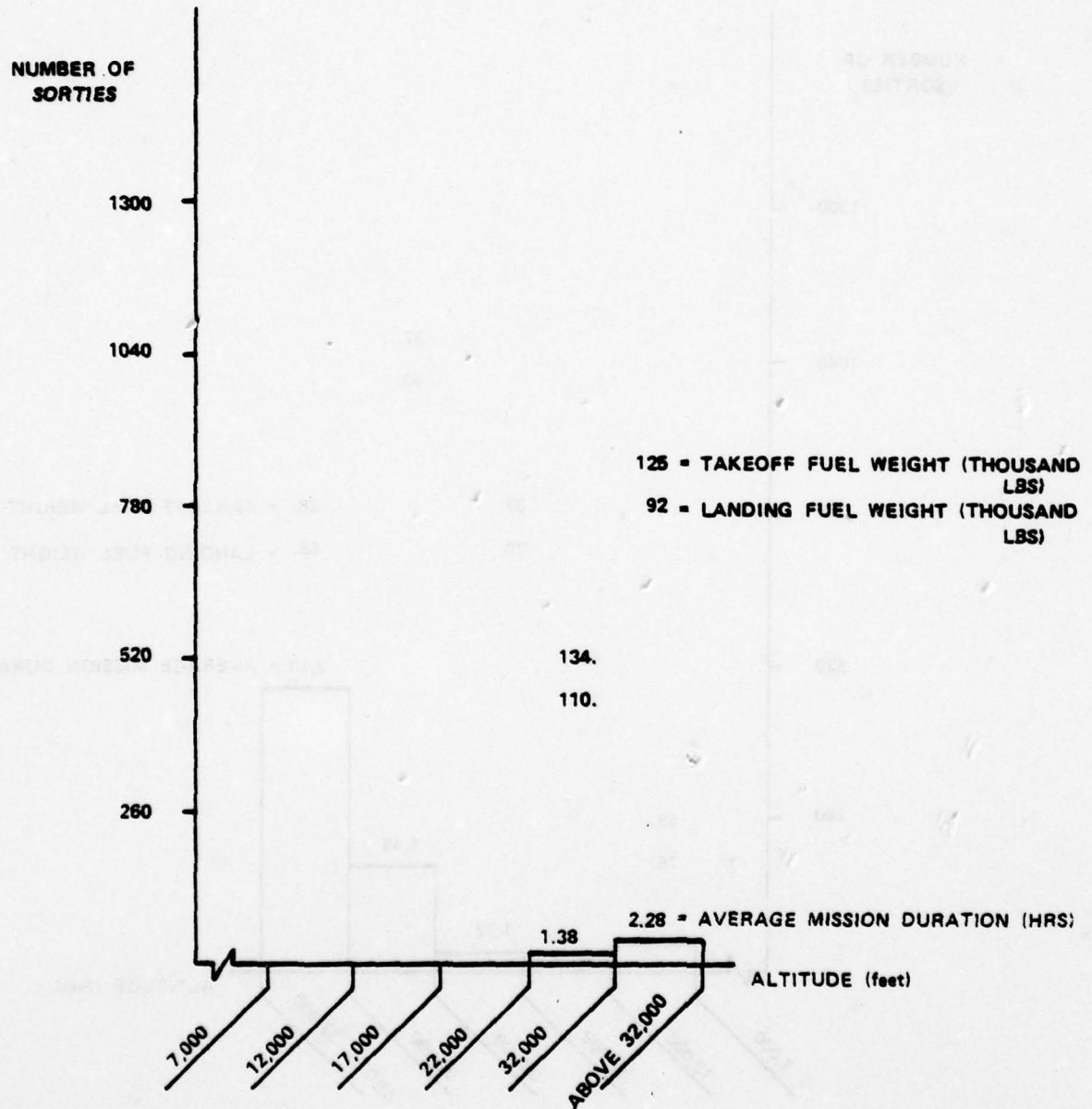


Figure 7.1-8

C-141
DISTRIBUTION OF LEVEL OFF ALTITUDES
TAKE OFF GROSS WEIGHT - 200,000 - 240,000 pounds
MISSION DURATION - 3 - 6 hours

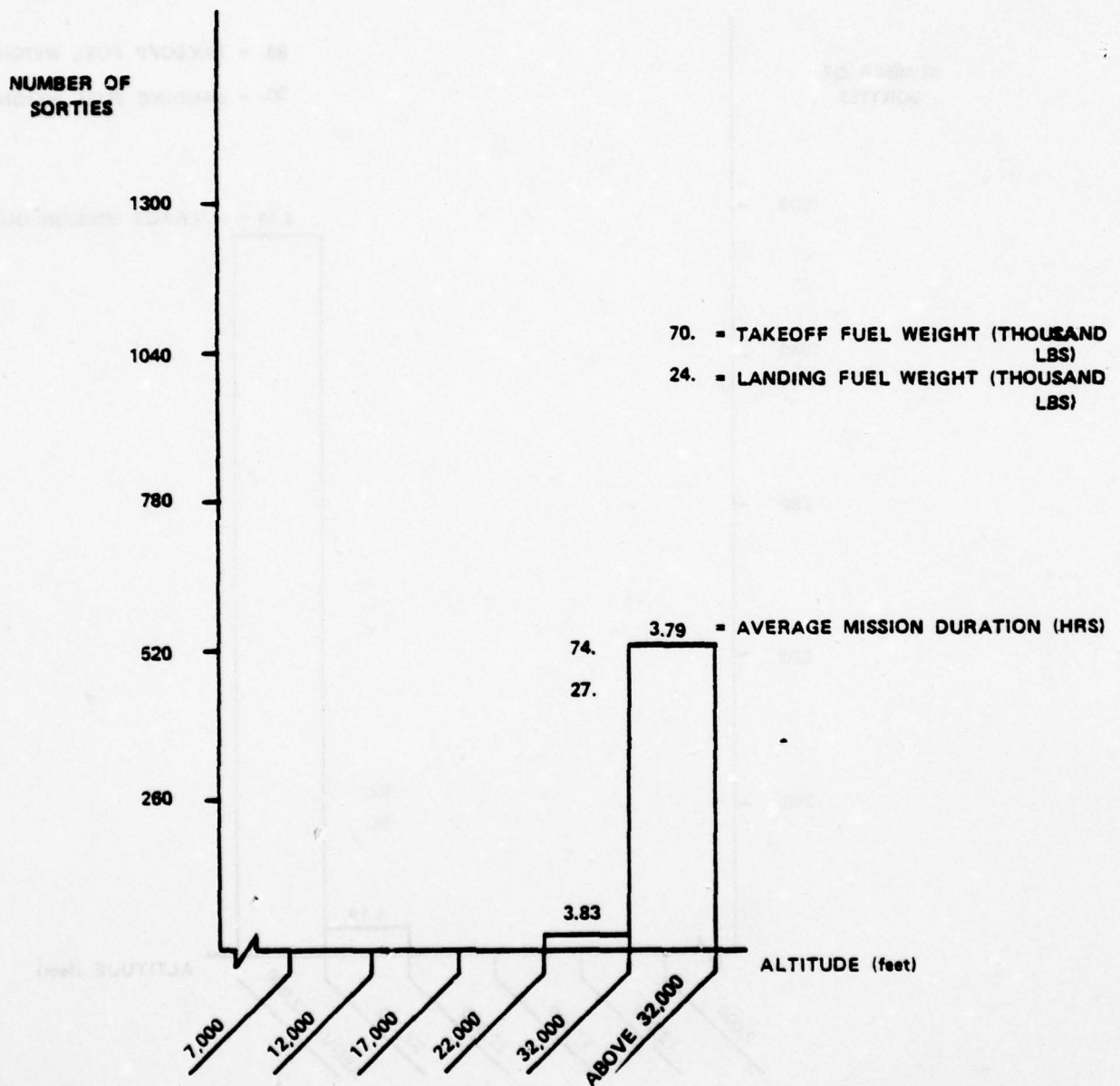


Figure 7.1-9

C-141
DISTRIBUTION OF LEVEL OFF ALTITUDES
TAKE OFF GROSS WEIGHT - 240,000 - 280,000 pounds
MISSION DURATION - 3 - 6 hours

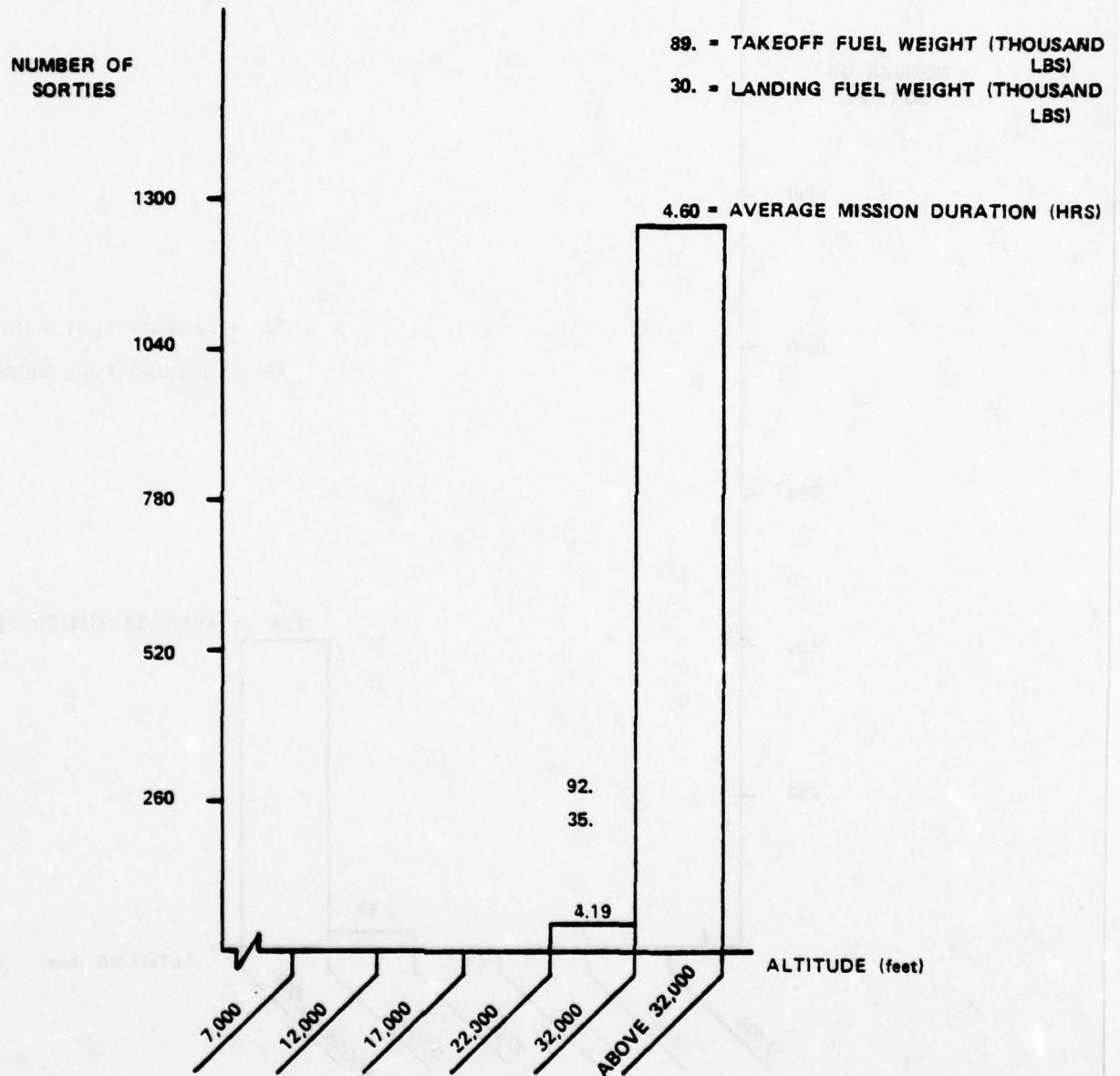


Figure 7.1-10

C-141
DISTRIBUTION OF LEVEL OFF ALTITUDES
TAKE OFF GROSS WEIGHT - 280,000 AND ABOVE
MISSION DURATION - 3 - 6 hours

NUMBER OF
SORTIES

1300

1040

780

520

260

121. = TAKEOFF FUEL WEIGHT (THOUSAND
LBS)

56. = LANDING FUEL WEIGHT (THOUSAND
LBS)

4.80 = AVERAGE MISSION DURATION (HRS)

ALTITUDE (feet)

7,000

12,000

17,000

22,000

32,000

ABOVE 32,000

Figure 7.1-11

C-141
DISTRIBUTION OF LEVEL OFF ALTITUDES
TAKE OFF GROSS WEIGHT - 240,000 - 280,000 Pounds
MISSION DURATION - 6 HOURS OR MORE

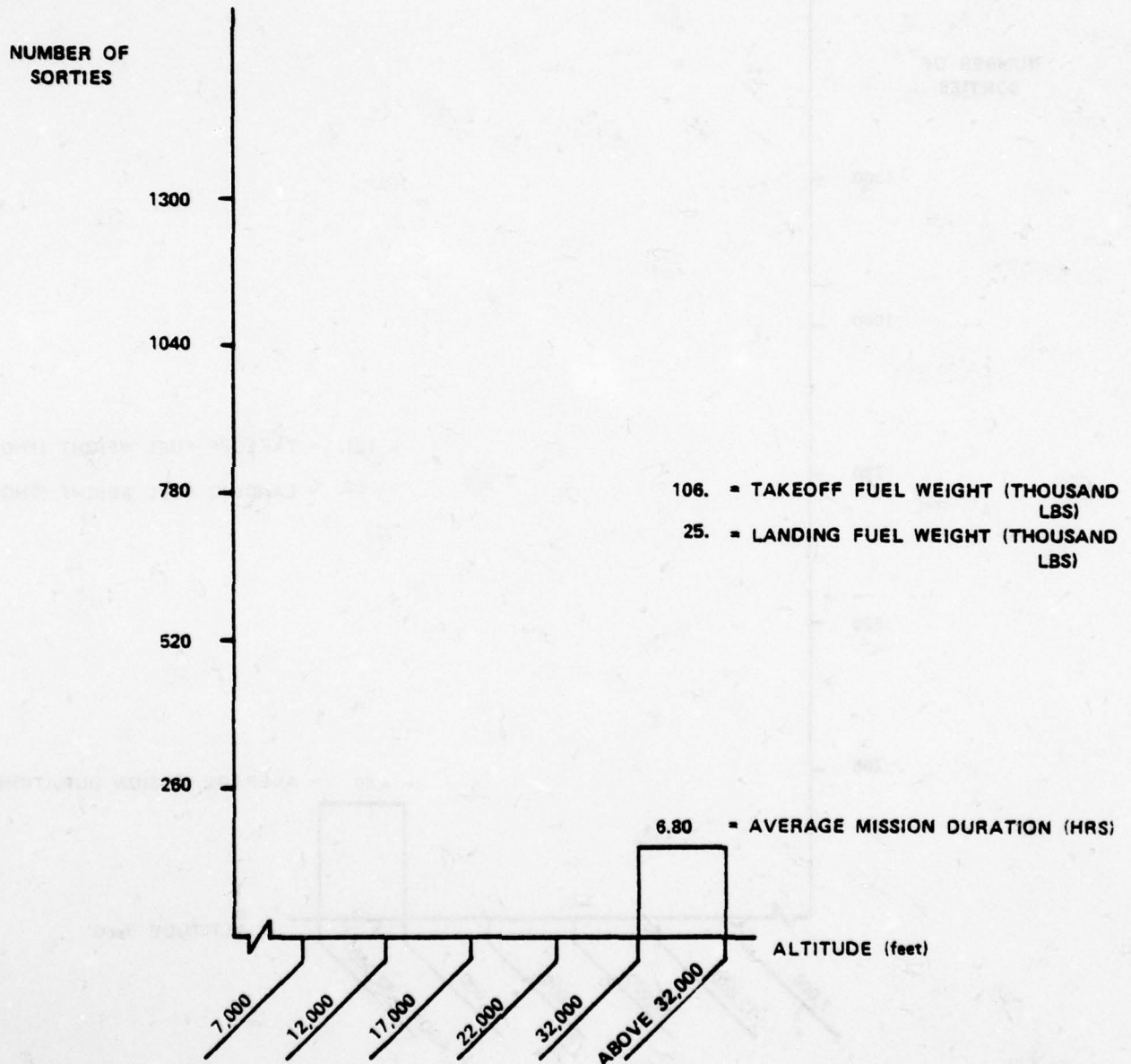
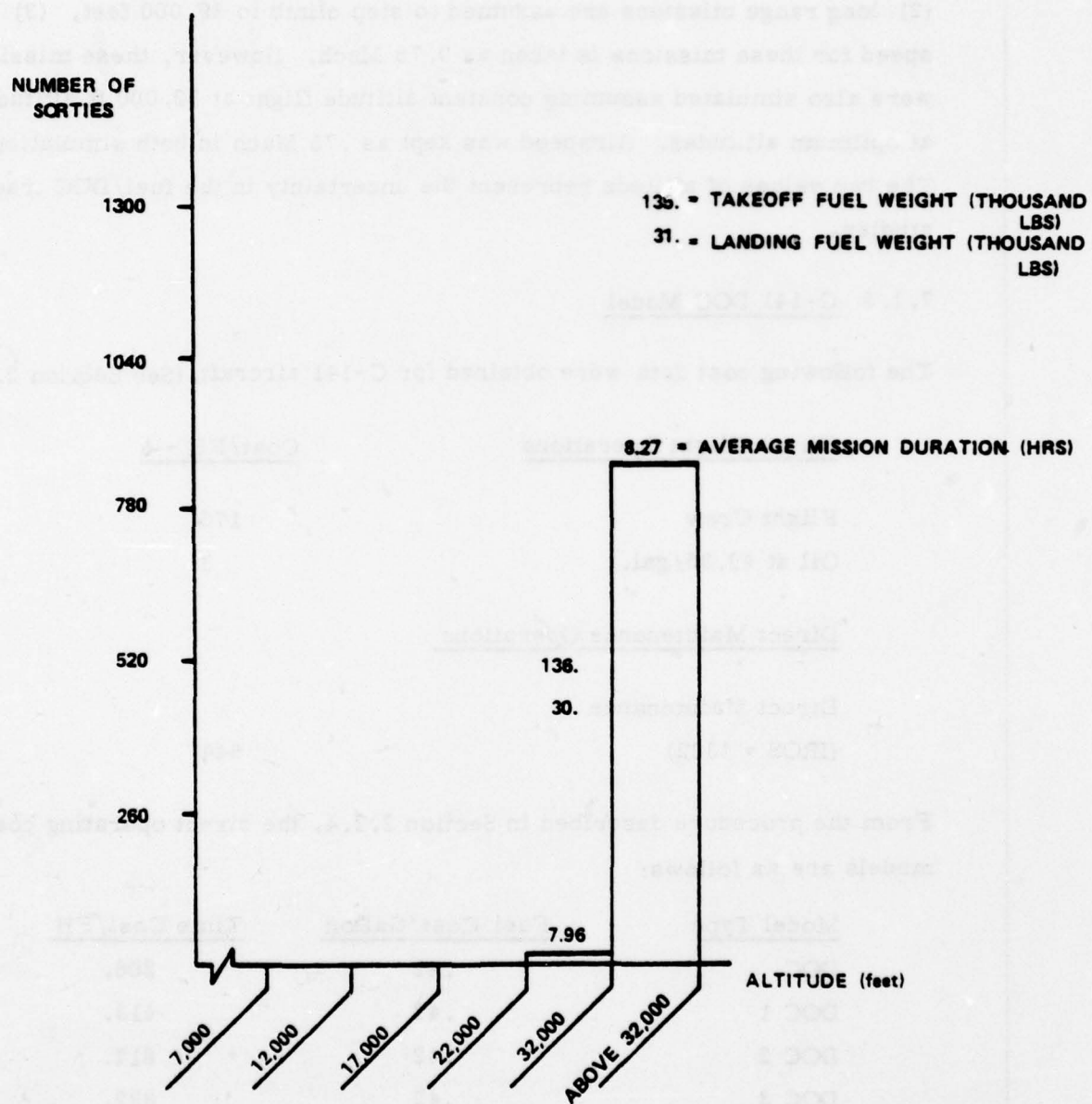


Figure 7.1-12

C-141
DISTRIBUTION OF LEVEL OFF ALTITUDES
TAKE OFF GROSS WEIGHT - 280,000 POUNDS
MISSION DURATION - 6 OR MORE HOURS



Note that most of the missions fly above 32,000 feet altitude and that airspeed for most of the missions is between .7 and .8 Mach number. There can be large variations between fuel consumed depending on the difference between actual and assumed altitude and airspeed between these bands. For analysis purposes, (1) initial level off altitude above 32000 ft is taken as 35,000 feet, (2) long range missions are assumed to step climb to 39,000 feet, (3) airspeed for these missions is taken as 0.75 Mach. However, these missions were also simulated assuming constant altitude flight at 32,000 ft altitude and at optimum altitudes. Airspeed was kept as .75 Mach in both simulation cases. The two values of altitude represent the uncertainty in the fuel/DOC trade studies.

7.1.3 C-141 DOC Model

The following cost data were obtained for C-141 aircraft. (See Section 2.2)

<u>Direct Flight Operations</u>	<u>Cost/FH - \$</u>
Flight Crew	175
Oil at \$9.35/gal.	3
<u>Direct Maintenance Operations</u>	
Direct Maintenance (IROS = \$322)	644

From the procedure described in Section 2.2.4, the direct operating cost models are as follows:

<u>Model Type</u>	<u>Fuel Cost/Gallon</u>	<u>Time Cost/FH</u>
DOC	.42	208.
DOC 1	.42	413.
DOC 2	.42	617.
DOC 3	.42	822.

Table 2.1-2 gives annual fuel consumed and flying hours during FY76 for the aircraft under study. Using those values and the above cost models, annual fuel and direct operating costs for C-141 are obtained as follows:

Fuel Cost	\$252.3 Millions
DOC	\$314.5 Millions
DOC 1	\$375.7 Millions
DOC 2	\$436.6 Millions
DOC 3	\$497.8 Millions

7.1.4 C-141 Aerodynamic and Propulsion Models

Aerodynamic and propulsion data for C-141 aircraft was obtained from Reference [41]. Using this data the following analytical models were developed for C-141.

7.1.4.1 C-141 Aerodynamic Model

Following the procedure outlined in Subsection 3.2, drag coefficient (C_D) is represented as a parabolic function of lift coefficients (C_L) for each Mach number.

$$C_D = C_{D_0} - B C_L + K C_L^2$$

$$\text{where coefficients } C_{D_0} = .016 + .125 \times 10^{-4} (M^* - M)^{-2.7}$$

$$B = .0072 + .152 \times 10^{-4} (M^* - M)^{-3.0}$$

$$K = .055 + .109 \times 10^{-5} (M^* - M)^{-4.6}$$

and

$$M^* = 0.9$$

This model is a very good representation (less than 2% error) of C_D up to a Mach number of .76. Beyond this number the error in C_D increases, but this model is adequate for this study since the C-141 generally operates at a Mach number of about .75 and the optimal Mach number from a fuel minimization viewpoint is even lower.

7.1.4.2 C-141 Thrust Model

Normal rated thrust (NRT) of each engine is represented as a polynomial function of normalized altitude (H_n) and Mach (M) on a standard day. The NRT equation is given by

$$\begin{aligned} \text{NRT} = 1000. [& 17.44 - 15.34H_n - 14.22M + .04 H_w^2 + 18.35 MH_n + \\ & 9.62M^2 - 5.92MH_n^2 - 11.81M^2H_n + .76M^2H_n^2] \end{aligned}$$

where

NRT = normal rated thrust (lb.)

H_n = normalized altitude

= altitude (ft)/40000.

This NRT model is applicable up to 41,000 ft altitude.

Idle engine thrust (T_{idle}) is also represented as a polynomial function of normalized altitude (H_n) and Mach (M). The representation is similar to NRT, only the constant coefficients are different. Thus, T_{idle} is given by

$$\begin{aligned} T_{idle} = 1000. [& 1.12 - 1.75H_n - 1.69M + 1.54 H_n^2 + 3.12 MH_n - 1.82M^2 \\ & - 1.7MH_n^2 + 1.38M^2H_n - .25M^2H_n^2] \end{aligned}$$

This idle thrust model is also applicable up to 41,000 ft. altitude. The maximum difference between actual idle thrust and theoretical idle thrust obtained using the above model is less than 75 lbs.

The above thrust models and the fuel flow models discussed next are generally good to within a 2% error over most of the regions of interest.

7.1.4.3 C-141 Fuel Flow Model

As discussed in Subsection 3.2, fuel flow rate, f , for the C-141 aircraft is a function of altitude, Mach, thrust setting and ambient temperature. However for analysis purposes fuel flow data is acceptably expressed as

$$f = f_n \delta \sqrt{\theta}$$

where

f = fuel flow rate - (lbs/hour/engine)

f_n = normalized fuel flow rate

δ = atmospheric pressure ratio

θ = temperature ratio

Normalized fuel flow rate, f_n , is expressed as a polynomial function of normalized thrust, T_n , and Mach (M). f_n is given by the equation:

$$f_n = 1000. [1.71 + 4.07 T_n + .71M + 6.15T_n^2 + 6.77MT_n + 1.18M^2]$$

where

T_n = normalized thrust/engine

$$= T/\delta/20000.$$

This fuel flow model degrades at idle thrust setting. Therefore a separate model was developed for normalized idle fuel flow rate $f_{n_{idle}}$ using idle thrust and fuel flow rate data. The functional form of $f_{n_{idle}}$ is similar to f_n , only the parameters are different:

$$f_{n_{idle}} = 1000. [.29 + 17.96T_n + .27M - 2.01T_n^2 + 13.22 MT_n + 4.66M^2]$$

This model is applicable up to 25,000 ft altitude. Above 25,000 ft. altitude idle fuel flow rate is 655 lbs/hr/engine and remains constant.

7.1.5 Evaluation of Airborne and Ground Operational Procedures

This subsection summarizes the results of the evaluation of fuel conservative operational procedures for the C-141. The technical approach follows the procedure outlined in Section 4. First, procedures which require trajectory optimization are discussed, then the results for fuel saving airborne procedures which do not require trajectory optimization are given. Then the evaluation of ground handling and maintenance procedures is presented.

7.1.5.1 Reduced Power Take-off

The average fuel savings due to reduced power takeoff for C-141 missions is estimated at less than one-half gallon, and the average take-off time increases by approximately 3 seconds per flight. These savings translate into 38,000 gallons of fuel and \$4,500 DOC annual savings for the C-141. Thus, the direct annual fuel/DOC savings due to reduced power take-off are small. However, indirect fuel savings due to reduced engine deterioration may be substantial. As mentioned in subsection 4.1, Reference [17] estimated fuel savings due to reduced engine deterioration to be as high as 2%. The 2% estimate is felt to be high by some Air Force personnel. To truly define the reduced engine deterioration due to reduced power take-off is felt to require closely controlled engine tests over an extended period of time.

7.1.5.2 Optimal Climb, Cruise and Descent Procedures

Climb, cruise and descent flight models for C-141 are first examined separately. The cruise segment is evaluated first since the optimal climb and descent algorithms developed in Appendix A utilize some parameters obtained from the optimal cruise solution. Results of the individual segment optimizations are combined to obtain the results for the complete trajectory.

Optimal Cruise-Climb Solution

Optimum cruise altitude and velocity are obtained by point extremization of the function given by Equation (A.31) in Appendix A. The solution of this equation depends upon the fuel/cost tradeoff parameter θ . Figure 7.1-13 depicts the fuel/cost trade-off obtained by varying the parameter θ in Equation (A.3). The solution corresponding to $\theta = 0$ is the minimum time solution and the solution corresponding to $\theta = 1$ is the minimum fuel solution. Both minimum cruise altitude and maximum cruise Mach were constrained in the simulation, and the minimum time solution shown was obtained under these constraints. As θ is increased fuel consumption decreases, however the flight time increases due to a decrease in optimum cruise Mach number. Optimum solution points corresponding to direct operating cost models DOC, DOC 1, DOC 2 and DOC 3 are shown on Figure 7.1-13. Since the ASIMIS tape data gives cruise velocity in bands the cruise velocity is not known exactly. However most of the long range and medium range missions fly above 0.7 Mach number, and for this study an average cruise velocity of .75 Mach is assumed. This cruise velocity corresponds to DOC 3. The minimum fuel cruise-climb solution occurs close to 0.72 Mach number. The "knee" in the curve occurs near the optimum solution for DOC 3. The optimum Mach number for DOC 1 is 0.745. The minimum fuel solution occurs for the following cruise conditions:

- Mach number = 0.717
- $W/\delta = 1.244 \times 10^6$ lb.
- Range Factor = 9226

This range factor has a 10% allowance for increased fuel flow as reported in Reference [42]. Note that this range factor has not been corrected for cruise climb conditions. For a cruise-climb profile, the average value of flight path angle for the C-141 is on the order of 0.02 deg. and the average value of range factor is 9164 which has 0.7% correction for energy gain during cruise-climb.

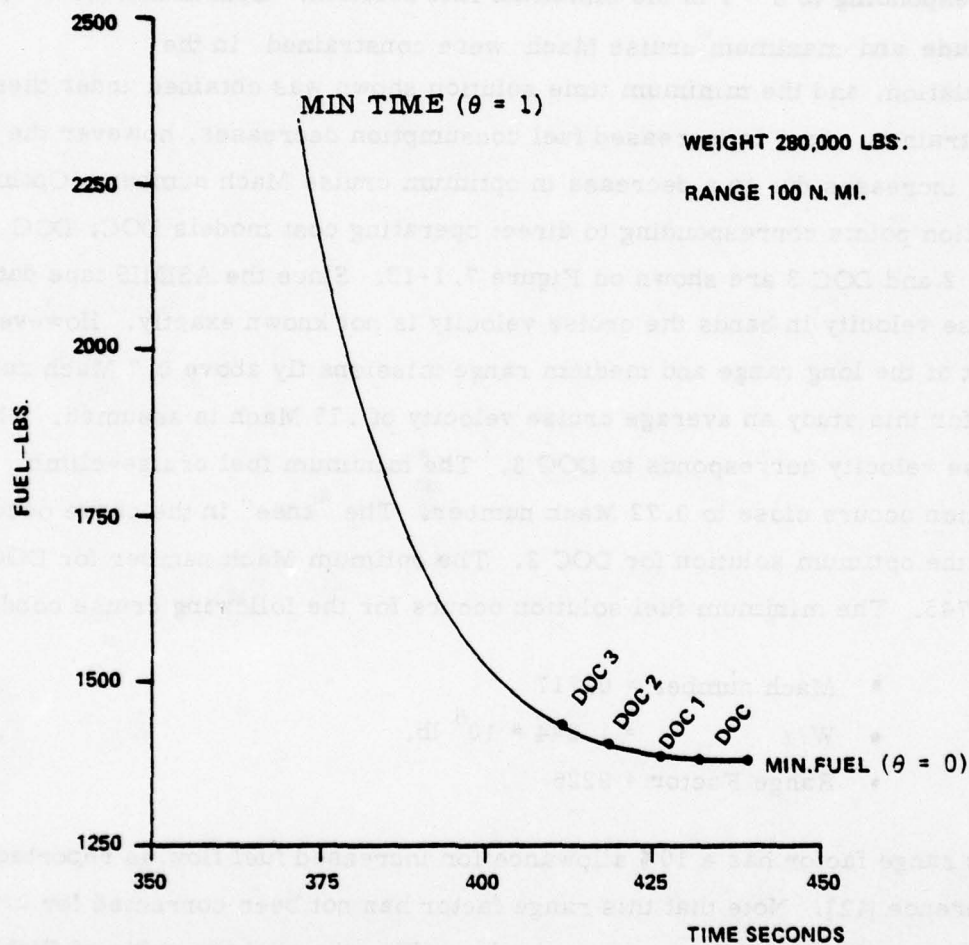


Figure 7.1-13 FUEL/TIME TRADE-OFF FOR THE C-141

CRUISE SOLUTION

Optimal Step-Climb Solution

The maximum cruise altitude for the C-141 is constrained to 41,000 feet due to pressurization requirements. The standard day cruise ceiling for the C-141 is more than 2000 feet above the cruise-climb altitude for this aircraft. Also best cruise altitude for the C-141 is always higher than 29,000 feet and it can only take 4,000 foot steps in altitude due to ATC restrictions. Note that the increase in fuel consumption caused by flying off the optimal cruise altitude is a parabolic function of altitude. Thus optimum step climb procedure for this aircraft is to initiate a level flight cruise at an altitude consistent with the direction of flight and as close as possible to 2,000 feet above cruise-climb altitude. Subsequent step climbs would be initiated as soon as gross weight decreases to a value that allows a step climb of 4,000 feet to the next level flight altitude that is less than 2,000 feet above the cruise climb ceiling. This procedure results in approximately 0.3% increase in fuel consumed over the cruise-climb procedure.

The following example illustrates a comparison of cruise-climb vs step-climb procedures for a typical C-141 cruise. Starting weight for cruise-climb was 293,600 lbs., altitude was 35,000 feet, cruise mach number was .717 and range was 1764 nm. For these conditions terminal cruise-climb altitude was 39,000 feet and fuel consumed during cruise-climb was 51,437 lbs. In order to keep initial and terminal conditions the same, level flight cruise was initiated at 35,000 feet altitude and a 4,000 foot step climb was initiated at 860 n.mi. range to 39,000 feet altitude. Climb was executed at NRT thrust setting. The remaining mission was performed in level flight at 39,000 feet. Fuel consumption for the step climb procedure was 51,576 lbs. Note that the step climb flight mode consumed 139 lbs more fuel than cruise-climb which is .27% more than the fuel consumption for the cruise-climb mode.

Conventional Climb Procedures

Conventional climb procedures simulated in this study were obtained from Reference [10]. Conventional climbs are executed at NRT power setting. Due to the ATC constraint, air speed below 10,000 feet altitude is 250 KCAS. Above

that altitude the C-141 conventional climbs are executed at 280 KCAS/.7 Mach number.

Optimum Climb Procedures

The optimum climb algorithm developed in Appendix A provides the optimum altitude (or equivalently air speed) and throttle setting for optimal climb segments. The ATC constraint on maximum climb speed can be enforced in the optimization algorithm. The optimum climb speed for the C-141 below 10,000 altitude is 250 KCAS due to this constraint. Optimum climb solutions have been obtained also by relaxing this constraint to assess the impact of this ATC constraint on optimal climb procedures. In general, both air speed and throttle setting vary continuously for optimal climb trajectories.

Parametric Optimal Climb

Parametric optimal climb is similar to conventional climb and is executed at NRT power setting. The air speed schedule follows a constant KCAS - constant Mach mode. Constant Mach is taken equal to optimum cruise Mach number and the constant KCAS is determined by parametric optimization. The parametric optimal climb procedure takes less time than the optimal climb solution and is easier to implement. Thus for actual implementation on aircraft this procedure may be preferable to the optimal climb procedures.

Comparison of Various Climb Procedures

Table 7.1-3 presents a comparison of various climb procedures for a typical C-141 climb segment. Initial and terminal conditions of all trajectories are the same and are given in the table. The optimal climb trajectory has a path length of 235 nm. The distance traversed during climb for the other climb modes is less than 235 n.mi and the climb segment is followed by a cruise segment at .717 Mach number which is the optimum speed for minimum fuel cruise. The optimum trajectory consumes 11,511 lbs of fuel which is 100 lbs less than the conventional climb.

Initial Conditions
Weight 290,000
Altitude 3,000
Airspeed 250 KCAS

Fuel Conditions
Range 235 NM
Altitude 36,000 ft
Airspeed .717 Mach

Type of Climb	Optimum	Optimum With ATC Constraint	Parametric Optimum 280KCAS/.717M	Conventional With ATC Constraint 250/280/.7M
Climb	235	223	138	134
Cruise	0	12	97	101
Total	235	235	235	235
Climb	11511	11249	8757	8641
Cruise	0	339	2809	2970
Total	11511	11588	11566	11611
Climb	2151	2075	1296	1285
Cruise	0	103	848	886
Total	2151	2178	2144	2171
Fuel	743.8	748.8	747.3	750.2
DOC	868.1	874.6	871.2	875.6
DOC1	990.6	998.7	993.3	999.3
DOC2	1112.5	1122.1	1114.9	1122.3
DOC3	1234.9	1246.1	1236.9	1245.9

Table 7.1-3 COMPARISON OF OPTIMUM VS CONVENTIONAL CLIMB - C-141

However, under the ATC constraint, the optimum trajectory consumes 11, 588 lbs. fuel which is only 23 lbs less than the conventional trajectory. Moreover, the constrained optimal solution takes 7 seconds more time than the conventional trajectory. Also note that the unconstrained parametric optimum trajectory consumes 55 lbs. more fuel (11566-11511) than the optimal solution which is only 0.5% of the climb fuel. Fuel and direct operating costs for the various climb profiles discussed above are also given in Table 7.1-3. Fuel/DOC savings due to the parametric optimal climb procedures are summarized in Table 7.1-4 for the C-141 mission spectrum. Fuel savings due to optimal climb procedures are negligible. Moreover optimal climbs have longer climb time and result in loss of direct operating costs.

Conventional Descent Procedures

Reference [10] outlines procedures for the "enroute" conventional descents simulated in this study for C-141 missions. The aircraft is kept in the clean configuration. Two engines are retarded to idle and two engines at fuel flow of 1500 lb/hrs. Air speed schedule during descent is Mach equal to .74 down to 300 KCAS at which time 300 KCAS is maintained down to 10,000 feet and 250 KCAS below, corresponding to the ATC constraint.

Optimal Descent Procedures

The optimal descent algorithm is similar to the optimal climb algorithm and provides the optimum altitude (or equivalently air speed) and throttle setting for the descent trajectory. Both optimal air speed and throttle setting vary continuously along an optimal descent path.

Parametric Optimum Descent Solution

Parametric optimal descent is executed at idle thrust setting with aircraft in the clean configuration. The air speed schedule is constant Mach/constant KCAS where Mach number is the optimum cruise Mach and KCAS is determined by parametric optimization. The difference between fuel consumed for EEM

COST	ANNUAL SAVINGS DUE TO PARAMETRIC OPTIMUM CLIMB	% SAVINGS
FUEL GALLONS	97,600	0.02
FUEL COST \$	41,000	0.02
DOC	10,300 (loss)	0.003 (loss)
DOC1	60,900 (loss)	0.02 (loss)
DOC2	111,200 (loss)	0.03 (loss)
DOC3	161,700 (loss)	0.03 (loss)

Table 7.1-4 FUEL/DOC SAVINGS DUE TO OPTIMAL CLIMB FOR C-141

optimal and parametric optimal is small, but parametric optimal procedure is easier to implement.

Comparison of Various Descent Procedures

Table 7.1-5 presents the comparison of various descent procedures for C-141. The optimal descent trajectory traverses a 143 nm. range which is taken as the mission range. The descent segment for other trajectories is initiated after a cruise segment so that total mission range for all trajectories is equal to 143 nm. The optimal descent consumes 411 lbs less fuel (2342-1931) than the conventional descent and take 231 seconds more time (1630-1399) for the same mission. The parametric optimum descent consumes only 27 lbs more fuel than the optimal descent (1958-1931) and takes 17 seconds more time (1647-1630) than the optimal descent. Conventional descent with all four engines retarded to idle setting consumes 92 lbs less fuel than "enroute" conventional descent fuel (2342-2250) and direct operating cost values for various descent procedures is also given in Table 7.1-5. Direct operating costs for the "enroute" conventional descent is less than the cost for the other descent procedures because this descent takes less time than the others.

Estimated fuel/DOC savings (loss) due to the parametric optimal descent procedure for C-141 missions are given in Table 7.1-6. A 0.56% fuel savings may be achieved by optimal descent procedures. However, optimal descent results in loss of direct operating cost for DOC 1 through DOC 3.

Integrated Optimal Trajectories

Mission spectrum data for C-141 obtained by processing ASIMIS tapes is given in Subsection 7.1.2. As mentioned earlier ASIMIS tape data for the C-141 gives cruise altitude and mach in bands. Since most of the long and medium range missions fly above 35,000 altitude and at an air speed between .71 and .8 mach, initial level-off altitude and mach number for these missions were assumed as 35,000 feet and 0.75 mach number, respectively. It was also assumed that for the long range mission a step climb to 39,000 feet altitude is performed.

Initial Conditions
 Weight 230,000
 Altitude 35,000
 Airspeed .7 Mach

Final Conditions
 Range 143 nm.
 Altitude 3,000 ft

Type of Descent	Optimal Descent [†]	Parametric Optimum at Idle Thrust	Conventional Descent at Idle Thrust	"En-Route" Conventional Descent
Cruise	0	28	57	36
Descent	143	115	86	107
Total	143	143	143	143
Cruise	0	682	1387	886
Descent	1931	1276	863	1456
Total	1931	1958	2250	2342
Cruise	0	250	508	322
Descent	1630	1397	882	1077
Total	1630	1647	1490	1399
Fuel	124.8	126.5	145.4	151.3
DOC	218.9	221.7	231.5	232.1
DOC1	311.8	315.4	316.3	311.8
DOC2	404.2	408.8	400.8	391.1
DOC3	497.0	502.6	485.6	470.7

† Note that the optimal descent solution is that for min fuel only

Table 7.1-5 COMPARISON OF OPTIMAL VS CONVENTIONAL DESCENT C-141

COST TYPE	ANNUAL SAVINGS DUE TO PARAMETRIC OPTIMAL DESCENT	% SAVINGS
FUEL GALLONS	3,398,000	0.56
FUEL COST \$	1,427,000	0.56
DOC	393,000	0.12
DOC1	626,000 (loss)	0.17 (loss)
DOC2	1,640,000 (loss)	0.38 (loss)
DOC3	2,660,000 (loss)	0.53 (loss)

Table 7.1-6 FUEL/DOC SAVINGS DUE TO OPTIMAL DESCENT - C-141

Conventional missions were simulated under these assumptions making 10% allowance for increased fuel flow rate reported in Reference [42]. Total fuel consumption for simulated missions was comparable to actual fuel consumption obtained from processing ASIMIS tapes. However, the missions which fly above 32,000 altitude were also simulated assuming that the missions were flown at optimum cruise altitudes (indicating best C-141 operation) and then assuming that the missions were flown at 32,000 feet altitude (indicating worst operating conditions). Table 7.1-7 indicates the difference of fuel and direct operating costs for the two extreme operating conditions compared to nominal operating conditions assumed for these missions. These values indicate the uncertainties in fuel/DOC savings due to trajectory optimization procedures for C-141 operations. The remaining integrated trajectory study results were obtained assuming the nominals mentioned earlier: a 35,000 foot altitude and an air speed of .75 mach.

As shown earlier, fuel savings due to optimal climb and descent procedures are small compared to conventional methods, especially under ATC constraints. Therefore conventional climb and descent procedures can be used in the determination of whether changes in the airborne procedures can produce fuel/DOC savings.

The trajectory parameters that impact fuel/DOC are altitude and air speed, and it is changes in these two parameters which will be investigated.

Figures 7.1-14 and 7.1-15 illustrate fuel and DOC savings due to reduced speed and increased altitudes for long range and medium range C-141 missions. Δ Mach indicates the decrease in cruise mach number from the average cruise mach number obtained from the ASIMIS tape. ΔH indicates the increase in cruise altitude from the average cruise altitudes of the mission spectrum. Since long range cruise altitudes were already assumed close to optimum cruise

COST TYPE	SAVINGS AT BEST CRUISE ALTITUDE	LOSS AT WORST (32,000 FT) CRUISE ALTITUDE
FUEL GALLONS	10,022,000	25,584,000
FUEL COST \$	4,209,000	10,745,000
DOC	4,039,000	10,115,000
DOC1	3,869,000	9,485,000
DOC2	3,699,000	8,855,000
DOC3	3,529,000	8,225,000

Table 7.1-7 COMPARISON OF THE FUEL/DOC FOR THE BEST AND WORST CRUISE ALTITUDES WITH RESPECT TO A NOMINAL OPERATING ALTITUDE OF 35,000 FT FOR C-141

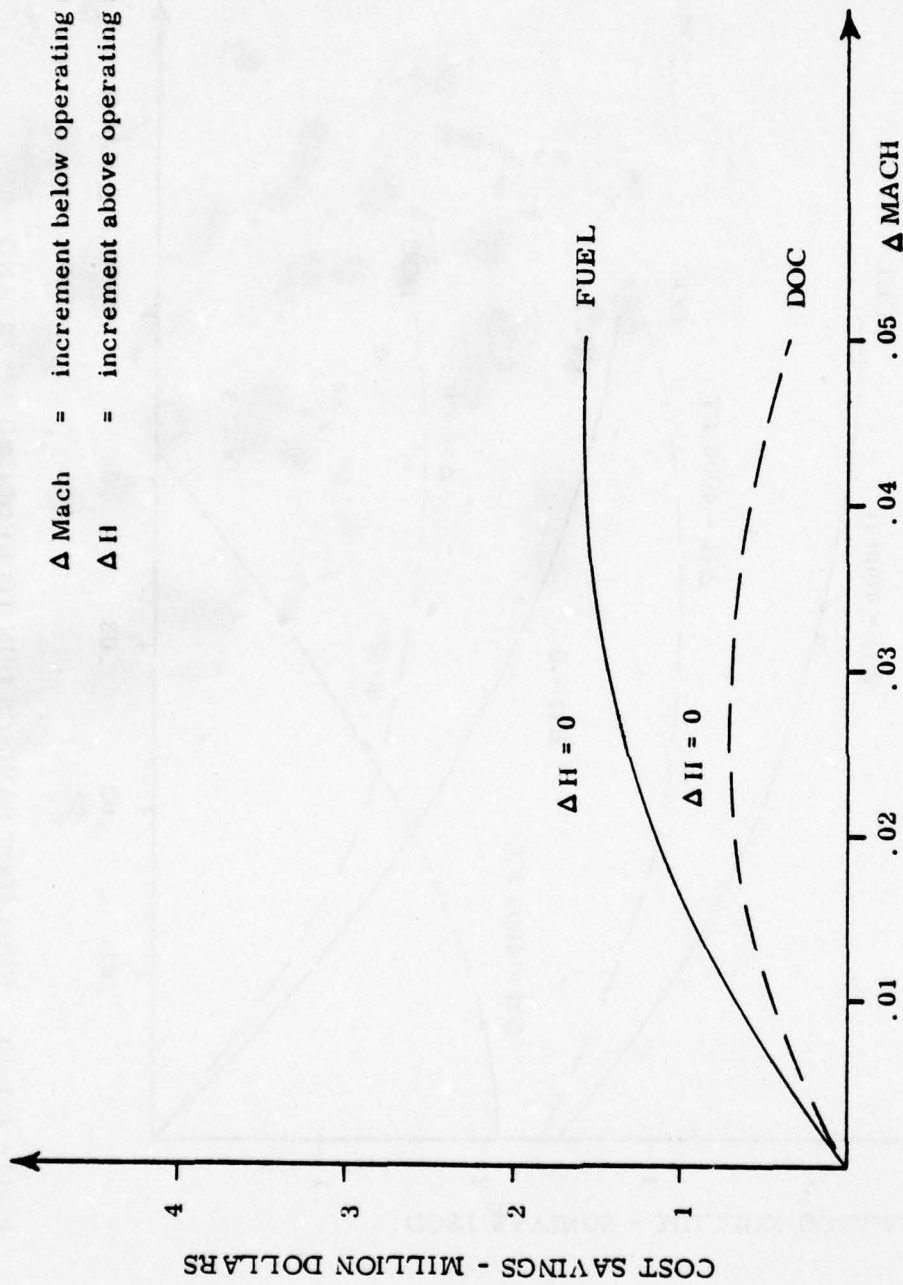


Figure 7.1-14 FUEL/DOC SAVINGS DUE TO REDUCED SPEED-C-141 LONG RANGE MISSIONS

Δ Mach = increment below operating air speed
 Δ H = increment above operating altitude

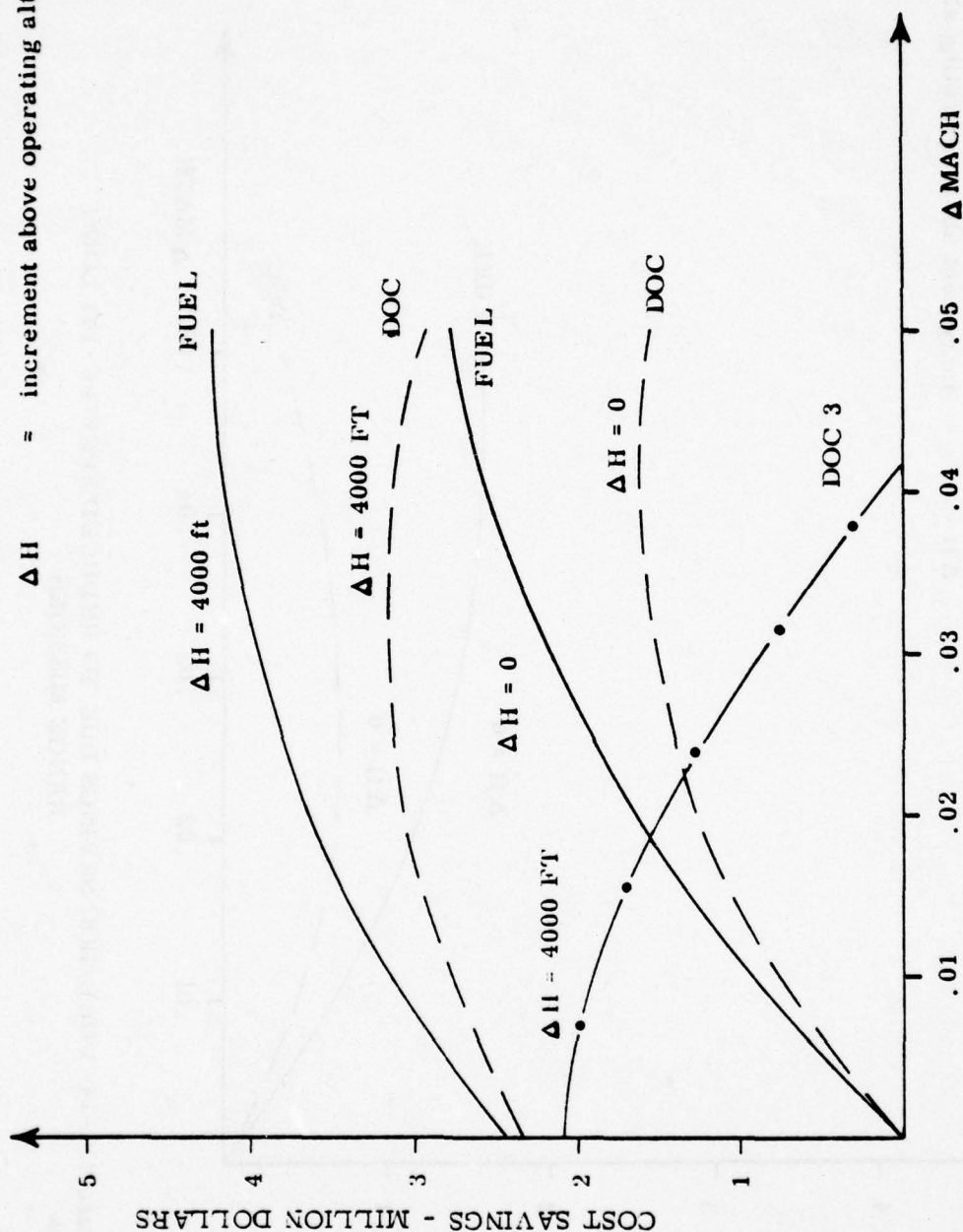


Figure 7.1-15 FUEL/DOC SAVINGS DUE TO REDUCED SPEED AND INCREASED ALTITUDES C-141 MEDIUM RANGE MISSIONS

altitudes, there is no altitude increment indicated for these missions. For the medium range case some of the missions were flown at optimal cruise altitudes and some were not. Results are presented in Fig. 7.1-15 for two cases: (1) for $\Delta H = 0$ none of the operating altitudes are changed and for $\Delta H = 4000$ ft those missions which were flown below their respective optimal altitudes have been raised by 4000 ft, the minimum increment allowed by ATC regulations at 29,000 feet and above. For long range missions the maximum fuel savings occurs with a reduction of .05 in the Mach number. The DOC savings in the case, however, peaks at a reduction of about .02 in the Mach number and decreases for further reductions. For the medium range missions the maximum fuel savings again occur for the largest reduction in Mach number investigated: namely, .05. For DOC the maximum occurs for smaller Δ Mach numbers, and for DOC 3, which weights time more heavily, the peak is at a Δ Mach of zero. In Fig. 7.1-15 it is seen that raising those missions flown at lower cruise altitudes to their optimal altitudes (the $\Delta H = 4000$ ft case) increases the fuel and DOC cost savings considerably.

Table 7.1-8 summarizes the results of the integrated optimal trajectory evaluation, including the short range mission. Graphs for the short range mission were not shown as a result of the large altitude variations which are possible and thus difficult to present in graphical form.

7.1.5.3 Delayed Flap Approach Procedure

Delayed flap approach procedures reduce both fuel consumed and time spent during the approach segment for C-141, thus resulting in both fuel and direct operating cost savings. Table 7.1-9 summarizes results of an evaluation of delayed flap approach procedure. The first column indicates the altitude above the runway where the aircraft attains a stable approach speed. For conventional approach this altitude is 1500 feet above the runway. Observe that fuel and DOC savings increase as the altitude for stable configuration is decreased. The maximum fuel savings due to delayed flap approach is about 0.5%.

7.1.5.4 AFT C.G. Operations

As mentioned in Section 4, the operation of an aircraft with c.g. further aft than

Mission Type	Maximum Savings					
	Fuel Gallon	Fuel Cost	DOC	DOC1	DOC2	DOC3
Long Range	3,764,300	1,581,000	687,600	241,000	22,500	0
Medium Range	10,077,000	4,232,300	3,136,700	2,556,200	2,149,600	2,059,000
Short Range	5,797,700	2,435,000	2,115,500	1,869,700	1,661,300	1,488,701
Total	19,639,000	8,248,300	5,939,800	4,666,900	3,833,400	3,647,700
\$ Savings	3.27	3.27	1.89	1.24	.88	.73

Table 7.1-8 C-141 ANNUAL SAVINGS DUE TO INCREASED ALTITUDES AND
REDUCED SPEED

Altitude for Stable Landing Speed	ANNUAL SAVINGS									
	Fuel/Gal.	%	Fuel Cost	%	DOC	%	DOC1	%	DOC2	%
1000	1,097,000	.18	460,700	.18	495,800	.16	530,400	.14	564,800	.13599, 400.12
500	2,149,000	.36	902,500	.36	961,100	.31	101,900	.27	107,600	.25113, 400.23
0	3,130,000	.52	1,314,800	.52	1,371,500	.44	142,700	.38	148,100	.34153, 900.31

Table 7.1-9 ANNUAL FUEL/DOC SAVINGS DUE TO DELAYED FLAP APPROACH - C-141

those being used, but within stability margin, results in reduced fuel consumption. Since the C-141 is a cargo aircraft, its c.g. can be shifted by the proper distribution of fuel and payload. During flight, burning fuel evenly towards aft c.g. also results in fuel savings.

In a prior study of fuel savings due to aft c.g. operations for the C-141, it was estimated that about 1% fuel savings were possible [33]. For this study fuel savings due to aft c.g. operations for C-141 were calculated by considering the average weights and cruise conditions for long range and medium range missions. For each mission, reduction in aerodynamic drag and the corresponding fuel savings were computed as a function of the shift in c.g. Final results were obtained by averaging over the mission spectrum. A 5%-MAC (mean aerodynamic chord) shift in c.g. towards aft results in 0.7% savings in fuel consumed for the C-141. This amounts to 4.2 million gallons fuel savings annually for C-141 operations. In order to fully realize the potential of aft c.g. operations each mission will require careful distribution of fuel and payload.

7.1.5.5 Reduced Reserve Fuel

Average landing fuel for each mission type is shown on histograms given in Subsection 7.1.2. These values indicate that the reserve fuel carried by the C-141 is much higher than required. Thus fuel savings can be realized by reducing the reserve fuel to the current requirements, which for most of the C-141 missions include an en route reserve, a destination-to-alternate reserve and fuel for 45 minutes of holding. In determining reserve fuel requirements it is assumed that an alternate is available within 200 nmi of the original destination. The C-141 has adequate navigational equipment: thus en route reserve may not be required. Also, the 45 minute holding time requirements may be relaxed, especially when an alternate is available. Thus fuel savings due to reduced reserve fuel have been determined under four options given below:

- 200 nm alternate plus en route reserve plus 45 minute holding time (current requirement)
- 200 nm alternate plus 45 minute holding time
- 200 nm alternate plus 15 minute holding time
- 200 nm alternate

Fuel and direct operating cost savings which can be achieved by reducing the reserve fuel carried on board are given in Table 7.1-10. Savings in fuel consumption by reducing the reserve fuel to the current requirement is 3.7%. However, by relaxing the reserve fuel requirements, up to a 5.7% fuel savings can be achieved. Note that optimal flight procedures will result in further reduction in reserve fuel requirements. However, the additional savings will not be significant.

7.1.5.6 Reduce Engine Load

Fuel savings can be realized by reducing accessory loads on engines and bleed air extraction. For C-141, use of wing and engine anti-icing results in a substantial increase (9%) in fuel consumption rate as mentioned in Subsection 4.3. Thus anti-icing should be used only when necessary. Power demands can be reduced by turning off unnecessary lights and equipment and by running the airplane warm. Assignment of a savings factor is unwarranted in this case since it is one of those operational procedures which require continued attention to achieve.

7.1.5.7 Reduce Engine Use and Taxi Time

Average fuel consumption for C-141 during ground operations is 100 lbs/minute with four engines operating. Fuel consumption during ground operations can be reduced by delaying engine starts until clearance to taxi is obtained, taking the shortest route to runway/ramp, and by using intersections for take-offs. Every minute of reduced taxi time amounts to an annual saving of 1.25 million gallons of fuel and \$804,000 in DOC for the C-141 fleet.

7.1.5.8 Partial Engine Taxi

Two engines may be shut down for taxi-in and parking for the C-141. Assuming 5 minute average taxi time, this procedure can save 3.1 million gallons of fuel and \$1.3 million DOC annually for C-141 operations.

Requirement Option	Savings Due to Reduced Reserve Fuel									
	Fuel		DOC		DOC1		DOC2		DOC3	
	Million Callons	\$ -1000	\$	\$ -1000	\$ -1000	\$	\$ -1000	\$	\$ -1000	\$
200 nmi. Alternate & 45 min. Holding & Enroute Reserve	22.4	9,400	3.7	9,490	9,560	2.5	9,610	2.2	9,670	1.9
200 nmi. Alternate & 45 min. Holding	28.1	11,820	4.7	11,890	11,970	3.2	12,050	2.8	12,120	2.4
200 nmi. Alternate & 15 min. Holding	32.2	13,540	5.4	13,630	13,730	3.7	13,820	3.2	13,920	2.8
200 nmi. Alternate	34.1	14,340	5.7	14,450	14,460	3.8	14,670	3.4	14,780	3.0

Table 7.1-10 FUEL/DOC SAVINGS DUE TO REDUCING RESERVE FUEL TO REQUIREMENTS
FOR C-141

7.1.5.9 Removing Excess Equipment

As mentioned in subsection 4.3.3, Reference [32] indicates that for the C-141 aircraft, 6477 pounds maximum weight reduction is possible. Out of this only 282 pounds reduction can be achieved for all missions and the remaining 6195 pounds is mission oriented. The average weight reduction for C-141 operations will be taken for this study as 2000 pounds. This weight reduction results in 3 million gallons annual savings in fuel for C-141 operations and the DOC savings amount to \$1.26 million/year. Fuel saving is almost 0.5% of annual fuel consumption for the C-141.

7.1.5.10 Maintenance to Reduce Drag

As mentioned in Subsection 4.3, aircraft surface irregularities, control surface rigging and seal leakages result in increased drag and thus increased fuel consumption. During the field visits the observed aircraft appeared in good state of maintenance and a direct quantification of savings in this case is inappropriate. However fuel/DOC savings due to aircraft maintenance may be estimated from the sensitivity plots given later in Subsection 7.1.6. There it is shown that a 1% reduction in zero lift drag due to aircraft maintenance amounts to a 0.7% reduction in annual fuel cost for the C-141 fleet.

7.1.5.11 Engine Maintenance

Reference [42] reports that average fuel flow rate during C-141 operations has increased by almost 10%. C-141 aircraft have been in use for some time, and TSFC has increased due to engine deterioration with use. However, this engine deterioration appears unavoidable, and the scheduled maintenance procedures are adequate. The fuel economy trim procedure outlined in Subsection 4.3 may offer some savings for the C-141. Fuel/DOC savings due to improved maintenance procedures may be estimated using Figure 7.1-18. For example, if improved maintenance procedures result in a 1.5% improvement in TSFC, Figure 7.1-18 indicates a 1.4% reduction in annual fuel consumption for C-141 operations.

7.1.6 Evaluation of Design Modification

Many design modifications are being considered by the Air Force for C-141 aircraft. These include lengthening the fuselage by 23.3 ft, retrofitting the aircraft with winglets and re-engining C-141's with TF-39 engines. This section evaluates the potential fuel saving for the design modifications being considered for C-141 aircraft.

7.1.6.1 Parametric Analysis of Aerodynamic and Propulsion Design Modifications

Following the general approach outlined in Section 5 for evaluation of design modifications, the generic plots illustrating changes in fuel and DOC as functions of changes in aircraft aerodynamic and propulsion parameters were developed. These plots were obtained by simulating the entire spectrum of missions for each perturbation in aircraft parameter. Thus these plots are representative of the entire C-141 fleet. Figures 7.1-16, 7.1-17 and 7.1-18 illustrate % variations in fuel/DOC as functions of % changes in zero lift drag, induced drag and thrust specific fuel consumption, respectively, for the C-141. Variation in fuel/DOC due to variation in TOGW is shown in Figure 7.1-19. These plots may be used to evaluate any design modification under consideration for the C-141. Specific design modifications considered in this study are winglets and re-engining the C-141 with TF-39 engines.

7.1.6.2 Evaluation of Winglets for the C-141

Winglet design data obtained from Reference [36] indicated approximately a 1.5% reduction in zero lift drag and an 11.0% reduction in induced drag for the C-141. The increase in operational empty weight will be approximately 700 lbs. Based on this data and Figs. 7.1-17, 7.1-18 and 7.1-20, the fuel savings is estimated to be 2.65% and the DOC savings are estimated to be 2.12%. Annual fuel and DOC savings turn out to be 15.92 million gallons of fuel and \$6.67 million DOC.

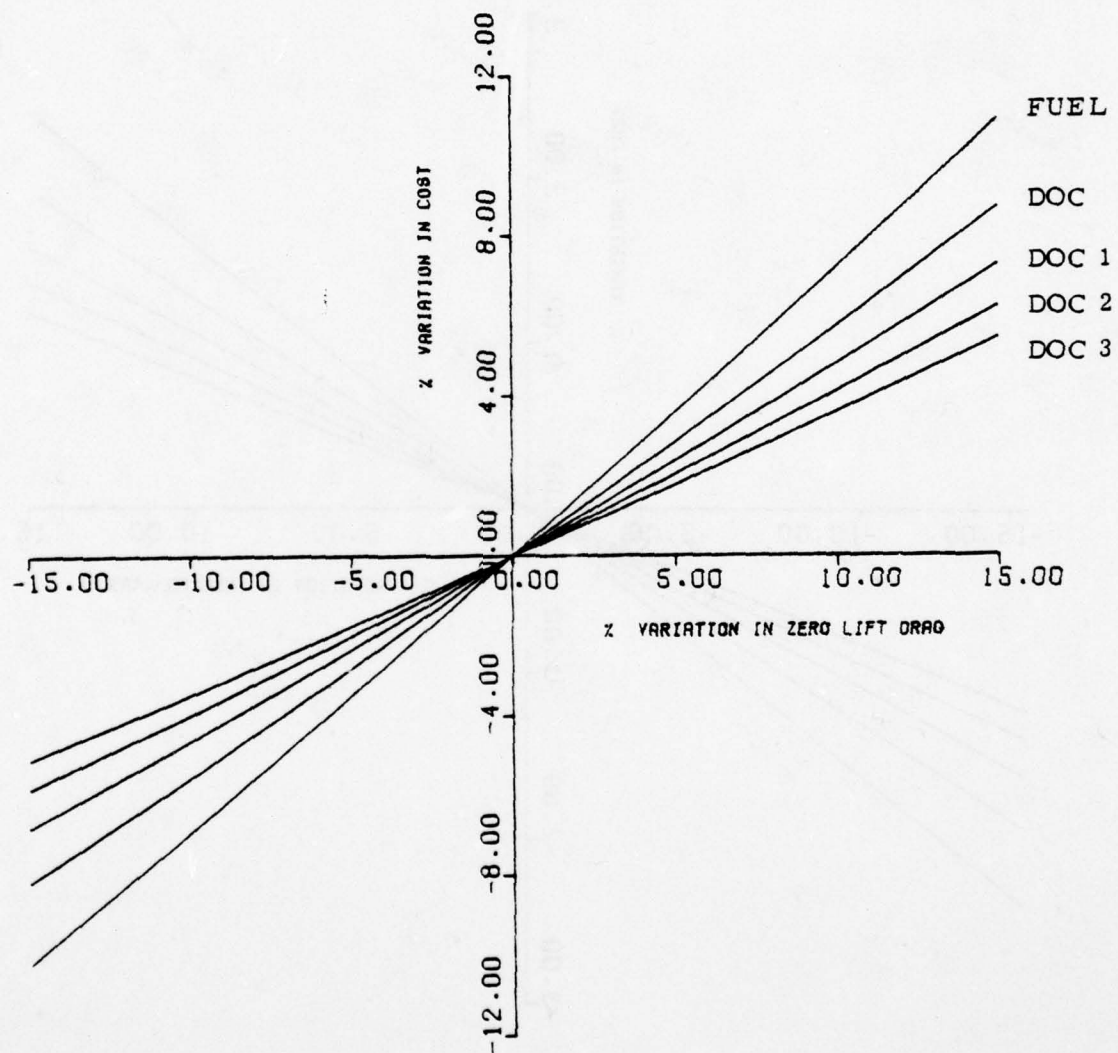


Figure 7.1-16 Sensitivity of Fuel/DOC to Variations in Zero Lift Drag - C-141A

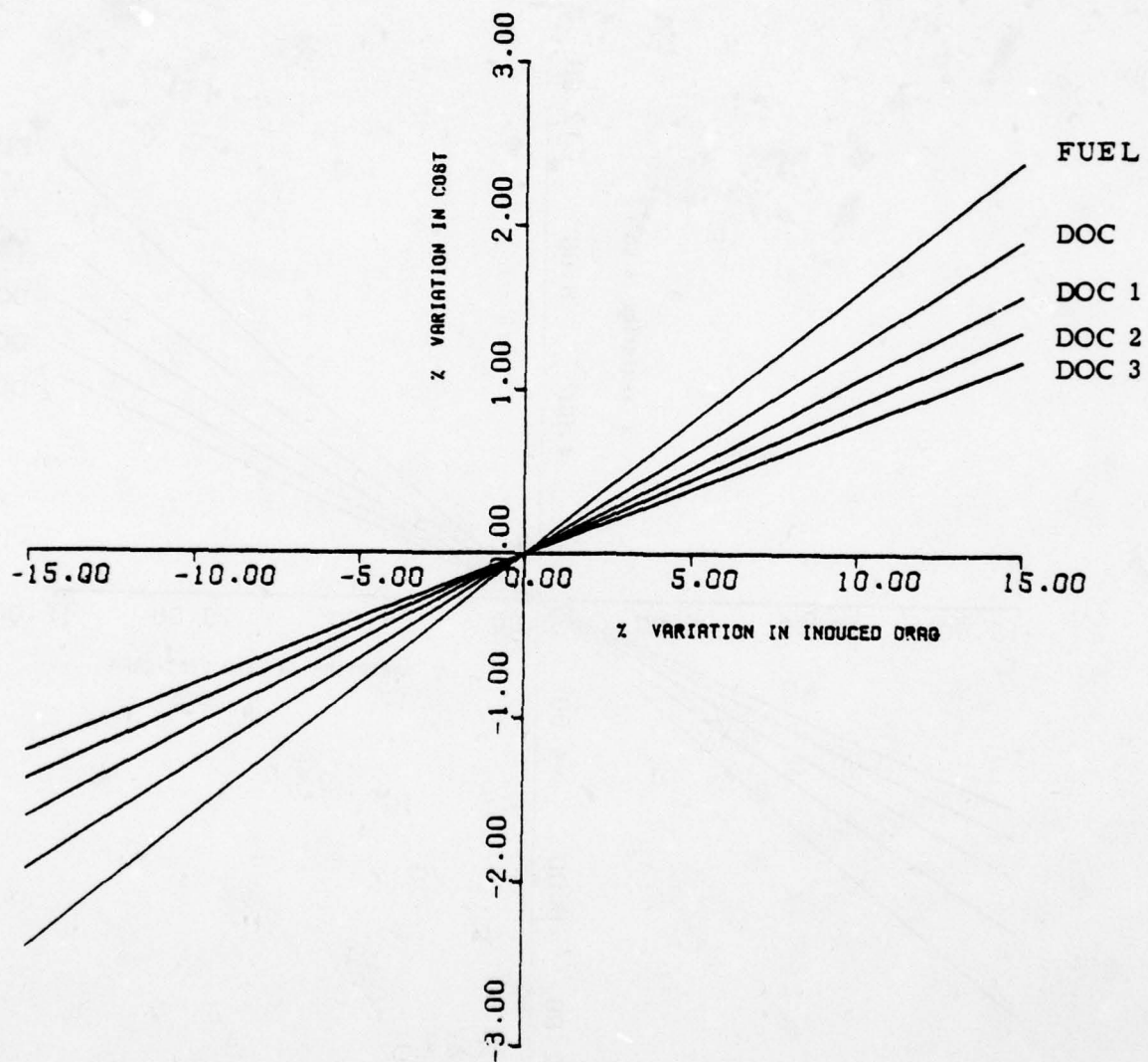


Figure 7.1-17 Sensitivity of Fuel/DOC to Variations in Induced Drag - C-141A

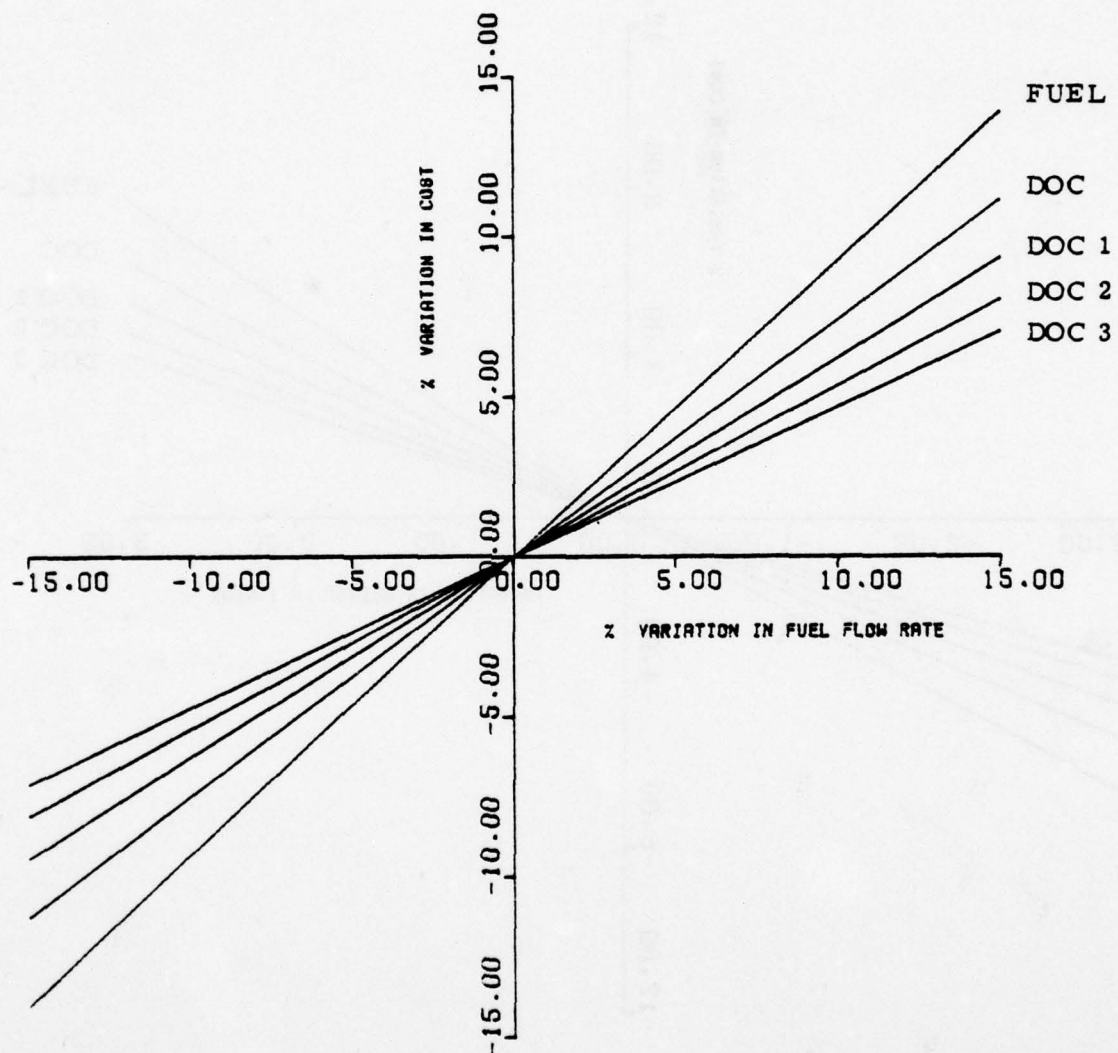


Figure 7.1-18 Sensitivity of Fuel/DOC to Variations in Thrust Specific Fuel Consumption
C-141A

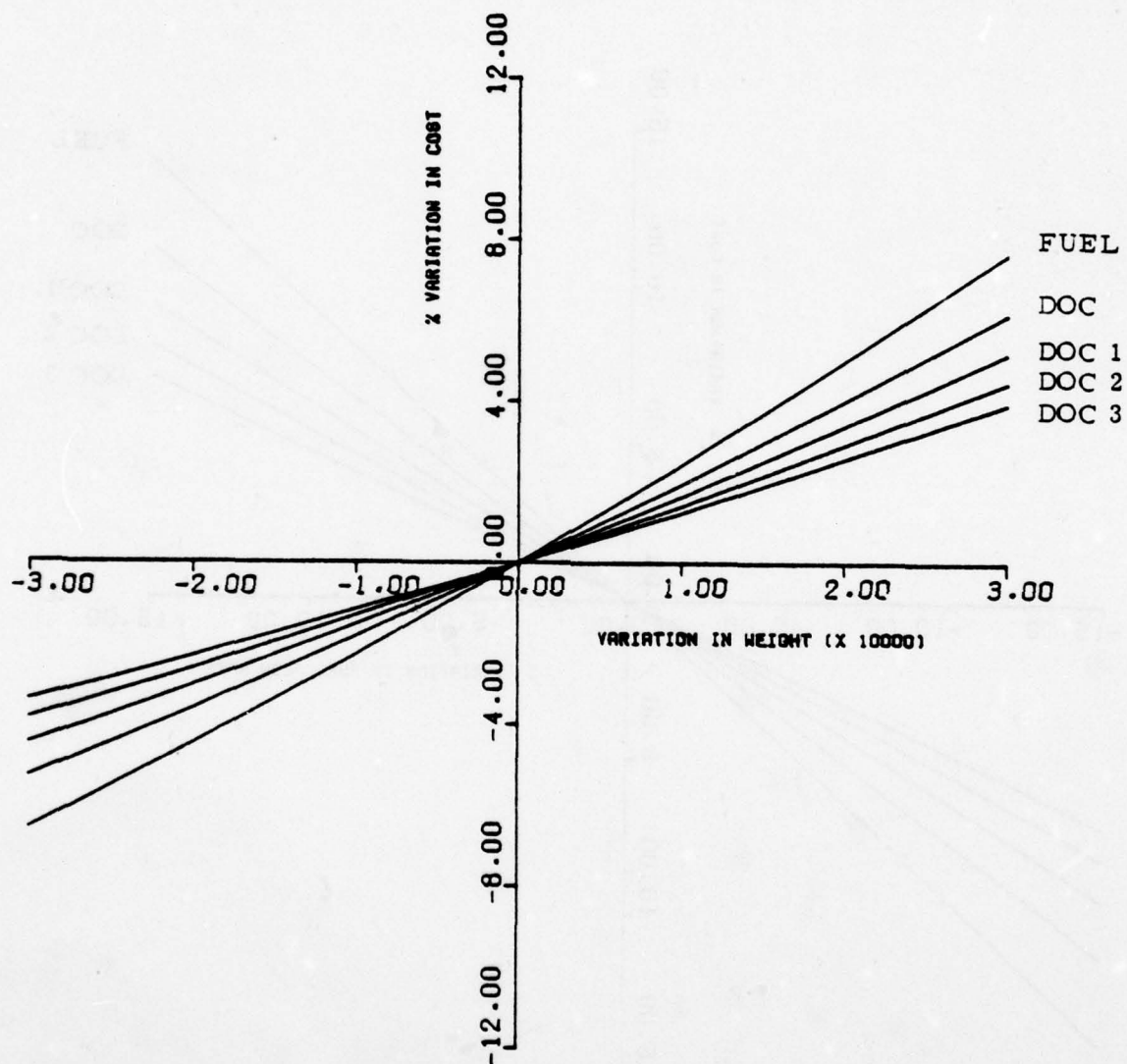


Figure 7.1-19 Sensitivity of Fuel/DOC to Variations in Weight - C-141

By extrapolating the cost estimates for the KC-135 given in Ref. [43] the estimated cost of retrofitting winglets on C-141 will be approximately \$20.0 million. Figure 7.1-20 illustrates accumulated fuel cost savings in 1978 dollars. These estimates indicate that the cost of retrofitting winglets on C-141 can be recovered within three years.

Fuel cost savings can also be obtained under the assumption that airplanes will fly at optimum altitude and Mach and most of the missions will be close to basic design mission. Due to engine deterioration specific fuel consumption of C-141 aircraft has increased approximately 10% as reported in Reference [42]. Thus average range factor for minimum fuel flight condition is 9045. This range factor has a 2% correction for power and bleed extraction plus a climbing cruise correction. Table 7.1-1 gives data for the basic range mission [41]. For evaluation of winglets the following aircraft parameters are considered:

Operating Empty Weight	132,600 lbs.
Payload	72,000 lbs.
Range	2,000 n.mi.

Based on these conditions, fuel consumed is found to be 50632 lbs. Note that no allowance has been made for the reserve fuel.

Now from Figures 7.1-24 and 7.1-25 (Section 7.1.7) which show the sensitivity of range factor to variations in zero lift drag and induced drag, respectively, for C-141, a 1.5% decrease in zero lift drag results in a 0.94% increase in RF, and an 11% decrease in induced drag gives a 4.8% increase in RF. Thus the total improvement in RF due to winglets is 5.74%. Using this value and increasing OEW by 700 lbs, fuel consumption for the basic mission with winglets is calculated as 47751 lbs. Thus under optimum operating conditions fuel saving due to winglets is 5.69% for the basic mission. Based on this value annual fuel savings increase to 34.18 million gallons. Ferry mission range will increase by 5.35%.

COST/SAVINGS TRADEOFF (1978 DOLLARS JP-4 @ 42 CENTS GALLON)

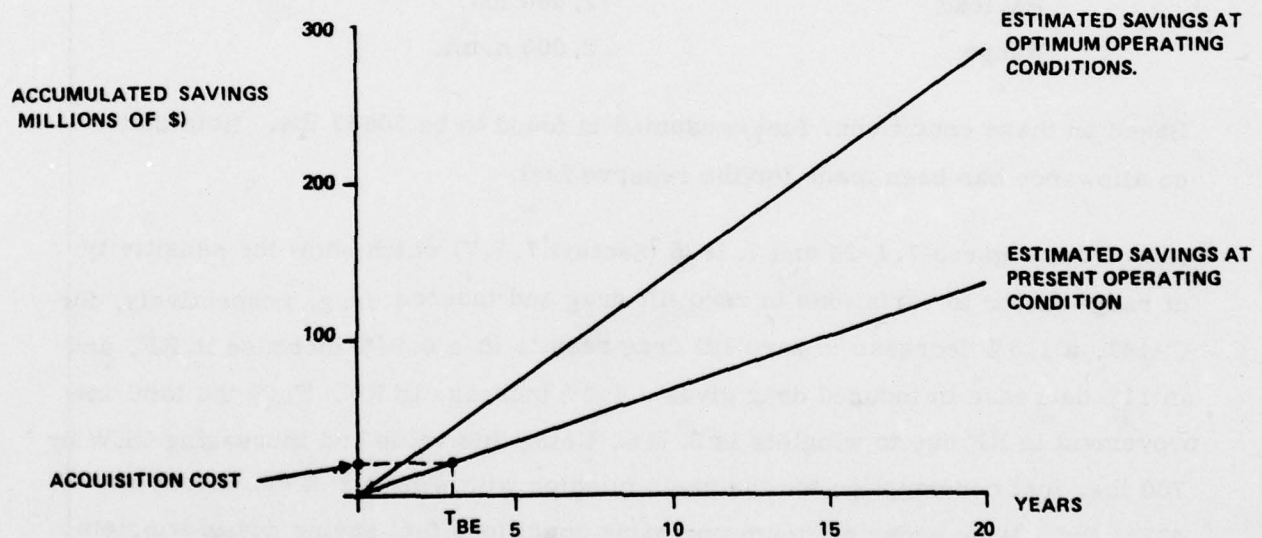


Figure 7.1-20 SAVINGS DUE TO RETROFITTING C-141 WITH WINGLETS

7.1.6.2 Reengining C-141 With TF-39 Engines

The TF-39 turbofan engine is a high bypass unit using the latest technological improvements of all engines presently being used in the military and commercial fields. It is the most economical in fuel consumption. A Rand Corporation study [33] indicates potential savings by replacing the currently installed TF-33-P7 with TF-39 on a 2-for-1 basis. Since C-141 has external pod-mounted engines, the technological risk associated with making the necessary design change to accommodate the new engines are substantially reduced. In considering the TF-39 engine, there is the obvious advantage in that the engine is already developed and non-recurring development costs do not have to be expended.

Mathematical models describing propulsion characteristics of TF-39 engines were developed for performance valuation of the C-5A aircraft under study. These propulsion models were used for evaluating potential savings from engine retrofitting. This evaluation was conducted under the assumption that operating conditions will not change appreciably due to re-engining. Thus range, altitude, airspeed and landing fuel weight values were kept the same as obtained from the ASIMIS tapes. The weight of 2 TF-39 engines is about 4,000 lbs less than that of 4 TF-33 engines. Thus take-off gross weight of the entire mission spectrum was adjusted to account for this difference in engine weight and reduced fuel required by TF-39 engines to perform the same missions. The simulation results indicate 24% savings in fuel consumed and 19.4% savings in DOC. Thus 144.2 million gallons of fuel and \$61 million DOC savings per year are possible for the C-141 fleet. Under optimum operating conditions the average range factor with TF-39 engines is 11674 which is 29% higher than current value. Considering the same basic design mission as for winglet evaluation and reducing OEW of C-141 by 4,000 lbs, fuel consumption for the basic design mission is reduced by 26%. The difference between savings based on the entire mission spectrum and on the basic design mission is 2%, which is small compared to the estimated 24% savings. Ferry mission range will increase by 31.4%.

Unit acquisition cost for reengining the entire C-141 fleet would be approximately \$8.4 million in 1978 dollars. Thus the cost of reengining C-141 is estimated as \$2,285 million. Based on these estimates Fig. 7.1-21 illustrates the cost/savings trade-off for retrofitting TF-39 engines on C-141. The acquisition cost of \$2285 million is much higher than the estimated savings for the next 20 years and thus does not appear in the graph.

7.1.6.4 C-141 Vortex Generator Removal

Small rectangular vortex generators were originally built onto the C-141 wing to improve aileron effectiveness and handling qualities in the stall regime. It has been suggested that the vortex generators may no longer be required with the present stick pusher, and efforts are being directed toward their removal. A savings on the order of 35 gal/hr is expected to result from eliminating the extra drag from the wing surface. Figure 7.1-22 shows the accumulated savings and non-recurring cost tradeoff. These estimates were obtained from Reference [32]. The break even period is less than 3 months.

7.1.6.5 C-141 Fillet Revision

The C-141 wing-to-fuselage fillet can be revised to reduce air flow separation resulting in a decrease in drag. The prototype version of the stretched C-141 has such a revised fillet and considerably more information about its effect will be known after testing is conducted. If the entire C-141 fleet is stretched, the intent of this revision will be carried out; however, if a decision is made to not convert all aircraft, consideration of only the fillet modification might be worthwhile. A fuel savings of approximately 117 gal/hr is anticipated. Cost of this modification is estimated at \$50 million in 1978 dollars. Figure 7.1-23 shows the cost/savings tradeoff. The break even period is less than 4 years.

7.1.7 Sensitivity Analysis

This subsection presents sensitivity results for C-141 aircraft due to changes in environmental conditions, instrumentation errors and uncertainties in aircraft parameters.

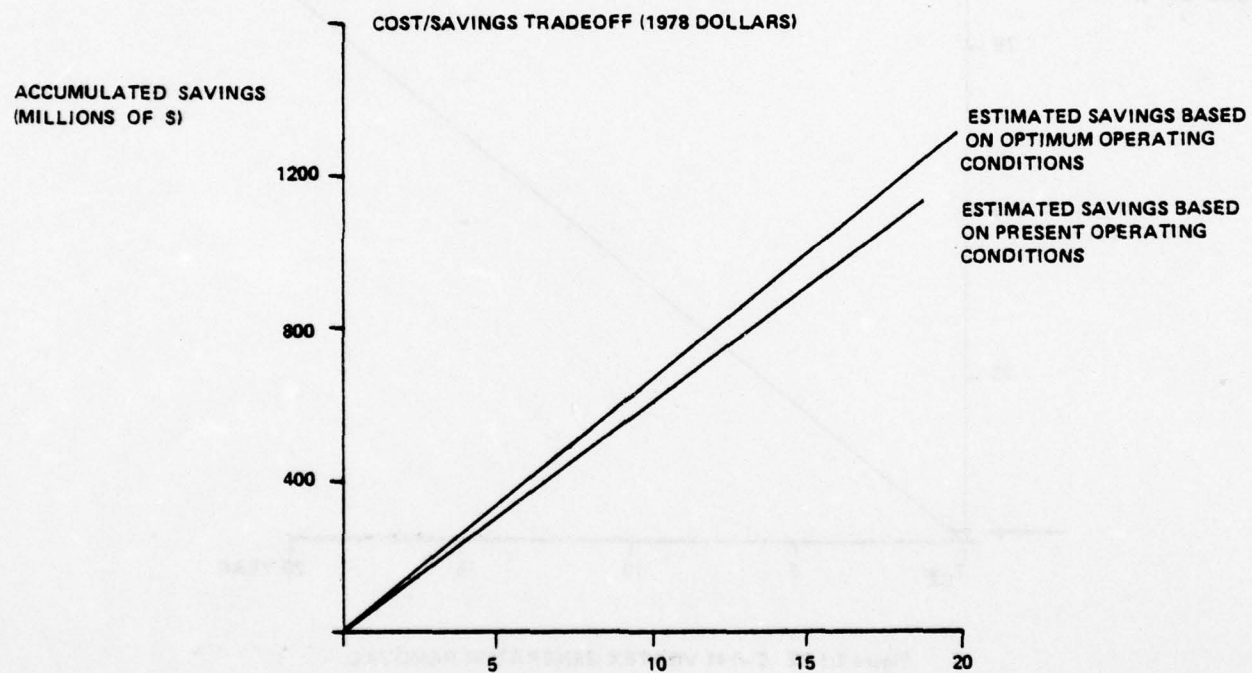


Figure 7.1-21 SAVINGS DUE TO REENGINEING C-141

COST/SAVINGS TRADEOFF (1978 DOLLARS, GAS. @ 42 CENTS GALLON)

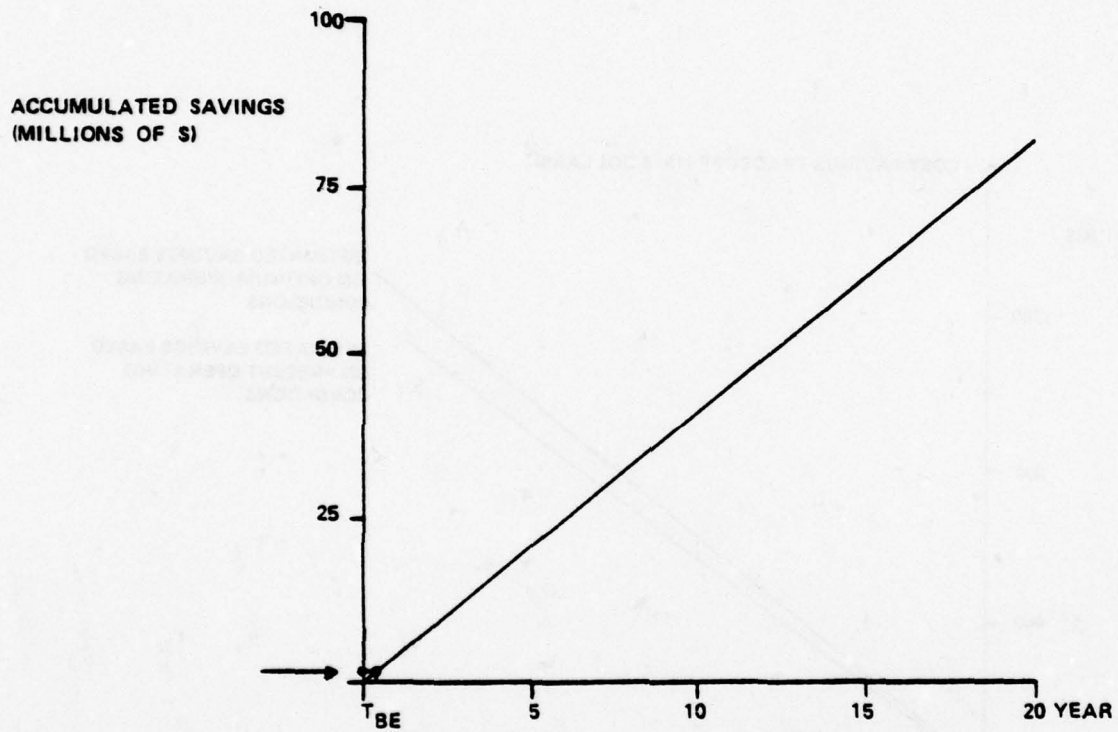


Figure 7.1-22 C-141 VORTEX GENERATOR REMOVAL

COST/SAVINGS TRADEOFF (1978 DOLLARS, GAS @ 42 CENTS GALLON)

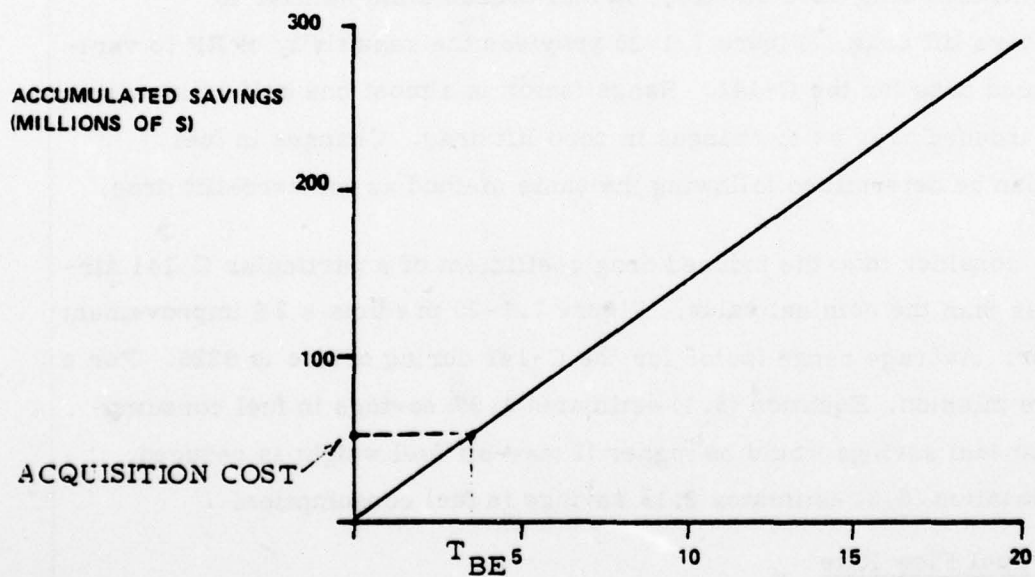


Figure 7.1-23 C-141 FILLET REVISION

7.1.7.1 Uncertainties In Aircraft Parameters

Since no two aircraft are alike, the optimal cruise performance varies for aircraft of the same type due to differences in aerodynamic and propulsion parameters and system weight. The sensitivity of fuel/DOC due to variations in these parameters is presented in this subsection.

Sensitivity to Zero-Lift Drag

Since fuel consumption during cruise depends upon the aerodynamic forces acting on the aircraft, a change in the zero lift drag coefficient directly impacts the fuel consumption. Figure 7.1-24 illustrates the sensitivity of range factor (RF) to changes in zero-lift drag coefficient for the C-141. If the take-off gross weight and mission range remain constant, Figure 7.1-24 can be used to obtain the change in RF due to a change in zero-lift drag. Then Equation (6.1) may be used to obtain the change in fuel consumption.

Sensitivity to Induced Drag

Variations in induced drag have an effect on fuel consumption similar to variations in zero lift drag. Figure 7.1-25 provides the sensitivity of RF to variations in induced drag for the C-141. Range factor is almost one half as sensitive to changes in induced drag as to changes in zero lift drag. Changes in fuel consumption can be determined following the same method as for zero-lift drag.

For example, consider that the induced drag coefficient of a particular C-141 aircraft is 5% less than the nominal value. Figure 7.1-25 predicts a 2% improvement in range factor. Average range factor for the C-141 during cruise is 9226. For a 100 nm. range mission, Equation (6.1) estimates 1.9% savings in fuel consumption. Note that fuel savings would be higher if take-off fuel weight is reduced. In that case Equation (6.2) estimates 2.1% savings in fuel consumption.

Sensitivity to Fuel Flow Rate

Range factor, RF, is inversely proportional to fuel flow rate. Thus an increase in TSFC consumption results in a decrease in RF. Then the change in fuel consumption for a specified mission can be obtained using Equation (6.1).

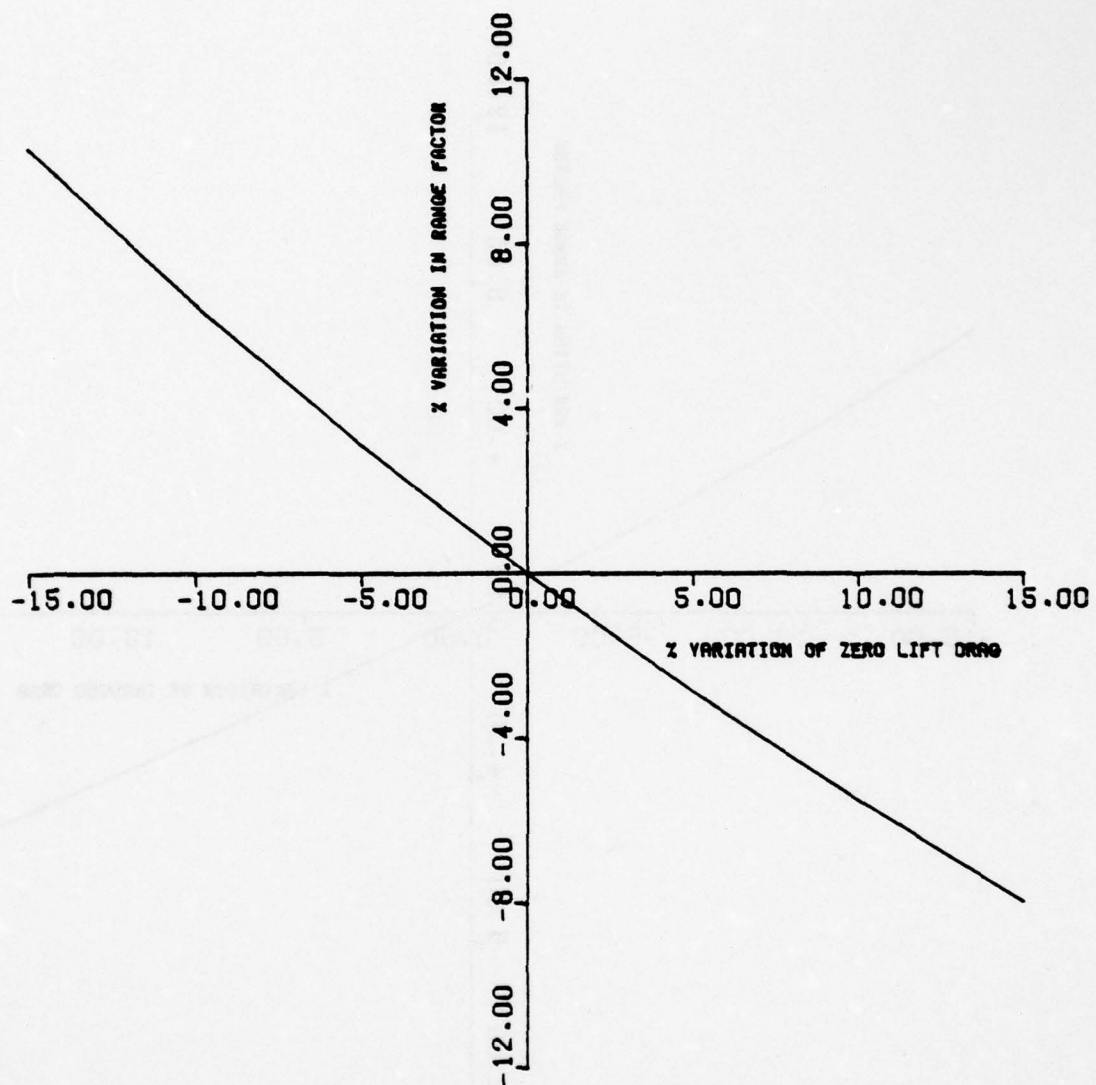


Figure 7.1-24 Sensitivity of Range Factor to Variations in Zero-Lift Drag for C-141

AD-A062 609

DYNAMICS RESEARCH CORP WILMINGTON MASS SYSTEMS DIV
AN ANALYSIS OF FUEL CONSERVING OPERATIONAL PROCEDURES AND DESIG--ETC(U)
JUL 78 R K AGGARWAL

F/G 1/3

F33615-76-C-3104

UNCLASSIFIED

R-247U

AFFDL-TR-78-96-VOL-2

NL

3 OF 6
ADA
062 609



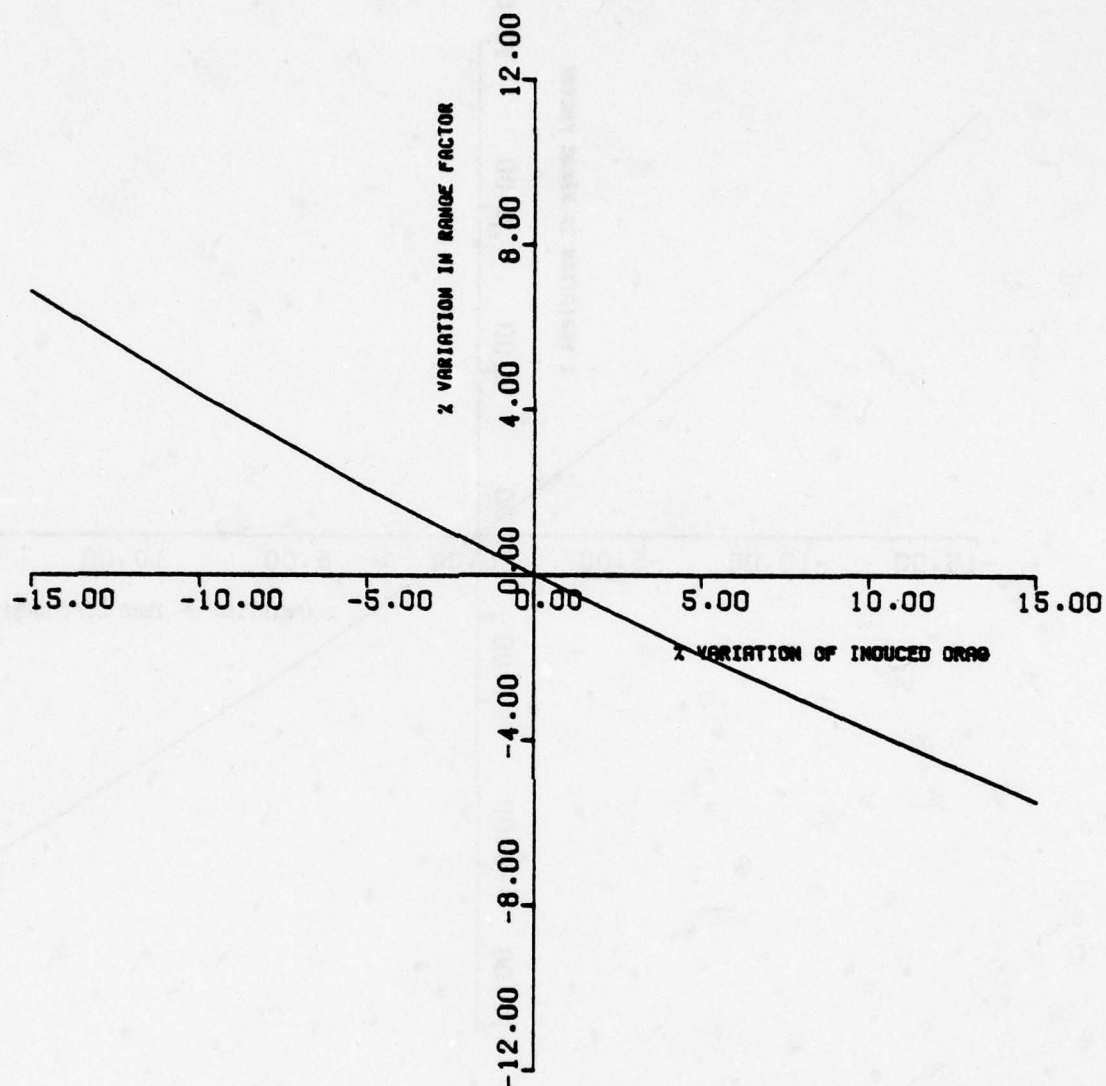


Figure 7.1-25 Sensitivity of Range Factor to Variations in Induced Drag for C-141

For example, consider a 5% increase in TSFC for a C-141 aircraft. The range factor (RF) for C-141 aircraft is 9045. From Eq. (6.1) the fuel consumption will increase by 4.7% for a 1,000 nm. mission. Observe that this result is based on the assumption that the aircraft was already carrying extra fuel. However, if the landing weight is assumed the same as for the nominal, then from Eq. (6.2) the fuel consumption will increase by 5.3%.

Sensitivity to System Weight

Changes in fuel consumed for a mission are proportional to changes in system weight. For example, a 5% increase in TOGW will result in approximately a 5% increase in fuel consumption. Note that the same relation holds for changes in landing weight. Thus a 5% increase in landing weight results in approximately a 5% increase in fuel consumption.

Sensitivity to Variations In Maximum Thrust

Variations in NRT impact the optimum cruise performance through its effect on cruise ceiling. A decrease in NRT lowers cruise ceiling. So long as cruise ceiling remains above optimum cruise altitude, optimum cruise performance is not affected by variations in NRT. Figure 7.1-26(a) depicts variations in cruise ceiling due to variations in NRT for a 293,600 pound C-141 aircraft. Optimal cruise altitude for this aircraft is 35,000 feet. Observe that a 10% decrease in NRT does not effect the cruise altitude.

However a 15% decrease in NRT lowers the cruise altitude by 1,400 feet. Figure 7.1-26(b) illustrates the impact of flying-off optimum cruise altitude on range factor (or equivalently specific fuel consumption). Specific fuel consumption increases by 0.4%.

Variations of NRT also impact the climb performance. However, for most of the missions the change in total fuel consumption will be negligible so long as cruise altitude is not constrained due to variations in NRT.

7.1.7.2 Sensitivity to Atmospheric Variations

The following describes the impact of changes in wind velocity and ambient temperatures on the optimal cruise performance of C-141.

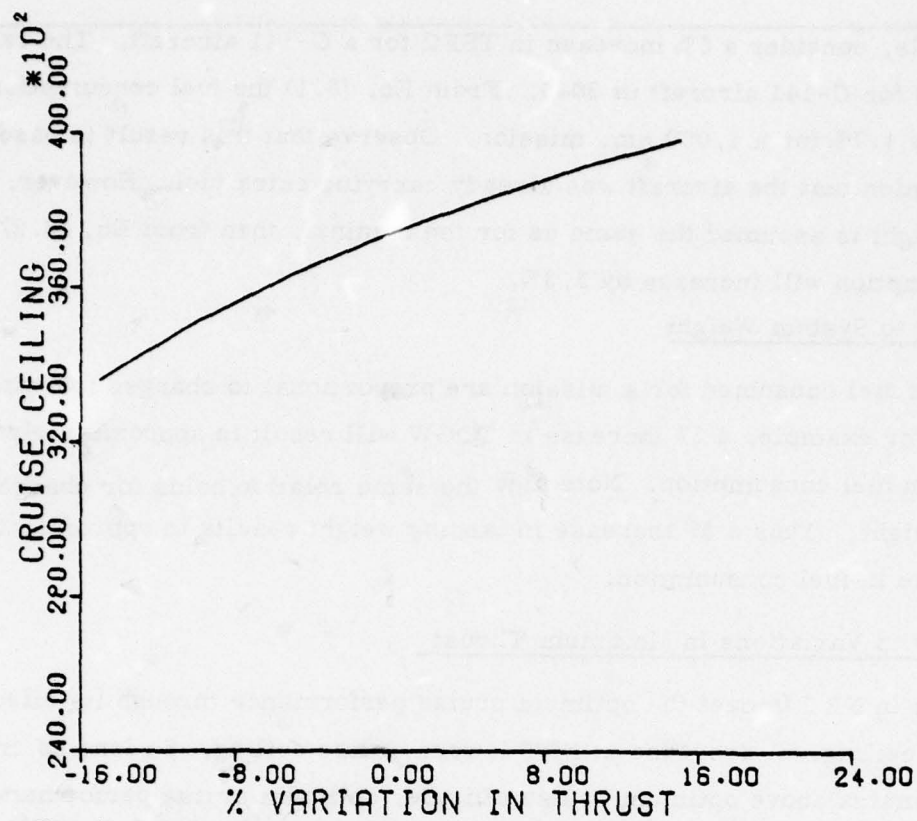


Fig. 7.1-26(a) Impact of Thrust Variation on Cruise Ceiling for C-141

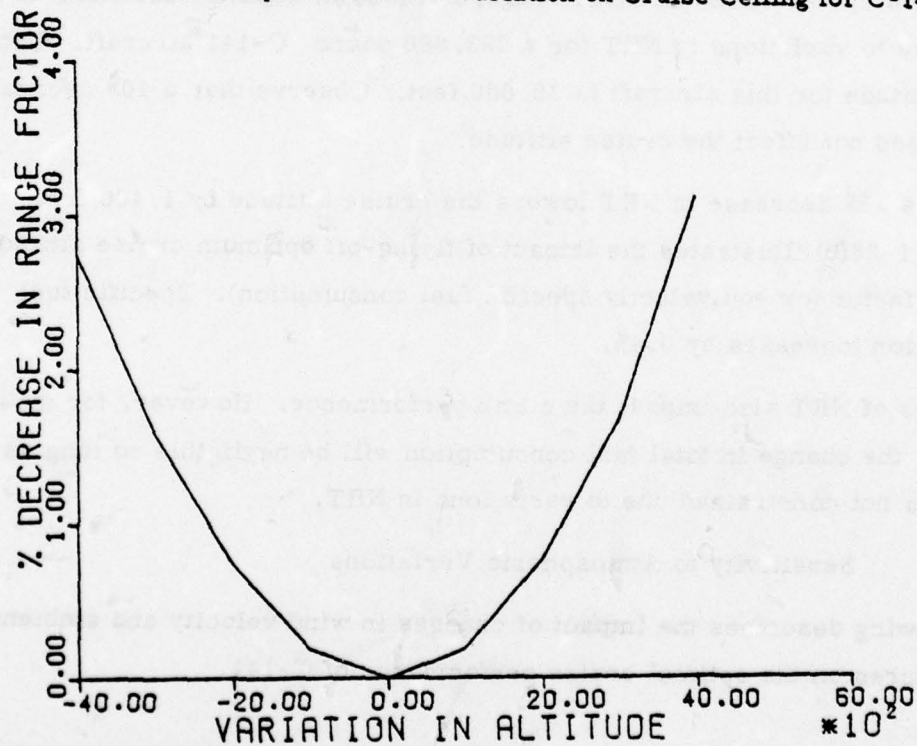


Fig. 7.1-26(b) Decrease in Range Factor due to Flying Off Optimum Cruise Altitude

Temperature Effects

Temperature deviations from the ICAO standard day have no effect on fuel consumed when less than normal rated thrust is required. However, cruise time is modified slightly due to change in true airspeed. For the C-141, each degree centigrade above standard reduces cruise ceiling by approximately 120 feet. Thus for most of the C-141 missions, temperature variation will not affect the fuel consumption. However, impact of temperature may be assessed by first obtaining the cruise altitude ceiling. If this altitude is less than optimum cruise altitude, Figure 7.1-30 may be used to estimate changes in fuel consumption.

Deviations in atmospheric temperatures also impact the climb performance. However, changes in total fuel consumption will be negligible so long as cruise altitude is not affected by ambient temperature.

Wind Effects

Winds have a large impact on the total fuel consumed in flying between two points. Headwinds increase fuel consumption whereas tail winds decrease it. However, the effect of winds on the optimum cruise mach is small as shown in Figure 7.1-27. Head winds increase the optimum cruise mach number slightly where as tail winds decrease it. Changes in specific range due to wind are illustrated in Figure 7.1-28 for a C-141 aircraft with a 293,600 pound weight. Note that a 100 knot headwind decreases the specific range by 24%, and a 100 knot tail wind increases it by almost the same amount.

7.1.7.3 Sensitivity To Traffic Density

An increase in air traffic near an airport generally results in delays in take-off/landing times which in turn result in increased fuel consumption and DOC. Thus the impact of air traffic density can be assessed in terms of increased engine use and taxi time before take-offs and increased holding times before landings. The C-141 aircraft consume an average of 100 lbs fuel/minute during ground operations with all four engines operating. Thus increased fuel consumption due to increased ground time can be easily computed.

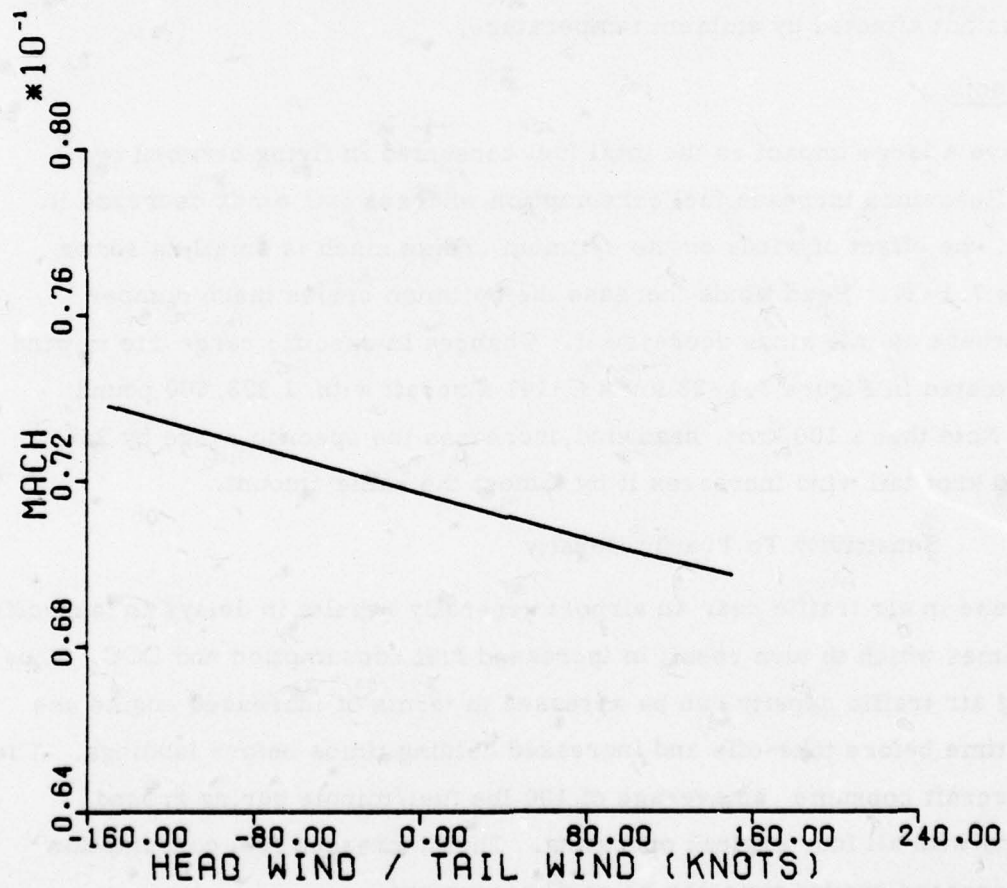


Figure 7.1-27 Impact of Wind on Optimum Cruise Mach Number for C-141

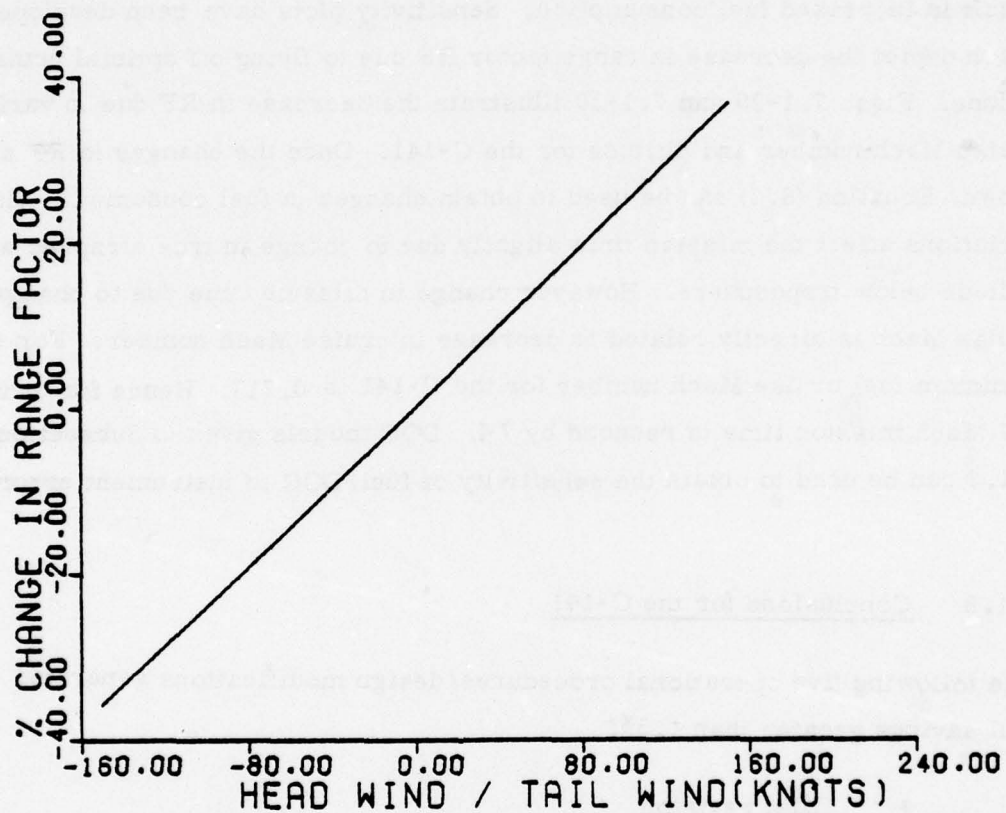


Figure 7.1-28 Impact of Wind on Range Factor for C-141

Fuel consumed/minute during holding varies with holding altitude and aircraft weight. Based on an average landing weight of 200,000 pounds and an optimum holding altitude, the fuel flow rate during holding is 130 lbs/minute. Now the increased fuel consumption due to holding can be calculated by multiplying 130 by the holding time in minutes.

7.1.7.4. Sensitivity To Instrument Errors

Deviations from optimal altitude and air speed due to instrumentation errors result in increased fuel consumption. Sensitivity plots have been developed which depict the decrease in range factor RF due to flying off optimal cruise conditions. Figs. 7.1-29 and 7.1-30 illustrate the decrease in RF due to variations in cruise Mach number and altitude for the C-141. Once the changes in RF are known, Equation (6.1) can be used to obtain changes in fuel consumed. Altitude variations affect the mission time slightly due to change in true airspeed with altitude below troposphere. However change in mission time due to change in cruise Mach is directly related to decrease in cruise Mach number. For example, minimum fuel cruise Mach number for the C-141 is 0.717. Hence for cruise at .77 Mach, mission time is reduced by 7%. DOC models given in Subsection 7.1.3 can be used to obtain the sensitivity of fuel/DOC to instrument errors.

7.1.8 Conclusions for the C-141

The following five operational procedures/design modifications generated fuel savings greater than 1.5%:

- fillet revision
- retrofitting winglets
- removal of vortex generators
- flying at optimum altitude and air speed
- reduced reserve fuel

The C-141 wing-to-fuselage fillet can be revised to reduce air flow separation. The annual fuel savings will be approximately 5.8%, and the modification cost can be recovered within 4 years.

Under present operating conditions winglets offer a 2.7% fuel savings. Even higher savings are possible under optimum operating conditions. The cost of retrofitting winglets can be recovered within three years based on present operating conditions.

Annual fuel savings of 1.7% have been estimated due to removal of vortex generators from the C-141. The modification cost can be recovered within three months.

An annual fuel savings of 3.3% can be achieved by flying at higher altitudes and slower air speed. Since the ASIMIS tape data for the C-141 missions is not precise, the estimated fuel savings can be as high as 7.6% and as low as 1.6%.

The ASIMIS tape data indicates that reserve fuel carried by this aircraft is much higher than required. A 3.7% savings in fuel annually has been estimated for the reduction of reserve fuel to the maximum set of requirements. An additional 2% savings is achievable with a more moderate set of requirements.

All other fuel conserving procedures investigated produced annual fuel savings of 1.5% or less, or a specific savings factor could not be assigned as a result of input variable uncertainties.

These conclusions are summarized in Table 7.1-11.

The potential fuel savings can be categorized as follows:

- | | |
|-----------------------------------|--------------|
| • Design modifications | 10.2 - 13.2% |
| • Airborne operational procedures | 4.8 - 5.8% |
| • Ground operational procedures | 6.7 - 9.2% |

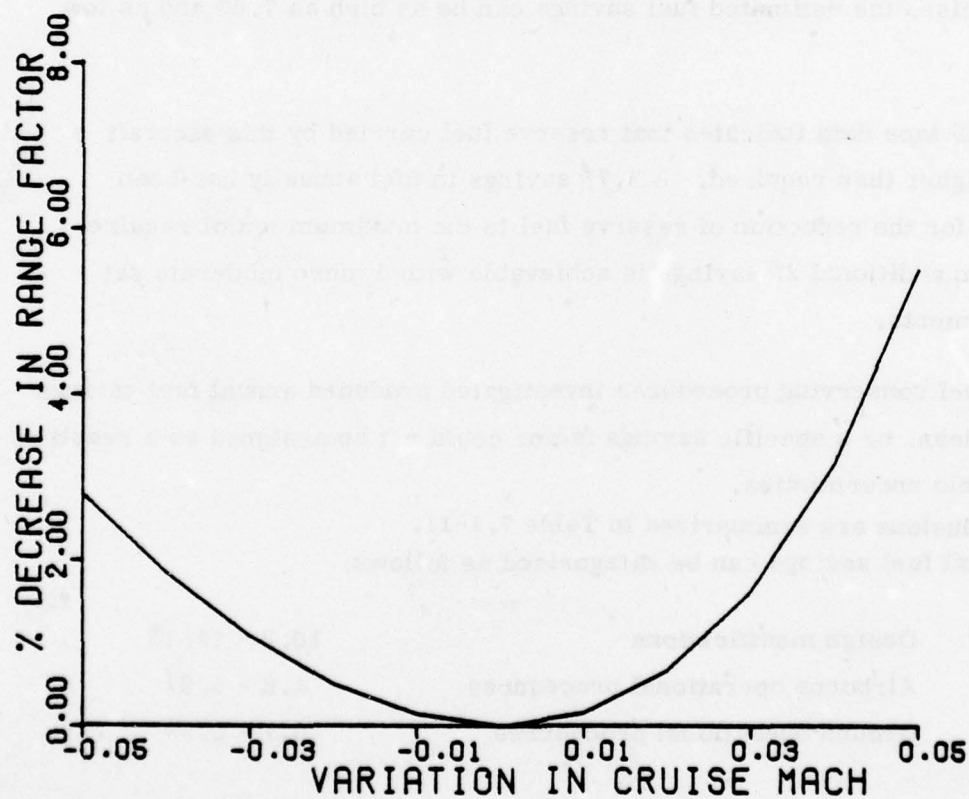


Figure 7.1-29 Decrease in Range Factor Due to Flying Off Optimum Cruise Mach Number

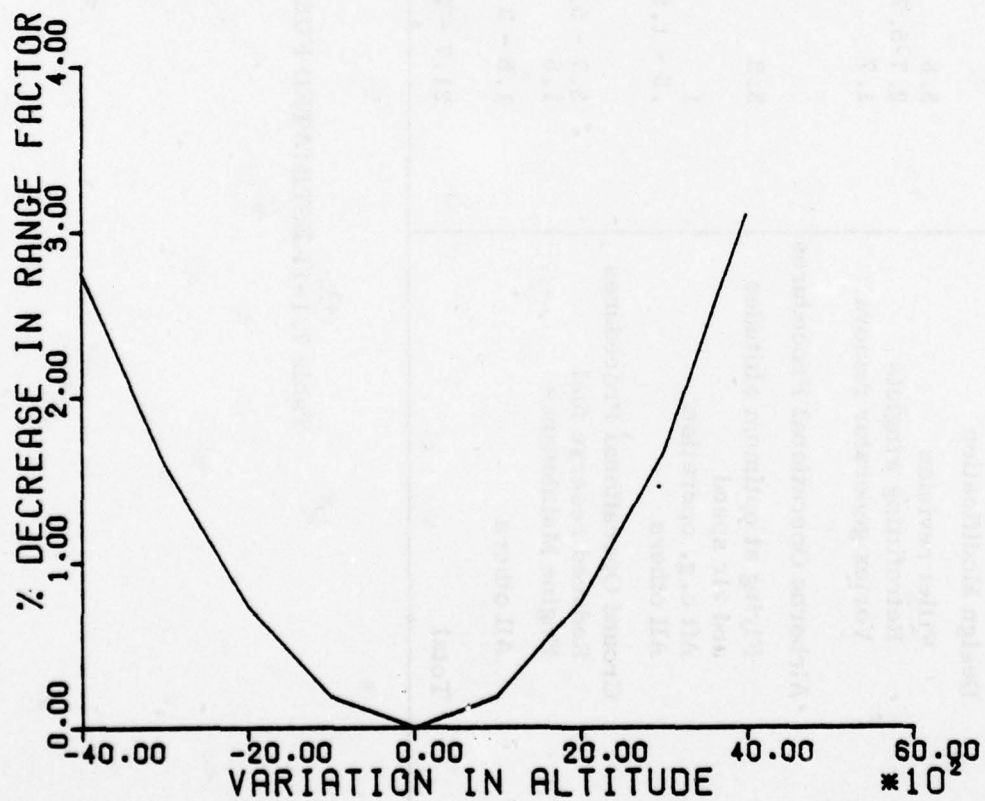


Figure 7.1-30 Decrease in Range Factor due to Flying Off Optimum Cruise Altitude

Procedures	Estimated Percentage Annual Fuel Savings	Break Even Period Years	Confidence In Estimates
Design Modification			
Fillet revision	5.8	3.4	Medium
Retrofitting winglets	2.7-5.7	1.4-3.	High
Vortex generator removal	1.7	.25	Medium
Airborne Operational Procedures			
Flying at optimum altitudes and air speed	3.3	-	Medium
Aft c.g. operations	1	-	High
All others	.5 - 1.5	-	Medium
Ground Operational Procedures			
Reduced reserve fuel	3.7 - 5.7	-	High
Engine Maintenance	1.5	-	Medium
All others	1.5 - 2	-	High
Total	21.7 - 28.2		

Table 7.1-11 ESTIMATED FUEL SAVINGS FOR THE C-141

7.2 C-5A AIRCRAFT

The Lockheed C-5A Galaxy is a four engine, long range, heavy transport aircraft with a primary mission of airlifting personnel and cargo. It is powered by General Electric TF-39 turbine engines rated at 41,000 pounds of thrust each.

The Air Force selected Lockheed, in September 1965, to build the C-5 with the procurement decision to purchase a total of 81 aircraft coming in 1969. Of that number, 77 are active in the inventory today: three were lost in ground accidents, and one crashed in Southeast Asia. The C-5 is involved in three major modification programs: the wing, cargo ramp door fastening system, (whose failure was blamed for the crash of the aircraft in Southeast Asia) and the cargo floors.

7.2.1 Design Mission Data

Typical design mission data for C-5A aircraft is presented in Table 7.2-1. The basic mission has a combat radius of 1000 n.mi., a combat range of 1710 n.mi., and a payload of 265,000 lbs. The maximum take-off gross weight of the C-5A is 762,500 lbs, the maximum payload is 265,000 lbs, the maximum fuel carried is 49,000 gallons, the maximum ferry range is 7,330 n.mi., and the OEW is 325,244 lbs. The design mission data presented in Table 7.2-1 was obtained from Reference [44].

7.2.2 Mission Model

The number of missions flown by C-5A during FY76 was 8800, and the total fuel consumed during FY76 by C-5A was 142.6 million gallons. Total flying time was 42,235 hours [45]. For the purpose of this study the missions are separated into two categories: airlift missions and training missions.

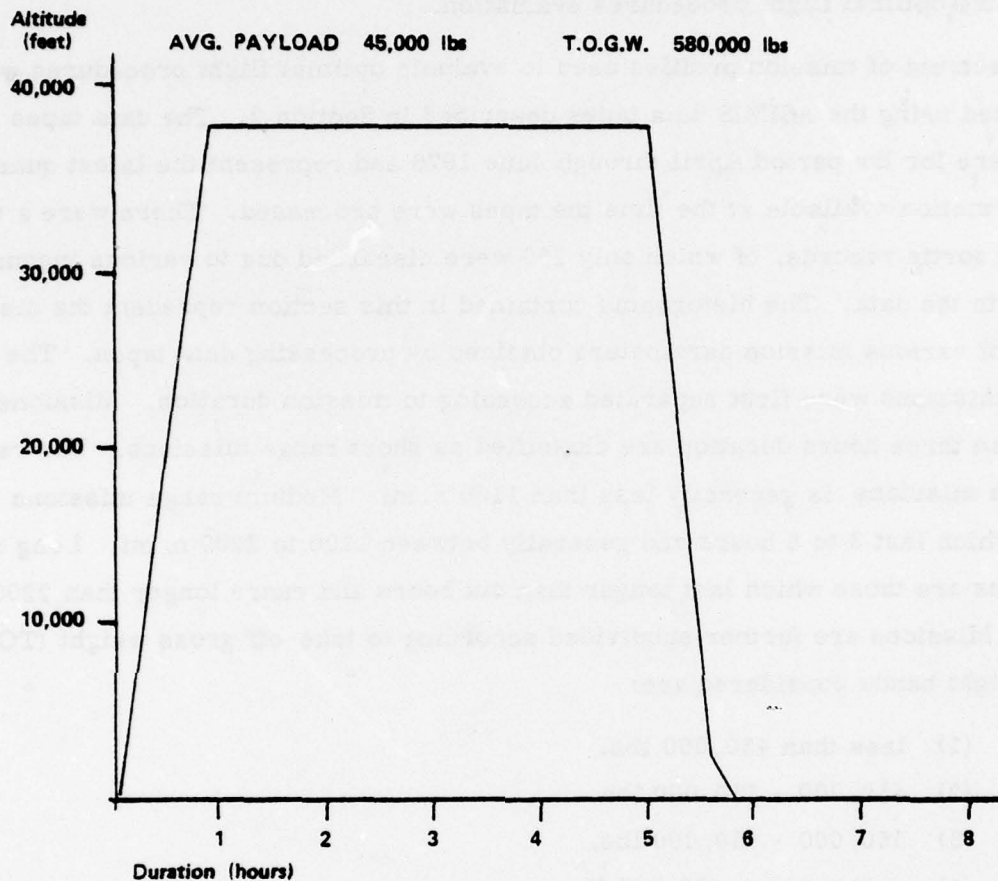
Airlift missions are considered those missions which are flown above 10,000 feet altitude and do not involve multiple take-offs and landings. A typical airlift mission for C-5A is shown in Figure 7.2-1. Airlift missions constitute 66% of the total sorties and 79% of the total flying hours for C-5A. These missions are the ones considered for the evaluation of optimal flight procedures for C-5A.

CONDITIONS		BASIC MISSION	MAX. CARGO MISSION	MAX. RANGE	HIGH SPEED MISSION	PERRY RANGE
TAKE-OFF WEIGHT	lbs	706, 634	769, 000	732, 500	712, 000	643, 774
fuel		116, 390	178, 756	307, 256	186, 756	318, 500
payload	lbs	265, 000	265, 000	100, 000	200, 000	0
COMBAT RANGE	nmi	1, 710	2, 721	5, 872	2, 910	7, 330
average cruising speed	kn	440	440	440	460/440	440
initial cruising altitude	ft	32, 800	28, 100	29, 700	29, 850	33, 600
final cruising altitude	ft	34, 400	34, 280	41, 100	33, 900	46, 150
total mission time	hr	4	6.3	13.4	6.4	16.7
FIRST LANDING WEIGHT	lbs	641, 150	664, 290	559, 670	603, 280	-
COMBAT RADIUS	nmi	1, 000	1, 630	3, 140	1, 740	-
average cruising speed	kn	440	440	440	460/444	-
average cruising altitude	ft	30, 800	28, 100	29, 700	29, 850	-
final cruising altitude	ft	46, 700	46, 500	46, 150	46, 500	-
total mission time	hr	4.7	7.6	14.4	7.9	-
LANDING WEIGHT	lbs	336, 520	339, 700	346, 240	340, 110	346, 840

OEW = 325, 244

Table 7.2-1 C-5A Typical Mission Data

Figure 7.2-1 C-5 TYPICAL AIRLIFT MISSION



Phase	IAS/Mach	TIME	Air Distance	Fuel Used	End Altitude	End Gross Weight
Climb	*270	0.61	195	19,300	38,000	560,700
Cruise	.77	4.74	2100	97,500	38,000	463,200
Descent	*250	.30	96	1,260	3,000	462,000
Traffic Pattern	160	0.25	40	5,200	0	456,800
TOTAL		5.9	2431	123,260		

*250 KIAS below 10,000'
270 KIAS to 29,000'
0.70M above 29,000'

**0.70 down to 250 KCAS

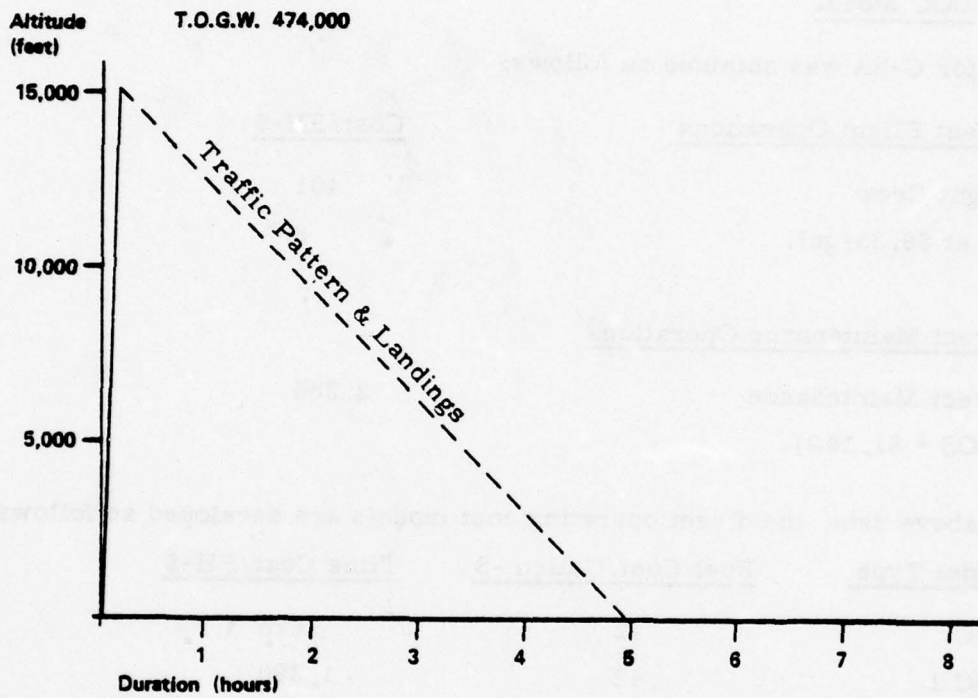
Training missions generally involve multiple take-offs and landings. Figure 7.2-2 shows a typical training mission for the C-5A. These missions constitute 34% of the sorties and 21% of the flying hours. The impact of optimal flight procedures on training missions will be small; therefore these missions are neglected during the optimal flight procedures evaluation.

The spectrum of mission profiles used to evaluate optimal flight procedures were generated using the ASIMIS data tapes described in Section 2. The data tapes used were for the period April through June 1976 and represent the latest quarterly information available at the time the tapes were processed. There were a total of 2009 sortie records, of which only 150 were discarded due to various inconsistencies in the data. The histograms contained in this section represent the distribution of various mission parameters obtained by processing data tapes. The airlift missions were first separated according to mission duration. Missions of less than three hours duration are classified as short range missions. The range of these missions is generally less than 1100 n.mi. Medium range missions are those which last 3 to 6 hours and generally between 1100 to 2200 n.mi. Long range missions are those which last longer than six hours and range longer than 2200 n.mi. Missions are further subdivided according to take-off gross weight (TOGW). The weight bands considered are:

- (1) less than 450,000 lbs.
- (2) 450,000 - 550,000 lbs.
- (3) 550,000 - 650,000 lbs.
- (4) greater than 650,000 lbs.

Figures 7.2-3, 4 and 5 depict the histograms of level off altitude for short range missions. Since there were only six short range missions for TOGW above 650,000 lbs., they were excluded from analysis. Take-off fuel weight, landing fuel weight and average mission duration information is also shown on these histograms. For each altitude band the first two numbers represent the average take-off fuel weight and landing fuel weight; the bottom number is the average mission duration.

Figure 7.2-2 C-5 TYPICAL TRAINING MISSION



Phase	IAS/Mach	TIME	Air Distance	Fuel Used	End Altitude	End Gross Weight
Climb	-	.09	22	6,800	15,000	467,200
Traffic Pattern	160	3.51	562	75,200	0	392,000
TOTAL		3.60	584	82,000		

Figures 7.2-6, 7 and 8 are the histograms of level-off altitude for medium range missions. Here again missions for TOGW above 650,000 lbs. are negligible.

Figures 7.2-9, 10, 11 are the level off altitude histograms for long range missions. There are no long range missions for TOGW less than 450,000 lbs.

7.2.3 DOC Model

Cost data for C-5A was obtained as follows:

<u>Direct Flight Operations</u>	<u>Cost/FH-\$</u>
Flight Crew	401
Oil at \$9.35/gal.	6
 <u>Direct Maintenance Operations</u>	
Direct Maintenance	2,366
(IROS = \$1,183)	

From the above data, the direct operating cost models are developed as follows:

<u>Model Type</u>	<u>Fuel Cost/Gallon -\$</u>	<u>Time Cost/FH-\$</u>
DOC	.42	698
DOC 1	.42	1,390
DOC 2	.42	2,081
DOC 3	.42	2,773

Annual fuel and direct operating costs for the C-5A aircraft obtained by using the above cost model and the annual flying hours and fuel consumed given in Table 2.1-2 are given below:

Fuel Cost	\$59.9 million
DOC	\$89.4 million
DOC 1	\$118.6 million
DOC 2	\$147.8 million
DOC 3	\$177.0 million

Figure 7.2-3
C-5
DISTRIBUTION OF LEVEL OFF ALTITUDES
TAKE OFF GROSS WEIGHT - 450,000 Pounds
MISSION DURATION - LESS THAN 3 hrs.

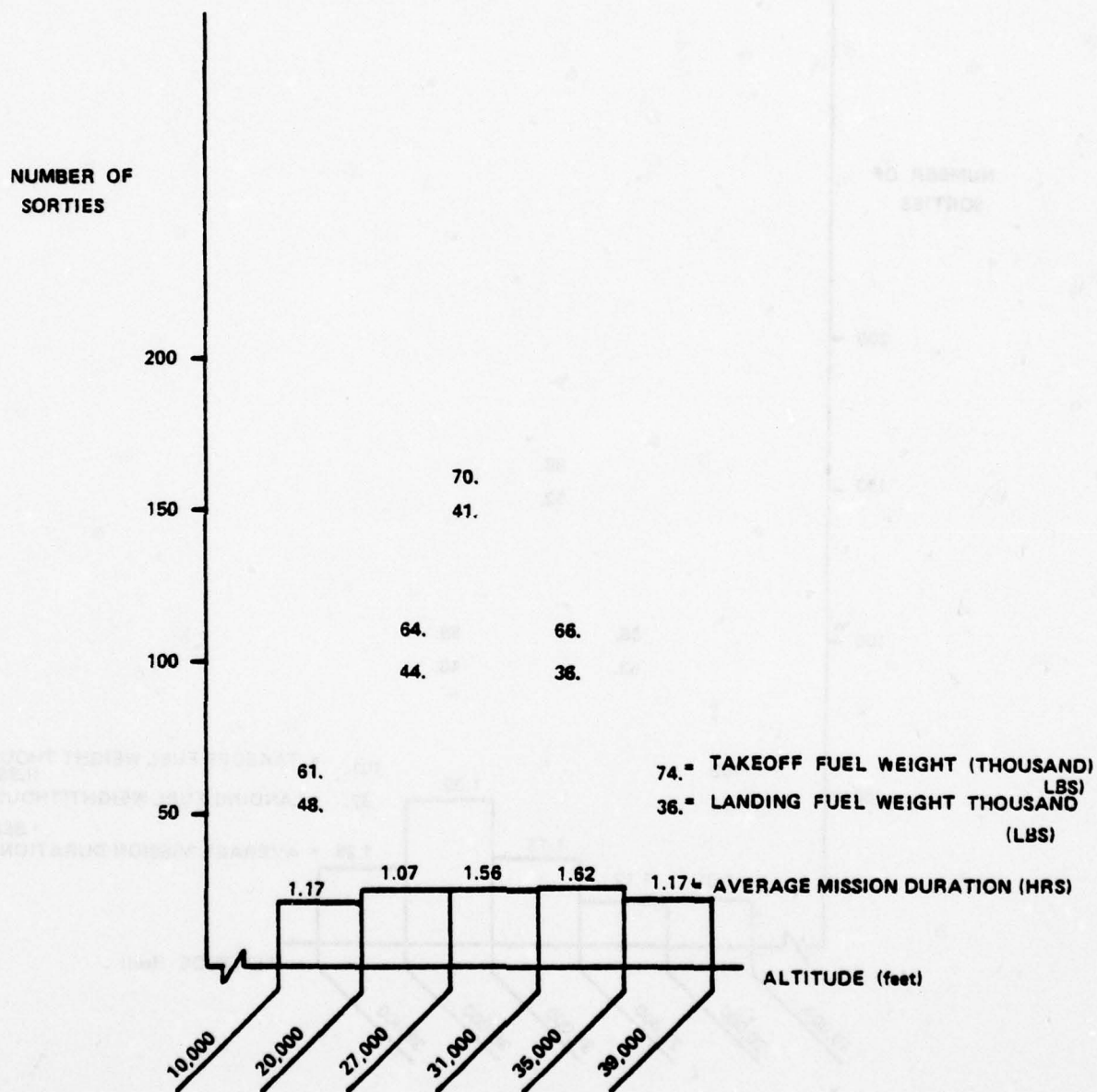


Figure 7.2-4
C-5
DISTRIBUTION OF LEVEL OFF ALTITUDES
TAKE OFF GROSS WEIGHT - 450,000 - 550,000 pounds
MISSION DURATION - LESS THAN 3 hrs.

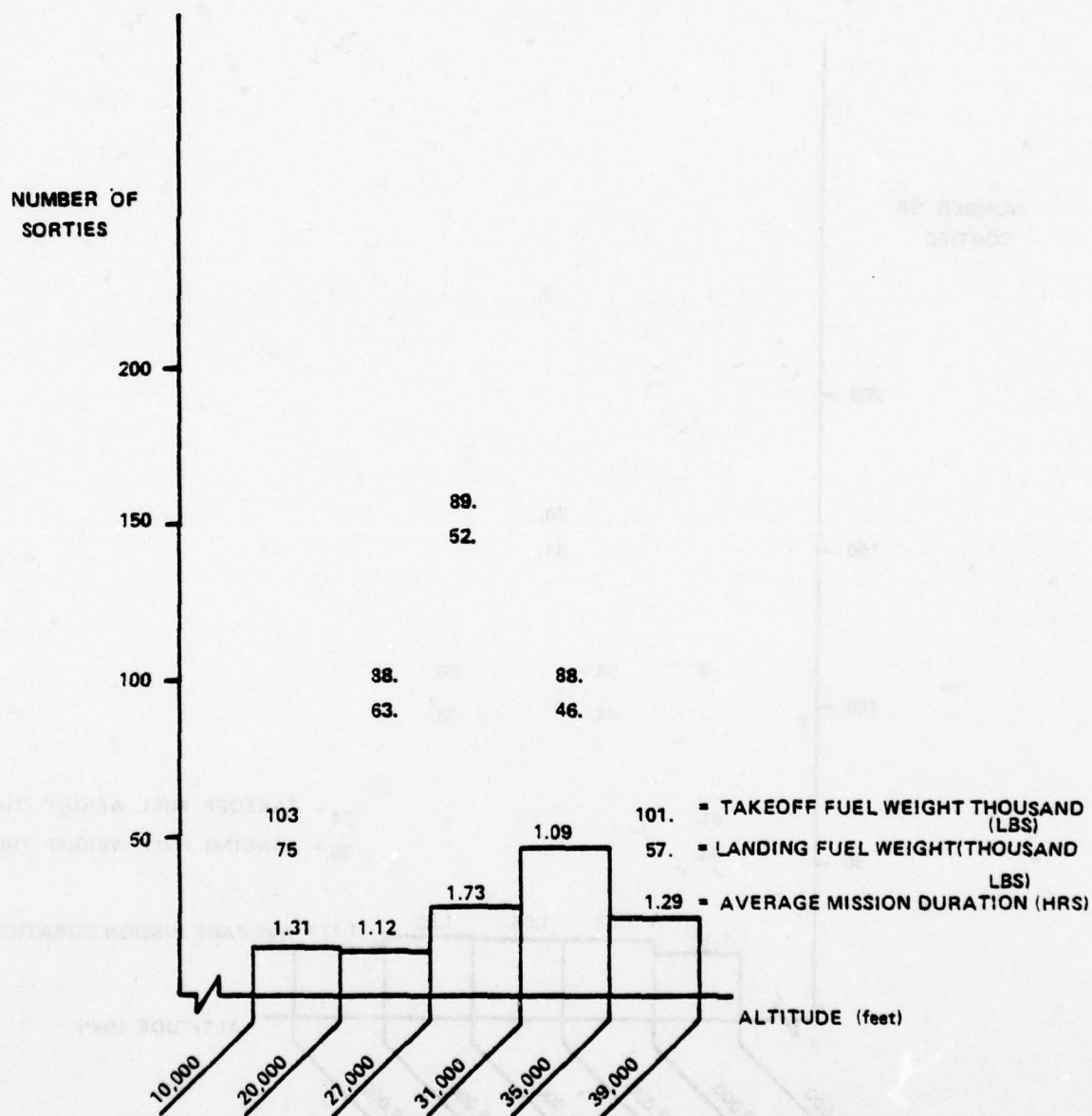


Figure 7.2-5
 C-5
 DISTRIBUTION OF LEVEL OFF ALTITUDES
 TAKE OFF GROSS WEIGHT - 550,000 - 650,000 pounds
 MISSION DURATION - LESS THAN 3 hrs.

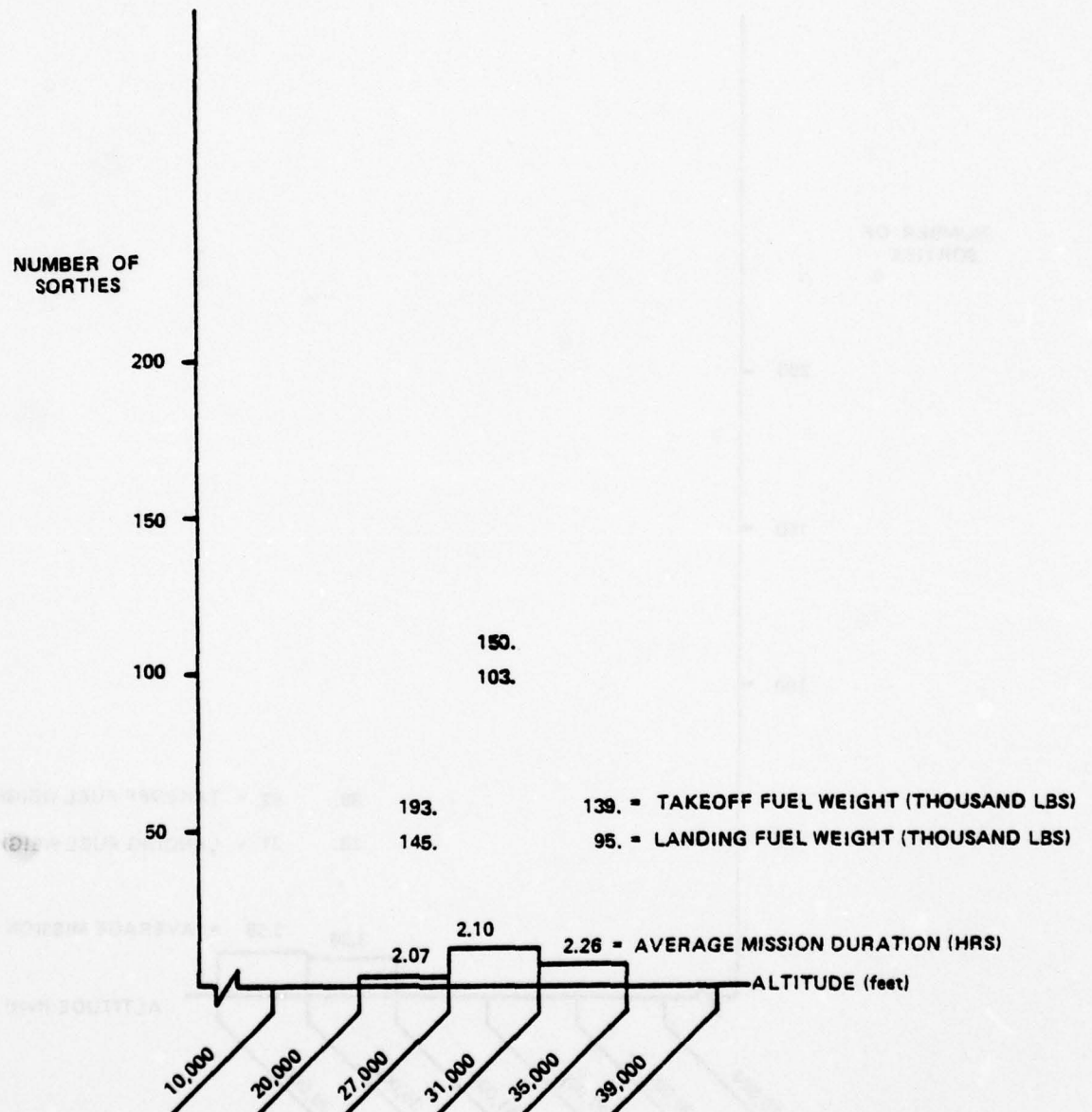


Figure 7.2-6

C-5

DISTRIBUTION OF LEVEL OFF ALTITUDES
TAKE OFF GROSS WEIGHT - UP TO 450,000 pounds
MISSION DURATION - 3 - 6 hours

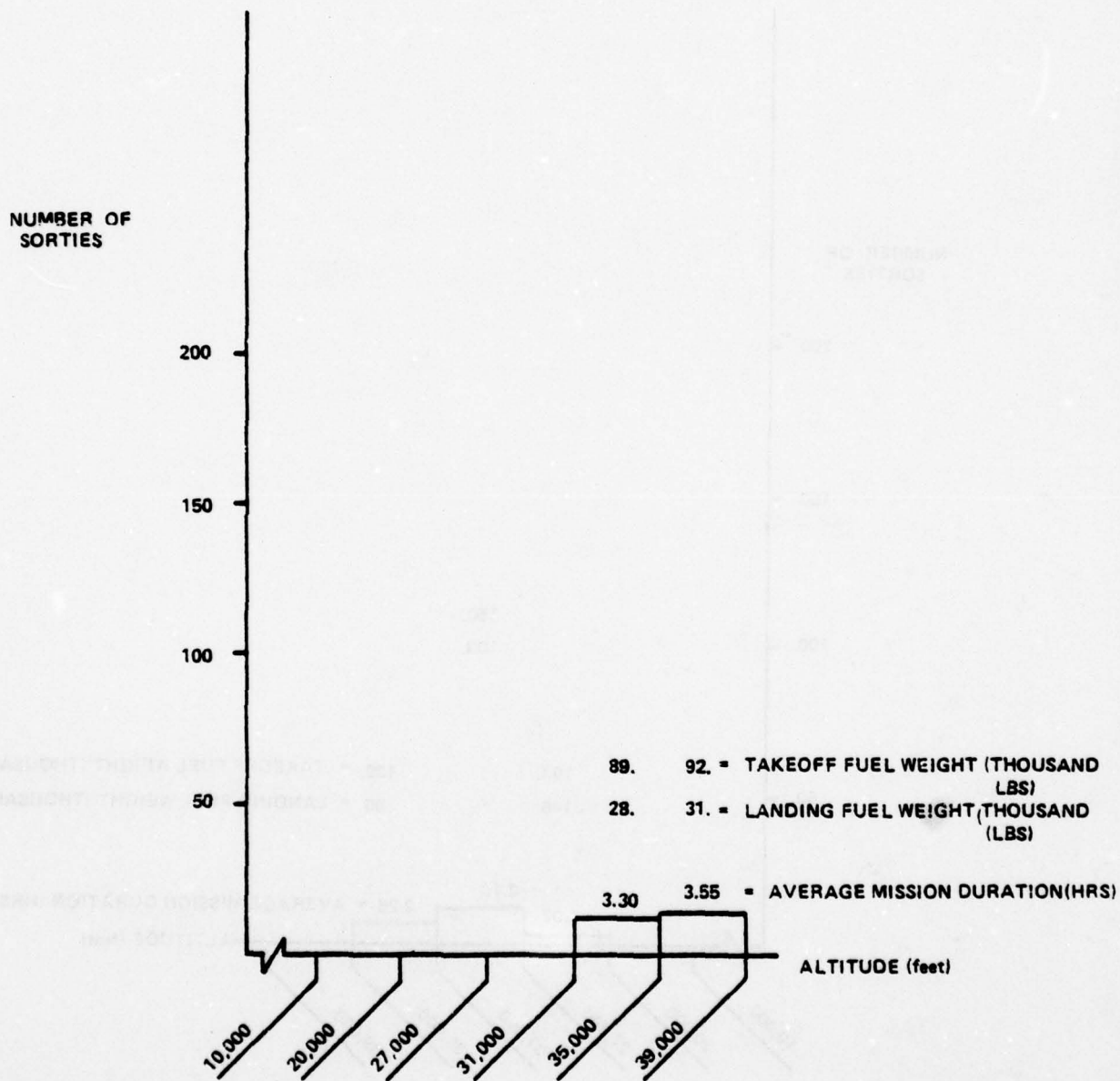


Figure 7.2-7

C-5

DISTRIBUTION OF LEVEL OFF ALTITUDES
TAKE OFF GROSS WEIGHT - 450,000 - 550,000 pounds
MISSION DURATION - 3 - 6 hours

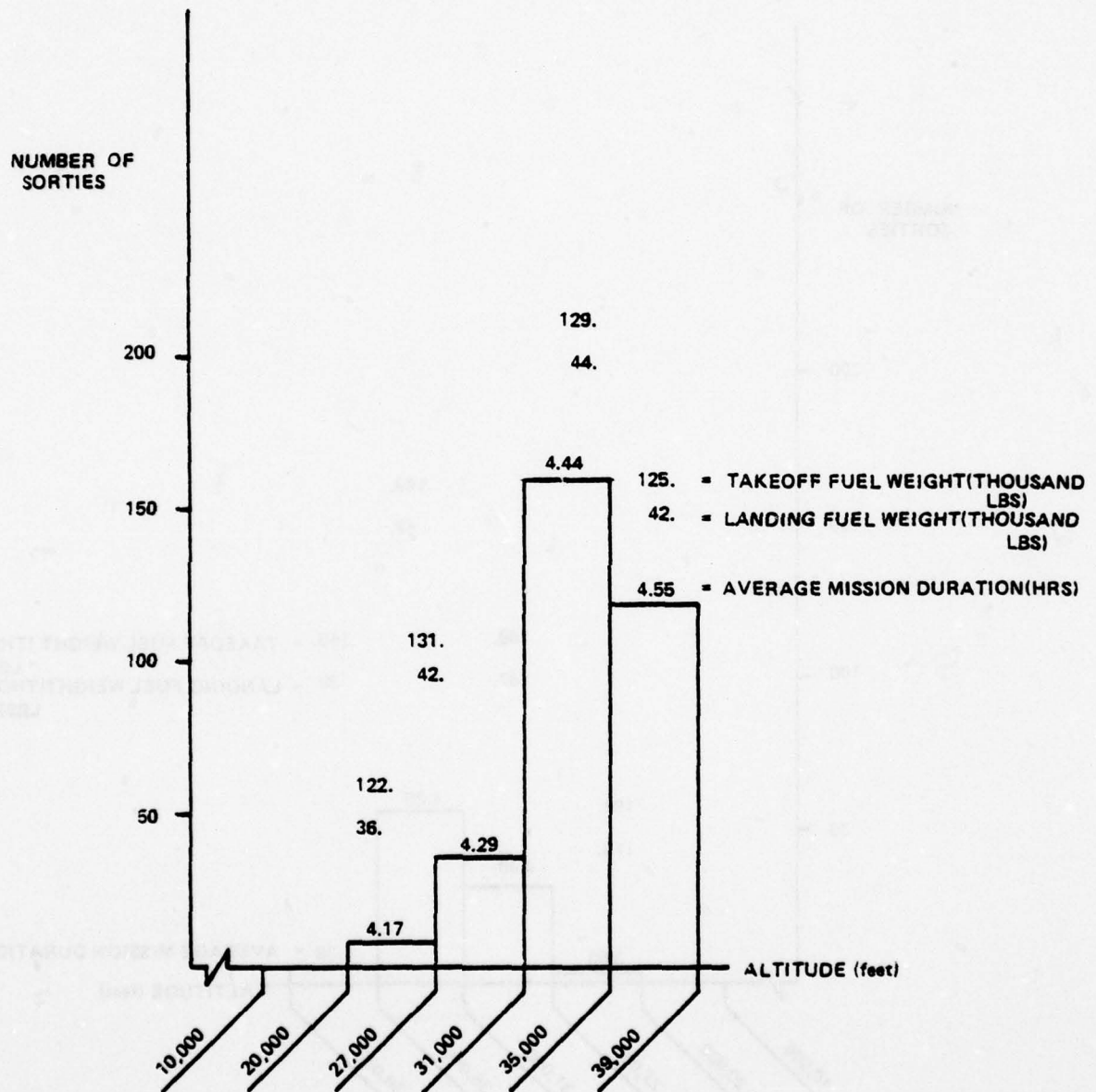


Figure 7.2-8

C-5

DISTRIBUTION OF LEVEL OFF ALTITUDES

TAKE OFF GROSS WEIGHT - 550,000 - 650,000 pounds

MISSION DURATION - 3 - 6 hours

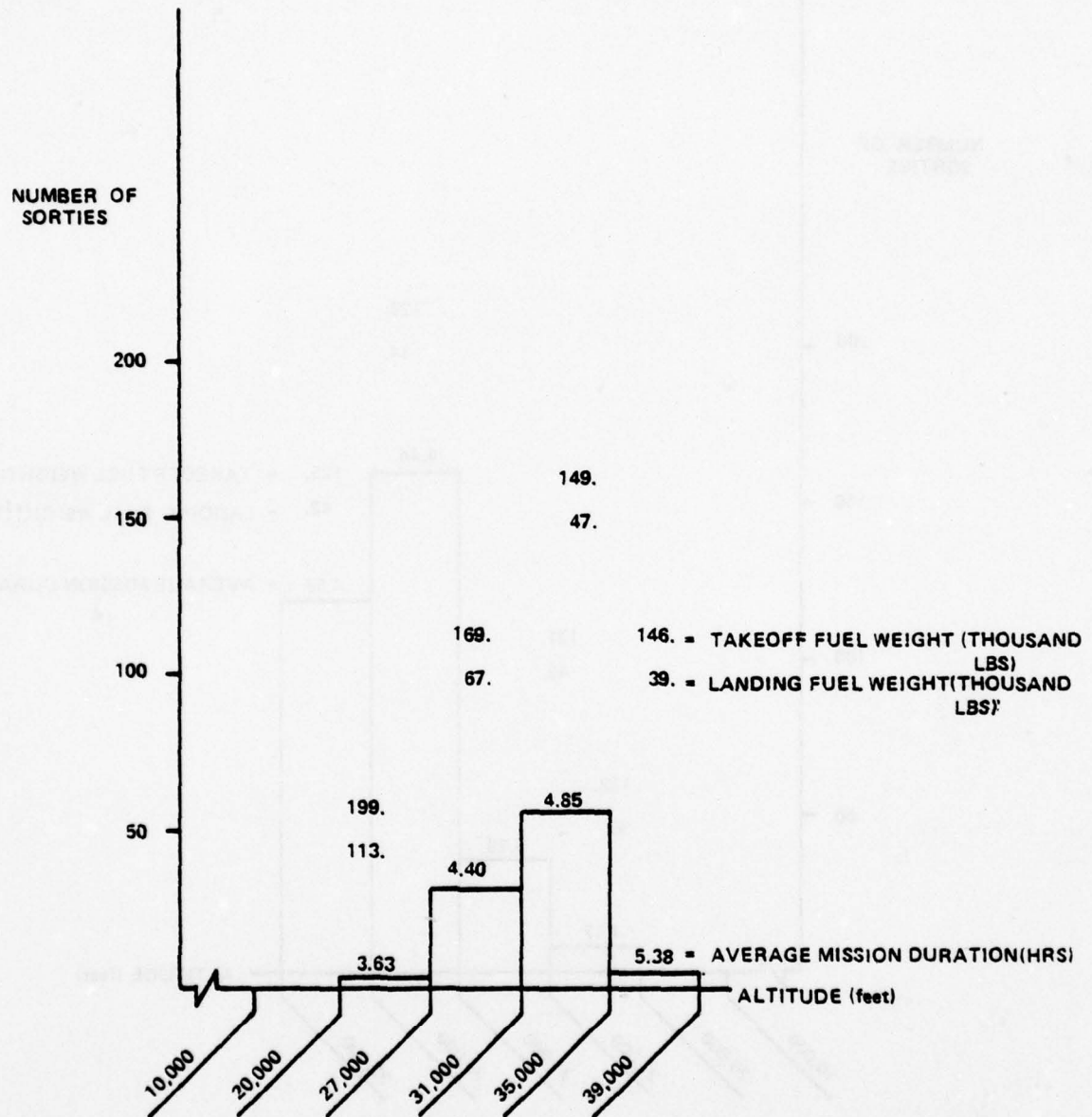


Figure 7.2-9

C-5
DISTRIBUTION OF LEVEL OFF ALTITUDES
TAKE OFF GROSS WEIGHT - 450,000 - 550,000 pounds
MISSION DURATION - 6 hours OR MORE

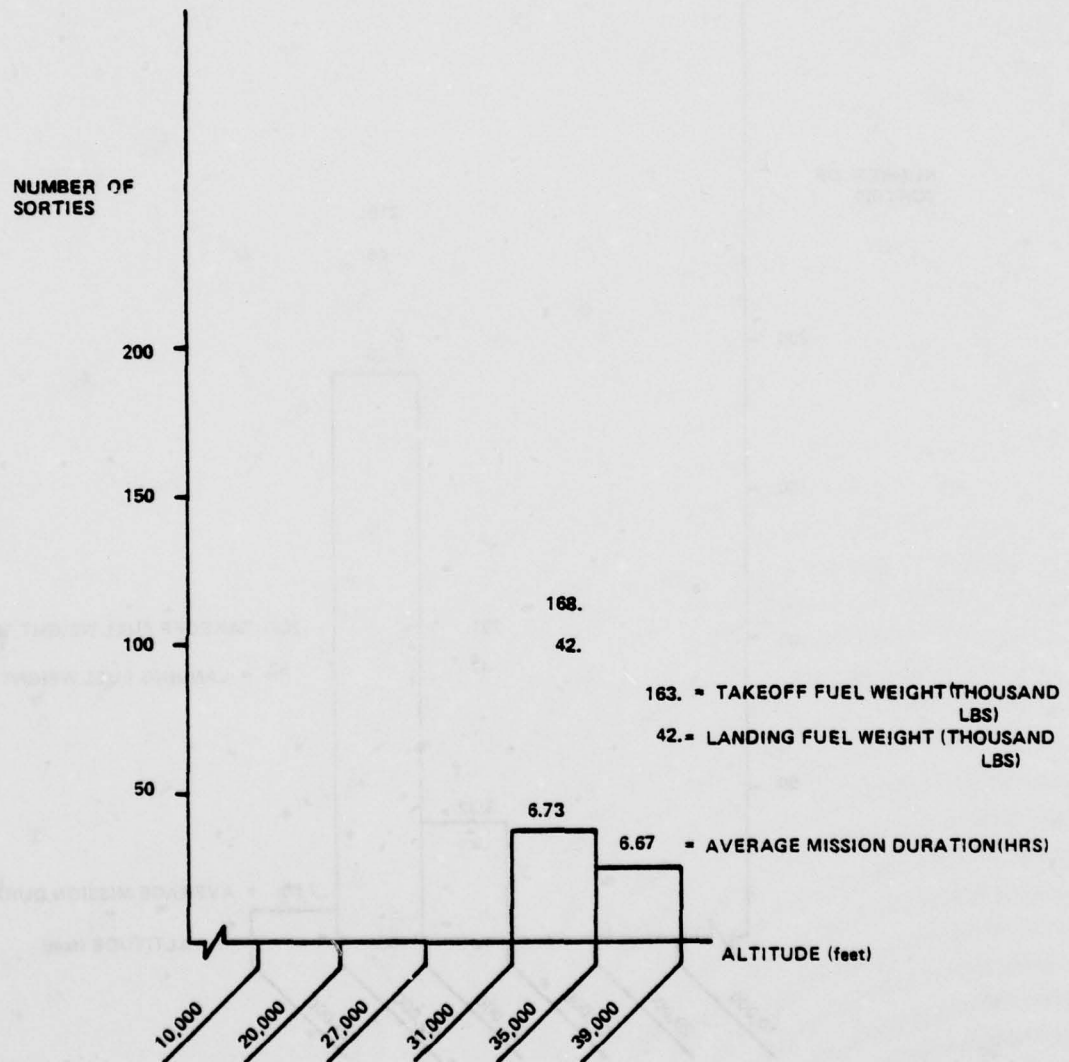


Figure 7.2-10

C-5
DISTRIBUTION OF LEVEL OFF ALTITUDES
TAKE OFF GROSS WEIGHT - 550,000 - 650,000 pounds
MISSION DURATION - 6 hours OR MORE

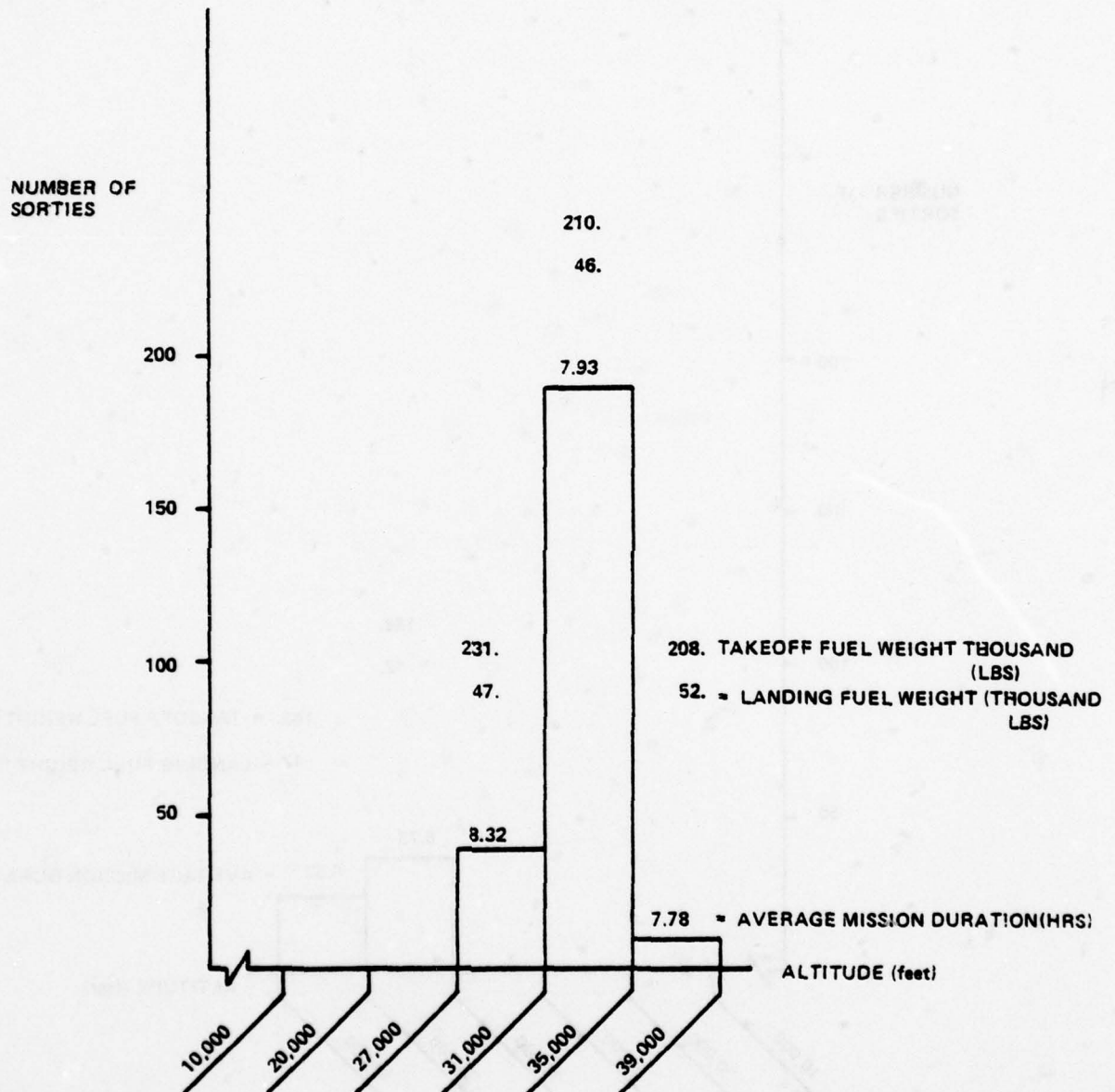


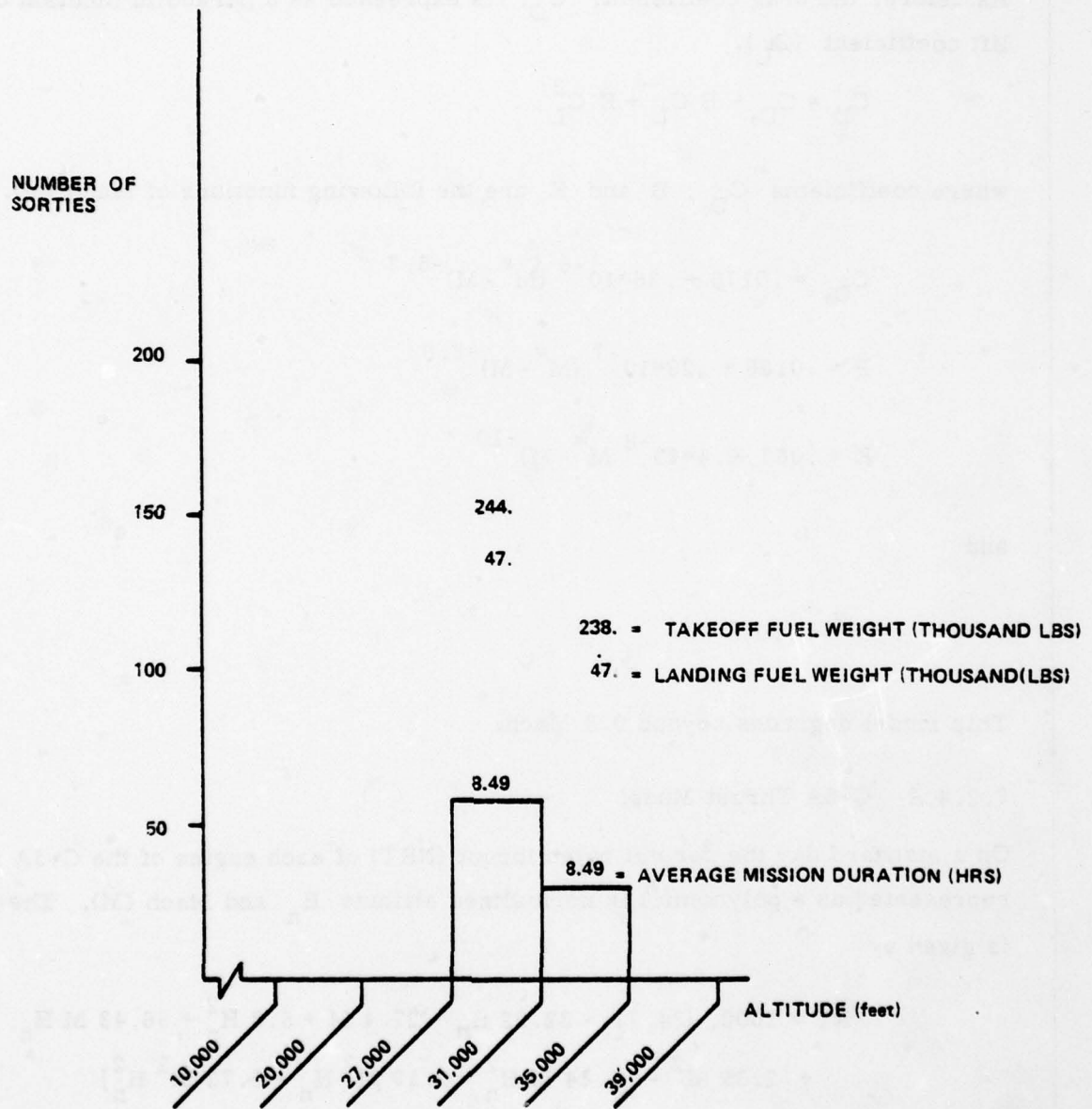
Figure 7.2-11

C-5

DISTRIBUTION OF LEVEL OFF ALTITUDES

TAKE OFF GROSS WEIGHT - 650,000 pounds and above

MISSION DURATION - 6 hours OR MORE



7.2.4 C-5A Characteristics

The aerodynamic and propulsion data used to develop analytical models for the C-5A were obtained from Reference [44].

7.2.4.1 C-5A Aerodynamic Models

As before, the drag coefficient, C_D , is expressed as a parabolic function of lift coefficient (C_L).

$$C_D = C_{D_0} - B C_L + K C_L^2$$

where coefficients C_{D_0} , B and K are the following functions of Mach (M).

$$C_{D_0} = .0176 + .36 \cdot 10^{-6} (M^* - M)^{-5.7}$$

$$B = .0166 + .29 \cdot 10^{-7} (M^* - M)^{-8.0}$$

$$K = .063 + .4 \cdot 10^{-8} (M^* - M)^{-10}$$

and

$$M^* = 1.0$$

This model degrades beyond 0.8 Mach.

7.2.4.2 C-5A Thrust Model

On a standard day the normal rated thrust (NRT) of each engine of the C-5A is represented as a polynomial in normalized altitude H_n and Mach (M). The NRT is given by

$$\begin{aligned} \text{NRT} = 1000. [& 34.71 - 32.22 H_n - 27.4 M + 5.8 H_n^2 + 36.43 M H_n \\ & + 2.65 M^2 - 11.64 M H_n^2 + 3.19 M^2 H_n - 5.72 M^2 H_n^2] \end{aligned}$$

where

NRT = normal rated thrust (lb)

H_n = altitude (ft)/40000

This model of NRT is applicable in the troposphere. Another NRT model developed for the stratosphere is given by

$$\begin{aligned} \text{NRT} = 1000. [& 30.06 - 34.74 H_n + 7.25 M + 12.11 H_n^2 - 1.12 M H_n \\ & - 13.96 M^2 - 5.46 M H_n^2 + 11.82 M^2 H_n - .01 M^2 H_n^2] \end{aligned}$$

As explained in Subsection 3.2, these two representations cause a discontinuity thrust at tropopause. However, this discontinuity does not affect the optimal trajectory algorithm.

Idle thrust (T_{idle}) is given by the following polynomial function, which is similar to the NRT equation in form.

$$\begin{aligned} T_{\text{idle}} = 1000. [& .687 - 3.62 H_n + 3.58 M + 1.69 H_n^2 + 9.36 M H_n \\ & - 25.06 M^2 - 5.74 M H_n^2 + 21.11 M^2 H_n - 5.6 M^2 H_n^2] \end{aligned}$$

where

T_n = normalized thrust/engine

= $T/5/20000$

δ = pressure ratio

The normalized fuel flow rate obtained from the above expression is a good representation of actual data in the troposphere. Beyond the troposphere the actual f_n increases with altitude. Thus a correction factor is used for altitude beyond the troposphere: the fuel flow rate is increased by 0.4% for each 1000 ft. increment in altitude beyond tropopause. The idle fuel flow rate model was also

developed for C-5A using idle thrust and idle fuel flow rate data. Thus normalized idle fuel flow rate, $f_{n \text{ idle}}$, is given

$$f_{n \text{ idle}} = 1000 \cdot [1.98 - .6 T_n - 9.73 M + 25.5 T_n^2 + 41.24 M T_n + 27.81 M^2]$$

This model is used up to tropopause. Beyond tropopause the idle fuel flow rate remains constant at a value of 550 lbs/hr/engine.

For most of the operating regions, the errors in the above aerodynamic and propulsion models are less than 2%.

7.2.5 Evaluation of Airborne and Ground Operational Procedures

Section 4 identified potential fuel saving airborne and ground operational procedures for the aircraft under study and outlined the analysis approach for evaluation of these procedures. This subsection carries out the analysis of fuel saving operational procedures for the C-5 aircraft.

7.2.5.1 Reduced Power Take-Off

Like the C-141 aircraft, direct fuel savings due to reduced power take-off for the C-5A aircraft are small. Depending upon take-off gross weight, average savings per mission due to reduced power take-off is less than one-half gallon and average take-off time increases by 3 seconds. Thus annual fuel/DOC savings due to reduced power take-offs are negligible. Indirect fuel savings due to reduced engine deterioration may be substantial. As mentioned in subsection 4.1, indirect fuel savings can only be estimated by prolonged experimentation.

7.2.5.2 Optimal Climb, Cruise and Descent Procedures

Section 4.1 outlined the general approach for evaluation of optimal climb, cruise and descent procedures. These three flight modes are first examined individually. Results derived from individual optimization are then used to assist in complete trajectory optimization. The cruise segment is examined first, as the terminal conditions for the climb phase and initiation point for the descent phase

are determined by the cruising flight conditions.

Optimal Cruise-Climb Solution

During the cruise phase, at any point on the trajectory, optimal cruise altitude and velocity are obtained by the extremization of Equation (A-31) in Appendix A. By changing the value of fuel/cost trade-off parameter, θ , different optimal solutions are obtained. Figure 7.2-12 illustrates the relationship between the fuel consumed and flight time as θ is varied between 0 and 1. The solution corresponding to $\theta = 0$ is the minimum time solution, while that corresponding to $\theta = 1$ is the minimum fuel solution. Since both minimum cruise altitude and maximum cruise velocity were constrained in the optimization routine, the minimum time solution was obtained under these constraints. As the value of θ is increased, optimum cruise velocity and fuel consumption decreases; however, the flight time increases. Optimum solution points corresponding to direct operating cost models DOC, DOC 1, DOC 2, and DOC 3 are shown on Figure 7.2-12. From processing of ASIMIS tape data it was observed that most of the missions fly at .77 Mach during cruise. This cruise mach number is close to the optimum cruise mach number corresponding to DOC 3. The "knee" in the curve is close to the optimal solution for DOC, which corresponds to a 0.75 Mach. The minimum fuel cruise-climb solution corresponds to a 0.72 Mach. For the C-5A the aircraft optimal cruise altitude is constrained by the cruise altitude ceiling. Thus the optimum cruise-climb solution corresponds to the cruise altitude ceiling.

Optimal Step-Climb Solution

Since the cruise altitude for the C-5A is constrained by the cruise ceiling, it can step climb only to the cruise ceiling and not above. This sets the C-5A apart from the C-141, KC-135, and B-52's which are not constrained by the cruise ceiling. Therefore the difference between optimum cruise-climb and optimum step-climb solutions for this aircraft is much higher than for the C-141, KC-135 and B-52 aircraft. Most of the C-5A flights requiring step-climb procedures cruise above 29,000 feet altitude and only 4000 foot altitude steps are permitted above this altitude by the ATC constraints. For the 4000 foot step climb solution

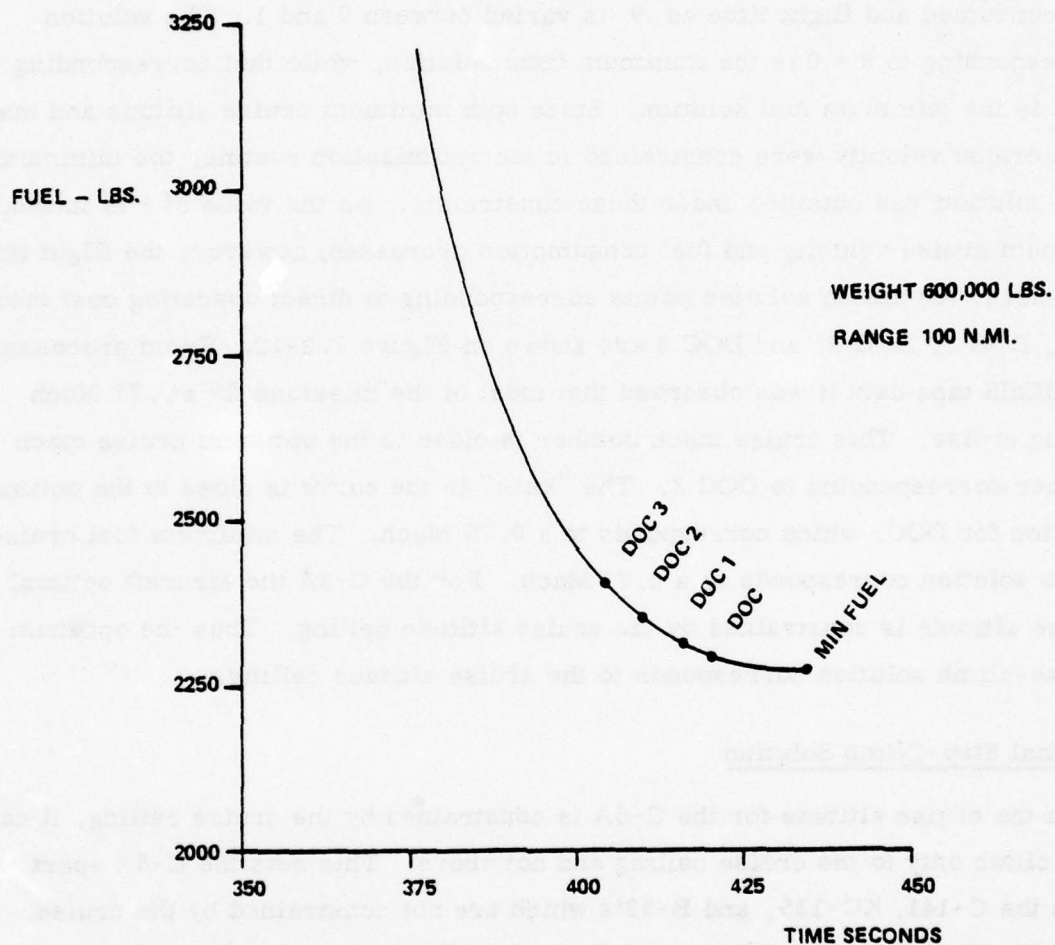


Figure 7.2-12 FUEL/TIME TRADE-OFF FOR THE C-5
CRUISE SOLUTION

the fuel consumption is 1.7% more than the cruise climb solution for the C-5A aircraft. If 2000 foot climb steps were allowed above a 29,000 foot altitude, then this fuel consumption difference would reduce to 0.6%. Note that the step climb solution was evaluated for a constant Mach number cruise.

Conventional Climb Procedures

The conventional C-5A climb segments simulated in this study follow the handbook schedules documented in Reference [11]. Conventional climbs are performed at a normal rated thrust (NRT) setting. Below a 10,000 ft. altitude the air speed is 250 KCAS due to ATC constraint. Above 10,000 ft. the conventional climb is executed at 270 KIAS/0.7 Mach number speed schedule.

Optimal Climb Procedures

Optimum altitude (or equivalently air speed) and throttle setting for optimal climb procedures are obtained by the solution of Equations (A-31), (A-32) and (A-47) of Appendix A. Solution for optimal climb under ATC constraint is obtained by constraining the maximum air speed to 250 KCAS below 10,000 ft. altitude in the optimization algorithm. For C-5A aircraft the optimal climb profiles below 10,000 feet ride the 250 KCAS constraint bound. Optimal climb solutions have also been obtained without ATC constraint to obtain the sensitivity of optimal climb solution to ATC constraint. In general, both optimal air speed and throttle setting vary continuously along an optimal climb profile.

Parametric Optimal Climb Solution

As described in Section 4.1, the parametric optimal climb procedure is similar to conventional climb methods. Climb is executed at a NRT throttle setting. The air speed schedule during climb follows a constant-KCAS/constant Mach number mode in which the air speed is set equal to the optimum cruise Mach number; however, the constant KCAS is determined by the parametric optimization method.

Comparison of Various Climb Procedures

Table 7.2-2 shows a comparison of optimal, parametric optimal and conventional climb solutions for C-5A aircraft. All the trajectories start at the same initial conditions and terminate at the same final conditions as summarized in Table 7.2-2. The optimal climb trajectory has a path length of 194 n.mi., which is taken as the reference length. The path length of the other climb trajectories is less than 194 n.mi.; their climb segment is followed by a cruise segment at 0.72 Mach, which is the minimum fuel optimal cruise speed. The optimal climb trajectory consumes 15,247 lbs. of fuel which is 166 lbs. less than the conventional climb; however, it takes 30 seconds more to travel the same path. The parametric optimal climb consumes only 87 lbs. (0.57% of climb fuel) more fuel than optimal climb and takes 3 seconds less than optimal climb. The ATC constraint results in a 46 lb. increase in fuel consumption and a 16 second increase in mission time for optimal mission profiles. The values of fuel and direct operating costs for the different climb profiles discussed above are also given in Table 7.2-2. Table 7.2-3 summarizes results of fuel/DOC savings (loss) due to parametric optimal climb procedures. Note that fuel savings due to optimal climb procedures are insignificant. There is a loss in direct operating cost due to longer time taken by optimal climbs.

Conventional Descent Procedures

Conventional descent segments simulated in this study follow the procedures for "en route" descent outlined in Reference [11]. For "en route" descent, all four engines are retarded to flight idle setting, the aircraft is kept in a clean configuration and the air speed schedule is Mach 0.7 down to 250 KCAS at which time 250 KCAS is maintained. These procedures result in a relatively low rate of descent.

Initial Conditions
Weight 570,000
Altitude 3,000
Air speed 250 KCAS

Final Conditions
Range 194 NM
Altitude 36,000
Air speed .72 Mach

Type of Climb	Optimum †	Optimum † with ATC Constraint	Parametric Optimum 260KCAS/.72M	Conventional with ATC Constraint
Climb	194	192.5	188	183
Range	0	1.5	6	11
n.mi.	194	194	194	194
Climb	15247	15224	15044	14880
Fuel	0	69	292	533
lbs.	15247	15293	15336	15413
Climb	1880	1883	1820	1756
Time	0	13	57	94
sec.	1880	1896	1877	1850
Fuel	\$985.2	\$988.2	\$990.9	\$995.9
DOC	1349.7	1355.8	1354.8	1354.6
DOC 1	1711.1	1720.3	1715.6	1710.2
DOC 2	2071.9	2084.2	2075.9	2065.3
DOC 3	2433.3	2448.6	2436.7	2420.9

† Note that these trajectories were optimized for fuel only.

Table 7.2-2 Comparison of Optimum vs Conventional Climb - C-5A

Cost	Annual Savings Due Parametric Optimal Climb	% Savings
Fuel	69,000 gallons	0.05
Fuel Cost	\$29,000	0.05
DOC	\$13,600 (Loss)	0.02 (Loss)
DOC 1	\$55,800 (Loss)	0.05 (Loss)
DOC 2	\$98,000 (Loss)	0.07 (Loss)
DOC 3	\$140,200 (Loss)	0.08 (Loss)

Table 7.2-3 Fuel/DOC Savings Due to Optimal Climb for C-5A

Optimal Descent Procedures

Optimum altitude (or equivalently air speed) and throttle setting for optimal descent procedures are obtained by the solution of optimal algorithm equations given in Appendix A. Optimal descent air speed for C-5A is less than 250 KCAS. Therefore the ATC constraint does not affect the optimal descent solution. Both optimal air speed and throttle setting vary continuously along an optimal descent path.

Parametric Optimum Descent Solution

The parametric optimum descent procedure is similar to the conventional descent procedure. Descent is performed at flight idle thrust setting with the aircraft in a clean configuration. The air speed schedule is constant Mach/constant KCAS where the Mach is set equal to the optimum cruise Mach number and the constant KCAS is determined by the parametric optimization method.

Comparison of Various Descent Procedures

Table 7.2-4 summarizes the results of a comparison of optimal, parametric optimal and conventional descent procedures for C-5 aircraft. All trajectories start at the same initial conditions and terminate at the same final conditions. The total mission range is taken equal to the range traversed by the optimal descent trajectory, which is 128 n.mi. Since descent range for other procedures is less than 128 n.mi., descent initiation is started after a short cruise segment such that total mission range is the same for all trajectories. The optimal descent trajectory consumes 2374 lbs. of fuel which is 395 lbs. less than for the conventional descent. However, it takes 250 seconds more to traverse the same path. The parametric optimum consumes only 26 lbs. more fuel than the optimal descent and takes 40 seconds more than optimal descent. Fuel and direct operating cost values for different descent procedures are also given in Table 7.2-4. Direct operating costs for the conventional descent are less than the DOC's for both the optimal and parametric optimal descents. This is due to the fact that the conventional descent takes much less time.

Initial Conditions
 Weight 480,000
 Altitude 33,000
 Air speed .72 Mach

Final Conditions
 Range 128
 Altitude 3,000

Comparison of Optimal vs Conventional Descent - C-5A

Type of Descent		Optimal† Descent	Parametric Optimal .72M/200KCAS	Conventional Descent .7M/250KCAS
Range n. mi.	Cruise	0	26	47
	Descent	128	102	81
	Total	128	128	128
Fuel lbs	Cruise	0	1062	1921
	Descent	2374	1328	848
	Total	2374	2390	2769
Time Sec.	Cruise	0	225	404
	Descent	1555	1370	890
	Total	1555	1595	1294
Cost \$	Fuel	153.4	154.4	178.9
	DOC	454.9	463.7	429.8
	DOC 1	753.8	770.2	678.5
	DOC 2	1052.3	1076.4	926.9
	Doc 3	1351.2	1383.0	1175.6

†Note that this trajectory is optimized for fuel only

Table 7.2-4 Comparison of Optimal vs Conventional Descent - C-5A

Cost	Annual Savings Due To Parametric Optimal Descent	% Savings
Fuel	360,000 gallons	.25
Fuel	\$151,000	.25
DOC	\$200,000 (Loss)	.22 (loss)
DOC 1	\$548,000 (Loss)	.46 (loss)
DOC 2	\$895,600 (Loss)	.6 (loss)
DOC 3	\$1,243,000 (Loss)	.7 (loss)

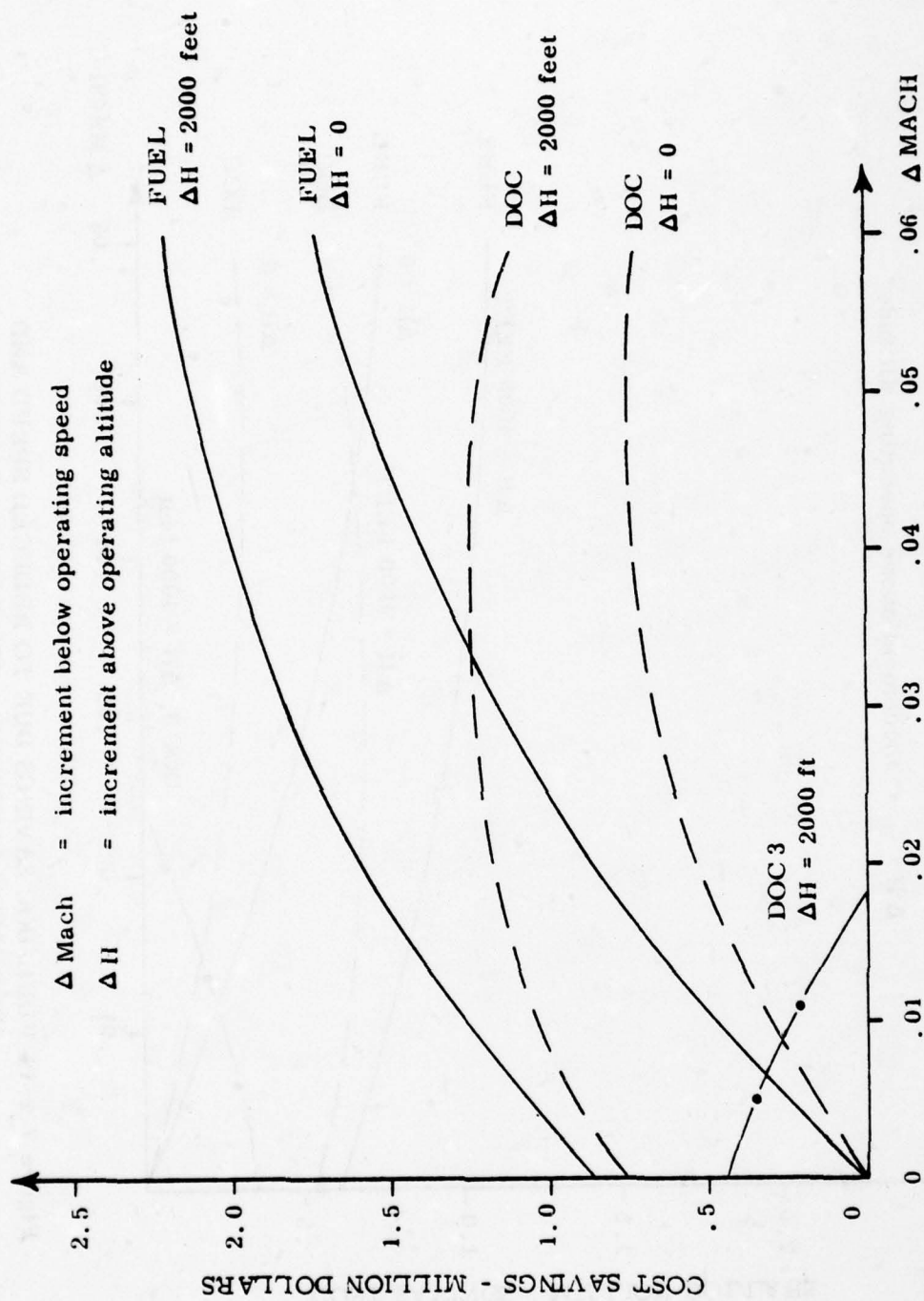
Table 7.2 - 5 Fuel/DOC Savings Due to Optimal Descent C-5A

Table 7.2-5 shows estimated fuel/DOC savings of parametric optimal descent with respect to conventional descent. The fuel savings are small (.25%). Moreover, the optimal descents cause a loss in direct operating costs, the magnitudes of the loss varying with the cost model.

Integrated Optimal Trajectories

Actual mission spectrum data for C-5A aircraft were obtained by processing the ASIMIS tapes. The average cruise velocity for most of the missions obtained from the ASIMIS tapes is .77 Mach, which is much higher than the cruise velocity for minimum fuel consumption. In addition, the cruise altitudes for most of the missions were lower than the optimum cruise altitudes. Thus fuel savings can be achieved by flying closer to the optimum altitudes and air speed. Since ATC constraints restrict aircraft to fly at discrete altitude levels with 2000 ft. spacing below a 29,000 foot altitude and 4000 ft. above, the optimal trajectories are simulated under these constraints. Also cruise air speed is restricted to constant values. Thus optimization is performed under a constant Mach cruise with optimal step climbs under ATC restrictions. As mentioned before, fuel savings due to optimal climb and descent procedures are small compared to conventional methods for C-5A. Thus conventional climb and descent procedures are simulated for this evaluation. Since there were only a few C-5A missions flown below a 27,000 foot altitude, they were neglected in this study. Long range, medium range and short range missions were simulated separately.

Figures 7.2-13, 14 and 15 illustrate fuel and DOC savings due to reduced speed and increased altitudes for long range, medium range and short range C-5A missions. Δ Mach indicates a decrease in cruise mach number from the average cruise mach number obtained from ASIMIS tapes. These average cruise mach numbers are close to 0.77 for most of the missions. Δ H indicates an increase in cruise altitude from the average cruise altitudes within the histogram bands in Figs. 7.2-3 through 7.2-11. When Δ H = 0, none of the operating altitudes are changed. When Δ H equals some positive value (such as 4000 feet), this indicates that those missions flow below their respective optimal altitudes have been raised to their optimal altitudes, as long as the increase



FUEL/DOC SAVINGS DUE TO REDUCED SPEED AND INCREASED ALTITUDE - C5A LONG RANGE MISSIONS

Figure 7.2-13

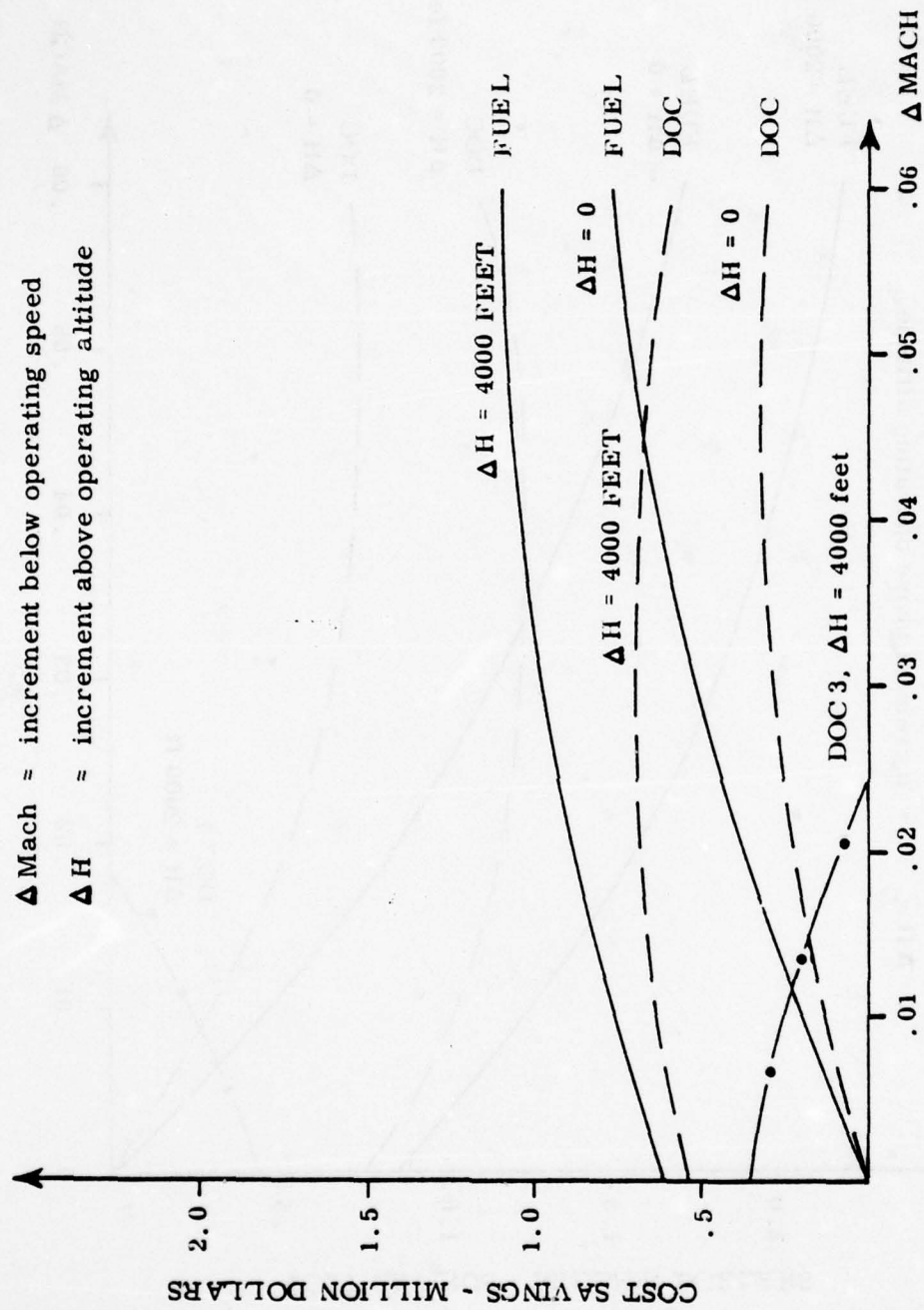


Figure 7.2-14 FUEL/DOC SAVINGS DUE TO REDUCED SPEED AND INCREASED ALTITUDE - C5A MEDIUM RANGE MISSIONS

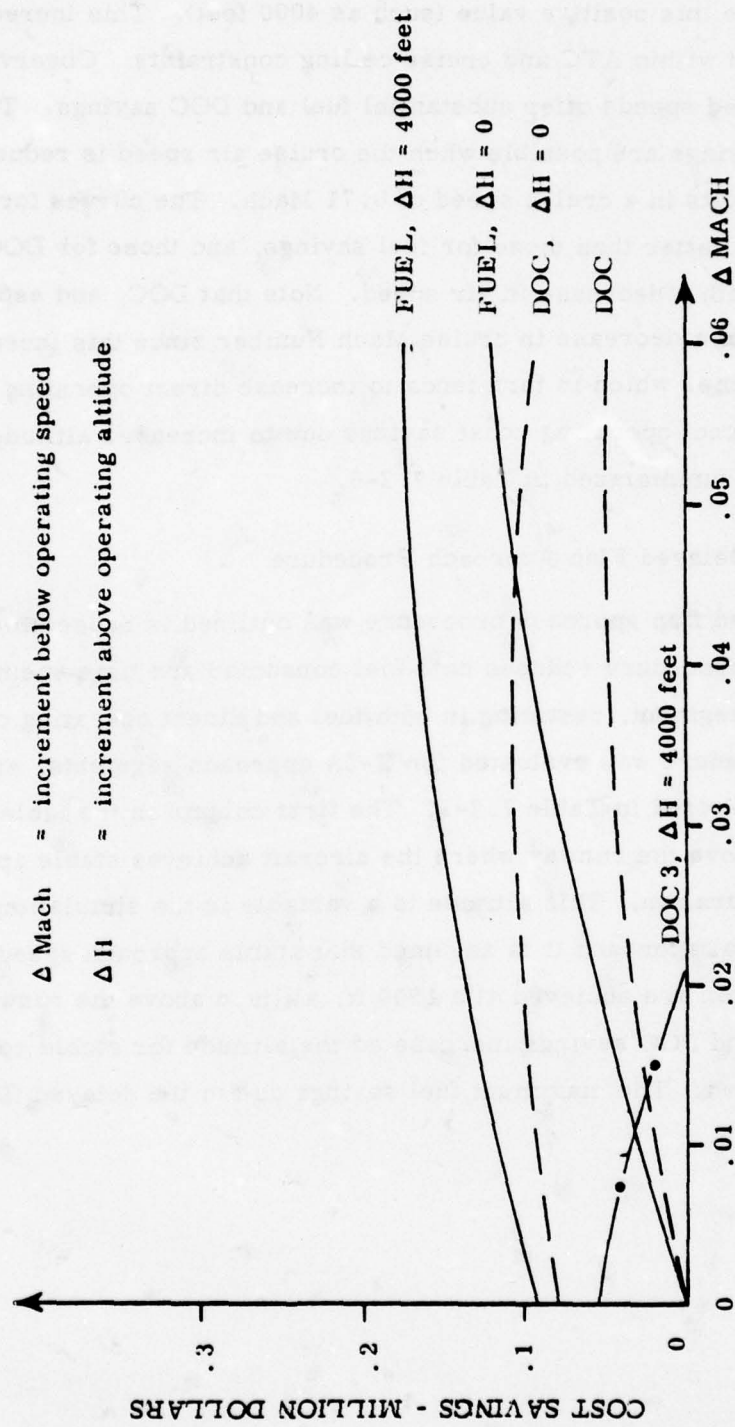


Figure 7.2-15 FUEL/DOC SAVINGS DUE TO REDUCED SPEED AND INCREASED ALTITUDE - C5A SHORT RANGE MISSIONS

is no more this positive value (such as 4000 feet). This increase in altitude is performed within ATC and cruise ceiling constraints. Observe that both altitudes and reduced speeds offer substantial fuel and DOC savings. The maximum amount of fuel savings are possible when the cruise air speed is reduced by 0.06 Mach which results in a cruise speed of 0.71 Mach. The curves for the DOC savings are much flatter than those for fuel savings, and those for DOC 3 move downward sharply with a decrease in air speed. Note that DOC, and especially DOC 3, are sensitive to a decrease in cruise Mach Number since this increases the mission time, which in turn tends to increase direct operating costs. Annual fuel and direct operating cost savings due to increased altitude and reduced speed are summarized in Table 7.2-6.

7.2.5.3 Delayed Flap Approach Procedure

The delayed flap approach procedure was outlined in Subsection 4.1.1. This approach procedure reduces both fuel consumed and time spent during the approach segment, resulting in both fuel and direct operating cost savings. This procedure was evaluated for C-5A approach segments, and the results are summarized in Table 7.2-7. The first column in the table is the altitude above the runway where the aircraft achieves stable approach speed and configuration. This altitude is a variable in the simulation. For a conventional approach it is assumed that stable approach speed and configuration are achieved at a 1500 ft. altitude above the runway. Observe that fuel and DOC savings increase as the altitude for stable configuration is decreased. The maximum fuel savings due to the delayed flap approach is 0.39%.

Mission Type	Maximum Savings					
	Fuel Gallons	Fuel Cost	DOC	DOC 1	DOC 2	DOC 3
Long Range	5,279,000	2,217,000	1,253,000	768,400	543,900	440,300
Medium Range	2,628,000	1,104,000	688,000	482,600	404,200	336,900
Short Range	419,000	176,000	104,000	67,600	54,200	41,500
Total	8,326,000	3,497,000	2,045,000	1,318,600	1,002,300	818,700
% Savings	5.84	5.84	2.29	1.11	0.68	0.46

Table 7.2-6 C-5A Annual Savings Due to Increased Altitudes and Reduced Speed

Altitude for Stable Landing Speed		ANNUAL SAVINGS											
		Fuel/gal	%	Fuel Cost	%	DOC	%	DOC 1	%	DOC 2	%	DOC 3	%
1000		190,500	.13	80,000	.13	102,300	.11	124,400	.1	146,500	.1	168,600	0.1
500		378,200	.26	158,800	.26	201,800	.22	244,400	.21	286,900	.2	329,500	.19
0		562,600	.39	236,300	.39	298,200	.33	359,700	2.3	421,000	.29	482,400	.27

Table 7.2-7 Annual Fuel/DOC Savings Due to Delayed Flap Approach - C-5A

7.2.5.4 Aft C.G. Operations

The operation of an aircraft with c.g. further aft than those being used results in reduced aerodynamic drag and attendant fuel savings. Since the C-5A is a cargo aircraft, its c.g. can be readily influenced by the proper fuel load and payload distribution. During flight tighter fuel management and burning fuel evenly towards aft c.g. will also reduce drag. For C-5A the fuel savings due to aft c.g. operations were calculated by taking the average weights during cruise segments of long range and medium range missions. Corresponding cruise altitudes and air speeds were obtained from the ASIMIS tape data. Then for each mission the reduction in aerodynamic drag and the corresponding fuel savings were computed. Final savings were obtained by averaging over the mission spectrum data. A .5%-MAC (mean aerodynamic chord) shift in c.g. towards aft results in a 0.7% savings in fuel consumed, which amounts to a savings of one million gallons in annual fuel consumed. Note that the actual estimate of savings due to aft c.g. operation will require a detailed study of actual fuel and load distributions and the means of changing this distribution to shift c.g. towards aft. Moreover, each mission will require careful distribution of fuel and payload.

7.2.5.5 Reduced Reserve Fuel

Histograms of C-5A mission spectrum given in Section 7.2.2 indicate that the landing fuel is much higher than required; thus fuel savings can be achieved by reducing the reserve fuel to requirements. In addition to fuel required for 45 minutes of holding, enroute reserve and destination to alternate, 2% extra fuel is required for aileron uprig [34]. In determining fuel savings due to reduced reserve fuel, allowance has been made for this requirement. It is assumed that an alternate is available within 200 n.mi. As discussed in Section 4.3, an alternate airport within 200 n.mi. of the original destination is

generally available except for a few overseas bases. Since the C-5A has sophisticated navigation equipment, the en route reserve may not be required. The fuel requirement for a 45 minute holding time appears excessive. Thus fuel savings for the C-5A have been determined under the four options given below.

- 200 n.mi. alternate plus en route reserve plus 45 minutes holding time
- 200 n.mi. alternate plus 45 minutes holding time
- 200 n.mi. alternate plus 15 minutes holding time
- 200 n.mi. alternate

A fuel allowance for aileron uprig has been made for all options. Table 7.2-8 summarizes the results for these four options. The savings in fuel consumption by reducing reserve fuel to the maximum requirements (the first option) is less than 1%. However by relaxing the reserve fuel requirements further, a fuel savings of more than 2% can be achieved. These fuel savings were obtained assuming that missions are flown at the cruise altitudes and air speeds obtained from ASIMIS tapes. Optimal flight procedures will result in a further reduction in reserve fuel requirements; however, this further reduction will not be significant.

7.2.5.6 Reduce Engine Load

As discussed in Section 4.2.2, fuel savings can be effected through a reduction in accessory loads on engines and bleed air extraction. Power demands can be reduced by turning off unnecessary lights, radios, etc. and by maintaining cabin temperatures at a higher setting than they currently are. Minimizing use of anti-icing also results in fuel savings. Discussions with people involved in the operation of these aircraft indicated that accessory equipment is used only when required, i.e., accessory loads are being run at a minimum now. This fact combined with the lack of real data on the subject has prevented the assignment of a savings factor in this case.

Requirement Option	Savings Due to Reduced Reserve Fuel											
	Fuel			DOC		DOC1		DOC2		DOC3		
	Gallons	\$	%	\$	%	\$	%	\$	%	\$	%	
200 nmi alternate + 45 min holding + enroute reserve	1, 269, 000	533, 000	. 9	553, 000	. 6	573, 000	. 5	590, 000	. 4	610, 000	. 3	
200 nmi alternate + 45 min holding	2, 390, 000	1, 004, 000	1. 7	1, 037, 000	1. 2	1, 071, 000	. 9	1, 100, 000	. 7	1, 140, 000	. 6	
200 nmi alternate + 15 min holding	2, 879, 000	1, 209, 000	2. 0	1, 250, 000	1. 4	1, 291, 000	1. 1	1, 330, 000	. 9	1, 370, 000	. 8	
200 nmi alternate	3, 119, 000	1, 310, 000	2. 2	1, 345, 000	1. 5	1, 398, 000	1. 2	1, 440, 000	1. 0	1, 480, 000	. 8	

Table 7.2-8 Fuel/DOC Savings Due to Reducing Reserve Fuel for C-5A

7.2.5.7 Reduce Engine Use and Taxi Time

Average fuel consumption for C-5A during ground operations is 120 lbs/minute with four engines operating. Some measures which may reduce engine use during ground operations were outlined in Section 4.3.2. These include delaying engine start until clearance to taxi is obtained, taxi the shortest route to runway, etc. If for each mission the taxi time were reduced by one minute, this would result in annual savings of 162,500 gallons of fuel and \$170,600 in DOC.

7.2.5.8 Partial Engine Taxi

It may be possible to shut down two engines for taxi-in and parking of the C-5A. A two-engine taxi for an average five minute taxi time can save 406,000 gallons of fuel and \$426,000 in DOC annually for C-5 operations.

7.2.5.9 Removing Excess Equipment

Carrying excess equipment results in the burning of additional fuel to carry that weight. Thus removal of equipment not required for a mission results in fuel conservation. No excess equipment has been specifically identified for C-5A operations and an overall savings factor is not appropriate in this case. However, a 1000 lb. reduction in equipment per mission would result in approximately a 140,000 gallon reduction in fuel consumption annually.

7.2.5.10 Maintenance to Reduce Drag

Section 4.3 details various reasons for an increase in aerodynamic drag. These include aircraft surface irregularities, control surface rigging and seal leakages. From the field visits the observed aircraft appeared in a good state of maintenance. Thus a direct quantification of savings due to aircraft maintenance is inappropriate. Fuel/DOC savings due to aircraft maintenance which reduces drag may be obtained from the sensitivity plots given in Section 7.2.6.

7.2.5.11 Engine Maintenance

The TF-39 engines powering C-5A aircraft are relatively new, and the deterioration of engine TSFC is minor compared to other aircraft under study. The scheduled maintenance procedures for these engines appear adequate. The fuel economy trim procedure outlined in Section 4.3 may result in some fuel savings; however, the assignment of a savings factor in this case is difficult. The fuel/DOC savings due to improvement in TSFC may be calculated from the sensitivity plots in Section 7.2.6.

7.2.6 Evaluation of Design Modifications

The C-5A is a result of relatively new technology and was introduced into the inventory in the late 1960s. The TF-39-GE-1 turbofan engine is a high bypass unit using the latest technological improvements, and of all the engines being used, it is still the most economical in fuel consumption. Thus there are no specific propulsion design modifications being considered for this aircraft. The C-5A is involved in a wing modification program which would extend the aircraft's operational life and increase the pay load capability to 235,000 lbs. Retrofitting winglets may offer potential fuel savings and will be evaluated in this section.

7.2.6.1 Parametric Analysis of Aerodynamic and Propulsion Design Modifications

The generic plots illustrating variations in fuel and DOC as functions of the variations in aerodynamic and propulsion parameters have been developed for C-5A. These plots are based on the entire mission spectrum and may be used to evaluate any design modifications following the approach outlined in Section 5. Variations in fuel/DOC as functions of variations in zero-lift drag, induced drag and thrust specific fuel consumption for the C-5A are shown in Figures 7.2-16, 17 and 18, respectively. Changes in fuel/DOC due to changes in TOGW are illustrated in Figure 7.2-19. The use of these plots to evaluate a potential winglet design will be discussed in the next subsection.

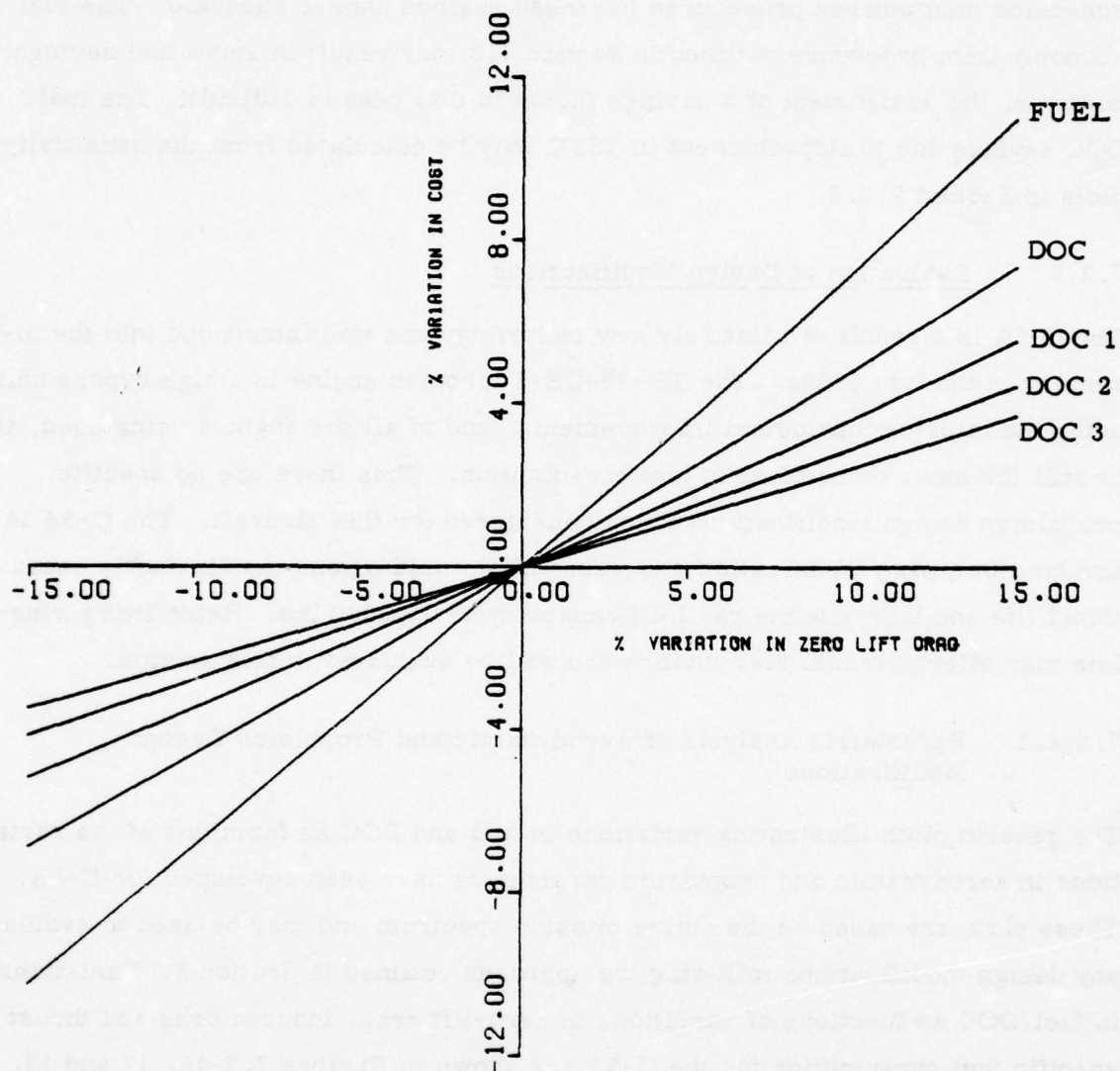


Figure 7.2-16 Sensitivity of Fuel/DOC to Variations in Zero-Lift Drag - C-5A

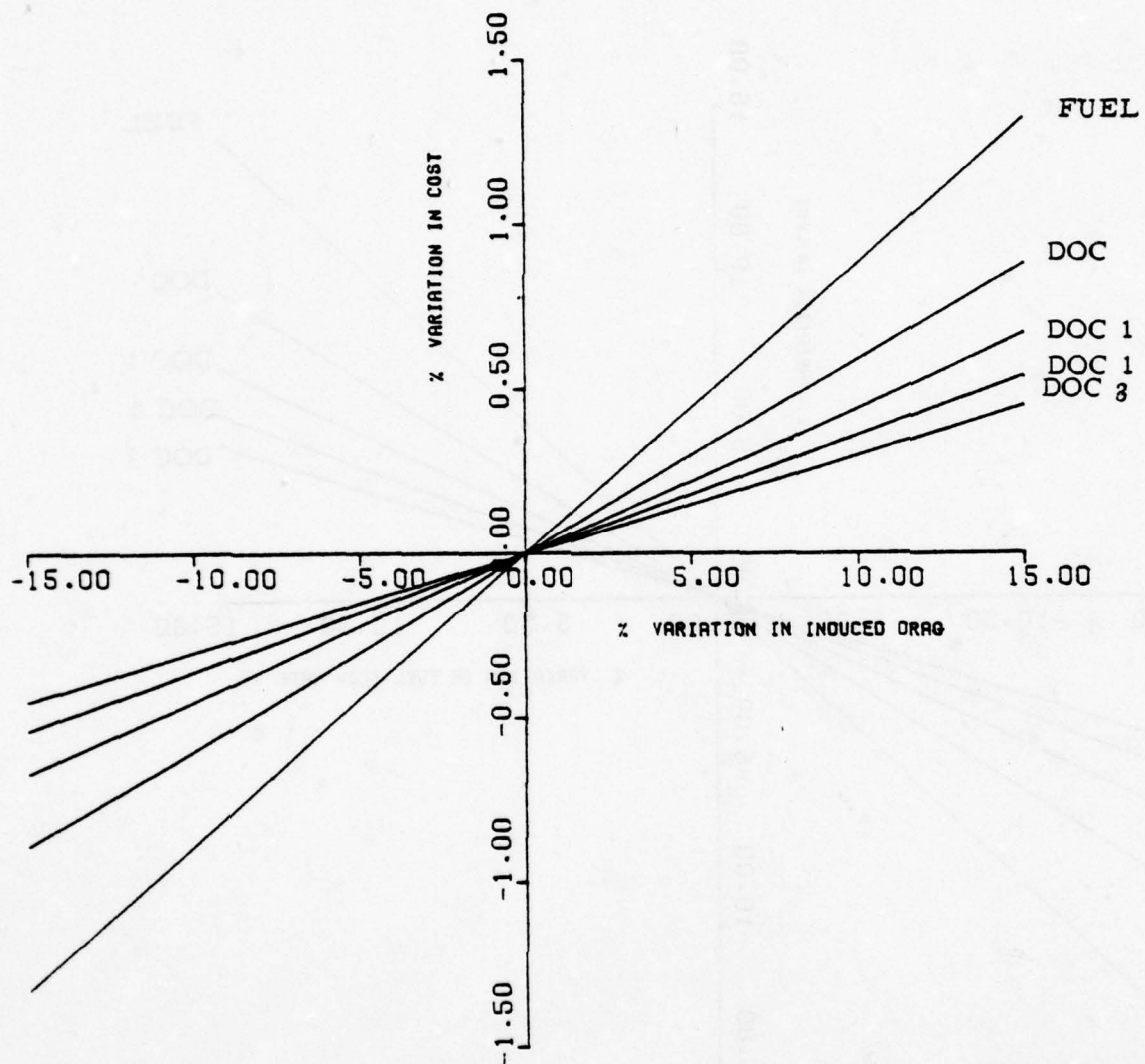


Figure 7.2-17 Sensitivity of Fuel/DOC to Variations in Induced Drag - C-5A

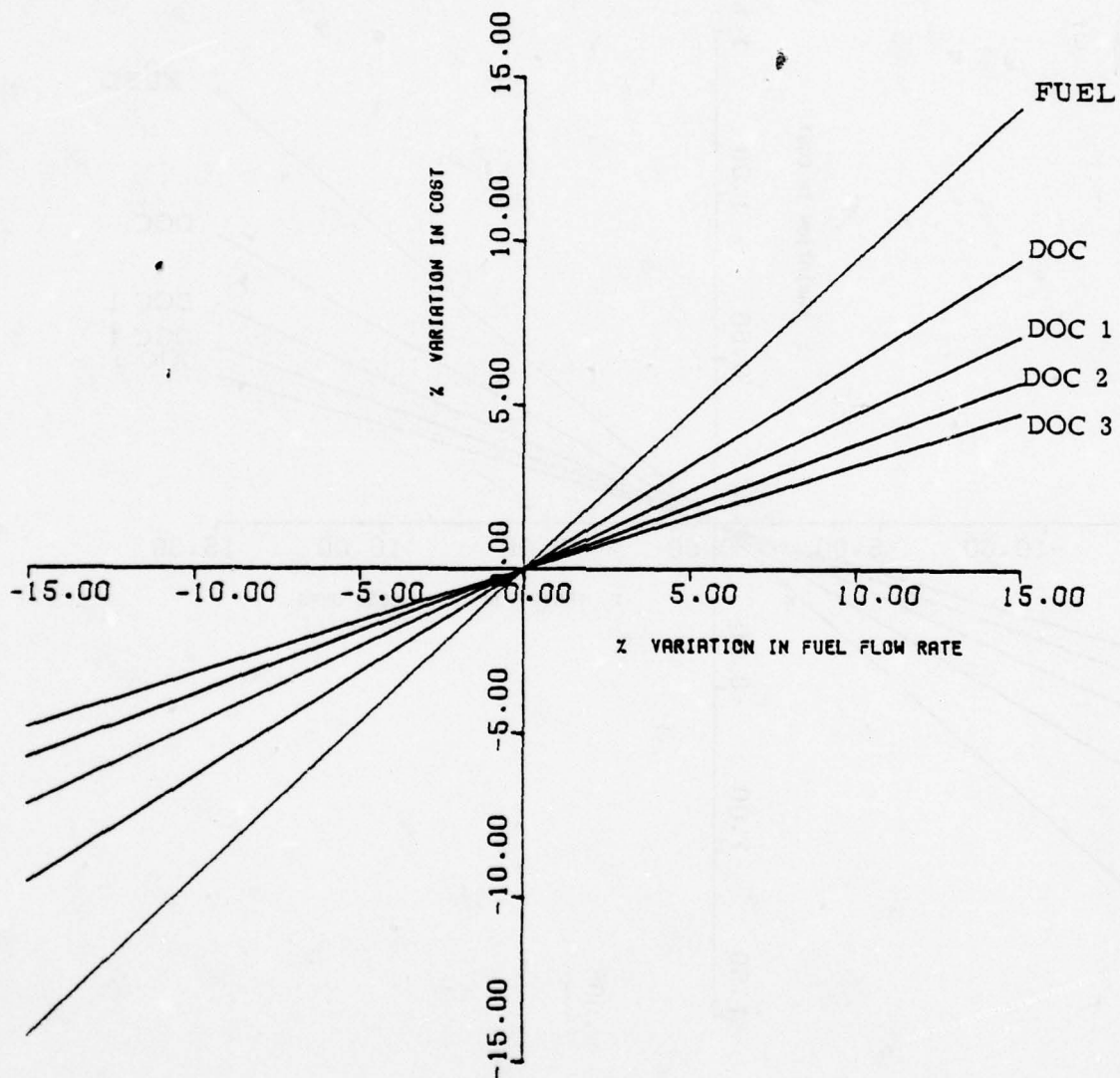


Figure 7.2-18 Sensitivity of Fuel/DOC to Variations in Thrust Specific Fuel Consumption - C-3A

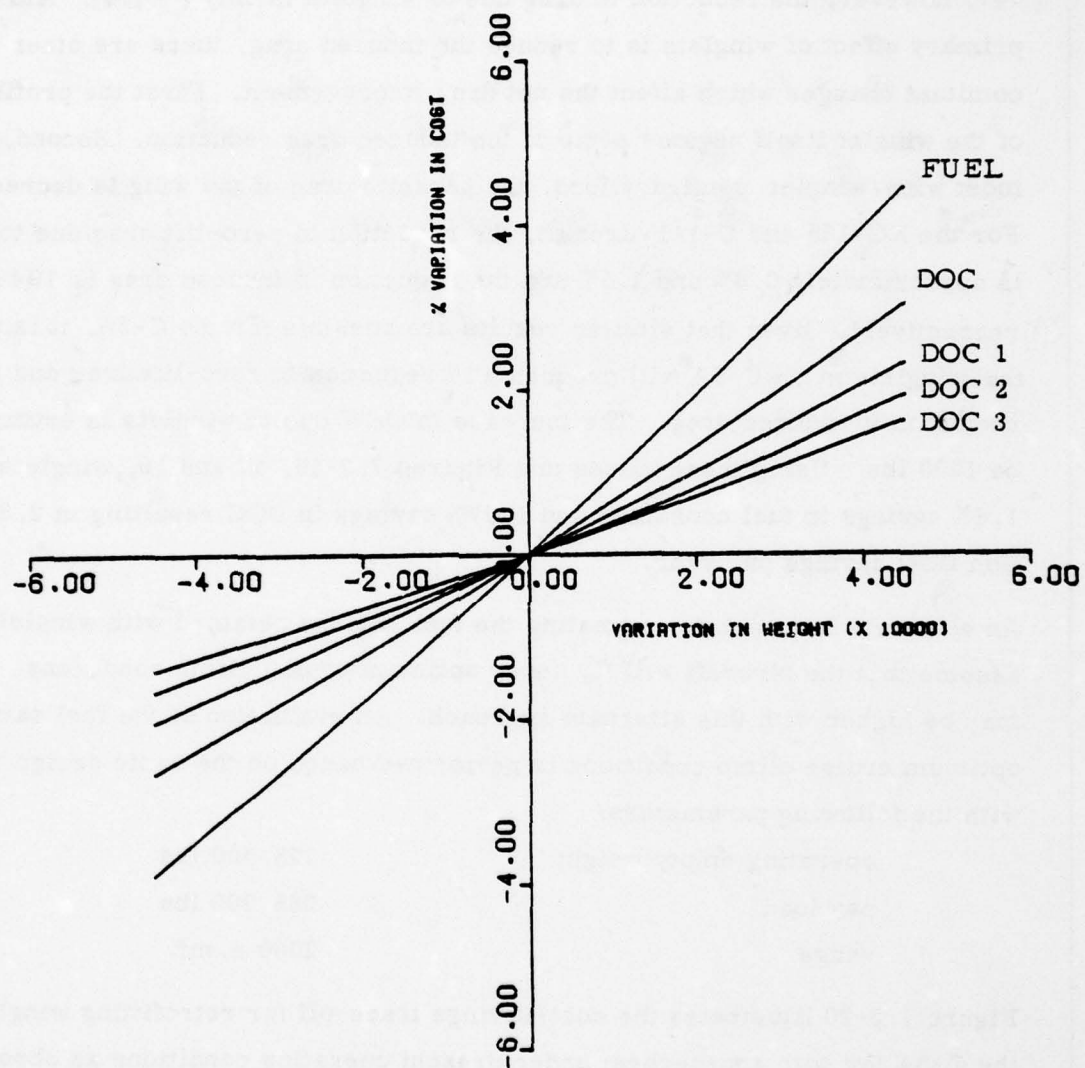


Figure 7.2-19 Sensitivity of Fuel/DOC to Variations in Weight - C-5A

7.2.6.2 Evaluation of Winglets for the C-5A

No prior study has been performed for the design and analysis of winglets for the C-5A, as was done for the C-141 and KC-135 aircraft. The C-141 and KC-135 studies indicate a 5.6% and 7% reduction in airplane drag, respectively. On a 747, however, the reduction in drag due to winglets is only 3% [36]. Although the primary effect of winglets is to reduce the induced drag, there are other concomitant changes which affect the net drag improvement. First the profile drag of the winglet itself negates some of the induced drag reduction. Second, for most wing/winglet configurations, the parasite drag of the wing is decreased. For the KC-135 and C-141 aircraft, the reduction in zero-lift drag due to winglets is approximately 0.8% and 1.5% and the reduction in induced drag is 19.4% and 11% respectively. Given that similar results are possible for the C-5A, it is assumed that winglets on the C-5A will produce a 1% reduction in zero-lift drag and an 11% reduction in induced drag. The increase in OEW due to winglets is estimated to be 1000 lbs. Using these values and Figures 7.2-16, 17 and 19, winglets offer a 1.6% savings in fuel consumed and 1.07% savings in DOC resulting in 2.82 million DOC savings per year.

An alternate approach to estimating the fuel savings obtained with winglets is to assume that the aircraft will fly under optimum cruise climb conditions. Savings may be higher with this alternate approach. An evaluation of the fuel savings for optimum cruise climb conditions is performed based on the basic design mission with the following parameters:

operating empty weight	325,500 lbs
pay load	265,000 lbs
range	2000 n. mi.

Figure 7.2-20 illustrates the cost/savings trade-off for retrofitting winglets on the C-5A for both approaches: under present operating conditions as observed from the ASIMIS tapes and under optimum conditions. With the acquisition cost estimated to be \$8 million, the break-even time (T_{BE}) is estimated to be 3.4 years for present operating conditions.

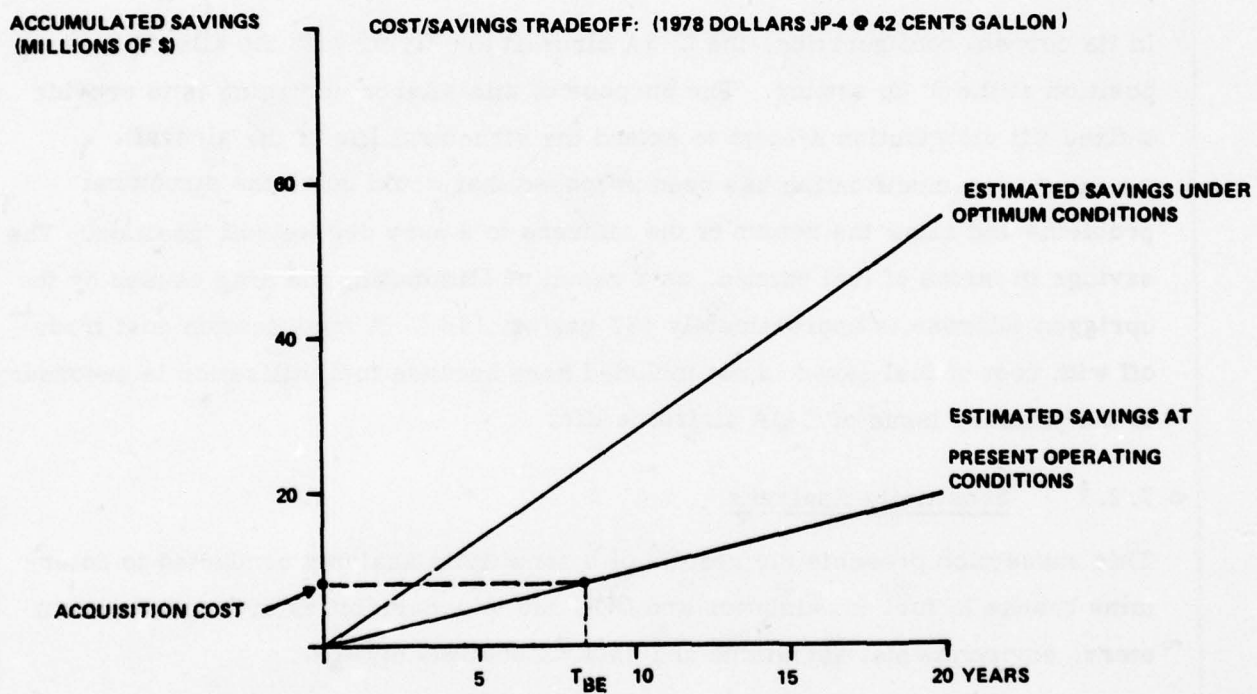


Figure 7.2-20 SAVINGS DUE TO WINGLETS FOR C-5A

The cost savings for the optimum cruise climb case are obtained using Figures 7.2-21 and 7.2-22, which show the sensitivity of range factor to variations in zero lift drag and induced drag, respectively. With a 1% reduction in zero-lift drag and an 11% reduction in induced drag, these figures give a 4.6% increase in range factor (0.8% from Figure 7.2-21 and 3.8% from Figure 7.2-22). The average value of range factor for the C-5A is 12270. From these values the fuel savings due to winglets for the C-5A under optimum operating conditions is calculated to be 4.5% for the basic mission. Based on this value, the annual fuel savings increase to 6.56 million gallons. Figure 7.2-20 shows a cost/savings trade-off for retrofitting winglets on the C-5A.

7.2.6.3 C-5A Outer Wing Modification

In its current configuration, the C-5A aircraft are flying with the aileron null position at the 6° up setting. The purpose of this aileron uprigging is to provide a fixed lift distribution system to extend the structural life of the aircraft. An outer wing modification has been proposed that would solve the structural problems and allow the return of the ailerons to a zero degree null position. The savings in terms of fuel burned, as a result of eliminating the drag caused by the uprigged ailerons, is approximately 133 gal/hr [46]. A modification cost trade-off with cost of fuel saved is not included here because fuel utilization is secondary to the primary issue of C-5A airframe life.

7.2.7 Sensitivity Analysis

This subsection presents the results of a sensitivity analysis conducted to determine change in fuel consumption and DOC due to uncertainties in aircraft parameters, environmental variations and instrumentation errors.

7.2.7.1 Uncertainties in Aircraft Parameters

The sensitivity of fuel consumption and DOC to variations in zero-lift drag, induced drag, fuel flow rate and system weight have been determined for best cruise performance by varying the aerodynamic and propulsion model coefficients about their nominal value in the simulation.

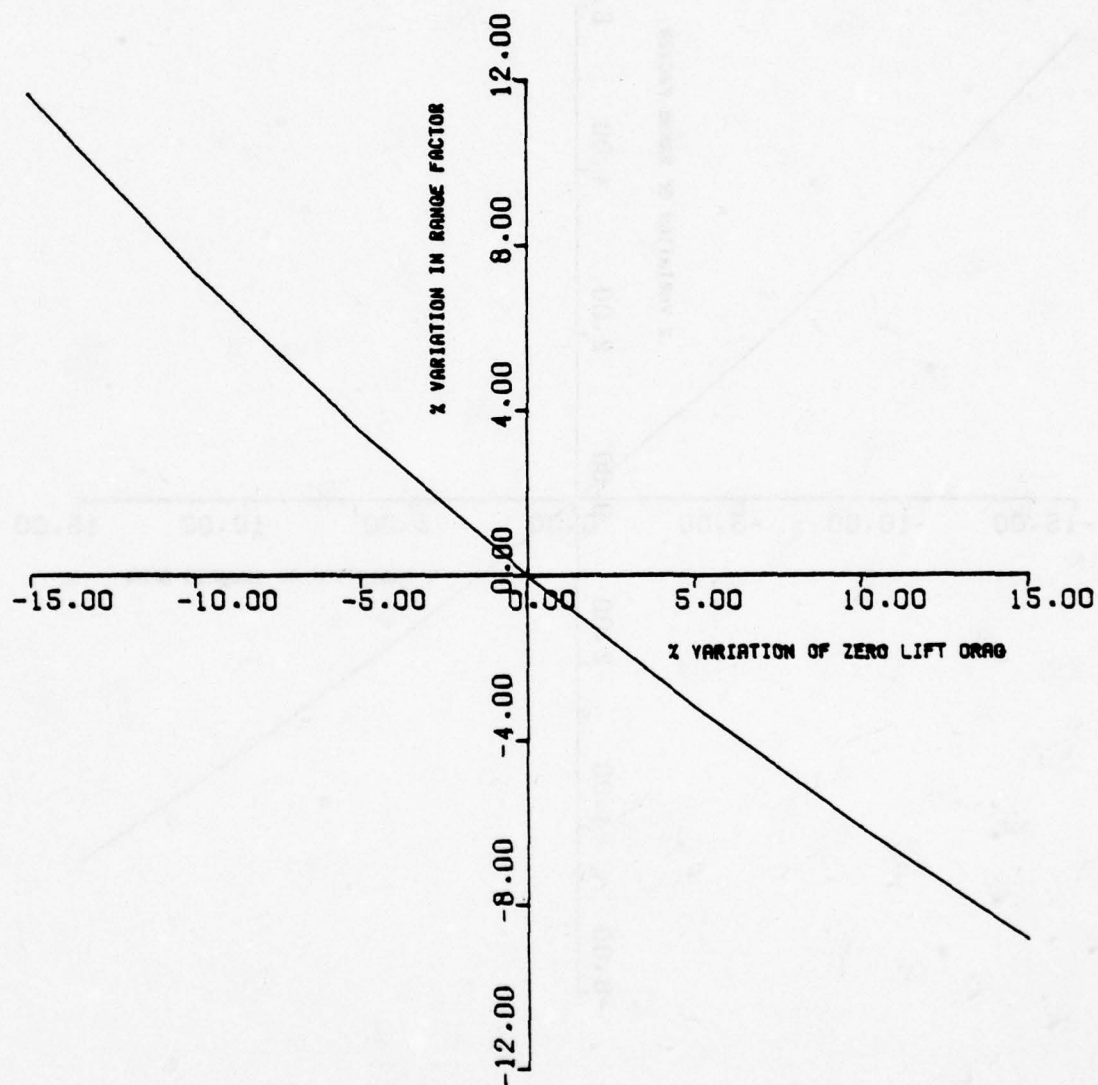


Figure 7.2-21 SENSITIVITY OF RANGE FACTOR TO VARIATION
IN ZERO-LIFT DRAG FOR C-5A

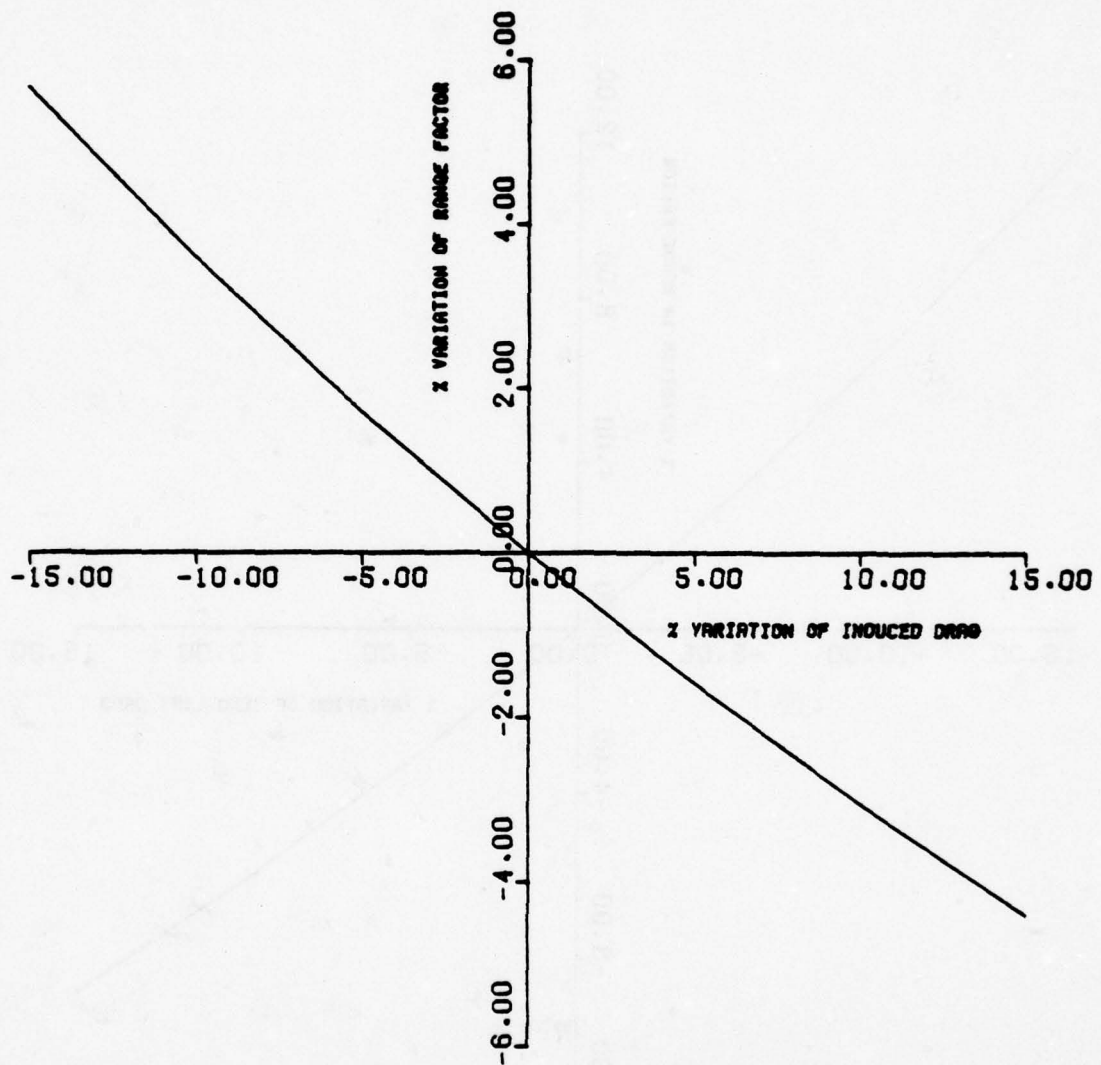


Figure 7.2-22 SENSITIVITY OF RANGE FACTOR TO VARIATIONS
IN INDUCED DRAG FOR C-5

Sensitivity to Zero-Lift Drag

An increase in the zero-lift drag coefficient results in an increased aerodynamic force and the attendant fuel consumption. Figure 7.2-21 depicts the sensitivity of range factor (RF) to variations in zero-lift drag for the C-5A. If mission range and take-off gross weight remain constant, then a knowledge of the change in RF, enables one to compute the fuel savings using Equation (6.1). For example, if the zero-lift drag coefficient of a particular C-5A aircraft is 5% less than the nominal value, from Figure 7.2-21 the range factor for that aircraft is 3.5% higher than nominal. By taking the average RF equal to 12270 for a 1000 n.mi. range mission, one computes that the fuel consumption will be 3.35% less than the average fuel consumption.

If it is known beforehand that the zero-lift drag coefficient is 5% less, then the take-off fuel weight may be reduced and fuel savings can be estimated using Equation (6.2). For the above example the fuel savings would amount to 3.65%.

Sensitivity to Induced Drag

The effect of variations in induced drag on fuel consumption is similar to that of zero-lift drag. Figure 7.2-22 provides the sensitivity of RF to variations in induced drag. Observe that the sensitivity of RF to changes in induced drag is almost one-half of the sensitivity to zero-lift drag. Changes in fuel consumption can be estimated following the same method as for zero-lift drag.

Sensitivity to Fuel Flow Rate

A uniform increase (decrease) in fuel flow rate results in a proportional decrease (increase) in range factor (RF). Thus for a given mission, the change in fuel consumption may be estimated using Equation (6.1) if TOGW remains the same, or Equation (6.2) if landing weight remains unchanged.

Sensitivity to System Weight

For a given mission the variation in fuel consumed due to variations in initial weight or terminal weight may be obtained using Equations (6.3) and (6.4). Note that the variation in fuel consumed is linearly proportional to variations in system weight.

Sensitivity to Variations in Thrust

As mentioned in Section 6.1.5, variations in maximum thrust (NRT) impact the optimum cruise performance through its effect on the cruise ceiling. For the C-5A the optimum cruise altitude is constrained by cruise ceiling. An increase in NRT raises the cruise ceiling, thus enabling the aircraft to cruise at the optimum cruise altitude resulting in reduced fuel consumption. However, a decrease in NRT lowers the cruise ceiling which decreases cruise altitude and increases fuel consumption. Fig. 7.2-23 illustrates the impact of a variation in NRT on cruise ceiling for a 600,000 pound aircraft weight. A 5% decrease in NRT results in lowering cruise altitude by 1300 feet. From Section 7.2.7-4, sensitivity to instrument errors, it is seen that this 1300 foot drop in altitude results in a 0.9% increase in the specific fuel consumption.

Variations of NRT also impact the climb time. However, if the cruise altitude is not constrained due to a change in NRT, then the change in total fuel consumed will be negligible for most of the missions.

7.2.7.2 Sensitivity to Atmospheric Variation

Atmospheric variations which impact the optimal flight procedures are the wind velocities and ambient temperatures.

Temperature Effects

Temperature deviations from a standard day have negligible effects on specific fuel consumption during cruise when less than normal rated thrust is required. However, atmospheric temperatures which are warmer than standard have the effect of decreasing the cruise altitude ceiling. For the C-5A each °C above standard reduces the cruise ceiling by approximately 300 feet. Thus the effect of temperature on fuel consumption is similar to the impact of NRT variation on fuel consumption. Knowing the change in cruise ceiling, Fig. 7.2-27 can be used to estimate changes in fuel consumption. Since true air speed varies

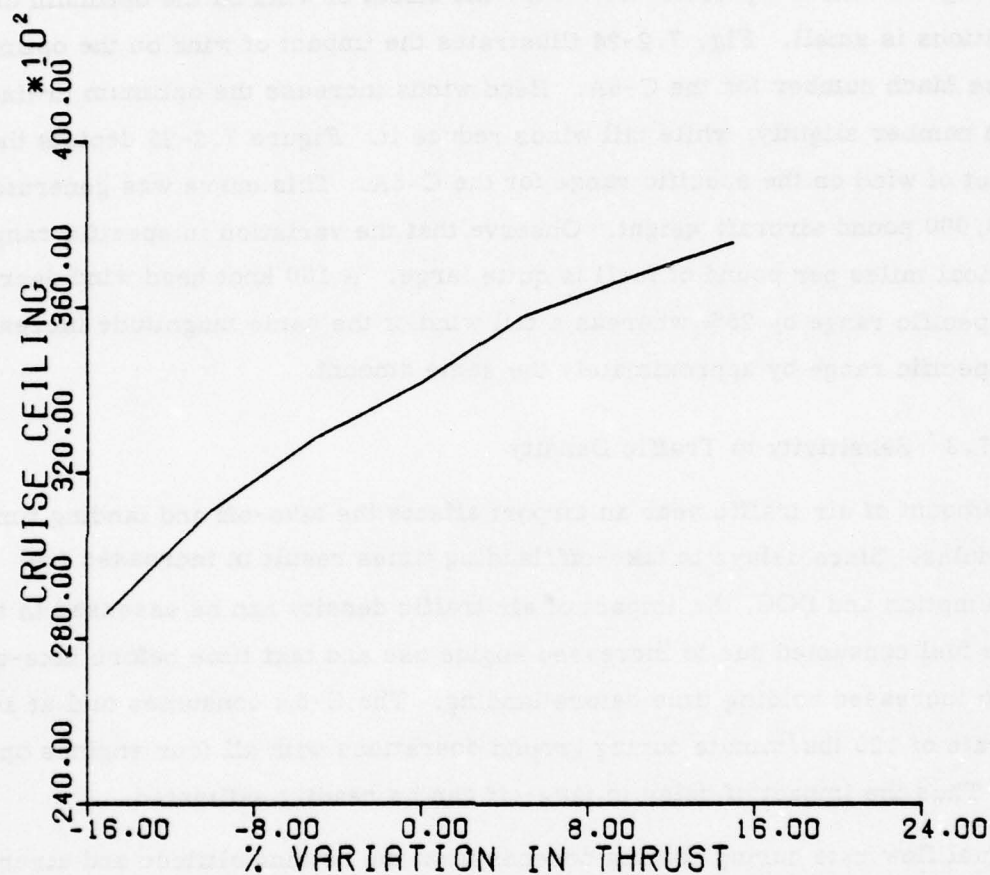


Figure 7.2-23 IMPACT OF THRUST VARIATION OF CRUISE
CEILING FOR C-5

with temperature, total mission time is affected by the changes in ambient temperature, assuming no wind change in mission time can be estimated using Eq. (6.6).

Wind Effects

As mentioned in Section 6.2, winds have a large impact on the fuel consumed in flying between two points. However, the effect of wind on the optimum cruise conditions is small. Fig. 7.2-24 illustrates the impact of wind on the optimum cruise Mach number for the C-5A. Head winds increase the optimum cruise Mach number slightly, while tail winds reduce it. Figure 7.2-25 depicts the impact of wind on the specific range for the C-5A. This curve was generated for a 600,000 pound aircraft weight. Observe that the variation in specific range (nautical miles per pound of fuel) is quite large. A 100 knot head wind decreases the specific range by 25%, whereas a tail wind of the same magnitude increases the specific range by approximately the same amount.

7.2.7.3 Sensitivity to Traffic Density

The amount of air traffic near an airport affects the take-off and landing time schedules. Since delays in take-off/landing times result in increased fuel consumption and DOC, the impact of air traffic density can be assessed in terms of the fuel consumed due to increased engine use and taxi time before take-off and due to increased holding time before landing. The C-5A consumes fuel at an average rate of 120 lbs/minute during ground operations with all four engines operating. Thus the impact of delay in take-off can be readily estimated.

The fuel flow rate during holding depends upon the holding altitude and aircraft weight. Assuming an average landing weight of 480,000 pounds and an optimum holding altitude, the fuel flow rate is 240 lbs/minute. The increased fuel consumption due to a delay in clearance for landing can be estimated using this fuel flow rate and actual holding time.

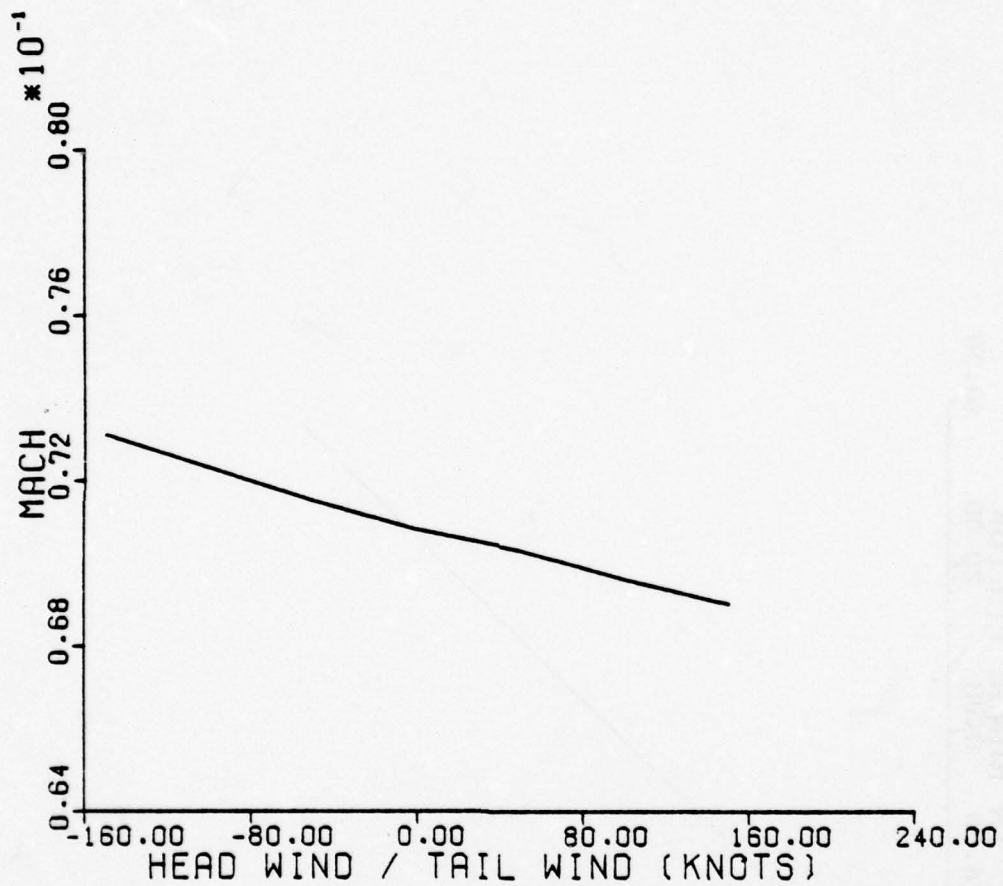


Figure 7.2-24 IMPACT OF WIND ON OPTIMUM
CRUISE MACH NUMBER FOR C-5

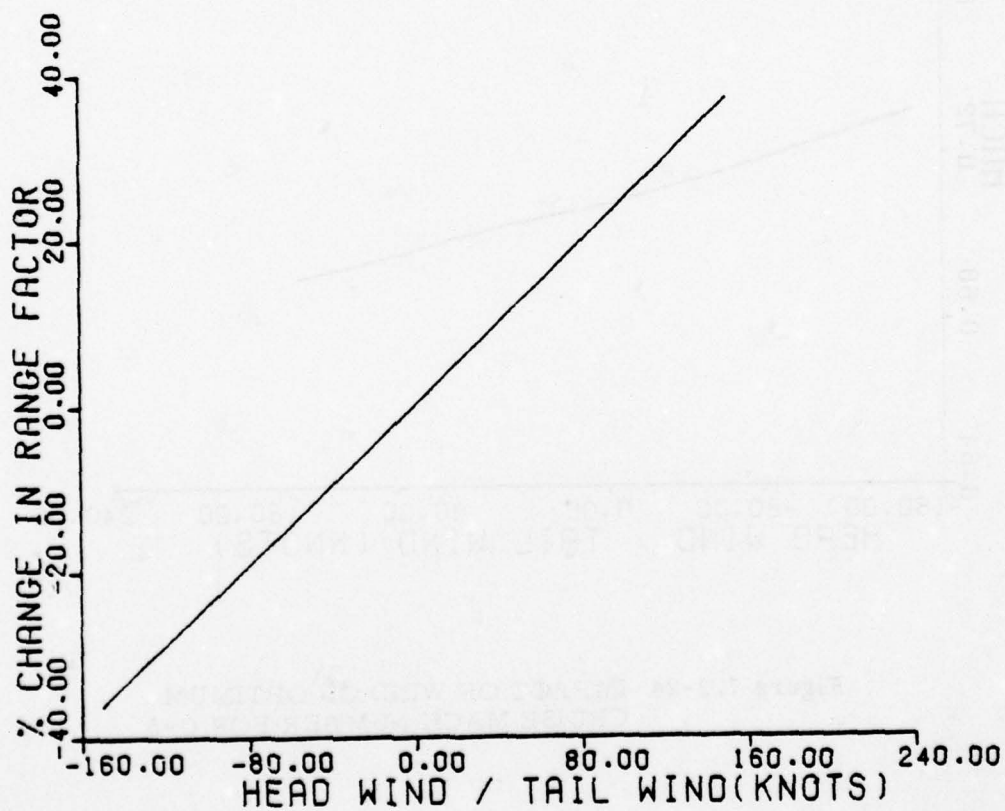


Figure 7.2-25 Impact of Wind on Range Factor

for C-5

7.2.7-4 Sensitivity to Instrument Errors

Instrumentation errors can cause an aircraft to fly at off-optimal cruise conditions resulting in increased fuel consumption. Impact of instrument errors on fuel consumption can be assessed from the sensitivity of fuel consumption to variations in air speed and altitude.

Figures 7.2-26 and 27 depict the sensitivity of range factor (RF) to changes in cruise mach number and cruise altitude for the C-5A. Once changes in RF have been determined, Eq. (6.1) can be used to obtain the change in fuel consumed. Change in mission time is directly proportional to change for cruise Mach number. Then the DOC models given in Section 7.2.3 may be used to obtain the sensitivity of fuel/DOC to instrument errors.

7.2.8 Conclusions for the C-5

The two items which produced more than a 1% fuel savings annually are both operational procedures: namely,

- cruising at optimum altitude and air speed
- reduced reserve fuel

An annual fuel savings of 5.8% can be achieved by flying at optimum altitude and air speed. A fuel savings of 0.9 is possibly by reducing reserve fuel to the maximum set of requirements, and an additional 1.3% savings can be generated by establishing a more moderate set of reserve fuel requirements.

These conclusions are summarized in Table 7.2-9. Note that no design modifications are seriously being considered for the C-5A.

The potential fuel savings can be categorized as follows:

- Airborne operational procedures 6.8 - 7.3%
- Ground operational procedures 1.9 - 4.2%

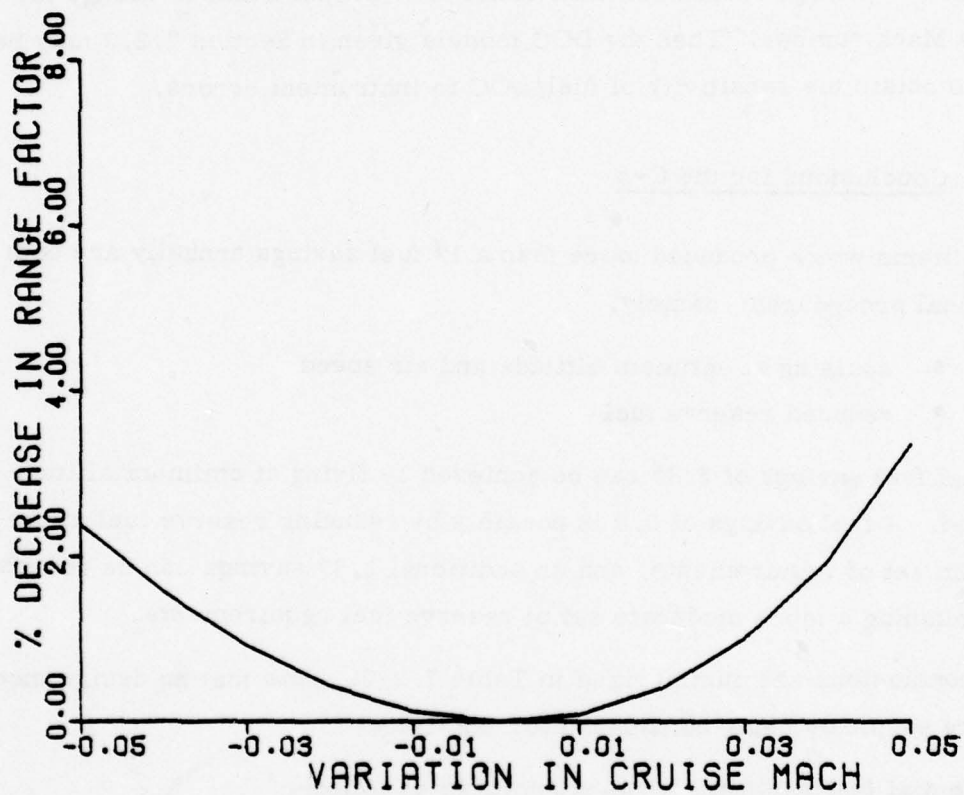


Figure 7.2-26 DECREASE IN RANGE FACTOR DUE TO
FLYING OFF OPTIMUM CRUISE MACH
NUMBER - C-5A

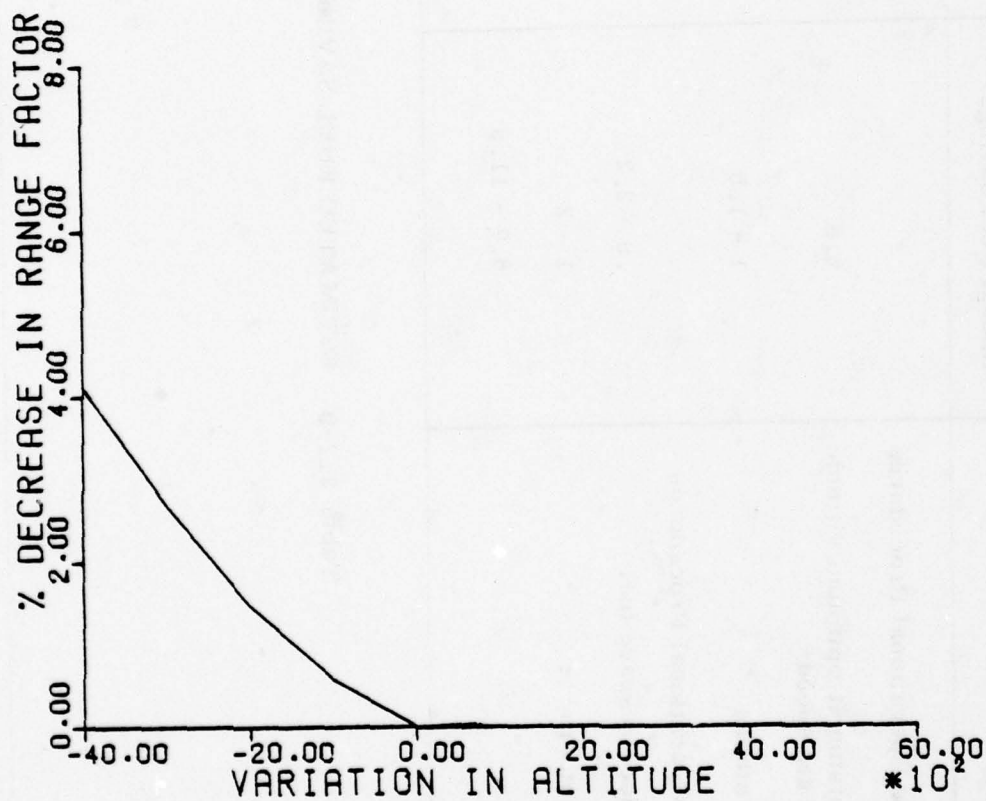


Figure 7.2-27 DECREASE IN RANGE FACTOR DUE TO
FLYING OFF OPTIMUM CRUISE ALTITUDE
- C-5A

Procedures	Estimated Percentage Annual Fuel Savings	Break Even Period Years	Confidence In Estimates
Airborne Operational Procedures			
Cruising at optimum altitude and air speed	5.8	-	High
All others	1 - 1.5	-	High
Ground Operational Procedures			
Reduce reserve fuel	.9 - 2.2	-	High
All others	1 - 2	-	High
Total	8.7 - 11.5		

Table 7.2-9 ESTIMATED FUEL SAVINGS FOR THE C-5A

7.3 C-130E AIRCRAFT

The Lockheed C-130 Hercules is a four engine, turboprop, medium transport aircraft with a primary mission of tactical airlift of cargo and personnel. The C-130E is powered by Allison T56-A-7 engines which are rated at 4,050 effective shaft horsepower (eshp). The first C-130 was built in 1956 and was designed as a straight cargo/personnel transport. The aircraft has over the years been modified for over 45 specialized applications. The first C-130H aircraft was received in March 1975 and used the same basic airframe as the C-130E, but with more powerful engines, a more efficient air-conditioning unit, a new auxiliary power unit, and larger engine inlet scoops. There are 15 C-130H aircraft which are C-130E's modified with the T56-A-15 engines in addition to the production C-130H aircraft. For this fuel conservation study only the C-130E aircraft performing MAC missions are considered. There are 217 C-130E aircraft performing this function.

7.3.1 Design Mission Data

Table 7.3-1 summarizes the data for the Basic and other design missions of the C-130E aircraft [47]. The Basic Mission has a 45,000 lb payload and carries 33,278 lbs in fuel. The Maximum Overload Maximum Cargo Mission has the same payload, but carries 57,108 lbs fuel and has a 2,972 n. mi. range.

7.3.2 Mission Model

During FY76 C-130E aircraft flew 44,600 missions for a total of 147,888 hours and consumed 116.09 million gallons of fuel. This aircraft performs a variety of missions including tactical missions, air drop missions, cargo airlift missions, training missions, etc. However, 75% of the C-130E missions are airlift missions with an average mission profile similar to the one shown in Figure 7.3-1. These missions are considered for evaluation of optimal flight procedures for C-130E aircraft.

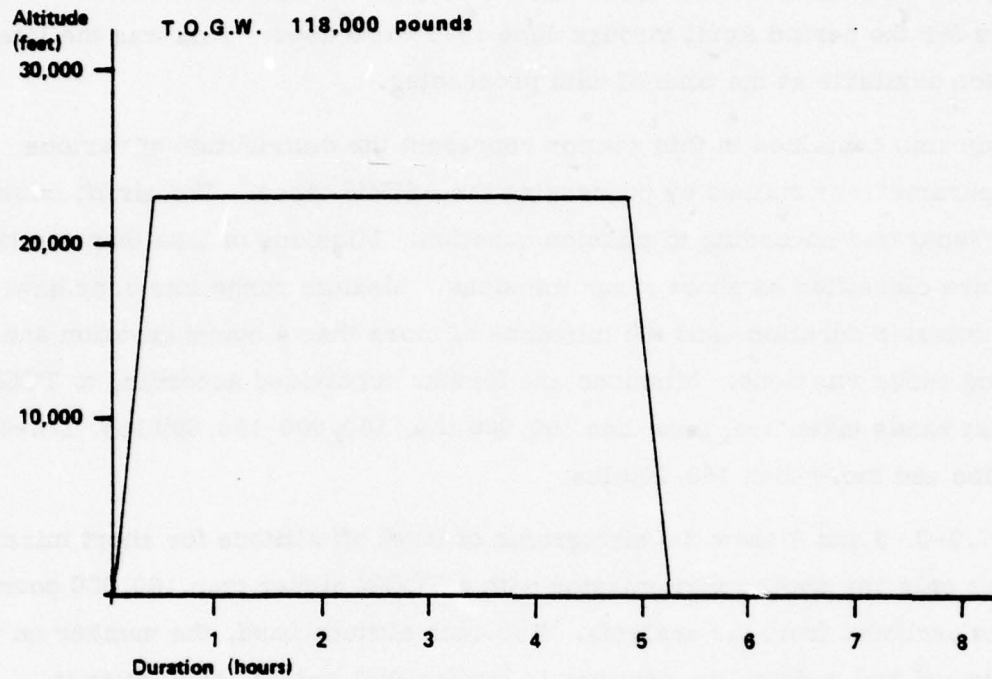
The remaining C-130E missions are classified as training missions in this study. These include air drop missions, local training missions with multiple take-offs

Conditions	Basic Mission	Max. Overload Max. Cargo	ADS Mission	Paratroup Mission	Ferry Range
TAKE-OFF WEIGHT	lb	175,000	155,000	152,172	135,228
fuel	lb	57,108	47,722	62,920	62,920
payload	lb	45,000	35,000	16,640	0
COMBAT RANGE	nmi	2,972	-	-	4,531
average cruise speed	kn	282	-	-	289
initial cruise altitude	ft	16,700	-	-	24,900
final cruise altitude	ft	37,900	-	-	37,900
mission time	hr	12.3	-	-	15.8
FIRST LANDING WEIGHT	lb	141,870	-	-	-
COMBAT RADIUS	nmi	1,699	1,497	2,053	-
average cruise speed	kn	282	290	290	-
initial cruise altitude	ft	16,700	20,700	21,300	-
final cruise altitude	ft	37,900	38,200	37,900	-
mission time	hr	12.6	10.8	14.7	-
LANDING WEIGHT	lb	77,467	76,374	77,475	77,164

OEW = 72,892

Table 7.3-1 C-130E Typical Mission Data

Figure 7.3-1 C-130 TYPICAL AIRLIFT MISSION



Phase	IAS/Mach	TIME	Air Distance	Fuel Used	End Altitude	End Gross Weight
Climb	174	.25	50	2,700	22,000	115,300
Cruise	196	5.58	1551	21,700	22,000	93,600
Descent	250	.25	38	1,200	0	92,400
TOTAL		6.08	1639	25,600		

and landings. Since the impact of optimal flight procedures on these missions is small, these missions are excluded from the optimal trajectory evaluation. Also there were several airlift missions flown below a 10,000 ft altitude, but the number of these missions is so small, they have been excluded from the evaluation.

The ASIMIS tape data, as described in Section 2, was used to generate the mission profile spectrum required to evaluate optimal flight procedures for C-130E. The data tapes for the period April through June 1976 were used. This was the latest information available at the time of data processing.

The histograms contained in this section represent the distribution of various mission parameters obtained by processing the ASIMIS tapes. The airlift missions are first separated according to mission duration. Missions of less than two hours duration are classified as short range missions. Medium range missions have a 2-4 hour mission duration, and the missions of more than 4 hours duration are called long range missions. Missions are further subdivided according to TOGW. The weight bands taken are: less than 100,000 lbs, 100,000-130,000 lbs, 130-000-160,000 lbs and more than 160,000 lbs.

Figures 7.3-2, 3 and 4 show the histograms of level off altitude for short missions. There was only one short range mission with a TOGW higher than 160,000 pounds, and it was excluded from the analysis. For each altitude band, the number on the top is take-off fuel weight, the next one is landing fuel weight, both given in thousands of pounds. The bottom one is mission duration in hours.

Figures 7.3-5, 6 and 7 are the histograms of level-off altitude for medium range missions. There were no medium range missions with a TOGW higher than 160,000 lbs.

Figures 7.3-8 and 9 are the level-off altitude histograms for long range missions. There was no long range mission with a TOGW higher than 160,000 lbs. There were only 9 missions with a TOGW less than 100,000 lbs, and they were excluded from the analysis.

Figure 7.3-2

C-130
DISTRIBUTION OF LEVEL OFF ALTITUDES
TAKE OFF GROSS WEIGHT - UP TO 100,000 pounds
MISSION DURATION - less than 2 hours

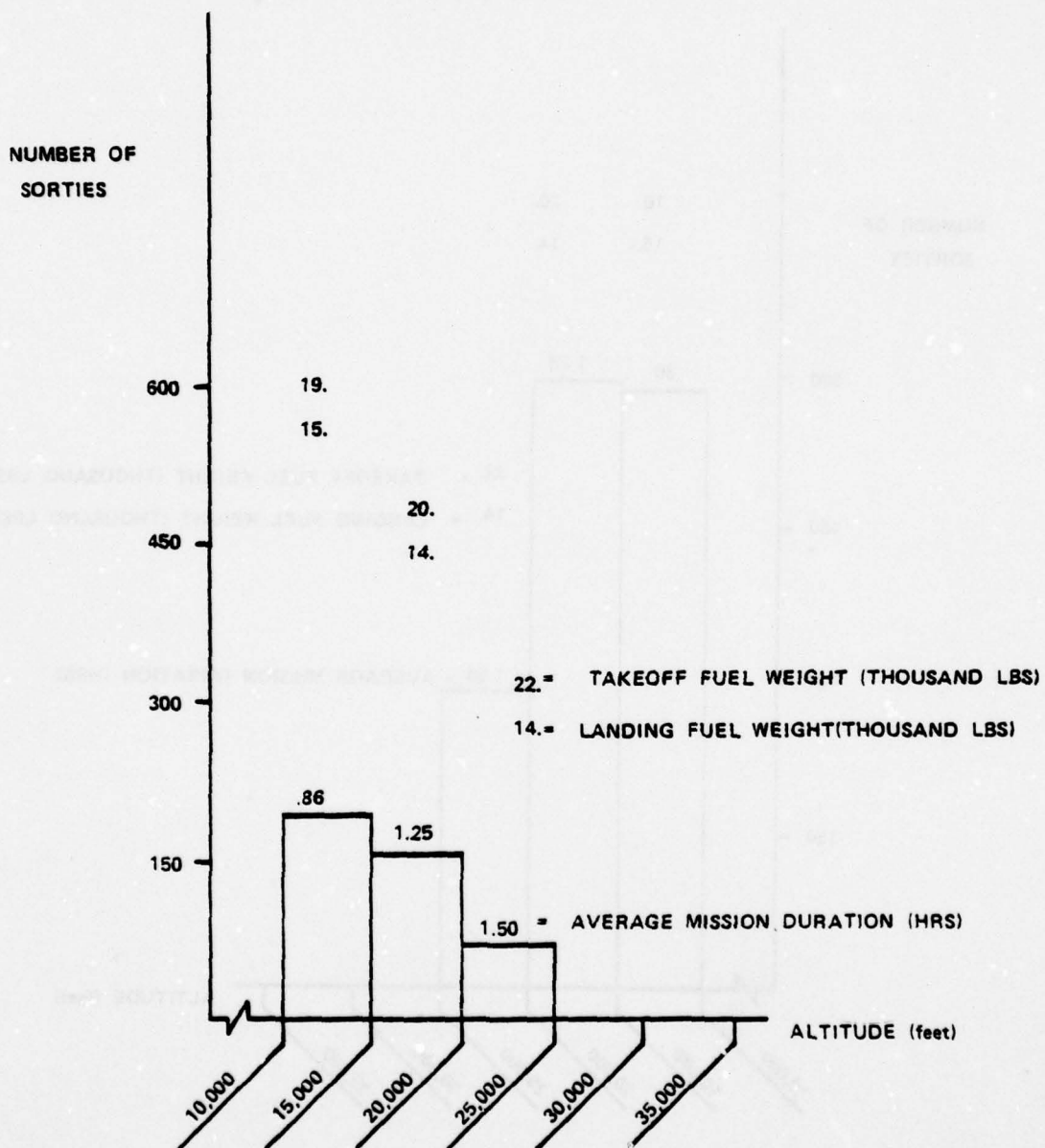


Figure 7.3-3

C-130
DISTRIBUTION OF LEVEL OFF ALTITUDES
TAKE OFF GROSS WEIGHT - 100,000 - 130,000 pounds
MISSION DURATION - less than 2 hours

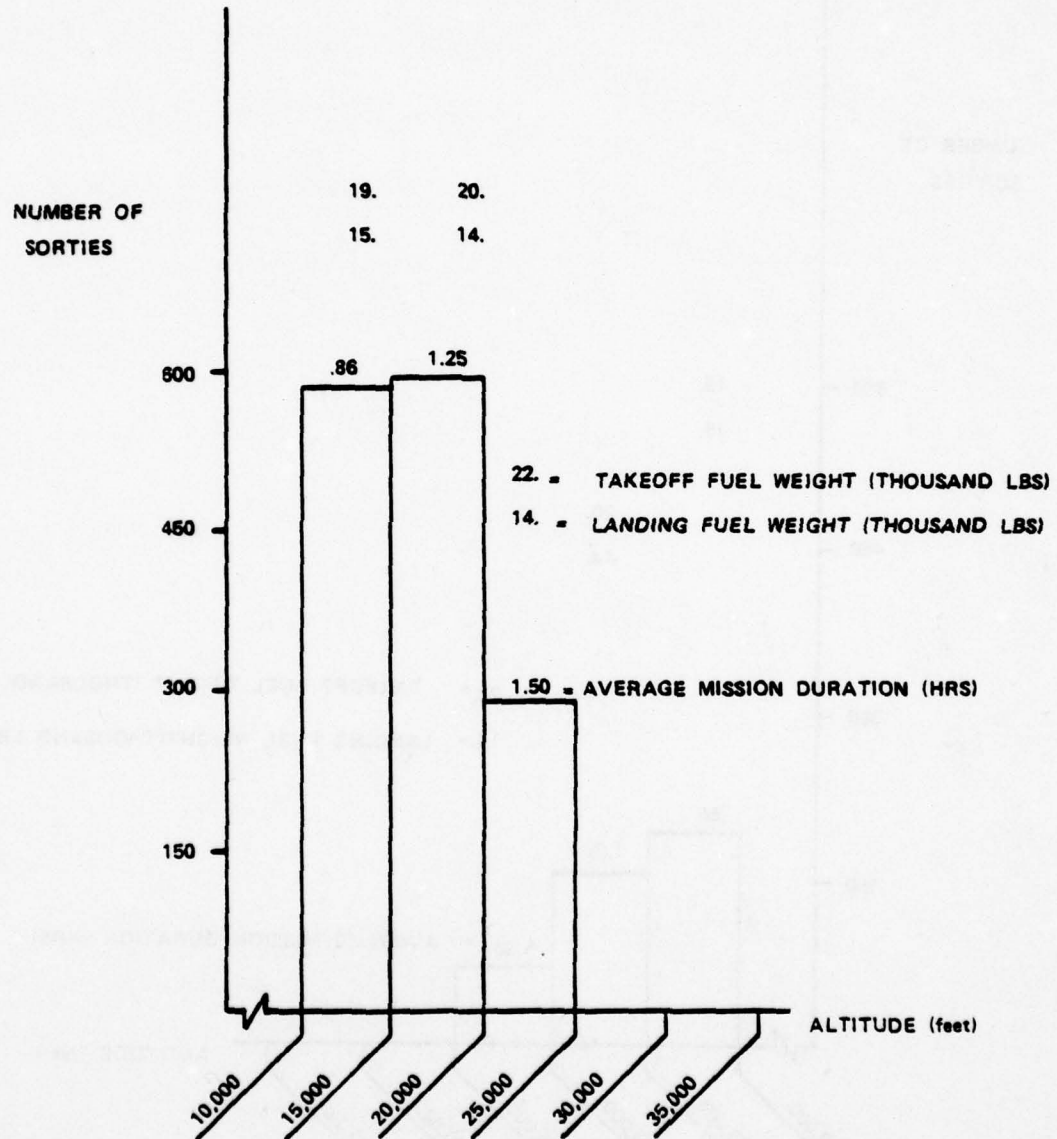


Figure 7.3-4

C-130
DISTRIBUTION OF LEVEL OFF ALTITUDES
TAKE OFF GROSS WEIGHT - 130,000 - 160,000 pounds
MISSION DURATION - less than 2 hours

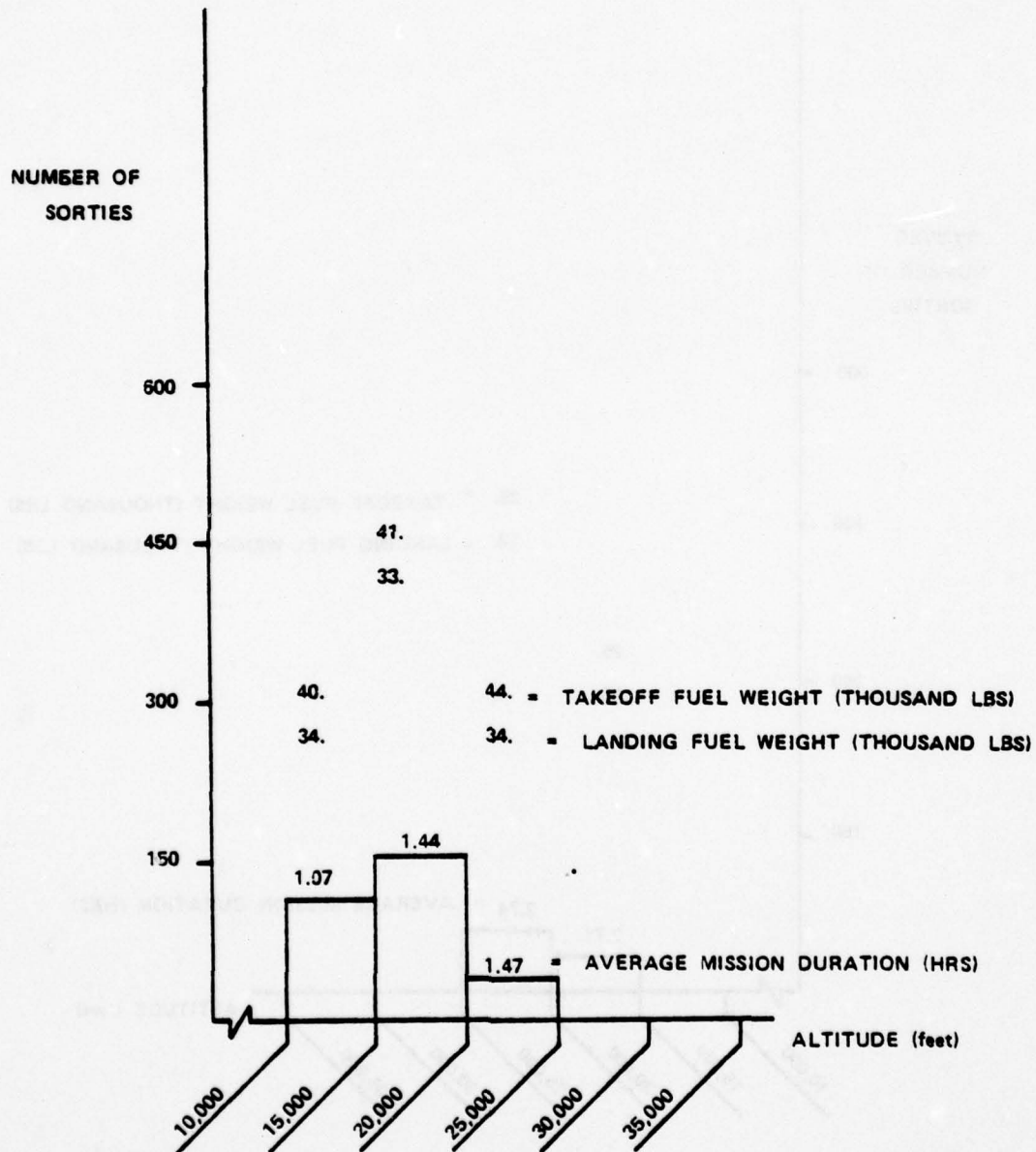


Figure 7.3-5

C-130
DISTRIBUTION OF LEVEL OFF ALTITUDES
TAKE OFF GROSS WEIGHT - up to 100,000 pounds
MISSION DURATION - 2 - 4 hours

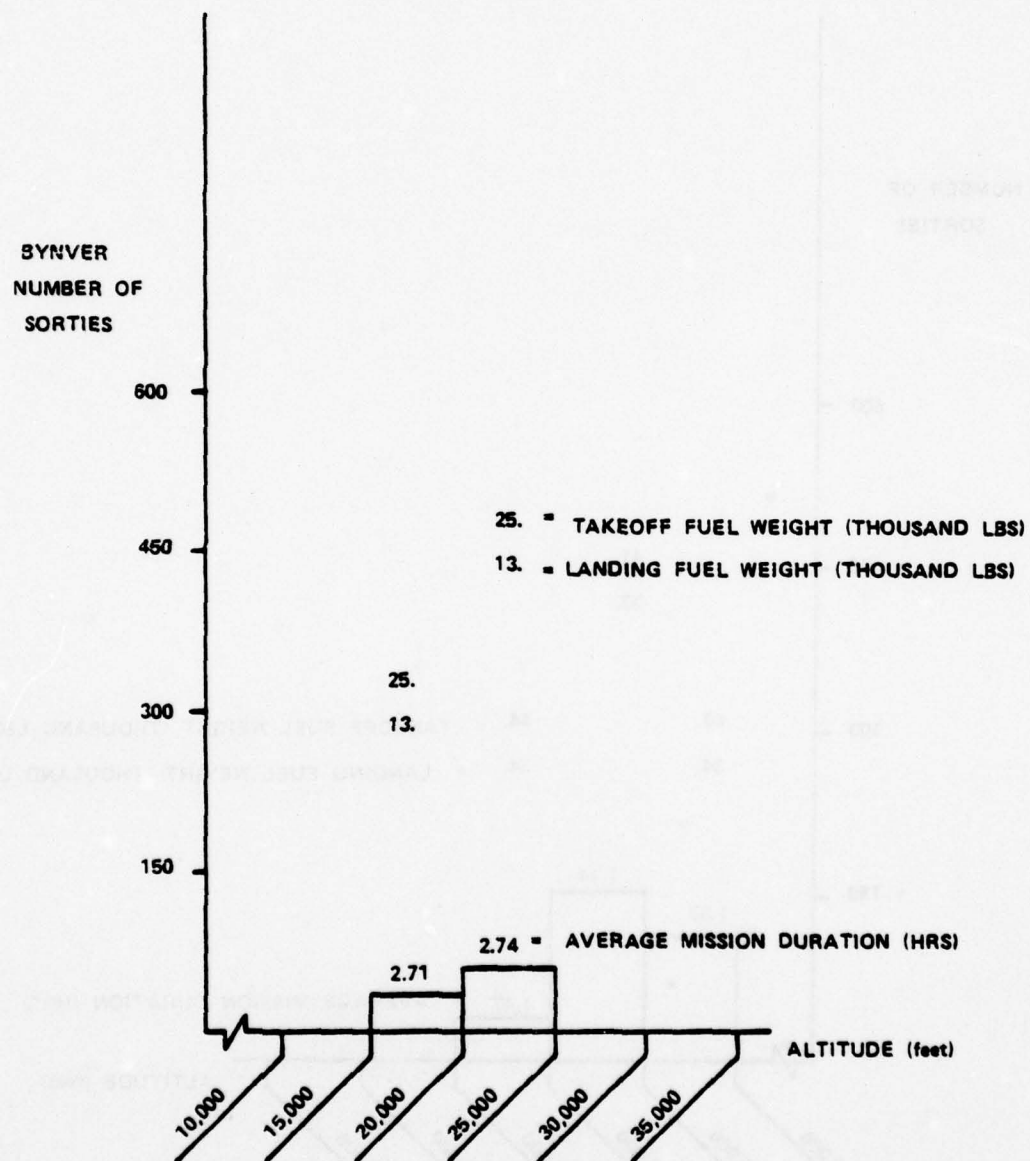


Figure 7.3-6

C-130
DISTRIBUTION OF LEVEL OFF ALTITUDES
TAKE OFF GROSS WEIGHT - 100,000 - 130,000 pounds
MISSION DURATION - 2 - 4 hours

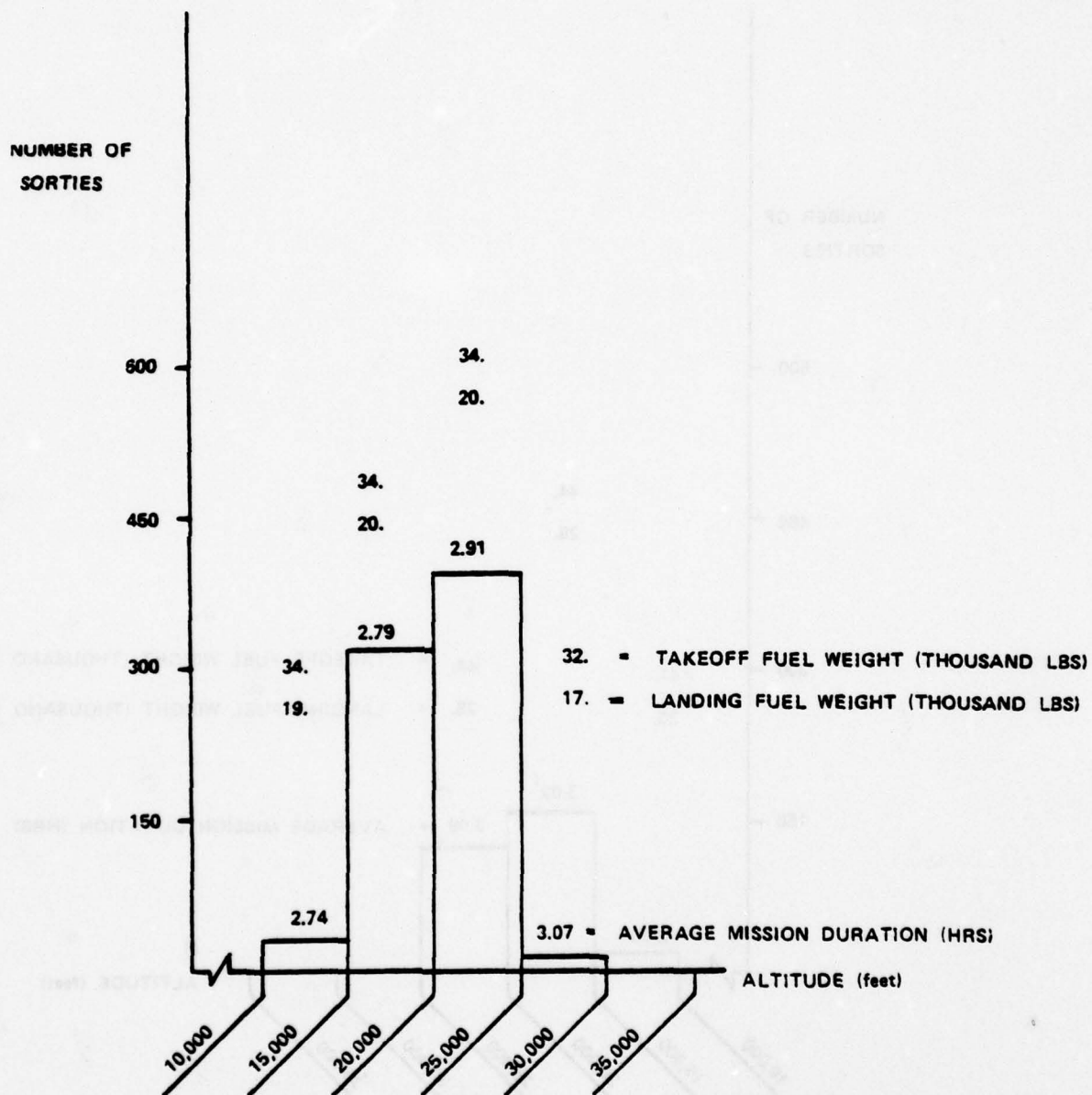


Figure 7.3-7

C-130
DISTRIBUTION OF LEVEL OFF ALTITUDES
TAKE OFF GROSS WEIGHT - 130,000 - 160,000 pounds
MISSION DURATION - 2 - 4 hours

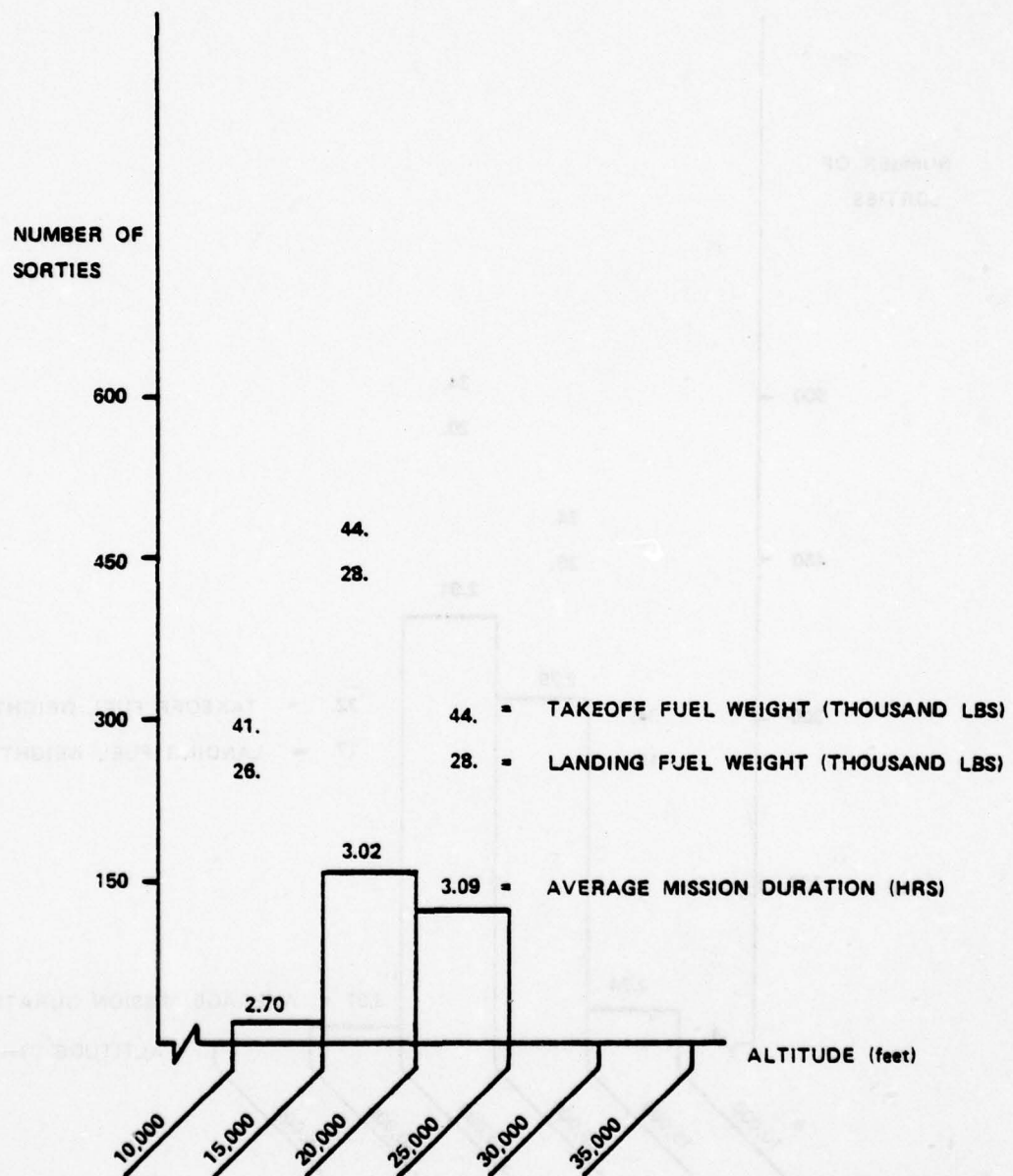


Figure 7.3-8

C-130
DISTRIBUTION OF LEVEL OFF ALTITUDES
TAKE OFF GROSS WEIGHT - 100 - 130,000 pounds
MISSION DURATION - greater than 4 hours

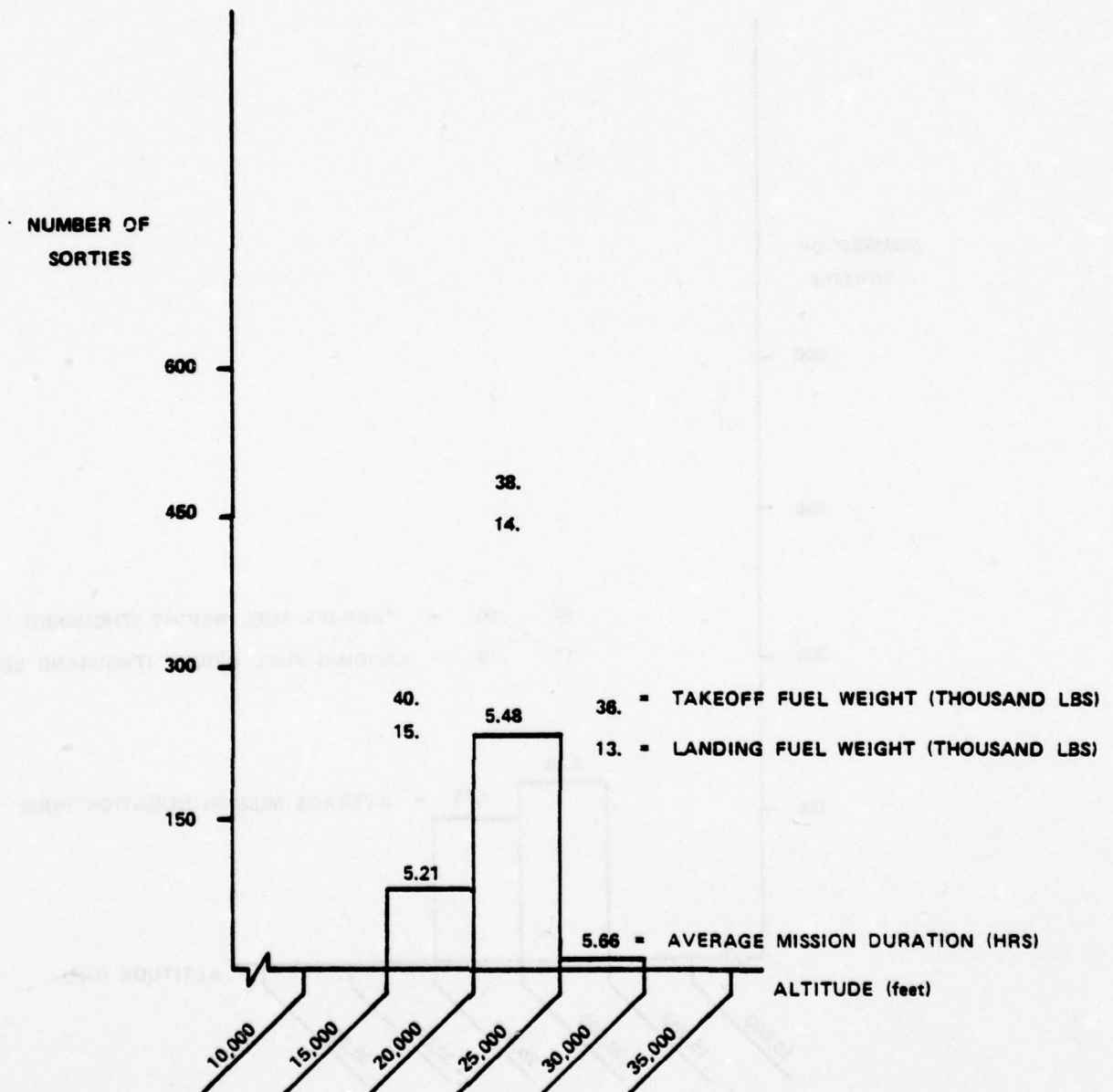
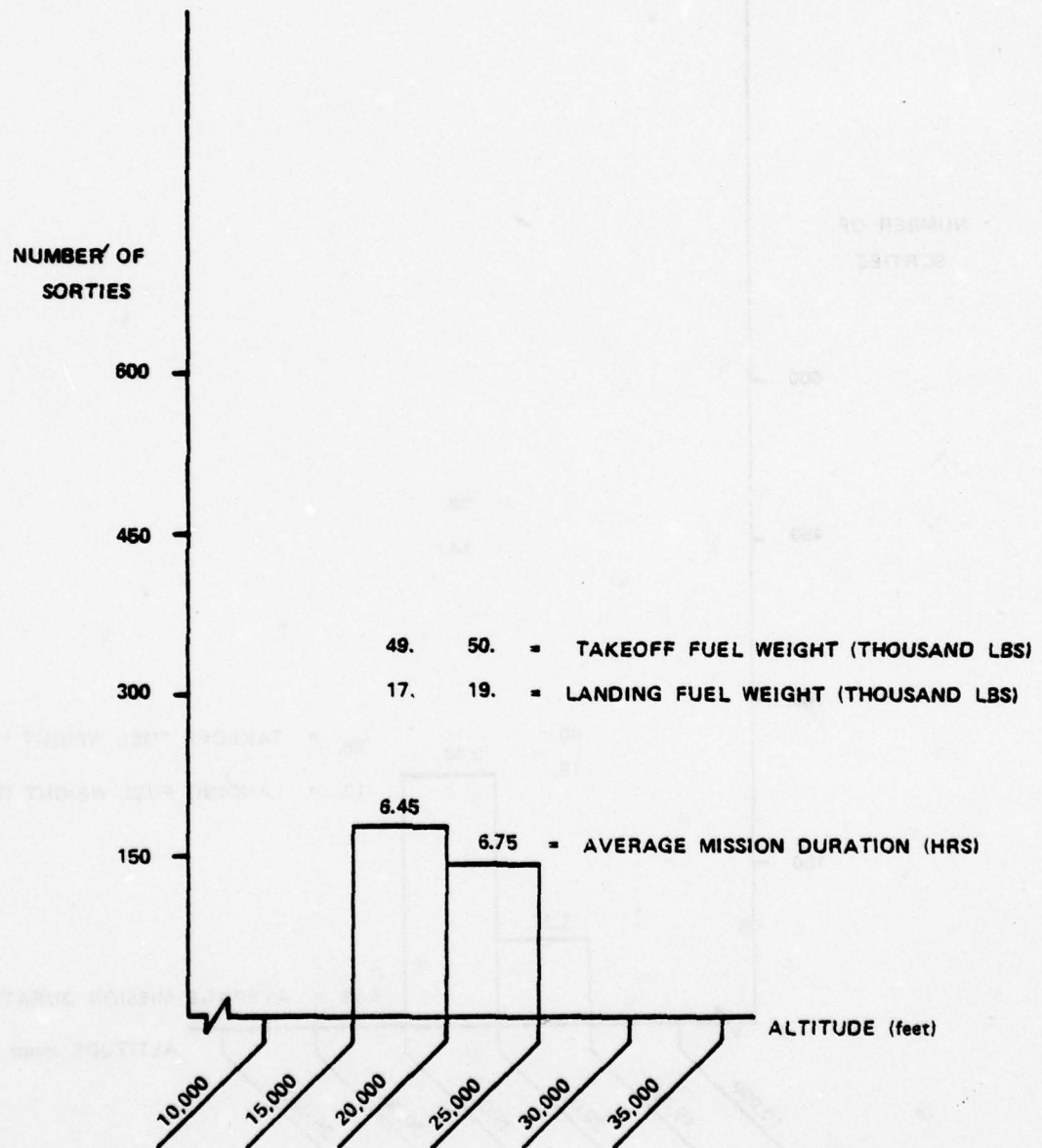


Figure 7.3-9

C-130
DISTRIBUTION OF LEVEL OFF ALTITUDES
TAKE OFF GROSS WEIGHT - 130,000 - 160,000 pounds
MISSION DURATION - greater than 4 hours



7.3.3 DOC Model

The following cost data was obtained for C-130E aircraft.

<u>Direct Flight Operations</u>	<u>Cost/FH - \$</u>
---------------------------------	---------------------

Flight Crew	278
-------------	-----

Oil at \$9.35/gal.	1
--------------------	---

<u>Direct Maintenance Operations</u>

Direct Maintenance (IROS = \$ 291)	582
---------------------------------------	-----

Following the same procedure as before, direct operating cost models for the C-130E are

<u>Model Type</u>	<u>Fuel Cost/Gallon - \$</u>	<u>Time Cost/FH - \$</u>
DOC	.42	216
DOC1	.42	431
DOC2	.42	646
DOC3	.42	861

Using these cost models and annual aircraft utilization data given earlier, annual fuel and direct operating costs for C-130E during FY76 were as follows:

Fuel Cost	\$48.76 million
DOC	\$80.70 million
DOC1	\$112.50 million
DOC2	\$144.30 million
DOC3	\$176.09 million

7.3.4 C-130E Characteristics

The aerodynamic and propulsion data for the C-130E were obtained from Ref. [47]. This data was used to develop the analytical models described below.

7.3.4.1 C-130E Aerodynamic Model

The procedure for developing the drag model is outlined in Section 3.2. Drag coefficient C_D is represented as a parabolic function of lift coefficient C_L .

$$C_D = C_{D_0} - B C_L + K C_L^2$$

where coefficients C_{D_0} , B and K are expressed as functions of Mach (M) given by

$$C_{D_0} = .0328 + .184 \times 10^{-5} (M^* - M)^{-4.1}$$

$$B = .0234 + .22 \times 10^{-20} (M^* - M)^{-2.4 \times 10^{19}}$$

$$K = .0558 + .45 \times 10^{-6} (M^* - M)^{-6.0}$$

and

$$M^* = 0.8$$

7.3.4.2 C-130E Power Model

Reference [47] provides nomographs of four engine normal bleed torque, Q , net jet thrust F_n , and fuel flows. Indicated torque, Q is given as a function of Mach, altitude ambient temperature and turbine inlet temperature. The relationship between Q and the propeller shaft horsepower, P_e is

$$P_e = Q/4.56 - \Delta \text{SHP}$$

where

$$\Delta \text{SHP} = \text{horsepower loss from propeller gearbox and accessories}$$

The equation for the total thrust horsepower available is

$$P_a = (P_{en} + \frac{F_n V}{325}) N$$

where

P_a = total thrust horsepower available

P_e = shaft horsepower available per engine

η = propeller efficiency

F_n = net jet thrust per engine

V = true airspeed in knots

N = number of engines

Net jet thrust, F_n , is a function of altitude, Mach, ambient temperature and turbine inlet temperature. Propeller efficiency, η is a function of altitude true airspeed and shaft horsepower.

Using the above mentioned relationships, Ref. [47] has computed thrust horsepower available as a function of altitude, true airspeed and turbine inlet temperature for normal bleed and standard atmosphere. This data forms the basis for the analytical C-130E power model used in this study. In this model the available thrust horsepower, P_a , for a 4 engine operation is represented by a polynomial in normalized altitude (H_n), normalized true airspeed (V_n) and normalized turbine inlet temperature (T_{in}). The equation for P_a is given by

$$P_a = 1000. [-19.31 + 16.01H_n - .55V_n + 36.83T_{in} + .88H_n^2 - 5.77V_n^2 - 11.19T_{in}^2 - 4.35H_nV_n - 25.93H_nT_{in} + 17.49V_nT_{in}]$$

where

P_a = available thrust horsepower - H.P.

H_n = normalized altitude
= altitude (ft)/40000

V_n = normalized velocity
= true airspeed (kn)/300

T_{in} = normalized turbine inlet temperature
= turbine inlet temperature $^{\circ}\text{C}/1000$

Idle engine thrust is represented as a polynomial function of normalized altitude (H_n) and normalized velocity (V_n).

$$T_{idle} = 1000 [.09 - 2.14H_n - 4.02V_n + 1.42H_n^2 + 8.63V_nH_n + 3.15V_n^2 - 5.62V_nH_n^2 - 6.11V_n^2H_n + 4.21V_n^2H_n^2]$$

where

T_{idle} = idle thrust - lbs/engine

7.3.4.3 C-130E Fuel Flow Model

For C-130E, an Equivalent Specific Fuel Consumption (ESFC) model has been developed. Here ESFC is defined as fuel consumed per hour per thrust horsepower available. ESFC values were calculated from the available thrust horsepower and fuel flow data as functions of altitude, true airspeed and turbine inlet temperature. Then ESFC was represented as a polynomial in normalized altitude (H_n), normalized true airspeed (V_n) and normalized turbine inlet temperature (T_{in}). The equation for ESFC is given by

$$\text{ESFC} = 4.64 - .31H_n - 1.08V_n - 7.74T_{in} + .18H_n^2 + .77V_n^2 + 4.38T_{in}^2 + .1H_nV_n + .13H_nT_{in} - .38V_nT_{in}$$

where the units for ESFC are lbs/hr/ P_a .

Idle fuel flow data for the C-130E is given as a function of altitude and true airspeed. Thus idle fuel flow rate, f_{idle} , is represented as a polynomial in normalized altitude and normalized true airspeed.

$$f_{idle} = 1000. [.58 - .68 H_n + .04 V_n + .27 H_n^2 - .07 H_n V_n + .04 V_n^2]$$

This model is applicable for the entire range of operation of the C-130E.

The above thrust and fuel flow models are generally good to within a 2% error over the regions of interest.

7.3.5 Evaluation of Airborne and Ground Operational Procedures

This subsection describes the operational procedures which result in fuel/DOC savings for the C-130E and quantifies the savings possible by implementing these procedures.

7.3.5.1 Optimal Departure Procedures

Generally the runway length available imposes the most stringent limits on the take-off performance of the C-130E. Conventional departure procedures for this aircraft are close to optimal, and fuel savings during the departure phase are negligible.

7.3.5.2 Optimal Climb, Cruise and Descent Procedures

Since the C-130E is the only turboprop aircraft considered in this study, the conventional procedures for this aircraft are different than those for the other aircraft. This subsection evaluates optimal climb, cruise and descent procedures of the C-130E and compares them with conventional procedures.

Optimal Cruise-Climb Solution

The optimum cruise altitude of the C-130E is constrained by the cruise ceiling. Optimum cruise parameters are obtained by the extremization of Equation (A.31) in Appendix A under cruise ceiling constraint. The fuel/time trade-off curve in Figure 7.3-10 is generated by varying the parameter θ in Equation (A.31). The solution corresponding to $\theta = 1$ is the minimum fuel solution. As θ is decreased to zero, the optimum air speed and fuel consumption increase and the mission time decreases. However, the maximum air speed is constrained by the maximum continuous power (932° C TIT). The optimum solution points corresponding to direct operating cost models DOC, DOC1, DOC2 and DOC3 are shown in Figure 7.3-10. The minimum fuel solution corresponds to a 265 TAS. The minimum fuel cruise climb path for the C-130E coincides with the cruise ceiling.

Optimal Step-Climb Solution

ATC regulations restrict the C-130E to fly a constant altitude cruise with a step-climb to the next cruise level whenever possible. Since the cruise altitude for this aircraft is constrained by the cruise ceiling, it can only step climb to this ceiling altitude and not above it. Most of the C-130E missions requiring a step-climb procedure cruise below a 29,000 foot altitude, and a minimum step of 2,000 feet is allowed below this altitude. Thus the optimum step-climb procedure for the C-130E is to initiate a level flight at an altitude (below cruise ceiling) consistent with the direction of flight and as close as possible to the cruise ceiling. Subsequent step climbs will be initiated as soon as the gross weight has been reduced to a value such that after a 2000 ft step climb the aircraft altitude will coincide with cruise ceiling. This procedure results in approximately 0.8% more fuel consumption than the optimum cruise-climb procedure.

Conventional Climb Procedures

Conventional climb is usually performed at maximum continuous power (932° C TIT) and an air speed schedule which results in the maximum rate of climb. This air speed, which is dependent on altitude and aircraft weight, varies continuously

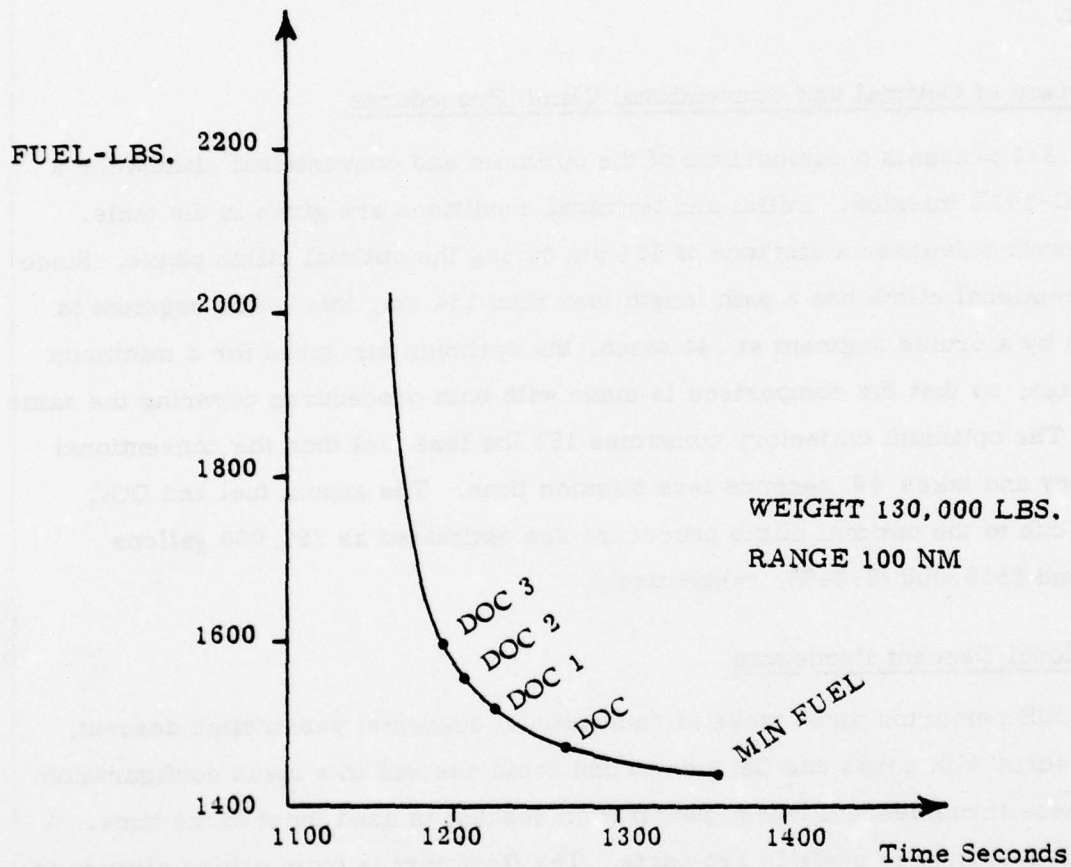


Figure 7.3-10 FUEL/TIME TRADE-OFF FOR THE
C-130E CRUISE SOLUTION

during climb. Since air speed during climb is less than 250 KIAS, ATC constraints do not have any impact on the climb performance of the C-130E.

Optimal Climb Procedure

The optimal climb algorithm derived in Appendix A is used to obtain air speed and thrust setting during climb. The optimum climb speed for the C-130E is less than 250 KIAS. Thus the ATC constraint does not affect the climb performance of this aircraft.

Comparison of Optimal and Conventional Climb Procedures

Table 7.3-2 presents a comparison of the optimum and conventional climbs for a typical C-130E mission. Initial and terminal conditions are given in the table. The aircraft traverses a distance of 154 nm during the optimal climb phase. Since the conventional climb has a path length less than 154 nm, this climb segment is followed by a cruise segment at .44 mach, the optimum air speed for a minimum fuel cruise, so that the comparison is made with both procedures covering the same range. The optimum trajectory consumes 151 lbs less fuel than the conventional trajectory and takes 89 seconds less mission time. The annual fuel and DOC savings due to the optimal climb procedure are estimated as 691,000 gallons (0.6%) and \$515,000 (0.64%), respectively.

Conventional Descent Procedure

The C-130E performs three types of conventional descents; penetration descent, rapid descent with gears and flaps down and rapid descent in a clean configuration. Out of these three descent types, penetration descent is used most of the time. A penetration descent is made in two parts. The first part is from cruise altitude to 20,000 feet at maximum lift over drag speeds with throttles at flight idle and gear and flaps up. The second part is from 20,000 feet down at a constant 250 KIAS. This descent procedure is used in the mission profile analysis program to simulate conventional trajectories.

Final Conditions
 Range 154 nm
 Altitude 25,000 ft
 Air Speed .44 Mach

Initial Conditions
 Weight 130,000
 Altitude Sea Level

Type of Climb	Optimum †	Conventional
Climb	154	90
Cruise	0	64
Total	154	154
Range nm		
Climb	3190	2409
Cruise	0	932
Total	3190	3341
Fuel lbs		
Climb	2356	1564
Cruise	0	881
Total	2356	2445
Time sec		
Fuel	206.1	215.9
Cost \$		
DOC	347.5	362.6

† Note that the optimum climb solution is for minimum fuel only

Table 7.3-2 Comparison of Optimum vs Conventional Climb C-130E

Optimal Descent Procedures

Air speed and throttle setting for optimal descent is obtained from the optimal control algorithm of Appendix A. Air speed varies continuously along an optimal descent path; however throttle setting is at flight idle during most of the descent. The optimum descent speed for this aircraft is less than 250 KIAS. Therefore the ATC constraint has no impact on the optimal descent segments.

Comparison of Optimal and Conventional Descents

The results of a comparison of optimal and conventional descent procedures are summarized in Table 7.3-3. The optimal trajectory traverses 91 nm during descent compared to 39 nm for the conventional descent. So that the comparison is made on the basis of equal ranges, the conventional descent is given a 52 nm cruise segment before the descent is initiated. The optimal trajectory consumes 758 lbs of fuel, which is 211 lbs less than the conventional descent. However the mission time for the optimal case is 259 seconds more than the conventional case. As a result, the optimal descent provides a \$2 loss in DOC. The annual fuel savings due to optimal descent procedures are estimated as 723,000 gallons which is .62% of the annual fuel consumption for the C-130E. However, the optimal descents result in annual loss of \$65,000 in DOC.

Optimal Cruise Conditions

This section investigates the effect of employing optimal altitudes and air speeds. Conventional ascent and descent procedures are used in conjunction with these optimal cruise conditions.

Histograms of level-off altitudes for the C-130E mission spectrum are given in Section 7.3.2. This mission spectrum data was obtained by processing ASIMIS tapes. Average cruise velocity for most of the missions is higher than cruise velocity for minimum fuel consumption, and the cruise altitudes are lower

Initial Conditions

**Weight 130,000 lbs.
Altitude 25,000 ft
Air Speed .44 Mach**

**Fuel Conditions
Range 91 nm
Altitude 3,000 ft**

Type of Descent	Optimum	Conventional
Cruise	0	52
Descent	91	39
Total	91	91
Cruise	0	747
Descent	758	222
Total	758	969
Cruise	0	707
Descent	1416	450
Total	1416	1157
Fuel	49.0	62.6
Cost	134.0	132.0
\$ DOC		

Table 7.3-3 Comparison of Optimal vs Conventional Descent - C-130E

than the cruise ceiling altitudes. Thus fuel savings can be achieved by flying at higher altitudes and slower air speeds. The fuel savings due to optimal cruise procedures were estimated by simulating long, medium and short range missions in the mission profile analysis program.

Figures 7.3-11, 12 and 13 illustrate the fuel and DOC savings due to higher cruise altitudes and reduced cruise speeds for long, medium and short range missions, respectively. Δ Mach indicates a decrease in cruise air speed and ΔH indicates an increase in cruise altitude from the averages within the histogram bands of Figs. 7.3-2 through 7.3-9. When ΔH is some positive value (say 10,000 feet), this indicates that those missions flown below their respective optimal altitudes have been raised to their respective optimal altitudes, but the maximum increase allowed is the noted positive value (say 10,000 feet).

Table 7.3-4 gives the maximum fuel and direct operating costs savings due to increased altitudes and reduced cruise speed. DOC 3 savings occur mostly due to increased altitudes.

7.3.5.3 Optimal Approach Procedures

Conventional ILS approach procedures were originally developed for turboprop aircraft, and these procedures are close to optimal for C-130E aircraft.

7.3.5.4 Aft C.G. Operations

Since the C-130E is a cargo transport, its c.g. can be readily influenced by proper distribution of fuel and payload. Burning fuel evenly towards aft c.g. during flight will further reduce drag. The fuel savings due to operation of the C-130E at c.g. locations further aft than those under present operations were estimated assuming an average 5%-MAC shift in C-130E missions. Average weights and cruise conditions were considered for all mission types, and fuel savings were calculated due to the c.g. shift. Then the savings for individual missions were averaged over the mission spectrum. The 5%-MAC shift in c.g. towards aft saves 0.52% in annual fuel consumption. This is equivalent to a 0.6 million gallon fuel savings annually for C-130E operations.

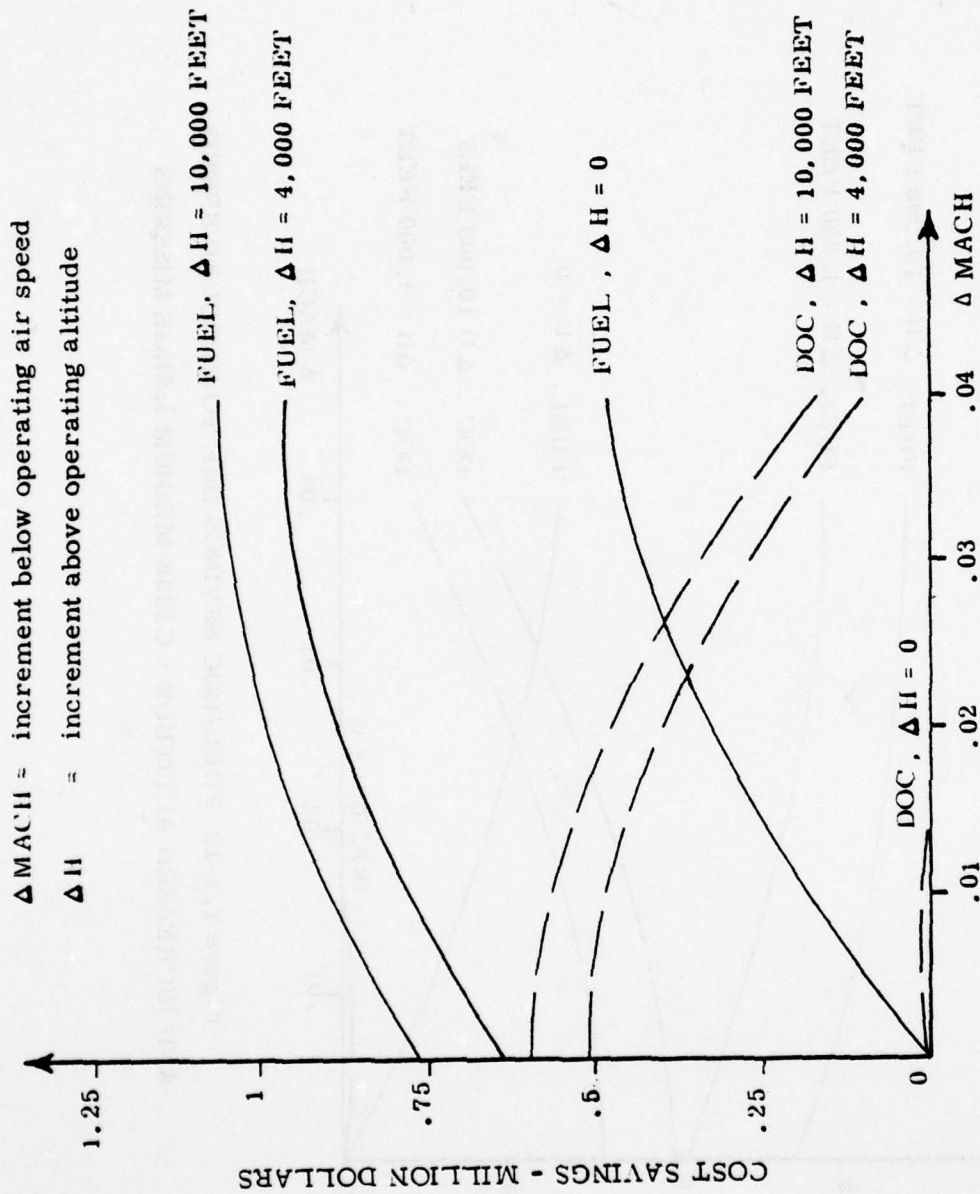


Figure 7.3-11 FUEL/DOC SAVINGS DUE TO REDUCED SPEED
 AND INCREASED ALTITUDE - C130E LONG RANGE MISSIONS

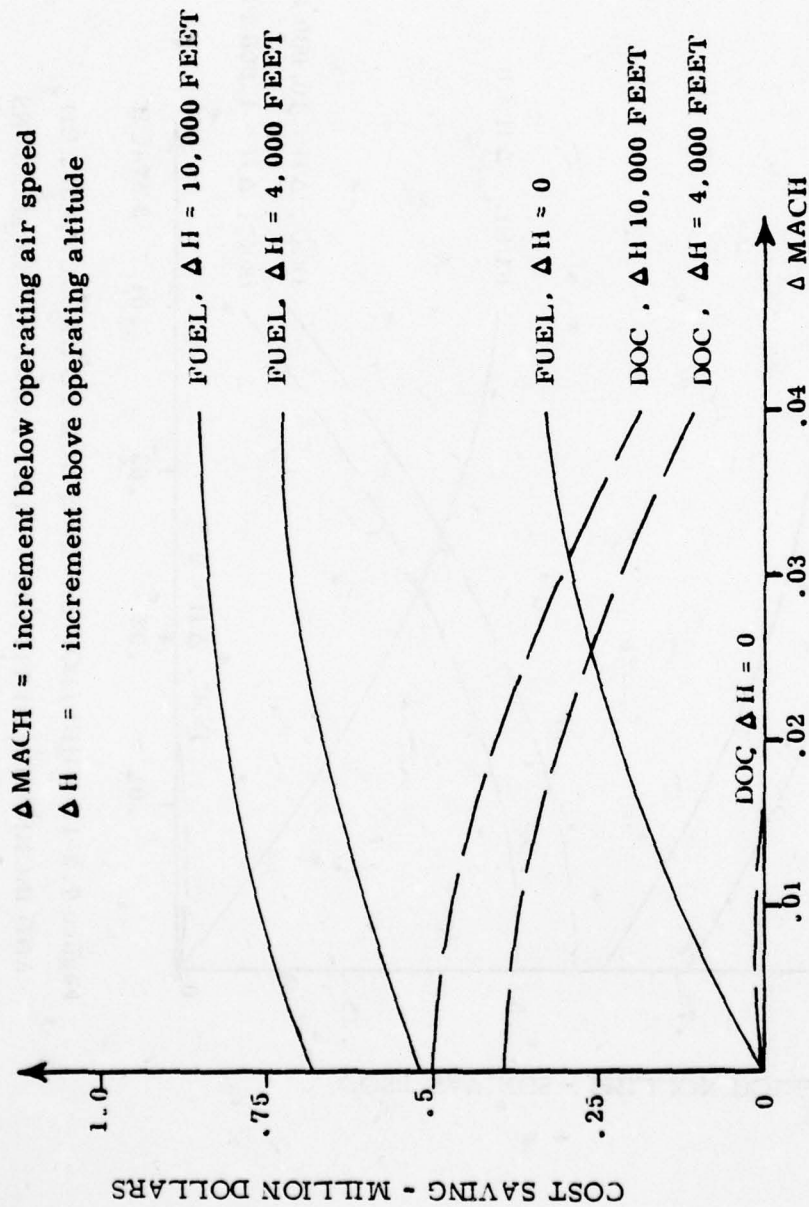


Figure 7.3-12 FUEL/DOC SAVINGS DUE TO REDUCED SPEED
 AND INCREASED ALTITUDE - C130E MEDIUM RANGE MISSIONS

ΔMACH = increment below operating air speed
 ΔH = increment above operating altitude

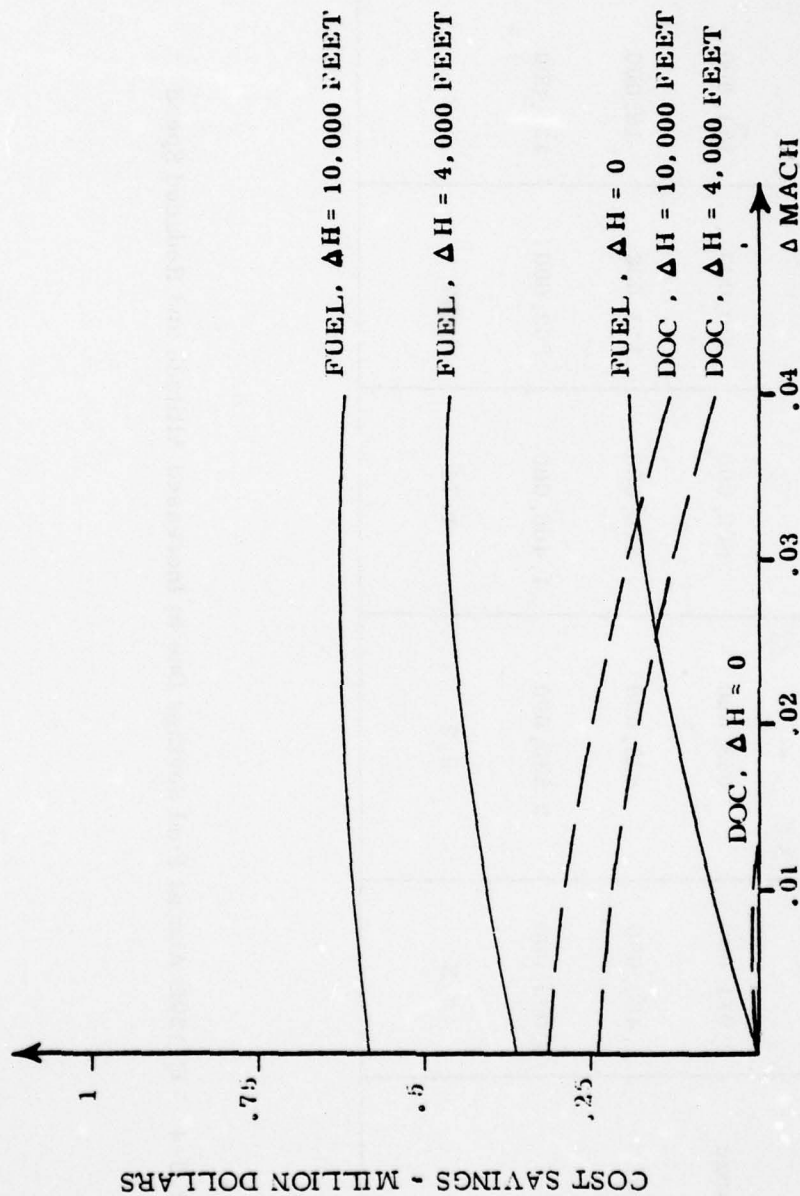


Figure 7.3-13 FUEL/DOC SAVINGS DUE TO REDUCED SPEED AND INCREASED ALTITUDE - C130E SHORT RANGE MISSIONS

AD-A062 609

DYNAMICS RESEARCH CORP WILMINGTON MASS SYSTEMS DIV
AN ANALYSIS OF FUEL CONSERVING OPERATIONAL PROCEDURES AND DESIGN--ETC(U)
JUL 78 R K AGGARWAL

F/G 1/3

F33615-76-C-3104

UNCLASSIFIED

R-247U

AFFDL-TR-78-96-VOL-2

NL

4 OF 6
ADA
062609



Mission Type	Maximum Savings					
	Fuel Gallon	Fuel Cost	DOC	DOC 1	DOC 2	DOC 3
Long Range	2,519,000	1,058,000	595,000	429,000	264,000	126,000
Medium Range	2,031,000	853,000	500,000	320,000	151,000	40,000
Short Range	1,488,000	625,000	313,000	113,000	16,000	3,000
Total	6,038,000	2,536,000	1,408,000	862,000	431,000	169,000
% Savings	5.2	5.2	1.74	.77	.3	.1

Table 7.3-4 C-130E Annual Fuel Savings Due to Increased Altitude and Reduced Speed

7.3.5.5 Reduce Reserve Fuel

The average landing fuel for each mission type is given on the histograms in Section 7.3.2. An examination of landing fuel indicates that the reserve fuel carried for C-130E missions is much more than required, and fuel savings may be achieved by reducing the reserve fuel. The maximum reserve fuel requirement for the C-130E includes an en route reserve, fuel required for an alternate airport, and fuel for 1 hour 15 minutes of holding at the destination. These reserve fuel requirements appear excessive. Therefore fuel savings were also computed under several sets of relaxed reserve fuel requirements. The following options were considered:

- En route reserve plus 200 n.mi. alternate plus 1.25 hours holding time
- 200 n.mi. alternate plus 1.25 hours holding time
- 200 n.mi. alternate plus .75 hour holding time
- 200 n.mi. alternate plus .25 hour holding time
- 200 n.mi. alternate

Table 7.3-5 summarizes the fuel and direct operating cost savings achievable by reducing the reserve fuel requirements to those defined by the above five options. Fuel savings can be as high as 2.2% or 2.5 million gallons annually for C-130E. Note that these fuel savings are estimated for missions flown at altitudes and air speeds obtained from the ASIMIS tapes. However, if the missions were flown under optimum cruise conditions, there would be a further reduction in the reserve fuel requirements and a corresponding increase in fuel savings.

7.3.5.6 Reduce Engine Load

The compressor bleed air used to operate the air-conditioning and pressurization system; the engine anti-icing system and the wing and tail surface anti-icing system subtract from the engine power delivered to the propeller. For the C-130E the use of the anti-icing system results in approximately a 10-15% increase

Reserve Fuel Requirements	Annual Savings				
	Fuel		DOC		
	Gallons	\$	%	\$	%
En route reserve + 200 nmi alternate + 1.25 hours holding time	1,564,000	657,000	1.35	724,000	0.9
200 nmi alternate + a. 25 hours holding time	1,831,000	769,000	1.58	843,000	1.04
200 nmi alternate + 45 minutes holding time	2,124,000	892,000	1.83	976,000	1.21
200 nmi alternate + 15 minutes holding time	2,405,000	1,010,000	2.1	1,102,000	1.37
200 nmi alternate	2,526,000	1,061,000	2.18	1,152,000	1.43

Table 7.3-5 Annual Fuel/DOC Savings Due to Reduced Reserve Fuel for C130E

in fuel flow rate. Thus minimizing power and air bleed extraction can result in fuel savings. However a quantification of the annual savings factor is difficult in this case since the data required to perform this analysis is not available.

7.3.5.7 Reduce Engine Use and Taxi Time

The C-130E consumes an average of 50 lbs/minute fuel during ground operations. Thus fuel/DOC savings can be realized by reducing engine use during ground operations. Some of the procedures which may be used include absorbing delays at the gate, taxiing the shortest route to runway/ramp and using intersections for take-offs. A one minute average reduction in taxi time per mission can save 343,000 gallons of fuel annually for C-130E operations. This saving is approximately 0.3% of the annual fuel consumption for the C-130E.

7.3.5.8 Partial Engine Taxi

Shutting down two engines after landing may be an acceptable procedure for fuel conservation. A two engine taxi for an average 5 minutes taxi time per mission can save 0.86 million gallons (.75%) of fuel annually for the C-130E fleet.

7.3.5.9 Removing Excess Equipment

Reference [32] describes the items which may be removed from C-130E aircraft to reduce the aircraft take-off gross weight. A maximum weight reduction of 7,459 pounds is possible. This includes 276 lbs from the galley and oven, 1,555 lbs from external tanks including 166 lbs of unusable fuel, and the remaining 5,628 lbs are mission oriented. If the average weight reduction for C-130E missions were taken as 3,000 pounds, this weight reduction would save 0.9 million gallons of fuel annually for the C-130E fleet. Fuel savings are almost 0.8% of the annual fuel consumption.

7.3.5.10 Maintenance to Reduce Drag

Section 4.3 outlined the causes and effects of increased airplane drag. An exact quantification of fuel savings due to aircraft maintenance is not possible.

However the fuel/DOC savings may be estimated from the plots given in the next subsection depicting the sensitivity of fuel/DOC to variations in aircraft drag. Assuming aircraft maintenance results in a 1% reduction in zero-lift drag for the entire C-130E fleet, Figure 7.3-14 indicates a 0.65% savings in the annual fuel consumption.

7.3.5.11 Engine Maintenance

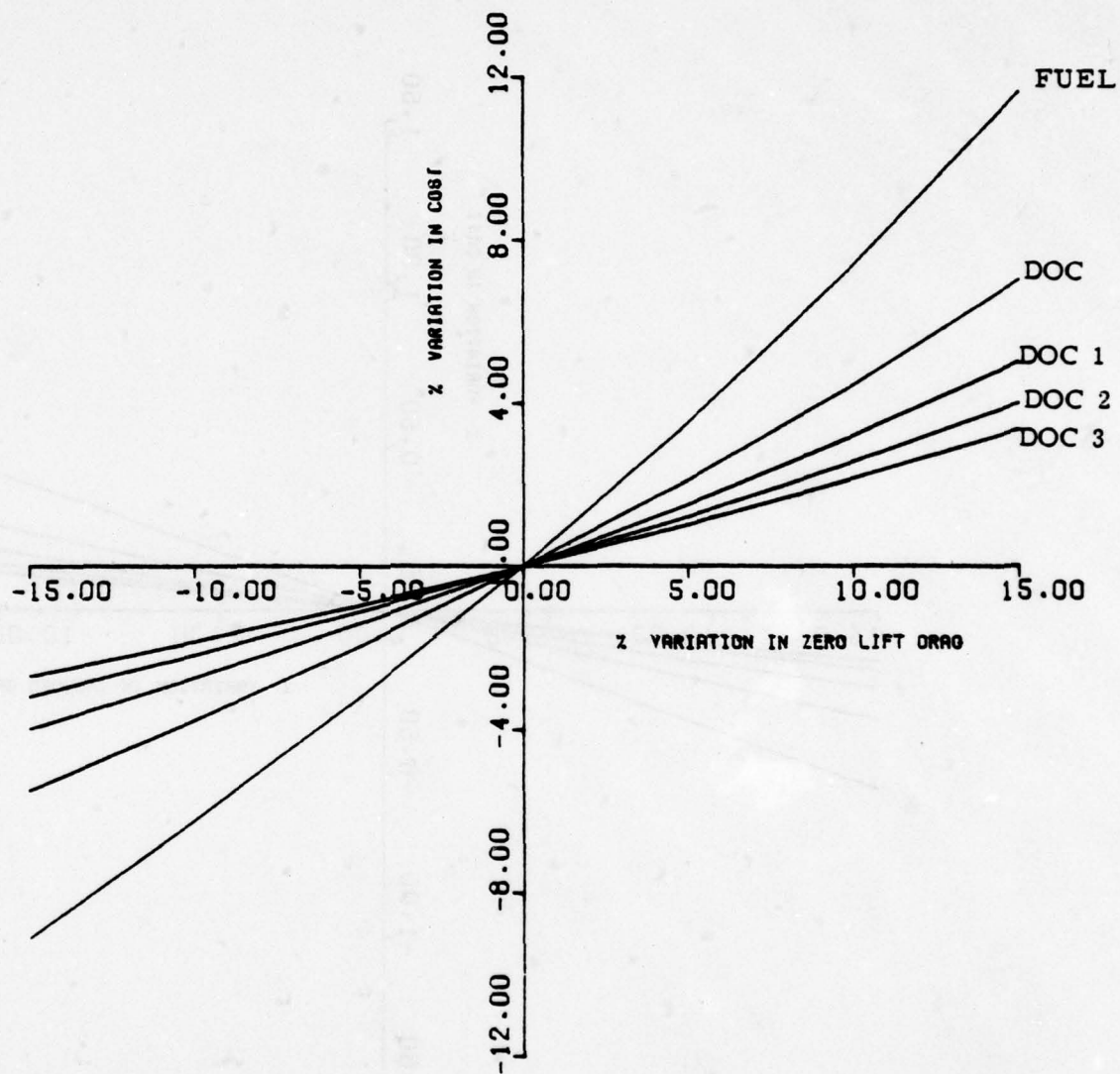
Improved engine maintenance procedures can result in increased engine efficiency. Section 4.3 discussed some procedures which may help reduce engine deterioration with use and time. Fuel savings due to improved maintenance procedures may be estimated using Figure 7.3-16. If a 1.5% improvement in fuel consumption per shaft horsepower could be realized through improved engine maintenance, Figure 7.3-16 indicates a 1.47% reduction in the annual fuel consumption.

7.3.6 Evaluation of Design Modifications

The specification on which the Hercules is based was issued by TAC in 1951, and since then the aircraft has been modified for many special applications. The C-130E is an extended-range development of the C-130B model with larger under wing fuel tanks. No specific propulsion modifications are under consideration for the C-130E aircraft at present except that the newer version, C-130H, has more powerful engines. The addition of fuselage afterbody-strakes is under consideration; this modification will be evaluated in this section.

7.3.6.1 Parametric Analysis of Aerodynamic and Propulsion Design Modifications

The generic plots of variations in fuel/DOC as functions of the variations in the aerodynamic and propulsion parameters have been developed for the C-130E. Figs. 7.3-14, 15, 16 and 17 illustrate variations in fuel/DOC due to variations in zero-lift drag, induced drag, specific fuel consumption/available horsepower and the take-off gross weight for the C-130E. These plots which were developed by simulating the entire mission spectrum obtained by processing ASIMIS tapes,



7.3-14 SENSITIVITY OF FUEL/DOC TO VARIATIONS
IN ZERO LIFT DRAG - C130E

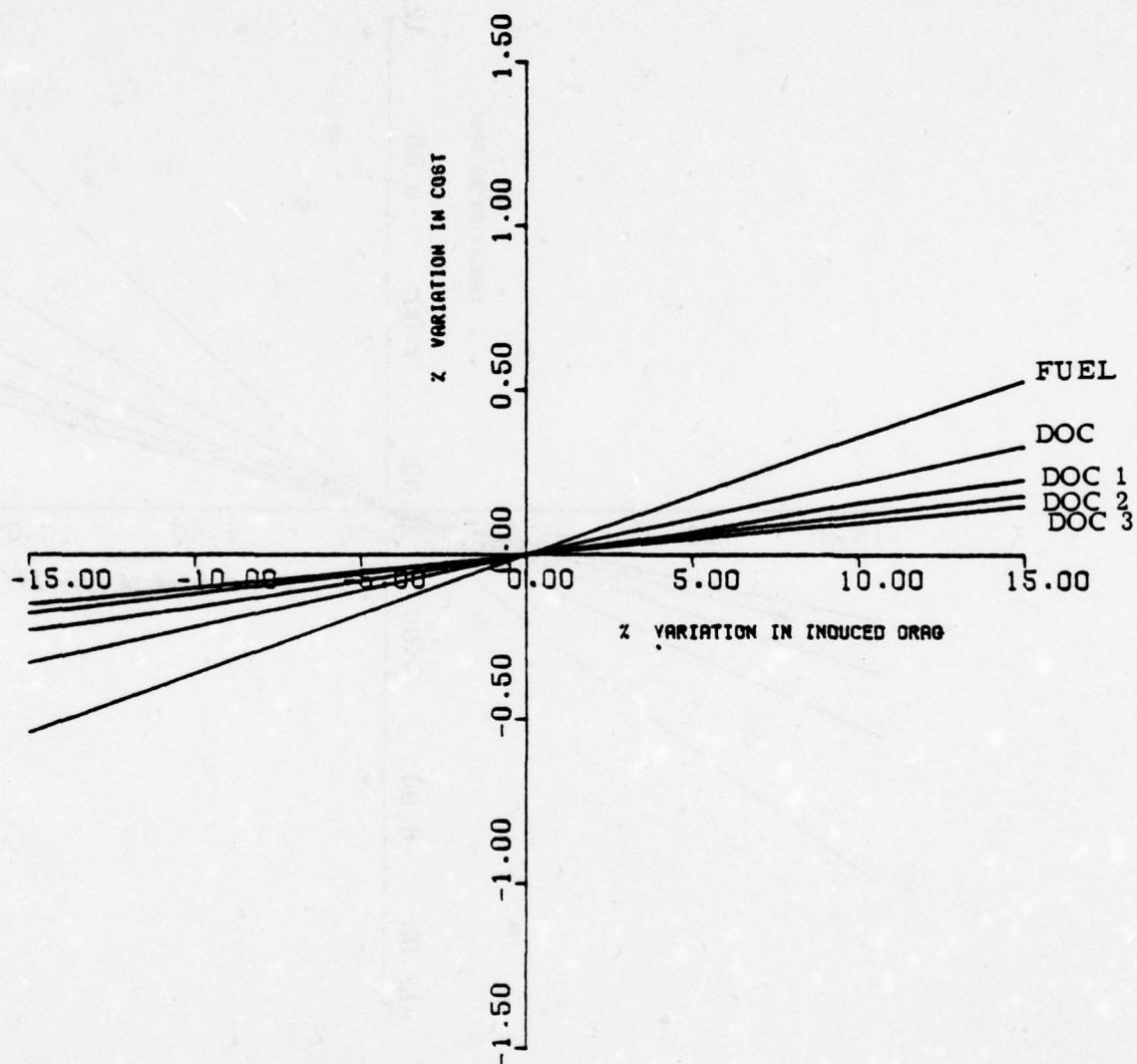


Figure 7.3-15 SENSITIVITY OF FUEL/DOC TO VARIATIONS
IN INDUCED DRAG - C130E

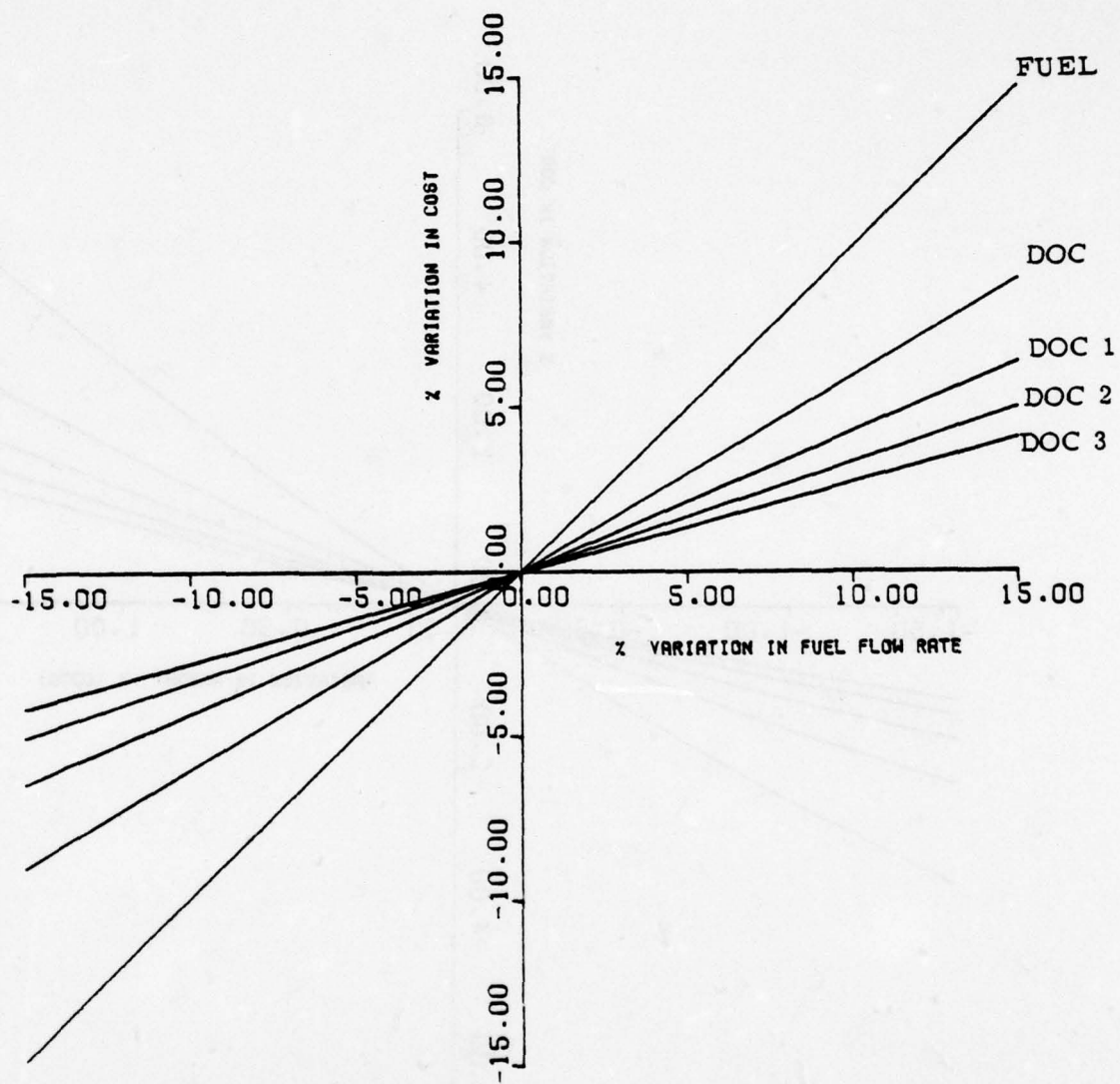


Figure 7.3-16 SENSITIVITY OF FUEL/DOC TO VARIATIONS
IN SPECIFIC FUEL CONSUMPTION PER HORSE POWER - C130E

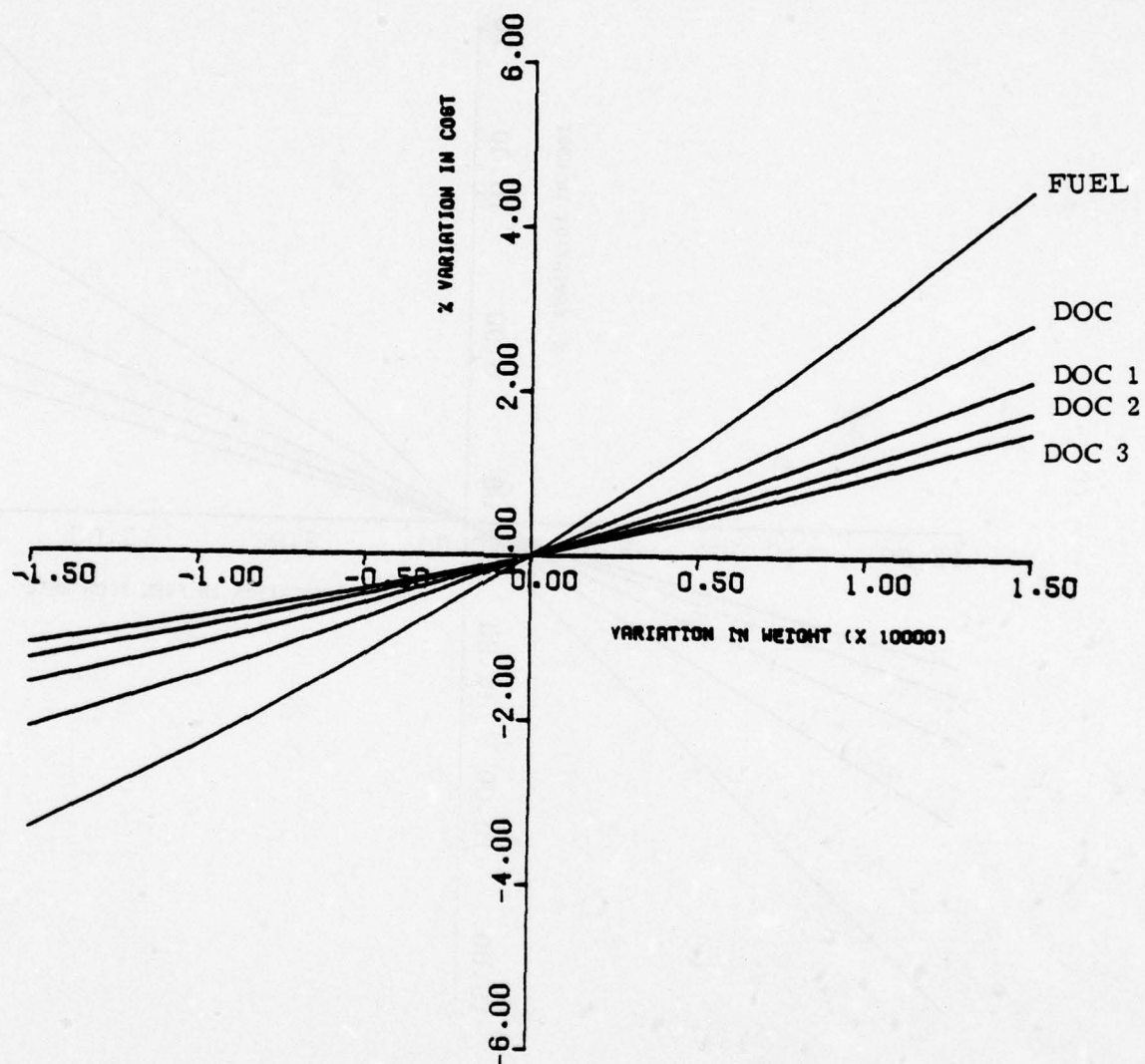


Figure 7.3-17 SENSITIVITY OF FUEL/DOC TO VARIATIONS
IN WEIGHT - C130E

can be used to evaluate any design modifications which may be considered in the future.

7.3.6.1 C-130E Aft Body Strakes

Fuselage afterbody-strakes for the C-130 aircraft have been proposed. The additions to the fuselage would be installed on both sides of the aft cargo opening and would reduce drag by revising the fuselage air flow patterns and hence reducing air flow separation. It has been estimated that savings of approximately 39 gal/hr could be expected [32]. Total fuel savings for C-130E aircraft are estimated to be 5.76 million gallons/year. The total modification cost is estimated to be \$7.5 million in 1978 dollars. Figure 7.3-13 shows a cost/savings trade-off in which the break-even period is less than 3.5 years.

7.3.7 Sensitivity Analysis

The results of a study to determine the sensitivity of fuel consumption and DOC for the C-130E due to changes in aircraft parameters and environmental factors are presented in this subsection.

7.3.7.1 Uncertainties in Aircraft Parameters

Aircraft parameters which impact fuel consumption are the zero-lift drag coefficient, induced drag coefficient, fuel consumption per shaft horsepower, and changes in maximum continuous power and the system weight.

Sensitivity to Zero-Lift Drag

Fig. 7.3-13 illustrates the sensitivity of fuel consumption to changes in the zero lift drag for C-130E aircraft. This plot was generated for a typical C-130E mission under optimum cruise conditions. Aircraft weight and mission range remain constant. Observe that fuel consumption is very sensitive to changes in the zero-lift drag coefficient.

ACCUMULATED SAVINGS

COST/SAVINGS TRADEOFF: (1978 DOLLARS)

(MILLIONS OF \$)

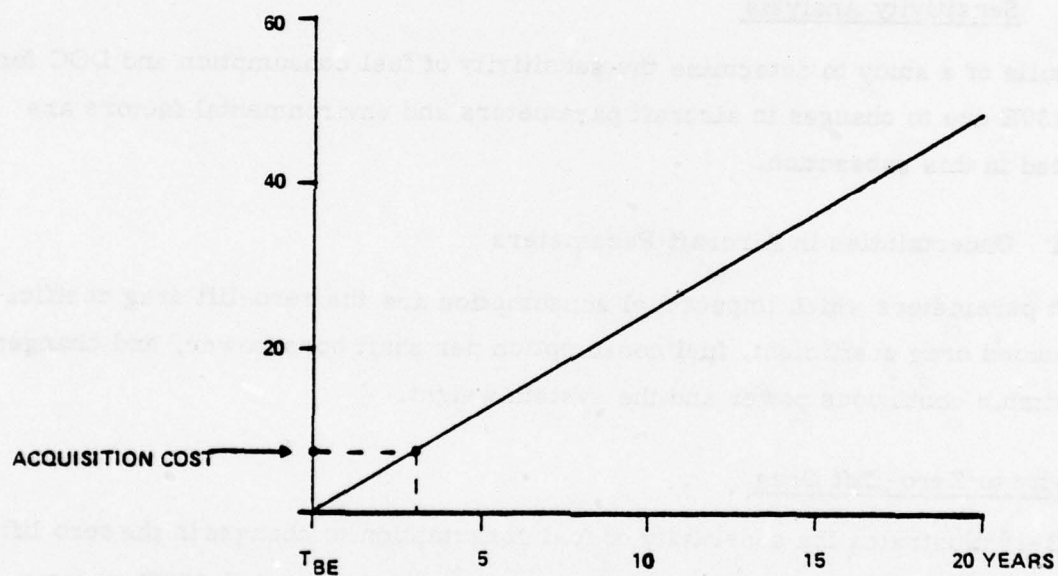


Figure 7.3-18

SAVINGS DUE TO C-130E AFT BODY STRAKES

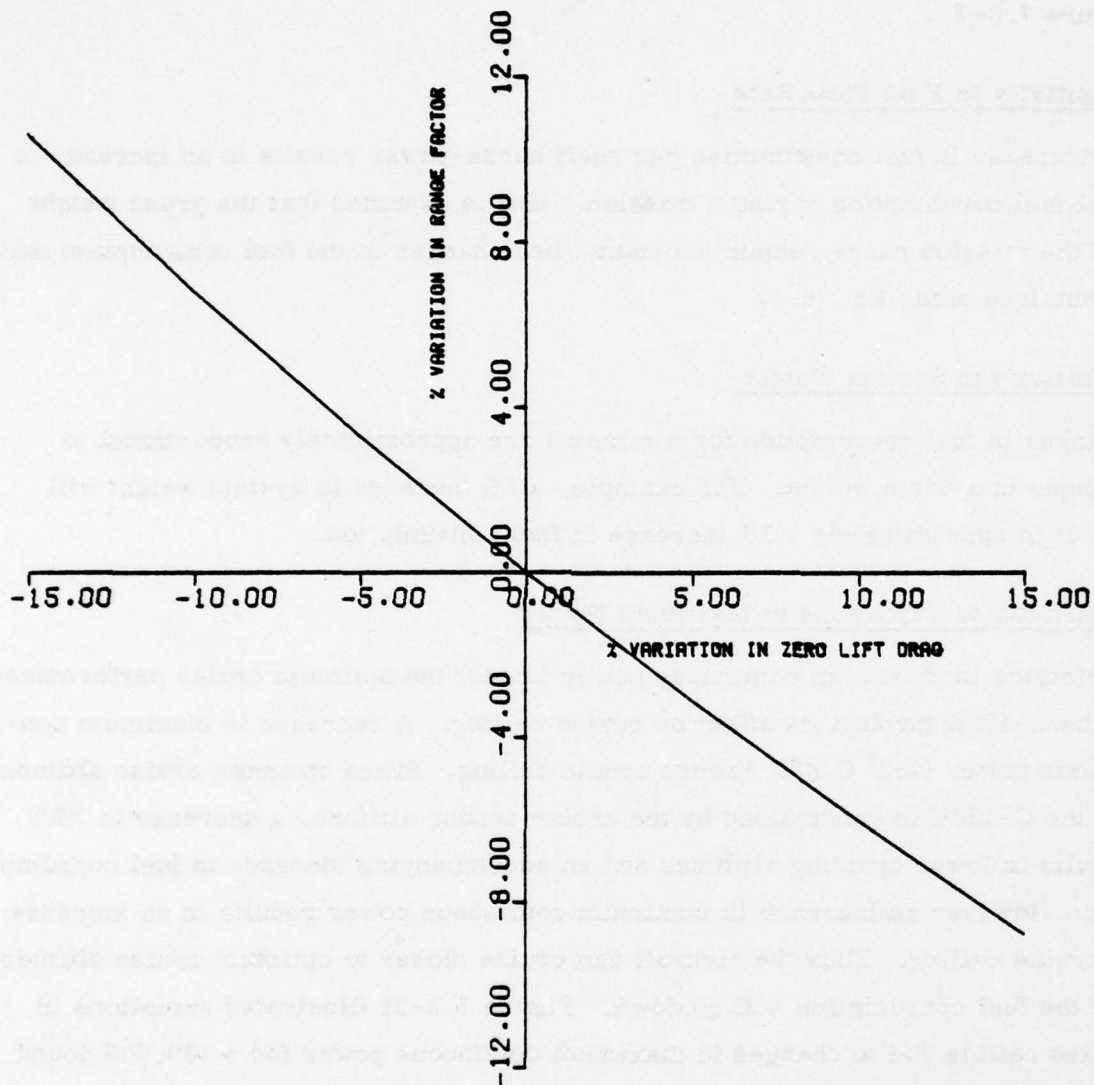


Figure 7.3-19 SENSITIVITY OF RANGE FACTOR TO VARIATIONS
IN ZERO LIFT DRAG FOR C130E

Sensitivity to Induced Drag

Changes in the induced drag coefficient affect the fuel consumption in a similar way as changes in the zero-lift drag coefficient. However the fuel consumption is not as sensitive to changes in the induced drag coefficient, as is evident from Figure 7.3-23.

Sensitivity to Fuel Flow Rate

An increase in fuel consumption per shaft horse-power results in an increase in total fuel consumption during a mission. If it is assumed that the gross weight and the mission range remain constant, then changes in the fuel consumption may be obtained using Eq. (6.1).

Sensitivity to System Weight

Changes in fuel consumption for a mission are approximately proportional to changes in system weight. For example, a 1% increase in system weight will result in approximately a 1% increase in fuel consumption.

Sensitivity to Variations in Maximum Power

Variations in maximum continuous power impact the optimum cruise performance of the C-130E through its effect on cruise ceiling. A decrease in maximum continuous power (932° C TIT) lowers cruise ceiling. Since optimum cruise altitude for the C-130E is constrained by the cruise ceiling altitude, a decrease in NRT results in lower cruising altitudes and an accompanying increase in fuel consumption. However an increase in maximum continuous power results in an increase in cruise ceiling. Thus the aircraft can cruise closer to optimum cruise altitudes and the fuel consumption will go down. Figure 7.3-21 illustrates variations in cruise ceiling due to changes in maximum continuous power for a 130,000 pound aircraft. A 10% decrease in power lowers the cruise ceiling altitude by 1,500 feet. Figure 7.3-25 shows the impact of flying off the optimum cruise altitude on specific fuel consumption. The specific fuel consumption increases by 1.3%.

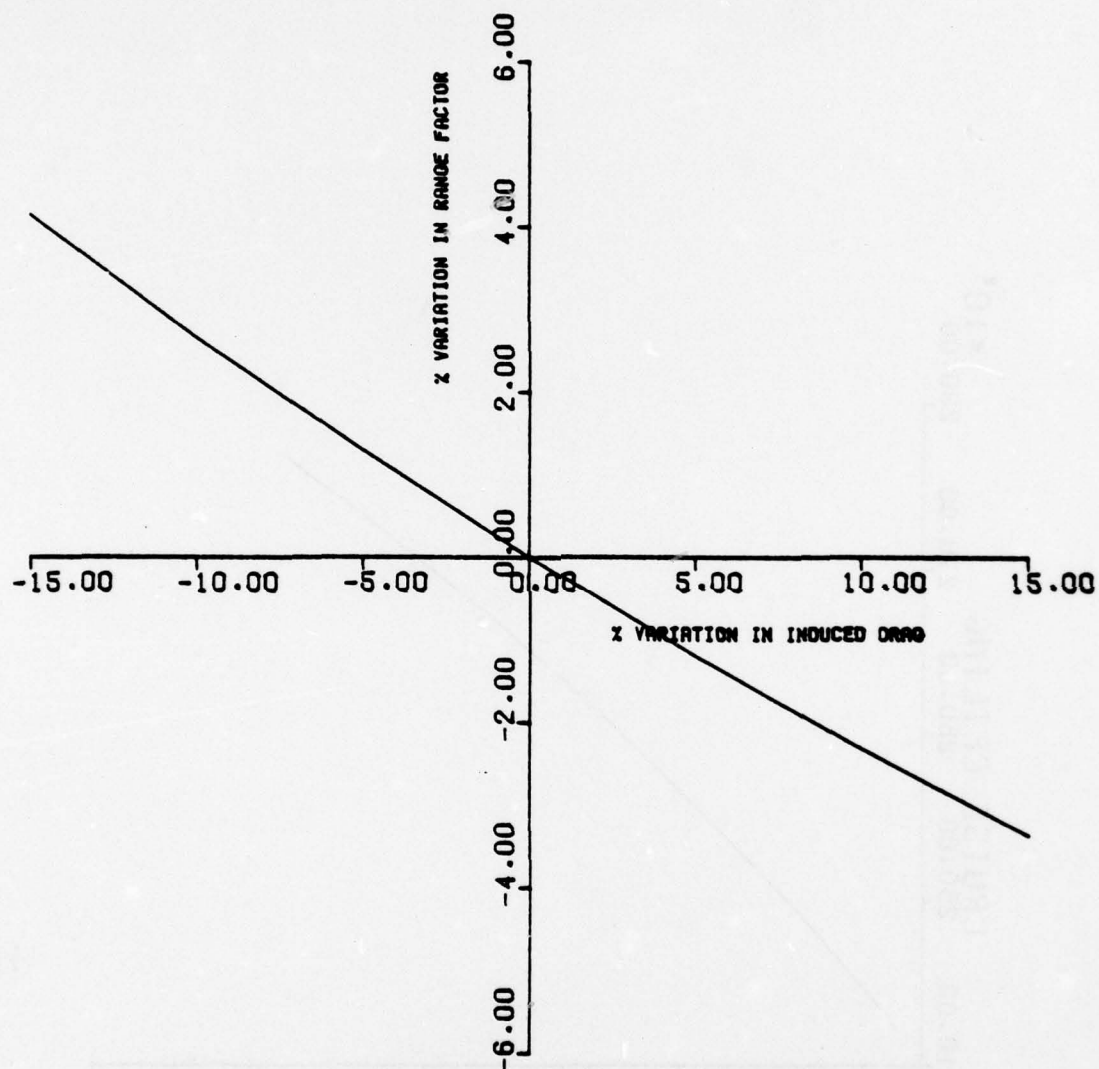


Figure 7.3-20 SENSITIVITY OF RANGE FACTOR TO VARIATIONS
IN INDUCED DRAG - C130E

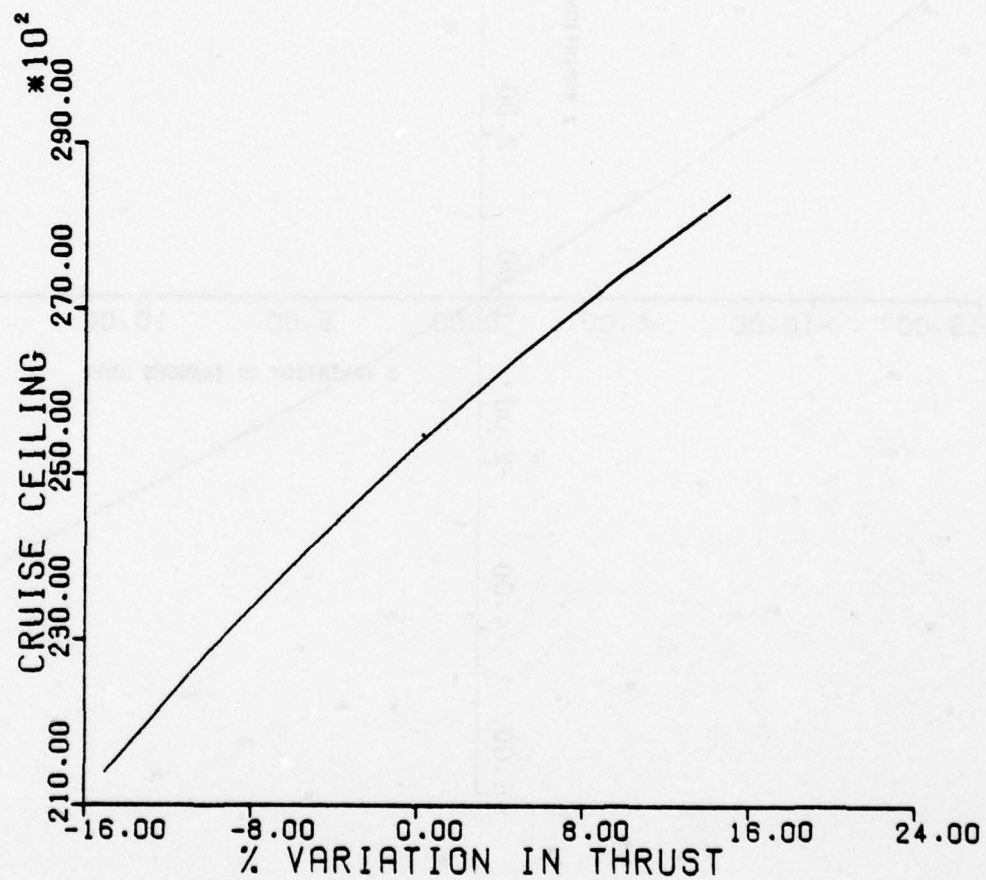


Figure 7.3-21 IMPACT OF VARIATIONS IN MAXIMUM CONTINUOUS
POWER ON CRUISE CEILING

Variations in the maximum continuous power also impact the climb performance. However, for most of the mission the impact of climb performance on total fuel consumed will be negligible.

7.3.7.2 Sensitivity to Atmospheric Variations

Changes in wind velocity and ambient temperatures have a large impact on the fuel consumption for C-130E missions.

Wind Effects

The cruise air speed for the C-130E is approximately 140 knots less than that for the other aircraft under study. Therefore atmospheric winds have a larger impact on the total fuel consumption in flying between two points for this aircraft. Headwinds increase fuel consumption while tail winds decrease it. The effect of wind on the optimum air speed is small. Head winds increase the air speed; however, the speed may be increased only up to the point at which maximum continuous power is required. The tail winds decrease the air speed somewhat. Changes in range factor due to wind are illustrated in Figure 7.3-22 for a 130,000 pound aircraft. Note that a 70 knot headwind decreases the range factor by 25% whereas a tail wind of the same magnitude increases it by almost the same amount.

Temperature Effects

Outside air temperature has a significant effect on the airplane performance. An increase in ambient temperature from the ICAO standard day lowers the cruise altitude ceiling. Lower cruise altitude results in increased fuel consumption. However a decrease in ambient temperature reduces fuel consumption due to an increase in aircraft cruise altitude. Figure 7.3-23 illustrates the impact of ambient temperature on the cruise ceiling for C-130E aircraft with 130,000 lbs. weight. Observe that a 5°C increase in temperature above the ICAO standard day temperature lowers the cruise ceiling by approximately 900 feet, resulting in a .7% decrease in specific range. Changes in temperature have a large impact on

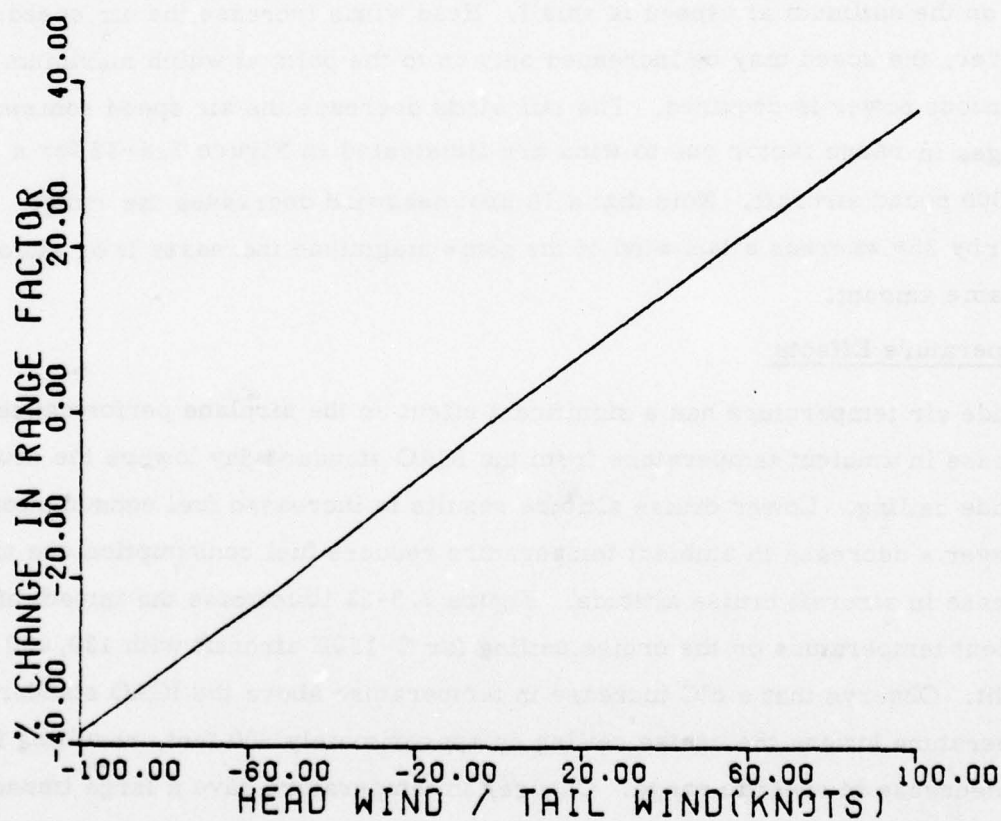


Figure 7.3-22 Sensitivity of Range Factor to Atmospheric Winds - C130E

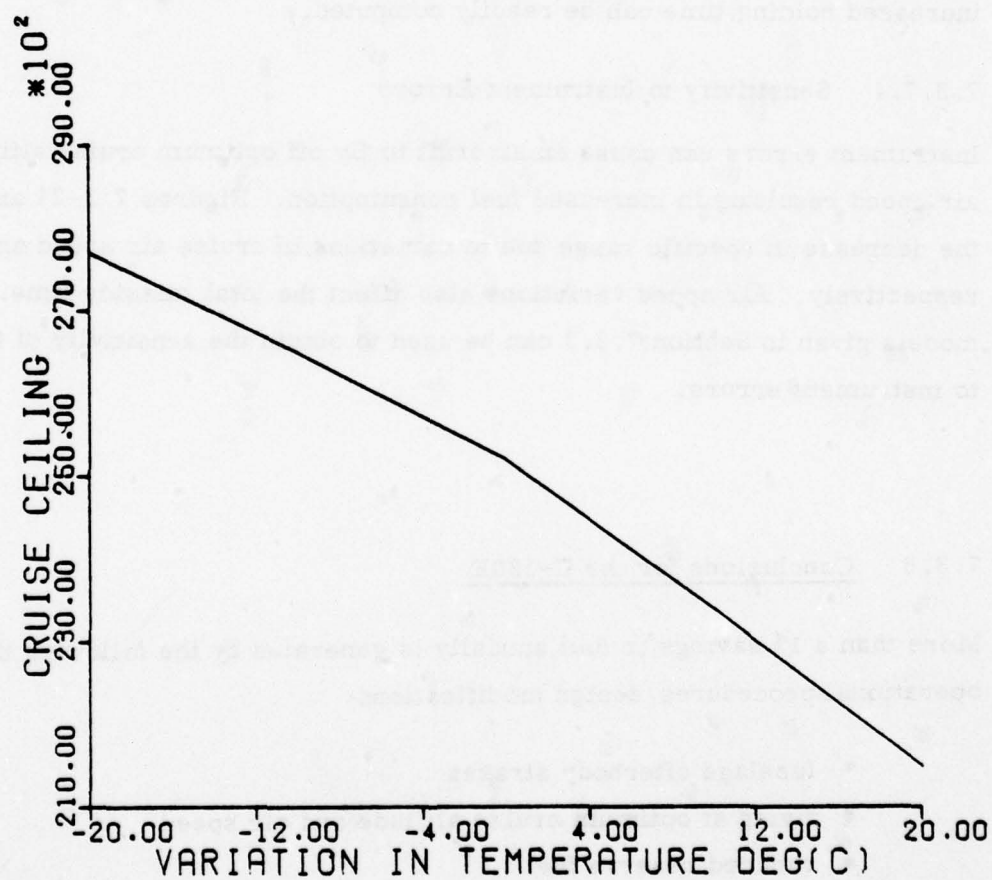


Figure 7.3-23 IMPACT OF AMBIENT TEMPERATURES ON
CRUISE CEILING - C130E

fuel consumed and distance traversed during climb. However the change in specific range during climb is negligible.

7.3.7.3 Sensitivity to Traffic Density

The impact of air traffic density on aircraft operations may be assessed in terms of increased fuel consumption due to take-off delays and increased holding time before landings. The C-130E consumes fuel at an average of 50 lbs/minute during ground operations. Fuel consumption during holding varies with altitude, air speed and aircraft weight. Based on an average landing weight of 100,000 pounds and optimum endurance altitude and air speed, the fuel flow rate during holding is 61 lbs/minute. Thus increased fuel consumption due to take-off delays and increased holding time can be readily computed.

7.3.7.4 Sensitivity to Instrument Errors

Instrument errors can cause an aircraft to fly off optimum cruise altitude and air speed resulting in increased fuel consumption. Figures 7.3-24 and 25 depict the decrease in specific range due to variations in cruise air speed and altitude, respectively. Air speed variations also affect the total mission time. DOC models given in Section 7.3.3 can be used to obtain the sensitivity of fuel/DOC to instrument errors.

7.3.8 Conclusions for the C-130E

More than a 1% savings in fuel annually is generated by the following three operational procedures/design modifications:

- fuselage afterbody strakes
- flying at optimum cruise altitude and air speed
- reduced reserve fuel

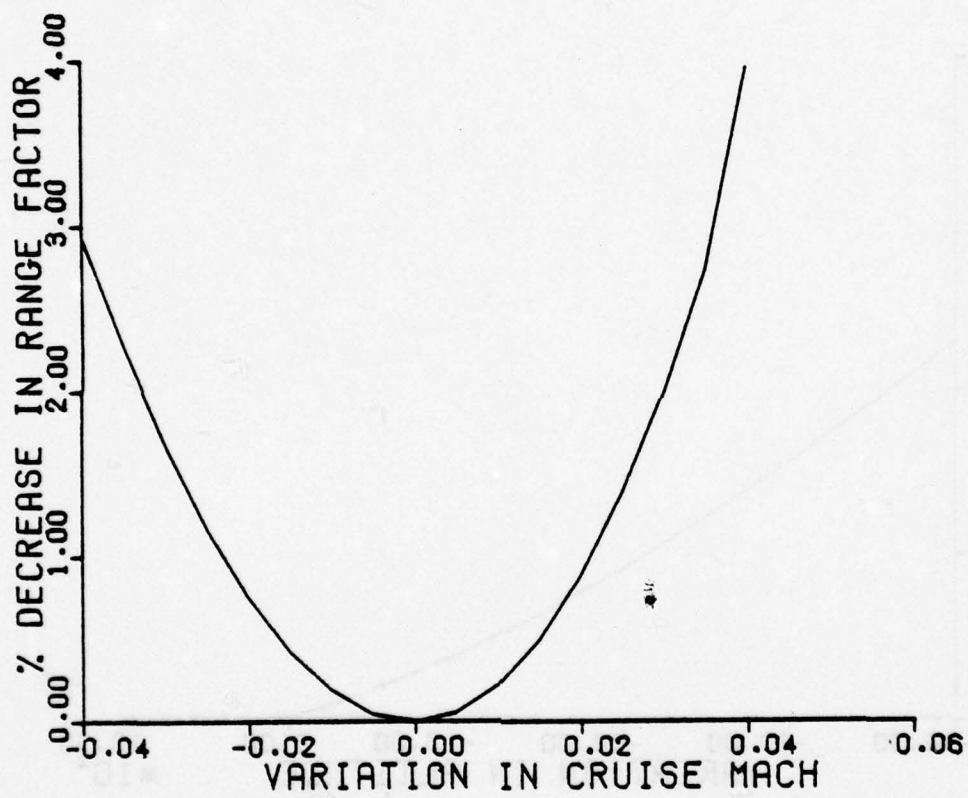
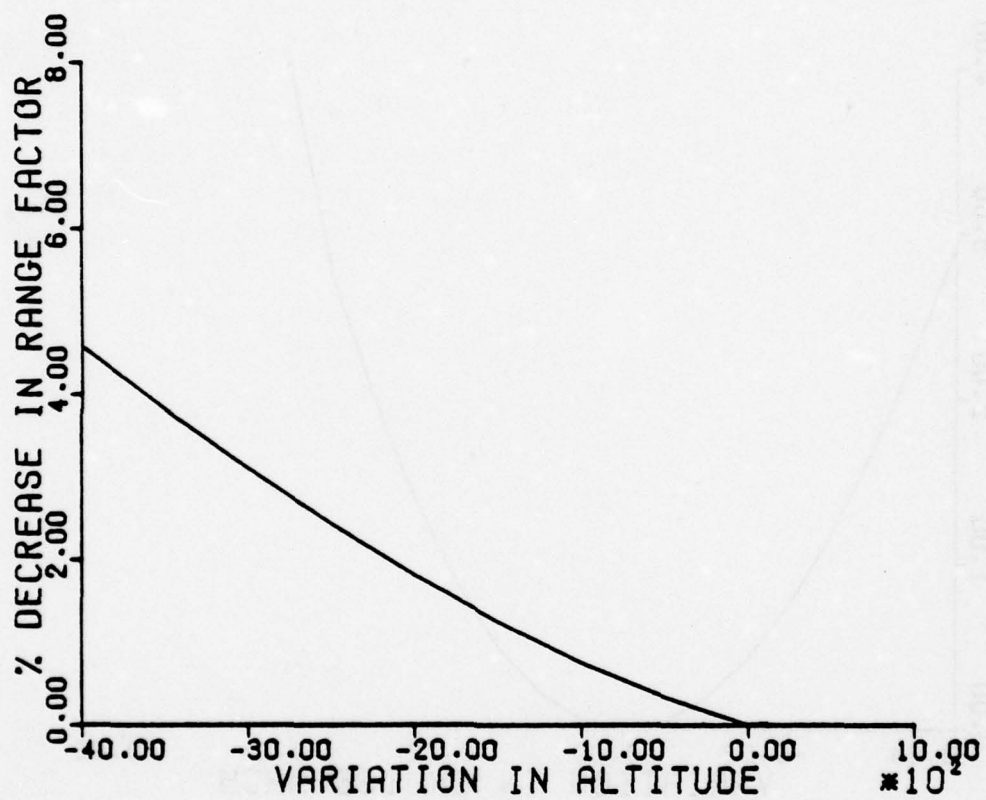


Figure 7.3-24 IMPACT OF FLYING OFF OPTIMUM CRUISE
SPEED ON RANGE FACTOR - C130E



7.3-25

IMPACT OF FLYING OFF OPTIMUM CRUISE
ALTITUDE ON RANGE FACTOR - C130E

Fuselage afterbody strakes revise the fuselage air flow patterns to reduce air flow separation and the resulting drag. The annual fuel savings estimate is 5%, and the associated modification cost can be recouped in 3.5 years.

Annual fuel savings of 5.2% are possible by optimum cruise procedures.

Annual fuel savings of 1.3% are produced by reducing the reserve fuel to the maximum set of requirements, and an additional 0.8% in fuel savings is possible with a more moderate set of reserve fuel requirements.

Each of the other items investigated generated less than a 1% fuel savings. The above conclusions are summarized in Table 7.3-6. The potential fuel savings due to the various items can be categorized as follows:

- | | |
|-----------------------------------|------------|
| • Design modifications | 5% |
| • Airborne operational procedures | 7.2 - 7.7% |
| • Ground operational procedures | 3.3 - 5.6% |

Procedures	Estimated Percentage Annual Fuel Savings	Break Even Period Years	Confidence In Estimates
Design Modifications			
Fuselage after body strakes	5	3.5	Medium
Airborne Operational Procedures			
Flying at optimum cruise altitude and airspeed	5.2	-	High
All others	2-2.5	-	High
Ground Operational Procedures			
Reduce reserve fuel	1.3 - 2.1	-	High
All others	2 - 3.5	-	High
Total	15.5 - 18.3		

Table 7.3 - 6 ESTIMATED FUEL SAVINGS FOR THE C-130E

7.4 B-52G AIRCRAFT

The Boeing-52 Stratofortress is an eight engine bomber with the primary mission of strategic air attack. Progressive refinement of the B-52, including installation of new equipment and more powerful engines in successive versions, have enabled it to continue as the major piloted component of the current SAC inventory. About 400 of the 744 production B-52's built between 1954 and 1962. Other versions still operational, but used only for training are the B-52D and B-52F. The B-52G, which is powered by J57-P-43 engines, introduced important changes including a redesigned wing containing an integral fuel tank and fixed underwing tanks, a new tail fin of reduced height and broader chord, a remotely controlled tail turret which allowed the gunner to be repositioned with the rest of the crew and the ability to carry two AGM-28 Hound Dog air to surface missiles on missions of a round-trip range of more than 10,000 miles. Deliveries of the B-52G began in 1959, and 193 were built. Under a major Air Force program initiated in 1971, the B-52G are being modified to carry 20 AGM-69A Short Range Attack Missiles (SRAM), six under each wing and eight in the bomb bay [48]. This section continues with an analysis of the B-52G model. The B-52H is covered separately in Section 7.5.

7.4.1 Design Mission

Typical design mission data for B-52G aircraft are presented in Table 7.4-1 [49]. The basic mission has a 3,550 n.mi. combat radius and carries 303,031 lbs of fuel and a 10,000 lb payload (bombs). Maximum take-off gross weight for the B-52G is 488,000 lbs, operation empty weight is 171,125 lbs, the maximum fuel carried is 48,030 gallons and the maximum missile load carried is 44,310 lbs. The maximum ferry range for B-52G is 7,335 n.mi.

7.4.2 Mission Model

The B-52G flew 9,316 missions in FY76 for a total of 70,664 hours and consumed 293.4 million gallons of fuel. The B-52 flies three basic missions: Normal

CONDITIONS	BASIC MISSION	DESIGN LOAD	MAX BOMB LOAD	MISSILE LOAD	FERRY RANGE
TAKE-OFF WEIGHT					
Fuel Load	lb.	488,000	488,000	488,000	485,556
Pay Load (Bombs)	lb.	303,031	277,631	248,718	312,195
Pay Load (Chaff, Flares)	lb.	10,000	35,400	44,310	None
	lb.	720/168	720/168	720/168	None
COMBAT RANGE	n.m.	-	-	-	7,335
COMBAT RADIUS	n.m.				
Average Cruise Speed	kn.	3,415	3,170	2,350	-
Initial Cruising Altitude	ft.	453	453	453	453
Target Altitude	ft.	31,700	31,700	31,700	31,800
Target Speed	kn.	44,250	43,200	40,900	-
Final Cruising Altitude	ft.	473	473	490	-
Total Mission Time	hr.	50,200	50,250	49,300	50,350
		15.1	14.0	10.6	16.25
LANDING WEIGHT	lb.	194,123	193,241	202,740	194,970

OEW = 171,125 lbs.

Table 7.4-1 B-52G TYPICAL MISSION DATA

Profile (Fig. 7.4-1), No Low Level (Fig. 7.4-2) and Pilot Proficiency (Fig. 7.4-3). The profiles shown are typical, and the parameter values are taken from a standard flight plan.

The ASIMIS tape data for the B-52 was also processed; however, this data provides only fragmentary information. Included on the tapes is take-off gross weight, landing gross weight and mission duration. Additional information is provided for air-refueling segments and low level segments including segment duration, altitude, airspeed, start gross weight and end gross weight. However, it does not indicate at what time during the mission these segments were flown. More important, no other information is available for the rest of the mission. Therefore the average mission profiles illustrated in Figs. 7.4-1, 2 and 3 are used for the trajectory optimization study.

7.4.3 DOC Model

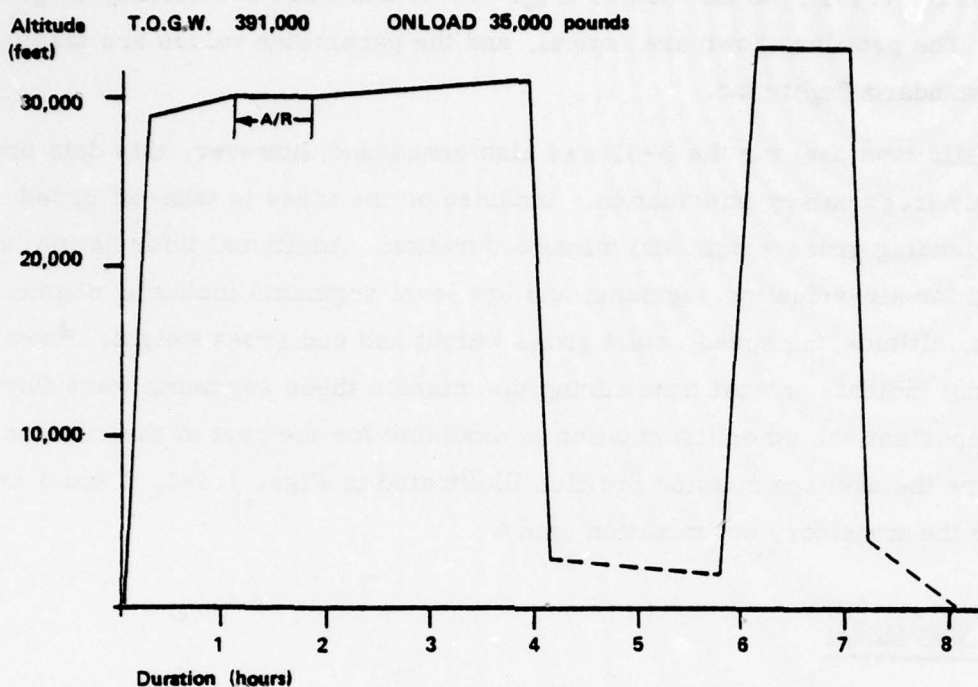
Cost data for the B-52G is given below.

<u>Direct Flight Operations</u>	<u>Cost/FH - \$</u>
Flight Crew	628
Oil at \$9.35/gal	6
<u>Direct Maintenance Operations</u>	
Direct Maintenance	1,708
(IROS = \$854)	

From the above data the following direct operating cost models are developed for the B-52G.

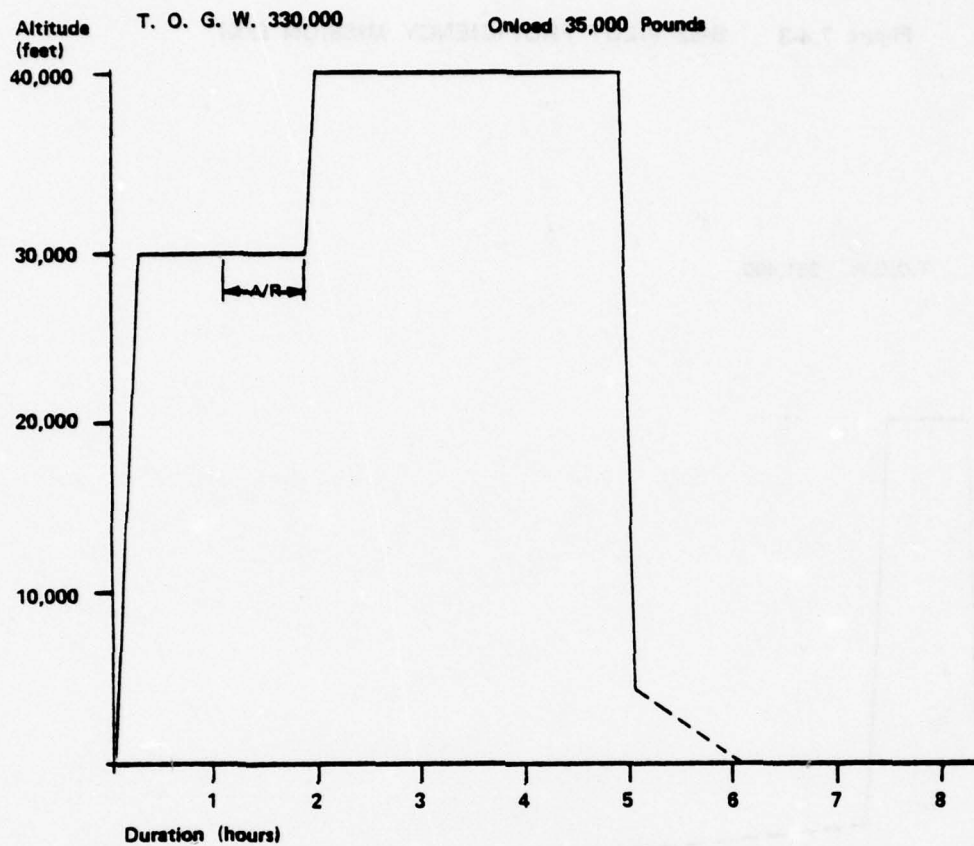
<u>Model Type</u>	<u>Fuel Cost/Gal. - \$</u>	<u>Time Cost/FH - \$</u>
DOC	.42	590
DOC1	.42	1,174
DOC2	.42	1,758
DOC3	.42	2,342

Figure 7.4-1 B-52 NORMAL PROFILE MISSION (76%)



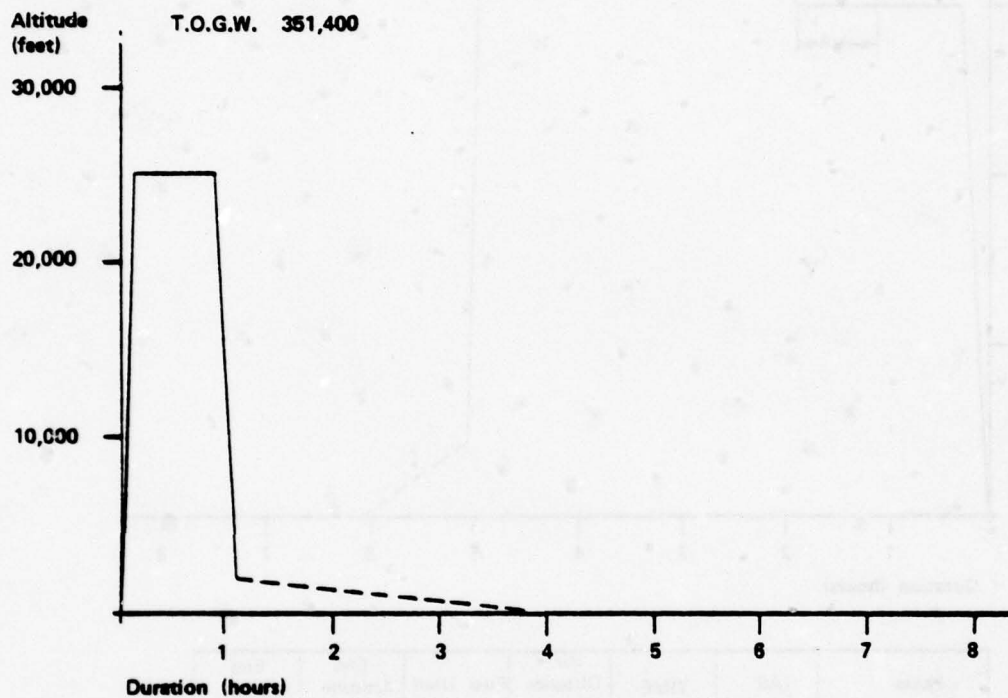
Phase	IAS	TIME	Air Distance	Fuel Used	End Altitude	End Gross Weight
Climb	280	0.22	96	17,500	29,000	373,500
Cruise	280	0.83	363	17,088	30,000	356,412
Air Refueling	255	0.72	289	20,800	30,000	370,612
Cruise	280	2.17	968	44,180	31,000	326,432
Descent	280	0.25	90	3,900	3,000	322,532
Low Level	280/325	1.65	516	41,900	2,000	280,632
Climb	280	0.33	123	8,900	33,000	271,732
Cruise	275	0.90	402	14,932	33,000	256,800
Descent	240	0.20	80	5,000	4,000	251,800
Traffic Pattern	160	0.85	140	39,000	0	212,800
TOTAL		8.12	3,067	213,200		

Figure 7.4-2 B-52 TRAINING (NO LOW LEVEL) - (17%)



Phase	IAS	TIME	Air Distance	Fuel Used	End Altitude	End Gross Weight
Climb	280	0.23	83	16,300	30,000	313,700
Cruise	280	0.83	363	14,110	30,000	299,590
Air Refueling	255	0.72	289	17,280	30,000	317,310
Climb	280-233 .77M	0.10	33	2,000	40,000	315,310
Cruise	233	3.00	1408	48,000	40,000	267,310
Descent	240	0.14	44	860	4,000	266,450
Traffic Pattern	160	1.00	165	48,100	0	220,350
TOTAL		6.02	2,385	144,650		

Figure 7.4-3 B-52 PILOT PROFICIENCY MISSION (7%)



Phase	IAS	TIME	Air Distance	Fuel Used	End Altitude	End Gross Weight
Climb	280	0.30	93	12,400	25,000	339,000
Cruise	280	0.75	276	20,200	25,000	318,800
Descent	240	0.20	80	5,000	4,000	313,800
Traffic Pattern	160	2.75	448	104,700	0	209,100
TOTAL		4.00	897	142,300		

Total flying hours for the B-52G during FY76 were 70,664 and the fuel consumed was 293.4 million gallons. From these values and the above cost model, the annual fuel and direct operating costs for the B-52G are as follows:

Fuel Cost	\$123.2 Millions
DOC	\$164.9 Millions
DOC 1	\$206.2 Millions
DOC 2	\$247.4 Millions
DOC 3	\$288.7 Millions

7.4.4 B-52G Characteristics

The aerodynamics and propulsion data for the B-52G were obtained from References [50-51]. This data was used to develop the analytical models described below.

7.4.4.1 B-52G Aerodynamic Model

The drag coefficient (C_D) representation for the B-52G follows the same method as for the aircraft described before. Thus C_D is represented as a parabolic function of the lift coefficient (C_L)

$$C_D = C_{D_0} - B C_L + K C_L^2$$

and coefficients C_{D_0} , B and K are functions of Mach (M) given by

$$C_{D_0} = .0152 + .3 \cdot 10^{-6} (M^* - M)^{-5.0}$$

$$B = .0136 + .28 \cdot 10^{-6} (M^* - M)^{-6.2}$$

$$K = .0643 + .74 \cdot 10^{-6} (M^* - M)^{-6.35}$$

and

$$M^* = 1.0$$

This model degrades beyond .825 Mach.

7.4.4.2 B-52G Thrust Model

Normal rated thrust (NRT) for each engine of the B-52G is given by the following polynomial of normalized altitude (H_n) and Mach (M) on a standard day

$$\begin{aligned} \text{NRT} = 1000. [& 8.58 - 5.22H_n - 2.86M - .95H_n^2 + 3.49MH_n + 1.79M^2 \\ & -.21MH_n^2 - 2.35M^2H_n + 1.27M^2H_n^2] \end{aligned}$$

where

NRT = normal rated thrust, (lb)/engine

H_n = altitude, (ft)/40000

This NRT model is applicable in the troposphere

For the stratosphere, the following NRT equation is used:

$$\begin{aligned} \text{NRT} = 1000. [& 9.7 - 9.23H_n + 2.1M + 2.27H_n^2 - 4.37MH_n + 2.01M^2 \\ & + 1.93MH_n^2 - 1.3M^2H_n + .08M^2H_n^2] \end{aligned}$$

Idle thrust (Tidle) for the B-52G is given by the following polynomial function of Mach (M) and normalized altitude (H_n)

$$\begin{aligned} \text{Tidle} = 1000. [& .36 + .25H_n - .57M + .1H_n^2 + 2.12MH_n - .75M^2 \\ & - 1.52MH_n^2 - .6M^2H_n + .93M^2H_n^2] \end{aligned}$$

where

T_{idle} = idle thrust, lbs/engine

7.4.4.3 B-52G Fuel Flow Model

The fuel flow model for the B-52G has a representation similar to the C-141 aircraft. The normalized fuel flow, f_n , is given by the following polynomial equation:

$$f_n = 1000 \cdot [.06 + 11.88 T_n + 3.5 M + 6.32 T_n^2 + 2.58 M T_n - 1.75 M^2]$$

where

$$T_n = T/\delta/20000$$

T = thrust, lbs/engine

δ = pressure ratio

In the stratosphere the actual f_n increases with altitude. Thus a correction factor is used for altitudes above the tropopause. Fuel flow rate is increased by 0.45 percent for each 1000 ft altitude increment above the tropopause

An idle fuel flow model was also developed for the B-52G using idle thrust and fuel flow data. The normalized idle fuel flow rate, f_{idle} , is represented by

$$f_{idle} = 1000 [.128 + .96 T_n + 1.77 M + 17.75 T_n^2 - 16.4 M T_n + .4 M^2]$$

This model is used up to a 25,000 ft altitude; beyond that altitude the actual fuel flow rate is 650 lbs/hr/engine.

The above thrust and fuel flow models are generally good to within 2% error over the regions of interest.

7.4.5 Evaluation of Airborne and Ground Operational Procedures

This subsection presents the results of an analysis of fuel conservation operational procedures for the B-52G aircraft. This analysis is based on the three average mission profiles given in Subsection 7.4.2.

7.4.5.1 Reduced Power Take-off

Fuel savings due to reduced power take-off are negligible; the average fuel savings per mission are approximately one-half gallon. Moreover the average take-off time increases by 7 seconds. However, the reduced power take-off procedure results in reduced engine deterioration. Indirect fuel savings due to reduced engine deterioration may be substantial. Therefore reduced power during take-off should be employed whenever feasible.

7.4.5.2 Optimal Climb, Cruise and Descent Procedures

Optimum climb, cruise and descent procedures are first evaluated separately and compared with the conventional procedures employed during these segments. Then the individual results are used to obtain integrated optimal trajectories.

Optimum Climbing Cruise Solution

The extremization of Equation (A.31) in Appendix A provides optimum cruise altitude and Mach number. Observe that as parameter θ is changed, the fuel consumed and the time required to execute a mission change. Figure 7.4-4 illustrates the fuel/time trade-off curve obtained by varying parameter θ in Equation (A.31). The minimum time solution corresponds to $\theta = 0$. As θ increases, fuel consumption decreases and the mission time increases. The minimum fuel solution corresponds to $\theta = 1$. The optimum solutions corresponding to various cost models are noted on Figure 7.4-4. The optimum cruise mach numbers corresponding to DOC, DOC 1, DOC 2 and DOC 3 are .785, .795, .805 and .81, respectively. Note that these cruise mach numbers vary with system weight. However, the parameters for the minimum fuel solution remain constant. For B-52G aircraft these parameters are as follows:

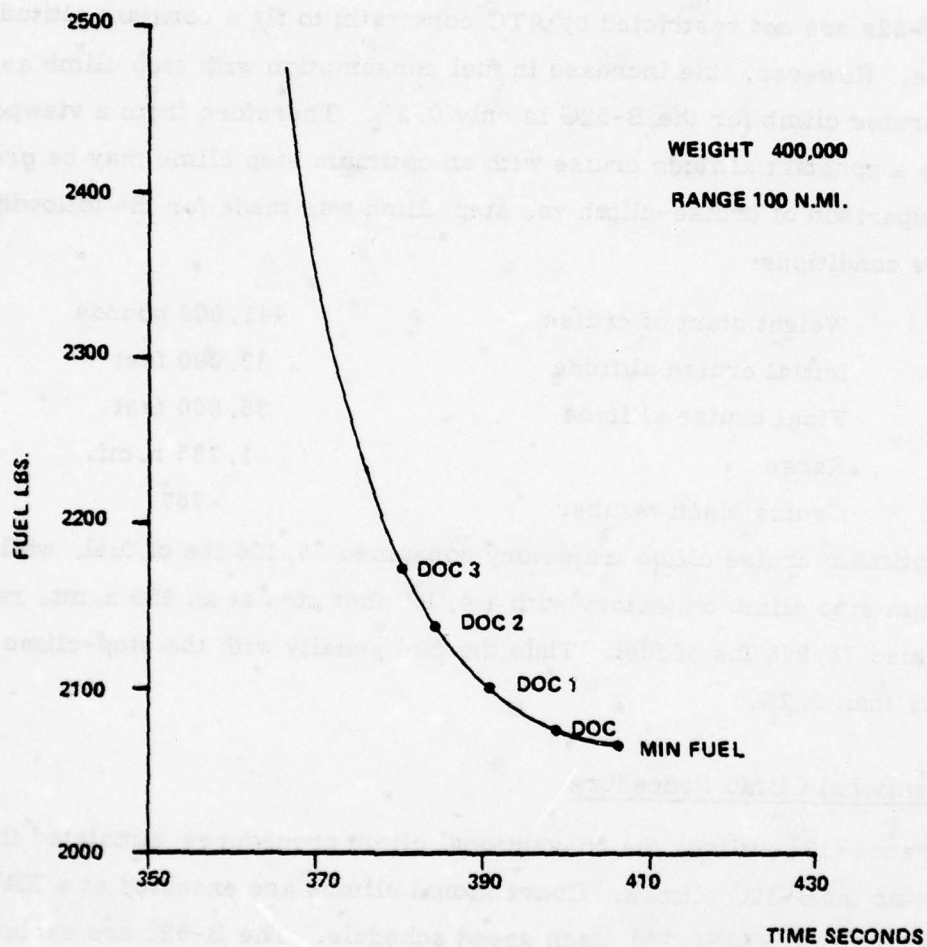


Figure 7.4-4

FUEL/TIME TRADE-OFF FOR THE B-52G

CRUISE SOLUTION

- Cruise Mach Number = .767
- Range Factor = 9224

Note that this range factor has not been corrected for power and bleed air extraction and the energy gain during cruise-climb. The energy required for cruise climb reduces the range factor by 0.7%.

Optimum Step Climb Solution

The B-52s are not restricted by ATC constraint to fly a constant altitude cruise. However, the increase in fuel consumption with step climb as opposed to a cruise climb for the B-52G is only 0.2%. Therefore from a viewpoint of safety a constant altitude cruise with an optimum step climb may be preferable. A comparison of cruise-climb vs. step climb was made for the following cruise conditions.

Weight start of cruise	441,000 pounds
Initial cruise altitude	32,000 feet
Final cruise altitude	36,000 feet
Range	1,735 n.mi.
Cruise Mach number	767

The optimum cruise climb trajectory consumed 76,126 lbs of fuel, while the optimum step climb trajectory with a 4,000 foot step at an 850 n.mi. range consumed 76,276 lbs of fuel. Thus the fuel penalty with the step-climb procedure is less than 0.2%.

Conventional Climb Procedure

Reference [13] outlines the conventional climb procedures simulated in this study for the B-52G climbs. Conventional climbs are executed at a NRT power setting and 280 KIAS/.765 Mach speed schedule. The B-52s are excluded from the ATC constraint of a 250 knot maximum climb speed below a 10,000 foot altitude.

Optimum Climb Procedure

The optimum climb air speed and power setting are obtain from the optimum climb algorithm. For an optimal climb trajectory, both the air speed and throttle setting vary with altitude. This optimal climb and the parametric optimal climb discussed next are optimized with respect to minimum fuel and compared to a conventional climb in the following material.

Parametric Optimum Climb Procedure

Parametric optimum climb is similar to conventional climb in that it follows a constant KCAS/constant mach speed schedule. However, instead of employing an air speed of 280 knots during climb, the best single speed at low altitudes is determined by parametric optimization. This speed varies with aircraft weight.

Comparison of Various Climb Procedures

Table 7.4-2 summarizes the results of a comparison of the three climb procedures discussed above. Initial and terminal conditions for all three trajectories are the same. The optimal trajectory traverses a 189 n.mi. distance during climb. Both parametric optimum and conventional climb segments are followed by short cruise segments at .767 mach number. The optimum trajectory consumes 15,727 pounds of fuel, which is 211 pounds less than the conventional climb, and it takes 99 seconds less time for the mission. The parametric optimum trajectory consumes only 1 pound more fuel than the EEM optimal trajectory; however, it takes 47 seconds more time to accomplish the mission. Table 7.4-2 also indicates the cost associated with each trajectory. Observe that the optimum trajectory has the least cost. However, the difference between the fuel consumed between optimum and parametric optimum is negligible. Annual savings due to parametric optimum climb procedures are computed to be 110,000 gallons of fuel (.04%) and \$156,000 DOC (.09%). However, the slight increase in time and fuel used with the conventional 280 knot climb is not considered critical for most missions [13].

Initial Conditions
 Weight = 415,000 lbs.
 Altitude = 3,000 ft.
 Airspeed = 250 KIAS

Final Conditions
 Range = 189 NM
 Altitude = 34,100 ft.
 Airspeed = .767 Mach

Type of Climb	Optimum	Parametric Optimum 310KIAS/.767M	Conventional 280KIAS/.767M
Climb	189	120	117
Cruise	0	69	72
Total	189	189	189
Climb	15727	12703	12808
Cruise	0	3023	3130
Total	15727	15726	15938
Climb	1592	1075	1107
Cruise	0	564	584
Total	1592	1639	1691
DOC	1277.1	1284.7	1306.9

Table 7.4-2 COMPARISON OF OPTIMUM CLIMB VS. CONVENTIONAL CLIMB - B-52G

Moreover an increase in climb speed will result in increased noise and air pollution. Therefore a start climb speed of 280 KIAS is used for all missions unless otherwise required for special mission operations.

Conventional Descent Procedures

The conventional descent procedures simulated for the B-52 evaluation were obtained from Reference [13]. Normal descent is accomplished at 240 knots IAS or Mach .75, whichever is slower. The airplane configuration during the normal descent is with landing gear down, airbrakes in position 4, flaps up and eight engines at idle.

The descent to the low level tactic was simulated at 280 KIAS or Mach .765, whichever is slower. The airplane configuration during the descent is with airbrakes in position 6, flaps up and eight engines at idle.

Optimal Descent Procedures

Air speed and throttle settings for optimal descent are obtained using the optimization algorithm developed in Appendix A. Both air speed and throttle setting vary with altitude during descent.

Comparison of Various Descent Procedures

The results of a comparison of various descent procedures for a B-52G aircraft are given in Table 7.4-3. The optimal descent trajectory traverses a 135 n. mi. range during descent. Other trajectories have a cruise segment before descent initiation so that the total mission range for all trajectories is the same. The optimal trajectory consumes 1563 pounds less fuel than the "normal" descent trajectory. Note that the conventional descent with the aircraft in a clean configuration and with a 240 KIAS air speed consumes only 322 lbs more fuel than the optimal descent, and it takes 235 seconds less time than the optimal descent. If the air speed were reduced lower than 240 KIAS, the fuel consumption decreases and mission time increases. Direct operating cost begins to increase if air speed

is reduced. A good compromise between fuel and time savings is a conventional descent at .75 mach/240 KIAS speed schedule with the aircraft in a clean configuration and eight engines retarded to idle setting since the compromise produces the minimum DOC. Table 7.4-4 gives estimates of fuel and direct operating cost savings which may be achieved by keeping the aircraft configuration clean during descent. Annual fuel savings will be 3.1 million fallons of fuel which is approximately 1.1% of the total fuel consumed for B-52G operations. However, due to increased mission times the annual DOC savings is only 0.5%.

Integrated Optimal Trajectories

Refueling requires special coordination between a tanker and a receiver. Normally refueling is accomplished in level flight. It is always better for a receiver to sacrifice altitude instead of speed to perform a successful refuel because slow speeds and high altitudes more often result in disconnects. With boom type refueling the receiver will always be flying in the down wash of the tanker and thus the receiver will have to use more power than in normal level flight. The refueling altitude is generally limited by the receiver performance at the end of transfer on outbound refueling and by tanker performance on inbound refueling [15]. The B-52 missions which require refueling are analyzed in the light of the above discussion.

Figure 7.4-1 illustrates the average profile for the normal missions of B-52G aircraft. Observe that there is a small cruise segment before the air refueling phase. The refueling altitude is restricted to 30,000 feet. The aircraft could save a small amount of fuel by initially climbing to a 36,000 foot altitude, cruising at this altitude, and then descending for air refueling. However, since special flying techniques are required for the refueling, there may not be enough time for the B-52 to climb to a higher altitude, descend, and be ready for refueling. Therefore no altitude change is considered until after the air refueling is accomplished.

After the refueling phase the B-52G can climb to a 36,000 foot altitude and cruise at that altitude before descending for the low level segment. No change in the low level segment is considered because of mission constraints. However, after completing the low level segment the aircraft can climb to a 41,000 foot altitude and

Initial Conditions
 Weight = 256,000
 Altitude = 35,000
 Airspeed = .75 Mach

Final Conditions
 Range 135
 Altitude 3,000 ft.

Type of Descent	Conventional with Air-brakes and Gear Down	Conventional in Clean Configuration	Optimal in Clean Configuration
Cruise	104	29	0
Descent	31	106	135
Total	135	135	135
Cruise	3372	931	0
Descent	516	1716	2315
Total	3888	2647	2315
Cruise	855	233	0
Descent	355	1197	1668
Total	1210	1433	1668
DOC	449.5	405.9	422.9

Table 7.4-3 COMPARISON OF OPTIMAL VS. CONVENTIONAL DESCENT - B-52G

COST	ANNUAL SAVINGS DUE TO CLEAN A/C CONFIGURATION DURING DESCENT	% SAVINGS
FUEL GALLON	3,138,000	1.07
FUEL COST \$	1,318,000	1.07
DOC \$	830,000	.5
DOC1 \$	346,500	.17
DOC2 \$	136,700 (loss)	.06 (loss)
DOC3 \$	620,000 (loss)	.21 (loss)

Table 7.4-4 ANNUAL FUEL/DOC SAVINGS DUE TO CLEAN AIRCRAFT
CONFIGURATION DURING DESCENT - B-52G

cruise before initiating the final descent. Under these conditions aircraft can save 326 gallons of fuel per mission with respect to the average profile. However, the mission time will increase by 159 seconds. Annual fuel savings will amount to 2.3 million gallons, and the annual savings in DOC will be \$780,000.

No change in cruise altitude is considered before the refueling segment of the training missions. After refueling has been accomplished, the aircraft climbs to a 40,000 foot altitude, which is close to the optimum cruise altitude. Some savings can be accomplished by flying at 42,000 feet altitude. However, due to an increase in TSFC at higher altitudes the savings at a 42,000 foot altitude are negligible.

Pilot proficiency missions generally involve local training and multiple take-offs and landings, and the chances of fuel savings due to trajectory optimization are negligible.

From the previous discussion, it is obvious that most of the B-52G mission segments are constrained by practical operational consideration and mission requirements. Based on information received from SAC on typical mission profiles these missions are being flown near to optimal.

7.4.5.3 Delayed Flap Approach Procedure

The fuel/DOC savings due to a delayed flap approach procedure for B-52G aircraft are summarized in Table 7.4-5. Altitude above the runway where the aircraft attains stable approach speed is shown in the first column. This altitude is 1,500 feet for the conventional approach. The maximum fuel savings due to the delayed approach for B-52G aircraft is 0.2%.

7.4.5.4 Aft C.G. Operations

For the B-52 bomber the possibility of shifting the c.g. further aft than those being used by the proper distribution of fuel and payload (bombs and missiles) is rather limited due to operational constraints. During flight, burning fuel evenly towards aft c.g. may result in some fuel savings. A 5%-MAC (mean aerodynamic

Altitude for Stable Landing Speed -ft.	ANNUAL SAVINGS					
	Fuel/Gal.	Fuel Cost	DOC	DOC1	DOC2	DOC3
1000	202,100	84,900	122,600	159,900	197,200	234,500
500	404,500	169,900	247,200	323,700	400,200	476,700
0	607,400	255,100	373,700	491,000	608,500	726,700

Table 7.4-5 Annual Fuel/DOC Savings Due to Delayed Flap Approach - B-52G

cord) shift in c.g. towards aft results in a 0.8% savings in fuel consumed for the B-52G.

7.4.5.5 Reduce Reserve Fuel

Since the ASIMIS tape data for B-52G does not provide any information on the landing fuel for B-52 missions, it is not possible to quantify fuel savings by reducing reserve fuel. Therefore, only the sensitivity of fuel savings due to reduced reserve fuel for B-52G operations can be determined. If the fuel reserve could be reduced an average 5000 pounds per mission, this would result in 1.2 million gallons of fuel saved annually for B-52G operations.

7.4.5.6 Reduce Engine Load

With the engine and nacelle anti-icing system in operation the fuel flow increases by approximately 2.5% at high altitudes and 4.8% at low altitudes for B-52G aircraft [13]. The use of bleed air for operations of the air conditioning system results in a decrease in fuel mileage. In general fuel savings can be achieved by reducing power and bleed air extraction. However, it is inappropriate to define a savings factor in this case because of the variability in conditions from one mission to another and the lack of specific data.

7.4.5.7 Reduce Engine Use and Taxi Time

The average fuel consumption for the B-52G with all eight engines operating during ground operations is 210 lbs/minute. Fuel consumption during ground operation can be reduced by following some of the procedures described in Section 4.3. Every minute of reduced taxi time can save 301,000 gallons of fuel and \$218,000 in DOC annually for B-52G operations.

7.4.5.8 Partial Engine Taxi

Shutting down four engines during taxi-in and parking may be a feasible operational procedure for the B-52G. Assuming a five minute average taxi time, this procedure can save 752,000 gallons of fuel annually for the B-52G.

7.4.5.9 Remove Excess Equipment

No excess equipment has been identified on the B-52's. Figure 7.4 -8 depicts the sensitivity of fuel/DOC to variations in system weight for the B-52G. This plot may be used to determine the fuel savings due to the removal of any equipment.

7.4.5.10 Maintenance to Reduce Drag

As discussed in Subsection 4.3, aircraft surface roughness, misrigged control surfaces and improperly adjusted hatch filters result in increased aerodynamic drag. If the spoilers on one wing are up 1° (one unit of trim), the aircraft drag is increased by 1%. The forward edge of improperly adjusted hatch lifters will raise from the fuselage skin at high airspeeds. When a hatch lifter gaps in this manner, the drag increase is dependent on the height of the lifter and the number of lifters raised on the aircraft. This effect will be more pronounced at the high indicated airspeed employed for low level [13]. Thus aircraft maintenance results in reduced fuel consumption. A direct quantification of savings is not possible in this case. Sensitivity plots depicting changes in fuel/DOC due to variations in aircraft are given in Section 7.4.6. These plots may be used to estimate fuel savings due to aircraft maintenance.

7.4.5.11 Engine Maintenance

The interior of the engines are aerodynamic surfaces and therefore any deterioration such as nicks, roughness from water residue, distortion due to creep and overheat will result in increased fuel consumption. Improved maintenance procedures may result in improved engine efficiency. SAC is doing considerable work in this area. Fuel savings due to improved maintenance procedures may be estimated using Figure 7.4-7. On the assumption that improved engine maintenance will reduce TSFC by 1.5%, the annual fuel savings will be approximately 3.9 million gallons.

7.4.6 Evaluation of Design Modifications

The B-52 Stratofortress has been modified and refined progressively over the years. Even today the B-52 is involved in a major modification to carry 20 short range attack missiles, six under each wing and eight in the bomb-bay. An engine retro-fit study was conducted to replace J-57's with TF-38's but was found to be uneconomical [37]. Winglets may offer potential fuel savings; however, this requires a detailed analysis because of other equipment and munitions carried under the wings. Manual engine surge bleed valve override offers substantial fuel savings and will be discussed in this section.

7.4.6.1 Parametric Analysis of Aerodynamic and Propulsion Design Modifications

Generic plots have been developed to illustrate the functional relationships between the variation in fuel/DOC and variations in the aerodynamic and propulsion parameters for B-52G aircraft. Figures 7.4-5, 6, 7 and 8 represent changes in fuel/DOC due to changes in zero-lift drag, induced drag, thrust specific fuel consumption and take-off gross weight for the B-52G. These plots, which were generated by simulating the three average mission profiles given in Section 7.4.2, can be used for any future design evaluation.

7.4.6.2 Manual Engine Surge Bleed Valve Override

The B-52G has an automatic air bleed valve which remains open when the engine is in the possible stall (low level) region, increasing the specific fuel consumption between 8 and 10 percent. By a modification to allow manual operation of the valve, it can be closed at all times other than when actually required to be open.

It has also been suggested that a procedure could be implemented that would allow four engines to be operated at power settings where the surge bleed valves would be automatically closed and the other four engines would be operated at high power with the valves manually operated by the co-pilot [52]. In this manner, all engines would be in the closed valve configuration, resulting in an approximate savings of 9 percent, while only requiring a modification for four engines. The modification cost is currently estimated at between \$3.5 - 4.5 million. The potential savings

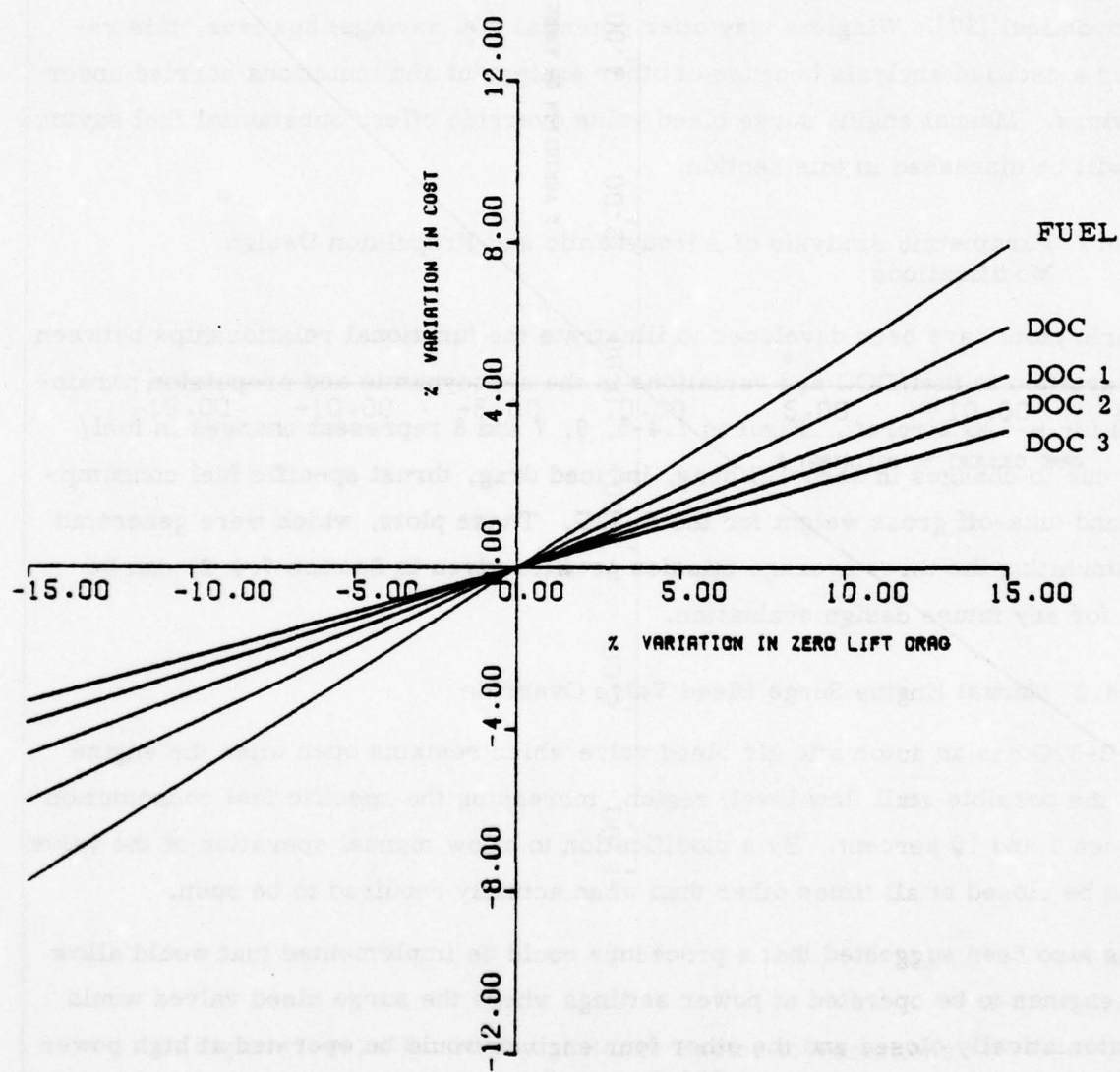


Figure 7.4-3 Sensitivity of Fuel/DOC to Variations in Zero-Lift Drag - B52G

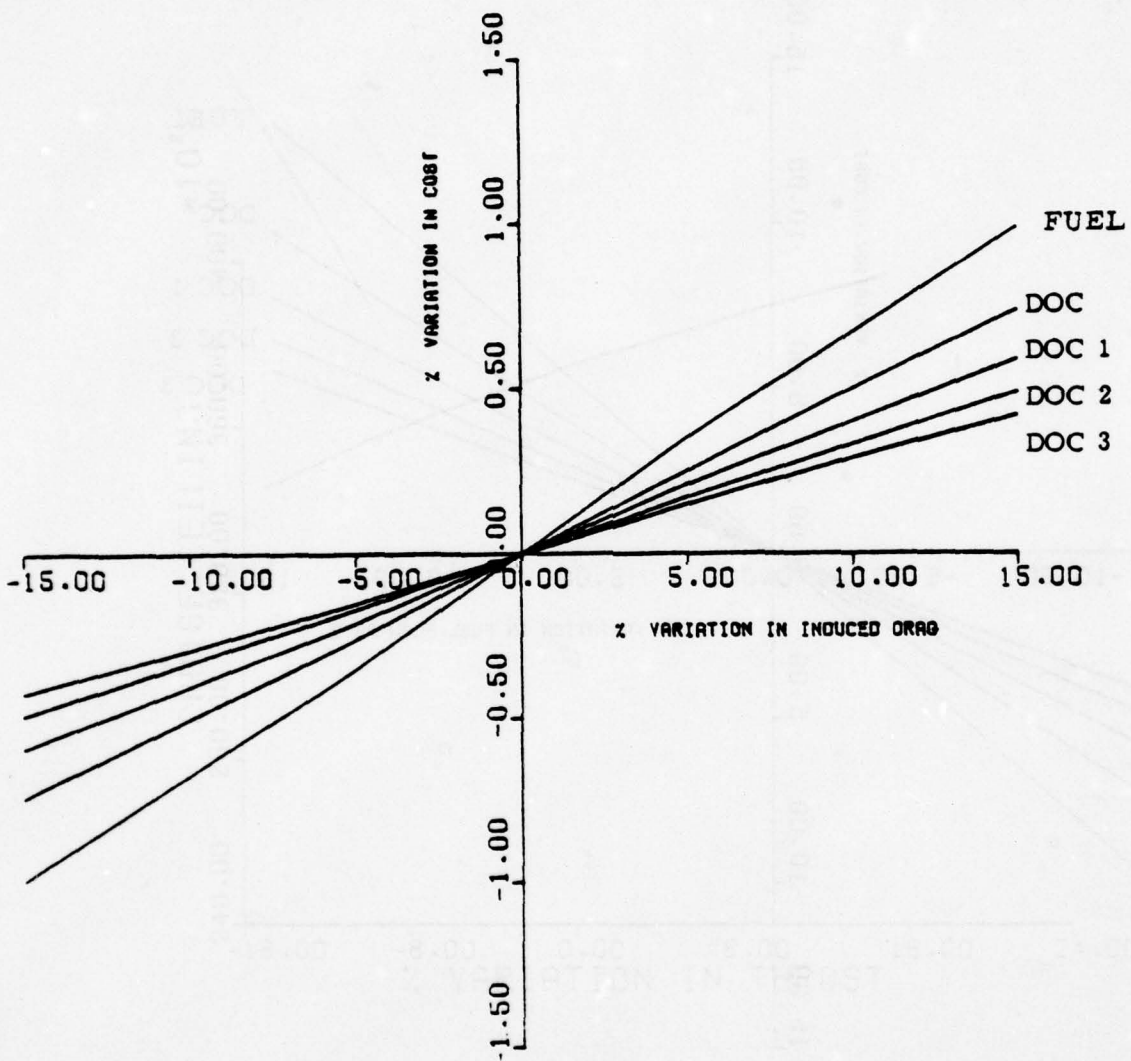


Figure 7.4-6 Sensitivity of Fuel/DOC to Variations in Induced Drag - B52G

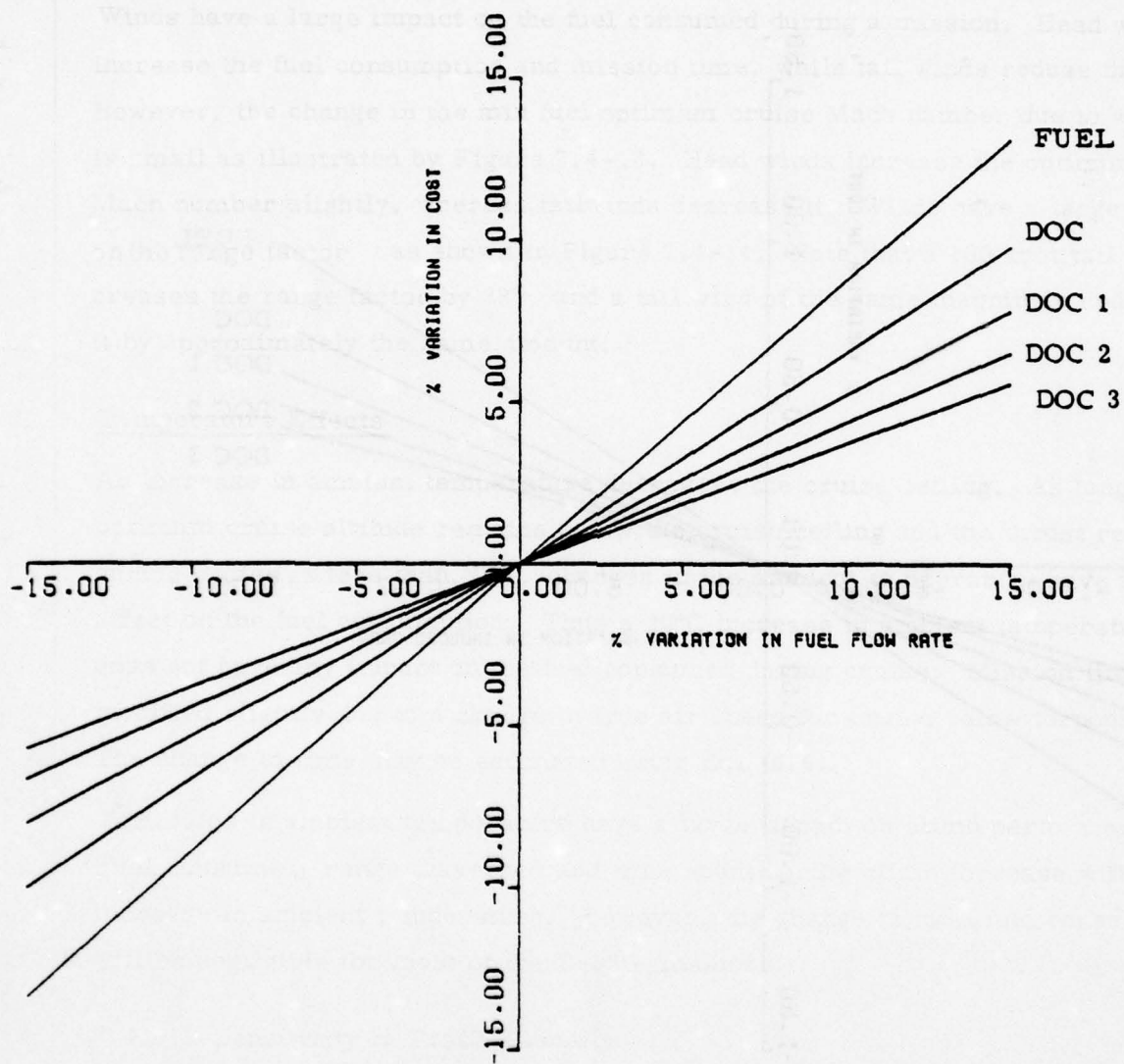


Figure 7.4-7 Sensitivity of Fuel/DOC to Variations in Thrust Specific Fuel Consumption - B52G

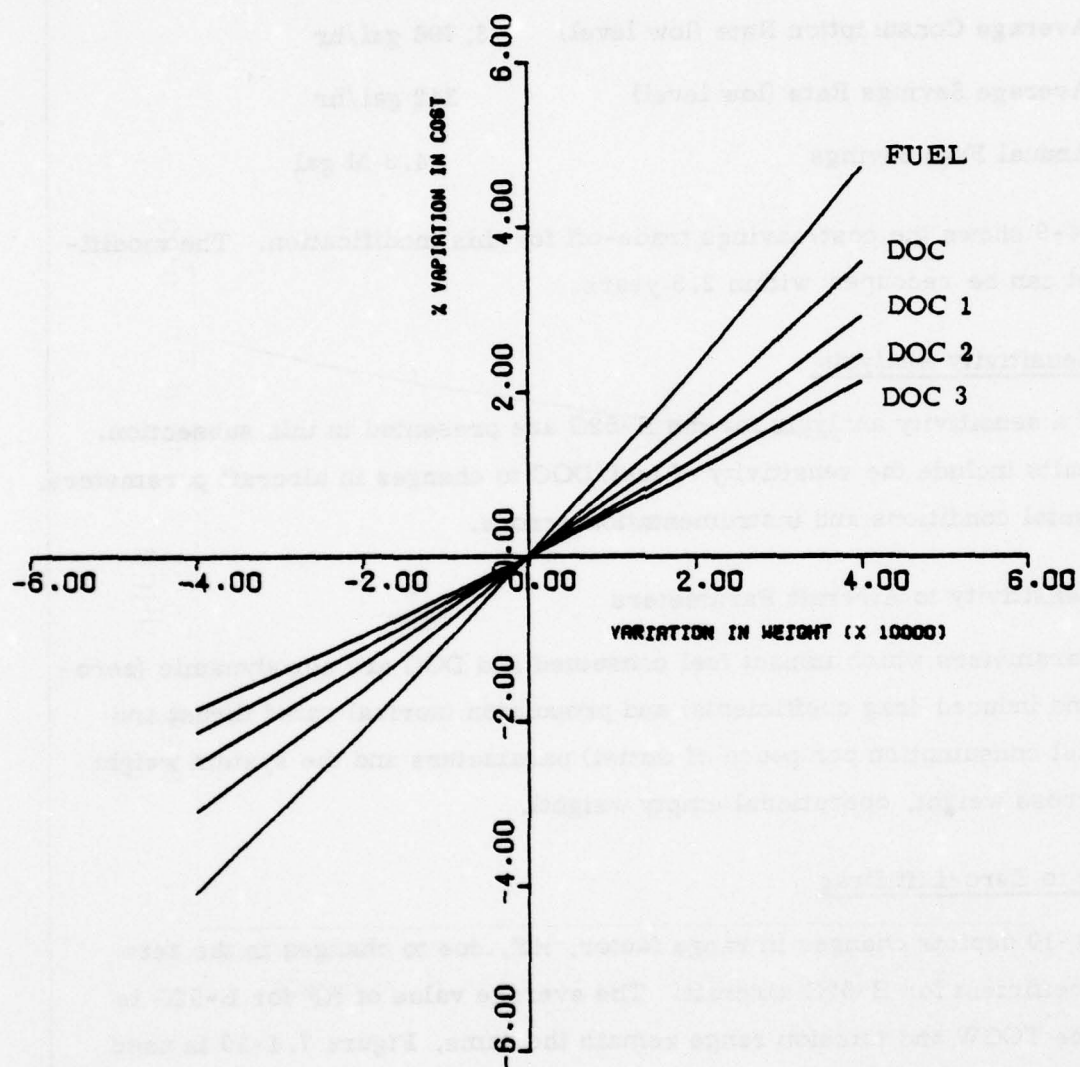


Figure 7.4-8 Sensitivity of Fuel/DOC to Variations in Weight - B52G

are calculated as follows:

Annual Fuel Consumed (low level)	47.8 M gal
Annual Flying Time	70,664 hours
Annual Flying Time (low level)	12,578 hours
Average Consumption Rate (low level)	3,798 gal/hr
Average Savings Rate (low level)	342 gal/hr
Annual Fuel Savings	4.3 M gal

Figure 7.4-9 shows the cost/savings trade-off for this modification. The modification cost can be recouped within 2.5 years.

7.4.7 Sensitivity Analysis

Results of a sensitivity analysis for the B-52G are presented in this subsection. These results include the sensitivity of fuel/DOC to changes in aircraft parameters, environmental conditions and instrumentation errors.

7.4.7.1 Sensitivity to Aircraft Parameters

Aircraft parameters which impact fuel consumed and DOC are aerodynamic (zero-lift drag and induced drag coefficients) and propulsion (normal rated thrust and specific fuel consumption per pound of thrust) parameters and the system weight (take-off gross weight, operational empty weight).

Sensitivity to Zero-Lift Drag

Figure 7.4-10 depicts changes in range factor, RF, due to changes in the zero lift drag coefficient for B-52G aircraft. The average value of RF for B-52G is 9224. If the TOGW and mission range remain the same, Figure 7.4-10 is used to determine the change in RF due to a change in zero lift drag, and then Eq. (6.1) provides the change in fuel consumption. As an example, consider that the zero-lift drag coefficient of an aircraft increased by 5% due to combat damage. The corresponding decrease in RF is 3.2%. Based on a 1,000 n.mi. combat range, the fuel consumption will increase by 3%.

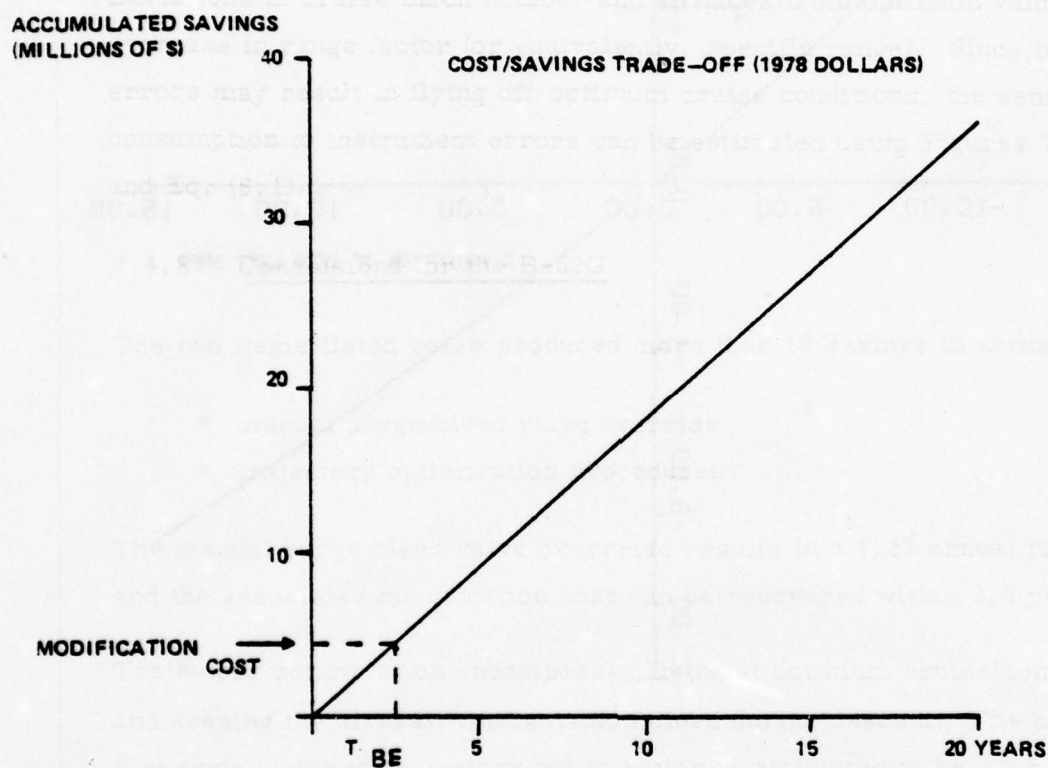


Figure 7.4-9 SAVINGS DUE TO MANUAL SURGE BLEED VALVE OVERRIDE

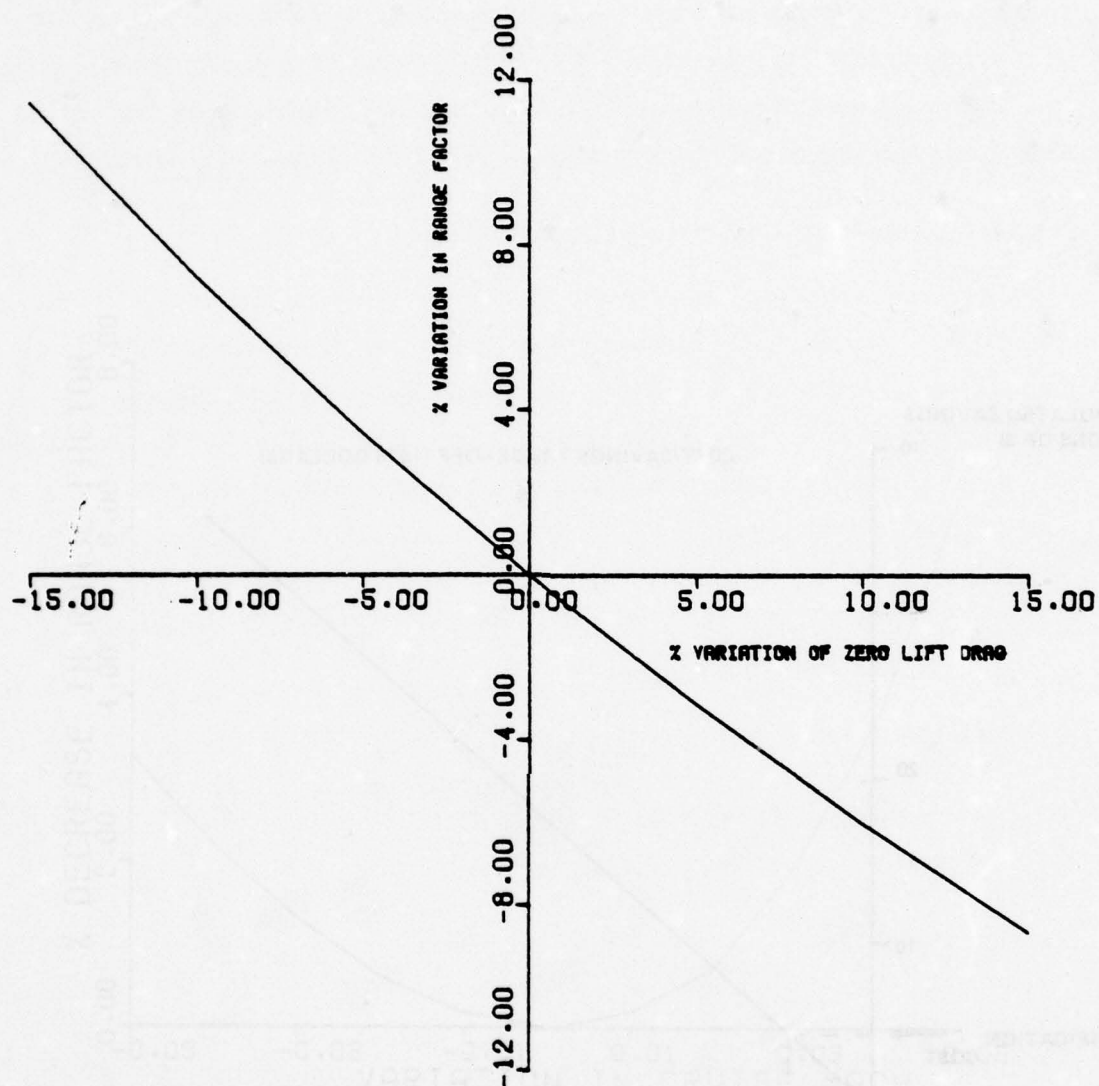


Figure 7.4-10 Sensitivity of Range Factor to Variations in Zero-Lift Drag - B-52G

Sensitivity to Induced Drag

Impact of changes in induced drag on fuel consumption for a B-52G mission can be assessed by using Figure 7.4-11 and Eq. (6.1). This figure depicts the sensitivity of RF to variations in induced drag. Observe that the sensitivity of RF to changes in induced drag is almost one half of the sensitivity to zero lift drag.

Sensitivity to Fuel Flow Rate

An increase in TSFC results in a decrease in range factor since RF is inversely proportional to fuel flow rate. Equation (6.1) may be used to determine the changes in fuel consumed for a given mission. Note that this equation is based on the assumption that TOGW remains the same as for the nominal case. Increased fuel consumption may also be computed under the assumption that the landing weight remains the same. Equation (6.2) provides the fuel consumption in this case.

Sensitivity to System Weight

Equation (6.3) may be used to estimate the change in fuel consumption due to a change in aircraft weight. For example a 5% increase in OEW results in approximately a 5% increase in fuel consumption.

Sensitivity to Variations in NRT

Figure 7.4-12 illustrates the impact of changes in NRT on the cruise altitude ceiling for a B-52G aircraft weighing 441,000 pounds. The optimum cruise altitude for this aircraft is 32,000 feet. Note that a 15% decrease in NRT does not affect the cruise altitude. Thus for most of the B-52G missions up to a 15% variation in NRT does not have any impact on the cruise solution.

Variations in NRT do have an impact on the range traversed and time spent during climb. However, the impact of variations in NRT on the total fuel consumed during a mission will be negligible.

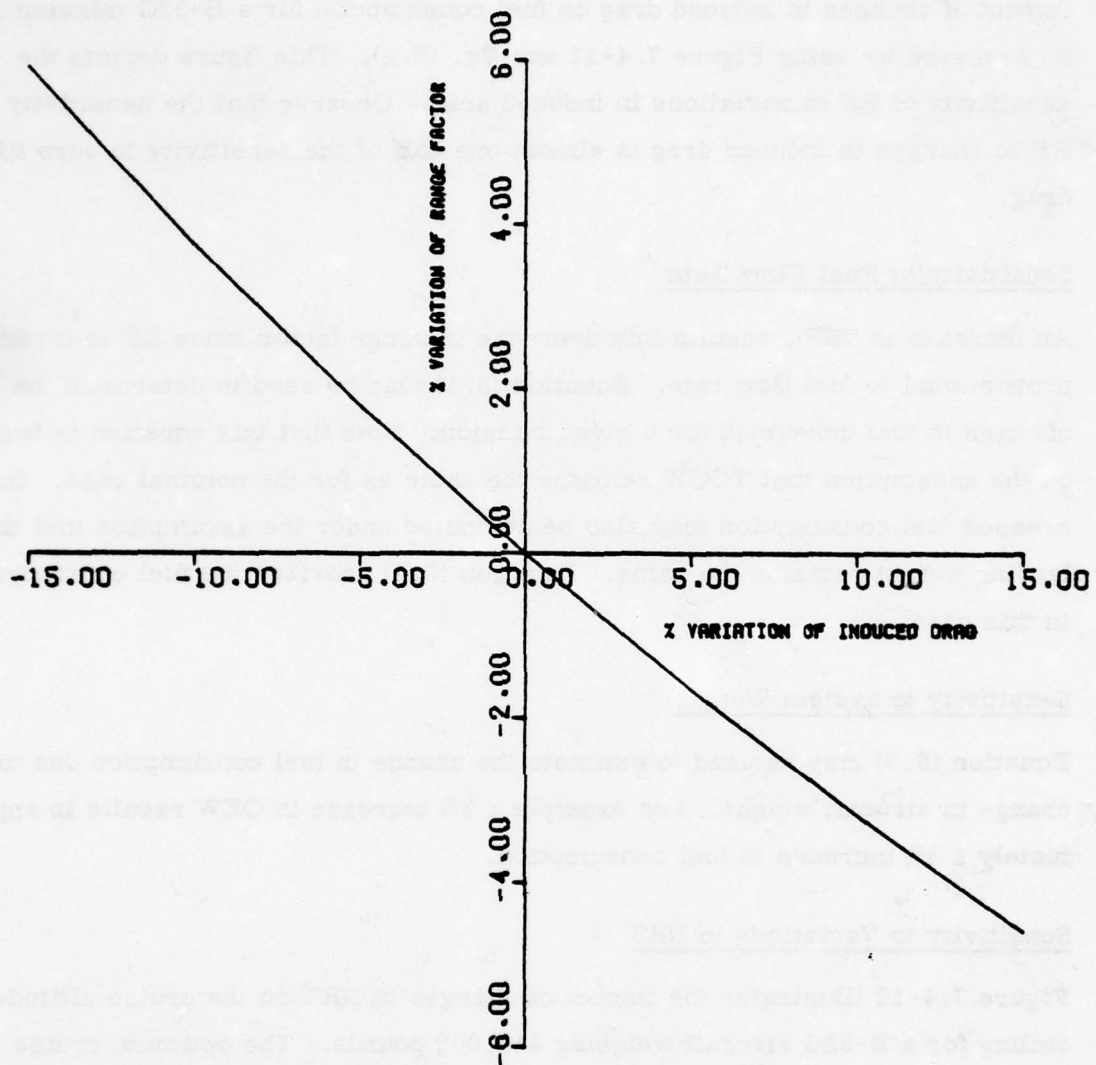


Figure 7.4-11 Sensitivity of Range Factor to Variations
in Induced Drag - B-52G

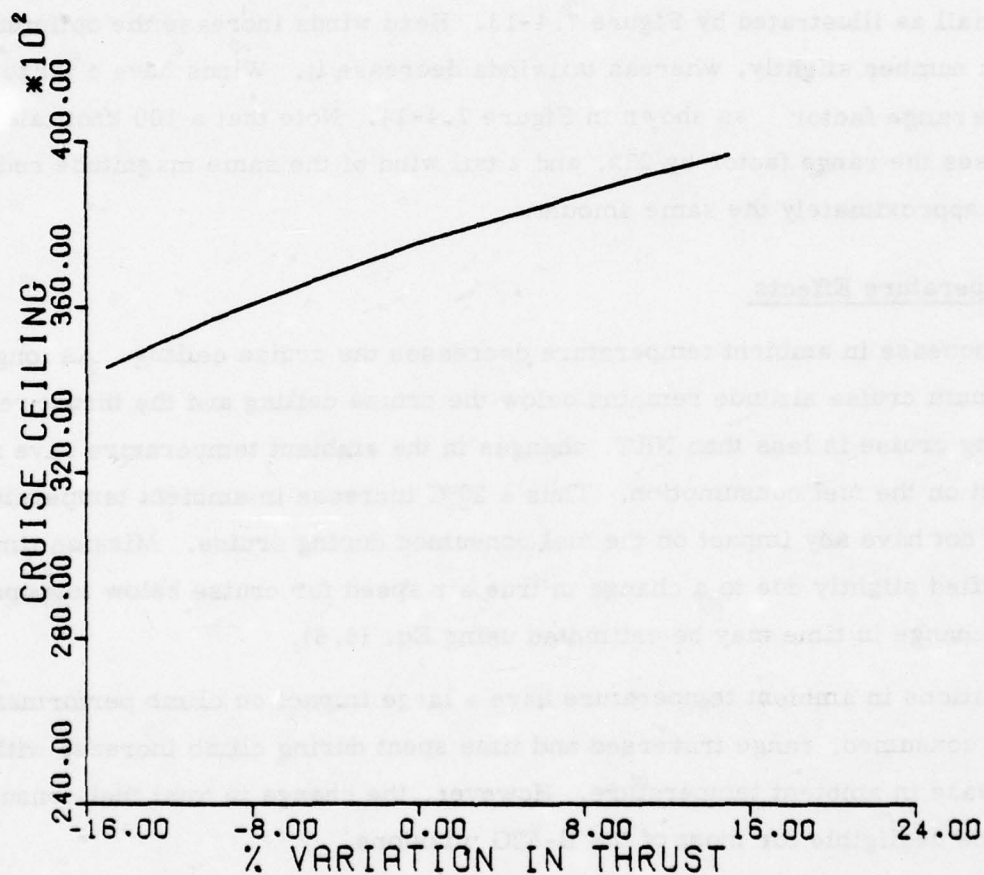


Figure 7.4-12 IMPACT OF VARIATIONS IN NRT ON
CRUISE CEILING FOR B-52G

7.4.7.2 Sensitivity to Atmospheric Variations

Variations in wind velocity and ambient temperatures have an impact on the fuel consumed during a mission.

Wind Effects

Winds have a large impact on the fuel consumed during a mission. Head winds increase the fuel consumption and mission time, while tail winds reduce them. However, the change in the min fuel optimum cruise Mach number due to winds is small as illustrated by Figure 7.4-13. Head winds increase the optimum cruise Mach number slightly, whereas tailwinds decrease it. Winds have a large impact on the range factor as shown in Figure 7.4-14. Note that a 100 knot tail wind increases the range factor by 23%, and a tail wind of the same magnitude reduces it by approximately the same amount.

Temperature Effects

An increase in ambient temperature decreases the cruise ceiling. As long as the optimum cruise altitude remains below the cruise ceiling and the thrust required during cruise is less than NRT, changes in the ambient temperature have no effect on the fuel consumption. Thus a 20°C increase in ambient temperature does not have any impact on the fuel consumed during cruise. Mission time is modified slightly due to a change in true air speed for cruise below torpopause. The change in time may be estimated using Eq. (6.6).

Variations in ambient temperature have a large impact on climb performance. Fuel consumed, range traversed and time spent during climb increase with an increase in ambient temperature. However, the change in total fuel consumed will be negligible for most of the B-52G missions.

7.4.7.3 Sensitivity to Traffic Density

Average fuel flow rate during ground operations for B-52G aircraft with all eight engines running is 210 lbs/minute. Since the increase in air traffic near an airport results in take-off delays, increased fuel consumption due to these delays can be calculated if the delay time is known. Generally take-off delays can be

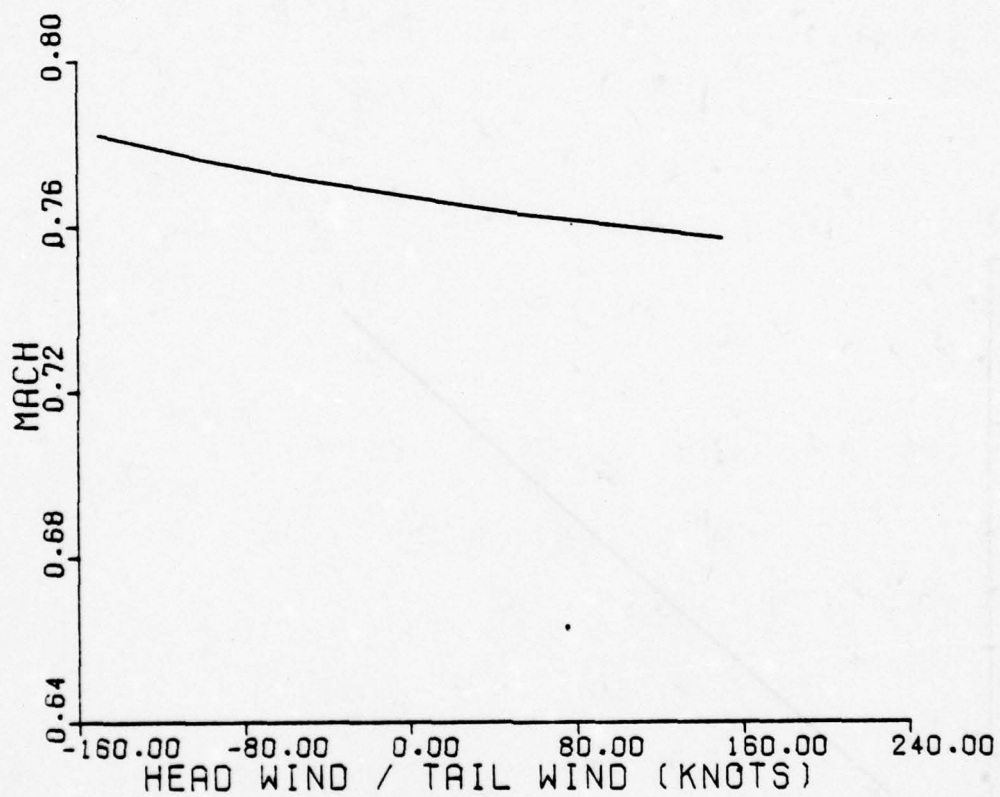


Figure 7.4-13 IMPACT OF WIND ON MIN FUEL OPTIMUM CRUISE
MACH NUMBER FOR B-52G

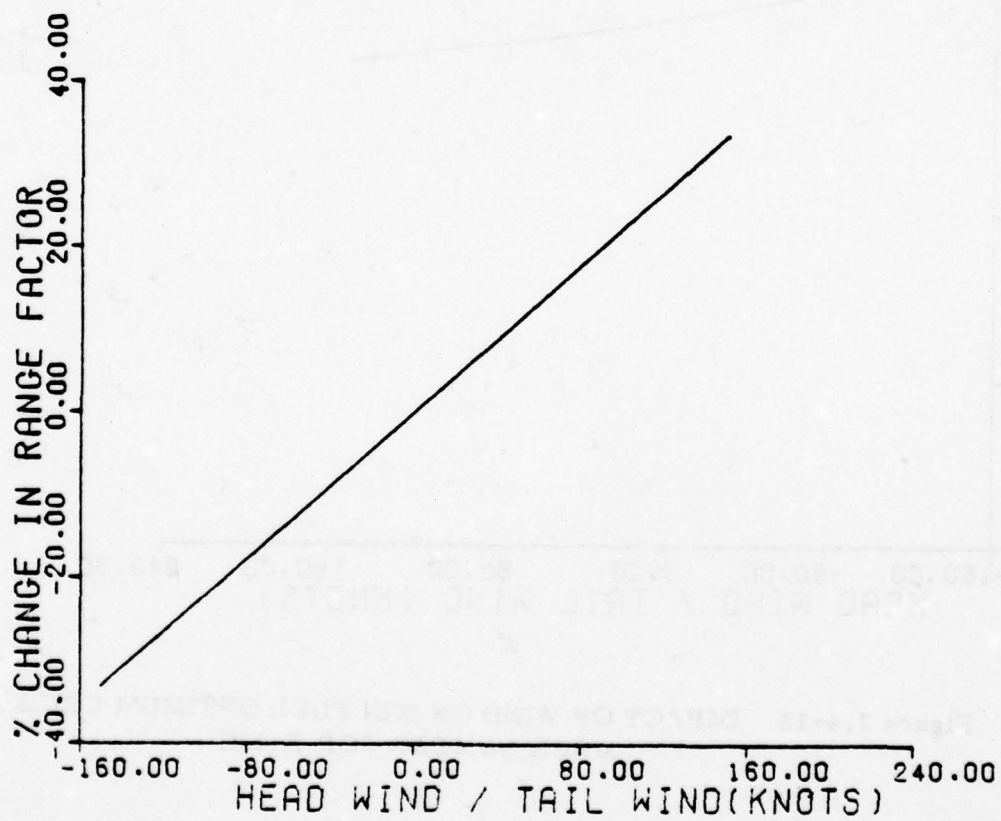


Figure 7.4-14 Impact of Wind on the Range Factor for B-52G

absorbed at the gate; however, increased air density also results in increased holding time for some aircraft. Based on an assumed average holding weight of 240,000 pounds, the fuel flow rate during holding at optimum holding altitude is 192 lbs/minute. Thus the sensitivity to traffic density can be determined by estimating the increased fuel consumed due to an increase in holding time.

7.4.7.4 Sensitivity to Instrument Errors

Figures 7.4-15 and 16 illustrate the sensitivity of range factor to variations in the optimum cruise mach number and optimum cruise altitude, respectively. Deviations in cruise mach number and altitudes from optimum values result in a decrease in range factor (or equivalently, specific range). Since instrument errors may result in flying off optimum cruise conditions, the sensitivity of fuel consumption to instrument errors can be estimated using Figures 7.4-15 and -16 and Eq. (6.1).

7.4.8 Conclusions for the B-52G

The two items listed below produced more than 1% savings in annual fuel:

- manual surge bleed valve override
- trajectory optimization procedures

The manual surge bleed valve override results in a 1.5% annual fuel savings, and the associated modification cost can be recovered within 2.5 years.

Trajectory optimization encompasses flying at optimum cruise conditions and keeping the aircraft configuration clean during descent. The annual fuel savings due to trajectory optimization is estimated to be 2.1%.

The fuel savings due to each of the remaining procedures investigated is estimated to be less than 1%.

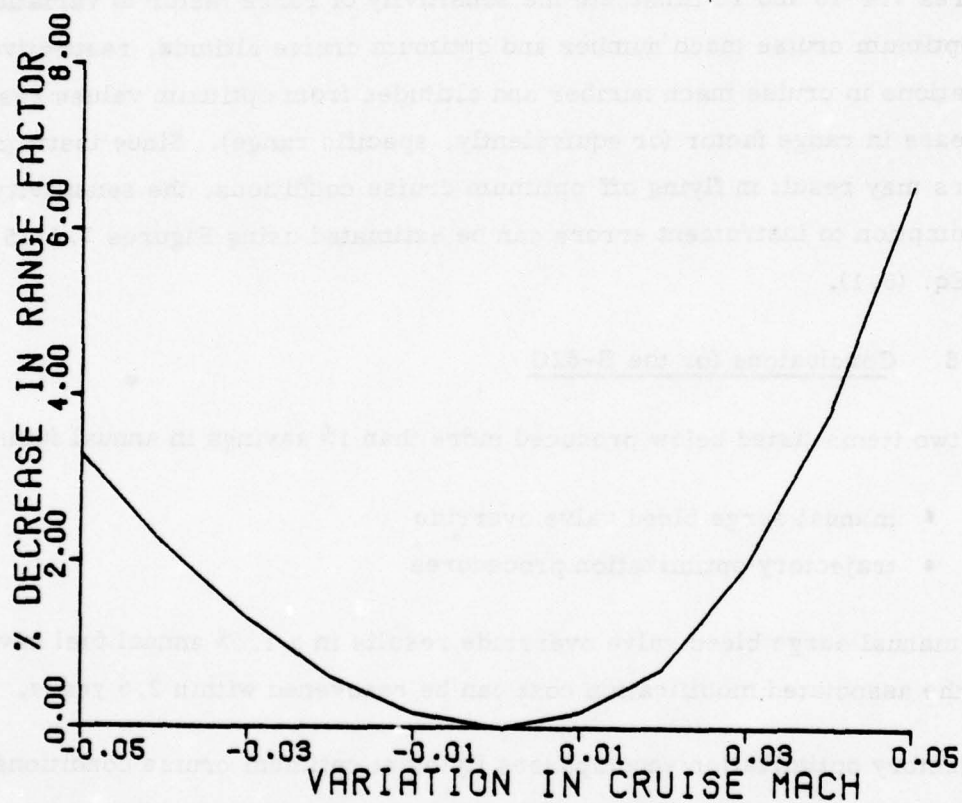


Figure 7.4-15 IMPACT OF FLYING OFF OPTIMUM
CRUISE MACH ON RANGE FACTOR-
B-52G

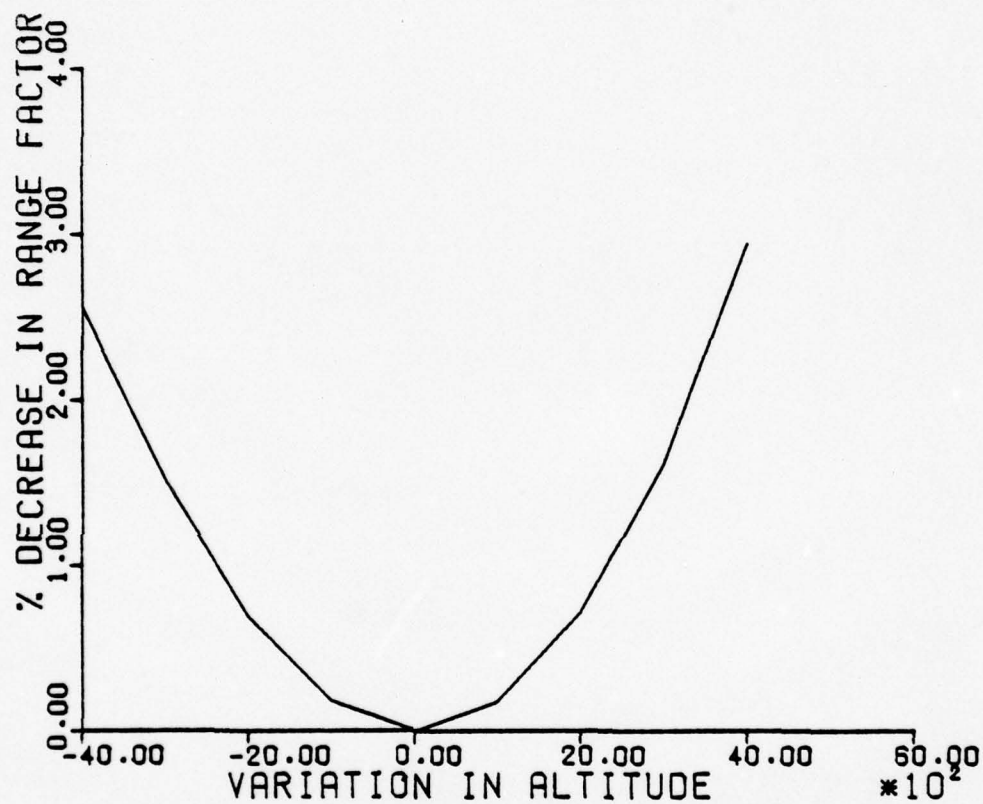


Figure 7.4-16 IMPACT OF FLYING OFF OPTIMUM CRUISE ALTITUDE ON RANGE FACTOR - B-52G

These conclusions are summarized in Table 7.4-6.

The potential fuel savings due to all the procedures investigated can be categorized as follows:

- | | |
|-----------------------------------|------------|
| • Design modifications | 1.5% |
| • Airborne operational procedures | 2.1 - 3.1% |
| • Ground operational procedures | 2.3 - 3% |

Procedures	Estimated Percentage Annual Fuel Savings	Break Even Period Years	Confidence In Estimates
Design Modifications			
Manual surge bleed valve override	1.5	2.5	Medium
Airborne Operational Procedure			
Trajectory optimization procedures	2.1	-	High
All others	0 - 1	-	Medium
Ground Operational Procedures			
Engine maintenance	1-1.5	-	Medium
All others	.8 - 1.5	-	Medium
Total	5.4 - 7.6		

Table 7.4-6 ESTIMATED FUEL SAVINGS FOR THE B-52G

7.5 B-52H AIRCRAFT

The B-52H, the final version of the B-52 bomber, is powered by Pratt and Whitney TF33-P-3 turbofan engines and has improved defensive armament, including a Vulcan multibarrel tail gun and underwing pods of penetration rockets. 102 of these planes were built with deliveries starting in May 1961. Like B-52G's, the "H's" are also being modified to incorporate the SRAM missile capability. In addition, nearly all of the B-52G and H models have been equipped with AN/ASO-151 Electro-optical Viewing System (EVS), using forward-look infrared (FLIR) and low-light level TV sensors to improve low-level flight capability [48].

7.5.1 Design Mission

Table 7.5-1 summarizes the design mission data for B-52H aircraft [49]. The basic mission has a 10,000 pound bomb load, carries 298,299 pounds of fuel, and has a combat radius of 4,176 n.mi. Maximum take-off gross weight for the B-52H is 488,000 lbs, operational empty weight is 175,723 lbs, the maximum fuel carried is 47,700 gallons and maximum missile load carried is 44,130 pounds. Ferry range for the B-52H is 8,756 n.mi.

7.5.2 Mission Model

The B-52H flew 4,784 missions in FY76 for a total of 36,280 hours and consumed 123.17 million gallons of fuel. The average mission profiles for the B-52H are similar to the B-52G mission profiles illustrated in Figures 7.4-1, 2 and 3; only the fuel consumption data will be different. Therefore the average profiles are not repeated in this section. The ASIMIS tape data was also processed for the B-52H, but again the tapes had incomplete mission information similar to that for the B-52G. Thus the average mission profile parameters presented in Figures 7.4-1, 2 and 3 are used for the trajectory optimization study.

CONDITIONS	BASIC MISSION	DESIGN LOAD	MAX BOMB LOAD	MISSILE LOAD	FERRY RANGE
TAKE-OFF WEIGHT [†]	488,000	488,000	488,000	488,000	498,00
Fuel Load	298,299	290,599	272,899	244,724	310,024
Pay Load	10,000	17,700	35,400	44,130	None
Pay Load (Chaff, Flares)	720/168	720/168	720/168	720/168	None
COMBAT RANGE	-	-	-	-	8756
COMBAT RADIUS	4,176	4,061	3,780	2,810	-
Average Cruise Speed	453	453	453	453	453
Initial Cruising Altitude	31,950	31,950	31,950	31,900	32,200
Target Altitude	45,900	45,300	44,900	43,200	-
Target Speed	470	470	470	487	-
Final Cruising Altitude	50,000	50,100	50,200	49,300	50,000
Total Mission Time	17.86	17.36	16.1	12.7	19.36
LANDING WEIGHT	199,143	198,758	197,873	206,959	199,729

OEW = 175,723.

Table 7.5-1 B-52H TYPICAL MISSION DATA

7.5.3 DOC Model

The flight crew salary and maintenance cost data for the B-52 aircraft was not available separately for the B-52G and H models. Therefore, the direct operating cost models used in this study for the B-52H are the same as for the B-52G and are obtained as follows.

<u>Model Type</u>	<u>Fuel Cost/Gal. - \$</u>	<u>Time Cost/FH - \$</u>
DOC	.42	590
DOC1	.42	1,174
DOC2	.42	1,758
DOC3	.42	2,342

From these cost models and the aircraft utilization data given in Section 7.5.2, the annual fuel and direct operating costs for the B-52H during FY76 were as follows:

Fuel Cost	\$51.73 Millions
DOC	73.13 Millions
DOC 1	94.32 Millions
DOC 2	115.51 Millions
DOC 3	136.70 Millions

7.5.4 B-52H Characteristics

Data required to develop mathematical models for aerodynamics and propulsion characteristics of the B-52H were obtained from References [50] and [53].

7.5.4.1 B-52H Aerodynamic Model

From the procedure of Section 3.2, the drag coefficient (C_D) is represented as a parabolic function of lift coefficient (C_L).

$$C_D = C_{D_0} - B C_L + K C_L^2$$

where coefficients C_{D_0} , B and K are represented by the following functions of Mach (M):

$$C_{D_0} = .0167 + .3 \cdot 10^{-5} (M^* - M)^{-4}$$

$$B = .0135 + .26 \cdot 10^{-5} (M^* - M)^{-5}$$

$$K = .0613 + .95 \cdot 10^{-6} (M^* - M)^{-6.17}$$

and

$$M^* = 1.0$$

The drag coefficient model degrades beyond .83 Mach.

7.5.4.2 B-52H Thrust Model

Normal rated thrust (NRT) for each engine has a functional form similar to B-52G aircraft. Thus NRT is expressed as a polynomial function of Mach (M) and normalized altitude (H_n) on a standard day.

$$\begin{aligned} \text{NRT} = 1000. [& 13.33 - 9.46H_n - 7.84M - .47H_n^2 + 4.86MH_n + .88M^2 \\ & + 2.06MH_n^2 + 6.44M^2H_n - 6.14M^2H_n^2] \end{aligned}$$

where

NRT = normal rated thrust, lbs/engine

H_n = altitude, (ft)/40000.

This NRT model is used for altitudes below the tropopause. In the stratosphere, NRT is obtained from the following equation:

$$NRT = 1000. [14.56 - 14.58H_n + .25M + .377H_n^2 - 5.46MH_n + 2.57M^2 + 3.5MH_n^2 + .22M^2H_n - 1.26M^2H_n^2]$$

Idle engine thrust (T_{idle}) is also represented by a polynomial function of Mach (M) and normalized altitude (H_n). This function is given by

$$T_{idle} = 1000. [.76 + .75H_n + .02M - .12H_n^2 - 4.91MH_n - 3.6M^2 + 3.16MH_n^2 + 9.1M^2H_n - 4.73M^2H_n^2]$$

where

T_{idle} = idle thrust, lbs/engine

7.5.4.3 B-52H Fuel Flow Model

Normalized fuel flow rate, f_n , is represented by the following function of normalized thrust (T_n) and Mach (M).

$$f_n = 1000. [.3 + 7.73T_n + 3.26M + 3.47T_n^2 + 6.81MT_n - 2.04M^2]$$

where

$T_n = T/\delta/20000$

T = thrust, lbs/engine

δ = pressure ratio

Since the fuel flow rate increases with altitude in the stratosphere, a correction factor is used for altitudes in the stratosphere. The fuel flow rate is increased by 0.4 percent for each 1000 ft altitude increment above the tropopause.

The normalized idle fuel flow model for the B-52H is given by

$$f_{idle} = 1000. [.896 + 2.23T_n + .75M + 21.68T_n^2 + 7.75MT_n + .81M^2]$$

This model is applicable up to 25000 ft altitude. Idle fuel flow rate is 650 lbs/hr/engine above 25000 ft altitude.

7.5.5 Evaluation of Airborne and Ground Operation Procedures

The results of an analysis of fuel conserving operational procedures for the B-52H aircraft are presented in this section. Most of the results are similar to the results for the B-52G presented in Section 7.4.

7.5.5.1 Reduced Power Take-off

Direct fuel savings due to reduced power take-off are negligible. However, reduced power take-off procedures result in reduced engine deterioration. Thus there will be an indirect fuel savings due to better engine efficiency.

7.5.5.2 Optimal Climb, Cruise and Descent Procedures

Optimal procedures for each segment are first examined separately. Then the results for integrated optimal trajectories are presented.

Optimal Cruise Climb Solution

Figure 7.5-1 shows the fuel/time trade-off curve for the B-52H. This curve was generated for a 400,000 pound aircraft. Optimum cruise solutions corresponding to various cost models are indicated on this curve. The optimum cruise mach numbers corresponding to DOC, DOC 1, DOC 2 and DOC 3 are .785, .795, .805 and .81, respectively. The optimum minimum fuel cruise solution parameters are given below:

- Cruise mach number = .767
- W/δ = 1.82×10^6
- Range Factor = 10394

The energy gain during cruise climb reduces this range factor by 0.7%.

Optimum Step Climb Solution

As mentioned in Section 7.4.5, the B-52s are permitted to fly a cruise climb path. However, like B-52G the increase in fuel consumption due to an optimum 4,000 step climb procedure is less than 0.2%. Therefore from a safety consideration, an optimum step climb procedure may be preferable to a cruise climb.

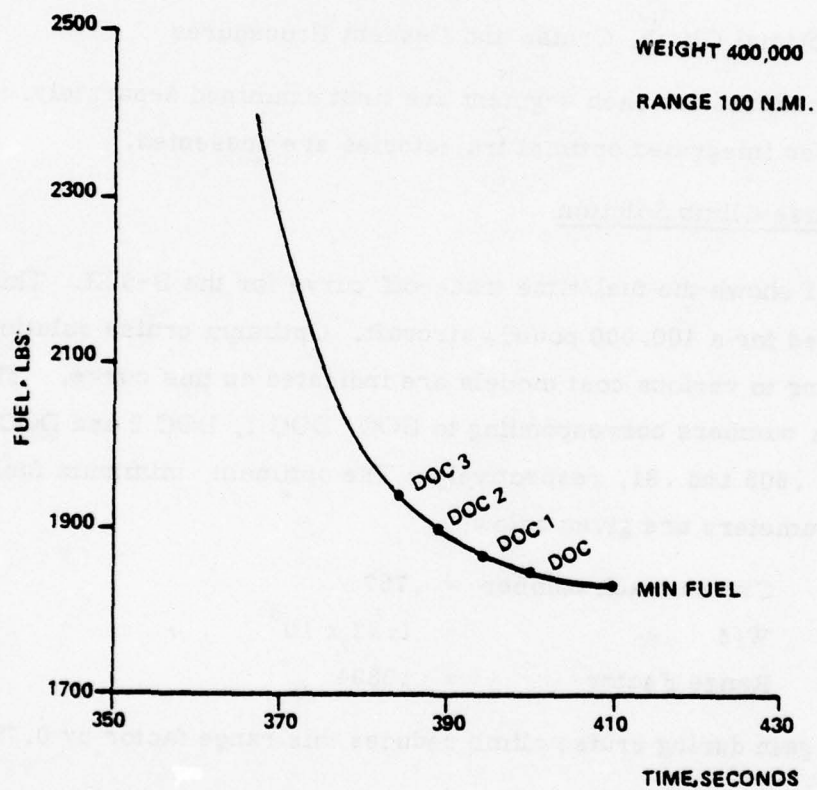


Fig. 7.5-1

FUEL/TIME TRADE-OFF FOR THE B-52H
CRUISE SOLUTION

Conventional Climb Procedure

The conventional climb procedure for the B-52H is the same as for the B-52G given in Section 7.4.5 [14].

Optimum Climb Procedure

Optimum climb air speed and throttle settings are obtained from the optimum climb algorithm. This optimal climb and the parametric optimal climb discussed next are both optimized with respect to minimum fuel.

Parametric Optimum Climb Procedure

The parametric optimum climb is similar to conventional climb; however, instead of climbing at 280 KIAS at low altitudes, a best climb speed is determined by parametric optimization. This optimum speed varies with aircraft weight.

Comparison of Various Climb Procedures

Table 7.5-2 presents the results of a comparison of EEM optimum, parametric optimum and conventional climb procedures for the B-52H aircraft. The optimal climb trajectory traverses a 164 n. mi. distance. Both the conventional and the parametric optimum climbs are followed by a short cruise segment such that the total range for all three trajectories is the same. The optimum trajectory consumes 90 lbs less fuel than the conventional trajectory and takes 56 seconds less mission time. The parametric optimum trajectory consumes only 24 lbs more fuel and takes 14 seconds more time than the EEM optimum.

The annual fuel savings of the parametric optimum climb with respect to the conventional climb is estimated to be 23,000 gallons, which is only .02% of the annual fuel consumption. The slight increase in time and fuel used with the conventional 280 KIAS climb is not considered critical for most missions [14]. Moreover an increase in climb speed will increase noise and air pollution. Therefore a start climb speed of 280 knots is used for all missions unless otherwise required for special mission operations.

Initial Conditions
Weight 415,000 lbs.
Altitude 3,000 ft.
Airspeed 250 KCAS

Final Conditions
Range 164 NM
Altitude 36,500 ft.
Airspeed .767 M

Type of Climb	Optimum [†]	Parametric Optimum [†] 300KCAS/.767M	Conventional 280KCAS/.767M
Climb	164	103	100
Cruise	0	61	64
Total	164	164	164
Climb	12765	10410	10358
Cruise	0	2379	2597
Total	12765	12789	12855
Climb	1396	914	926
Cruise	0	500	525
Total	1396	1414	1451
DOC	\$ 1053.6	1058.1	1068.4

† The trajectory was optimized for fuel.

Table 7.5-2 COMPARISON OF OPTIMUM VS. CONVENTIONAL CLIMB - B-52H

Conventional Descent Procedures

Conventional descent procedures are outlined in Reference [14]. These procedures are the same as for the B-52G aircraft described in Section 7.4.5.

Optimal Descent Procedures

The optimal descent algorithm of Appendix A provides the air speed and thrust settings for the optimal descent trajectory. Air speed varies with altitude during descent.

Comparison of the Descent Procedures

Table 7.5-3 summarizes the results of a comparison of conventional (normal) descent, optimal descent and conventional descent in clean aircraft configuration. Initial and final conditions are given in the table. Note that the optimal trajectory consumes 760 pounds less fuel than normal descent. Although the optimal trajectory takes 20 seconds less time, this gain in time is partially due to high air speeds at low altitudes, which is not an acceptable practice.

Conventional descent in clean aircraft configuration consumes 713 lbs less fuel than normal descent and spends 270 seconds more time during the mission. If airspeed is reduced further, then fuel consumption decreases, but mission time increases excessively. Thus the conventional descent at a .75 mach/240 KIAS speed schedule with the aircraft in a clean configuration offers a good compromise between fuel and time in that it minimizes DOC. Table 7.5-4 gives estimates of fuel and direct operating cost savings achievable by keeping the aircraft clean during descent. Almost one million gallons of fuel can be saved annually for the B-52H operations.

Integrated Optimal Trajectories

The basic mission profiles for B-52 are shown in Section 7.4.2. As mentioned in the case of B-52G, no altitude change is considered for the normal mission profile before the aerial refueling has been accomplished. After refueling the aircraft can climb to a 36,000 foot altitude and cruise at that altitude before descending for the low level segment. No change in the low level segment is

Initial Condition
 Weight = 256,000 lbs.
 Altitude = 33,000 ft.
 Airspeed = .75 Mach

Final Conditions
 Range 112 NM
 Altitude 3,000 ft.

Type of Descent	Conventional with Air-brakes and Gear Down	Conventional in Clean Configuration	Optimal in Clean Configuration
Cruise	80	0	38
Descent	32	112	74
Total	112	112	112
Cruise	2443	0	1142
Descent	724	2454	1265
Total	3167	2454	2407
Cruise	658	0	311
Descent	374	1302	701
Total	1032	1302	1012
DOC	373.8	371.9	321.4

Table 7.5-3 COMPARISON OF OPTIMAL VS. CONVENTIONAL DESCENT - B-52H

Cost	Annual Savings Due to Clean A/C Configuration During Descent	% Savings
Fuel	gallon	
Fuel Cost	\$ 978,600	0.8
DOC	\$ 411,000	0.8
DOC 1	\$ 32,000	0.04
DOC 2	\$ 343,000 (loss)	.36 (loss)
DOC 3	\$ 718,000 (loss)	.62 (loss)
	\$ 1,093,000 (loss)	.8 (loss)

Table 7.5-4 Annual Fuel/DOC Savings Due to Clean Aircraft
Configuration During Descent - B-52H

considered. However, after completing the low level segment, the aircraft may climb to a 42,000 foot altitude and cruise there before initiating the final descent. Under these conditions the B-52H can save almost 650 gallons of fuel per mission. However mission time will increase by 187 seconds. Annual fuel and DOC savings will be 2.36 million gallons and \$880,000, respectively. For the training mission no change in cruise altitude was considered before completion of air refueling segment. After refueling the aircraft climbs to a 40,000 foot altitude which is close to the optimum altitude. The fuel savings attained by flying at the somewhat higher optimum altitudes are negligible.

Pilot proficiency missions involve mostly multiple take-offs and landings. These missions account for only 4% of the total flight hours. Trajectory optimization does not appear feasible in this case.

Since most of the mission segments for B-52H are constrained by mission requirements, trajectory optimization procedures do not offer significant fuel savings.

7.5.5.3 Delayed Flap Approach Procedure

Fuel/DOC savings due to the delayed flap approach procedure for B-52H are summarized in Table 7.5-5. Maximum annual savings due to this procedure will be 283,000 gallons, which is approximately 0.2% of the annual fuel consumption for the B-52H fleet.

7.5.5.4 Aft C.G. Operations

The possibility of influencing the C.G. through fuel and payload (bombs and missiles) is limited for bombers. During flight, some fuel savings may be attained by burning fuel evenly towards the aft C.G. A 5%-MAC shift in the C.G. towards aft saves 0.7% fuel annually for the B-52H.

7.5.5.5 Reduce Reserve Fuel

As mentioned before, the B-52 ASIMIS tapes have no information on landing fuel. Therefore, no specific fuel/DOC savings can be estimated. However, the

Altitude for Stable Landing Speed	ANNUAL SAVINGS					
	Fuel/Gal.	Fuel Cost	DOC	DOC1	DOC2	DOC3
1000	79,500	33,400	51,600	69,600	87,600	105,600
500	159,300	66,900	103,300	139,300	175,300	211,300
0	238,100	100,000	154,300	208,000	261,800	315,500

Table 7.5-5 ANNUAL FUEL/DOC SAVINGS DUE TO DELAYED FLAP APPROACH - B-52H

sensitivity of fuel savings due to reduced reserve fuel was determined for a 5,000 pound average reduction in fuel carried per mission. The resulting fuel savings is estimated at 510,000 gallons.

7.5.5.6 Reduce Engine Load

For B-52H the fuel flow rate increases by 6.2% at high altitudes and 7.8% at low altitudes due to engine and nacelle anti-icing [14]. Thus the fuel penalty for anti-icing is higher for the B-52H than for the B-52G model. Like the other aircraft under study, a fuel savings potential exists for reduced engine loads. However, no savings factor is computed due to large expected variations in conditions from one mission to another with no data available to quantify these variations.

7.5.5.7 Reduce Engine Use and Taxi Time

Average fuel flow rate during ground operations with all eight engines operating is 200 lbs/minute. Thus procedures which reduce time taken during ground operations result in fuel savings. Every minute of reduced taxi time/mission can save 147,000 gallons of fuel and \$62,000 in DOC annually for B-52H operations.

7.5.5.8 Partial Engine Taxi

Shutting down four engines during taxi-in and parking can save 368,000 gallons of fuel annually for an average taxi time of five minutes per mission.

7.5.5.9 Removing Excess Equipment

As mentioned in Section 7.4, no excess equipment has been identified on the B-52's. However, Figure 7.5-5 which illustrates sensitivity of fuel/DOC to variations in system weight may be used to estimate fuel savings due to removal of excess equipment.

7.5.5.10 Maintenance to Reduce Drag

A direct quantification of savings due to aircraft maintenance is not possible. Plots showing sensitivity of fuel/DOC to variations in aircraft drag, which are given in Section 7.5.6, may be used to estimate fuel savings due to maintenance which results in reduced aerodynamic drag.

7.5.5.11 Engine Maintenance

Figure 7.5-4 illustrates the sensitivity of fuel/DOC to changes in thrust specific fuel consumption for B-52H. This figure may be used to estimate fuel savings due to maintenance procedures which result in increased engine efficiency. Assuming a 1.5% improvement in TFSC, the annual fuel savings are estimated to be 1.7 million gallons.

7.5.6 Evaluation of Design Modifications

No potential fuel saving aerodynamic design modifications are under consideration at present for the B-52H. Winglets may offer fuel savings; however, a detailed analysis is required because currently B-52H are powered by TF-33 turbofan engines, and some potential fuel saving modifications are possible for these engines. This section presents the general approach for evaluating future design modifications for the B-52H and discusses the fuel savings potential of engine modifications.

7.5.6.1 Parametric Analysis of Aerodynamic and Propulsion Design Modifications

A general approach of evaluating aerodynamic and propulsion design modifications is outlined in Section 5. These design modifications may be characterized by the resulting aerodynamic and propulsion changes and the change in TOGW of the aircraft. Thus generic plots illustrating the sensitivity of annual fuel/DOC to variations in aerodynamic and propulsion characteristics and TOGW of the B-52H are developed. Figures 7.5-2, 3, 4 and 5 represent the sensitivity of fuel/DOC to changes in zero lift drag, induced drag, thrust specific fuel consumption and TOGW of B-52H aircraft. Thus knowing the amount of aerodynamic, propulsion or

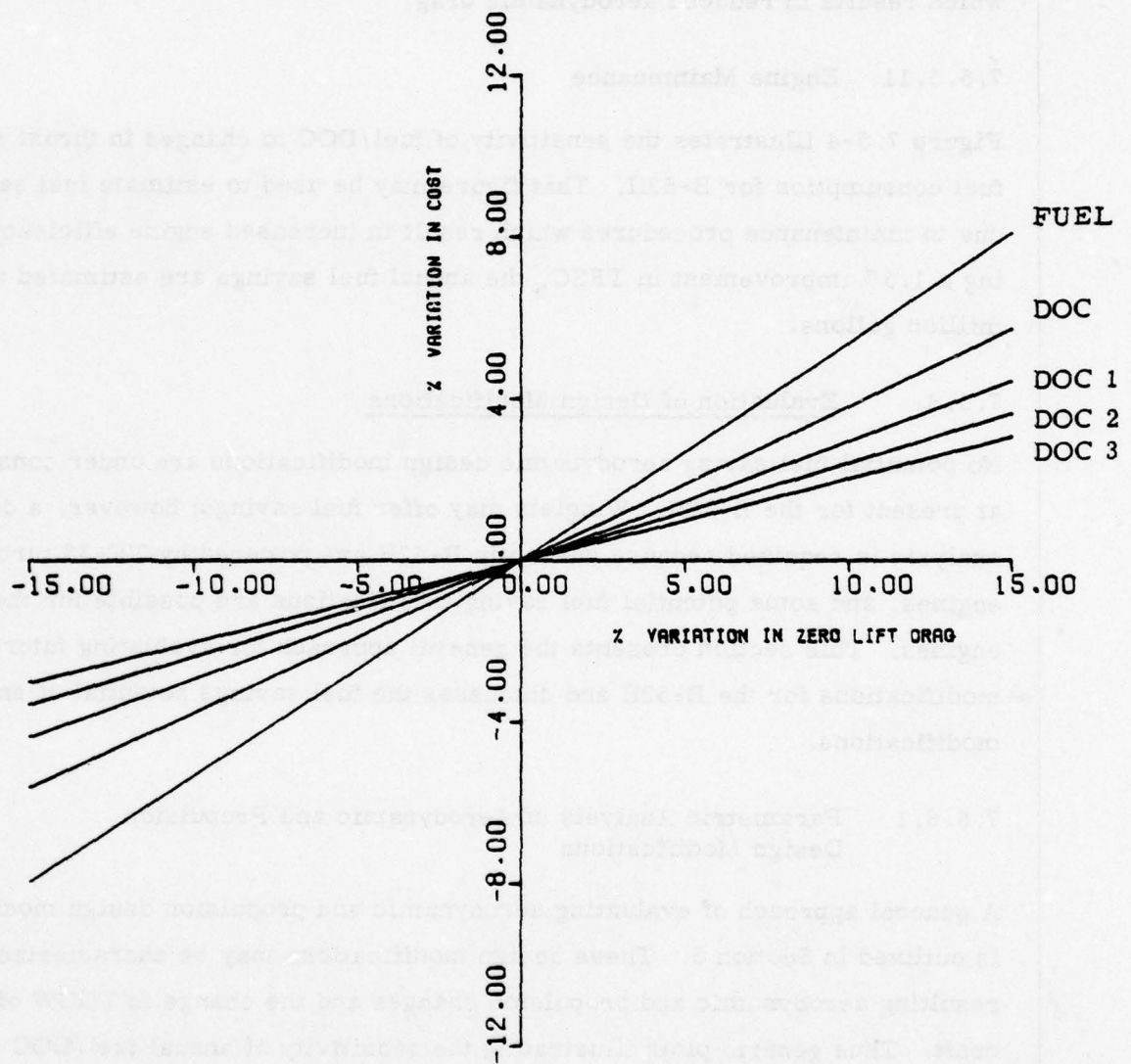


Figure 7.5-2 Sensitivity of Fuel/DOC to Variations in Zero-Lift Drag - B-52H

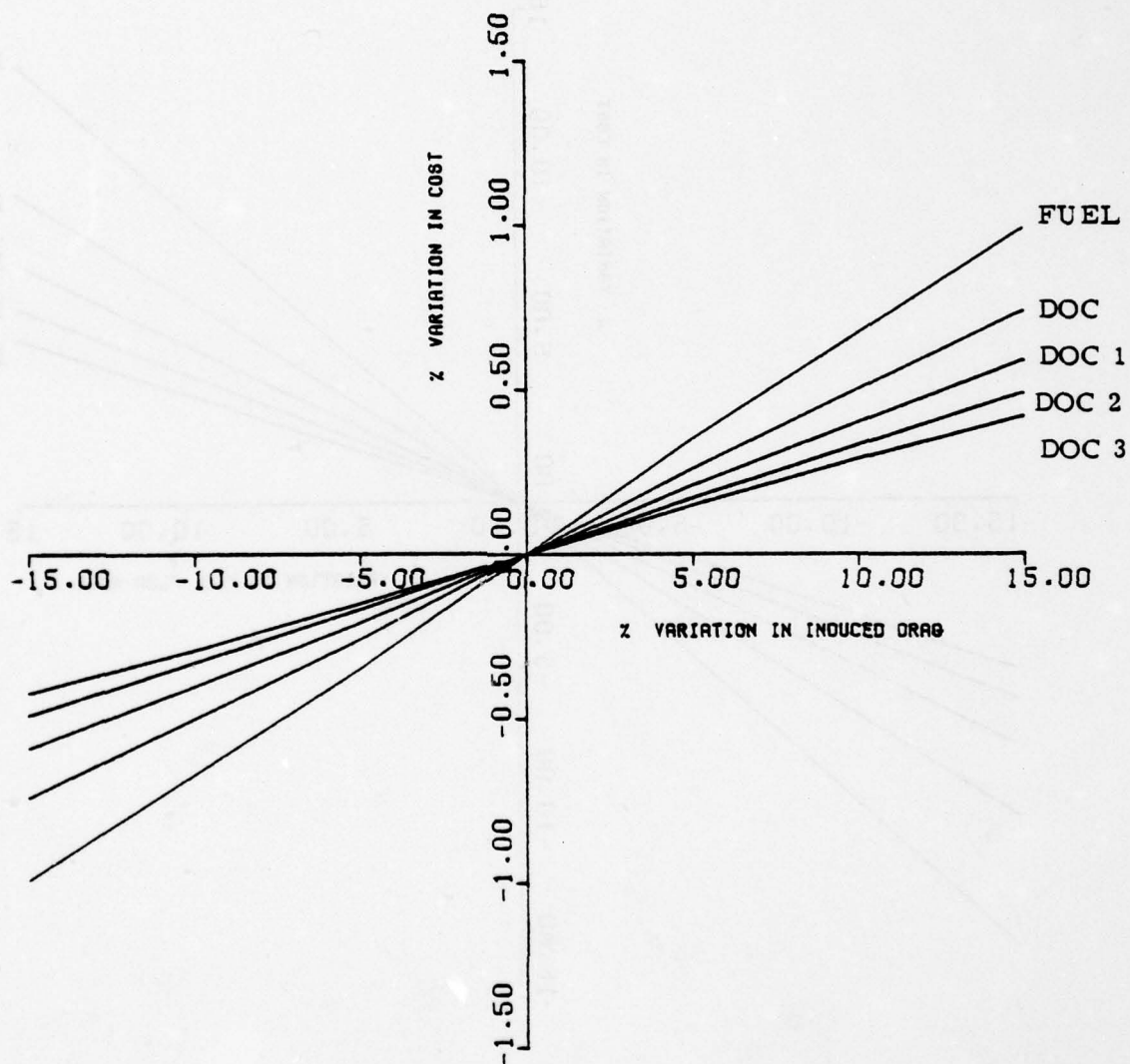


Figure 7.5-3 Sensitivity of Fuel/DOC to Variations in Induced Drag - B-52H

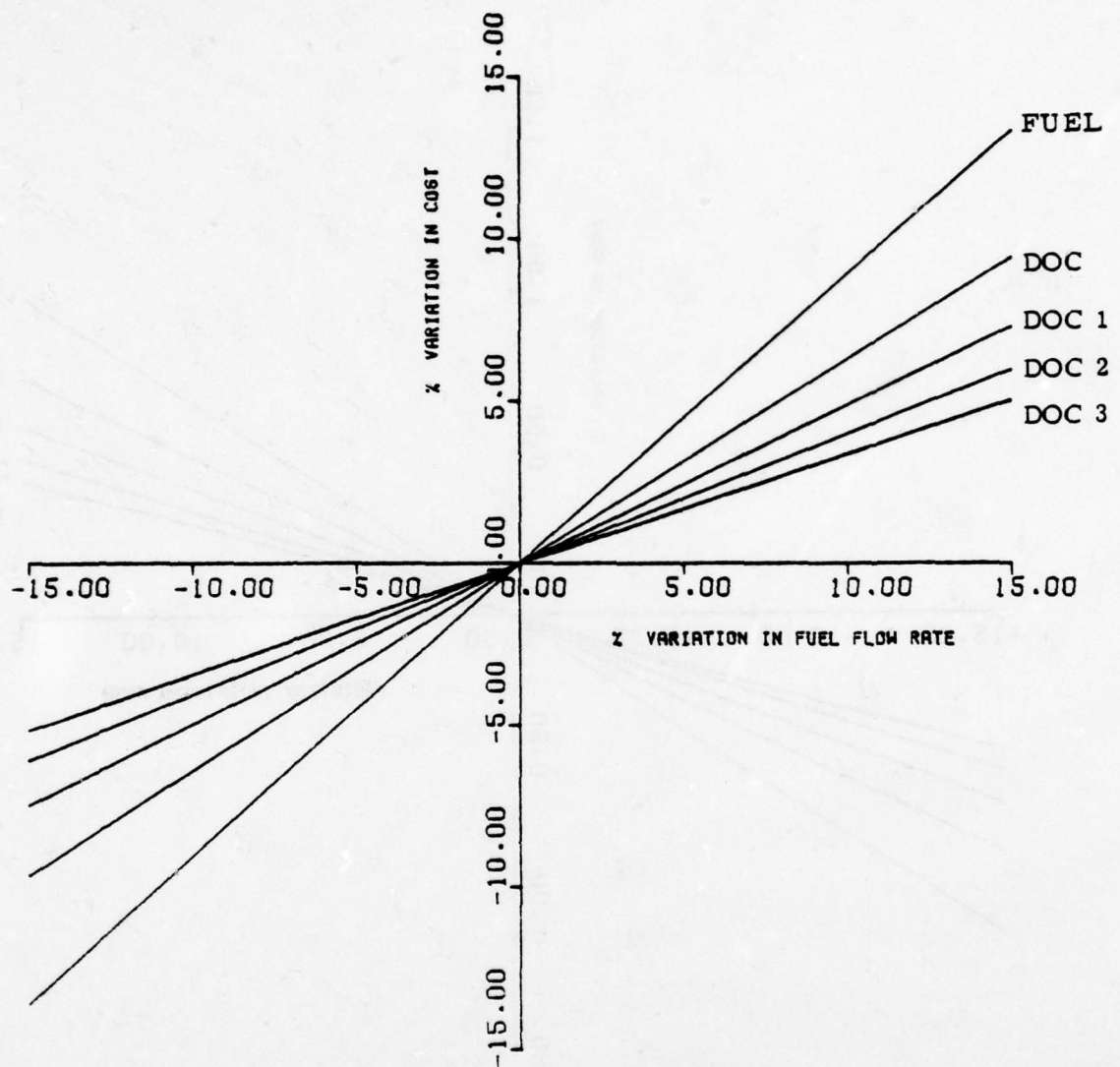


Figure 7.5-4 Sensitivity of Fuel/DOC to Variations in Thrust Specific Fuel Consumption - B-52H

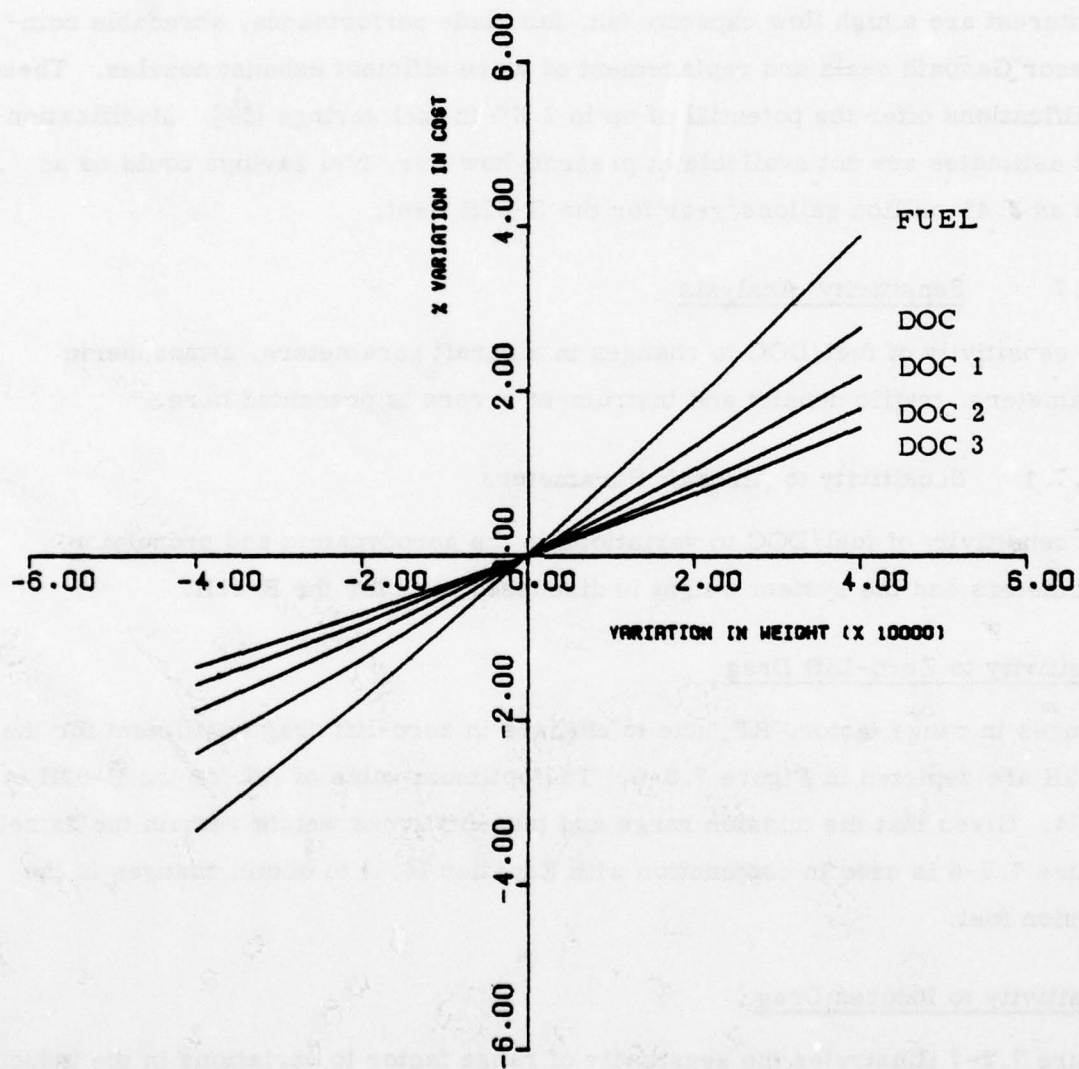


Figure 7.5-5 Sensitivity of Fuel/DOC to Variations in Weight - B-52H

weight change in aircraft due to a design modification, these generic plots can be used to calculate the resulting changes in fuel and DOC.

7.5.6.2 Turbo-Fan Engine Modifications

Several potential retrofit modifications are possible for reducing specific fuel consumption of turbo-fan engines. For the JT3D (TF-33) class engines, areas of interest are a high flow capacity fan, fan blade performance, abradable compressor Gaspath seals and replacement of more efficient exhaust nozzles. These modifications offer the potential of up to 2.8% in fuel savings [54]. Modification cost estimates are not available at present; however, fuel savings could be as high as 3.45 million gallons/year for the B-52H fleet.

7.5.7 Sensitivity Analysis

The sensitivity of fuel/DOC to changes in aircraft parameters, atmospheric parameters, traffic density and instrument errors is presented here.

7.5.7.1 Sensitivity to Aircraft Parameters

The sensitivity of fuel/DOC to variations in the aerodynamic and propulsion parameters and the system weight is discussed here for the B-52H.

Sensitivity to Zero-Lift Drag

Changes in range factor, RF, due to changes in zero-lift drag coefficient for the B-52H are depicted in Figure 7.5-6. The optimum value of RF for the B-52H is 10394. Given that the mission range and take-off gross weight remain the same, Figure 7.5-6 is used in conjunction with Equation (6.1) to obtain changes in the mission fuel.

Sensitivity to Induced Drag

Figure 7.5-7 illustrates the sensitivity of range factor to variations in the induced drag coefficient. Again Equation (6.1) may be used along with this figure to obtain changes in mission fuel. For example, if the induced drag coefficient of a particular B-52H aircraft is 2% less than the nominal value, Figure 7.5-7 indicates that

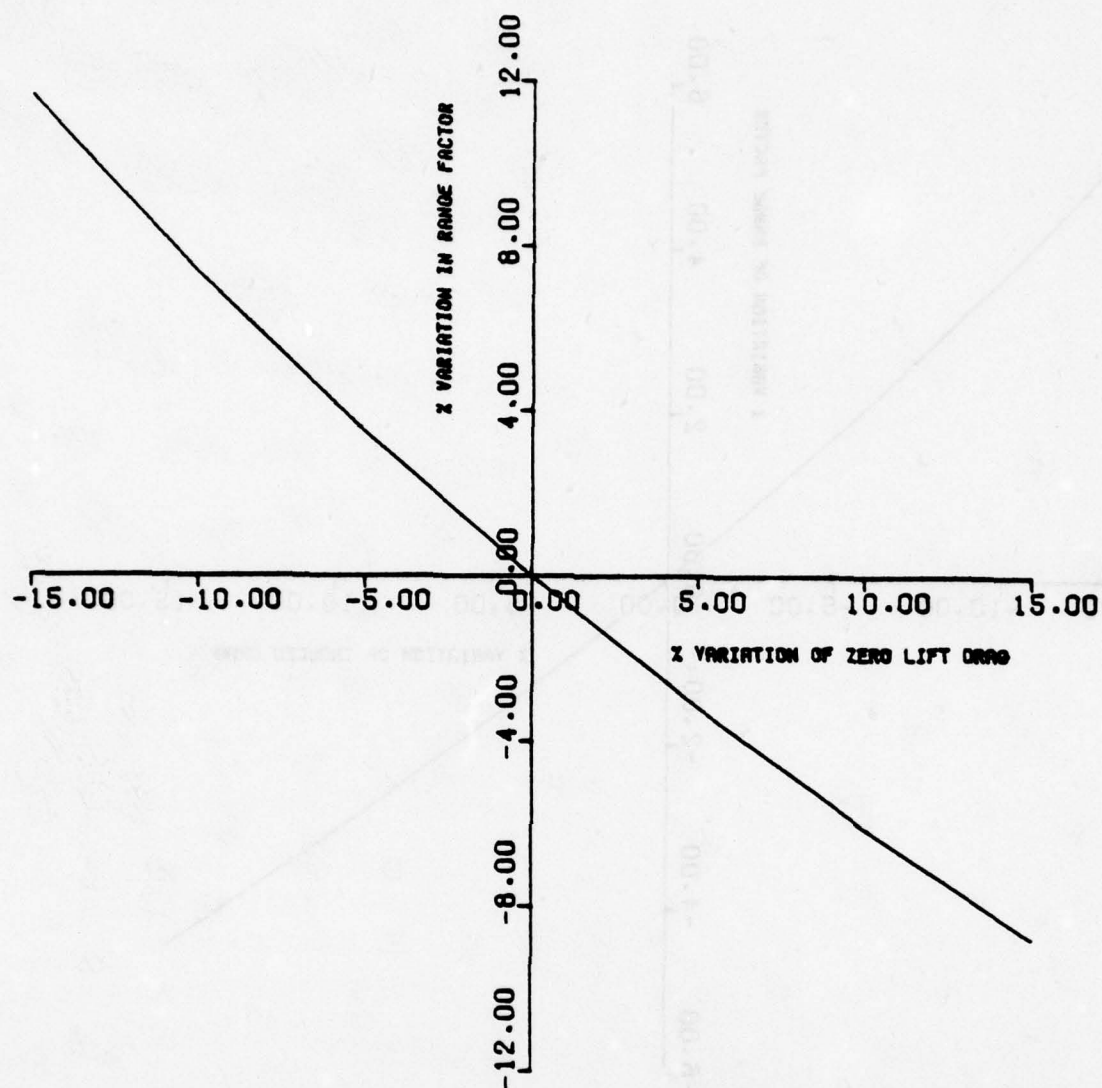


Figure 7.5-6 Sensitivity of Range Factor to Variations in Zero-Lift Drag Coefficient for B-52H

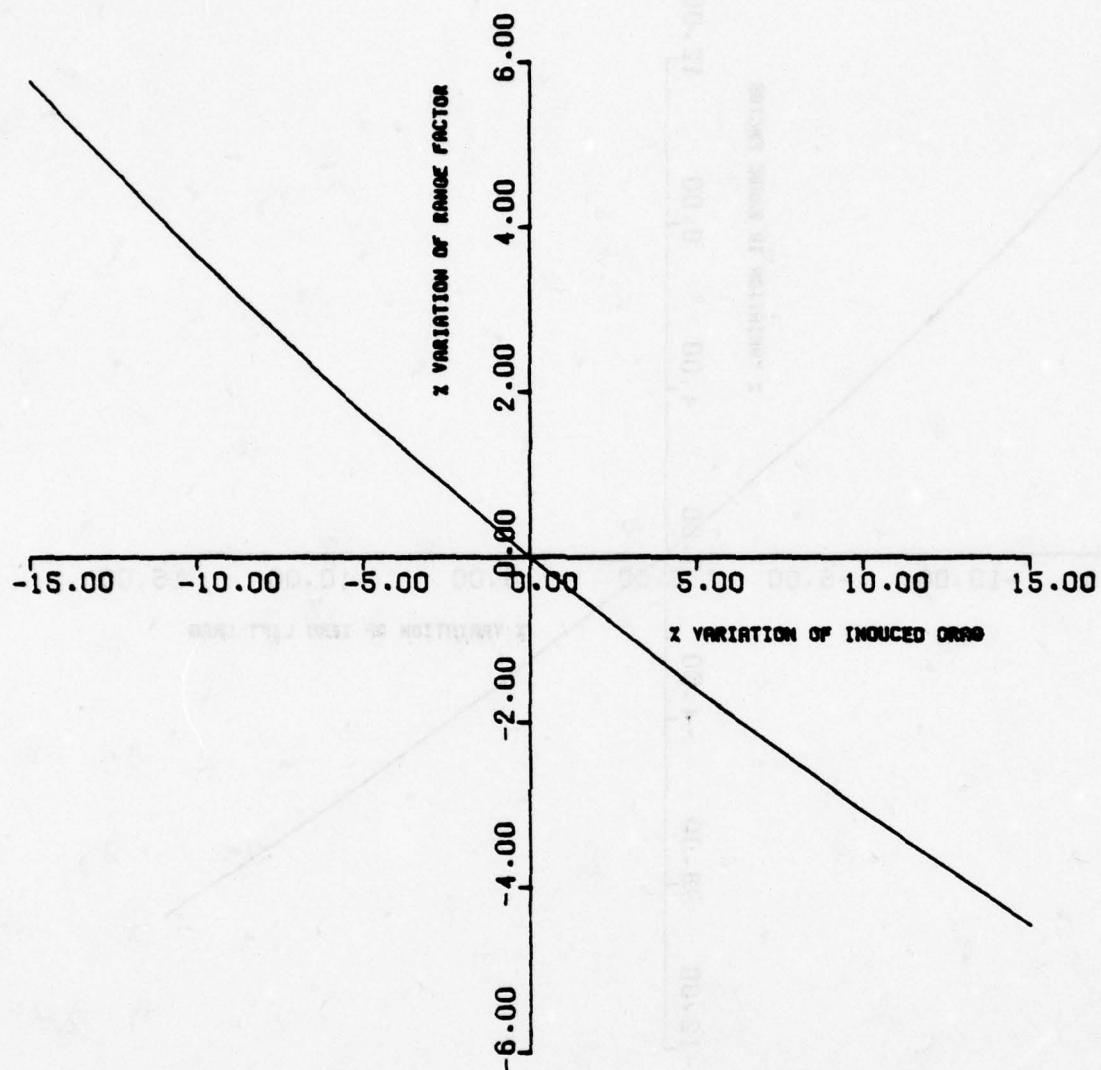


Figure 7.5-7 Sensitivity of Range Factor to Variations in Induced Drag Coefficient for B-52H

the optimum range factor will be 0.7% higher. The corresponding fuel savings for a 1,000 n.mi. mission will be 0.67%.

Sensitivity to Fuel Flow Rate

Since range factor is inversely proportional to fuel flow rate, an increase in TSFC results in a decrease in RF. Once a change in RF is determined, Eq. (6.1) may be used to estimate changes in mission fuel. Thus a 5% improvement in TSFC results in a 4.76% reduction in mission fuel.

Sensitivity to Variations in NRT

Changes in NRT impact the cruise ceiling as shown in Figure 7.5-8. This cruise ceiling was generated for a B-52H aircraft with a 470,000 pound weight, which is typical of B-52H missions. Cruise altitude for this aircraft is 33,000 feet. A 15% decrease in NRT has no effect on cruise altitude and hence fuel consumed during cruise. Variations in NRT have a substantial impact on the range traversed and the time taken during the climb segment; however, the overall impact on the total mission will be negligible.

7.5.7.2 Sensitivity to Atmospheric Variations

Atmospheric winds have a large impact on fuel consumption and direct operating costs; however, the effect of variations in temperatures from the ICAO standard day on the fuel consumption for B-52H is negligible.

Wind Effects

For all aircraft head winds increase fuel consumption and mission time, while tail winds reduce them. Figure 7.5-9 illustrates the impact of winds on optimum range factor for a 470,000 pound B-52H aircraft. Note that a head wind of 100 knots velocity reduces range factor by 22%. Impact of wind on optimum cruise Mach number is small as is evident from Figure 7.5-10.

Temperature Effects

Changes in ambient temperatures have an inverse impact on the cruise ceiling; an increase in ambient temperature lowers the cruise ceiling. However, for a

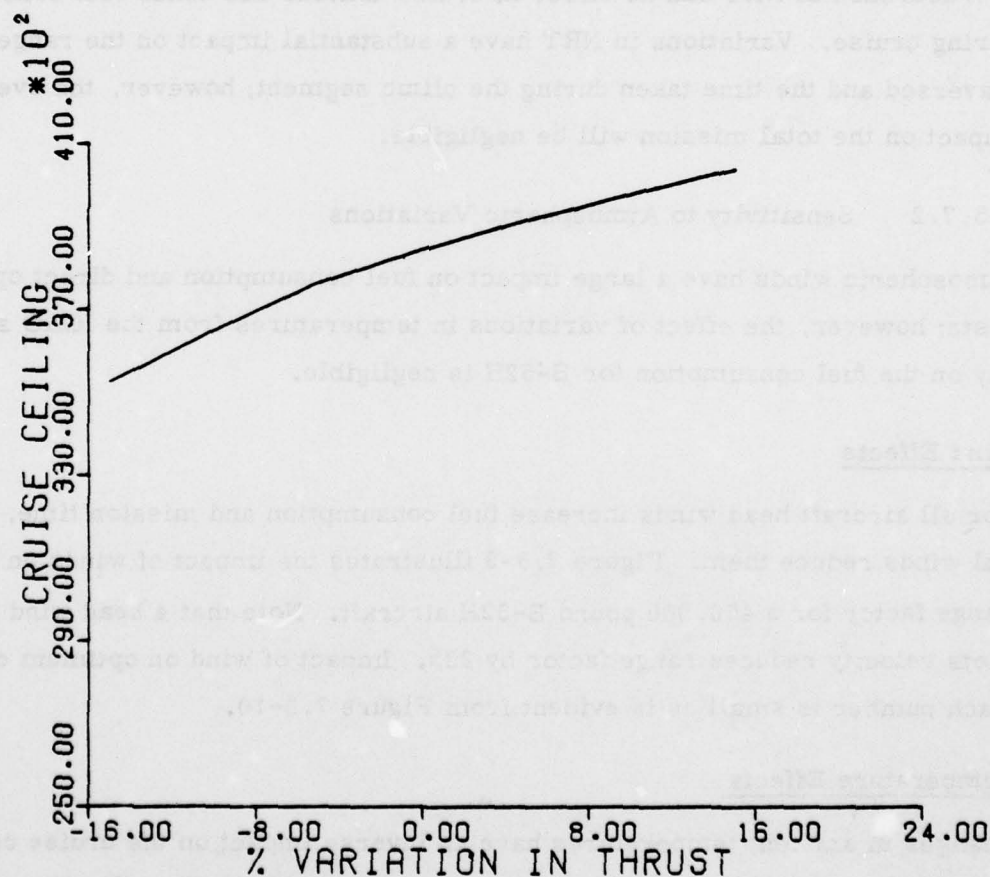


Figure 7.5-8 Impact of Variations in NRT on Cruise Ceiling for B-52H

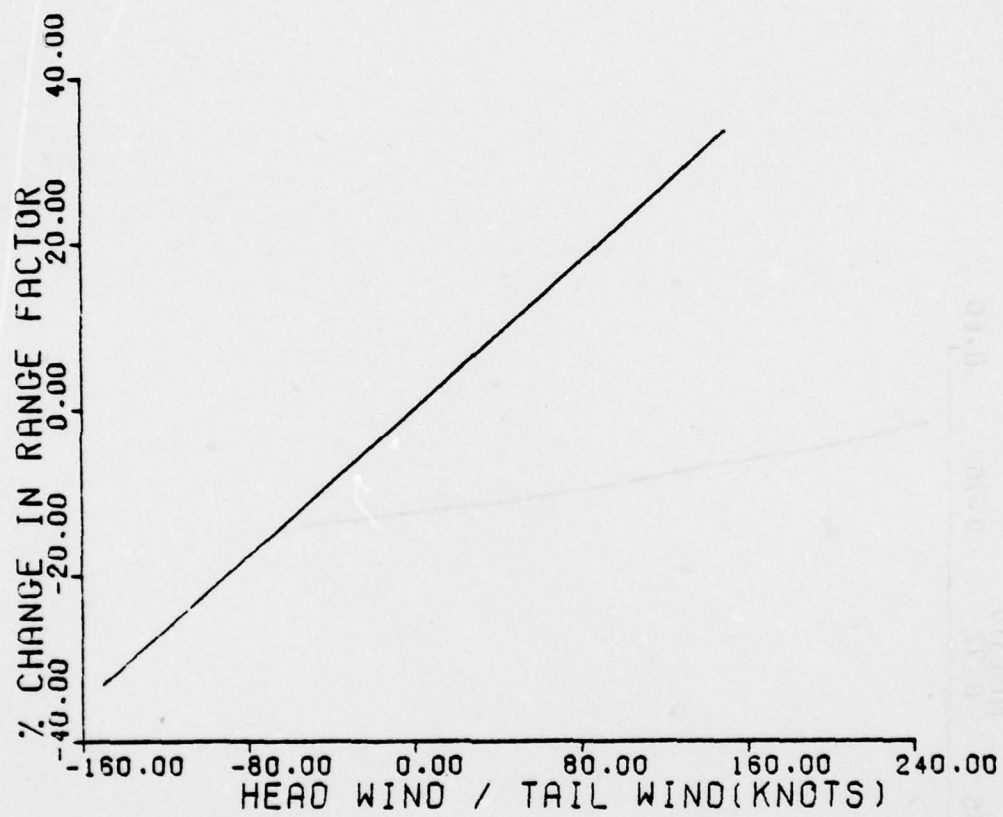


Figure 7.5-9 Impact of Wind on Range Factor for a B-52H Aircraft

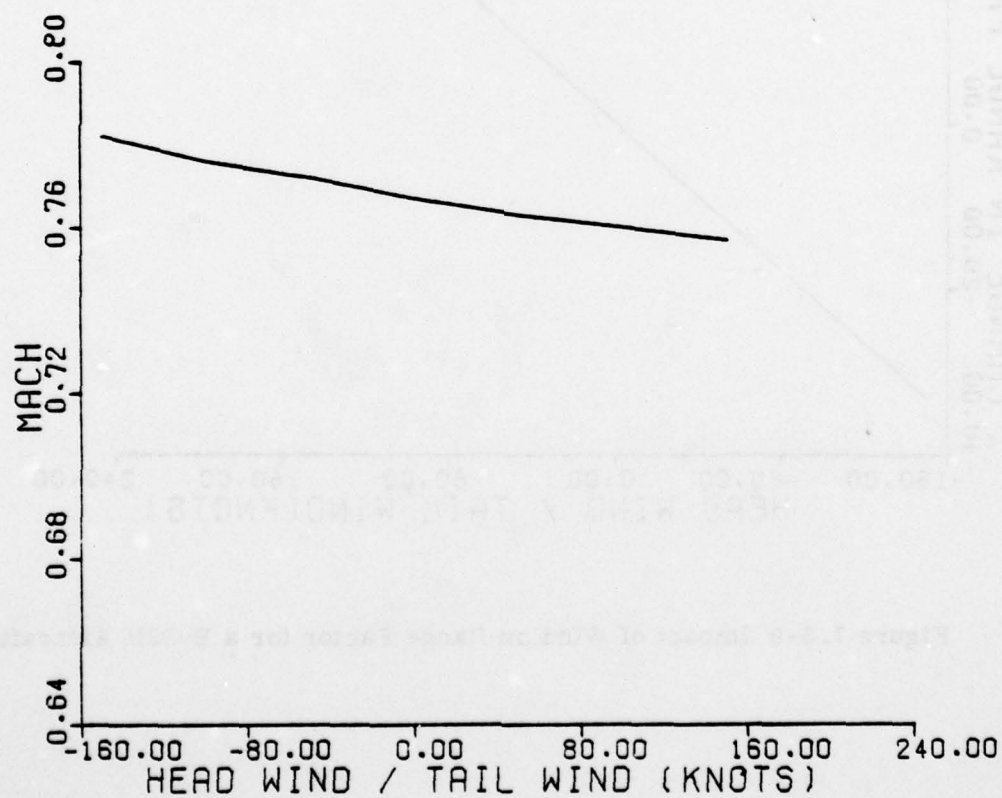


Figure 7.3-1) Impact of Wind on Optimum Cruise Mach Number for B-52H Aircraft

20°C increase in temperature, the cruise ceiling is lowered by approximately 2,000 feet and the optimum cruise altitude remains below the cruise ceiling. Therefore ambient temperature has no impact on the fuel consumption during cruise for B-52H. However, mission time is modified slightly for a constant mach number cruise in the troposphere. The change in time may be estimated using Equation (6.6). Changes in ambient temperatures have a large impact on range traversed and time spent during climb. However, the change in total fuel consumed during the mission will be negligible.

7.5.7.3 Sensitivity to Traffic Density

Since an increase in air traffic near an airport results in take-off delays and increased holding time, the impact of air traffic density on fuel/DOC is evaluated by estimating the increased fuel consumption due to take-off delays and increased holding times. During ground operations the B-52H consumes an average 200 lbs of fuel/minute, and for an average landing weight of 240,000 lbs, the fuel flow rate during holding at optimum altitude is 162 lbs/minute. Thus increased fuel consumption can be estimated using these average fuel flow rates and increased mission time.

7.5.7.4 Sensitivity to Instrument Errors

The decrease in range factor due to flying-off the optimum cruise mach number and optimum cruise altitudes is depicted by Figures 7.5-11 and 12. These figures in conjunction with Equation (6.1) may be used to obtain the increase in fuel consumption due to flying off the optimum cruise conditions.

7.5.8 Conclusions for the B-52H

The following two items result in more than a 1.5% savings in annual fuel consumption:

- turbofan engine modifications
- trajectory optimization

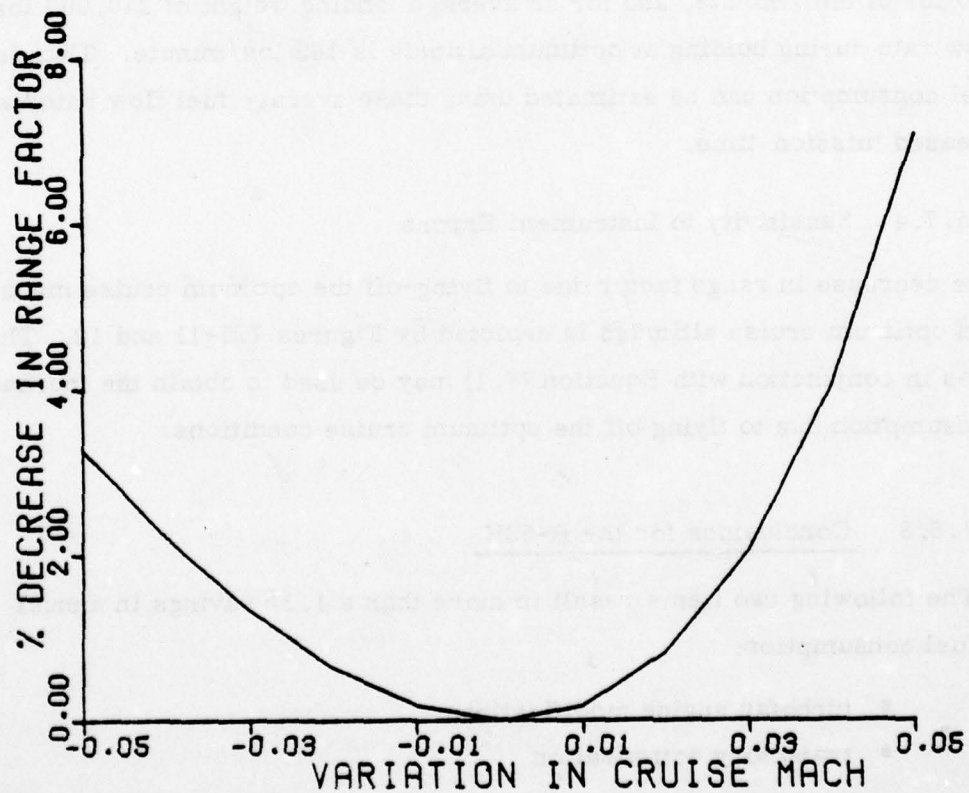


Figure 7.5-11 Impact of Flying-Off Optimum Cruise Mach Number on Range Factor - B-52H

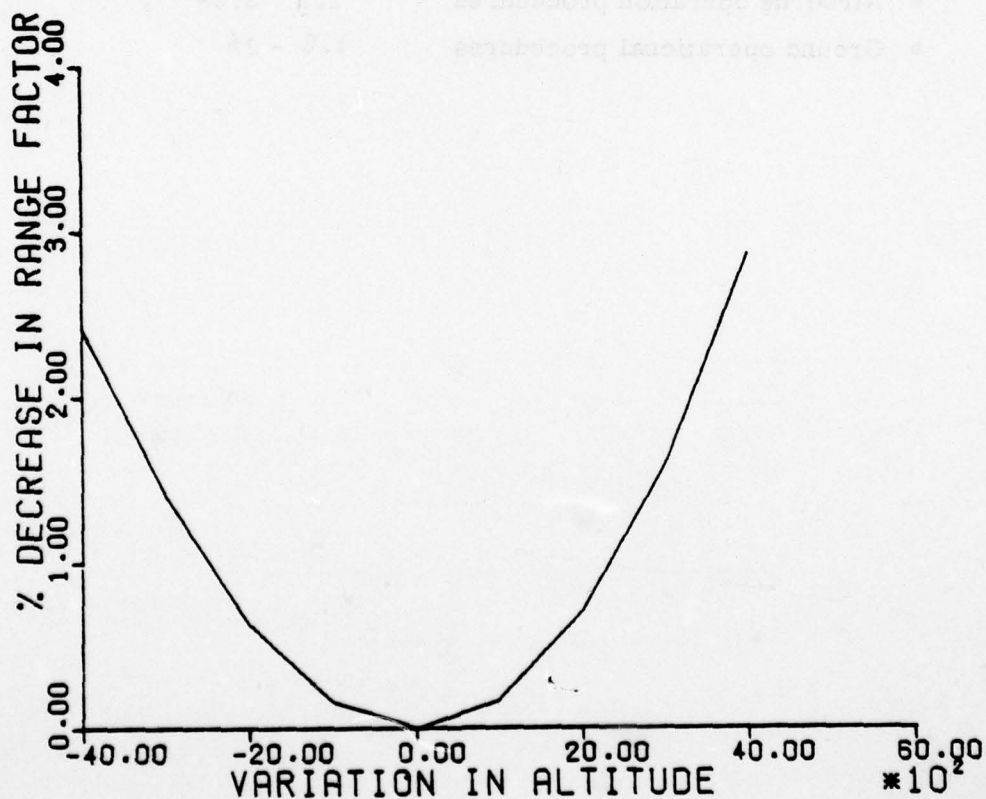


Figure 7.5-12 Impact of Flying-Off Optimum Cruise Altitude on Range Factor - B-52H

Several potential retrofit modifications are possible for reducing the SFC of turbofan engines. These modifications offer up to a 2.8% savings in fuel. The modification cost estimates are not available at present.

The trajectory optimization involves cruising at optimum altitude and air speed and descending with the aircraft in a clean configuration. An annual fuel savings of 2.9% has been estimated due to these optimization procedures.

Each of the other fuel conservation items produced fuel savings of 1.5% or less. The above conclusions are summarized in Table 7.5-6. The annual fuel savings due to all the items investigated can be categorized as follows:

- | | |
|---------------------------------|------------|
| • Design modifications | 2.8% |
| • Airborne operation procedures | 2.9 - 3.9% |
| • Ground operational procedures | 1.8 - 3% |

Procedures	Estimated Percentage Annual Fuel Savings	Break Even Period Years	Confidence In Estimates
Design Modifications			
Turbofan engine modifications	2.8	Not known at Present	Low
Airborne Operational Procedures			
Trajectory optimization procedures	2.9	-	High
All others	0-1	-	Medium
Ground Operational Procedures			
Engine maintenance	1 - 1.5	-	Medium
All others	.8 - 1.5	-	Medium
Total	7.5 - 9.7		

Table 7.5 - 6 ESTIMATED FUEL SAVINGS FOR THE B-52H

AD-A062 609

DYNAMICS RESEARCH CORP WILMINGTON MASS SYSTEMS DIV
AN ANALYSIS OF FUEL CONSERVING OPERATIONAL PROCEDURES AND DESIG--ETC(U)
JUL 78 R K AGGARWAL

F/G 1/3

F33615-76-C-3104

UNCLASSIFIED

R-247U

AFFDL-TR-78-96-VOL-2

NL

5 of 6
ADA
062609



7.6 KC-135 AIRCRAFT UTILIZATION MODEL

The Boeing KC-135 Stratotanker is a four engine strategic tanker with the primary mission of inflight refueling of bombers, tactical fighters, and transports, at high speed and at high altitude. The KC-135 is powered by Pratt & Whitney J57-P-59W turbojet engines rated at 12,925 pounds of thrust each. The first KC-135's were delivered to the Air Force in June, 1957. The average tanker is 16 years old with an average of approximately 7,500 flight hours with some aircraft approaching 17,000 hours logged.

Several studies are underway to improve the capability and extend the life of the KC-135 including re-engining (which is discussed in Section 7.6.7), retrofitting winglets, an update of navigation capability, and the installation of a VHF communications system. A wing modification program is also underway to eliminate wing fatigue constraints on aircraft service life.

7.6.1 Design Missions

The design mission data presented in Table 7.6.1 was obtained from Reference [49]. The basic mission has a 1000 n.mi. combat radius and carries 119,200 pounds of fuel for transfer. Maximum take-off gross weight is 300,800 pounds, and the operational empty weight is 104,450 pounds. The maximum ferry range is 7,537 n.mi.

7.6.2 Mission Model

KC-135 flew 39,400 missions during FY76 for a total duration of 178,154 hours and consumed 458.1 million gallons of fuel.

For the purposes of this section, the KC-135 missions have been separated into the following four profiles: (1) Air Refueling at an air speed of 275 KIAS or lower of aircraft such as B-52s and C-5s (Figure 7.6-1), (2) Air Refueling at an air speed greater than 275 KIAS of high performance aircraft such as FB-111s and tactical fighters (Figure 7.6-2), (3) Non-Air Refueling missions such as ferry or navigational training at altitudes over 21,000 feet (Figure 7.6-3), and (4) Non-Air Refueling missions such as local training at 21,000 feet or below

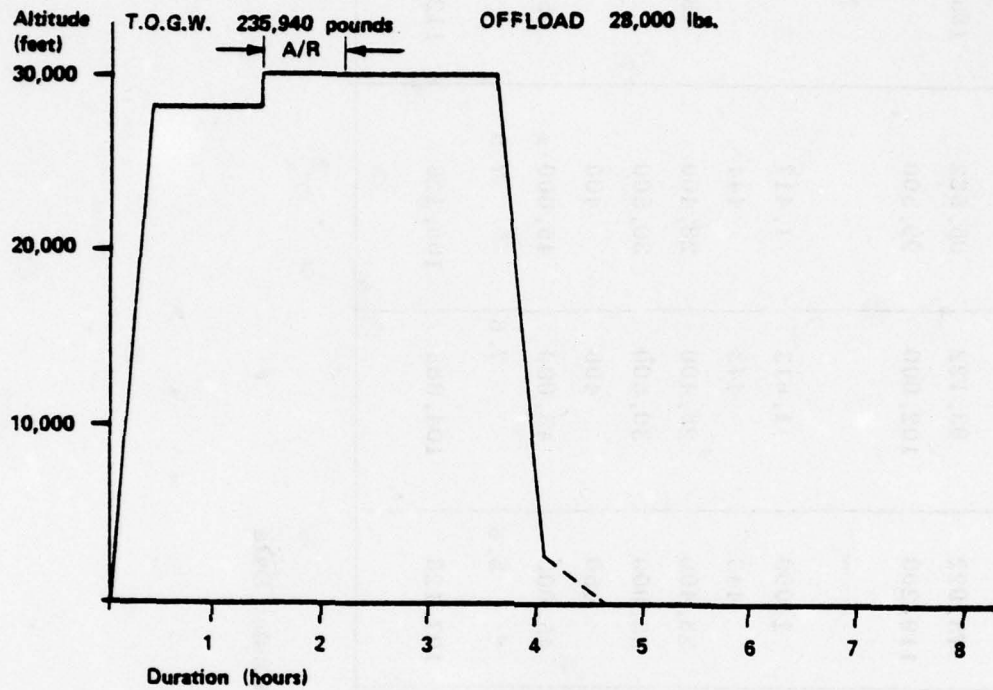
Conditions	Basic Mission	B-52G Buddy Refuel	B-52G Rendezvous Refuel	Ferry Range
TAKE-OFF WEIGHT	300,800	300,800	300,800	300,800
fuel load	75,922	93,122	95,622	195,122
payload (transfer fuel)	119,200	102,000	99,500	-
COMBAT RANGE	-	-	-	7,537
COMBAT RADIUS	1,000	1,613	1,417	-
average cruising speed	443	443	444	444
initial cruising altitude	28,400	28,400	28,400	28,400
refuel altitude	35,000	30,500	30,500	-
refuel speed	450	400	400	-
final cruising altitude	45,000	45,000	45,000	45,000
total mission time	5.6	7.6	7.5	17.1
LANDING WEIGHT	107,128	104,888	108,128	112,928

OEW = 104,450

Table 7.6-1 KC-135A Typical Mission Data

Figure 7.6-1 KC-135 AVERAGE AIR REFUELING (34%)

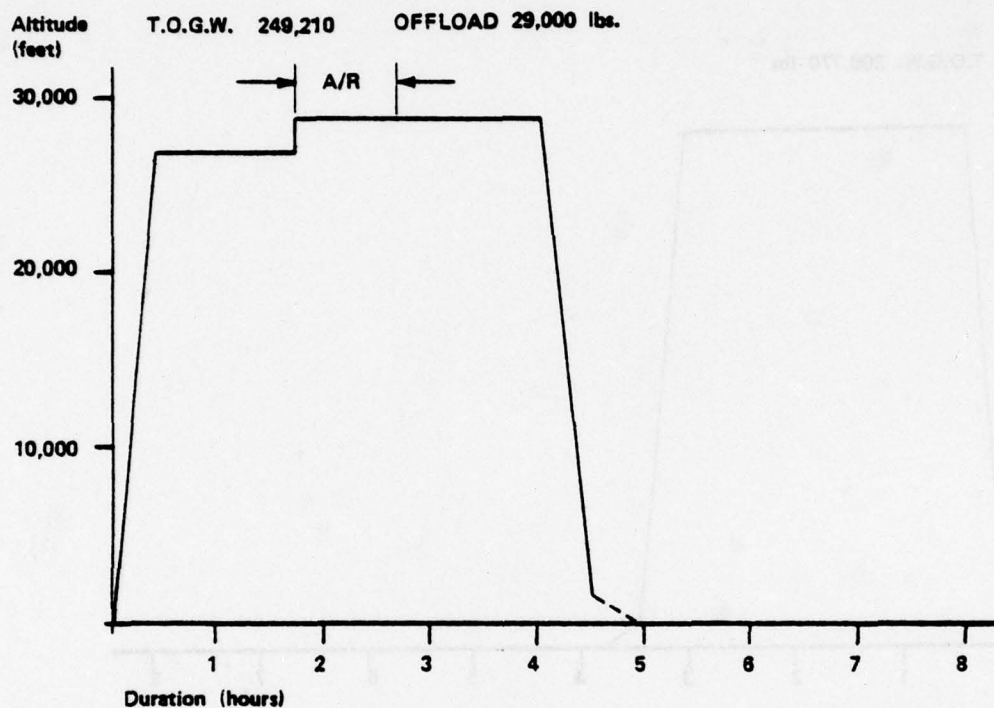
Refueling Airspeed - 275 KIAS or less



Phase	IAS	TIME	Air Distance	Fuel Used	End Altitude	End Gross Weight
Climb	273	0.39	133	10,510	28,000	225,430
Cruise	284	1.04	361	13,730	28,000	211,700
Air Refueling	257	0.72	299	8,840	30,000	174,860
Cruise	269	1.47	628	14,900	30,000	159,960
Descent	253	0.48	154	5,390	2,000	154,570
Traffic Pattern	155	0.54	85	7,890	0	146,680
TOTAL		4.64	1,660	61,260		

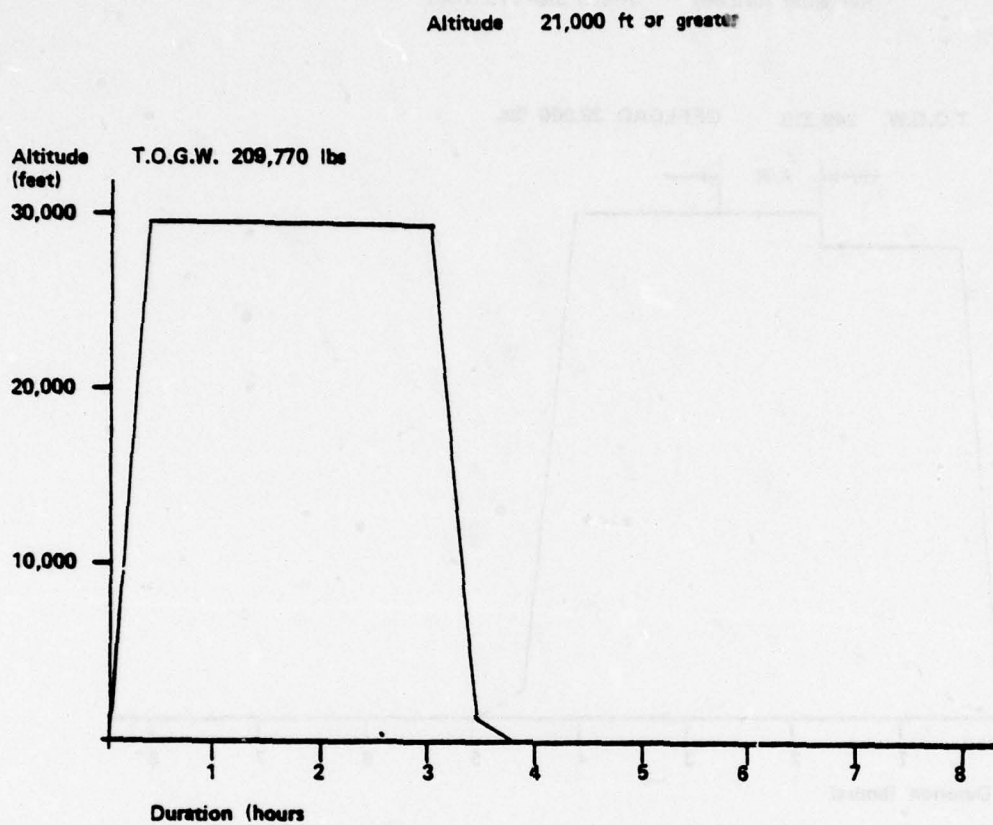
Figure 7.6-2 KC-135 AVERAGE AIR REFUELING (13%)

Refueling Airspeed Greater than 275 KIAS



Phase	IAS	Time	Air Distance	Fuel Used	End Altitude	End Gross Weight
Climb	280	0.39	131	11,100	26,000	238,110
Cruise	292	1.34	587	19,770	26,000	218,340
Air Refueling	311	0.96	465	14,940	27,000	174,400
Cruise	287	1.39	609	15,880	27,000	158,520
Descent	253	0.45	140	5,320	1,500	153,200
Traffic Pattern	158	0.40	64	4,817	0	148,383
TOTAL		4.93	1,996	71,827		

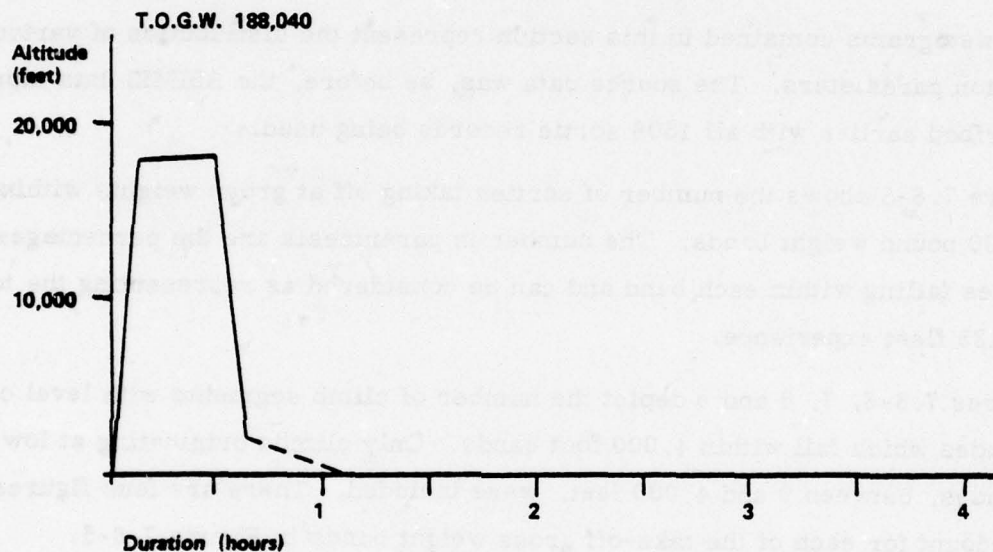
Figure 7.6-3 KC-135 AVERAGE NON-REFUELING (45%)



Phase	IAS	TIME	Air Distance	Fuel Used	End Altitude	End Gross Weight
Climb	274	0.38	116	9,550	29,000	200,220
Cruise	286	2.72	1,230	31,680	29,000	168,540
Descent	261	0.46	150	5,080	1,500	163,460
Traffic Pattern	158	0.30	44	6,870	0	156,590
TOTAL		3.84	1,540	53,180		

Figure 7.64 KC-135 AVERAGE NON-REFUELING (8%)

Altitude - 21,000 ft. or less



Phase	IAS	TIME	Air Distance	Fuel Used	End Altitude	End Gross Weight
Climb	276	0.25	86	7,130	18,000	180,910
Cruise	274	0.71	191	8,730	18,000	172,180
Descent	242	0.31	82	4,160	2,000	168,020
Traffic Pattern	158	0.90	161	25,160	0	142,860
TOTAL		2.17	520	45,180		

(Figure 7.6-4). The parameter values in Figures 7.6-1 through 7.6-4 are averages of all the sorties which had the basic profile phase pattern shown in the particular figure.

These profiles have been generated by the computer programs using the ASIMIS data tapes described in Section 2. The data tapes used were for the periods January through March 1975 and January through March 1976. There were a total of 1506 sortie records of applicable KC-135 missions. Of this number, only 1134 records were complete enough to be used in generating the profiles.

The histograms contained in this section represent the distribution of various mission parameters. The source data was, as before, the ASIMIS data tapes described earlier with all 1506 sortie records being used.

Figure 7.6-5 shows the number of sorties taking off at gross weights within four 40,000 pound weight bands. The number in parenthesis are the percentages of sorties falling within each band and can be considered as representing the total KC-135 fleet experience.

Figures 7.6-6, 7, 8 and 9 depict the number of climb segments with level off altitudes which fall within 4,000 foot bands. Only climbs originating at low altitudes, between 0 and 4,000 feet, were included. There are four figures to account for each of the take-off gross weight bands in Figure 7.6-5.

Figure 7.6-10 shows the number of sorties landing at gross weights falling within the four selected weight bands. The number in parenthesis are the percentages of sorties falling within each band and can be considered as being representative of the total KC-135 fleet experience.

The ASIMIS data tapes for KC-135 do not have fuel-off load information for refueling missions. Since refueling missions constitute 47% of the total KC-135 missions, it was decided to use the average mission profiles shown in Figures 7.6-1, 2, 3 and 4 for the analysis task. With these mission profiles, it is possible to estimate the fuel consumed from the performance charts given in the T.O. (Technical Order) for this aircraft.

FIGURE 7.6-5
KC-135
DISTRIBUTION OF TAKEOFF GROSS WEIGHT

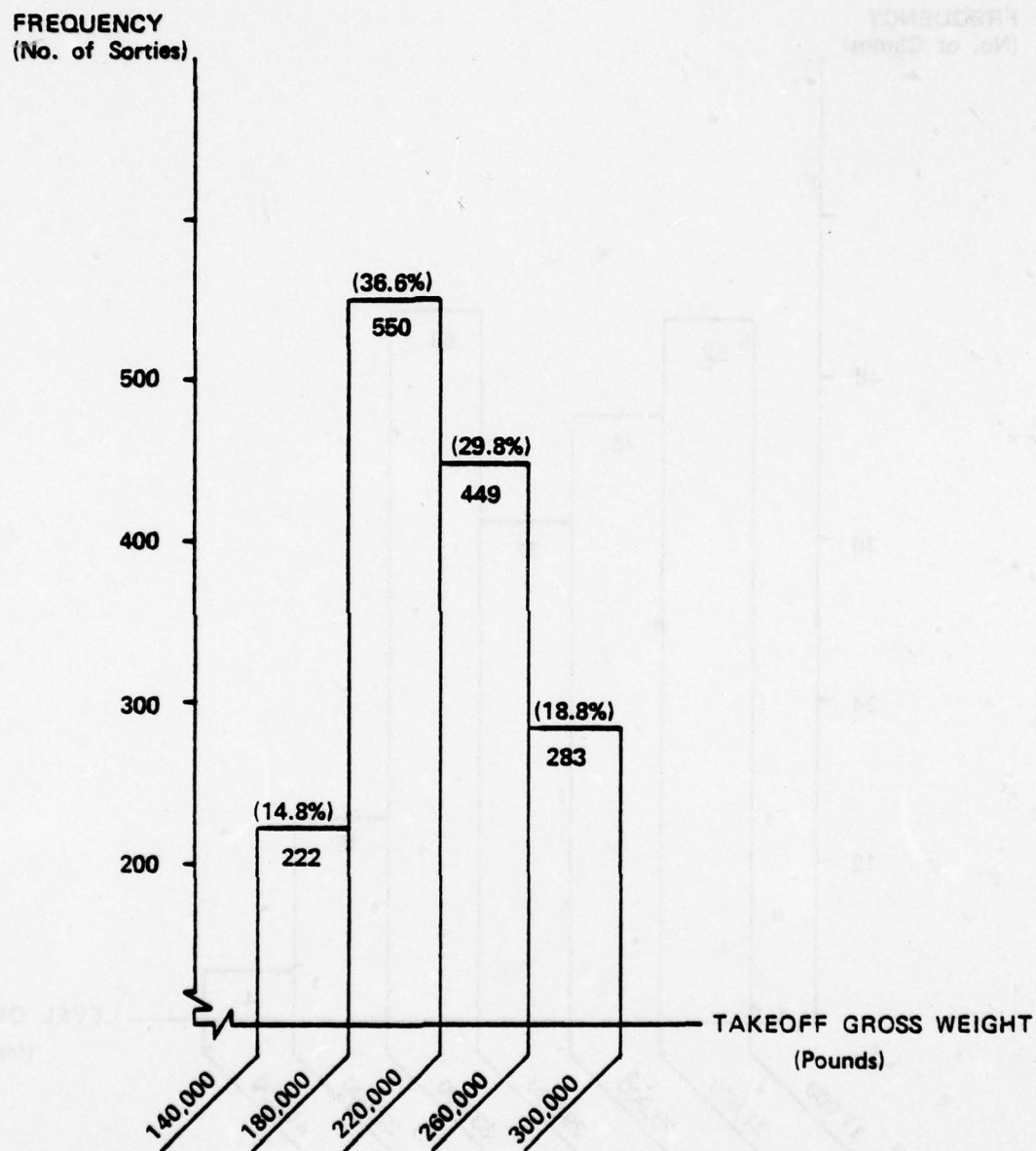


FIGURE 7.6-6
KC-135
DISTRIBUTION OF LEVEL OFF ALTITUDES (CLIMB)
START CLIMB ALTITUDE 0 - 4,000 FEET
START CLIMB GROSS WEIGHT 140,000 - 180,000 POUNDS

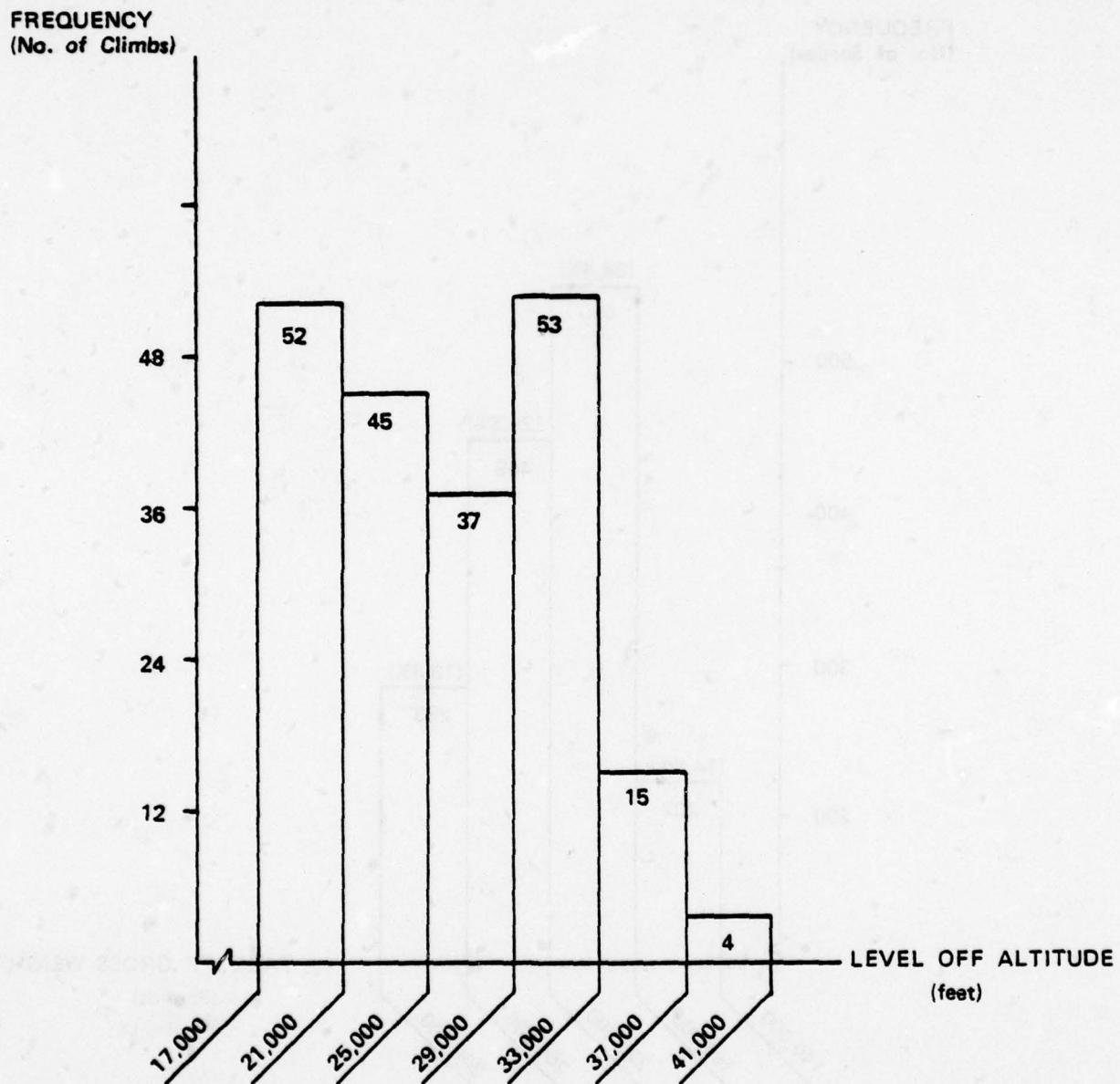


FIGURE 7.6-7
KC-135
DISTRIBUTION OF LEVEL OFF ALTITUDES (CLIMB)
START CLIMB ALTITUDE 0 - 4,000 FEET
START CLIMB GROSS WEIGHT 180,000 - 220,000 POUNDS

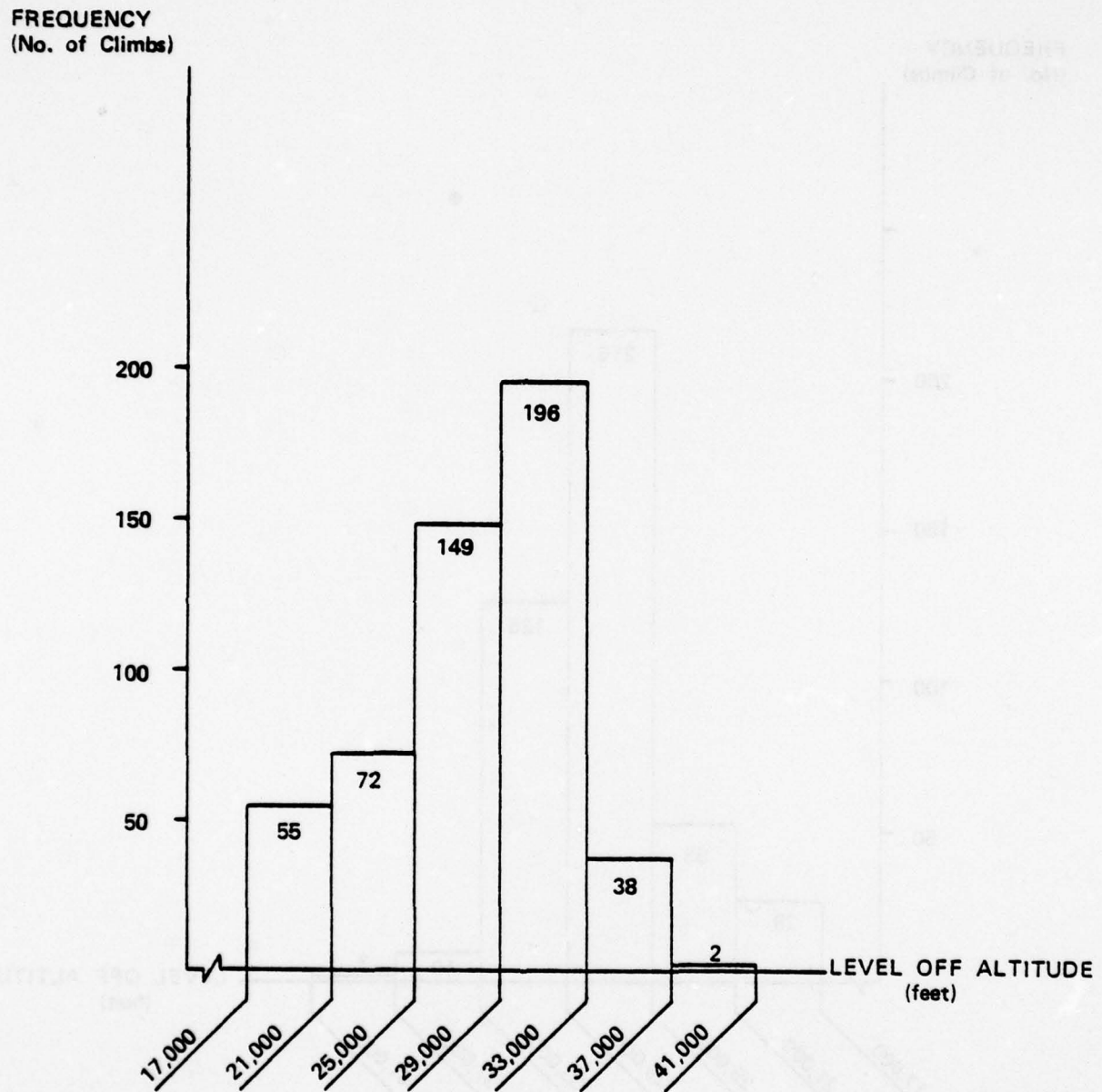


FIGURE 7.6-8
KC-135
DISTRIBUTION OF LEVEL OFF ALTITUDES (CLIMB)
START CLIMB ALTITUDE 0 - 4,000 FEET
START CLIMB GROSS WEIGHT 220,000 - 260,000 POUNDS

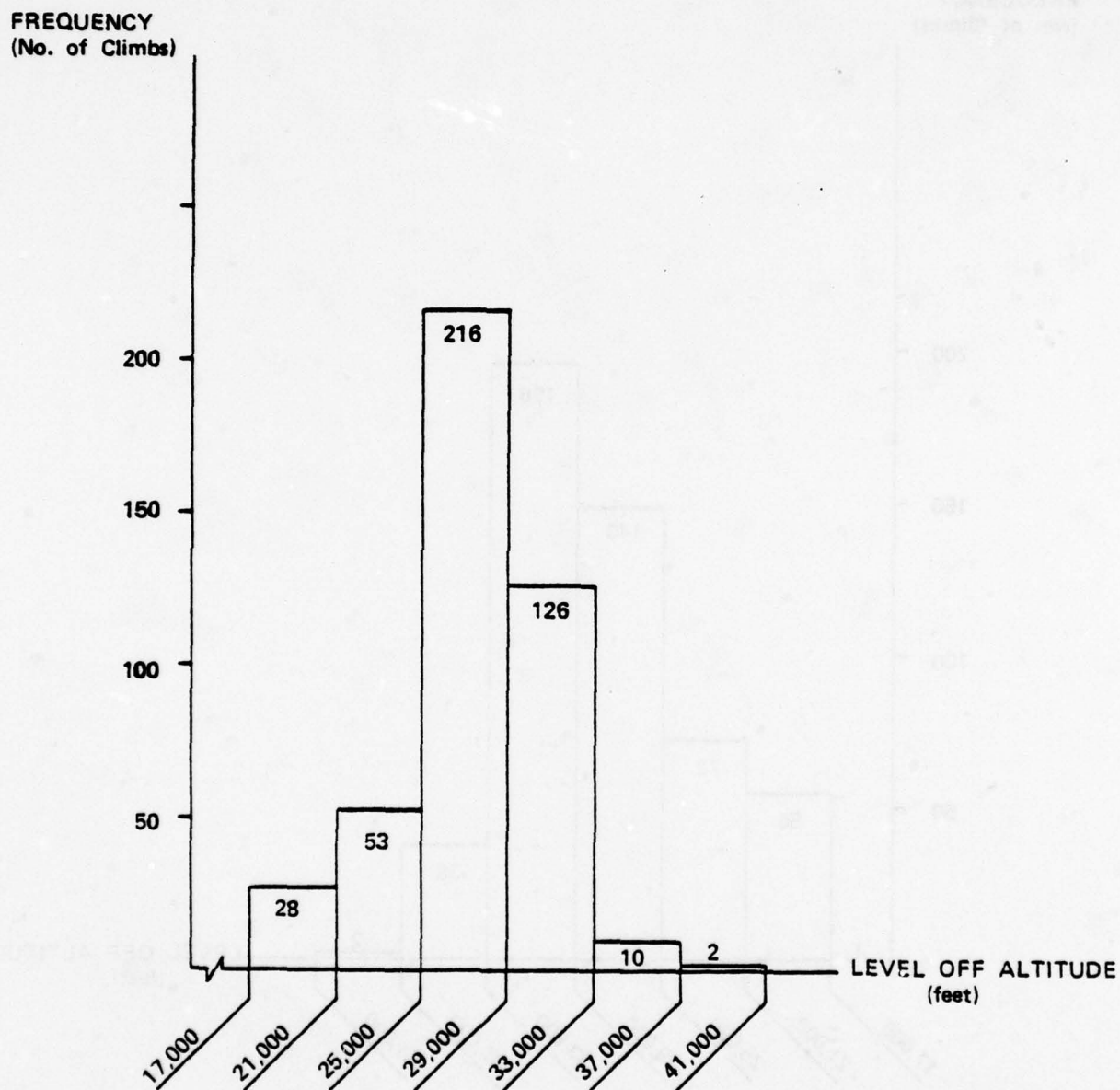


FIGURE 7.6-9

KC-135

DISTRIBUTION OF LEVEL OFF ALTITUDES (CLIMB)

START CLIMB ALTITUDE 0 - 4,000 FEET

START CLIMB GROSS WEIGHT 260,000 - 300,000 POUNDS

FREQUENCY
(No. of Climbs)

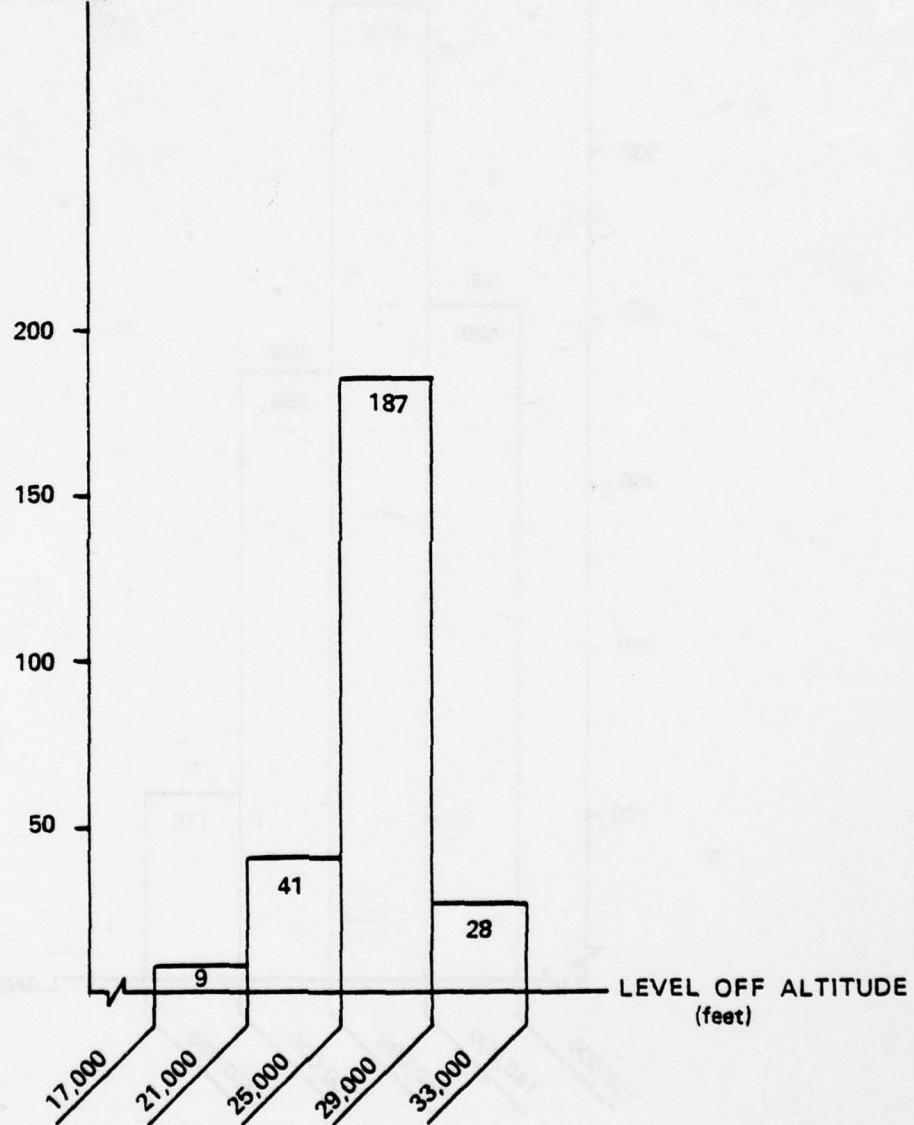
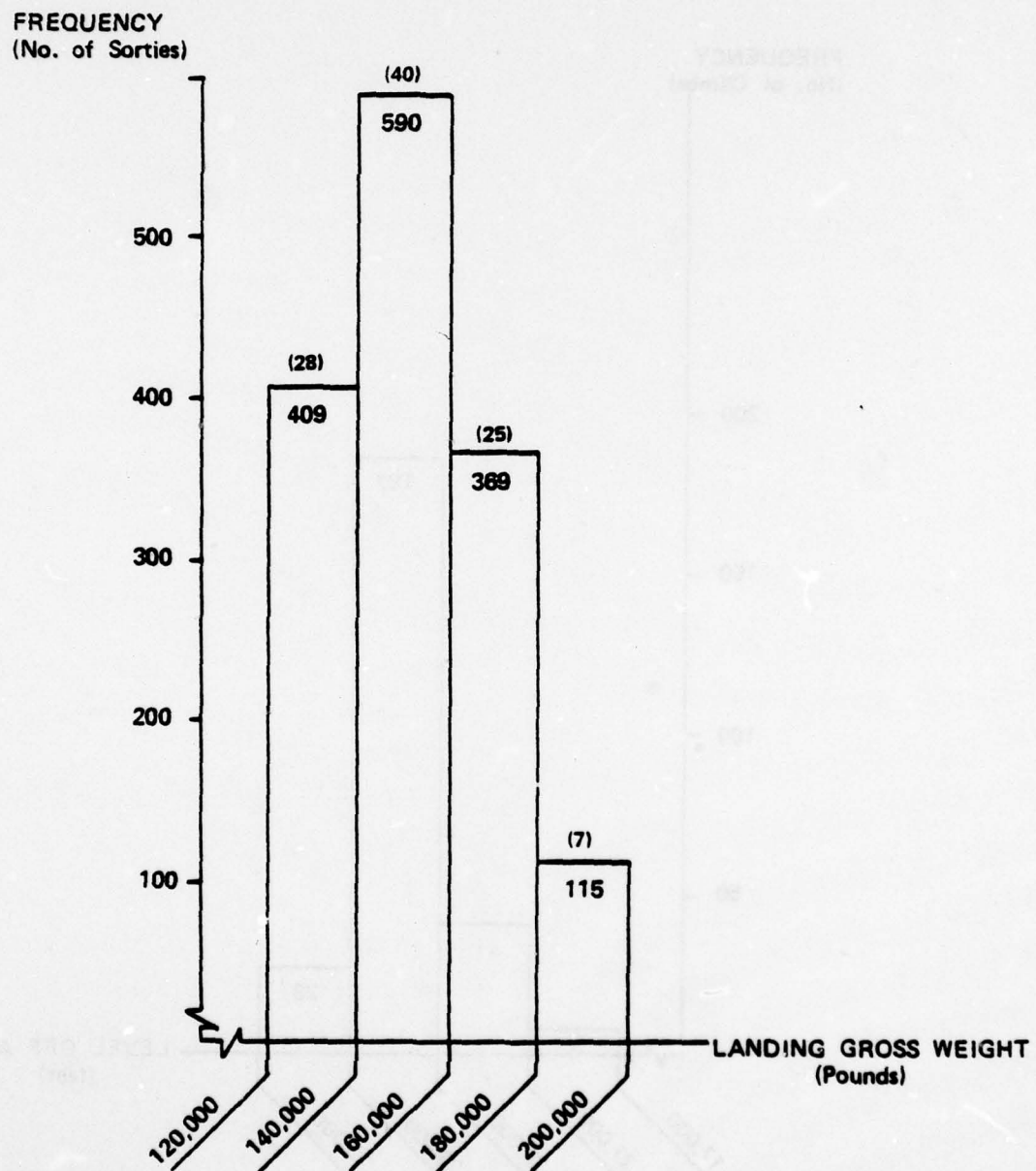


FIGURE 7.6-10
KC-135
DISTRIBUTION OF LANDING GROSS WEIGHTS



7.6.3 DOC Model

Cost data obtained for KC-135 is as follows:

<u>Direct Flight Operations</u>	<u>Cost/FH - \$</u>
Flight Crew	504
Oil at \$9.35/gal.	6
<u>Direct Maintenance Operations</u>	
Direct Maintenance	888
(IROS = \$444)	

From the same formulas as before, the direct operating cost models for KC-135 are given as follows:

<u>Model Type</u>	<u>Fuel Cost/Gal. - \$</u>	<u>Time Cost/FH - \$</u>
DOC	.42	354
DOC 1	.42	702
DOC 2	.42	1,050
DOC 3	.42	1,398

Based on FY76 utilization data, the annual fuel and direct operating costs for the KC-135 are calculated as follows:

Fuel Cost	\$192.4 million
DOC	\$255.5 million
DOC 1	\$317.5 million
DOC 2	\$379.5 million
DOC 3	\$441.5 million

7.6.4 KC-135 Characteristics

Aerodynamic and propulsion data used to develop mathematical models for KC-135 were taken from References [55] and [56].

7.6.4.1 KC-135 Aerodynamic Model

The procedure used to develop the mathematical model of drag coefficient (C_D) as a function of lift coefficient (C_L) and Mach (M) is outlined in Section 3.2. C_D is represented as a parabolic function of C_L as follows:

$$C_D = C_{D_0} - B C_L + K C_L^2$$

where

coefficients C_{D_0} , B and K are obtained as the following functions of M .

$$C_{D_0} = .0165 + .89 \cdot 10^{-8} (M^* - M)^{-6.9}$$

$$B = .015 + .165 \cdot 10^{-5} (M^* - M)^{-5.2}$$

$$K = .073 + .744 \cdot 10^{-5} (M^* - M)^{-5.0}$$

and

$$M^* = 1.0$$

This model degrades beyond a mach number of .82.

7.6.4.2 KC-135 Thrust Model

Normal rated thrust (NRT) per engine for KC-135 is expressed as a polynomial function of Mach (M) and normalized altitude (H_n).

$$\begin{aligned} \text{NRT} = 1000. [& 8.58 - 5.22H_n - 2.86M - .95H_n^2 + 3.49MH_n + 1.79M^2 \\ & - .21MH_n^2 - 2.35M^2H_n + 1.27M^2H_n^2] \end{aligned}$$

where

NRT = normal rated thrust, (lb)/engine

H_n = altitude, (ft)/40000

The above NRT model is used in the troposphere only. For operations in the stratosphere the following NRT model is used:

$$\text{NRT} = 1000. [9.7 - 9.23H_n + 2.1M + 2.27H_n^2 - 4.37MH_n + 2.01M^2 + 1.93MH_n^2 - 1.3M^2H_n + 0.8M^2H_n^2]$$

The idle thrust (T_{idle}) model for KC-135 has the same functional representation as NRT except the constant coefficients are different. The equation for T_{idle} is given by

$$T_{\text{idle}} = 1000. [.36 + .25H_n - .57M + .1H_n^2 + 2.12MH_n - .75M^2 - 1.52MH_n^2 - .6M^2H_n + .93M^2H_n^2]$$

where

T_{idle} = idle thrust, lbs/engine

7.6.4.3 KC-135 Fuel Flow Model

Normalized fuel flow rate, f_n , for KC-135 is represented by the same functional form as for B-52G. Thus f_n is given by the following polynomial function of normalized thrust (T_n) and Mach (M).

$$f_n = 1000. [.06 + 11.88T_n + 3.5M + 6.32T_n^2 + 2.58MT_n - 1.75M^2]$$

$$T_n = T/5/20000$$

where

f_n = normalized fuel flow rate

T = thrust, lbs/engine

δ = pressure ratio

In the stratosphere the fuel flow rate obtained from the above expression is increased by 0.45 % for each 1000 foot altitude increment above the tropopause.

The idle fuel flow model for KC-135 was developed using idle thrust and idle fuel flow data. The normalized idle fuel flow rate, f_{idle} , is represented by the following equation.

$$f_{\text{idle}} = 1000. [.128 + .96T_n + 1.77M + 17.75T_n^2 - 16.4MT_n + .4M^2]$$

Beyond a 25,000 foot altitude the idle fuel flow rate remains constant at 650 lbs/hr/engine.

The above thrust and fuel flow models are generally good to within a 2% error over the regions of interest.

7.6.5 Evaluation of Airborne and Ground Operational Procedures

Section 4 outlined the technical approach for evaluation of fuel conserving airborne and ground operational procedures. The results of this evaluation for KC-135 aircraft are summarized in this section.

7.6.5.1 Reduced Power Take-off

The direct fuel savings for KC-135 due to reduced power take-off procedures are negligible. The average savings per mission due to reduced power take-off is less than one-fourth of a gallon, and the average take-off time increases by approximately 4.5 seconds. However, indirect savings due to reduced engine deterioration may be substantial. Thus this procedure should be used whenever possible.

7.6.5.2 Optimal Climb, Cruise and Descent Procedures

Following the same procedures as for the other aircraft under study, the climb, cruise and descent procedures are first examined separately. Results of the individual optimizations are then used for a complete trajectory optimization under operational constraints.

Optimal Cruise-Climb Solution

Optimum cruise parameters are obtained by the extremization of Eq. (A.31). The fuel consumed and time required to execute a mission change as the value of parameter θ is changed. Figure 7.6-11 illustrates the relationship between mission fuel and mission time for various values of θ . The solution corresponding to $\theta = 0$ is the minimum time solution while that corresponding to $\theta = 1$ is the minimum fuel solution. The minimum cruise altitude and maximum cruise mach number were constrained in the simulation, and the minimum time solution was obtained under these constraints. As θ increases, fuel consumption decreases and the mission time increases. Solution points corresponding to the direct operating cost models developed in Section 7.6.3 are indicated on Figure 7.6-11. The optimum cruise mach number corresponding to DOC, DOC 1, DOC 2 and DOC 3 are 0.79, 0.8, .81 and .815, respectively. The minimum fuel solution occurs for the following cruise conditions.

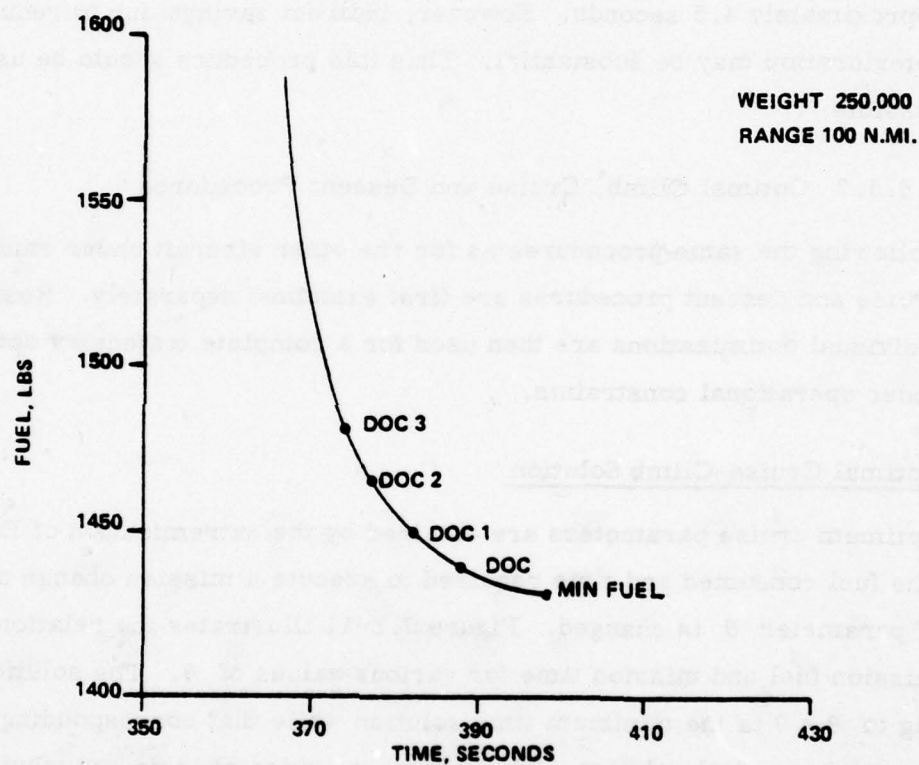


Fig. 7.6-11 FUEL/TIME TRADE-OFF FOR THE
KC-135 CRUISE SOLUTION

- Mach Number = 0.776
- W/s = 0.912×10^6 lbs
- Range Factor = 8323

This range factor has not been corrected for power and bleed air extraction and the energy required for climbing-cruise. The energy gain during the cruise climb profile reduces the range factor by 0.7%.

Optimal Step-Climb Solution

KC-135 aircraft are not restricted to fly at constant cruise altitude by ATC constraints. However, for safety considerations, a constant altitude cruise with optimum step-climbs may be a preferable flight procedure, if the associated fuel penalty is small. The standard day cruise ceiling for KC-135 is close to 2,000 feet above the cruise-climb altitude. Thus, the optimum step-climb procedure for this aircraft is similar to the one described in Section 7.1.5 for C-141.

A comparison of cruise-climb vs. step-climb was made for the following cruise condition.

Aircraft weight at start of cruise	247,600 pounds
Initial Cruise Altitude	32,000 feet
Final Cruise Altitude	36,000 feet
Range	1,563 n.mi.
Cruise Mach Number	.766

Both cruise climb and step climb trajectories were simulated. The cruise climb trajectory consumed 42,686 pounds of fuel, and the optimum step climb procedure with a 4,000 foot step at a 960 n.mi. range consumed 42,769 pounds of fuel. Thus step-climb trajectory consumed close to 0.2% more fuel than cruise-climb solution.

Conventional Climb Procedure

The conventional climbs simulated in this study follow the procedures outlined in Reference [15]. Under normal conditions, conventional climbs are performed at NRT power setting. En route climb speed is 280 KCAS below 32,500 feet and Mach 0.78 above 32,500 feet. KC-135 aircraft are excluded from the ATC constraint of a 250 KCAS maximum speed below 10,000 feet altitude.

Optimum Climb Procedure

The optimum climb air speed and power setting are obtained from the optimum climb algorithm derived in Appendix A. Both air speed and throttle setting vary continuously for optimal climb trajectories. This optimal climb and the parametric optimal climb discussed next are both optimized with respect to minimum fuel.

Parametric Optimal Climb

The parametric optimal climb is similar to conventional climb and is performed at NRT power setting. The air speed schedule is also similar to that of conventional climb and follows a constant KCAS/constant mach mode. However, the value of constant KCAS is determined by parametric optimization. This value varies with aircraft weight.

Comparison of Various Climb Procedures

A comparison of various climb procedures was made for a typical KC-135 climb trajectory, and the results are summarized in Table 7.6-2. Initial and terminal conditions for all three climb trajectories are the same. The optimal trajectory has a path length of 259 n.mi. The distance traversed during climb for both the parametric optimum and conventional trajectories is less than 259 n.mi.; thus their climb segments are followed by a cruise segment at 0.776 mach number, which is the optimum speed for the minimum fuel cruise. The optimum trajectory consumes 12,780 pounds of fuel which is 118 lbs less than the conventional trajectory, and it takes 116 seconds less time than the conventional

trajectory. The parametric optimum trajectory consumes only 6 pounds more fuel than the optimal trajectory, and it takes 52 seconds more than optimal trajectory. Table 7.6-2 also indicates the cost associated with each trajectory. Observe that of all three trajectories the optimum trajectory has the least cost. However, as mentioned earlier the optimum climb is not very practical to implement and the minimum fuel difference between optimum and parametric optimum is small. Table 7.6-3 shows the annual fuel/DOC savings due to the parametric optimum climb procedure. The total fuel savings is seen to be small. Also note that the optimum climb speed is higher than the conventional 280 KCAS. The J-57 engines already violate noise and air pollution limits at a 280 KCAS climb speed; an increase in this speed would result in further increases in noise and air pollution. In summary, it appears that the conventional climb procedures are preferable.

Conventional Descent Procedures

En route conventional descent procedures simulated in this study were obtained from Reference [15]. The two outboard engines are retarded to idle and the two inboard engines are set at a thrust setting schedule which maintains pressurization. The speed schedule followed is 0.78 Mach/280 KCAS above 10,000 feet and 250 KIAS from 10,000 feet to sea-level.

Optimal Descent Procedures

The optimum descent algorithm derived in Appendix A provides the air speed and throttle setting during descent. For an optimal trajectory both altitude and air speed may vary continuously.

Initial Conditions
 Weight 260,000 lbs
 Altitude 3,000 ft
 Air speed 250 KCAS

Final Conditions
 Range 259 NM
 Altitude 31,800 ft
 Air speed .776 M

Type of Climb	Optimum	Parametric Optimum 300 KCAS/.776M	Conventional 280 KCAS/.776M
Climb	259	224	219
Range	0	35	40
n.m. Total	259	259	259
Climb	12780	11744	11706
Fuel	0	1042	1192
lbs. Total	12780	12786	12898
Climb	2236	2011	2034
Time	0	277	318
sec Total	2236	2288	2352
Fuel	825.8	826.2	833.4
Cost	1045.7	1051.2	1064.7
\$	1261.8	1272.4	1292.0
DOC1	1478.0	1493.5	1519.4
DOC2	1694.1	1714.7	1746.8
DOC3			

Table 7.6-2 Comparison of Optimum vs Conventional Climb - KC-135

Cost		Annual Savings Due to Parametric Optimum Climb	% Savings
Fuel	gallons	109, 800	0.02
Fuel	Cost \$	46, 000	0.02
DOC	\$	156, 000	0.06
DOC 1	\$	263, 500	0.08
DOC 2	\$	372, 200	0.1
DOC 3	\$	481, 000	0.11

Table 7.6-3 Fuel/DOC Savings Due to Optimum Climb for KC-135

Parametric Optimum Descent Solution

The parametric optimum descent is accomplished at an idle thrust setting with the aircraft in a clean configuration. The air speed schedule is constant Mach/constant KCAS where the air speed is set at the min fuel mach and the KCAS is varied parametrically to obtain the minimum value of fuel consumed.

Comparison of Various Descent Procedures

Table 7.6-4 summarizes the results of a comparison of various descent procedures. The en route conventional descent trajectory traverses a 126 n.mi. range, which is the maximum range traversed during descent. The other trajectories have a cruise segment before the descent is initiated such that total mission range for all trajectories is 126 n.mi. The optimal descent trajectory consumes 821 lbs less fuel than the conventional descent trajectory; however, it takes 157 seconds more mission time. The conventional trajectory with all four engines retarded to idle setting consumes 320 lbs less fuel and takes 140 seconds less time than the "en route" conventional descent. The differences in fuel consumed between the parametric and EEM optimum solutions was small; however, the parametric optimum trajectory takes more time than the EEM trajectory, and the DOC for the parametric optimum will be even higher than those shown in Table 7.6-4 for the EEM optimum.

If descent speed is reduced to 250 KCAS at idle thrust setting the minimum DOC solution is obtained. It is interesting to note that the average descent speed calculated from the ASIMIS tapes is close to 250 KCAS. Compared to a conventional descent at idle thrust and 250 KCAS air speed, the optimal descent will result in a 2 million gallon (.44%) annual fuel savings; however, there will be a loss of \$87,000 (.03) in DOC and \$2.9 million (.66%) in DOC 3.

Initial Conditions
Weight 160,000
Altitude 28,000
Air speed 280 KCAS

Final Conditions
Range 126 n. mi.
Altitude 3,000 ft.

Type of Descent	† Optimal Descent	Conventional at Idle Thrust 250 KCAS	Conventional at Idle Thrust 280/250 KCAS	Conventional Descent 280/250 KCAS
Cruise	6	43	51	0
Range	120	83	75	126
n. mi.	126	126	126	126
Total				
Cruise	156	1117	1325	0
Descent	1270	645	592	2247
Fuel	1426	1762	1927	2247
lbs.				
Total				
Cruise	52	373	443	0
Descent	1494	930	806	1389
Time	1546	1303	1249	1389
sec.				
Total				
Fuel	92.1	113.8	124.5	145.2
DOC	244.1	241.9	247.3	281.8
DOC 1	393.6	367.9	368.1	416.1
DOC 2	542.2	493.8	488.8	550.3
DOC 3	692.5	619.8	557.8	684.6

† This is a minimum fuel descent.

Table 7.6-4 Comparison of Optimum vs Conventional Descent KC-135

Integrated Optimal Trajectories

Obtaining optimum results with air refueling requires careful mission planning supported by special flying techniques and coordination between tanker and receiver. The refueling altitude is generally limited by the receiver weight or performance at the end of transfer on outbound refueling and by tanker performance on inbound refueling. Refueling is generally accomplished in level flight, but refueling in a descent is possible if made necessary by weather conditions, engine thrust limitations or abnormal airplane drag. It is always better for the receiver to sacrifice altitude instead of speed to perform a successful refuel. The extra fuel burned during climb back to cruise altitude will be less than the extra fuel that will be burned if trouble is experienced from disconnects at slow speeds and high altitude. For most operations the altitude limit is set by the receiver because of the tanker down wash which necessitates the receiver to use more power, or because it is at cruise altitude at the completion of refueling [15]. The average refueling profiles for KC-135 given in Section 7.6.2 are now examined in the light of the above discussions.

Figure 7.6-1 illustrates the average profile for refueling B-52's and C-5's at an air speed of 275 KIAS or lower. Observe that the refueling is done at a 30,000 foot altitude; however, the KC-135 initially cruises at 28,000 feet for almost one hour. Between the cruise and the refueling, there is a time period during which the KC-135 orbits while waiting for the receiver. The ASIMIS data tapes do not provide information on the time duration of this orbit. For the average aircraft weight the best orbit altitude is close to 28,000 feet, and the best cruise altitude is close to 32,000 feet. However, from a practical viewpoint it appears best to avoid both of these altitudes. Since refueling is accomplished at a 30,000 foot altitude, a practical procedure is to initially level-off at 30,000 feet and remain there until refueling is finished. After refueling has been accomplished the tanker may climb to a 39,000 foot altitude and cruise there for the rest of the mission before initiating descent. This procedure will result in a 2,527 lb. fuel saving and a 144 second time saving per mission, which amounts to 5.18 million gallons of fuel savings and \$2.36 million in DOC per year.

The average mission profile for air refueling high performance aircraft is illustrated in Figure 7.6-2. Again a practical procedure is to level-off at a 27,000 foot altitude and remain there until refueling has been accomplished. After the refueling phase the procedure consists of a climb to a 39,000 foot altitude and a cruise there for the rest of the mission before initiating descent. This procedure will result in a fuel savings of 4.119 lbs. The total mission will increase by only 15 seconds. The annual fuel and DOC savings will amount to 3.12 million gallons and \$1.3 million, respectively.

The average mission profile for non-refueling such as ferry or navigation training missions is shown in Figure 7.6-3. The initial level-off cruise altitude for this mission type may be as high as 36,000 feet. A constant altitude cruise at 36,000 feet and a speed of .77 mach will save 6.87 million gallons of fuel and \$2.37 million in DOC per year for KC-135 operations. Note that this is a conservative estimate. Savings will be a little higher if a cruise-climb or step-climb procedure is employed.

For the average short range non-refueling mission (Figure 7.6-4), 675,000 gallons of fuel and \$616,000 in DOC can be saved annually by climbing to a 30,000 foot altitude.

Table 7.6-5 summarizes the results of trajectory optimization for KC-135. From the total of the four missions analyzed, it is seen that approximately 16 million gallons of fuel can be saved annually.

7.6.5.3 Delayed Flap Approach Procedure

Results of an evaluation of fuel and DOC savings due to a delayed flap approach procedure for KC-135 are summarized in Table 7.6-6. The first column in this table shows the altitude above the runway where the aircraft attains stable approach speed. For conventional approaches, this altitude is generally 1500 feet. The maximum fuel savings (the zero altitude case) with respect to the 1500 foot altitude figure is estimated at 2.3 million gallons/year which is 0.5% of the annual fuel consumption for KC-135.

Mission Type	Annual Savings					
	Fuel Gallons	Fuel Cost \$	DOC \$	DOC 1 \$	DOC 2 \$	DOC 3
Air Refueling Below 275 KIAS (B-52 and C-5A)	5,180,000	2,176,000	2,360,000	2,546,000	2,736,000	2,920,000
Air Refueling Above 275 KIAS (High Performance Aircraft)	3,120,000	1,310,000	1,303,000	1,294,000	1,289,000	1,281,000
Non-Refueling Mission (Ferry or Navigation)	6,786,000	2,850,000	2,373,000	1,908,000	1,441,000	974,000
Non-Refueling Mission (Local Training)	675,000	283,000	616,000	943,000	1,271,000	1,598,000
Total	15,761,000	6,619,000	6,652,000	6,691,000	6,737,000	6,773,000
%	3.44	3.44	2.6	2.11	1.78	1.53

Table 7.6-5 Annual Fuel/DOC Savings Due to Trajectory Optimization for KC-135

Altitude for Stable Landing Speed	ANNUAL SAVINGS											
	Fuel/Gal.	%	Fuel Cost	%	DOC	%	DOC1	%	DOC2	%	DOC3	%
1000	775,200	.17	325,600	.17	368,300	.14	410,300	.13	452,300	.12	494,200	.11
500	1,551,700	.34	651,700	.34	733,400	.29	813,700	.26	894,000	.24	974,300	.22
0	2,319,000	.5	974,000	.5	1,095,000	.43	1,208,000	.38	1,332,900	.35	1,451,900	.33

7.6.5.4 Aft C.G. Operations

Aft c.g. operations for aircraft result in fuel savings. However, for a tanker, the possibility of influencing c.g. location through proper distribution of transferable fuel is limited. Burning fuel evenly towards aft c.g. may result in small fuel savings. The sensitivity of fuel savings due to a shift in c.g. location for KC-135 was estimated by considering average weights and cruise conditions for the four typical KC-135 missions given in Section 7.6.2, and the results were averaged. A 5%-MAC shift in c.g. aft of the nominal location results in a 0.65% savings in fuel consumed during the cruise phase. This represents a savings of 1.95 million gallons annually.

7.6.5.5 Reduced Reserve Fuel

The KC-135 average mission profiles obtained by processing ASIMIS tapes indicate that the actual landing weights are higher than those estimated based on the assumption that the exact amount of transferable fuel was carried. Since this assumption does not appear to be realistic, it is difficult to distinguish excess reserve fuel from excess transferable fuel. Therefore the fuel savings due to reduced reserve fuel for KC-135 operations were estimated on a sensitivity basis only. If on the average the fuel carried per mission could be reduced by 5,000 pounds, the annual fuel savings would be 6.67 million gallons, which is equivalent to a 1.48% reduction in the annual fuel consumption for KC-135 aircraft.

7.6.5.6 Reduce Engine Load

Fuel savings can be realized for KC-135 by reducing accessory load on engines and bleed air extraction. Since fuel flow increases by 2% when the anti-icing system is in operation [15], minimizing the use of anti-icing can produce some fuel savings. Normally during descent two engines are set at idle thrust setting and the other two at the thrust required to meet cabin air conditioning requirements. However, the power setting can be reduced beyond this point if the pilot is prepared to accept lower cabin temperatures at higher altitudes and rising cabin temperatures as he descends. Reduced power setting during descent will result in fuel savings. Further fuel savings may be realized by turning off unnecessary lights and equipment. On the average, the accessory power loads and the bleed air extraction result in approximately a 1.25% increase in TSFC. Thus the total saving due to reduced engine load cannot be more than 1%. The assignment of a specific savings factor in this case is inappropriate.

7.6.5.7 Reduce Engine Use and Taxi Time

The average fuel consumption during ground operations for KC-135 is approximately 105 lbs/minute. Thus fuel savings can be realized by reducing the engine use during ground operations. Procedures which may result in reduced engine use and taxi time were outlined in Section 4.3. An average reduction of one minute in taxi time per mission can save 636,000 gallons of fuel and \$0.5 million in DOC per year for the KC-135 fleet.

7.6.5.8 Partial Engine Taxi

It may be possible to shut down two engines after landing. For a five minute average taxi time, this procedure can save 1.59 million gallons of fuel (.35%) annually.

7.6.5.9 Removing Excess Equipment

Carrying excess equipment translates into increased fuel consumption. Some procedures to reduce weight were outlined in Section 4.3. However no excess

equipment has been specifically identified on KC-135 aircraft. Figure 7.6-15 illustrates the sensitivity of fuel/DOC to variations in system weight for KC-135. This plot may be used to estimate fuel savings due to removal of excess equipment.

7.6.5.10 Maintenance to Reduce Drag

A direct quantification of savings is difficult in this case. Fuel/DOC savings due to aircraft maintenance which results in reduced drag may be estimated from the plots depicting sensitivity of fuel/DOC to changes in aircraft drag. These plots are given in Section 7.6.6. For example, a one percent reduction in zero lift drag due to maintenance results in 0.6% savings in annual fuel consumption for KC-135.

7.6.5.11 Engine Maintenance

Thrust specific fuel consumption (TSFC) on J-57 engines deteriorates almost 3-6% between overhauls. Because of parts replacements during a series of overhauls, the average engine performance is deteriorated about 5% [26]. A specific approach to reducing engine deterioration is an engine trending technique used by airlines. SAC has done considerable work in this area and now has their entire fleet of KC-135 participating in an Engine Inflight Monitoring System [27]. Fuel savings due to improved maintenance procedures may be estimated using Figure 7.6-14 which depicts changes in fuel/DOC due to changes in TSFC for KC-135. On the assumption that improved engine maintenance procedures result in a 1.5% improvement in TSFC, Figure 7.6-14 indicates a corresponding 1.4% reduction in annual fuel consumption.

7.6.6 Evaluation of Design Modifications

Since the KC-135A introduction, significant technological improvements have been developed that now may be applied to airplanes to improve their effectivity. As mentioned earlier, several studies are underway to enhance the capability and extend the life of the KC-135. The Air Force is planning to install winglets on KC-135 to improve the efficiency of the tanker fleet. As a result of the structural

fatigue tests, the lower wing surfaces of the tankers are being reskinned. This modification will give the airframe an additional 27,000 hours of useful life. A re-engining program is under consideration which would take advantage of this increased service life and at the same time overcome the environmental and operational problems of the existing J57 engines [43]. This section evaluates some of the design modifications under consideration for KC-135 aircraft.

7.6.6.1 Parametric Analysis of Aerodynamic and Propulsion Design Changes

Figures 7.6-12, 13 and 14 are the generic plots of % variation in fuel/DOC as a function of % variations in zero-lift drag, induced drag and thrust specific fuel consumption, respectively for KC-135. Figure 7.6-15 illustrates changes in fuel/DOC due to changes in TOGW. These plots were generated by using the four mission profiles given in Section 7.2. As mentioned in Section 5, these generic plots are generated under the assumption that design modifications will not appreciably impact the operational procedures. For example, the primary mission of the KC-135 tanker is to refuel other aircraft. Thus the cruise altitude of KC-135 is constrained by the refueling requirements. The generic plots reflect constraints such as these and are extremely useful in evaluating design modifications for the KC-135 as long as its mission profiles are generally the same.

7.6.6.2 Retrofitting KC-135 with Winglets

As mentioned in Section 5, Reference [36] carries out a design and analysis of winglets for KC-135 and provides data for retrofitting winglets on KC-135. This data was used in Section 5.5.1 to analytically evaluate the improvement in performance/cost due to winglets for KC-135. Note that the analytical evaluation in Section 5.5.1 assumes optimum operational conditions for a ferry mission and indicates a 7.6% improvement in ferry range. The winglet design data used in Section 5.5.1 shows a 19.4% reduction in induced drag, a 0.81% reduction in zero-lift drag and a 592 lb. increase in OEW. From Figure 7.6-12 a 0.81% reduction in zero-lift drag results in a 0.5% reduction in fuel consumption and a 0.37% reduction in DOC. From an extrapolation of Figure 7.6-13, a 19.4% reduction in induced drag

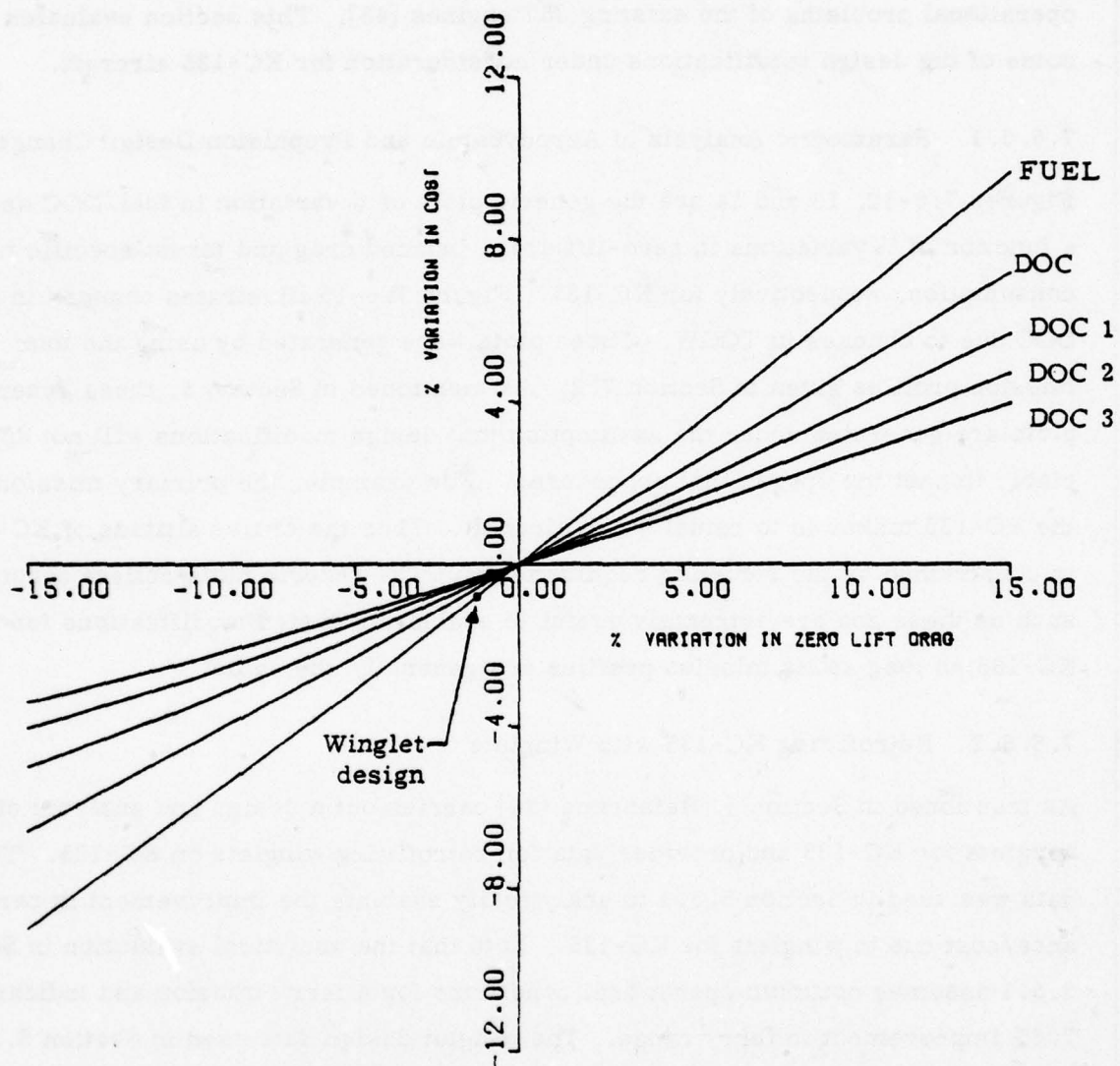


Figure 7.6-12 SENSITIVITY OF FUEL/DOC TO VARIATIONS IN ZERO LIFT DRAG -KC135

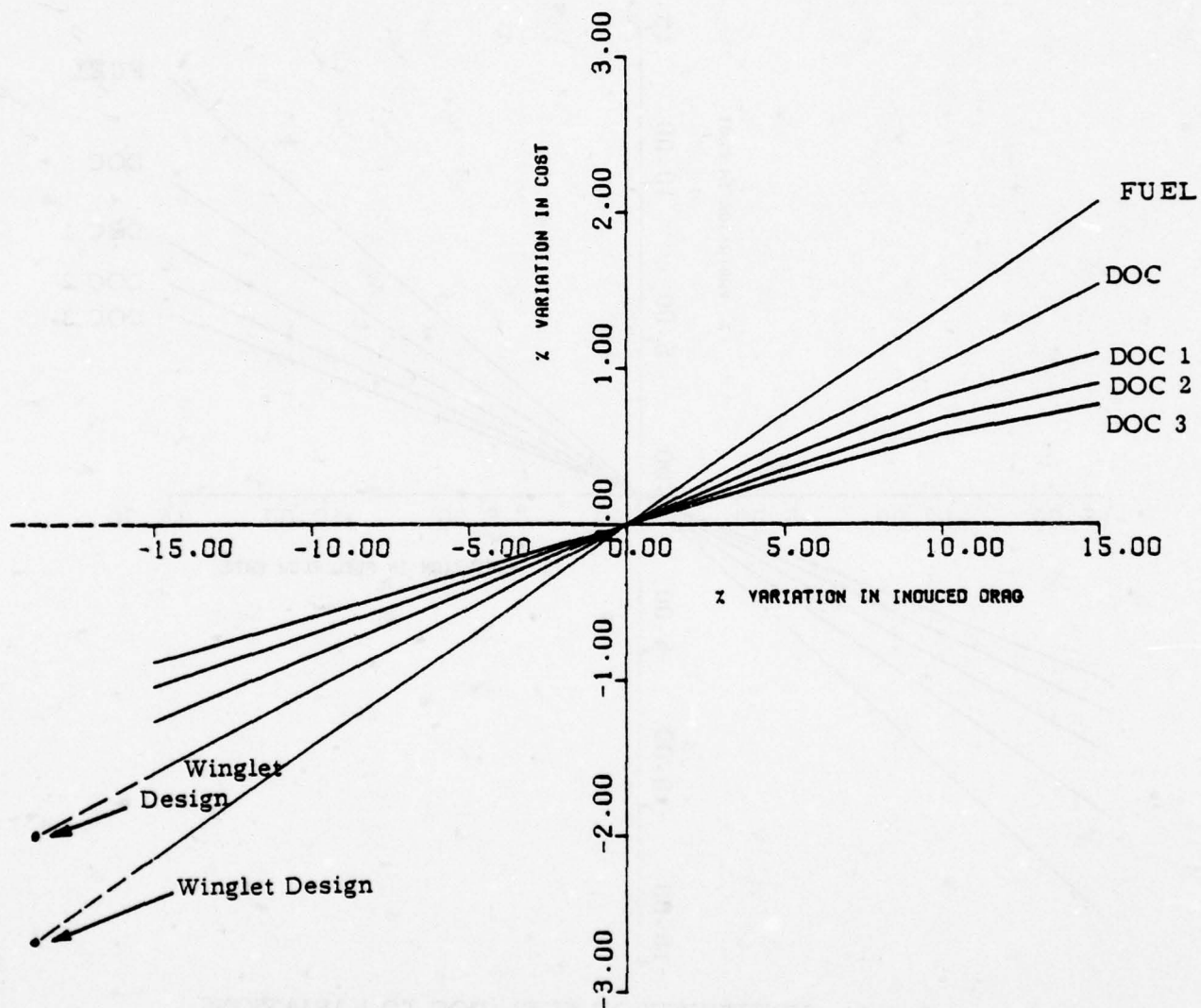


Figure 7.6-13 SENSITIVITY OF FUEL/DOC TO VARIATIONS IN
INDUCED DRAG KC-135

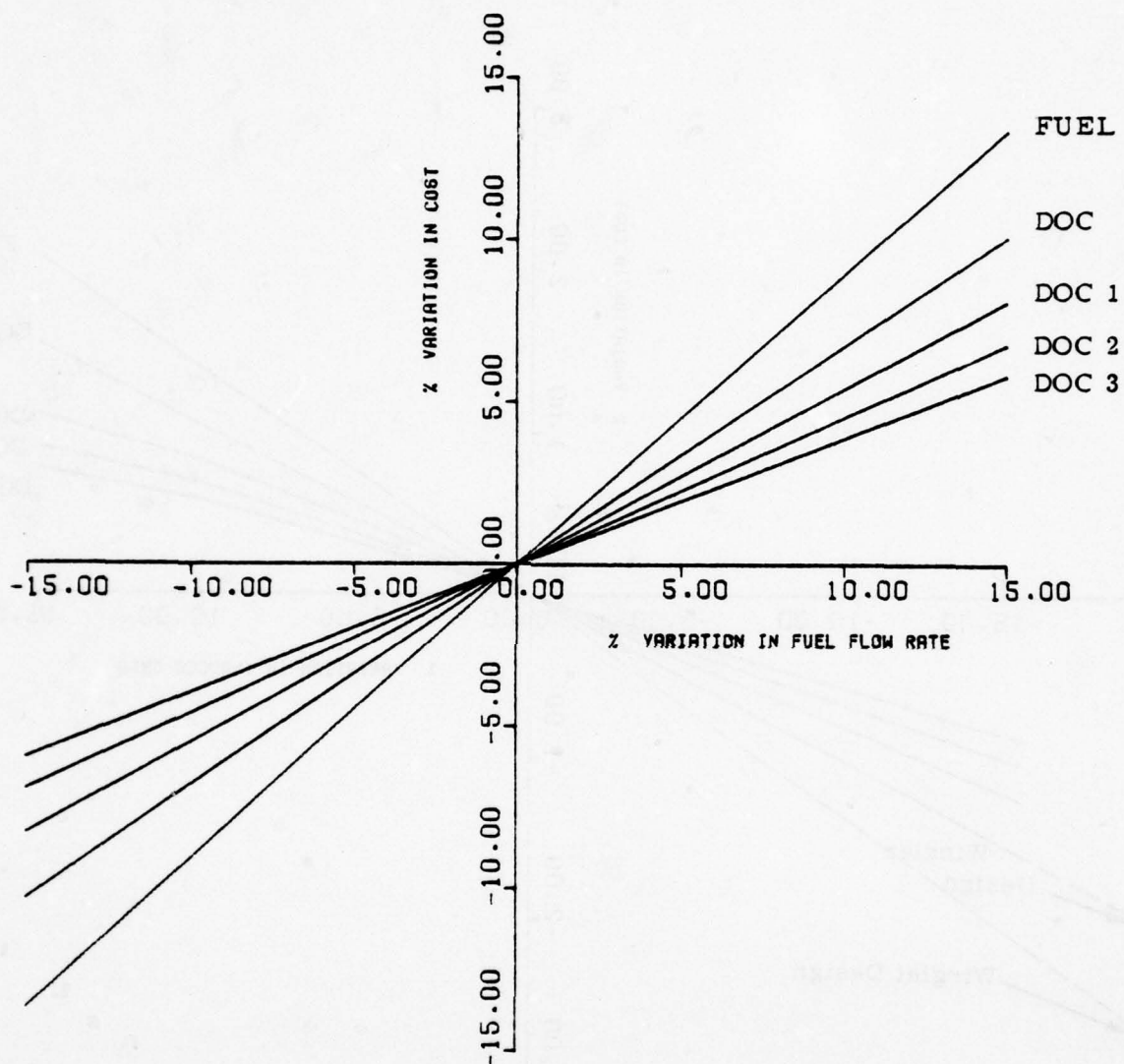


Figure 7.6-14 SENSITIVITY OF FUEL/DOC TO VARIATIONS
IN THRUST SPECIFIC FUEL CONSUMPTION
KC-135

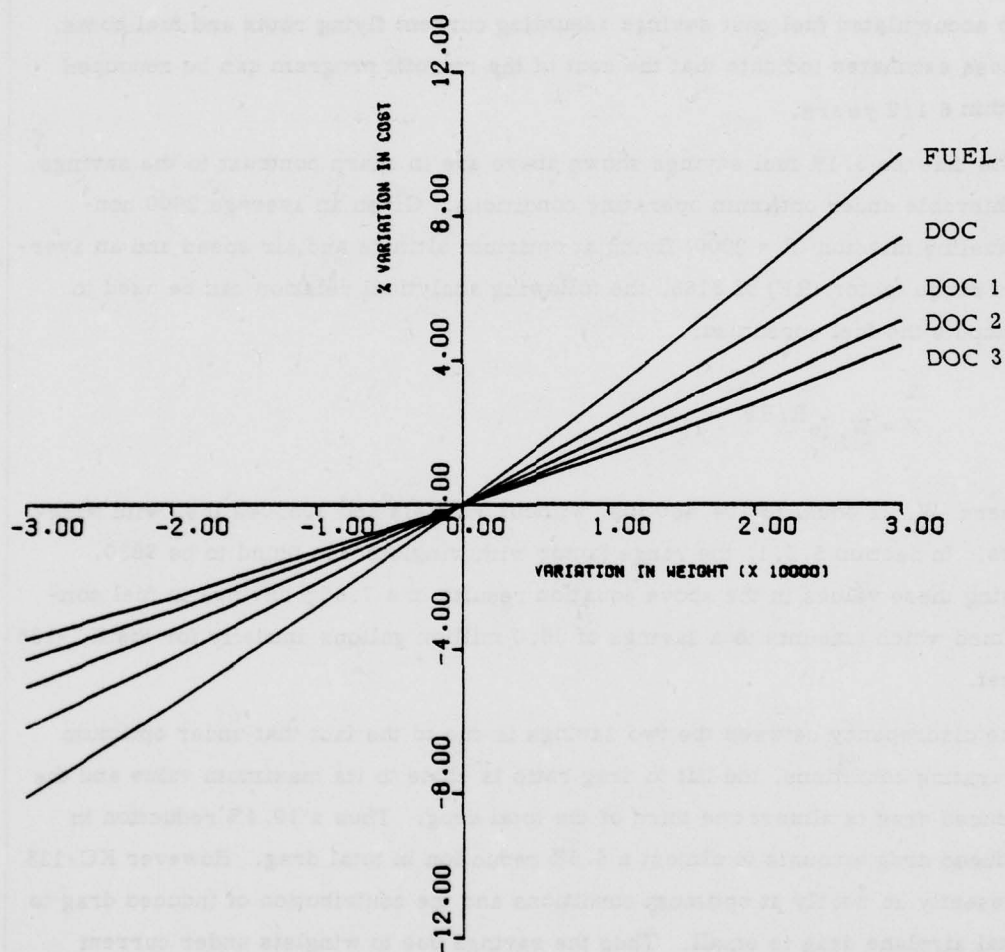


Figure 7.6-15 SENSITIVITY OF FUEL/DOC TO VARIATIONS
IN WEIGHT - KC-135

yields a 2.77% reduction in fuel consumed and a 2.06% reduction in DOC. Figure 7.6-15 gives an 0.17% increase in fuel consumption and 0.13% increase in DOC due to a 592 lb. increase in aircraft weight. The total net savings in fuel and DOC amount to 3.1% and 2.30%, respectively. This results in 14.2 million gallons of fuel and \$5.9 million in DOC savings annually. The estimated cost of retrofitting winglets on KC-135 is \$37.9 million[43]. Figure 7.6-16 illustrates the accumulated fuel cost savings assuming current flying rates and fuel costs. These estimates indicate that the cost of the retrofit program can be recouped within 6 1/2 years.

Note that the 3.1% fuel savings shown above are in sharp contrast to the savings achievable under optimum operating conditions. Given an average 2000 non-refueling mission ($R = 2000$) flying at optimum altitude and air speed and an average range factor (RF) of 8168, the following analytical relation can be used to compute the fuel consumed:

$$F = W_f [e^{R/RF} - 1]$$

where W_f is equal to 104,450 lbs. without winglets and 105,042 lbs. with winglets. In Section 5.5.1, the range factor with winglets was found to be 8830. Using these values in the above equation results in a 7.86% savings in fuel consumed which amounts to a savings of 36.0 million gallons annually for the KC-135 fleet.

The discrepancy between the two savings is due to the fact that under optimum operating conditions, the lift to drag ratio is close to its maximum value and the induced drag is almost one third of the total drag. Thus a 19.4% reduction in induced drag amounts to almost a 6.5% reduction in total drag. However KC-135 presently do not fly at optimum conditions and the contribution of induced drag to total airplane drag is small. Thus the savings due to winglets under current operating conditions are small compared to savings under optimum conditions.

ACCUMULATED SAVINGS
(MILLIONS OF \$)

COST/SAVINGS TRADEOFF: (1978 DOLLARS JP-4 @ 42 CENTS GAL.)

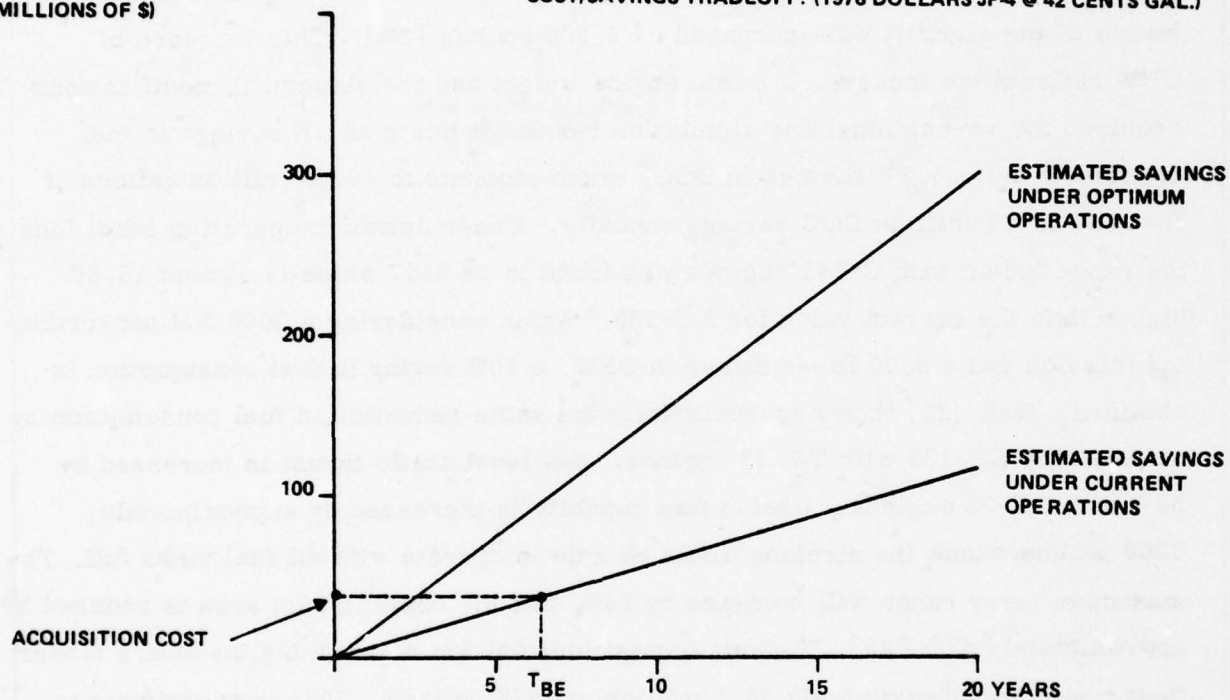


Figure 7.6-16 RETROFITTING KC-135 WITH WINGLETS

7.6.6.2 Re-engine KC-135

As mentioned in Section 5.4, several alternatives for re-engining the KC-135 are under consideration. One of the re-engined configurations replaces all four existing J57-P-59W turbojet engines with P&WA TF-33-P7 turbofan engines like those presently used on C-141 aircraft. Since mathematical models describing propulsion characteristics of TF-33 engines were developed in this study, these models were used for simulating KC-135 missions. Mission range, cruise altitude and air speed, and the landing fuel weight were kept the same. Operational empty weight of the aircraft was increased by 6,300 pounds [39]. This increase in OEW reflects the increase in basic engine weight and the structural modifications required for re-engining. The simulation results indicate an 8% savings in fuel consumed and a 6.3% savings in DOC, which amounts to 36.65 million gallons of fuel and \$16.1 million DOC savings annually. Under optimum operating conditions, the range factor with C-141 engines was found to be 9457 which is almost 15.8% higher than the current value for KC-135. Again considering a 2000 NM non-refueling mission and a 6300 lb. increase in OEW, a 10% saving in fuel consumption is obtained. Ref. [39] shows approximately the same reduction in fuel consumption by re-engining KC-135 with TF-33 engines. Sea level static thrust is increased by 53% with TF-33 engines. Usable fuel capacity is increased by approximately 2000 gallons since the airplane would be able to operate with all fuel tanks full. The maximum ferry range will increase by 14%, and the noise impact area is reduced by approximately 87% [39]. The unit acquisition cost for re-engining the entire tanker fleet would be approximately \$5.5 million in 1978 dollars. This cost estimate is based on the information given in Ref. [39] where an 8% inflation factor has been used. Thus total acquisition cost will be \$3,146 million in 1978 dollars. Savings in maintenance cost will be approximately equal to the difference between the direct maintenance costs of C-141 and KC-135 aircraft given in Sections 7.1.3 and 7.6.3. This savings amounts to \$243/FH. The assumption here is that the difference in maintenance costs of C-141 and KC-135 are due to differences in engines. Thus based on FY76 flying hours the total savings in fuel and maintenance cost will amount to \$58.7 million annually. Based on these values the break-even time period is more than the expected life of KC-135 fleet. Figure 7.6-17 shows

ACCUMULATED SAVINGS
(MILLIONS OF \$)

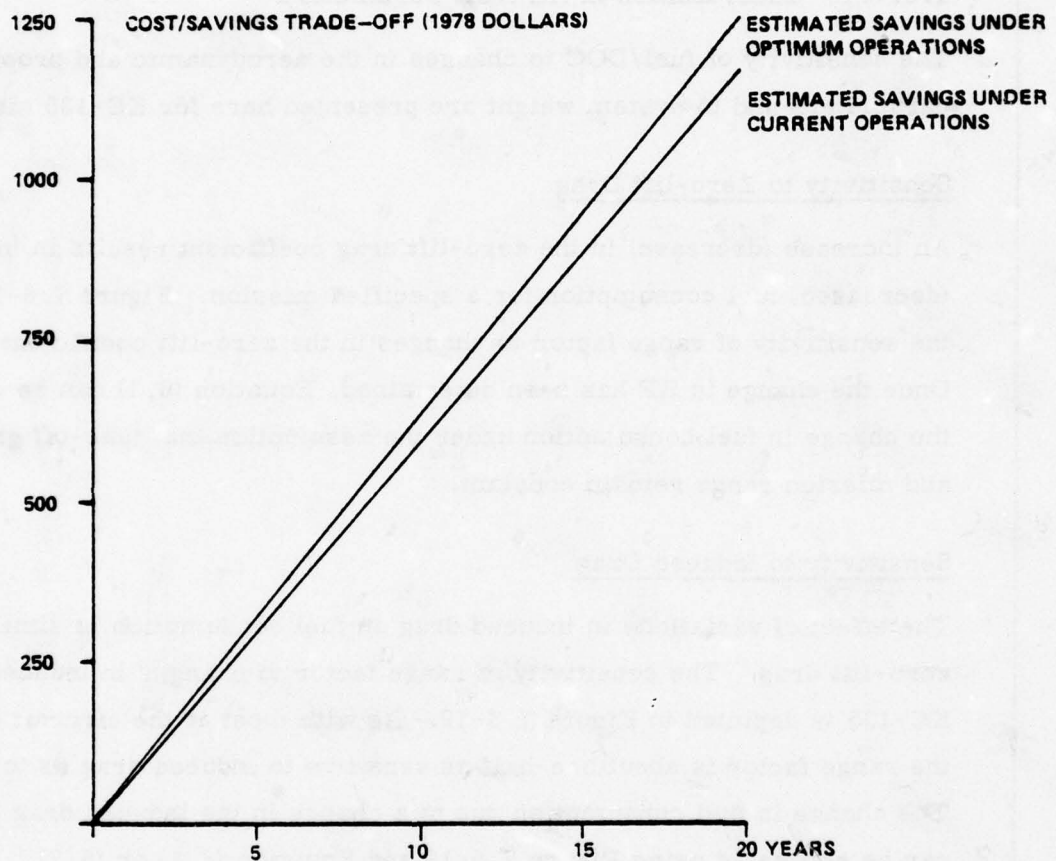


Figure 7.6-17 SAVINGS DUE TO REENGINEING KC-135
WITH TF-33

the estimated total savings over the next 20 years. Accumulated savings are much smaller than the acquisition cost; thus re-engining the KC-135 with TF-33 does not seem to be cost effective.

7.6.7 Sensitivity Analysis

This section summarizes the results of the sensitivity analyses conducted for the KC-135.

7.6.7.1 Uncertainties in Aircraft Parameters

The sensitivity of fuel/DOC to changes in the aerodynamic and propulsion parameters and to system weight are presented here for KC-135 aircraft.

Sensitivity to Zero-lift Drag

An increase (decrease) in the zero-lift drag coefficient results in increased (decreased) fuel consumption for a specified mission. Figure 7.6-18 depicts the sensitivity of range factor to changes in the zero-lift coefficient for KC-135. Once the change in RF has been determined, Equation (6.1) can be used to obtain the change in fuel consumption under the assumption that take-off gross weight and mission range remain constant.

Sensitivity to Induced Drag

The effect of variations in induced drag on fuel consumption is similar to that of zero-lift drag. The sensitivity of range factor to changes in induced drag for KC-135 is depicted in Figure 7.6-19. As with most of the aircraft under study, the range factor is about one-half as sensitive to induced drag as to zero-lift drag. The change in fuel consumption due to a change in the induced drag coefficient can be estimated using Figure 7.6-19 and Equation (6.1) or (6.2).

As an example, consider that the induced drag coefficient of a particular KC-135 aircraft is 5% higher than the nominal value. Figure 7.6-19 shows a 1.5% reduction in range factor. The average range factor for KC-135 aircraft is 8168. On the assumption that landing weight and mission range remain constant, Eq. (6.2) estimates a 1.6% increase in fuel consumption for a 1000 n.mi. mission.

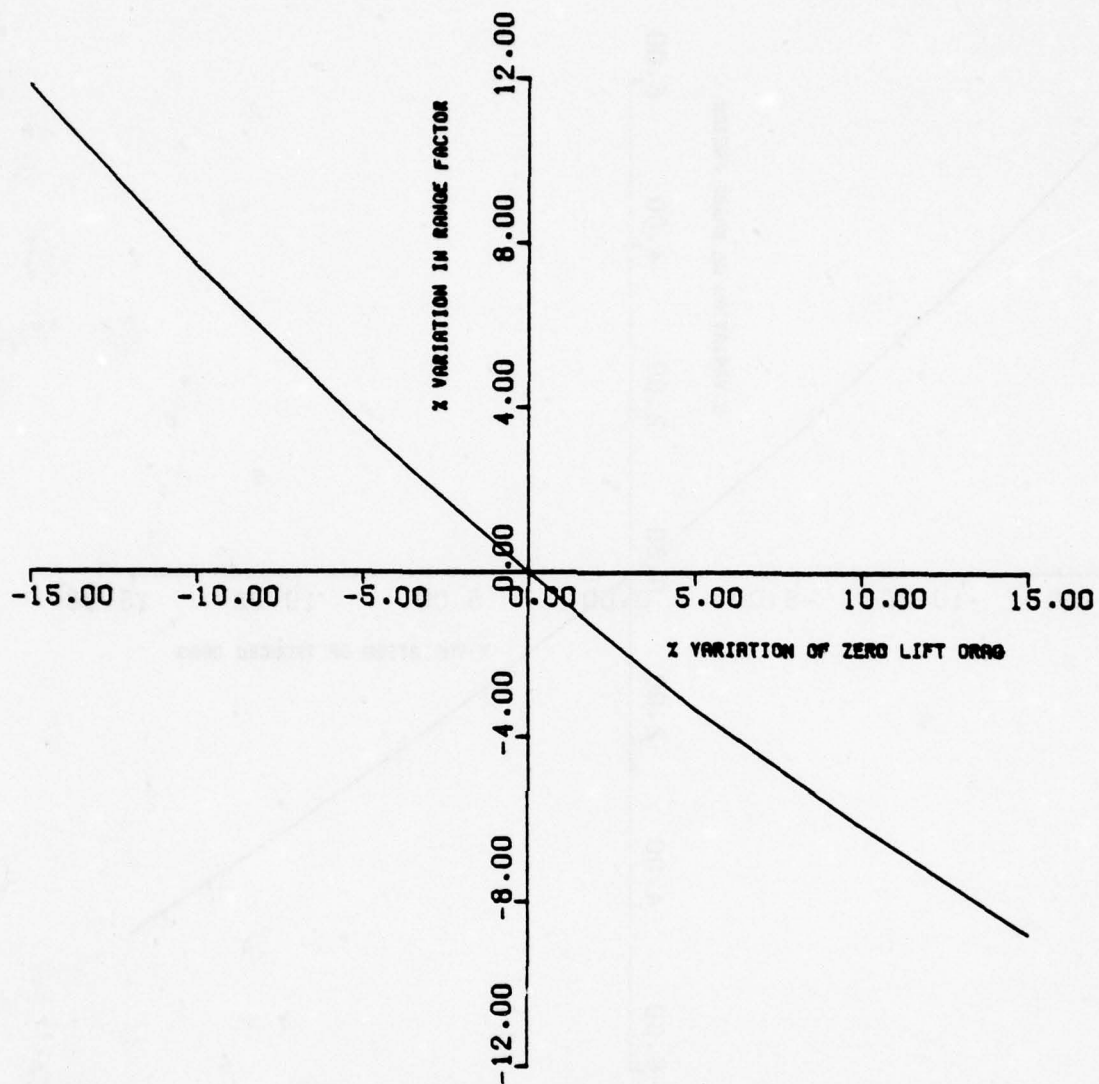


Figure 7.6-18 SENSITIVITY OF RANGE FACTOR TO VARIATIONS
IN ZERO-LIFT DRAG - KC-135A

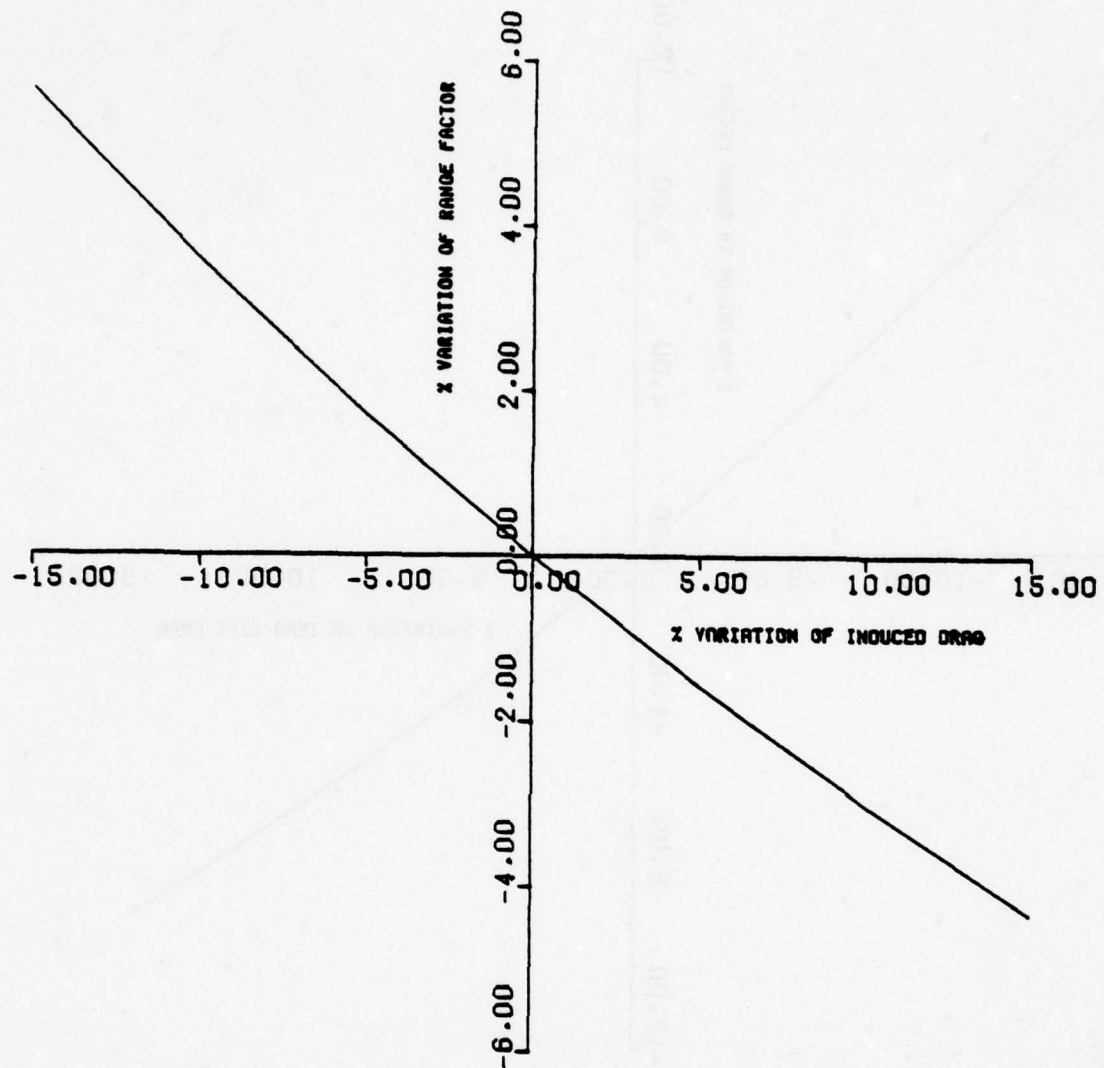


Figure 7.6-19 SENSITIVITY OF RANGE FACTOR TO
VARIATIONS IN INDUCED DRAG-
KC-135A

Sensitivity to Fuel Flow Rate

Since range factor is inversely proportional to fuel flow rate, an increase in TSFC reduces range factor. Given the reduction in RF Equation (6.2) may be used to compute the increase in fuel consumption. Note that Equation (6.2) was derived under the assumption that landing weight and mission range remain constant. For example, a 5% increase in TSFC results in a 5.3% increase in fuel consumed for a 1000 n. mi. mission.

Sensitivity to System Weight

Equation (6.3) provides the relation between change in fuel consumption and change in system weight. From this equation a 5% reduction in TOGW results in approximately a 5% savings in fuel consumption.

Sensitivity to Variations in Maximum Thrust

As mentioned in Section 6.1, a decrease in NRT lowers the cruise ceiling. So long as optimum cruise altitude remains below cruise ceiling, the cruise solution is not affected by the changes in NRT. Figure 7.6-20 illustrates the variation in cruise altitudes due to variations in NRT for a 247,600 pound aircraft. The optimum cruise altitude is 32,000 feet. Observe that a 10% reduction in NRT results in a 3400 foot decrease in cruise altitude. Figure 7.6-24 illustrates the impact of flying-off optimum cruise altitude on RF. From this figure it is seen that the range factor will decrease by 2% for a zero lift decrease in cruise altitude. The climb performance is also affected by the changes in NRT. However for most of the missions, the impact on fuel consumed will be negligible so long as the optimum altitude is below the cruise ceiling.

7.6.7.2 Sensitivity to Atmospheric Variations

Atmospheric variations which impact fuel consumption are wind velocities and ambient temperatures.

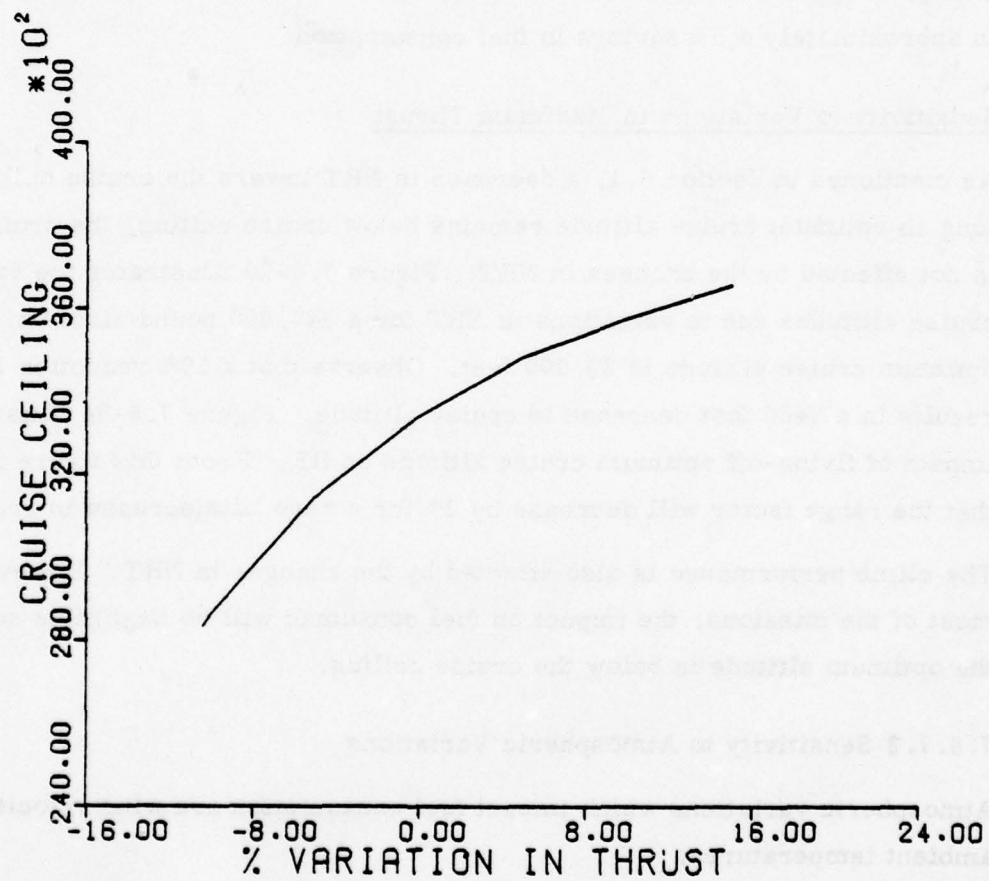


Figure 7.6-20 IMPACT OF THRUST VARIATION ON
CRUISE CEILING FOR KC - 135

Temperature Effects

As long as the thrust required during cruise is less than NRT, changes in ambient temperature do not affect the fuel consumption. Mission time is modified slightly due to the change in true air speed for cruise below tropopause. The change in time may be estimated using Equation (6.6). For most of the KC-135 missions the temperature variations do not affect the fuel consumption.

Deviations in temperature have a large effect on climb performance. However, changes in fuel consumed during a mission will be small if the cruise altitude remains below the cruise ceiling.

Wind Effects

Head winds increase the fuel consumption, and tail winds reduce it. Winds have a small effect on the optimum min fuel cruise Mach number for KC-135 as shown by Figure 7.6-21. Head winds increase the optimum cruise Mach number slightly whereas tail winds reduce it. Figure 7.6-22 illustrates changes in range factor due to wind for a KC-135 aircraft. Observe that a 100 knot head wind decreases the range factor by 22%, whereas a tail wind increases it by approximately the same amount.

7.6.7.3 Sensitivity to Traffic Density

An increase in air traffic density near an airport generally results in take-off delays and increased holding times. The average fuel flow rate during ground operations for KC-135 is 105 lbs/minute. Thus the increase in fuel consumption due to a take-off delay can be estimated if the delay time is known. The fuel consumption rate during holding varies with holding altitude and aircraft weight. Given an average holding weight of 125,000 pounds the fuel flow rate during holding at the optimum holding altitude is 115 lbs/minute.

7.6.7.4 Sensitivity to Instrument Errors

Instrument errors may result in flying off the optimum altitude and cruise mach number, thus resulting in an increase in fuel consumption. Figures 7.6-23 and

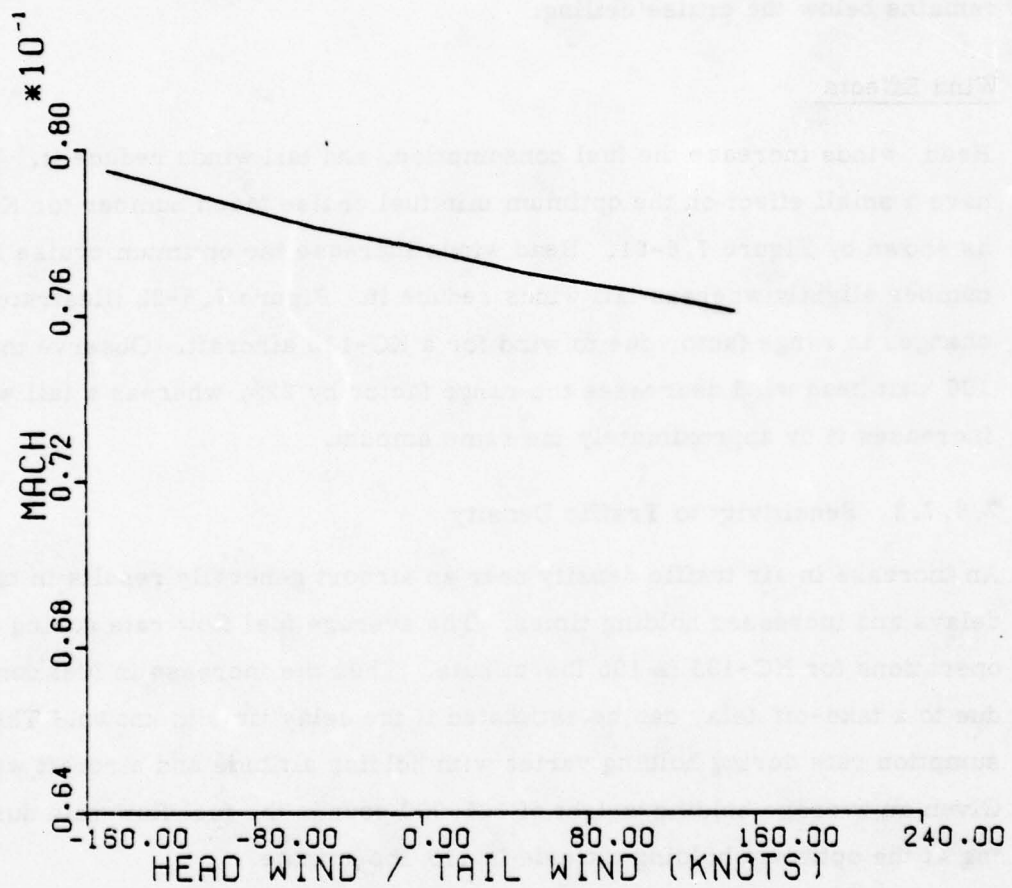


Figure 7.6-21 IMPACT OF WIND ON OPTIMUM CRUISE
MACH NUMBER FOR KC - 135

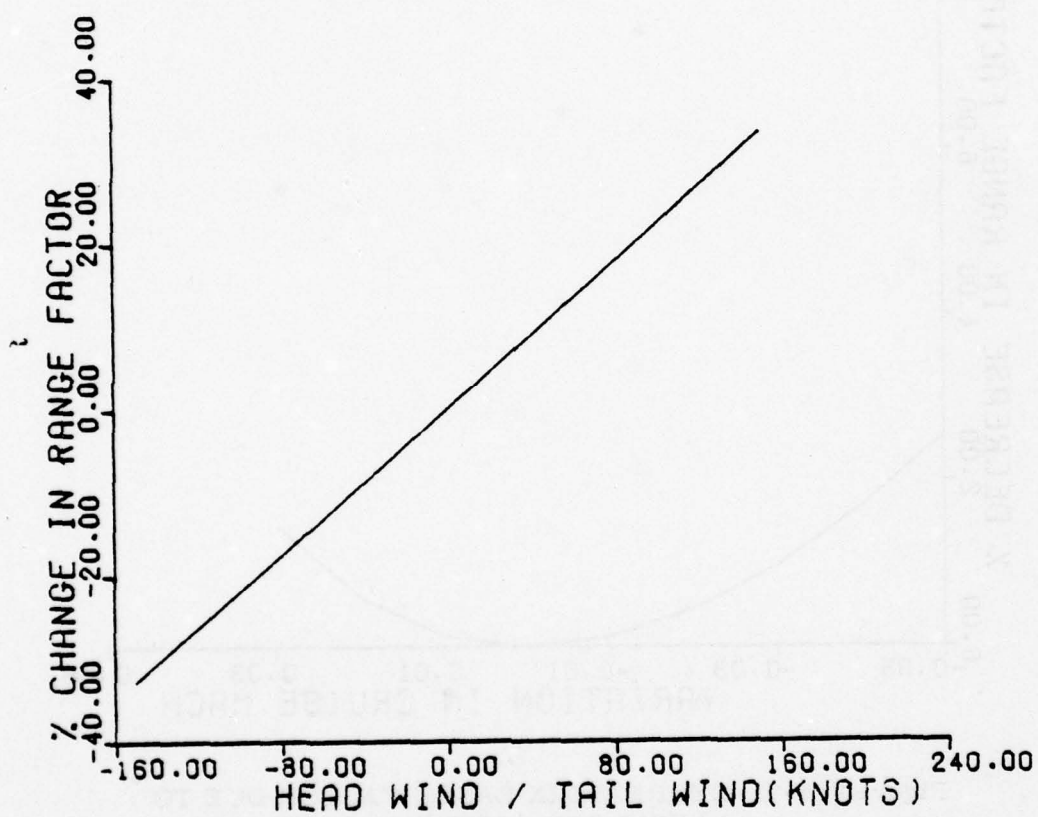


Figure 7.6-22 Impact of Wind on Range Factor for KC-135

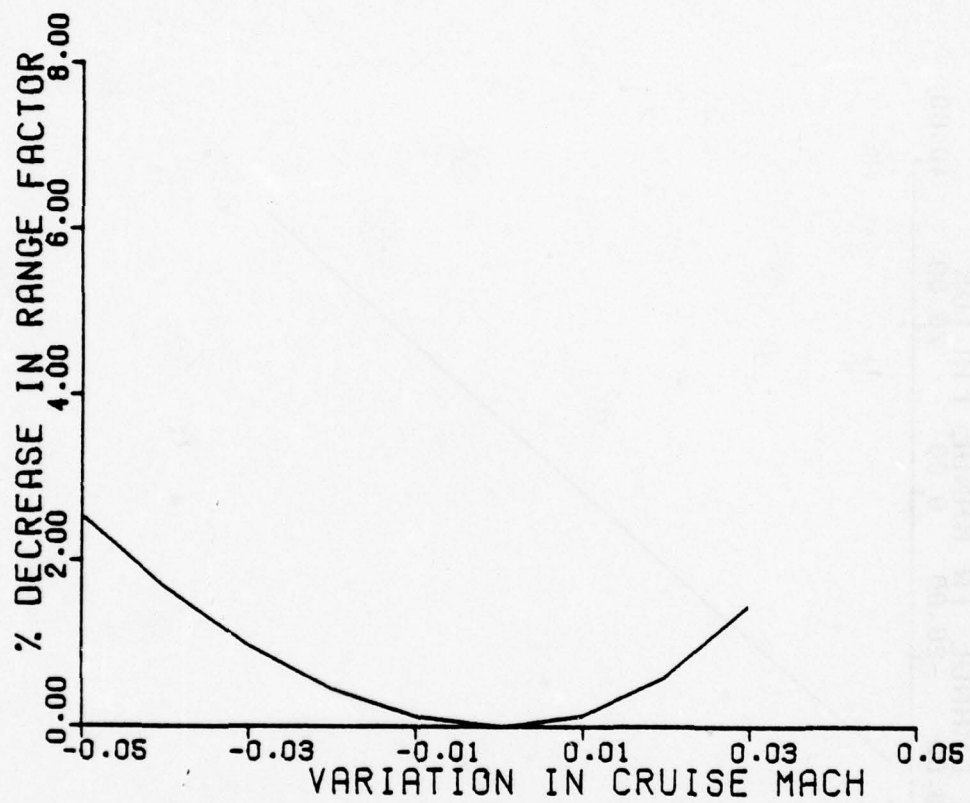


Figure 7.6-23 DECREASE IN RANGE FACTOR DUE TO
FLYING OFF OPTIMUM CRUISE MACH
NUMBER - KC-135

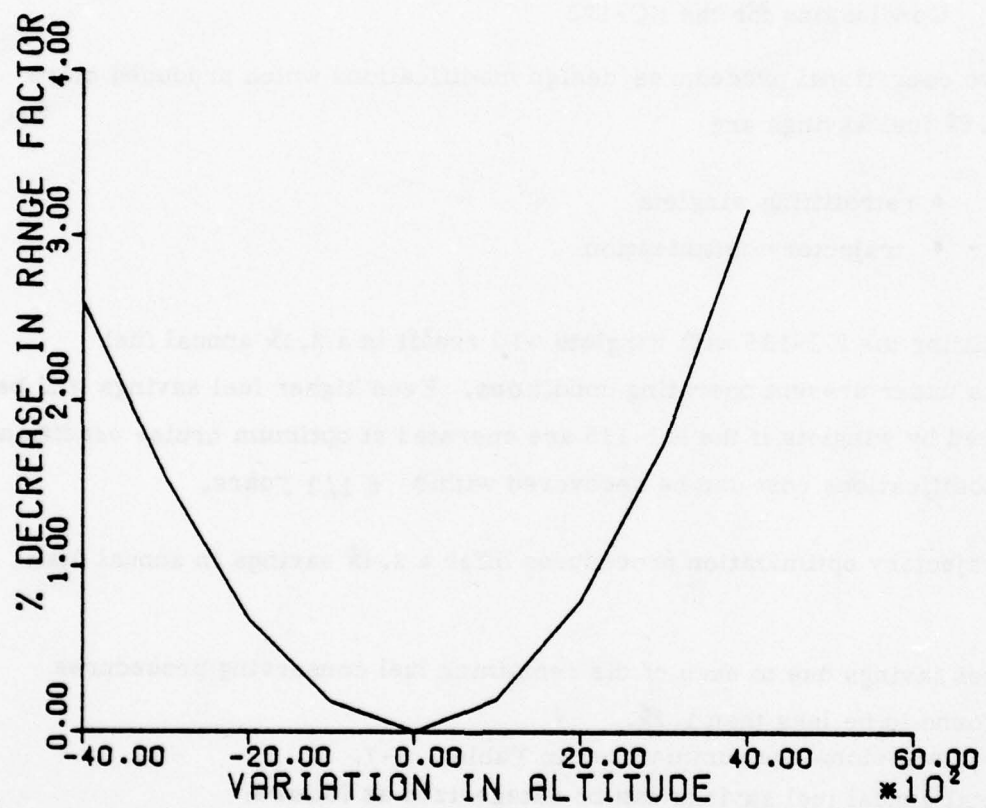


Figure 7.6-24 DECREASE IN RANGE FACTOR DUE TO FLYING
OFF OPTIMUM CRUISE ALTITUDE - KC-135

24 illustrate the sensitivity of range factor, RF, to deviations from the optimum cruise mach number and altitude, respectively. These plots can be used in conjunction with Equation (6.1) to obtain the increase in fuel consumption due to instrument errors. Changes in cruise mach also affect the mission time, which in turn affect the DOC. Altitude variations also impact mission time because for a constant mach cruise the true air speed will vary with altitudes. The DOC models given in Section 7.6.3 can be used to obtain the sensitivity of the DOC to instrument errors.

7.6.8 Conclusions for the KC-135

The two operational procedures/design modifications which produced more than 1.5% fuel savings are

- retrofitting winglets
- trajectory optimization

Retrofitting the KC-135 with winglets will result in a 3.1% annual fuel savings under present operating conditions. Even higher fuel savings will be produced by winglets if the KC-135 are operated at optimum cruise conditions. The modifications cost can be recovered within 6 1/2 years.

The trajectory optimization procedures offer a 3.4% savings in annual fuel.

The fuel savings due to each of the remaining fuel conserving procedures were found to be less than 1.5%.

These conclusions are summarized in Table 7.6-7.

The total annual fuel savings can be categorized as follows:

• Design modification	3.1 - 7.8%
• Airborne operational procedures	3.9 - 4.9%
• Ground operation procedures	3.0 - 4.2%

Procedures	Estimated Percentage Annual Fuel Savings	Break Even Period Years	Confidence In Estimates
Design Modifications			
Retrofitting winglets	3.1 - 7.8	2.5 - 6.4	High
Airborne Operational Procedures			
Trajectory optimization	3.4	-	High
All others	.5 - 1.5	-	Medium
Ground Operational Procedures			
Engine maintenance	1 - 1.5	-	Medium
Reduce reserve fuel	1 - 1.5	-	Medium
All others	.5 - 1.2	-	Medium
Total	9.5 - 16.9		

Table 7.6-7 ESTIMATED FUEL SAVINGS FOR THE KC-135

SECTION 8

IMPACT OF REDUCED FUEL ALLOCATION ON OPERATIONAL READINESS

This section will discuss the effect of reduced fuel allocations on operational readiness. Due to rising costs and increased scarcity, fuel allocations to SAC and MAC are far below pre-1973 levels. In 1974, the United States Air Force consumed less jet fuel (all grades) than in any previous year since 1958. Consumption levels dropped from a high of 202.5 million barrels in 1969, to 150.2 million barrels in 1973, to a low of 94.2 million barrels in 1974. While part of this decline can be attributed to a termination of Air Force involvement in Southeast Asia, the decline in the early 70's was due to the impact of rising costs and the short-lived Arab oil embargo. Consumption climbed slightly in 1975, but was still short of pre-1973 levels. In light of the reduced availability and rising costs of fuel, the Air Force has had to reduce flying hours and the total number of aircraft in the inventory (see Table 8-1).

Congress through the Government Accounting Office (GAO), the President through the Office of Management and Budget (OMB), and the Office of the Secretary of Defense (OSD) all have a common goal: a reduction in military flying time by FY81. This reduction in flight time is easiest to accomplish by reducing the fuel available to the military; thus forcing the various using commands such as SAC and MAC to develop more efficient fuel management procedures and flying programs in order to meet operational commitments and training objectives. Now that many of the available measures to achieve efficiency have been put into effect, further reductions tend to become much more difficult to absorb without compromising the readiness of the aircraft fleet or aircrew. It will be our purpose here to discuss the impact of a hypothetical ten percent reduction in fuel allocation on this aircrew readiness.

Table 8.1-1
FLYING HOURS VS. FUEL CONSUMPTION (USAF)

Fiscal Year	Flying Hours	Aircraft Inventory	Jet Fuel (millions of barrels)
1968	7,485,277	14,270	194.2
1969	7,475,392	13,719	202.5
1970	6,808,525	13,026	176.8
1971	5,963,705	12,124	155.3
1972	5,302,298	10,996	150.7
1973	4,744,688	10,414	150.2
1974	3,655,109	10,170	94.2
1975	3,492,488	9,587	100.8
1976	3,110,160	7,260	101.6

8.1 OPERATIONAL EFFECTIVENESS

For a flightcrew to be operationally effective, it must be ready to perform all missions set forth for a particular aircraft in all environments without additional training. Although normal operational missions provide some contingency training, the conventional means of assuring this operational effectiveness is to provide separate training missions when flying hour allocations permit. As fuel became scarcer and more expensive after 1973, these training flights were reduced and a greater dependence on alternatives, such as simulator training, were considered.

Figure 8.1-1 shows the total amount of fuel used by the aircraft evaluated in this study for fiscal year 1976.

Figure 8.1-2 breaks this information down further by displaying how SAC and MAC apportioned their fuel between operational missions and training missions. Calculation of these figures was based upon the mission and fuel consumption data collected from SAC and MAC presented in earlier chapters. In regard to the B-52, only pilot proficiency missions were considered in the training segment even though all B-52 missions could essentially be considered training. Also, all exercise missions and non-refueling missions (KC-135) were considered as training to calculate fuel usage. Consequently, the fraction of missions that are training related might seem high, but it was the purpose of this section to separate true operational missions from other types of missions.

There are few alternatives open to a using command when fuel allocations have been cut. For example, with a ten percent fuel allocation reduction, the using commands may either reduce the number of sorties

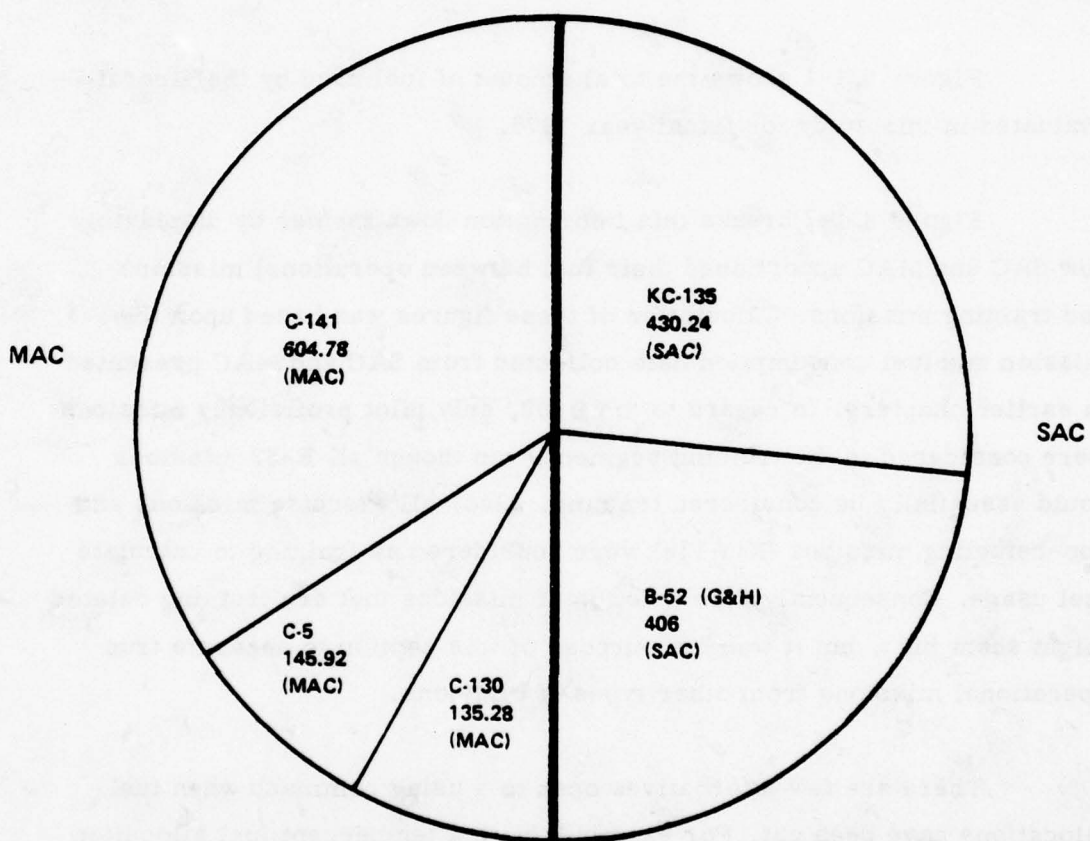


Figure 8.1-1 AIRCRAFT FUEL CONSUMPTION FY 1976 (millions of barrels)

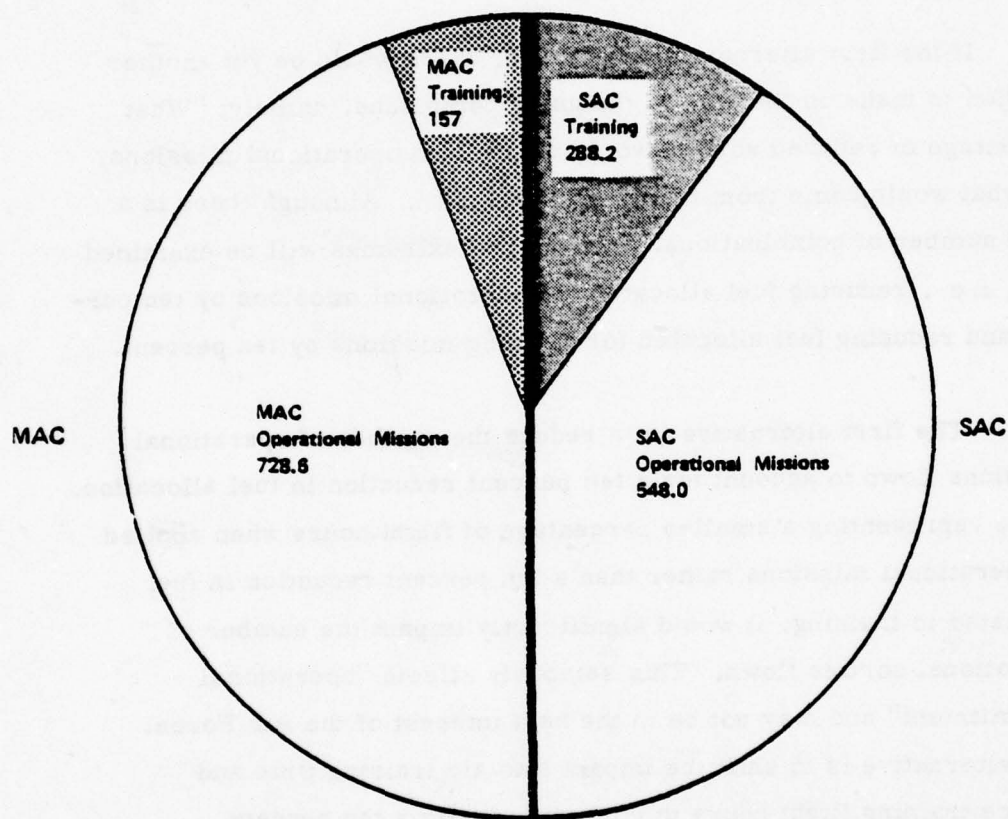


Figure 9.1-2 FUEL UTILIZATION (FY 1976) BY COMMAND
(millions of barrels).

flown to correspond with the ten percent full reduction, or else reduce the fuel per aircraft per sortie by ten percent. The latter option would reduce range and endurance, but, since most SAC and MAC missions are fixed as to time spent in the air and distance flown, this alternative is not realistic. A small percentage of flights could accept a reduced fuel allocation without significant impact, but could not absorb the total fuel reduction.

If the first alternative were taken, there would be yet another decision to make on the part of the using commands, namely; "What percentage of reduced sorties would come from operational missions, and what would come from training missions?". Although there is a large number of combinations, only the two extremes will be examined here, i.e., reducing fuel allocated for operational missions by ten percent and reducing fuel allocated for training missions by ten percent.

The first alternative is to reduce the number of operational missions flown to account for a ten percent reduction in fuel allocation. While representing a smaller percentage of flight hours when applied to operational missions rather than a ten percent reduction in fuel allocated to training, it would significantly impact the number of operational sorties flown. This seriously affects "operational commitment" and may not be in the best interest of the Air Force. The alternative is to shift the impact into air training time and reduce training flight hours to correspond with a ten percent reduction in fuel allocation.

Since training flights are flown to maintain and improve flight crew proficiency and train aircrews in mission procedures and emergency contingencies, a reduction in fuel of ten percent could seriously affect readiness in these areas if some other means of training were not substituted. Flight simulators could provide a partial solution to this problem, as could the combination of more operational and training missions. Significant simulator hardware and software development has taken place in the Air Force in the past few years much of which has been directed at training aircrews for the aircraft in this study. This simulator development became more cost effective as flight hour costs rose due to fuel costs and the other inflationary driven factors.

8.2 SIMULATORS

One of the major problems that became evident after the fuel reductions of 1973-1974 was that the Air Force had not kept up with the state-of-the-art in simulators, nor were there enough of the present simulators to ensure realistic supplemental training for aircrews. The design of flight simulators had advanced to the point where they were capable of accurately portraying the aerodynamic responses of aircraft to control inputs and of reproducing realistic cockpit instrument indications for almost all flight situations [57]. This capability had come about as a result of commercial airlines concern for training costs and from NASA space research efforts.

The Air Force had been slow in taking advantage of this capability and in utilizing the experience gained by both the private airlines and NASA's use of simulators. The reasons are varied and range from a lack of knowledge of the available capability to a lack of sufficient budgetary funds for both aircraft development/acquisition and for simultaneous support of a large simulator development effort. Some of these problems were expressed by Lt. General William V. McBride in the Commander's Digest dated 15 August 1974. In that article, General McBride stated reasons such as "preoccupation with the war in Vietnam, budgeting restraints, maintenance problems on the few experimental models (simulators) which have been purchased during that period (since WWII), or maybe because the sheer human reluctance to adapt to new techniques." [58].

Prompted by declining O&S budgets, increasing fuel costs, and interest in fuel conservation, a resurgence of interest in ground-based simulators has come about since 1973. During the Arab oil embargo, the cost of jet fuel climbed from 14.9 cents per gallon in the fall of 1973 to 27.7 cents per gallon in February 1974. Further price increases pushed the level up to 43.3 cents per gallon in 1977. Relating this to the cost of flying training missions, in April 1973 it cost about \$5,400 to fill the tanks of a B-52H or a C-5A, while in October of that same year that figure had jumped to \$17,000. From the beginning of 1974 to the beginning of 1975, the cost per flying hour increased more than \$800 per hour, and the cost of training a new pilot had increased more than \$17,500 due to the increased cost of fuel [59]. To show how that has affected today's 'training' costs, Boeing charges commercial airlines \$1400/hour to train a pilot in an aircraft while charging only \$280/hour to train in a simulator. .

These figures show why Air Force using commands turned their attention toward simulator development. SAC trailed MAC in simulator development and use, relying upon older rail car mounted procedural trainers for the B-52 and KC-135. These simulators did not lend themselves to optimum ground simulation of flight conditions and had low in-commission time due to numerous maintenance problems. The down time and unavailability of simulators did not provide the necessary training capability.

MAC, on the other hand, had been making optimum use of simulators for initial, refresher, and proficiency training programs. While keeping abreast of the state-of-the-art, MAC's only problem was not having enough simulators to reduce flight training significantly. MAC's first approach to solving this problem was to supplement its supply of simulators by using those offered by other commands and commercial contractors.

Simulator technology has continued to advance in recent years as a result of commercial airlines and NASA development programs. A current assessment of simulator technology in regard to military bombers and transports aircraft is presented below in Table 8.2-1.

Table 8.2-1

SIMULATOR TECHNOLOGY ASSESSMENT

	Bomber			Transport		
	Motion	Visual	Sensor	Motion	Visual	Sensor
Taxi	1	1		1	1	
Takeoff	1	1		1	1	
Approach	1	1		1	1	
Landing	1	1		1	1	
Instrument Qualification	1			1		
Formation Flying				1	2	
Air-to-Surface Attack	1	3	3			
Refueling	1	2		1	2	
Navigation Exercises	1	3	3	1	3	2

Note: (1) Developed (2) Inadequate Simulation Capability
(3) Not Developed

These technological capabilities allow for effective training of military aircrews and for considerable savings in flight time for training purposes. Significant strides are being made to link visual systems to motional systems to provide a more realistic and effective training device. Considerable development yet remains, but with the resurgence of interest in more cost-effective simulators, significant advances should be seen in the next few years.

At the present time, SAC is investing approximately \$800 million over a five-year span to purchase combination full-mission simulators and part-task trainers for the B-52/KC-135 programs. Prototype part-task trainers are being developed to simulate aerial refueling for use by B-52 flight crews and KC-135 boom operators. Simulators for the B-52 offensive and defensive avionic stations will soon be available. These development programs will utilize state-of-the-art technology and as much off-the-shelf hardware as possible.

MAC is addressing the problem of continually upgrading their simulators to allow for the latest advances in the state-of-the-art while increasing their number of simulators to meet the ever-increasing demand for their use. In 1974 MAC acquired two visual systems multiplexed between two C-5 and two C-141 simulators. While proving to be a very good system, MAC continued to expand its simulator capabilities by including flight simulators with six degrees-of-freedom and expanded visual systems. Six degrees-of-freedom motion provides simulation of roll, pitch, yaw, heave, lateral sway, and longitudinal surge. The expanded visual systems that will be used by both MAC and SAC in future simulators will be similar to the General Electric Compu-scene display system (see Figure 8.2-1) developed ten years ago during the NASA Apollo program. These visual systems provide a 200 x 200 nautical mile computer-generated, out-the-window display with visibility ranges from zero to ceiling and visibility unlimited.

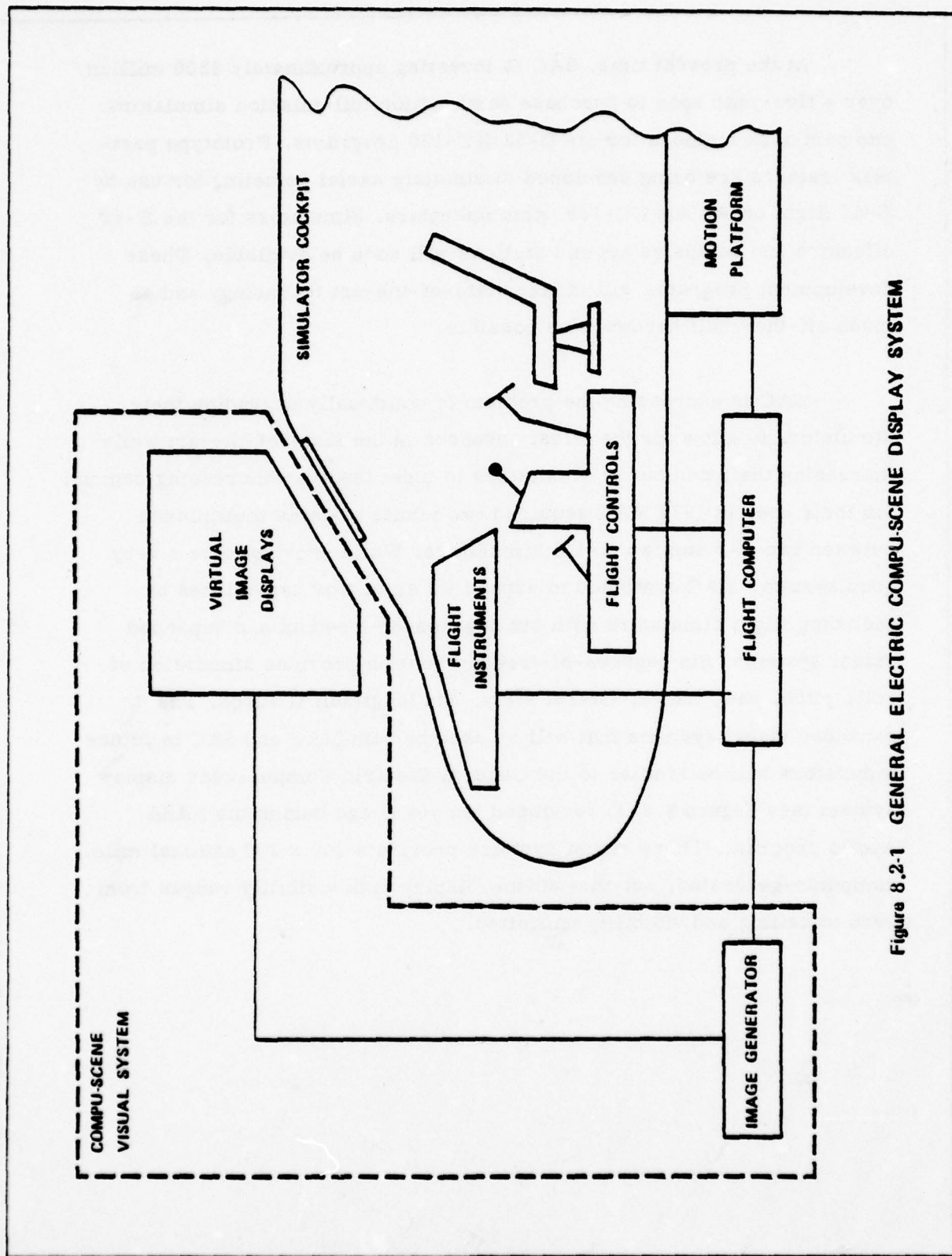


Figure 8.2-1 GENERAL ELECTRIC COMPU-SCENE DISPLAY SYSTEM

The C-5A and C-141 aircraft are successfully incorporating limited visual systems to reduce flying hours. Flying time for training pilots on these aircraft has been reduced 30 percent and 40 percent, respectively, due to the use of simulators. Simulators for the C-130 have proven to be incapable of satisfying all requirements and therefore, flying time for training can be reduced by only a small amount for this aircraft.

"The role of simulators as an integral part of current and future training programs has been established beyond question; research now should concentrate on how best to incorporate them into the total training environment in such a way as to reduce both complexity and cost. The tools for doing so are analysis, transfer studies, and controlled operational demonstrations."

In this statement, Colonel Fulgham and Dr. Hazin of the Flying Training Division of the Air Force Human Resources Laboratory, Brooks AFB, Texas, are identifying a problem that has been prevalent in many simulator training programs; namely, that the simulators were not used efficiently and effectively. Emphasis on both of these areas is critical to a quality training program. To teach a pilot the skills needed in an operational aircraft is considered effective training, but this is not enough; the simulator training must be cost-effective.

Existing systems, while not providing long acceleration or deceleration effects and not having the capability to generate inner ear responses such as those felt in actual flight conditions, can provide very realistic flight simulation. Given pilots with the proper attitude toward this type of training, these systems can be effectively used to simulate actual flight conditions.

In addition to reducing fuel consumption, which was the catalyst to the resurgence in simulator use, simulators also reduce noise and air pollution and have other benefits to provide. With fewer flights necessary through the use of simulators, there is a corresponding reduction in air traffic, a reduction in air space and air field requirements for the purposes of training, a freedom from weather constraints (which forced cancellation of many training flights), improved and increased training capability, and a better student retention (chiefly because the simulator allows the instructor to freeze conditions while discussing problems with his student). Training is also done on a no-risk basis where a pilot can take his "plane" to the edge of the aircraft's performance limits without jeopardizing human lives or expensive hardware. A major benefit is the significant cost saving that can result.

Table 8.2-2 is a comparative analysis of cost per flight hour versus cost per simulator training hour for the aircraft in this study. The major driver to this cost differential is of course the cost of fuel utilized per flight hour. Table 8.2-3 displays a breakdown of the anticipated number of flight hours to be saved in FY 1978 by the utilization of simulators, the resultant fuel savings in thousands of gallons based on present flight hour consumption rates, and the resultant dollar savings. As can be readily seen, simulators can save the Air Force some 117.7 million dollars in fuel costs during FY78 alone. As similar technology improves and a resultant increase in flight hour/simulator hour trade-off occurs, this fuel savings will increase.

Table 8.2-2

SAVINGS PER FLIGHT HOUR UTILIZING
SIMULATORS BY AIRCRAFT TYPE

Aircraft	Cost per FH(\$) (DOC + Fuel)	Simulator Cost/Hr. (\$)	Savings/Hr. (\$)
C-5	2194	263 - 329	1931 - 1865
B-52	2191	263 - 329	1928 - 1862
KC-135	1467	176 - 220	1291 - 1247
C-141	1293	155 - 194	1138 - 1099
C-130	556	67 - 83	489 - 473

Table 8.2-3

PROJECTED FY78 FUEL SAVINGS DUE TO SIMULATORS

Aircraft	Flight Hour Savings	Fuel Savings (thousands of gallons)	Dollar Savings (thousands)
B-52G	8,978	35,957	15,569
B-52H	4,996	16,936	7,333
C-5	16,823	58,123	25,167
C-130	17,688	13,885	6,012
C-141	26,554	53,772	23,283
KC-135	38,541	93,077	40,302

It should be noted that there are additional dollar savings from simulator utilization besides the resultant dollar savings in fuel. Although actual dollar values are not currently available, savings will be realized from reduced flight time of the aircraft due to fewer aircraft accidents, extended airframe life, reduced maintenance actions, reduced engine wear, reduced consumption of spares, and reduced missiles and munitions expended for purposes of training.

In conclusion, it is felt that further reduction in fuel allocation for either MAC or SAC would impair its present readiness capability. Reduction of fuel allocated to operational missions would seriously degrade the using command's capability to meet present operational commitments. A shift of this reduction in fuel allocation into the area of training flights would also present a significant impact on readiness; however, this impact could be partially offset by conducting more training during operational missions and by the increased development and use of simulators and part-task trainers. In addition, it is felt that the increased development and usage of simulators and part-task trainers can be beneficial both from a cost savings aspect and in providing a more efficient pilot/crew training program. However, simulators cannot replace all inflight training because it is essential to operate the hardware in the environment for which it was designed. With the human element involved, you need to operate the equipment where the mental awareness of criticality can be developed and the response to stress measured. These requirements cannot be realized in a trainer.

SECTION 9

CONCLUSIONS AND RECOMMENDATIONS

This study addressed improvements in design and operational procedures for the C-141, C-5A, C-130E, B-52G, B-52H and KC-135 aircraft with fuel conservation as the major objective. The findings and results of this study lead to the following conclusions and recommendations.

1. Of all the operational procedures investigated, flying close to optimum altitude and air speed offers the best opportunity for fuel savings. Since these savings can be realized with little effort and cost, it is recommended that this item be given the highest priority. It should be noted that the Air Force and industry are currently involved in the development of on-board real time energy management systems whose function is to aid the pilot in flying at optimal altitudes, air speeds, and climb and descent trajectories.
2. Next in priority is a reduction in reserve fuel. The amount of reserve fuel carried by the aircraft under study (no data is available for the B-52's) is generally higher than required by the current Air Force regulations. Thus fuel savings can be achieved by reducing the reserve fuel to the current requirements. Also during the sensitivity study it was determined that additional fuel savings can be generated by relaxing the current reserve fuel regulations. These regulations, which have been in effect for years, should be re-evaluated with respect to the current operational environments. It is recommended that a study be conducted to assess the feasibility of relaxing the reserve fuel requirements and to determine the technical advancements required (e.g., in navigation and ATC equipment) to allow this relaxation in the requirements.
3. For the cargo transport aircraft in this study (C-141, C-5A and C-130E), fuel savings can be achieved by the aft c.g. operation since the c.g. location can be readily influenced by a proper distribution of the fuel load and payload. Thus a revision of the cargo loading procedures for these aircraft is recommended.
4. The potential fuel conserving design modifications investigated in this study vary with aircraft type. The following discusses these design improvements individually for each aircraft under study:

C-141 Design Modifications

- Fillet revision - It is estimated that the revised wing-to-fuselage fillet will save 35 million gallons of fuel (5.8%) annually. However, if the entire C-141 fleet is stretched, then this modification is not required. If the fleet is not converted, the fillet revision should be considered since the break-even period is estimated to be 3.4 years.
- Retrofitting winglets - A preliminary analysis of winglets indicates that almost 16 million gallons (2.7%) of fuel can be saved annually for the C-141 with a potential for higher fuel savings under optimum cruise conditions. Since the break-even period is estimated to be less than three years, it is recommended that a detailed design analysis be performed to assess the feasibility of retrofitting winglets on the C-141.
- Vortex generator removal - Elimination of vortex generators from the C-141 wing are estimated to produce annual fuel savings of 10.5 million gallons (1.7%). Since the break-even period is less than three months, the efforts directed toward the vortex generator are certainly cost-effective.

C-130E Design Modifications

- Fuselage afterbody strakes - These additions to the fuselage would reduce drag by revising the air flow patterns. An annual fuel savings of approximately 6 million gallons (5%) is estimated and the break-even period is less than 3.5 years. As a result of these figures, it is concluded that a more detailed investigation of this modification is warranted.

B-52G Design Modifications

- Manual engine surge bleed valve override - The B-52G aircraft has an automatic air bleed valve which remains open when the engine is in the possible stall region. An annual fuel savings of 1.5% can be achieved by operating four engines at power

settings where the surge bleed values will be automatically closed and the other four engines at high power with the values manually operated by the co-pilot. The cost of the modification to allow manual operation of these values can be recovered within 2.5 years. However, the procedure will result in an increased work load for the co-pilot. Thus, it is recommended that a work load study be conducted to determine the feasibility of this procedure before a final decision for modification is made.

KC-135 Design Modifications

- Retrofitting winglets-An annual fuel savings of 14.2 million gallons(3.1%) has been estimated for retrofitting winglets on the KC-135, and the break-even period is estimated to be 6.4 years. Based on these results, it is recommended that winglets be installed on the KC-135.
5. The use of JP-8 grade fuel instead of the JP-4 currently used by the Air Force would generate approximately 57 million gallons (3.3%) of fuel savings annually for the aircraft under study. Thus it is recommended that the use of JP-8 grade fuel be considered. The Air Force is already shifting from JP-4 to JP-8 at its bases in Britain.
 6. The individual contributions of the other fuel saving items investigated do not appear to be significant. However, collectively they can sum to significant amounts. These items include reduced engine use and taxi time, reduced power take-off, reduced accessory load on engines, delayed flap approach and partial engine taxi. It is suggested that these procedures be implemented whenever possible.
 7. A reduction in fuel allocations would impair the user command's capability to meet operational commitments, and in the area of training it would impact the command's state of readiness. This impact could be partially offset by conducting more training during operational missions and by the increased use of simulators for training.

8. During the field trips, discussions with maintenance and operations personnel have indicated that there may be some problems with pressurization losses, which ultimately result in increased fuel consumption. Further investigation in this area may be worthwhile.

REFERENCES

1. "An Appraisal of Logistics Support Costs Used in the Air Force IROS Program", United States Air Force Project Rand, February 1975.
2. Bryson, A. E., Desai, M. N. and Hoffman, W. E., "Energy State Approximation in Performance Optimization of Supersonic Aircraft", Journal of Aircraft, Vol. 6, Nov.-Dec. 1969, pp. 481-488.
3. Schultz, R. L. and Zagalsky, N. R., "Aircraft Performance Optimization", Journal of Aircraft, Vol. 9, No. 2, Feb. 1972, pp. 108-114.
4. Zagalsky, N. R., "Aircraft Energy Management", AIAA Paper 73-228, 1973.
5. Calise, A. J., "Extended Energy Management for Flight Performance Optimization", AIAA Journal, Feb. 1977.
6. Kokotovic, P. V., "A Control Engineer's Introduction to Singular Perturbations", in Singular Perturbations: Order Reduction in Control System Design, New York, ASME, 1972.
7. Kokotovic, P. V., O'Malley, Jr., R. E. and Sannuti, P., "Singular Perturbation and Order Reduction in Control Theory - An Overview", presented at the 6th World IFAC Congr., Aug. 1975, Paper 51:3.
8. Speyer, J. L., "Non-Optimality of the Steady-State Cruise for Aircraft", to be published.
9. Aggarwal, R., Calise, A. J., and Goldstein, F., "Singular Perturbation Analysis of Optimal Flight Profiles for Transport Aircraft" JACC San Francisco, Calif., June 1977.
10. Anon., "C-141A Flight Manual" Technical Order T.O. 1C-141A-1-1, 25 October 1968, Change 13 - 10 June 1975.
11. Anon., "C-5A Flight Manual" Technical Order T.O. 1C-5A-1-1, 27 July 1972, Change 7- 19 March 1975.
12. Anon., "C-130B, C-130E and C-130H Flight Manual" Technical Order T.O. 1C-130B-1-1S-5, 10 February 1976.
13. Anon., "B-52G Flight Manual" Technical Order T.O. 1B-52G-1-1, 15 May 1961, Change 50- 15 October 1975.
14. Anon., "B-52H Flight Manual" Technical Order T.O. 1B-52H-1-1, 1 February 1961, Change 50- 1 March 1975.

15. Anon., "KC-135A Flight Manual" Technical Order T.O. 1C-135(K) A-1-1, 15 June 1966 Change 28- 10 April 1975.
16. Stengel, R. F., Marcus, F. J., "Energy Management Techniques for Fuel Conservation in Military Transport Aircraft" Technical Report AFFDL-TR-75-156.13 February 1976.
17. Flight Operations Fuel Management Program, Branniff International, January 1974.
18. Bull, J. S., and Foster, J. D., "Jet Transport Energy Management for Minimum Fuel Consumption and Noise Impact in the Terminal Area" NASA-Ames Research Center.
19. "Fuel Conservation Possibilities for Terminal Area Compatible Aircraft", NASA CR-132608, May 1975 [D9209U, N75-19224].
20. "Improved Navigational Systems and Procedures for MAC Airlift Aircraft", Operational Test and Evaluation Final Report 1-19-73, Hq. MAC Directorate of Operational Requirements, July 1973.
21. "Life Cycle Cost Analysis for Selected Inertial Navigation Systems for B-1, B-52, C/KC-135, FB-111 Weapon Systems", Instrument Systems IM Division, Oklahoma City Air Logistics Center, 17 March 1976.
22. "3-D Area Navigation System Available for Boeing Jetliners", Boeing Airlines", April 1976.
23. "Airplane Maintenance for Fuel Conservation for Boeing 707/727/734/747 Jet Transports". Boeing Commercial Airplane Company, January 1976.
24. Duchnowski, E. M., "An Operations Approach to Reduce Fuel Consumption in C-141 Aircraft", Maxwell Air Force Base, Alabama, May 1974.
25. "Aircraft Fuel Conservation: An AIAA View", American Institute of Aeronautics and Astronautics, 30 June 1974.
26. "Air Force Energy R&D Programs Synopsis FY76-81", HQ USAF/RDPS, 3 December 1975, p. B-21.
27. "Engine Inflight Monitoring", Combat Crews. SAC/LGME, July 1976, p. 8-13.
28. Povinelli, F., Klineberg, J., and Kramer, J., "Improving Aircraft Energy Efficiency", NASA Aircraft Efficiency Office, OAST, Astronautics & Aeronautics, February 1976.

29. "Fuel Economy Trim", letter from Vice President, Engineering, United Airlines, 30 September 1974.
30. "Fuel Conservation Through Airplane Maintenance", Boeing Airliner, April 1976.
31. "Completion Report MEP Project GM 76-1E, Generator Sets, Diesel Powered", letter from Deputy Commander for Maintenance, 60 Military Airlift Wing, 10 September 1976.
32. "Fuel Conservation Opportunities" Air Force Flight Dynamics Laboratory Briefing.
33. J. R. Peele, "Feasibility Study of C-141A Fuel Conservation through Aft C.G. Operations", Lockheed-Georgia Co., Report No. AFFDL-TR-75-140, Dec. 1975.
34. "General Flight Rules" AF Regulation 60-16, Department of the Air Force, Headquarters U.S. Air Force, Washington, D. C., 15 August 1974.
35. Telephone Interview: Use of alternate jet fuel for USAF aircraft. Mr. Arthur Churchill, Chief, Fuels Branch, Air Force Aero Propulsion Laboratory, Wright-Patterson AFB, Ohio, 4 August 1976.
36. Ishimitsu, K. K., Van Devende, N., Dodson, R., "Design and Analysis of Winglets for Military Aircraft", Boeing Commercial Airplane Co., Report No. AFFDL-TR-76-6, February 1976.
37. E. D. Harris, D. Dreyfuss, W. D. Gosch and H. Watanake, "Potential for Advanced Technology to Reduce Military Airlift Energy Consumption for 1975 - 2000 (S)". The Rand Corporation, February 1976.
38. "Pratt and Whitney Engines", Jane's All the World's Aircraft 1972-1974.
39. Floyd Palmer, "KC-135 Re-engine Study", The Boeing Company, Report No. D3-11000-1, 1 March 1976.
40. Stephan, P. W., Sworde, S. C., "Fuel Management Computer Investigation". Hughes Aircraft Company, Report No. AFFDL-TR-70-148, December 1970.
41. "C-141A Aerodynamic Substantiating Data", Lockheed-Georgia Company Report No. ER-8330, January 1967.
42. "C-141 Aircraft Flying Heavy", Operational Test and Evaluation Final Report, May 1974.
43. Communications from the Air Force Flight Dynamics Laboratory, 1978.

44. "C-5A Aerodynamic Substantiating Data" Lockheed-Georgia Company Report No. LGIC-22-1-1, 24 June 1968.
45. "Fuel Consumption for Specific Aircraft", letter from Chief, Logistics Management Division, Directorate of Energy Management, San Antonio Air Logistics Center, San Antonio, Texas, to Dynamics Research Corporation, 12 November 1976.
46. "C-5 Outer Wing Modification Report", C-5 SPO (ASD/YAS), 22 April 1976.
47. "C-130E Substantiating Data" Report No. ER-7357 Lockheed-Georgia Company, 15 December 1964.
48. Young, S. H. H., "Gallery of Aircraft", Air Force Magazine, May 1977.
49. "Standard Aircraft Characteristics", Air Force Guide 2, Vol. 1, Addition 55, January 1973.
50. "B-52G Substantiating Data" Report No. D3-9776-2, The Boeing Company, 1975.
51. "B-52G Substantiating Data" Report No. D3-1633, The Boeing Airplane Company, 1961.
52. Interview, topic: Manual override for B-52G engine surge bleed valves. Mr. Norm Kirk, B-52 technical services, Oklahoma Air Logistics Center, Tinker AFB, Oklahoma, by telephone, 11 January 1977.
53. "B-52H Substantiating Data" Report No. D3-3183, Boeing Airplane Company, 1960.
54. D. E. Gray, "Study of Turbofan Engines Designed for Low Energy Consumption - Final Report", Pratt & Whitney Aircraft Division, United Technologies Corporation, Report No. NASA CR-135002, April 1976, p. 6-33.
55. "Substantiating Data Report for the KC-135A Flight Manual", Document No. DG-5595, The Boeing Company, 1969.
56. "Specification Engine Performance for Use in Airplane Performance Determination, J-57-P-59W", Document No. D-16906, The Boeing Company, 1965.
57. Illinois University Institute of Aviation, "Synthetic Flight Training Revisited", Urbana, Illinois, August 1972.
58. Lt. General William V. McBride, "Simulation in Undergraduate Pilot Training", Commander's Digest, Vol. 16, No. 7, August 15, 1974.

59. Colonel Craig C. McCall, "Operational Readiness and Conservation", Supplement to the Air Force Policy Letter for Commanders, No. 2-1975, February 1975.
60. Ertzberger, H., Barman, J. F., McLean, J. D., "Optimum Flight Profiles for Short Haul Missions", AIAA Guidance & Control Conference, Boston, Mass., August 1975.
61. Calise, A. J., "Singular Perturbation Analysis Approach for Systems with Highly Coupled Dynamics", Fourteenth Annual Allerton Conference on Circuits and System Theory, University of Illinois, Urbana-Champaign, September 29 - October 1, 1976.
62. Miller, L. E. & Koch, P. G., "Aircraft Flight Performance Methods", Air Force Flight Dynamics Laboratory, Technical Report No. AFFDL-TR-75-89, June 1975.

APPENDIX A

DERIVATION OF OPTIMAL FLIGHT PROCEDURES

This appendix carries out an analysis of optimal flight profiles for subsonic bomber/transport aircraft based on singular perturbation theory. Optimal climb, cruise and descent solutions for long range missions are derived. For a short range mission the optimal flight profile does not contain a cruise segment; a constrained matching technique is used to derive optimal short range solution.

Problem Formulation

The point mass 2-DOF equations of motion for an aircraft are:

$$\dot{x} = V \cos \gamma \quad (\text{A.1})$$

$$\dot{E} = (T - D)V/W \quad (\text{A.2})$$

$$\dot{h} = V \sin \gamma \quad (\text{A.3})$$

$$\dot{\gamma} = g (L - W \cos \gamma)/WV \quad (\text{A.4})$$

where x is down range position, W is weight, E is energy per unit weight, h is altitude, γ is flight path angle, V is velocity, T is thrust, D is drag and L is lift. These equations apply for a flight over a flat earth with thrust directed along the flight path. Thrust is a nonlinear function of h , V and power setting (η) and drag is a nonlinear function of h , V and L .

$$T = T(h, V, \eta) \quad (\text{A.5})$$

$$D = D(h, V, L) \quad (\text{A.6})$$

Lift (L) and power setting (δ) are the aircraft control variables. For the B-52, KC-135, C-141 and C-5A aircraft, the power setting (δ) is a function of the engine pressure ratio (EPR), and for the C-130E it is a function of the turbine inlet temperature T_{in} . However for the optimal control analysis, thrust (T) rather than power setting (δ) is considered as control variable. W_i , E_i and h_i are the aircraft weight, energy and altitude at the initial time. The terminal altitude h_f , energy E_f and the range x_f are specified.

The performance index is given by

$$J = \int_0^{t_f} [\sigma \theta f + (1 - \theta)] dt \quad (A. 7)$$

as described in Section 3.1 with fuel flow rate f given as

$$f = f(h, V, T)$$

Speed can be expressed as a function of E and h using

$$V = [2g(E - h)]^{1/2} \quad (A. 8)$$

The following aircraft constraints are imposed

$$L/W \leq G_{\max} \quad (A. 9)$$

$$L \leq q S C_{L_{\max}}(h, V) \quad (A. 10)$$

$$h_{\min} \leq h \leq h_{\max} \quad (A. 11)$$

$$V \leq V_{\text{limit}}(h) \quad (A. 12)$$

$$T_{\min}(h, V) \leq T \leq T_{\max}(h, V) \quad (A. 13)$$

The altitude (h) constraint encompasses the pressurization constraint, cruise ceiling constraint and ATC constraint on flight altitudes. The ATC constraint on climb and descent velocities is accounted for by the velocity constraint.

As explained in Section 3.6, the system dynamics are scaled by introducing epsilons (ϵ_i) in the left hand side of the equations such that $\lim_{\epsilon_i \rightarrow 0} \epsilon_i^{i+1}/\epsilon_i = 0$.

The ordering for equations (A.1-A.4) is as follows:

$$\dot{x} = V \cos \gamma \quad (\text{A.14})$$

$$\epsilon_1 \dot{E} = (T - D) V/W \quad (\text{A.15})$$

$$\epsilon_2 \dot{h} = V \sin \gamma \quad (\text{A.16})$$

$$\epsilon_3 \dot{\gamma} = g (L - W \cos \gamma)/WV \quad (\text{A.17})$$

The corresponding Euler-Lagrange equations are:

$$\dot{\lambda}_x = -\frac{\partial H}{\partial x} = 0 \quad (\text{A.18})$$

$$\epsilon_1 \dot{\lambda}_E = -\frac{\partial H}{\partial E} \quad (\text{A.19})$$

$$\epsilon_2 \dot{\lambda}_h = -\frac{\partial H}{\partial h} \quad (\text{A.20})$$

$$\epsilon_3 \dot{\lambda}_\gamma = -\frac{\partial H}{\partial \gamma} \quad (\text{A.21})$$

where

$$H = \lambda_x V \cos \gamma + \lambda_E (T - D) V/W + \lambda_h V \sin \gamma + \lambda_\gamma g [L/W - \cos \gamma]/V \\ + \theta f(h, V, T) + (1 - \theta) + \text{constraints} = 0 \quad (\text{A.22})$$

The optimality conditions on the controls are

$$\frac{\partial H}{\partial T} = 0, \quad \frac{\partial H}{\partial L} = 0 \quad (\text{A.23})$$

Reference [5] shows that this procedure reduces to solving a series of first order optimal control problems for which a feedback (point-wise optimization) solution results. The optimal control and trajectory solution is expanded in an "outer expansion" solution about $\epsilon = 0$

$$\bullet(t, \epsilon) = \bullet(t, 0) + \frac{\partial \bullet}{\partial \epsilon} \epsilon + \dots \quad (\text{A. 24})$$

where the \bullet denotes the state, adjoint and control variables. However, the expansion in (A. 24) is not uniformly valid in the intervals $0 \leq t \leq t_f$ since the fast states and their adjoints will not satisfy their respective boundary conditions at $t = 0$ and $t = t_f$. This leads to the occurrence of boundary layer or "inner expansion" solutions of

$$\bullet(\tau_i, \epsilon) = \bullet(\tau_i, 0) + \frac{\partial \bullet}{\partial \epsilon} \epsilon + \dots, \quad t = 0_0 \quad (\text{A. 25})$$

$$\bullet(\sigma_i, \epsilon) = \bullet(\sigma_i, 0) + \frac{\partial \bullet}{\partial \epsilon} \epsilon + \dots, \quad t = t_f \quad (\text{A. 26})$$

The solutions are derived using the time stretching transformations

$$\tau_i = t/\epsilon_i, \quad \sigma_i = \frac{T-t}{\epsilon_i} \quad (\text{A. 27})$$

about $t = 0_0$ and $t = t_f$ respectively. The total solution which, in effect, is the sum of (A. 24) - (A. 26) satisfies all the boundary conditions and is uniformly valid in the closed interval $0 \leq t \leq t_f$

Zero Order Outer Solution

Taking the limit as ϵ goes to zero and using the necessary conditions for optimality, the following conditions for the zero order outer solution are obtained:

$$H_0 = \lambda_x^T V + \sigma^T \theta f(h, V, T) + (1 - \theta) + \text{constraints} = 0 \quad (\text{A. 28})$$

$$T_0 = D_0, \quad L_0 = W, \quad \gamma_0 = 0 \quad (\text{A. 29})$$

$$E_0, h_0 = \arg \min_{E, h} \{H_0\} \quad (\text{A. 30})$$

Note that E and h have adopted the role of control variables. Equations (A. 28) and (A. 30) are equivalent to the following point extremization:

$$E_0, h_0 = \arg \max \{V/[\sigma \theta f + (1 - \theta)]\} \quad (\text{A. 31})$$

subject to constraints in (A. 9) - (A. 13) and (A. 29).

$$\lambda_{x_0} = [\{\sigma \theta f_0 + (1 - \theta)\} / V_0] \quad (\text{A. 32})$$

where

$$f_0 = f(h_0, V_0, D(h_0, V_0, W)) \quad (\text{A. 33})$$

$$V_0 = [2g(E_0 - h_0)]^{1/2} \quad (\text{A. 34})$$

For $\theta = 1$ (minimum fuel), Eq. (A. 31) can be recognized as the equation for the optimum specific range of an aircraft. As the aircraft burns fuel, its weight decreases and the optimum values of E and h given by Eq. (A. 31) increase unless the solution lies on the constraint bound. For example, if the ATC constraint on cruise altitude is ignored, the aircraft range and weight equations may be integrated forward in time to obtain the cruise-climb solution.

Minimum Fuel Cruise-Climb Solution

For the unconstrained minimum fuel case, the aircraft range and weight equations can be integrated analytically. The following derives the relation between aircraft range and weight during cruise-climb. From Eq. (A. 31) optimum energy

and altitude for minimum fuel cruise-climb are given by

$$E_{\text{opt}}, h_{\text{opt}} = \arg \max [V/f] \quad (\text{A. 35})$$

For all aircraft under study (except the C-130E) fuel flow (f) is given by

$$f = \sqrt{\theta} \delta f_n (M, T_r) \quad (\text{A. 36})$$

where $\sqrt{\theta}$ is temperature ratio, δ is pressure ratio and normalized fuel flow (f_n) is a function of Mach (M) and normalized thrust (T_r) as described in Section 3.2.

Using (A.29) and (A.36), the right hand side of Eq. (A.35) may be written as

$$\frac{V}{f} = \frac{1}{W} \left[\frac{Ma_0}{f_n(M, D_r)} \right] \frac{W}{\delta} \quad (\text{A. 37})$$

where normalized drag (D_r) is equal to

$$D_r = D/\delta = .5 \rho_0 a_0^2 M^2 C_{D_0} (M) - K^{-1} W/\delta + K (M) W^2/\delta^2 / .5 \rho_0 a_0^2 M^2 \quad (\text{A. 38})$$

according to the drag model described in Section 3.2.

In Eq. (A.37) the expression in the parenthesis is known as range factor (RF). Note that this expression is a function of Mach (M) and normalized weight (W/δ). Optimum values of mach (M^*), and normalized weight (W/δ)* are obtained by solving equations (A.39) and (A.40) simultaneously.

$$f_r (M, D_r (M, W/\delta)) - M \frac{\partial f_r}{\partial M} = 0 \quad (\text{A. 39})$$

$$f_r - W/\delta \frac{\partial f_r}{\partial (W/\delta)} = 0 \quad (\text{A. 40})$$

Optimum mach (M^*), normalized weight $(W/\delta)^*$ and range factor (RF^*) remain constant for an aircraft. Now from the aircraft range and weight equations

$$\frac{dx}{dW} = - \frac{V}{f} \quad (A.41)$$

For the minimum fuel cruise climb case Eq. (A.41) may be written as

$$\frac{dx}{dW} = - \frac{RF^*}{W} \quad (A.42)$$

Equation (A.42) is integrated analytically to obtain

$$\text{Range} = RF^* \log \frac{W_i}{W_f} \quad (A.43)$$

where W_i and W_f are the initial and final aircraft weight respectively.

For the C-141, B-52G, B-52H and KC-135 aircraft values of M^* , $(W/\delta)^*$ and RF^* are given in Section 7. For the C-5A and C-130E, altitudes are constrained by cruise ceiling.

Zero Order Energy Boundary Layer

The energy transition dynamics during climb are investigated using the time stretching transformation $\tau_1 = \frac{t}{\epsilon_1}$. Applying this transformation to (A.14) - (A.21) and letting $\epsilon_1 \rightarrow 0$ results in the following optimality conditions for climb:

$$H_0^1 = \lambda_{x_0} V + \lambda_E (T - D) V/W + \theta f + (1 - \theta) + \text{constraints} = 0 \quad (A.44)$$

$$\gamma_0^1 = 0, \quad L_0^1 = W \quad (A.45)$$

$$T_0^1, h_0^1 = \arg \min_{T, h} \{H_0^1\}_E, \quad T > D \quad (A.46)$$

where the superscript ("1") denotes a first boundary solution. Note that only one unknown adjoint (λ_E) is introduced by this procedure. Control variables are

altitude (h) and thrust (T). Equations (A.44) and (A.46) result in the following point wise extremal solution:

$$T_o^1, h_o^1 = \arg \max_{T,h} \lambda_{x_o} \frac{(T-D)V/W}{V+\theta f+(1-\theta)} \quad E, \quad T > D \quad (A.47)$$

$$\lambda_{E_o}^1 = - \frac{\lambda_{x_o} V_o^1 + \theta f_o^1 + (1-\theta)}{(T_o^1 - D_o^1) V_o^1 / W} \quad (A.48)$$

where

$$f_o^1 = f(h_o^1, V_o^1, T_o^1) \quad (A.49)$$

$$D_o^1 = D(h_o^1, V_o^1, W) \quad (A.50)$$

$$V_o^1 = [2 g (E - h_o^1)]^{1/2} \quad (A.51)$$

The algebraic solution of (A.47) subject to constraints in (A.9) to (A.13) and (A.45) yields T (or equivalently throttle setting) and is a function of energy (E) during climb. The boundary conditions on E around $t = 0$ are

$$E(\tau)/_{\tau=0} = E_i, \quad E(\tau)/_{\tau \rightarrow \infty} = E_o(0) \quad (A.52)$$

where E_i is the initial energy and $E_o(0)$ is the value of energy from the zero-order outer expansion solution. Hence the energy boundary layer solution during climb can be viewed as asymptotically approaching the zero order cruise conditions.

Zero order boundary layer equations for the energy transition during descent are obtained in a similar manner by using the time stretching transformation $\sigma_1 = (t_f - t)/\epsilon_1$ and requiring $T < D$. This results in an identical set of conditions as for climb.

There may be more than one extremal path for climb and descent, as was the case in [60] for a STOL aircraft, where one local and one global extremum were produced for the descent portion of the trajectory. Local extrema are not a problem in the point wise optimization of (A.47) since the search for maximization can be conducted over the complete range of T and h to choose the overall maximum.

Second and Third Boundary Layer Solution

The second and third boundary layer analysis addresses the h and γ dynamics for matching the initial conditions on h and γ to the optimal climb solution from (A.47). However, both altitude and flight path angle vary slowly for bomber/transport aircraft. Therefore these dynamics are neglected in this application.

Constrained Matching for Optimal Short Range Solution

The optimal aircraft trajectory contains the cruise segment only if the specified range x_f is greater than the sum of the horizontal distance travelled during climb to cruise altitude and in descent from the cruise to the terminal altitude. However, if this condition is not satisfied, then the optimal trajectory cannot attain the cruise altitude. In this case if both the climb and the descent trajectories are plotted in the (x, h) plane such that the climb trajectory starts at $x = 0$ and the descent trajectory terminates at x_f , then these two trajectories will be asymptotic to h_c and intersect (see Fig. A-1) at some altitude $h_1 < h_c$, where h_c is the optimum cruise altitude. However, the matching condition requires that there be a region of overlap in which both the initial and terminal boundary layers are in steady state ($\frac{dx}{dh} = 0$). This is achieved by following the procedure suggested in [61]. The altitude in the zero order outer expansion is constrained to h_{\max} . If, in the unconstrained optimal solution to the original problem, $h(t) < h_{\max}$ then it is convenient to think of $h < h_{\max}$ as an artificial constraint that does not alter the original problem statement. A logical choice

for h_{\max} is the value h_1 corresponding to the intersection of climb and descent solutions as shown in Fig. A-1. This produces new value for λ_x in (A.32) and new values of controls in (A.47) for climb and in a similar equation for descent. This results in a new set of curves for $x(h)$ that intersect at a lower value of h (h_2 in Fig. A-1). This procedure is iterated until a sufficiently small value of $\frac{dx}{dh}$ is observed at the point of intersection.

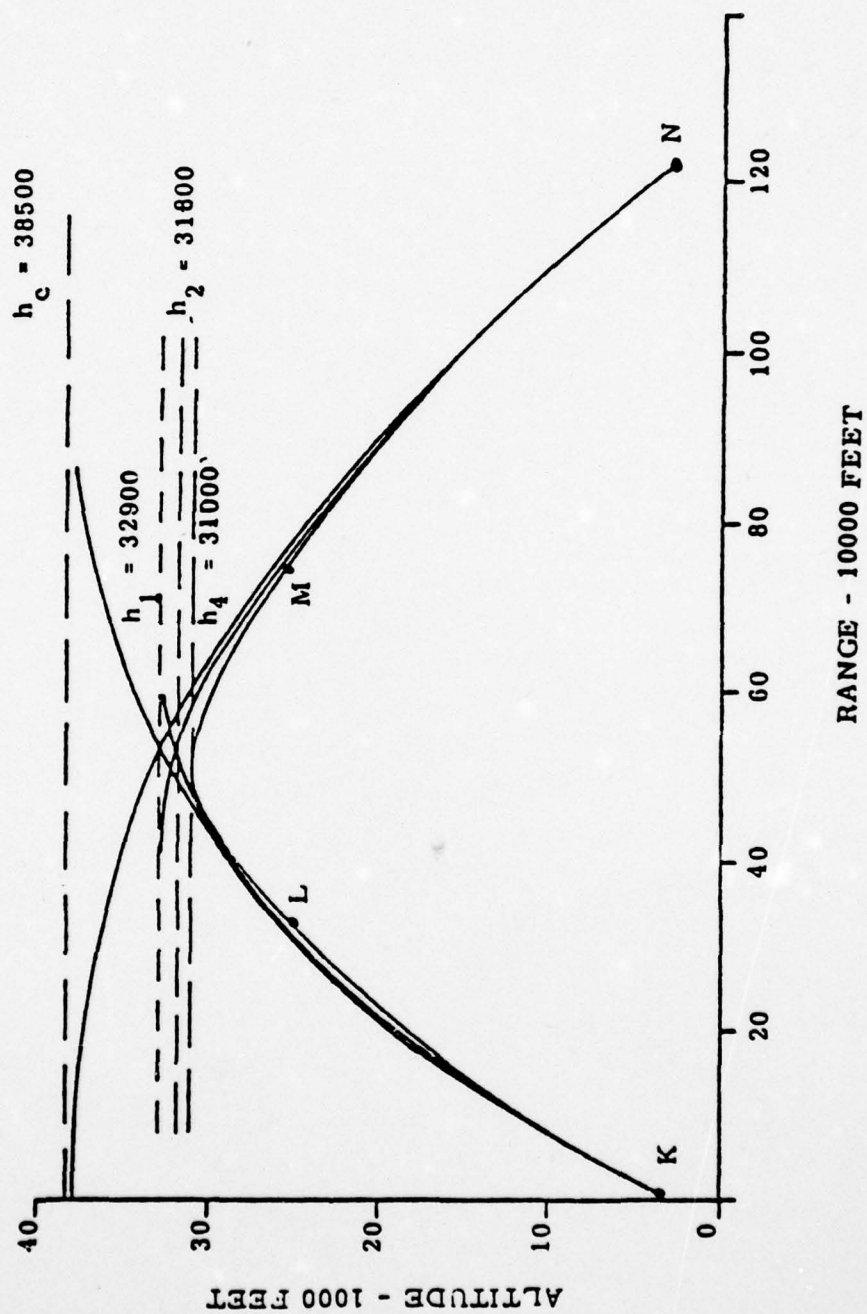


Figure A-1 Short Range Solutions

APPENDIX B

OPTIMALITY OF CRUISE SOLUTION

The object of this Appendix is to determine if the relaxed steady-state cruise fuel consumption (f_{rss}) exists for a class of subsonic transport aircraft. If so this would represent a lower bound on the fuel consumption below that of the steady-state cruise fuel consumption (f_{ss}). It is shown that for the C-5A and C-141 transports the f_{rss} does not exist and that f_{ss} is the lower bound on fuel consumption.

B.1 PROBLEM FORMULATION

The equations of motion of an aircraft are reduced to one-dimension where energy E is used as the dependent state variable and down range x is the independent variable. The dynamic equation of the energy-state approximation is

$$\frac{dE}{dx} = \bar{E} = T - D(V, E) \quad (B.1)$$

where T is thrust, V is velocity, D is drag, x is down range, and E , the energy, is

$$E = \frac{\Delta}{2} V^2 + gh \quad (B.2)$$

The thrust and velocity are considered control variables. Knowing E and V implies h by (B.2)

The object is to minimize the average fuel used given as

$$f_A = \frac{1}{x} \int_0^x \frac{df}{dx} dx \quad (B.3)$$

where

$$\frac{df}{dx} = \bar{f} = \frac{\dot{f}(V, E, T)}{V} \quad (B.4)$$

where $\dot{f}(V, E, T)$ is the mass rate of fuel. The minimization of f_A is subject to the dynamic constraints (B.1) and the inequality constraints on the control variables as

$$T_{\min}(V, E) \leq T \leq T_{\max}(V, E) \quad ; \quad V \geq 0 \quad (B.5)$$

The object of this study is to search for two static paths. If the hodograph formed by (B.1), (B.4) and (B.5) is convex, then the static steady-state cruise path is minimizing. If the hodograph is not convex, then the relaxed steady-state cruise path results forming a lower bound on the fuel consumption of subsonic aircraft. In Section B.4 the determination of the f_{rss} is described.

B.2 GIVEN FUNCTIONAL EQUATIONS

In this section the functional forms of the aerodynamics and engines are presented. Since the energy-state approximation is used, the lift is assumed to be in balance with the weight. As a result the drag force D is modeled as

$$D = \bar{a}_1(M) QS + \bar{a}_1(M) W + \bar{a}_2(M) W^2/QS \quad (B.6)$$

where M is the Mach Number, S is the reference surface area, and Q the dynamic pressure is

$$Q = \frac{1}{2} \rho V^2 \quad (B.7)$$

where ρ is the atmospheric density. The coefficients in (B.6) are explicitly modeled as

$$\bar{a}_i(M) = \alpha_i |M - M_0|^{\beta_i} + \gamma_i \quad i = 0, 1, 2 \quad (B.8)$$

where α_i , β_i , γ_i and M_0 are constants.

Since most aircraft fly in the stratosphere where an isothermal atmosphere is a very good approximation, we will assume an exponential atmosphere which means the density ρ is

$$\rho = \rho_0 e^{-h/\lambda_3} \quad (B.9)$$

where

$$\rho_0 = 2.1814 \times 10^{-2} e^{h_0/\lambda_3}, \quad h_0 = 37,000 \text{ ft}, \quad \lambda_3 = 20,886 \text{ ft}$$

Similarly, the pressure ratio $\delta = \frac{p(h)}{p(h_0)}$ is also exponential as

$$\delta = \delta_0 e^{-h/\lambda_3}, \quad \delta_0 = .214469 e^{h_0/\lambda_3} \quad (\text{B.10})$$

Using an isothermal atmosphere, the speed of sound and the absolute ($^{\circ}\text{R}$) temperature ratio θ are constants as

$$a = 963.03 \text{ ft/sec}, \quad \theta = .7519 \quad (\text{B.11})$$

The above simplifies the process of taking partial derivatives with respect to V and h and avoids table look ups on the computer.

The mass rate \dot{f} (lb/hr per engine) is of the form

$$\dot{f} = 1000 \delta \sqrt{\theta} \sum_{j=0}^2 \sum_{i=0}^2 (a_{ij} M^i) \left(\frac{T}{\delta N} \right)^j; \quad N = 20,000 \quad (\text{B.12})$$

The maximum thrust (lb per engine) is

$$T_{\max} = 1000 \sum_{j=0}^2 \sum_{i=0}^2 d_{ij} M^i \xi^j; \quad \xi = h/40,000 \quad (\text{B.13})$$

The minimum thrust is found from (B.12) where \dot{f} at idle (\dot{f}_{\min}) is given.

B.3 DETERMINATION OF STEADY STATE CRUISE FOR MIN FUEL

Since the two numerical examples considered (C-5A and C-141) have four engines, then in steady state cruise the thrust per engine is $T=D/4$. To find the optimum steady state cruise, the fuel function

$$\frac{df}{dx} = \bar{f} = \frac{1000 \delta \sqrt{\theta}}{V} \sum_{j=0}^2 \sum_{i=0}^2 \bar{a}_{ij} M^i \left[\frac{\bar{a}_0(M) Q + \bar{a}_1(M) W + \bar{a}_2(M) W^2 / Q A}{4 \delta N} \right]^j \quad (\text{B.14})$$

is minimized with respect to V and h .

This is done in a numerical algorithm by driving the gradients* \bar{f}_V and \bar{f}_h to zero where these gradients are given as

$$\begin{aligned} \bar{f}_h = & \frac{1000 \delta \sqrt{\theta}}{V} \sum_{j=0}^2 \sum_{i=0}^2 j \bar{a}_{ij} M^i \left(\frac{D}{4 \delta N} \right)^{j-1} \left[\bar{a}_0 - \bar{a}_2 \left(\frac{W}{Q} \right)^2 \frac{\partial D}{\partial V} / 4 \delta N \right. \\ & \left. - D \delta_h / 4 N \delta^2 \right] + \bar{f} \delta_h / \delta \end{aligned} \quad (\text{B.15})$$

$$\bar{f}_V = \frac{1000 \delta \sqrt{\theta} \bar{a}_{ij} M^i}{V} \left[\frac{D}{4 \delta N} \right]^j \frac{i}{V} + j \left[\frac{\partial D}{\partial V} / D \delta N \right] \bar{f} \quad (\text{B.16})$$

*For a scalar function $z(x)$ the symbol z_x denotes $\partial z / \partial x$.

AD-A062 609

DYNAMICS RESEARCH CORP WILMINGTON MASS SYSTEMS DIV F/G 1/3
AN ANALYSIS OF FUEL CONSERVING OPERATIONAL PROCEDURES AND DESIG--ETC(U)
JUL 78 R K AGGARWAL F33615-76-C-3104

UNCLASSIFIED

R-247U

AFFDL-TR-78-96-VOL-2

NL

6 OF 6
ADA
062609

SEE
PAGE 1

END
DATE
FILMED

3 -79
DDC

B.4 DETERMINATION OF THE RELAXED STEADY-STATE CRUISE FOR MIN FUEL

The object is to find the relaxed steady-state minimum fuel cruise by assuming that the hodograph of (\bar{E}, \bar{f}) for constant E is concave between T_{\max} and T_{\min} . If (df/dx) obtained by infinitely chattering between T_{\max} and T_{\min} at $\bar{E} = 0$ (this is the precise definition of f_{rss}) is superior to df/dx of the steady-state cruise, then we conclude that the hodograph is not convex and the relaxed steady-state cruise f_{rss} is the lower bound on the fuel consumption.

In $dE/dx = \bar{E}$ and $df/dx = \bar{f}$ space for a fixed value of E , curves for T_{\min} and T_{\max} are plotted in Figure B.1 as the velocity ranges from 0 to infinity. Note V_1 and V_2 correspond to velocities associated with T_{\min} and T_{\max} , respectively.

The line tangent to the curves for T_{\max} and T_{\min} determine the hull of the assumed concave hodograph. Where this line crosses the $\bar{E} = 0$ axis is the relaxed steady-state cruise. This line has the general form (four engine aircraft).

$$\bar{E} = \alpha \bar{f} + \beta \quad (\text{B.17})$$

When the line is tangent to the curve for T_{\min}

$$\alpha + \bar{f}(V_1) + \beta = 4T_{\min}(V_1) - D(V_1) \quad (\text{B.18})$$

When the line is tangent to the T_{\max} curve

$$\alpha + \bar{f}(V_2) + \beta = 4T_{\max}(V_2) - D(V_2) \quad (\text{B.19})$$

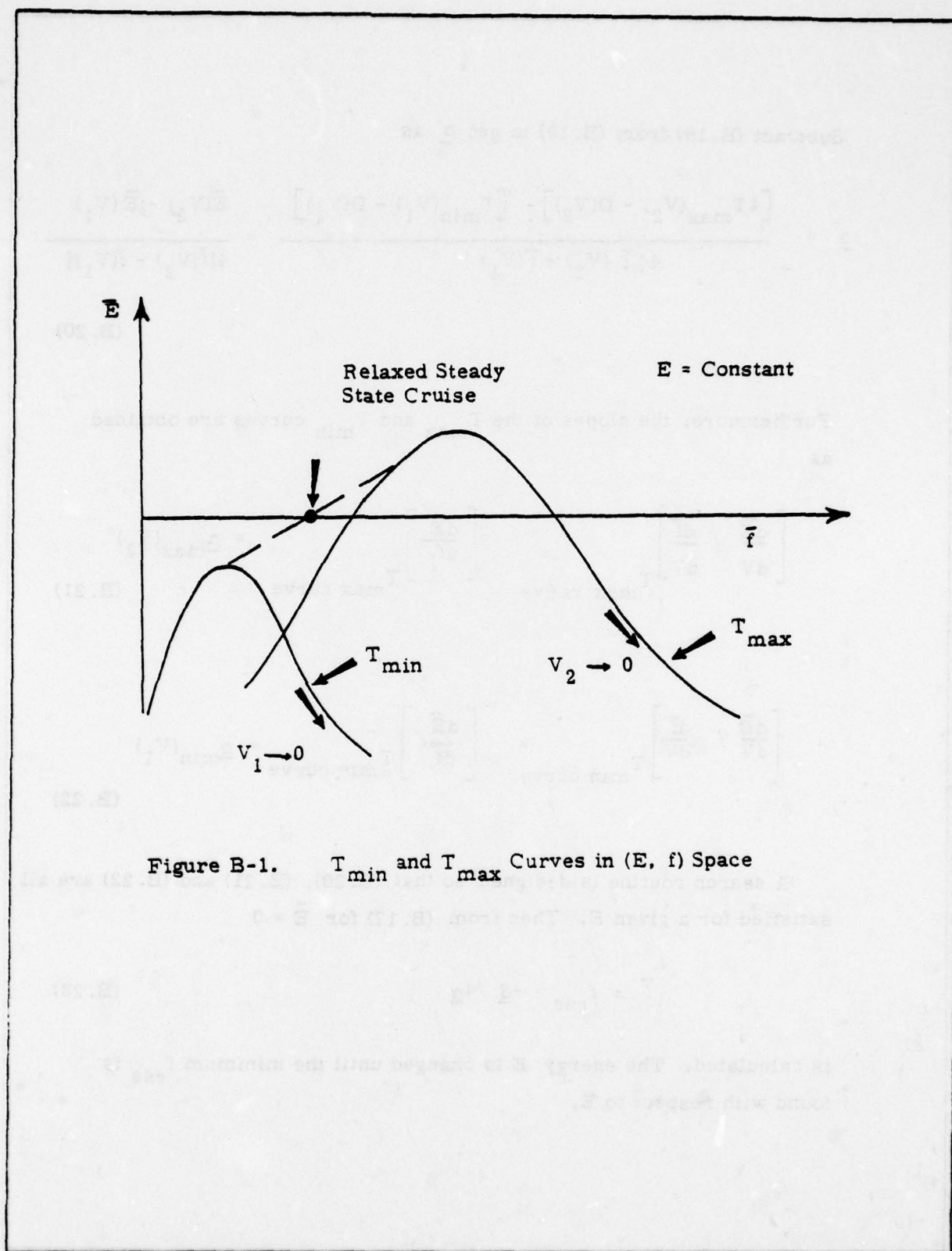


Figure B-1. T_{\min} and T_{\max} Curves in (E, \bar{f}) Space

Subtract (B.18) from (B.19) to get $\underline{\alpha}$ as

$$\underline{\alpha} = \frac{[4T_{\max}(V_2) - D(V_2)] - [T_{\min}(V_1) - D(V_1)]}{4[\bar{f}(V_2) - \bar{f}(V_1)]} = \frac{\bar{E}(V_2) - \bar{E}(V_1)}{4[\bar{f}(V_2) - \bar{f}(V_1)]} \quad (\text{B.20})$$

Furthermore, the slopes of the T_{\max} and T_{\min} curves are obtained as

$$\left[\frac{d\bar{E}}{dV} / \frac{d\bar{f}}{dV} \right]_{T_{\max} \text{ curve}} = \left[\frac{d\bar{E}}{d\bar{f}} \right]_{T_{\max} \text{ curve}} = \underline{\alpha}_{\max}(V_2) \quad (\text{B.21})$$

$$\left[\frac{d\bar{E}}{dV} / \frac{d\bar{f}}{dV} \right]_{T_{\min} \text{ curve}} = \left[\frac{d\bar{E}}{d\bar{f}} \right]_{T_{\min} \text{ curve}} = \underline{\alpha}_{\min}(V_1) \quad (\text{B.22})$$

A search routine is designed so that (B.20), (B.21) and (B.22) are all satisfied for a given E . Then from (B.17) for $\bar{E} = 0$

$$\bar{f} = f_{\text{rss}} = -\underline{\beta} / 4\underline{\alpha} \quad (\text{B.23})$$

is calculated. The energy E is changed until the minimum f_{rss} is found with respect to E .

B.5 NUMERICAL RESULTS

Two transport aircraft were considered in determining if f_{rss} was below f_{ss} . For these subsonic aircraft it is established that the hodograph is not concave since f_{ss} is of lower value than f_{rss} for all values of E .

The aerodynamic and engine data used in the functions of Section III for both aircraft is presented in Table B-1. Using this data the cruise point for the C-141 was

$$V = 694 \text{ ft/sec and } h = 37,533 \text{ ft.} \quad (\text{B.24})$$

with a fuel rate of

$$\bar{f} = f_{ss} = .00422 \text{ lb/ft.} \quad (\text{B.25})$$

For the C-5A the cruise point was

$$V = 700.7 \text{ ft/sec. and } h = 35,667 \text{ ft.} \quad (\text{B.26})$$

with a fuel rate of

$$\bar{f} = f_{ss} = .00748 \text{ lb/ft.} \quad (\text{B.27})$$

The results of determining the relaxed steady state fuel rate f_{rss} is shown in Figure B-2 for the C-141 and Figure B-3 for the C-5A where \bar{f} at $\bar{E} = 0$ is plotted against energy E . For these two aircraft minimum f_{rss} seem to be at an energy above that of the cruise energy. However, in both cases the $f_{rss} > f_{ss}$ for all energy. Note that the gap between f_{rss} and f_{ss} for the C-5A is considerably less than that for the C-141.

DRAG MODEL

	γ_0	γ_1	γ_2	α_3	α_1	α_2	β_0	β_1	β_2	M_0
C-141	.0161	-7.214×10^{-3}	.055	1.25×10^{-5}	-1.52×10^{-5}	1.094×10^{-6}	-2.705	-3.045	-4.625	.9
C-5A	.0176	-.0166	.063	3.6×10^{-7}	-2.94×10^{-8}	3.98×10^{-9}	-5.67	-7.97	-9.98	1

FUEL MODEL

	$\frac{d}{dt}$	$\frac{d}{dt}$	$\frac{d}{dt}$	$\frac{d}{dt}$	$\frac{d}{dt}$	$\frac{d}{dt}$	$\frac{d}{dt}$	$\frac{d}{dt}$	$\frac{d}{dt}$	$\frac{d}{dt}$
C-141	1.71	4.07	6.152	.709	6.77	0	1.19	0	0	655
C-5A	2.038	3.707	1.604	-4.383	5.936	0	12.995	0	0	555

MAX THRUST MODEL

	$\frac{d}{dt}$	$\frac{d}{dt}$	$\frac{d}{dt}$	$\frac{d}{dt}$	$\frac{d}{dt}$	$\frac{d}{dt}$	$\frac{d}{dt}$	$\frac{d}{dt}$	$\frac{d}{dt}$	$\frac{d}{dt}$
C-141	17.44	-15.34	.0393	-14.22	18.34	-.592	9.62	-11.81	.755	
C-5A	34.71	-32.22	5.8	-27.4	36.43	-11.64	2.65	3.19	-5.72	

C-141 W - 260,000 lb. S - 3228 ft.²

C-5A W - 600,000 lb. S - 6200 ft.²

TABLE B-1
AERODYNAMIC AND ENGINE DATA

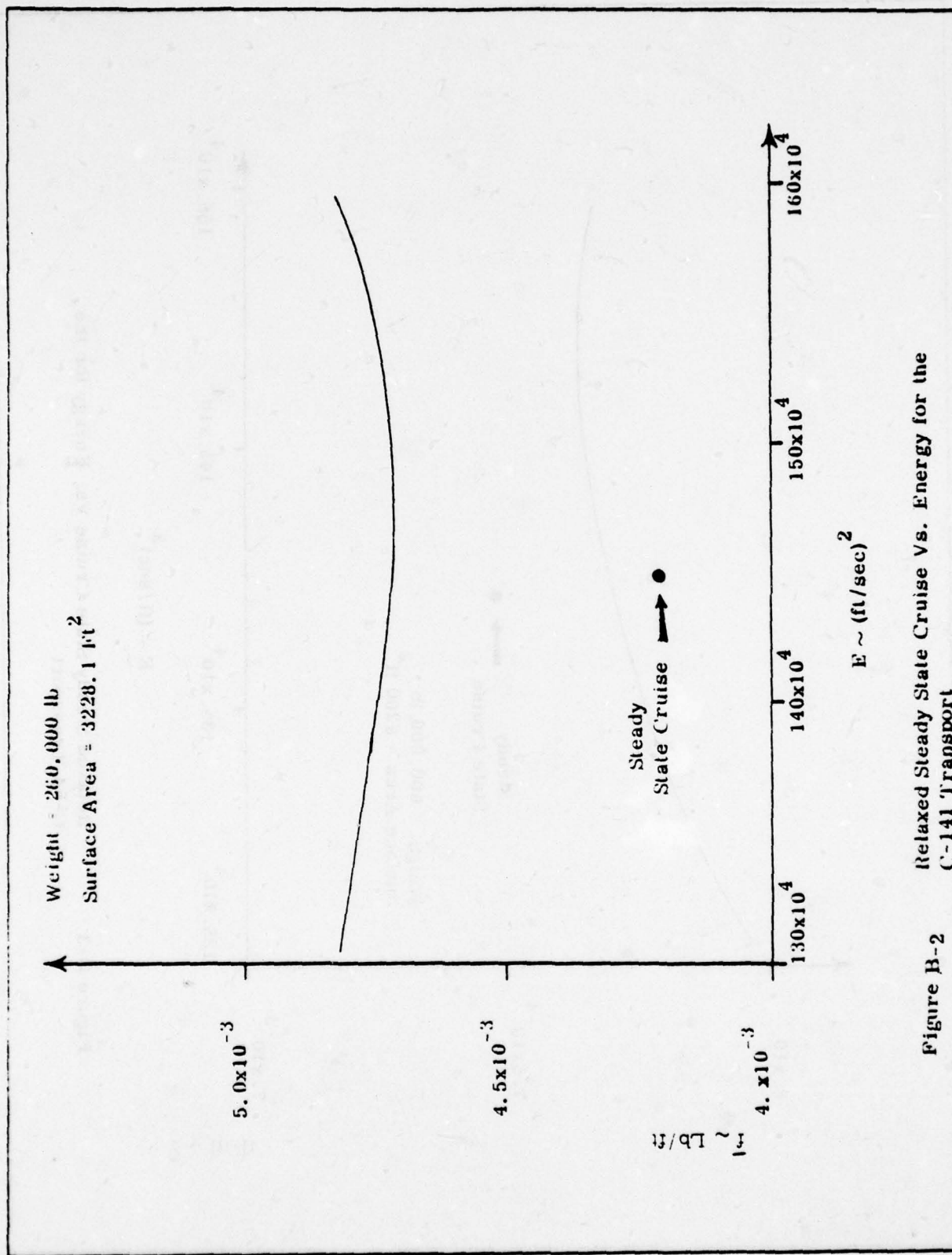


Figure B-2 Relaxed Steady State Cruise Vs. Energy for the C-141 Transport

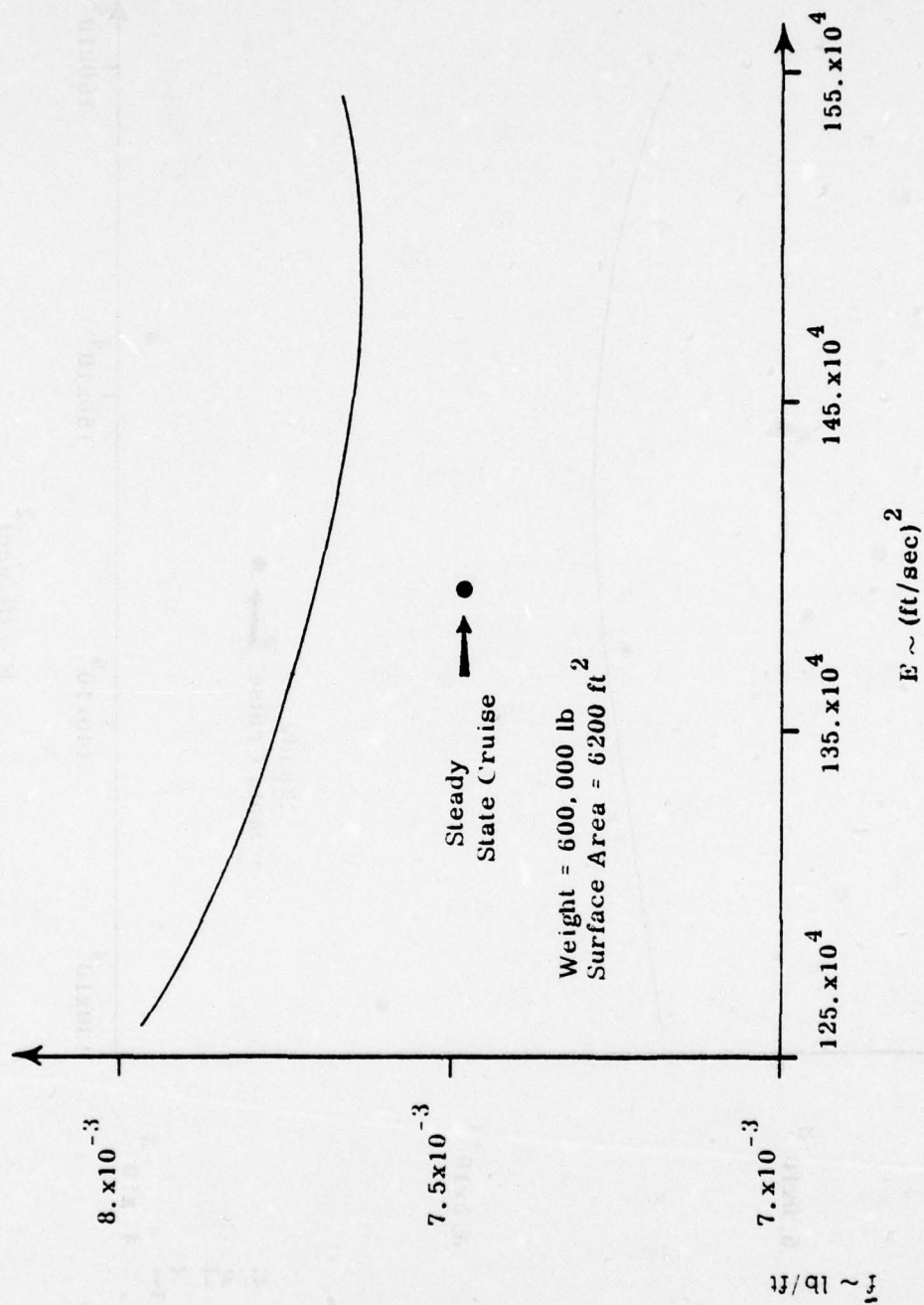


Figure B-3 Relaxed Steady State Cruise Vs. Energy for the G-5A Transport

APPENDIX C

FUNCTIONAL RELATIONSHIPS BETWEEN DESIGN MODIFICATIONS AND IMPROVEMENT IN PERFORMANCE/COST

Another way of evaluating the design modifications is based on the analytical relationship between various aircraft parameters and the range factor RF.

Range factor is defined as

$$RF = \frac{VW}{f} \quad (C.1)$$

Appendix A shows that minimum fuel consumption occurs at a cruise speed and altitude which maximizes range factor for a given weight.

Reference [62] carries out a sensitivity analysis of the range factor to changes in the aerodynamic and engine performance characteristics. The approach taken here is similar to reference [62] except for the differences in aerodynamic and fuel flow models. The drag model is assumed to be represented by

$$C_D = C_{D_0} + B C_L + K C_L^2 \quad (C.2)$$

where the coefficients C_{D_0} , B and K are Mach number dependent. Normalized fuel flow f_n is represented by

$$f_n = T_n \cdot f(M) \quad (C.3)$$

where $f(M)$ is equal to $TSFC/\sqrt{\theta}$, the normalized thrust specific fuel consumption. This assumption is in agreement with the fuel flow model described in Section 3. It is assumed that the value of normalized thrust specified fuel consumption, NTC, is the minimum value. The rationale for this assumption is that if the aircraft aerodynamics and engine are properly matched, then the throttle setting for cruise should be in the neighborhood of minimum $TSFC/\sqrt{\theta}$. Under these assumptions range factor may be written as

$$RF = \frac{Ma_2 W}{D \cdot NTC} \quad (C.4)$$

Drag D is represented by

$$D = S \lambda M^2 \delta c_{D_0} + BW + \frac{KW^2}{S \lambda M^2 \delta} \quad (C.5)$$

where

$$\lambda = .5 \rho_0 a_0^2 \quad (C.6)$$

and a_0 is the speed of sound at sea-level, ρ_0 is the air density at sea-level and S is reference area.

Under the assumption that aerodynamic coefficients C_{D_0} , B and K and normalized thrust specific fuel consumptions are functions of Mach only, range factor becomes a function of Mach and pressure ratio δ . Optimum cruise Mach and pressure ratio for maximizing RF can now be determined.

The necessary conditions for maximum range factor are

$$\frac{\partial}{\partial \delta} \left[\frac{a_0 M W}{D NTC} \right] = 0 \quad (C.7)$$

$$\frac{\partial}{\partial M} \left[\frac{a_0 M W}{D NTC} \right] = 0 \quad (C.8)$$

Substituting the value of drag (D) from (C.5) in (C.7) and carrying out the differentiation results in

$$W/\delta = S \lambda M^2 \sqrt{\frac{C_{D_0}}{K}} \quad (C.9)$$

Consequently $\frac{W}{\delta}$ is constant if M, C_{D_0} and K are constant.

Observe that for a given Mach, the maximum value of L/D occurs where

$$C_L = \sqrt{\frac{C_{D_0}}{K}} \quad (C.10)$$

This condition is the same as given by equation (C.9) which indicates that best cruise is at maximum (L/D).

Expanding Equation (C. 8) gives

$$\frac{1}{M} - \frac{1}{D} \frac{\partial D}{\partial M} - \frac{1}{NTC} \frac{\partial NTC}{\partial M} = 0 \quad (C.11)$$

From Equation (C. 5)

$$\frac{\partial D}{\partial M} = S\lambda \delta \left[2M c_{D_0} + M^2 \frac{\partial c_{D_0}}{\partial M} \right] + \frac{\partial B}{\partial M} + \frac{KW^2}{S\lambda \delta} \left[\frac{1}{M} \frac{\partial K}{\partial M} - \frac{2}{M^3} \right] \quad (C.12)$$

Substituting Equations (C. 9) and (C.12) in (C.11) and rearranging gives a function of Mach number

$$F(M) + \left[2\sqrt{c_{D_0}} K + B \right] \left[NTC - M \frac{\partial NTC}{\partial M} \right] - MNTC$$

$$\left[\sqrt{\frac{k}{c_{D_0}}} \frac{\partial c_{D_0}}{\partial M} + \frac{c_{D_0}}{K} \frac{dK}{dM} + \frac{\partial B}{\partial M} \right] = 0 \quad (C.13)$$

Equations (C.13) is nonlinear in M. An iterative technique is required to solve for best cruise Mach number M^* which remains constant. The optimum value range factor is

$$RF = \frac{Ma_0 (L/D) \max}{NTC} = Ma_0 / (2\sqrt{c_{D_0}} K + B) NTC \quad (C.14)$$

The value of $\frac{W}{S}$ and M^* obtained by solving equations (C. 9) and C.13) differ slightly from the ones obtained by using the actual fuel flow model without the assumption of Equation (C.3). However, the fuel flow representation of Equation (C.3) is more useful for carrying out the sensitivity analysis.

Rewriting Equation (C. 9) in logarithmic form and forming the total differential gives

$$\frac{d\delta}{\delta} = \frac{1}{2} \frac{dK}{K} - \frac{1}{K} - \frac{dc_{D_0}}{c_{D_0}} + \frac{d\left(\frac{W}{S}\right)}{W/S} - 2 \frac{dM}{M} \quad (C.15)$$

Pressure ratio δ can be approximately expressed as an exponential function of altitude h

$$\delta = \delta_R e^{-\mu h} \quad (C.16)$$

where δ_R and μ are defined as follows:

<u>Atmospheric Layer</u>	<u>δ_R</u>	<u>μ (Feet⁻¹)</u>
Troposphere	1.0	1/24700
Stratosphere	1.287	1/20600

Differentiating equation (C.16) and combining with (C.15) gives

$$dh = -\mu \frac{d\delta}{\delta} = -\frac{1}{2\mu} \frac{dK}{K} + \frac{1}{2\mu} \frac{dc_{D_0}}{c_{D_0}} - \frac{1}{\mu} \frac{d(W/S)}{W/S} + \frac{2}{\mu} \frac{dM}{M} \quad (C.17)$$

Note that a decrease in K gives an increase in h where a decrease in c_{D_0} gives a decrease in h

Expanding Equation (C.14) in logarithmic form and differentiating gives

$$\begin{aligned} \frac{dRF}{RF} &= \frac{dM}{M} - \frac{dNTC}{NTC} + \frac{d\left(\frac{L}{D}\right)_{\max}}{(L/D)_{\max}} \\ &= \frac{dM}{M} - \frac{dNTC}{NTC} - \frac{1}{2/(c_{D_0} K + B)} \left[\sqrt{c_{D_0} K} \frac{dc_{D_0}}{c_{D_0}} + \sqrt{c_{D_0} K} \frac{dK}{K} + B \frac{dB}{B} \right] \end{aligned} \quad (C.18)$$

Also from Appendix A, range R is given by

$$R = RF \log \frac{W_i}{W_f} \quad (C.19)$$

where W_i and w_f are initial and final aircraft weight.

Expanding Equation (C.18) in logarithmic form and differentiating results in

$$\frac{dR}{R} = \frac{dRF}{RF} + \left[\frac{W_i}{W_i} - \frac{dW_f}{W_f} \right] / \log \frac{W_i}{W_f} \quad (C.20)$$

If the total fuel is assumed to remain constant the equation (C.20) may be written as

$$\frac{dR}{R} = \frac{dRF}{RF} + \frac{dW_i}{W_i} \left[1 - e^{-R/RF} \right] \frac{RF}{R} \quad (C.21)$$

which is approximately equal to

$$dR/R = \frac{dRF}{RF} - \frac{dW_i}{W_i} \left[1 - .5 R/RF \right] \quad (C.22)$$

Equation (C.21) gives the increase in range due to design modifications. Note that the increase in range is a function of range.

If both range and fuel consumed are assumed to remain constant then Equation (C.20) can be written as

$$dW_i = W_i \frac{dRF}{RF} \left[1 - .5 \frac{R}{RF} \right] \quad (C.23)$$

If both range and payload remain constant then equation (C.20) may be written as

$$0 = \frac{dRF}{RF} + \left[\frac{dW_i}{W_i} - \frac{dW_i - dF}{W_i - F} \right] / (R/RF) \quad (C.24)$$

where F is the total fuel consumed and dF is the change in fuel consumed due to design modifications.

Equation (C.24) can be rewritten as

$$\frac{dF}{F} = \frac{dW_i}{W_i} - \frac{dRF}{RF} \left[\frac{R}{RF} - \frac{1}{e^{R/RF} - 1} \right] \quad (C.25)$$

which may be approximated by

$$\frac{dF}{F} = \frac{dW_i}{W_i} - \frac{dRF}{RF} \left[1 - .5 \frac{R}{RF} \right] \quad (C.26)$$

Equations (C.21), (C.22) and (C.25) define the relationships between design modifications and improvements in range, payload and fuel consumption. Note that all these relations are derived at optimum cruise conditions.

C .1 Example Application of the Analytical Functional Relationships

As mentioned in Section 5.3.2, reference [36] provides design data for retrofitting winglets on KC-135 aircraft. The final estimate of full-scale drag improvement on the KC-135 is given below:

Reduction in induced drag	=	-.00155
Reduction in zero lift drag	=	-.00013
Airplane induced drag without winglets	=	.016

This amounts to 19.4% reduction in induced drag and 0.81% zero lift drag reduction. Reference [36] also indicates an increase in cruise Mach number from .77 to .774 and an increase in NTC from 1.05 to 1.054. Using these values in equation (C.18) results in

$$\frac{dRF}{RF} = 0.071$$

Note that Equation (C.18) is derived from a first order expansion of range factor, RF, about its optimum value. However, for large variations in drag coefficients higher order expansion terms become important. In this case, Fig. 7.6-19 which shows sensitivity of RF to variations in induced drag, may be used by extrapolation. From that Figure, a 19.4% increase in induced drag amounts to 7.6% increase in RF, and from Fig. 7.6-18 a 0.81% reduction in zero lift drag coefficients results in 0.5% increase in RF. Thus, total increase in RF due to winglets for KC-135 is 8.1%. Now considering the ferry mission for the KC-135: maximum take-off gross weight is 297,000 lbs and OEW is 104,450 lbs. without winglets. Winglet weight is equal to 592 lbs. Since maximum take-off gross weight is limited by take-off considerations, assume take-off gross

weight is limited by take-off considerations, assume take-off gross weight remains 297,000 lbs. From equation (C.20), the maximum ferry range improves by 7.6%.

Fuel savings can be computed using these functional relationships, e.g. 7.86% for the KC-135 see(Section 7.6). However, in using these relationship it is assumed that optimum cruise-climb conditions are employed. They do not reflect the actual spectrum of aircraft mission profiles. When the generic fuel/DOC sensitivity plots generated under this study for each aircraft using the actual profile spectrum, the fuel savings for the KC-135 came out to be only 3.1%. This demonstrates that the analytic functional relations, because they do not reflect actual aircraft useage, do not give realistic estimates of the fuel savings. The generic fuel/DOC sensitivity plots should be used (see Section 7 for plots for each aircraft).

APPENDIX D

CENTER-OF-GRAVITY SHIFT EFFECTS ON FUEL CONSUMPTION

In this study only 2-DOF equations are used to describe aircraft motion. Thus total pitching moment on the aircraft is assumed to be zero, i.e., the aircraft is trimmed. As the aircraft c.g. moves aft, the pitching moment supplied by the tail is decreased resulting in a decrease in the magnitude of negative lift due to tail. The wing lift required for level flight is reduced by an amount equal to decrease in the magnitude of tail lift, resulting in a decrease in the total aircraft drag. This appendix derives the relation between the c.g. location and the aircraft fuel consumption.

The aerodynamic data for aircraft under study provides drag coefficient, C_D , as function of mach number, M and C_L . To express C_L as function of stabilator deflection angle and c.g. location additional modeling is required. Total lift coefficient may be expressed as

$$\begin{aligned} C_L &= C_{LB} - C_{LT} \\ &= C_{LB} - C_{L\delta} \delta \end{aligned} \tag{D-1}$$

where C_{LB} is the basic lift coefficient and C_{LT} is the lift coefficient due to stabilator deflection, δ .

The pitching moment due to stabilator deflection is given by

$$M = qSC_{LT}d = qSb C_{m\delta} \delta \tag{D-2}$$

where

- q = dynamic pressure
- S = reference area
- d = tail moment arm
- b = reference length
- $C_{m\delta}$ = pitching moment coefficient due to stabilator deflection

From equation (D-2) substituting value of C_{LT} in Equation (D-1), total lift coefficient may be written as

$$C_L = C_{LB} - \frac{b}{d} C_{m\delta} \quad (D-3)$$

Total pitching moment acting on an aircraft may be expressed as

$$C_m = C_{m_o} + C_{m_{C_L}} C_{LB} + C_{m\delta} - \left(\frac{CG - CG\phi}{b} \right) C_L + C_{m_T} \quad (D-4)$$

where

C_{m_o} = zero lift pitching moment

C_{m_T} = thrust induced pitching moment

$C_{m_{C_L}}$ = pitching moment due to lift

Note that a positive $(CG - CG\phi)$ corresponds to rearward shift of c.g.

Since total pitching moment, C_m , is assumed to be zero, using equations (D-3) and (D-4), C_L is expressed as

$$C_L = \frac{C_{LB} \left(1 + \frac{b}{d} C_{m_{C_L}} \right) + \frac{b}{d} (C_{m_o} + C_{m_T})}{\frac{b}{d} \left(\frac{CG - CG\phi}{b} \right)} \quad (D-5)$$

Either total lift coefficient (C_L) or the wing lift coefficient (C_{LB}) can be used to compute drag coefficient C_D . The first approach neglects the trim drag where as the trim drag is included in the second approach. To evaluate first order effects of c.g. shift, it may be assumed that change in C_{m_T} due to small decrease in thrust required is negligible. Under this

assumption change in wing lift coefficient (ΔC_{LB}) due to a c.g. shift (ΔCG) may be expressed as

$$\Delta C_{LB} = -\frac{b}{d} C_L \left[\frac{\Delta CG}{b} \right] / \left[1 + \frac{b}{d} C_{mC_L} \right] = \eta C_L \frac{\Delta CG}{b} \quad (D-6)$$

where

$$\eta = -b/d / \left[1 + \frac{b}{d} C_{mC_L} \right] \quad (D-7)$$

Equation (C-2) in Appendic C defines drag coefficient as a parabolic function of lift coefficient. This equation is used to obtain change in drag coefficient (ΔC_D) due to a change in wing lift coefficient.

$$\Delta C_D = B \Delta C_{LB} + 2K \Delta C_{LB} C_{LB} \quad (D-8)$$

which may be written as

$$\Delta C_D = \eta \frac{\Delta CG}{b} \left[B C_L + 2K C_L^2 \right] \quad (D-9)$$

where it is assumed that C_{LB} is approximately equal to C_L . Since thrust is equal to drag during cruise equation (D-9) is used to calculate reduction in thrust required and corresponding reduction in SFC due to a shift in c.g. towards aft.

As an example consider a C-141 aircraft cruising at 35,000 feet altitude and 0.75 mach number with average cruise weight 260,000 lbs. For these conditions following aircraft parameters are obtained

$$C_{mC_L} = -.219$$

$$b/d = .298$$

$$\begin{aligned}
 \eta &= .319 \\
 C_L &= .41 \\
 C_D &= .0236 \\
 T &= 14994 \text{ lbs.} \\
 \Delta C_D &= .506 * 10^{-2} \frac{\Delta C_G}{b} \\
 f &= 12719 \text{ lbs./hrs.}
 \end{aligned}$$

Assume a 5% MAC shift in c.g. toward aft of normal operating c.g.

This results in 161 lbs decrease in airplane drag and 145 lbs/hrs. reduction in fuel flow rate during cruise. Thus fuel savings due to 5% aft c.g. is 1.14% in this case.

Appendix E

SUMMARY OF VISITS

INTRODUCTION

As a part of the Data Acquisition phase of 'An Analysis of Fuel Conservation Procedures and Designs', numerous contacts were made with policy-making and operating personnel within the Air Force, industry, and the Federal Aviation Administration. These visits not only served as sources of considerable utilization information and fuel saving suggestions for our study but also as a sounding board for our conclusions and a means of validating our evaluation of data acquired from other sources.

The checklist shown in Table E-1 was used during air and ground crew interviews. Answers were generalized and formed the basis for much of the information included in the report for ground operations and operator variations. It should also be noted that most of the interviews provided additional leads to ideas and to publications which were added to the reference material. This appendix by no means includes all of the people that assisted this effort; however, we would like to express our appreciation for the contributions willingly provided by everyone contacted by the study team.

(Schedule of Visits)

(Alphabetical list of all persons contacted)

Table E-1

BASE CHECKLIST

Maintenance

- I. Engine Runs/Trim:
 - A. Frequency
 - B. Purpose
 - C. Required time
 - D. Fuel consumed
 - E. Suggested reductions

- II. Instrument Accuracy (altitude, airspeed, EPR, fuel quantity):
 - A. Frequency of calibration/check
 - B. Requirement
 - C. Deviations found

- III. Aerodynamic Cleaness:
 - A. Condition of surfaces and seals:
 - 1. Skin
 - 2. Doors
 - 3. Hatches
 - 4. Cowling
 - 5. Flight controls
 - 6. Panels
 - 7. Radome
 - B. Exterior sheet metal repairs:
 - C. Paint:
 - 1. Condition
 - 2. Number of layers (weight)
 - D. Control surface rigging:
 - 1. Rudder
 - 2. Spoilers
 - 3. Flaps, leading and trailing edge
 - E. Frequency of wash

- IV. Security of Pneumatic Systems (attempt to evaluate average aircraft condition - % of bleed air loss)

(continued)

V. Auxiliary Power Units:

- A. Operating durations
- B. Fuel consumption rate

VI. Taxi (reason, e.g., takeoff, trim pad, compass rose, hanger):

- A. Time
- B. Distance
- C. Number of engines used
- D. Base peculiarities

VII. Obtain Copies of:

- A. Instrument, pneumatic, and on-aircraft engine inspection requirements (-6)
- B. Aircraft historical records (samples)
- C. AFTO forms 349 for fuel quantity and engine trim discrepancies (samples)
- D. Fuel distribution logs (samples)
- E. AF form 1994 (samples)
- F. AFTO form 781 H (samples)

VIII. Recommendations/Suggestions:

- A. Procedural improvements
- B. Equipment modifications
- C. Future equipment design

(continued)

BASE CHECKLIST

Operations

- I. Taxi
 - A. Distance.
 - B. Number of engines.
 - C. Time.
 - D. Base peculiarities.
- II. Impact of Reducing Engine Loads:
 - A. Systems not used full time.
 - B. Higher cabin altitudes.
 - C. Lower cabin temperatures.
- III. Constraints to Mission Efficiency:
 - A. Air Traffic Control (ATC).
 - B. Policies and Directives.
 - C. Technical orders.
 - D. Regulations.
 - E. Area peculiarities.
- IV. Fuel Management Procedures:
 - A. Constraints to maintaining aft C. G.
- V. Power Setting Procedures:
 - A. Parameter used (EPR, F/F, EGT, RPM?).
 - B. Degree to which charted settings are used.
- VI. Degree to which Optimum Altitude is Maintained:
 - A. Ease of changing altitude enroute.
- VII. Obtain Copies of:
 - A. Flight plans (samples and procedures).
 - B. Flight logs (samples and procedures).
 - C. Fuel logs (samples and procedures).
- VIII. Recommendations/Suggestions:
 - A. Procedural improvements.
 - B. Equipment modifications.
 - C. Future equipment design.

SCHEDULE OF VISITS

LOCATION	AGENCY	DATE
SCOTT AFB	Visit HQ MAC	10-11 Aug. '76
HQ USAF	USAF/RDPS	20 Aug. '76
FAA	OPS & Proc. Branch	20 Aug. '76
OFFUTT AFB	Visit HQ SAC	23-25 Aug. '76
OKLAHOMA CITY - ALC	ASIMIS Branch; B-52, KC-135 SM; J-57, TF-33 IM	6-7 Sep. '76
SAN ANTONIO ALC	C-5 SM; T-56, TF-39 IM Energy Mgt. Office	18 Sep. '76
LITTLE ROCK AFB	314TAW (C-130)	9 Sep. '76
WARNER-ROBINS AFB	C-130/C-141 SM	14 Sep. '76
LOCKHEED-GEORGIA CO.	C-5/C-130/C-141	14 Sep. '76
CHARLESTON AFB	437 MAW (C-141)	15 Sep. '76
DOVER AFB	436 MAW (C-5A)	Apr. '77

PERSONNEL CONTACTED

Mr. G. Albers

Col. B. Backues
Mr. W. Baker
Lt. Col. H. Ball
Mr. D. Barnes
Col. J. Barnett
Capt. S. Bartosiak
SMSgt. T. Beaubien
Maj. J. Bell
Maj. J. Bennett
Capt. Bergers
Mr. J. Bias
SMSgt. D. Blankenship
Mr. G. Boire
Maj. L. Bonham
Lt. Col. D. Boone
Mr. E. Boss
Mr. T. Bridges
Capt. L. Bryant
Mr. E. Briesch
Lt. Col. R. Bustim

Mr. P. Cadwell
Mr. N. Cain
Mr. R. Callahan
MSgt. A. Calwell
Mr. O. Carlile
Col. F. Carter
CMSgt. J. Castlebury
CMSgt. B. Chase
MSgt. C. Chasi
Mr. B. Chaudoin
CMSgt. R. Cherry
Lt. Col. G. Clark
SMSgt. J. Clark
Capt. E. Coleman
Mr. R. Coleman
Mr. B. Connelly
Capt. L. Converse
Capt. M. Cotnoir
Mr. C. Curnane

Brannif Airlines

San Antonio Air Logistics Center
Lockheed-Georgia Co.
437th Military Airlift Wing
Oklahoma City Air Logistics Center
416th Bomb Wing
416th Bomb Wing
HQ Military Airlift Command
416th Bomb Wing
416th Bomb Wing
314th Tactical Airlift Wing
Oklahoma City Air Logistics Center
HQ Strategic Air Command
HQ Strategic Air Command
HQ Strategic Air Command
HQ Strategic Air Command
Warner Robins Air Logistics Center
FAA Representative, Pease AFB
416th Bomb Wing
Warner Robins Air Logistics Center
HQ Strategic Air Command

Oklahoma City Air Logistics Center
Oklahoma City Air Logistics Center
Oklahoma City Air Logistics Center
509th Bomb Wing
Pratt & Whitney
HQ Military Airlift Command
416th Bomb Wing
USAF Airlift Center
314th Tactical Airlift Wing
Warner Robins Air Logistics Center
437th Military Airlift Wing
314th Tactical Airlift Wing
416th Bomb Wing
416th Bomb Wing
Federal Aviation Administration
Oklahoma City Air Logistics Center
AMST System Program Office
HQ Strategic Air Command
Lockheed-Georgia Co.

TSgt Daniel
CMSgt. W. Daniel
Lt. Col. C. Davis
Mr. W. Davis
Lt. Col. J. Dayley
MSgt J. Debeve
MSgt. J. DeGout
1LT J. DeGroat
Mr. K. Denny
Mr. F. Dickson
Capt. B. Diggins
Mr. H. Ditcher

Mr. A. Eaffy
Mr. A. Elsasser

CMSgt. C. Feilds
MSgt. A. Fineman
Maj. C. Fontana
Mr. J. Freer
Mr. J. Fuller
Mr. J. Funk

Mr. V. Gammill
Maj. H. Barrette
TSgt. D. Gates
TSgt. A. Gatisman
MSgt. W. Goodwin
MSgt. W. Graham
Mr. E. Gray
SMSgt. F. Griffin
Col. S. Groening
Mr. W. Grosschese
Capt. G. Grosskopf
Maj. J. Gunkel
Mr. G. Gusdorf
SMSgt. Guzman

TSgt. V. Hasse
Mr. W. Harbins
Mr. D. Harris
Lt. Col. B. Hawes
Capt. R. Heddelston
MSgt. T. Henkel

HQ Strategic Air Command
416th Bomb Wing
HQ Strategic Air Command
Federal Aviation Administration
HQ Military Airlift Command
437th Military Airlift Wing
416th Bomb Wing
416th Bomb Wing
Oklahoma City Air Logistics Center
San Antonio Air Logistics Center
HQ Military Airlift Command
Lockheed-Georgia Co.

HQ USAF
San Antonio Air Logistics Center

437th Military Airlift Wing
HQ Strategic Air Command
HQ USAF
United Airlines
HQ Military Airlift Command
Boeing Aircraft Co.

Oklahoma City Air Logistics Center
HQ Military Airlift Command
416th Bomb Wing
416th Bomb Wing
416th Bomb Wing
HQ Military Airlift Command
Air Logistics
437th Military Airlift Wing
Warner Robbins Air Logistics Center
Oklahoma City Air Logistics Center
416th Bomb Wing
HQ Military Airlift Command
San Antonio Air Logistics Center
HQ Strategic Air Command

314th Tactical Airlift Wing
Warner Robins Air Logistics Center
San Antonio Air Logistics Center
HQ Military Airlift Command
416th Bomb Wing
416th Bomb Wing

Mr. B. Hensley
Maj. E. Herr
CMSgt. D. Hess
Mr. H. Hillard
CMSgt. W. Hoffs
Mr. B. Hollaway

Lt. Col. T. James
SMSgt. H. John
Mr. O. Johns
CMSgt. A. Johnson
TSgt. J. Johnson
Mr. J. Johnson
SMSgt. R. Johnson
Col. H. Jordan
Capt. G. Jungwirth

Mr. J. King
Capt. R. King
Mr. N. Kirk
Col. C. Kreklow
Lt. Col. K. Krouse
CMSgt. A. Kruger

Mr. A. Lackey
Mr. L. Lapp
MSgt. D. Lawhorn
Lt. Col. A. Lazarist
Lt. Col. D. Lehigh
Lt. Col. Lentz
Mr. T. Lewis
Mr. A. Liu
CMSgt. T. Lindsey
SMSgt. R. Lopez
Capt. Louden
TSgt. Lovell
Mr. C. Lowe
SMSgt. O. Lyree

Mr. R. Mackel
SSgt J. Major
TSgt. M. Martin
Col. P. Martin
Mr. J. Martinique

Oklahoma City Air Logistics Center
416th Bomb Wing
437th Military Airlift Wing
Warner Robins Air Logistics Center
314th Tactical Airlift Wing
San Antonio Air Logistics Center

Warner Robins Air Logistics Center
416th Bomb Wing
San Antonio Air Logistics Center
416th Bomb Wing
314th Tactical Airlift Wing
Oklahoma City Air Logistics Center
314th Tactical Airlift Wing
416th Bomb Wing
HQ Strategic Air Command

Lockheed-Georgia Co.
HQ Strategic Air Command
Oklahoma City Air Logistics Center
437th Military Airlift Wing
416th Bomb Wing
HQ Military Airlift Command

Oklahoma City Air Logistics Center
437th Military Airlift Wing
416th Bomb Wing
416th Bomb Wing
416th Bomb Wing
HQ Military Airlift Command
General Electric Co.
Oklahoma City Air Logistics Center
416th Bomb Wing
416th Bomb Wing
314th Tactical Airlift Wing
509th Bomb Wing
San Antonio Air Logistics Center
437th Military Airlift Wing

Lockheed-Georgia Co.
416th Bomb Wing
314th Tactical Airlift Wing
Oklahoma City Air Logistics Center
San Antonio Air Logistics Center

MSgt. Burton Matteson
Mr. J. McCarty
CMSgt. R. McCord
Lt. Col. E. McCormick
Lt. Col. McIntosh
Capt. B. McNamara
MSgt. J. Meade
Mr. R. Meadows
MSgt. J. Meeks
Mr. J. Mehallow
Mr. C. Miller
Lt. Col. D. Miller
Capt. R. Millnard
Lt. Col. M. Moake
Lt. Col. D. Moorhaus
CMSgt. H. Morillo
Mr. V. Morris

SMSgt. R. Naughton
Col. M. Nash
Maj. M. Nash
Mr. J. Nester
Mr. A. Nichols

Capt. D. Olsen
Col. D. Olson
Capt. G. Olson
Lt. Col. R. Olson
Maj. A. Orlando
Mr. C. Osborne

MSgt. J. Page
SMSgt. T. Paramore
MSgt. A. Pellertire
Maj. D. Powers
SMSgt. W. Prentice
Maj. T. Proffitt
Maj. K. Pruyne
Maj. R. Puchinski

Col. P. Rankin
CMSgt. Richie
Capt. W. Richies
Capt. Rickey
Col. P. Piede
Col. G. Robertson
Lt. Col. Rodeheaver

416th Bomb Wing
Warner Robins Air Logistics Center
HQ Strategic Air Command
San Antonio Air Logistics Center
HQ Strategic Air Command
416th Bomb Wing
437th Military Airlift Wing
Lockheed-Georgia Co.
416th Bomb Wing
HQ Military Airlift Command
Oklahoma City Air Logistics Center
314th Tactical Airlift Wing
314th Tactical Airlift Wing
416th Bomb Wing
HQ Strategic Air Command
437th Military Airlift Wing
HQ Military Airlift Command

437th Military Airlift Wing
San Antonio Air Logistics Center
HQ Military Airlift Command
San Antonio Air Logistics Center
437th Military Airlift Wing

HQ Strategic Air Command
HQ Military Airlift Command
HQ Military Airlift Command
HQ USAF .
HQ Strategic Air Command
Oklahoma City Air Logistics Center

314th Tactical Airlift Wing
437th Military Airlift Wing
509th Bomb Wing
HQ Military Airlift Command
HQ Military Airlift Command
HQ Strategic Air Command
HQ Military Airlift Command
314th Tactical Airlift Wing

Oklahoma City Air Logistics Center
HQ Strategic Air Command
437th Military Airlift Wing
314th Tactical Airlift Wing
314th Tactical Airlift Wing
HQ USAF
HQ Military Airlift Command

CMSgt. T. Salvator
Lt. Col. T. Satterwhite
Capt. F. Schneider
Mr. R. Schwake
Maj. Bernard Sher
Lt. Col. J. Sherrod
Maj. D. Short
Mr. E. Shuba
CMSgt. C. Skipper
TSgt. C. Smith
Maj. L. Smith
Mr. M. Smith
CMSgt. R. Snyder
Maj. S. Spivey
SMSgt R. Spurlock
MSgt. R. Strauss
CMSgt. P. Stephenson
Mr. D. Sulcliffe
MSgt. R. Sword

TSgt. T. Tallion
Mr. J. Tedder
Mr. D. Teet
Mr. B. Tisdale
Mr. J. Toeplitz
Mr. M. Toney
Lt. Col. W. Townsend
Lt. Col. R. Tranceur
Lt. Col. J. Trask
Lt. R. Turley
SMSgt. W. Turner
Capt. P. Tyler

TSgt. Van Dyke

Capt. J. Valaika

Mr. J. Wagner
Ms. E. Walls
Mr. A. Warkentin
SMSgt. D. Webber
Col. Wharton
SSgt. T. Whatley
Lt. Col. M. Wheeler
Col. D. White
Lt. Col. R. Winkler

Mr. J. Yanker
Lt. Col. D. Yarr

416th Bomb Wing
437th Military Airlift Wing
HQ Strategic Air Command
Oklahoma Air Logistics Center
437th Military Airlift Wing
HQ Strategic Air Command
437th Military Airlift Wing
Oklahoma City Air Logistics Center
437th Military Airlift Wing
416th Bomb Wing
437th Military Airlift Wing
Federal Aviation Administration
437th Military Airlift Wing
314th Tactical Airlift Wing
HQ Military Airlift Command
HQ Strategic Air Command
89th Military Airlift Wing
Boeing Aircraft Co.
314th Tactical Airlift Wing

437th Military Airlift Wing
Federal Aviation Administration
Oklahoma City Air Logistics Center
437th Military Airlift Wing
Oklahoma City Air Logistics Center
San Antonio Air Logistics Center
HQ USAF
416th Bomb Wing
416th Bomb Wing
HQ Military Airlift Command
416th Bomb Wing
HQ Military Airlift Command

509th Bomb Wing

HQ Strategic Air Command

Warner Robins Air Logistics Center
314th Tactical Airlift Wing
Oklahoma City Air Logistics Center
314th Tactical Airlift Wing
314th Tactical Airlift Wing
314th Tactical Airlift Wing
HQ Strategic Air Command
437th Military Airlift Wing
HQ USAF

HQ Military Airlift Command
314th Tactical Airlift Wing